Digitized by the Internet Archive
in 2023 with funding from
Kahle/Austin Foundation

https://archive.org/details/contributionsfro0017unse

UNIVERSITY OF ARIZONA
STEWARD OBSERVATORY
TUCSON, ARIZONA

Carnegie Institution of Washington

CONTRIBUTIONS

FROM THE

MOUNT WILSON OBSERVATORY

VOLUME XVII

NOS. 371–390

WITH TWENTY-SEVEN PLATES

APRIL, 1928—NOVEMBER, 1929

UNIVERSITY OF ARIZONA
LIBRARY

7B

Q28
v.17

UNIVERSITY OF ARIZONA
STEWARD OBSERVATORY
TUCSON, ARIZONA

CONTENTS

NO. PAGE

371. PHOTOGRAPHIC OBSERVATIONS OF SOME DOUBLE STARS. *Thomas H. Osgood* . . . 1

372. THE SPECTRUM AND RADIAL VELOCITY VARIATION OF RU CAMELOPARDALIS. *Roscoe F. Sanford* . . . 9

373. CONFERENCE ON THE MICHELSON-MORLEY EXPERIMENT, HELD AT MOUNT WILSON OBSERVATORY, FEBRUARY 4–5, 1927 . . . 17

374. REVISION OF THE VALUE OF e/m DERIVED FROM MEASUREMENTS OF THE ZEEMAN EFFECT. *Harold D. Babcock* . . . 79

375. IS THERE ARGON IN THE CORONA? *Henry Norris Russell* and *I. S. Bowen* . . . 85

376. A SPIRAL NEBULA AS A STELLAR SYSTEM, MESSIER 31. *Edwin Hubble* 99

377. A SPECTROSCOPIC DETERMINATION OF THE PRESSURE IN THE CALCIUM CHROMOSPHERE: AN EXPERIMENTAL TEST OF MILNE'S THEORY. *Albrecht Unsöld* . . . 155

378. ON THE PHYSICAL INTERPRETATION OF SPECTROHELIOGRAMS. *Albrecht Unsöld* . . . 173

379. ON THE THERMAL EXCITATION OF ATOMS IN THE REVERSING LAYER OF THE SUN. *Albrecht Unsöld* . . . 185

380. ENERGY SPECTRA OF THE STARS. *C. G. Abbot* . . . 193

381. THE SPECTRUM OF B.D.+11°4673. *Paul W. Merrill* . . . 213

382. SPECTROSCOPIC OBSERVATIONS OF R VIRGINIS. *Paul W. Merrill* and *Alfred H. Joy* . . . 263

383. ON THE COMPOSITION OF THE SUN'S ATMOSPHERE. *Henry Norris Russell* . . . 271

384. THE ELECTRIC-FURNACE SPECTRUM OF HAFNIUM. *Arthur S. King* . 343

385. ELEMENTS UNIDENTIFIED OR DOUBTFUL IN THE SUN. *Charles E. St. John* . . . 353

386. RONCHI'S METHOD OF OPTICAL TESTING. *J. A. Anderson* and *Russell W. Porter* . . . 369

175592

CONTENTS

NO. PAGE

387. THE RADIAL VELOCITIES OF 741 STARS. *W. S. Adams, A. H. Joy, R. F. Sanford,* and *G. Strömberg* 377

388. THE SPECTROHELIOSCOPE AND ITS WORK: PART I. HISTORY, INSTRUMENTS, ADJUSTMENTS, AND METHODS OF OBSERVATION. *George E. Hale* 407

389. THE UNIT CHARACTER OF MULTIPLETS. *Charles E. St. John* . . 455

390. EXCITATION POTENTIAL IN SOLAR PHENOMENA. *Charles E. St. John* 463

LIST OF PLATES

NO.		FACING PAGE
I.	SOUTH PRECEDING END OF MESSIER 31	154
II.	MESSIER 31	154
III.	CENTRAL REGION OF MESSIER 31	154
IV.	VARIABLES IN MESSIER 31	154
V.	MESSIER 31, REGION NO. 4	154
VI.	VARIABLES IN REGION NO. 4 OF MESSIER 31	154
VII.	CHROMOSPHERIC SPECTRUM WITH INTENSITY MARKS	161
VIII.	SPECTROGRAMS OF B.D.+11°4673	219
IX.	A SLIGHTLY IMPERFECT SPHERICAL CONCAVE MIRROR SEEN UNDER THE FOUCAULT KNIFE-EDGE TEST	372
X.	APPEARANCE OF GRATING PATTERNS ON A CONCAVE SILVERED MIRROR	373
XI.	GRATING PATTERNS SHOWN BY FIVE DIFFERENT LENSES	374
XII.	(*a*) PROMINENCES PHOTOGRAPHED WITH $H\alpha$ LINE; (*b*) DIRECT PHOTOGRAPH OF THE SUN; (*c*) HYDROGEN FLOCCULI, PHOTOGRAPHED WITH $H\alpha$ LINE; (*d*) CALCIUM FLOCCULI, PHOTOGRAPHED WITH K LINE; (*e*) COELOSTAT USED WITH 13-FOOT SPECTROHELIOSCOPE IN 1924; (*f*) OSCILLATING SLITS OF 13-FOOT SPECTROHELIOSCOPE, 1924	413
XIII.	COELOSTAT, SECOND MIRROR, AND TELESCOPE LENS	416
XIV.	OSCILLATING SLITS AND EYEPIECE OF SPECTROHELIOSCOPE	418
XV.	CONCAVE MIRRORS OF SPECTROHELIOSCOPE	418
XVI.	GRATING SUPPORT AND LINE-SHIFTER	418
XVII.	SECOND SLIT, DRIVING MECHANISM, AND LINE-SHIFTER	418
XVIII.	SPINNING DISK WITH RADIAL SLITS	425
XIX.	ANDERSON'S ROTATING PRISMS, FOR USE WITH FIXED SLITS	426
XX.	BRIGHT AND DARK HYDROGEN FLOCCULI	434
XXI.	(*a*) BRIGHT AND DARK HYDROGEN FLOCCULI; (*b*) DARK HYDROGEN FLOCCULUS, APPEARING AS A PROMINENCE WHERE IT PROJECTS BEYOND THE LIMB	434

LIST OF PLATES

NO.		FACING PAGE
XXII.	(*a*), (*b*), (*c*) HYDROGEN FLOCCULI PHOTOGRAPHED ON THREE SUCCESSIVE DAYS; (*d*) STRUCTURE OF HYDROGEN FLOCCULI NEAR LARGE BIPOLAR SUN-SPOT GROUP	434
XXIII.	(*a*) STRUCTURE OF HYDROGEN FLOCCULI NEAR SUN-SPOTS; (*b*) (*c*), (*d*), (*e*), (*f*) SAME REGION OF SUN, PHOTOGRAPHED AT CENTER OF $H\alpha$ AND AT INCREASING DISTANCES TOWARD THE VIOLET	436
XXIV.	(*a*) HYDROGEN FLOCCULI SURROUNDING THE SOUTHERN BIPOLAR SPOT GROUP, MT. WILSON NO. 2656; ACCELERATION OF THE RADIAL VELOCITY OF THE INFLOWING HYDROGEN, SHOWN BY THE LINE-SHIFTER OF THE SPECTROHELIOSCOPE	441
XXV.	COMBINED SPECTROGRAPH, SPECTROHELIOGRAPH, AND SPECTROHELIOSCOPE	448
XXVI.	SLITS, GRATINGS, AND SKELETON TUBE OF COMBINED SPECTROGRAPH, SPECTROHELIOGRAPH, AND SPECTROHELIOSCOPE SEEN FROM BELOW	450
XXVII.	CONCAVE MIRRORS OF SPECTROHELIOGRAPH AND SPECTROHELIOSCOPE	450

Contributions from the Mount Wilson Observatory, No. 371
Printed in the U.S.A.

PHOTOGRAPHIC OBSERVATIONS OF SOME DOUBLE STARS

By THOMAS H. OSGOOD[1]

ABSTRACT

The paper gives photographic measures of 59 double stars, the majority with separations between 2″ and 10″ and magnitudes between 6 and 10. The average probable error in the determination of the angular separation is 0″.007, and in position angle, 5′. All plates were taken at the 80-foot focus of the 60-inch reflector.

The photographic measures enable hypothetical parallaxes to be calculated for these stars, many of which have hitherto been classed as fixed. The results show reasonable statistical agreement with mean parallaxes derived by other methods.

Photographic methods of observing double stars, as developed by Hertzsprung and others, necessarily involve more labor than visual methods; but what they lose in speed they gain in accuracy. On the other hand, visual observations can be carried out for pairs of equal brightness whose separation is almost at the theoretical limit of resolution of a good telescope, while the lower limit for satisfactory photographic work is some fifteen times as great. The present paper gives photographic measures for 59 pairs between magnitudes 6 and 10, the separations for the majority being between 2″ and 10″; at the same time it provides material for calculating the hypothetical parallaxes of these stars, many of which have hitherto been classed as "fixed."

All the plates were taken with the Cassegrain arrangement of the 60-inch reflector (equivalent focal length, 80 ft.), the average exposure being about 20 seconds for an eighth-magnitude pair. Those dated earlier than 1927.30 were photographed and measured by van Maanen, the remainder by the writer. In general, fifteen exposures were made on each plate, in three rows of five: one group with exposures corresponding to the figures given, the others with exposures about 30 per cent more and 30 per cent less than these. The trail of a neighboring bright star served as a reference line in measuring the plate. Color filters were not used. Of the 59 plates,

---

[1] Fellow of the Commonwealth Fund.

TABLE I

β G.C.	α 1900	δ 1900	Mag.		Type	Δα	Δδ	P.E.		s	P	Date	Exp.	Dyn. π	Sp. and Trig. π
439......	0h44m5	+27°10′	6.3	6.3	F0	3″.964	1″.982	2	2	4″.432	296°34′	1925.79	38	0″.0050	+0″.008
1854......	3 40.1	+41 11	8.2	8.8	G6	6.267	5.346	3	3	8.237	49 32	.87	22	.042	.030
2440......	4 54 0	+50 7	8.7	8.7	G	3.438	2.804	2	4	4.436	129 12	1925.88	25	.055	.004
3587......	6 39.9	+55 49	6.3	6.3	F5	4.780	1.077	4	5	4.900	77 30	1926.03	25	.0087	.023
4601......	8 20.8	+27 16	6.4	6.9	A2	3.006	4.051	4	2	5.044	216 35	1927.26	23	.016	.009
4890......	55.8	+15 40	8.6	8.7	K5	1.224	5.063	3	4	5.209	193 35	1927.26	15	.041	.066
5516......	10 34.8	+42 41	7.8	7.8	F2	0.961	3.428	2	3	3.560	164 20	1926.19	25	.023	....
6210......	12 31.0	+11 57	8.3	8.3	G5	2.120	1.181	2	2	2.427	240 53	1926.29	25	.014	.018
6415......	13 7.3	+32 39	6.7	7.2	F8	0.545	1.840	5	3	1.919	343 30	1927.41	14	.024	.020
6527......	28.8	+49 39	8.1	8.3	G0	3.236	2.019	2	2	3.814	301 58	1926.29	25	.020	....
6558......	32.4	− 7 22	7.2	7.2	K2	1.767	2.037	6	4	2.697	40 56	1927.42	15	.0022	....
6561......	32.7	+30 36	8.7	9.7	G	18.796	7.769	7	11	20.338	67 33	.41	14	.045	....
6702......	14 8.4	+ 5 51	7.7	7.8	A3	1.077	4.745	4	7	4.866	192 47	.41	15	.0060	....
6837......	17.4	− 7 19	6.8	6.8	G0	0.898	5.573	3	7	5.645	170 51	.42	14	.026	.023
6869......	21.1	+24 6	9.0	9.5	M2	43.973	12.332	5	6	45.670	74 20	1927.42	10	.099	.076
6875......	22.0	+ 4 9	8.5	8.5	G0	0.737	2.630	3	3	2.731	15 39	1926.36	25	.0055	....
7059......	50.4	+34 30	8.5	10.2	G0	3.105	1.756	16	8	3.567	29 30	1927.47	9	.017	....
7127......	15 2.6	+ 9 36	6.7	6.7	G5	2.234	3.743	2	2	4.359	210 50	1926.36	25	.0084	....
7160......	7.9	+15 46	8.9	9.2	F8	1.929	1.423	8	8	2.397	53 35	1927.48	10	.0090	....
7212......	13.9	+44 10	8.6	8.6	G5	3.072	6.875	2	2	7.530	24 5	1926.36	24	.092	.013
7338......	33.7	− 8 15	8.9	9.4	G0	2.191	1.184	7	4	2.490	298 23	1927.42	12	.0055	....
7341......	33.8	+30 26	8.2	8.6	F8	4.435	2.090	5	4	4.903	295 14	.41	14	.030	.013
7389......	42.6	− 5 1	8.8	8.8	G5	3.534	0.591	6	4	3.583	80 30	.42	11	.015	....
7394......	42.9	+59 44	9.0	9.0	A3	18.357	5.901	7	6	19.282	72 11	.41	15	.048	....
7396......	43.9	− 2 56	8.3	8.5	A0	0.831	2.365	7	4	2.507	160 38	.48	11	.0043	....
7454......	53.7	− 2 48	8.0	8.3	G0	2.067	0.936	6	5	2.269	65 38	.42	15	.011	....
7461......	54.6	+22 5	8.6	8.8	KA2	1.781	3.582	8	6	4.001	206 26	.47	14	.013	....
7551......	16 8.6	+13 48	6.8	7.0	K0	1.424	3.849	5	4	4.104	339 42	.41	16	.036	+0.061
7556......	9.8	+29 0	7.6	9.4	F2	0.654	6.120	10	10	6.155	186 6	.48	17	.0078	....
7571......	12.9	− 2 2	8.3	8.5	A3	1.064	10.677	9	9	10.738	174 19	1927.47	15	0.011	....

7625......	$16^{h}20^{m}.6$	+37°15′	7.9	8.1	Ko	2″.365	8″.158	6	4	8″.494	343°50′	1927.41	15	0″.026	....
7658......	26.9	+56 49	8.1	8.1	Ko	3.433	1.489	3	5	3.742	66 33	.41	15	.0060	....
7712......	36.1	+29 6	8.1	8.6	K2	4.853	5.680	8	5	7.471	40 30	.47	15	.0013	....
7798......	50.3	− 5 1	8.8	8.8	Go	2.007	0.729	6	8	2.135	70 2	.42	15	.011	....
8030......	17 23.9	+30 29	8.9	10.6	F5	4.417	0.629	11	11	4.461	98 6	.48	16	.021	....
8167......	42.9	+51 59	8.7	9.0	K2	7.115	5.343	12	6	8.898	306 54	.48	15	.087	+0″.003
8243......	53.1	+18 21	6.7	6.7	A2	2.418	0.979	5	3	2.609	112 3	.42	15	.0061	....
8354......	18 1.1	+56 25	8.1	9.1	Ao	3.443	5.162	8	6	6.205	146 18	.48	15	.013	....
8579......	23.4	+19 14	7.6	8.0	F5	1.121	5.389	3	5	5.504	191 45	.41	15	.018	....
8684......	33.0	+41 12	6.9	6.9	Ao	1.848	4.902	4	4	5.239	339 21	1927.42	15	.016	....
8705......	34.8	+30 38	9.0	9.2	A	1.613	1.951	2	2	2.531	219 35	1926.53	22	.013	....
8798......	41.8	+59 29	8.7	9.2	K5	7.113	15.336	6	8	16.905	155 7	1927.42	7	.16	.285
9056......	19 4.1	+29 38	8.0	8.5	Ao	2.368	0.636	3	4	2.452	105 2	.41	15	.0014	....
9201......	14.3	+21 46	8.2	8.5	B8	1.497	2.098	5	5	2.577	324 29	.48	15	.0058	....
9248......	17.1	+39 0	8.9	10.9	A2	8.004	4.997	13	15	9.436	301 58	.48	10	.040	....
9262......	18.5	+ 9 19	8.3	8.3	Ao	0.103	8.678	6	6	8.678	180 41	.47	15	.011	....
9693......	48.2	+25 36	7.4	7.4	Ao	2.554	2.891	6	6	3.858	138 32	.48	16	.0060	....
9808......	55.8	+47 5	7.6	7.6	Ko	2.393	4.710	4	5	5.283	26 56	.42	15	.020	....
9818......	56.7	+10 28	6.9	7.1	F2	0.540	4.094	4	6	4.130	352 29	.41	15	.020	.016
9845......	58.0	+47 59	8.3	8.3	G5	3.814	2.007	3	3	4.310	242 15	.42	15	.012	....
9956......	20 5.5	+35 11	7.2	8.2	B3p	4.923	3.031	7	5	5.781	301 37	.48	15	.0091	....
9966......	6.4	− 4 53	8.8	9.8	Ao	4.874	11.570	13	9	12.554	202 51	.48	11	.020	....
10191......	20.4	− 8 37	9.2	9.4	G5	2.509	2.353	4	8	3.439	313 10	.47	13	.011	....
10215......	21.5	+63 53	8.8	9.4	B9	0.872	4.096	6	11	4.187	347 59	.48	14	.0020	....
10485......	40.1	+23 31	8.7	8.8	Ao	1.283	2.073	7	8	2.438	328 15	.48	12	.0020	....
10775......	21 4.8	+16 57	9.6	10.8	F8	15.654	6.663	8	8	17.013	293 3	.47	9	.091	.004
10946......	18.8	+ 3 56	8.3	8.8	Fo	2.591	0.633	9	10	2.667	103 44	.48	11	.012	....
11112......	32.9	+57 1	8.8	9.3	F5	10.262	.489	10	6	10.274	272 44	1927.48	15	.0060	....
11968......	22 42.7	− 4 45	6.7	7.2	Go	3.087	0.321	3	2	3.104	264 4	1925.88	25	0.029	+0.032

40 were measured on the comparator in Pasadena, the remainder on the instrument at the Cambridge Observatory, England.

The observations are collected in Table I. The first three columns identify the star according to its number in Burnham's *General Catalogue* and give its position for the epoch 1900. All are Struve stars with the exception of β G.C. 6415, 6869, 7712, 8030, 9693. Right ascension is quoted to the nearest tenth of a minute. In the sixth column is tabulated the separation in right ascension ($\Delta\alpha$) of the components of each binary; in the seventh, the separation in declination ($\Delta\delta$), both measured in seconds of arc. The next column, headed "P.E.," gives the probable errors, in thousandths of a second, of the measurements in the two preceding columns. The components of the separation are combined in the ninth column to give the angular separation $s=\sqrt{(\Delta\alpha)^2+(\Delta\delta)^2}$. It will be noticed that in only one case is s less than $2''$; according to the standards of visual observation the objects are therefore "easy" pairs. The position angle, tabulated under P, follows from the ratio $\Delta\alpha/\Delta\delta$. The probable error in P is of the order of $5'$. After the position angle is the date, and, in the column headed "Exp.," the number of exposures which were measured on each plate.

The hypothetical parallax of a double star can be determined if the orbital motion of the pair is known. If this motion covers only a very small arc, the parallax may still be calculated, provided we assume a circular orbit, and take an average value for the tilt of the orbital plane. Evidence has been accumulating during the last few years to show that parallaxes derived in this approximate manner can be relied on statistically, though they do not give accurate results in individual cases. It is difficult, from visual observations alone, to detect orbital motion with certainty unless it be large—say about $0\overset{\circ}{.}1$ per annum, if the observations extend over fifty years. With the help of one accurate photographic measurement, however, the sensitivity of the method is much increased. The diagrams in Figure 1 (β G.C. 5516) illustrate this. The essential point is that the photographic measure receives infinite weight—the curve passes through that point, and at the same time represents the older observations weighted approximately as follows: Burnham, Leavenworth, Comstock, Van Biesbroeck, Struve, Aitken, 10; Wirtz, Doolittle, Espin, 8; van den Bos, Doberck, 6; others, 1. For a few of the stars recent photographic measurements by Hertzsprung are available. These were, of course, given additional weight.

That it is legitimate to allocate an infinite weight to the photographic, as compared to the visual observations, may easily be realized from a consideration of the measures of so-called fixed pairs as given in Burnham's *General Catalogue.* About a dozen pairs (between 2″ and 10″) were chosen which showed no evidence of relative motion, and for each of which data were available at not fewer than eight epochs. The observations showed an average departure of 1°.03 from the mean in P, and of 0″.127 in s. Each observation, it must be remembered, is derived from measurements made on several nights—in the case under consideration the average was 3.1 nights. A comparison of these figures with those in the eighth column of Table I reveals the great improvement in accuracy when photographic methods are used. In practice it is more convenient to plot s and P separately against time; so that if ds/dt (in seconds) and dP'/dt (in radians, and corrected for precession) represent the annual change in s and P, the hypothetical parallax is given by

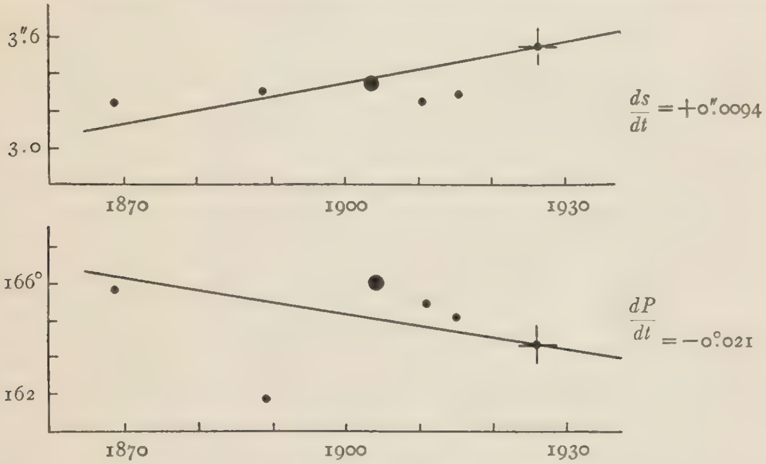

FIG. 1.—β G.C. 5516

$$p = 0.42 \sqrt[3]{\frac{s\left\{\left(\frac{ds}{dt}\right)^2 + s^2\left(\frac{dP'}{dt}\right)^2\right\}}{m_1 + m_2}} ,$$

where m_1 and m_2 are the masses of the components relative to the sun. As a first approximation $m_1+m_2=2$. To obtain a more reliable value of the parallax, it is necessary to reduce the visual to bolometric magnitudes; then the first value of p may be corrected[1] by adjusting both m_1 and m_2 with the help of Eddington's mass-luminosity curve. In compiling the fourth and fifth columns of Table I, where the requisite data are tabulated, it has been assumed that the magnitude and type quoted in the *Henry Draper Catalogue* refer to the brighter star of the pair; for the other component, the type is taken to be the same, and the difference in magnitude, if any, is derived from Burnham's *General Catalogue*. The magnitudes given in Table I, fourth column, are visual magnitudes. The hypothetical parallaxes are listed in the last column but one of this table.

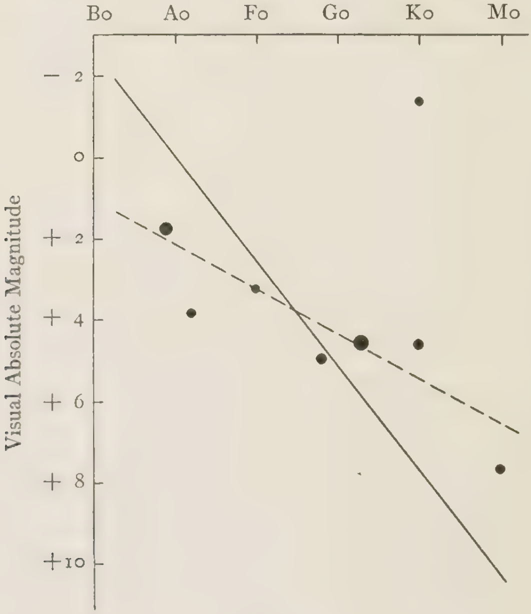

FIG. 2

For β G.C. 439, 3587, 6216, 6869, 7551, and 8798, both trigonometric and spectroscopic parallaxes are available; for β G.C. 1854, 2446, 4601, 4890, 6415, 6837, 7212, 7341, 8167, 9818, 10775, and 11968, spectroscopic ones only. The mean values, corrected for systematic errors as far as the trigonometric parallaxes are concerned, are given in the last column of Table I. I am under great obligation to Mr. W. S. Adams, who communicated many of the spectroscopic values to me in advance of publication. The agreement is in general quite good, except for β G.C. 2446, 7212, 8167, 8798, and 10775. While β G.C. 8798 is undoubtedly a physical pair, 2446 and 7212 are probably only optical double stars, while for 8167 and 10775 the measures give no evidence whether we are dealing with a physical pair or not.

---

[1] Russell, Dugan, and Stewart, *Astronomy*, **2**, 692, 1927.

Since the resolving power of telescopes is limited, the hypothetical parallaxes derived from the orbital motion of double stars are, on the average, considerably greater than the average for all stars of the same visual magnitude. In the present investigation still greater values are to be expected, since the minimum separation of the stars considered is about 2″; such a pair could be resolved by a telescope of very modest dimensions. On the other hand, the measurements in this work have excluded stars brighter than sixth magnitude and wide pairs. It follows that the absolute magnitudes of the stars in Table I will be brighter than the average for all stars of the same type, except in the case of very bright stars, when the discrepancy may be expected in the other direction. This is clearly shown by means of a Russell diagram in Figure 2. Instead of recording individual stars, however, the diagram gives the mean absolute magnitude for groups of stars of nearly similar type. The points were compiled as follows: B3 – A0, 11 stars; A1 – A4, 7 stars; A6 – F4, 6 stars; F5 – F9, 9 stars; G0 – G6, 16 stars; G7 – K3, 5 stars in the main sequence, 2 giants; K4 – M, 3 stars. The dotted line has been drawn to represent the observations as well as possible, while the full line indicates the main sequence. Two stars, β G.C. 6558 and 7712, are obviously giants.

Mention should be made of a paper by Redman[1] dealing with calculations of the same nature as those just described. He has computed hypothetical parallaxes for all stars with determined orbits, as well as for all in which visual observations reveal orbital motion. He adopts the refinement, as here, of applying Eddington's mass-luminosity relation to each component of the binary. His results show good statistical agreement with parallaxes derived by other methods.

---

[1] Redman, *Monthly Notices, R.A.S.*, **88**, 33, 1927.

My thanks are due to Dr. van Maanen and Professor H. N. Russell for much friendly counsel; and to the directors of the Cambridge Observatory, England, for their courtesy in placing their comparator at my disposal for two weeks. I am indebted to Dr. Aitken for furnishing me with measures, for the years between 1906 and 1927, of the stars in Table I.

Carnegie Institution of Washington
Mount Wilson Observatory
April 1928

Contributions from the Mount Wilson Observatory, No. 372
Reprinted from the *Astrophysical Journal*, Vol. LXVIII, pp. 408–415, 1928
Printed in the U.S.A.

THE SPECTRUM AND RADIAL-VELOCITY VARIATION OF RU CAMELOPARDALIS

By ROSCOE F. SANFORD

ABSTRACT

Light-elements.—Fifty-seven epochs of light minimum covering an interval of thirty-five years are satisfactorily represented by the formula

$$\text{Minimum} = \text{J.D. } 2417611.054 + 22^{\mathrm{d}}.1622E \text{ (G.M.A.T.)} .$$

Velocity-curve.—Twenty-four slit spectrograms were obtained between 1919 and 1928. The plot of the measured velocities against phases, computed by means of the foregoing formula, shows that the velocity oscillates periodically with the light through a total range of about 30 km/sec. The interval from velocity maximum to velocity minimum is 15 ± days, which is considerably more than half the period. Minimum and maximum light correspond closely to the epochs of the γ velocity on the rising and falling branches of the velocity-curve, and maximum and minimum velocity occur near the epoch of median magnitude on the rising and falling branches of the light-curve. The usual correspondence between velocity- and light-curves for Cepheids does not hold for RU Camelopardalis.

If the radial-velocity variation is interpreted as the result of a symmetrical pulsation of a spherical star, maximum light synchronizes with minimum diameter and minimum light with maximum diameter.

Spectrum.—The spectrum passes through three clearly recognizable stages: (1) class R0e with emission lines of hydrogen, phase $3^{\mathrm{d}}.3$–$6^{\mathrm{d}}.3$, which is near median magnitude on the rising branch of the light-curve and at velocity maximum; (2) class K0 with hydrogen lines in absorption, phase $8^{\mathrm{d}}.8$–$13^{\mathrm{d}}.0$, which is about symmetrical to light maximum; (3) class R0, with hydrogen lines still in absorption, over the remainder of the period, which includes the epoch of light minimum.

Possible explanation.—The relations between the light- and velocity-curves of RU Camelopardalis at the four crucial phases of maxima and minima for these curves could be explained by a radial pulsation in which maximum light and earliest spectral class go with minimum diameter and vice versa, without a phase-lag. An explanation by variable oblateness is possible but much less probable.

THE LIGHT-CURVE

The variability of the star B.D. $+69^{\circ}417$ was first detected by Mme Ceraski[1] in 1907 from an examination of plates taken by M. S. Blažko between 1899 and 1906. Shortly after, Blažko[2] derived its magnitudes from these plates and concluded that the star varies from 8.0 to 9.1 mag. in a period of $22^{\mathrm{d}}.27$, and with $M - m = 9^{\mathrm{d}}.5$. Several series of observations of the light of this variable (designated RU Camelopardalis) have been made. Especially important are those by Luizet,[1] Ichinohe,[2] Shapley,[3] Haas,[4] Silva,[5] and Leiner.[6] All except Haas and Leiner have published curves derived from their observations. Luizet and Ichinohe have indicated a very slight secondary minimum about midway between primary minima, while the other two have preferred to draw curves of continuous variation. It seems to the writer that the former might well have done likewise. In that case three of the four curves would have been nearly alike in shape with $M-m$ equal to 9 or 10 days. Shapley's curve differs somewhat in having $M-m$ equal to one-half the period. The work of Haas, Silva, and Leiner carries the photometric observations to 1923 and makes it desirable to readjust the formula for minimum light.

---

[1] *Astronomische Nachrichten*, **174**, 80, 1907.

[2] *Ibid.*, **175**, 327, 1907.

Luizet, Shapley, and Silva have given the dates of minimum indicated by their observations. Ichinohe has not done this, but his results agree with those of Luizet, and so need not be considered separately. Dates for minimum light have been derived by the writer from the observations of Haas and Leiner. In addition, three earlier dates are known when this star appeared to be unusually faint.

Table I gives the Julian Day in Greenwich Mean Astronomical Time for the fifty-four observed minima and for the three early dates. The residuals obtained by comparing these fifty-seven dates with those given by Luizet's formula (Minimum = J.D. 2417610.96 $+22^{\mathrm{d}}.172E$, G.M.A.T.) indicate that his formula needs revision. Slight modifications by trial and error were made in both epoch and period; in the first, in order to give a mean residual of zero for Nos. 4–29 in Table I, and in the second, to accomplish a like result for the last ten entries. The modified formula is

$$\text{Minimum} = \text{J.D. } 2417611.054 + 22^{\mathrm{d}}.1622\,E \text{ (G.M.A.T.)} .$$

The residuals are in the fourth column of Table I. Those for Nos. 4–57, inclusive, are little, if any, larger than residuals given by formulae derived from considerably shorter intervals. In addition, those for the three epochs when the star was unusually faint—in 1888, 1894, and 1896—are, at the worst, little in excess of one day. Since all known minima are accounted for over an interval of thirty-five years, the foregoing formula for light minimum has been adopted.

---

[1] *Ibid.*, p. 332; **193**, 83, 1912.

[2] *Ibid.*, **180**, 363, 1909.

[3] *Laws Observatory Bulletins*, **2**, 71 (No. 21), 1913. Discussion based on observations by Seares, Haynes, and Shapley.

[4] *Astronomische Nachrichten*, **220**, 342, 1924.

[5] *Società Astronomica Italiana, Memorie*, N.S., **2**, 191, 1922.

[6] *Astronomische Nachrichten*, **219**, 207, 1923.

TABLE I

MINIMA FOR RU CAMELOPARDALIS*

No.	J.D. (G.M.A.T.)	*E*	O−C	No.	J.D. (G.M.A.T.)	*E*	O−C
1.....	2410675	−313	$+0^{d}.7$	30.....	2418519.00	41	$-0^{d}.70$
2.....	2868	−214	−0.3	31.....	86.70	44	+ .51
3.....	3601	−181	+1.3	32.....	8741.90	51	+ .57
4.....	7676.5	3	−1.04	33.....	63.20	52	−0.29
5.....	99.0	4	−0.70	34.....	86.90	53	+1.25
6.....	7722.0	5	+ .14	35.....	8940.00	60	−0.79
7.....	44.0	6	− .03	36.....	63.00	61	+ .05
8.....	66.3	7	+ .11	37.....	9051.90	65	+0.30
9.....	88.2	8	− .15	38.....	74.80	66	+1.04
10.....	7855.1	11	+ .26	39.....	9140.70	69	+0.45
11.....	7943.6	15	+ .11	40.....	9229.60	73	+ .70
12.....	7966.0	16	+ .35	41.....	52.00	74	+ .94
13.....	8010.8	18	+ .83	42.....	9339.80	78	+ .10
14.....	32.1	19	− .04	43.....	9450.40	83	−0.12
15.....	54.3	20	.00	44.....	74.40	84	+1.72
16.....	77.0	21	+ .54	45.....	96.90	85	+2.06
17.....	99.0	22	+ .38	46.....	9539.70	87	+0.54
18.....	8121.1	23	+ .32	47.....	2420493.32	130	+1.18
19.....	43.0	24	+ .05	48.....	2487.40	220	+0.66
20.....	8364.5	34	− .07	49.....	2576.40	224	+1.01
21.....	87.4	35	+ .67	50.....	2641.75	227	−0.12
22.....	7655.20	2	− .18	51.....	2818.60	235	− .57
23.....	99.10	4	− .60	52.....	41.70	236	+ .37
24.....	7743.80	6	− .23	53.....	2907.80	239	− .02
25.....	67.00	7	+ .81	54.....	30.10	240	+ .12
26.....	8121.40	23	+0.62	55.....	3129.35	249	−0.09
27.....	44.60	24	+1.65	56.....	3283.40	256	−1.18
28.....	8232.00	28	+0.40	57.....	61.70	255	−0.72
29.....	8364.50	34	−0.07				

* Sources for data:

Minima Nos. 1, 2, 3, *Astronomische Nachrichten*, **174**, 80, 1907.
4–21, Haynes, *Laws Observatory Bulletins*, **2**, 71, 1913.
22–47, Luizet, *Astronomische Nachrichten*, **193**, 83, 1912.
48–56, Leiner, *ibid.*, **219**, 207, 1923.
57, Haas, *ibid.*, **220**, 342, 1924.

Silva[1] has published the four curves from the observations of Ichinohe, Luizet, Shapley, and himself. The curve at the bottom of Figure 1 is based on Leiner's observations, which have been grouped into normal places covering phase-intervals of one-half day, the phases being reckoned by the adopted formula. All the curves agree in showing a sharp minimum, a blunt maximum, and a variation that is probably continuous.

---

[1] *Op. cit.*, **2**, 201, 1922.

The shape of the light-curve presents some difficulties. Shapley[1] has interpreted it as the result of an ellipsoidal star in revolution on its minor axis, which, for $i = 90°$, would be 42 per cent of the major axis in the case of uniform brightness, or 62 per cent for complete darkening at the limb. Others have classified RU Camelopardalis as a Cepheid variable.

SPECTRUM AND RADIAL VELOCITY

The *Henry Draper Catalogue* contains the remark, "The spectrum varies. At maximum it is Ko, having a wide absorption band near the wave length 4227. At minimum it is of Class Ro."

Observations with a slit spectrograph were made at this Observatory from February, 1919, to May, 1928. The faintness and late spectral type of RU Camelopardalis, especially at minimum, make it at best a difficult object for spectrographic observation. Furthermore, it is too far north to be reached with the 100-inch reflector. It was necessary, therefore, to use the 60-inch reflector and a one-prism spectrograph with a short-focus camera giving a dispersion of 74 A per millimeter at $H\gamma$. The data for the twenty-four usable spectrograms are given in Table II. The velocities in each case are means of at least two measures, usually one with the Gaertner micrometer measuring machine and one with the Hartmann spectrocomparator.

The thirty-five-year interval during which light minima are represented by the adopted formula overlaps nearly one-half of the interval covered by the spectrograms. The formula should therefore give reliable phases for the spectrograms, to be used in finding the relation of the velocity- and light-curves. These phases appear in Table II.

The change in spectral type mentioned in the *Henry Draper Catalogue* is certainly present. Some of the slit spectrograms show another spectral distinction in that emission lines of hydrogen appear on a spectrum of class Ro. These are designated by Roe in Table II. For the two other types observed, Ko and Ro, the hydrogen lines are in absorption.

---

[1] *Op. cit.*, **2**, 82 (No. 21), 1913.

The top of Figure 1 shows the radial velocities plotted against phase. The phase durations for the three spectral classes are denoted by horizontal lines between brackets and shown below.

TABLE II

Observations of RU Camelopardalis

Plate No.	Date	G.M.A.T.	Phase	Vel. km/sec.	Type
γ 7873	1919 Feb. 13	$19^{h}20^{m}$	$4^{d}636$	− 8.9	Roe
7971	Mar. 17	19 55	14.498	35.0	Ro
8019	Apr. 9	16 55	15.210	36.8	Ro
8122	Apr. 20	19 35	4.160	14.6	Roe
12247	1923 Oct. 28	23 45	16.331	31.3	Ro
12255	Oct. 29	23 52	17.335	36.1	Ro
12412	1924 Jan. 18	21 20	9.580	24.2	Ko
12417	Jan. 19	17 40	10.428	30.4	Ko
12499	Feb. 18	18 22	18.296	33.4	Ro
12503	Feb. 19	19 12	19.330	28.7	Ro
12505	Feb. 20	16 30	20.218	30.1	Ro
13040	Oct. 18	0 21	16.761	31.8	Ro
13170	1925 Jan. 6	17 20	8.779	19.6	Ko
13342	Apr. 2	16 39	6.142	4.4	Roe
13736	Sept. 24	0 11	3.159	8.4	Roe
13742	Sept. 25	0 38	4.177	3.0	Roe
13992	1926 Jan. 25	17 00	16.048	26.4	Ro
14786	1927 Jan. 16	22 00	17.661	36.4	Ro
14855	Mar. 15	18 23	9.024	26.9	Ko
14870	Mar. 19	17 42	12.996	27.4	Ko
14930	Apr. 20	16 56	0.639	30.6	Ro
15318	Oct. 13	23 05	21.760	33.8	Ro
15612	1928 Mar. 6	18 35	11.437	23.2	Ko
15738	May 2	17 09	1.891	−22.2	Ro

The intervals are phase $3^{d}3$–$6^{d}3$ for Roe, $8^{d}8$–$13^{d}0$ for Ko, and $14^{d}2$–$1^{d}9$ for Ro. In other words, Ko covers maximum light, Ro extends from $8^{d}0$ before to $1^{d}9$ after minimum light, and Roe coincides roughly with maximum velocity. Within each interval are indications of progressive spectral changes. The emission lines of hydrogen appear to have their greatest strength near velocity maximum. The absorption of $H\gamma$ tends to increase with phase during the Ko stage. The spectrograms taken nearest to minimum light seem to have the strongest carbon bands. The bands appear weakest at the beginning of the Ro stage and at the end of the Roe stage.

The velocity evidently varies in the same period as the light. Although the variation in light and velocity cannot be interpreted as the result of orbital motion, the velocity variation is conveniently described by the six elements of such a motion. The period is assumed to be known, and the other five elements were found from the plotted velocities by Russell's[1] method. The curve based upon these elements is shown with the plot of the velocities and evidently gives as faithful an approximation to the observations as can be expected with the low dispersion used. The broken horizontal line shows the velocity of the system. The six elements are:

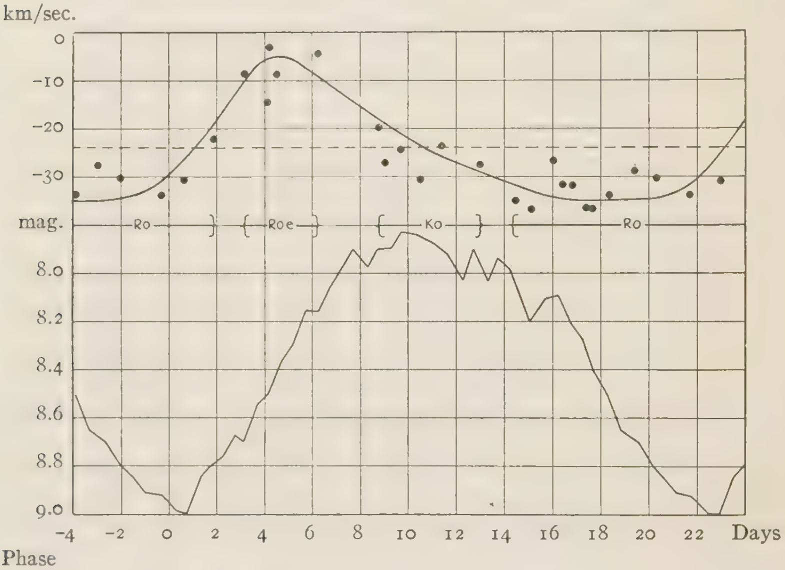

FIG. 1.—Upper part, radial velocities, and radial-velocity curve of RU Camelopardalis with the intervals for its three spectral types indicated underneath. The light-curve from Leiner's observations appears in the lower section of the figure.

$P = 22^{d}.1622$
$K = 14.9$ km/sec.
$e = 0.325$
$\omega = 322^{\circ}$
$T = 3^{d}.4$ after minimum light
$= $ J.D. 2417614.454 G.M.A.T.
$\gamma = -23.9$ km/sec.

---

[1] *Astrophysical Journal*, 40, 282, 1914.

Figure 1 shows that minimum light is nearly coincident with the epoch when the velocity changes from approach to recession, and maximum light with the change from recession to approach. Further, maximum velocity corresponds approximately to the phase of median magnitude on the rising branch of the light-curve, and minimum velocity to that magnitude on the falling branch.

The correspondence of the earliest spectral class with light maximum and of the latest with light minimum might be cited as evidence of Cepheid variation, were it not for the fact that in all other respects the evidence is against it. Velocity minimum does not correspond with light maximum nor velocity maximum with light minimum, and the interval from velocity maximum to velocity minimum is nearly 70 per cent of the period, whereas in the majority of Cepheids this interval has been found to be less than one-half of the period. It is well also to point out that if the velocity variation is the result of a symmetrical pulsation of a spherical star, light minimum is nearly coincident with maximum diameter and vice versa, and that no phase-lag of temperature with respect to velocity need be postulated as for Cepheids.

Furthermore, the existence of a variation in the radial velocity is inconsistent with Shapley's assumption that a single rotating ellipsoid explains the light-curve. Another way out, which he mentions as less likely, is to assume that the star is spotted; but difficulties arise in trying to explain with this mechanism the relation here found between the light- and the velocity-curves.

The light-curve could be harmonized with the velocity-curve were it permissible to make the rather artificial assumption of a spheroidal star whose axis of rotation points nearly toward the observer and which, with nearly constant volume, pulsates through varying degrees of oblateness with little if any change in surface brightness. At phase $10^{d}.7$ (Fig. 1) the stellar matter ceases to recede, the spheroid reaches its greatest oblateness, the surface presented to an observer on the earth is a maximum, and light maximum occurs. At phase $1^{d}.0\pm$ the stellar matter ceases to approach, least oblateness occurs, the disk presented to the observer is a minimum, and light minimum takes place. The median spheroids should be attained near the phases of maximum and minimum velocities which are nearly coincident with the two phases for median magnitude. The relations of light- and velocity-curves are thus accounted for at the four crucial points.

Whether the spectral changes, which must represent modifications of the conditions of temperature, pressure, gravity, etc., in the atmosphere of the star, can be accounted for by such a system is not clear. It is, however, futile to speculate upon the explanation until more is known about the difference between the atmospheres of stars of spectral classes K and R.

The appearance of emission lines at the time of maximum velocity of recession has an analogy in the spectra of some other stars. For example, emission lines in the spectra of the two components of the companion to Castor[1] are relatively stronger when their source is receding. Further, a study of the spectrum of AC Herculis now in progress shows that emission lines appear at maximum velocity of recession. No satisfactory explanation of these peculiarities has yet been found.

Carnegie Institution of Washington
Mount Wilson Observatory
September 1928

---

[1] *Mt. Wilson Contr.*, No. 320; *Astrophysical Journal*, **64**, 250, 1926.

Contributions from the Mount Wilson Observatory, No. 373
Reprinted from the *Astrophysical Journal*, Vol. LXVIII, pp. 341–402, 1928
Printed in the U.S.A.

CONFERENCE ON THE MICHELSON-MORLEY EXPERIMENT

HELD AT THE MOUNT WILSON OBSERVATORY
PASADENA, CALIFORNIA

FEBRUARY 4 AND 5, 1927

The presence of Professor A. A. Michelson and Professor H. A. Lorentz in Pasadena in the early months of 1927 offered an exceptional opportunity for a conference on the theoretical and practical aspects of the Michelson-Morley experiment. Since Professor Michelson had planned, with the co-operation of the Mount Wilson Observatory, to repeat the experiment, such a conference was especially desirable. This was arranged largely on the initiative of Dr. Charles E. St. John. The experimental side was further presented by Dr. Roy S. Kennedy. This was supplemented by a mathematical treatment of the light-path by Professor E. R. Hedrick, as developed by himself and Professor L. Ingold, and by an account presented by Professor P. S. Epstein of the Trouton-Noble experiment, recently repeated at the California Institute of Technology by Chase, and of other recent experimental investigations. Illuminating discussion followed the presentation of the general reports. The shorthand notes were taken by Dr. Fritz Zwicky and Glenn H. Palmer, of the California Institute. These have been reviewed by the authors.

The addresses by Professors Michelson and Lorentz were followed by a detailed account of the results obtained by Professor D. C. Miller, who, fortunately, was also able to be present.

REPORTS

I. PROFESSOR A. A. MICHELSON (UNIVERSITY OF CHICAGO)

In 1880 I conceived for the first time the idea that it should be possible to measure optically the velocity w of the earth through the solar system. There had been earlier attempts to discover first-order effects, based on the idea of a system moving through a stationary ether. (First-order effects are proportional to w/c, where c = light-velocity.) Talking in terms of the beloved old ether (which is now abandoned, though I personally still cling a little to it), one might have expected that the aberration of light would be different for a telescope filled with air and with water, respectively. The experiments, however, showed, contrary to the then-established theory of light, that no such difference was present.

Fresnel's theory was the first to account for this result. Fresnel assumed that matter was able to drag along the ether partially (entrainment of ether), giving it a velocity w', so that

$$w' = \rho w \, .$$

He was able to determine ρ (Fresnel's coefficient) in terms of the refractive index μ:

$$\rho = \frac{\mu^2 - 1}{\mu^2} \, .$$

This coefficient is easily obtained from the negative result of the following experiment. Two light-beams travel along the path (Fig. 1; 0, 1, 2, 3, 4, 5) in opposite directions and give rise to a set of interference fringes. I is a tube filled with water. Now if the whole system moves with the velocity w through the ether, a shift of fringes would be expected on moving the tube from position I to II. No displacement is observed. By assuming a partial entrainment of the ether, Fresnel's coefficient ρ may readily be determined from this experiment. It may also be found in a very simple and direct fashion with help of the Lorentz transformation.

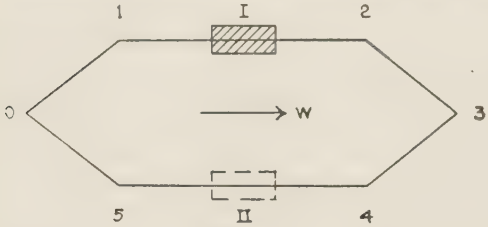

FIG. 1

Fresnel's result was accepted universally by investigators of his time, including Maxwell, who pointed out that, while there could be no first-order effects, there might, nevertheless, be second-order effects (proportional to w^2/c^2). Now with $w \sim 30$ km/sec. for the motion of the earth, $w/c=10^{-4}$, and $w^2/c^2=10^{-8}$, a quantity too small to be measured, according to Maxwell.

It seemed to me, however, that by making use of light-waves, one might devise an adequate arrangement for measuring such second-order effects. Consider an apparatus, including mirrors, moving with the velocity w through the ether. Suppose two light-beams to travel back and forth in the apparatus, one parallel to w, the other at right angles to w. According to the classical theory, the change in light-path resulting from w should be different for the two beams and produce an appreciable shift of the interference fringes. The first device tried for the measurement of second-order effects is indicated in Figure 2. This arrangement, however, involved very great difficulties and was soon abandoned; and fortunately, because it led to the construction of the interferometer, which has proved of great value in many subsequent experiments.

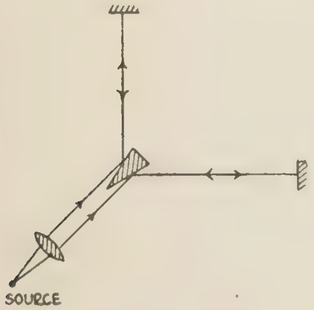

FIG. 2

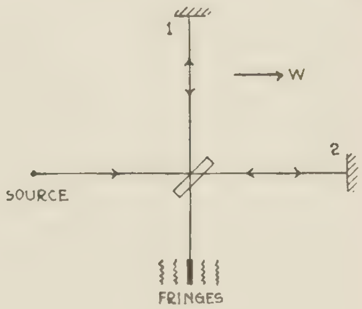

FIG. 3

The interferometer (Fig. 3) is known to all of you. A set of fringes is obtained by superposition of the two beams traveling from the source to a glass plate and then to mirrors 1 and 2, respectively, and back. If white light is used, the central fringe will be white and the side fringes will be colored. A motion of the apparatus with the velocity w through the ether should have much the same effect on the light as a stream of water would have on a boat trying to go once forth and back across the stream, and once down and then back up the stream. The time for getting forth and back a given distance will be different for the two cases. This is easily seen, because, however swift the current, the boat in its transverse journey could always return to the bank from which it started, whereas, in the second case, it might be unable to get back up stream against the current.

I tried the experiment at Berlin in Helmholtz' laboratory, but the vibrations of the city traffic made it impossible to get steady fringes. The apparatus was transferred to the observatory at Potsdam. I have forgotten the name of the director (I think it was Vogel), but I remember with pleasure that he was immediately interested in my experiment. Though he had never seen me before, he put the whole observatory with its staff at my disposition. I got a zero result in Potsdam. The accuracy was not very high, because I had a light-path of only about 1 m. Still it is interesting that the results were quite good. Coming back to America, I had in Cleveland the good fortune to secure the co-operation of Professor Morley. The apparatus then used was the same in principle as that used in Berlin, although the light-path was made longer by introducing a number of reflections instead of a single one. The path was in fact about 10–11 m long, which should have yielded a displacement of half a fringe, due to the orbital motion of the earth. But no displacement was found. The shift of fringes was certainly less than 1/20 and may be even 1/40 of that predicted by the theory. The result could be accounted for by the assumption that the earth drags the ether along nearly at its full speed, so that the relative velocity between the ether and the earth at the surface is zero or very small. This assumption, however, is a very dubious one because it contradicts some other important theoretical considerations. Lorentz then suggested another explanation (Lorentz contraction) which in its final form yielded as a result the famous Lorentz transformation equations. These contain the gist of the whole relativity theory. The Michelson-Morley experiment was continued by Morley and Miller, who again obtained a negative result. Miller then continued alone, and seems now to get some positive effect. This effect, however, has nothing to do with the orbital motion of the earth. It seems to be due to a velocity of the solar system relative to stellar space, which may be much greater than the orbital velocity.

The observations of Mr. Miller have stimulated new interest in the problem. An excellent piece of work has already been done by Mr. Kennedy, whose report you will hear. I intend myself to go over the experiments again, but several months may pass before I shall be able to give my results, which, I hope, will shed more light on the subject.

II. PROFESSOR H. A. LORENTZ (LEIDEN, HOLLAND)

The motion of the earth through a hypothetical ether (talking in historical terms) might have an effect on different phenomena. The first relevant phenomenon found experimentally was the aberration of light. It was discussed on the basis of the emission theory and also on the wave theory in the form Fresnel had given it. From Fresnel's point of view we may argue as follows: We draw our diagrams in a system of co-ordinates which is fixed to the earth. In this system all ponderable matter is at rest. But the ether may move through it. Say the velocity of the ether is w. If the ether does not move, then the velocity of light through matter would be $u=c/\mu$ (μ = index of refraction; c = velocity of light). Now let an elementary wave be formed around P. This after the time dt will be a sphere of radius udt. The center O of this wave will, however, not coincide with P, being displaced over a distance $kwdt$, where $1-k$ is Fresnel's coefficient $1-1/\mu^2=\rho$. Thus $k=1/\mu^2$. PQ is a ray of light. (We denote by v the velocity of the *rays* of light.)

We have then from Figure 4, in which $PQ=vdt$, $PO=kwdt$, and $OQ=udt$, the relation

$$PQ:PO:OQ=v:kw:u\,.$$

Thus

$$u^2=v^2+k^2w^2-2kv\cos\vartheta. \qquad (1)$$

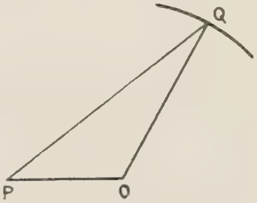

FIG. 4

The derivation of this formula is based on Huyghens' principle and Fresnel's entrainment. Huyghens' principle can be used in any case. One has simply to follow the elementary waves and to construct the successive wave fronts. As to the coefficient of entrainment, I mention that Fresnel found it at first on a mechanical basis from his elastic theory of light. This was a very remarkable performance at that time.

If we neglect terms in w^2 we find

$$v=u+kw\cos\vartheta\ ,$$

$$\frac{1}{v}=\frac{1}{u}-\frac{kw}{u^2}\cos\vartheta\ .$$

The course of a ray of light between given points is determined by the condition (Fermat's principle)

$$0=\delta\int\frac{ds}{v}$$

or

$$0=\delta\int\left(\frac{ds}{u}-\frac{kw}{u^2}\cos\vartheta\,ds\right)\ . \qquad (2)$$

Suppose now

$$\frac{k}{u^2}=\text{const.},$$

that is, k is inversely proportional to μ^2. For $\mu=1$, there is necessarily $k=1$. Thus it follows that

$$k=\frac{1}{\mu^2}\ .$$

The second term in (2) becomes then

$$\frac{1}{c^2}\int w\cos\vartheta\,ds\ .$$

Now let the motion of the ether in our diagram be irrotational, so that w depends on a velocity potential φ,

$$w=\text{grad}\ \varphi\ .$$

Then the integral

$$\int w\cos\vartheta\,ds$$

for a path between two given points P and P' becomes

$$\int_P^{P'}\frac{\partial\varphi}{\partial s}\,ds=\varphi_{P'}-\varphi_P\ .$$

This has the same value for all paths, and the condition (2) becomes simply

$$\delta\int\frac{ds}{u}=0\ ,$$

as if there were no ether motion. Thus we conclude that the course of the ray is not altered by the motion of the ether.

The considerations given above also include cases of reflection and diffraction.

Now let there be two paths, 1 and 2, for a ray of light from a given point P to another given point P'. The time required for light going over them is, for the first path,

$$\int_1 \frac{ds}{v} = \int_1 \frac{ds}{u} - \frac{1}{c^2}\int_1 w \cos\vartheta\, ds\,,$$

and, for the second path,

$$\int_2 \frac{ds}{v} = \int_2 \frac{ds}{u} - \frac{1}{c^2}\int_2 w \cos\vartheta\, ds\,.$$

The last terms in these expressions are equal. Therefore, the difference between the two times is not altered by the motion of the ether. This motion, then, has no influence on phenomena either of interference or of diffraction.

It may be remarked that the difference between the times just considered will be altered by the motion of the ether if this motion is not irrotational. The change is given by the difference of the two integrals

$$\int_1 w \cos\vartheta\, ds \qquad \text{and} \qquad \int_2 w \cos\vartheta\, ds$$

taken for the two paths between P and P'. For this difference one can write the line integral of the velocity w taken over the closed circuit formed by the two lines.

Let us consider, for instance, the earth's rotation. If the ether is stationary, its motion relative to the earth will be a rotation in the opposite direction. If now a large horizontal circuit fixed to the earth, e.g., a rectangular one, is traveled over in opposite directions by two beams of light, the relative motion of the ether will change the position of the fringes produced by the interference of these beams. This effect has been observed by Professors Michelson and Gale.

In the following there will be no question of the rotation of the earth; the annual aberration only will be considered. For the explanation of this the foregoing considerations suffice. If, at a point at some distance from the earth, the direction of the rays coming from a star is given in a system of co-ordinates in which the earth is moving, one can deduce from that the direction of the rays in a system of co-ordinates fixed to the earth, and the further course of these relative rays is determined by the ordinary laws of optics.

We proceed with the discussion of some special theories. In Fresnel's theory the ether is supposed to be at rest; its motion relative to the earth may be considered as a uniform translation, which, obviously, is irrotational. It is necessary to introduce the dragging coefficient because the ether moves through the ponderable bodies (lenses) contained in our instruments of observation.

Stokes proposed a theory in which the ether was supposed to have an irrotational motion, such that at all points of the earth's surface its velocity is equal to that of the earth. By this latter assumption he could avoid the introduction of Fresnel's coefficient.

However, at least when the ether is supposed to be incompressible, Stokes's assumptions contradict each other. If a sphere moves with a constant velocity in an incompressible medium, the motion of the medium is completely determined by the condition that it is irrotational and that, in the direction of the normal to the surface, a point of the sphere and the adjacent medium have the same velocity. In a tangential direction the two velocities will necessarily be different.

So far as aberration is concerned, a modification of Fresnel's theory is certainly admissible. When we admit his value of the dragging coefficient, we may assume the existence of any motion of the ether, provided that it be irrotational. In fact, this is a necessary condition. Suppose, for instance, that over a part of the earth's surface which may be considered as plane the ether flows in a horizontal direction x with a velocity w_x increasing with the height y above the earth. This motion would not be irrotational and would not lead to the observed aberration. Since the existence of a velocity potential requires the equality of the derivatives $\partial w_x/\partial y$ and $\partial w_y/\partial x$, the observed aberration can exist only when, in addition to the supposed motion in a horizontal direction, there is a vertical velocity of the ether of sufficient magnitude, varying from one point of the surface to the other.

So far there was question of first-order effects only, i.e., of effects that would be proportional to the first power of the ratio between the velocity of the earth and the speed of light. In almost all cases in which astronomers and physicists have tried to detect an influence of the earth's motion on optical and electromagnetic phenomena, only effects of this order of magnitude could have been observed. The fact that all these attempts have been fruitless, and that this could be accounted for by theoretical considerations of the kind just preceding, led by and by to the conviction that the motion of the earth can never produce a first-order effect. This conviction was greatly strengthened when Einstein developed his theory of relativity and simply postulated that the result of all experiments which we perform in our laboratories must be independent of the motion of the earth, whatever may be the refinement of our measurements and the order of the effects which we can reach by them. To the experimental evidence which we already had, the charm of a beautiful and self-consistent theory was then added.

Historically, I might add that before the relativity theory was developed the situation was somewhat similar to that which now characterizes the quantum problem. There were, of course, not so many people working in the field as there are now. Nevertheless, we had often very lively discussions about the subject. I remember especially the assembly of the German Society of Natural Sciences in Düsseldorf in 1898, at which numerous German physicists were present, Planck, W. Wien, Drude, and many others. We discussed especially the question of the first-order effects. Some devices with which such an effect might be observed were proposed, but none of these attempts was ever made, so far as I know. The conviction that first-order effects do not exist became by and by too strong. We even got, finally, into the habit of looking only at the summary of experimental papers which dealt with such effects. In case the result was properly negative we felt perfectly satisfied.

As to the second-order effect, the situation was much more difficult. The experimental results could be accounted for by transforming the co-ordinates in a certain manner from one system of co-ordinates to another. A transformation of the time was also necessary. So I introduced the conception of a local time which is different for different systems of reference which are in motion relative to each other. But I never thought that this had anything to do with the real time. This real time for me was still represented by the old classical notion of an absolute time, which is independent of any reference to special frames of co-ordinates. There existed for me only this one true time. I considered my time transformation only as a heuristic working hypothesis. So the theory of relativity is really solely Einstein's work. And there can be no doubt that he would have conceived it even if the work of all his predecessors in the theory of this field had not been done at all. His work is in this respect independent of the previous theories.

I shall have little to say about the theory of the Michelson-Morley experiment, which was the first ever made of those in which we are concerned with effects of the second order. That here again the result must be negative is immediately clear if we follow the theory of relativity. If, instead of that, we apply to the experiment our old stationary ether, we must carefully consider the paths of the interfering rays of light and the time in which the light is propagated along each of them from the source of the point where the interference takes place.

For this purpose we can again use the fundamental equation (1). Confining ourselves to the propagation in ether, we may put $u=c$, $k=1$ so that the equation becomes

$$c^2 = v^2 + w^2 - 2vw \cos\vartheta$$

Taking into account terms of the second order w^2/c^2, we deduce from it

$$v = c\left(1 + \frac{w}{c}\cos\vartheta - \frac{w^2}{2c^2}\sin^2\vartheta\right),$$

$$\frac{1}{v} = \frac{1}{c}\left\{1 - \frac{w}{c}\cos\vartheta + \frac{w^2}{c^2}\left(\cos^2\vartheta + \tfrac{1}{2}\sin^2\vartheta\right)\right\}.$$

Now let there be two paths, 1 and 2, along which light can go from the point P to the point P' (Fig. 5). For each of them the time required for propagation will be represented by expressions of the form

$$\int \frac{ds}{v} = \frac{1}{c}\int ds - \frac{1}{c^2}\int w \cos \vartheta \, ds + \frac{1}{c^3}\int w^2 \left(\cos^2 \vartheta + \tfrac{1}{2} \sin^2 \vartheta\right) ds \,, \qquad (3)$$

and we shall be able to calculate the two times, if we know the lines along which the integrals are to be taken. Let the lines l_1 and l_2 (Fig. 5) represent the paths of the two rays as they would be if the ether did not move through the diagram. As has been shown, these lines are not altered by the motion so long as we confine ourselves to terms of the order w/c. They may, however, be somewhat changed when, as is now proposed, quantities of the second order are taken into account. We shall then have, for instance, the dotted lines l_1' and l_2' whose distances from l_1 and l_2, reckoned along the normals to these lines, are of the second order. We must now calculate the times of propagation for the paths l_1' and l_2', say Tl_1' and Tl_2'. Since, however, T is a minimum for l_1, as compared with neighboring lines, and since the displacements from l_1 to l_1' are of the second order, the difference between Tl_1 and Tl_1' will be of the fourth order. This may be neglected when we confine ourselves to quantities of the second order. Similarly, we may replace Tl_2' by Tl_2. This means that, in the determination of the phase differences, we may use the values of (3) for the rays, such as they would be according to the ordinary laws of optics in the absence of the earth's motion.

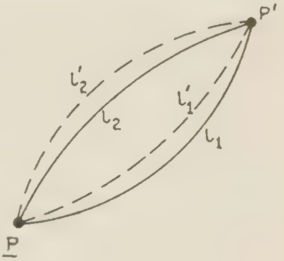

FIG. 5

We are thus led to the ordinary theory of the experiment, which would make us expect a displacement of the fringes, the absence of which is accounted for by the well-known contraction hypothesis (Lorentz contraction).

Asked if I consider this contraction as a real one, I should answer "yes." It is as real as anything that we can observe.

III. PROFESSOR DAYTON C. MILLER (CASE SCHOOL OF APPLIED SCIENCE)

The experiments on which I shall report today seem to lead to conclusions which are in contradiction to the common interpretation of the Michelson-Morley experiment. To make the story complete, I shall start with the conclusion of the experiments performed by Michelson and Morley in 1887, in Cleveland, which were interpreted as giving no indication of an ether drift. Dr. Lorentz, in 1895, proposed the first explanation for this unexpected result by assuming that the motion of translation of a solid through the ether might produce a contraction in the direction of the motion, with extension transversely, the amount of which is proportional to the square of the ratio of the velocities of translation and of light, and which might have a magnitude such as to annul the effect of the ether drift in the Michelson-Morley interferometer. The optical dimensions of this instrument were determined by the base of sandstone on which the mirrors were supported. If the contraction depends upon the physical properties of the solid, it was suggested that pine timber would suffer greater compression than sandstone, while steel might be compressed in a lesser degree. If the compression annuls the expected effect in one apparatus, it might in another apparatus give place to an effect other than zero, perhaps with the contrary sign.

At the International Congress of Physics, held in Paris in 1900, Lord Kelvin gave an address in which he considered theories of the ether. He remarked that "the only cloud in the clear sky of the theory was the null result of the Michelson-Morley experiment." Professor Morley and the writer were present, and in conversation Lord Kelvin expressed the conviction that the experiment should be repeated with a more sensitive apparatus. The writer, in collaboration with Professor Morley, constructed an interferometer about four times as sensitive as the one used in the first experiment, having a light-path of 214 feet, equal to about 130,000,000 wavelengths. In this instrument a relative velocity of the earth and ether equal to the earth's orbital velocity would be indicated by a displacement of the interference fringes equal to 1.1 fringes. This is the size of the instrument which has been used ever since. The optical parts were all new, and nothing was used from the original apparatus excepting the mercury tank and its wooden float.

Such an instrument with a base made of planks of pine wood was used at Cleveland, in 1902, 1903, and 1904, for the purpose of directly testing the Lorentz-FitzGerald effect, but the changes in the wooden frame due to the variations in humidity and temperature made it difficult to obtain accurate observations. A new supporting frame was designed by Professor F. H. Neff, of the department of civil engineering of the Case School of Applied Science, the purpose being to secure both symmetry and rigidity. This frame, or base, was made of structural steel and was so arranged that the optical dimensions could be made to depend upon distance-pieces of wood, or upon the steel frame itself. Observations were made with this apparatus in 1904. The procedure was based upon the effect to be expected from the combination of the diurnal and annual motions of the earth, together with the presumed motion of the solar system toward the constellation Hercules with a velocity of 19 km/sec. On the dates chosen for the observations there were two times of the day when the resultant of these motions would lie in the plane of the interferometer, about 11:30 A.M. and 9:00 P.M. The calculated azimuths of the motion would be different for these two times. The observations at these two times were, therefore, combined in such a way that the presumed azimuth for the morning observations coincided with that for the evening. The observations for the two times of day gave results having positive magnitudes but nearly opposite phases; when these were combined, the result was nearly zero. The result, therefore, was opposed to the theory then under consideration; but according to the ideas which will be set forth later in this address it now seems that the superposition of the two sets of observations of different phases was based upon an erroneous hypothesis and that the positive results then obtained are in accordance with a new hypothesis as to the solar motion. Our report of these experiments published in the *Philosophical Magazine* for May, 1905, concludes with the following statement: "Some have thought that this experiment only proves that the ether in a certain basement room is carried along with it. We desire therefore to place the apparatus on a hill to see if an effect can be there detected."

As an important factor I may mention the state of mind in which we then performed the experiment. It was proposed to look for a certain effect in order to check a certain theory. We had definite pictures in our minds as to what should happen. We calculated the magnitude and azimuth of the effect from the theory and discussed our experimental results in relation to these specific expectations. In every case we found that the result was negative as to these expectations. But it was never numerically zero, not even in the original Michelson and Morley experiment. It was zero in so far as the motion of the earth in its orbit is concerned. The remaining effect, however, was large enough to be measured. Experiments were performed to prove that it was not due to magnetic deformation of the frame, nor to temperature disturbances, since the effect was systematic. It was suggested that the ether might be entrained differently inside and outside of a masonry building.

In the autumn of 1905, Morley and Miller removed the interferometer from the laboratory basement to a site on Euclid Heights, Cleveland, free from obstruction by buildings, and having an altitude of about three hundred feet above Lake Erie and about eight hundred and seventy feet above sea-level. The house was purposely of very light construction, and was transparent (glass windows) in the direction of expected drift. Five sets of observations were made in 1905–1906, which give a definite positive effect of about one-tenth of the then-expected drift. Professor Morley retired from active work in 1906, and it devolved upon the present speaker to continue the experiments. It seemed desirable that further observations should be carried out at a much higher altitude, but numerous causes prevented the resumption of observations.

The deflection of the light from the stars by the sun, as predicted by the theory of relativity, was put to test at the solar eclipse of 1919. The results were widely accepted as confirming the theory. This revived the writer's interest in the ether-drift experiments, the interpretation of which had never been acceptable to him. Through the kindness of President Merriam and Directors Hale and Adams, a site was provided at the Mount Wilson Observatory on the top of Mount Wilson, at an elevation of about six thousand feet. The ether-drift interferometer was set up here in February, 1921, and observations were carried on during the succeeding five years.

Observations were begun in March, 1921, using the apparatus and methods employed by Morley and Miller in 1904, 1905, and 1906, with certain modifications and developments in details. The very first observation gave a positive effect such as would be produced by a real ether drift, corresponding to a relative motion of the earth and ether of about 10 km/sec. But before announcing such a result it seemed necessary to study every possible cause which might produce a displacement of fringes similar to that caused by ether drift; among the causes suggested were magneto-striction and radiant heat. In order to test the latter, the metal parts of the interferometer were completely covered with cork about one inch thick, and fifty sets of observations were made showing a periodic displacement of the fringes, as in the first observations, thus showing that radiant heat is not the cause of the observed effect.

In the summer of 1921 the steel frame of the interferometer was dismounted and a base of one piece of concrete, reinforced with brass, was cast in place on the mercury float. All the metal parts were made of aluminum or brass; thus the entire apparatus was free from magnetic effects and the possible effects due to heat were much reduced. In December, 1921, forty-two sets of observations were made with the non-magnetic interferometer. These show a positive effect as of an ether drift, which is entirely consistent with the observations of April, 1921. Many variations of incidental conditions were tried at this epoch. Observations were made with rotations of the interferometer clockwise and counter-clockwise, with a rapid rotation and a very slow rotation, with the interferometer extremely out of level, due to the loading of the float on one side. Many variations of procedure in observing and recording were tried. The results of the observations were not affected by any of these changes.

The entire apparatus was returned to the laboratory in Cleveland. During the years 1922 and 1923 many trials were made under various conditions which could be controlled and with many modifications of the arrangements of parts in the apparatus. An arrangement of prisms and mirrors was made so that the source of light could be placed outside of the observing-room, and a further complication of mirrors was tried for observing the fringes from a stationary telescope. Methods of photographic registration by means of a motion-picture camera were tried. Various sources of light were employed, including sunlight and the electric arc. Finally an arrangement was perfected for making observations with an astronomical telescope having an objective of five inches aperture and a magnification of fifty diameters. The source of light adopted was a large acetylene lamp of the kind commonly used for automobile headlights. An extended series of experiments was made to determine the influence of inequality of temperature and of radiant heat, and various insulating covers were provided for the base of the interferometer and for the light-path. These experiments proved that under the conditions of actual observation the periodic displacement could not possibly be produced by temperature effects. An extended investigation in the laboratory demonstrated that the full-period effect mentioned in the preliminary report of the Mount Wilson observations is a necessary geometrical consequence of the adjustment of mirrors when fringes of finite width are used and that the effect vanishes only for fringes of infinite width, as is presumed in the simple theory of the experiment.

In July, 1924, the interferometer was taken again to Mount Wilson and mounted on a new site where the temperature conditions were more favorable than those of 1921. The interferometer house was also mounted with a different orientation. Again the observations showed a real periodic displacement of the fringes, as in all the observations previously made at Mount Wilson and at Cleveland.

In spite of long-continued efforts, it was impossible to account for these effects as being due to terrestrial causes or to experimental errors. Very extended calculations were made in the effort to reconcile the observed effects with the accepted theories of the ether and of the presumed motions of the earth in space. The observations were repeated at certain epochs to test, one after another, the hypotheses which were suggested. At the end of the year 1924, when a solution seemed impossible, a complete calculation of the then-expected effects, for each month of the year, was made for the first time. This indicated that the effect should be a maximum about April 1, and further, that the direction of the effect should, in the course of the twenty-four hours of the day, rotate completely around the horizon. Observations were made for verifying these predictions in March and April, 1925. The effect was equal in magnitude to the largest so far observed; but it did not point successively to all points of the compass, that is, it did not point in directions 90° apart at intervals of six hours. Instead of this, the direction merely oscillated back and forth through an angle of about 60°, having, in general, a northwesterly direction.

Previous to 1925, the Michelson-Morley experiment has always been applied to test a specific hypothesis. The only theory of the ether which has been put to the test is that of the absolutely stationary ether through which the earth moves without in any way disturbing it. To this hypothesis the experiment gave a negative answer. The experiment was applied to test the question only in connection with specific assumed motions of the earth, namely, the axial and orbital motions combined with a constant motion of the solar system toward the constellation Hercules with the velocity of about 19 km/sec. The results of the experiment did not agree with these presumed motions. The experiment was applied to test the Lorentz-FitzGerald hypothesis that the dimensions of bodies are changed by their motions through the ether; it was applied to test the effects of magneto-striction, of radiant heat, and of gravitational deformation of the frame of the interferometer. Throughout all these observations, extending over a period of years, while the answers to the various questions have been "no," there has persisted a constant and consistent small effect which has not been explained.

The ether-drift interferometer is an instrument which is generally admitted to be suitable for determining the relative motion of the earth and the ether; that is, it is capable of indicating the direction and the magnitude of the absolute motion of the earth and the solar system in space. If observations were made for the determination of such an absolute motion, what would be the result, independent of any "expected" result? For the purpose of answering this general question, it was decided to make more extended observations at other epochs in 1925, and this was done in the months of July, August, and September.

It may be asked: Why was not such a procedure adopted before? The answer is, in part, that we were concerned with the verification of certain predictions of the so-called "classical" theories, and in part that it is not easy to develop a new hypothesis, however simple, in the absence of direct indication. Probably a considerable reason for the failure is the great difficulty involved in making the observations at all times of day at any one epoch. I think I am not egotistical, but am merely stating a fact when it is remarked that the ether-drift observations are the most trying and fatiguing, as regards physical, mental, and nervous strain, of any scientific work with which I am acquainted. The mere adjustment of an interferometer for white-light fringes and the keeping of it in adjustment, when the light-path is 214 feet, made up of sixteen different parts, and when it is in effect in the open air, requires patience as well as a steady "nerve" and a steady hand. Professor Morley once said, "Patience is a possession without which no one is likely to begin observation of this kind." The observations must be made in the dark; in the daytime, the interferometer house is darkened with black paper shades; the observations must be made in a temperature which is exactly that of the out-of-door air; the observer has to walk around a circle about twenty feet in diameter, keeping his eye at the moving eyepiece of the telescope attached to the interferometer, which is floating on mercury and is turning on its axis steadily, at the rate of about one turn a minute; the observer must not touch the interferometer in any way, and yet he must never lose sight of the interference fringes, which are seen only through the small aperture of the eyepiece of the telescope, about a quarter of an inch in diameter; the observer makes sixteen readings of the position of the interference fringes in each turn, at times indicated by an electrical clicker; these operations must be continued without a break through a set of observations, which usually lasts for about fifteen or twenty minutes, and this is repeated continuously during the several hours of the working period.

When observations are in progress, the interferometer to which the observing telescope is attached is caused to rotate on the mercury float so that the telescope points successively to all points of the compass, that is, it points to all azimuths. A relative motion of the earth and the ether should cause a periodic displacement of the interference fringes, the fringes moving first to one side and then to the other as referred to a fiducial point in the field of view, with two complete periods in each rotation of the instrument. Beginning when the telescope points north, the position of the fringes is noted at sixteen equidistant points around the horizon. The azimuth of the line of sight when the displacement is a maximum having been noted at two different times of day, it is a simple operation to calculate the right ascension and declination, or the "apex" of the presumed "absolute" motion of the earth in space. The determination of the direction of the earth's motion is dependent only upon the direction in which the telescope points when the observed displacement of the fringes is a maximum; it is in no way dependent upon the amount of this displacement or upon the adjustment of the fringes to any particular zero position. As the readings are taken at intervals of about three seconds, the position of the maximum is dependent upon observations covering an interval of less than ten seconds. A whole period of the displacement extends over only about twenty-five seconds. Thus the observations for the direction of the absolute motion are largely independent of ordinary temperature disturbances. The observation is a differential one, and can be made with considerable certainty under all conditions. A set of readings usually consists of twenty turns of the interferometer made in about fifteen minutes' time; this gives forty determinations of the periodic effect. The forty values are simply averaged to give one "observation." Any temperature effect, or other disturbing cause, which is not regularly periodic in each twenty seconds over an interval of fifteen minutes would largely be canceled out in the process of averaging. The periodic effect remaining in the final average must be real.

The position of the fringe system is noted in units of a tenth of a fringe-width. The actual velocity of the earth's motion is determined by the amplitude of the periodic displacement, which is proportional to the square of the relative velocity of the earth and the ether and to the length of the light-path in the interferometer. A relative motion of 30 km/sec., equal to the velocity of the earth in its orbit, would produce a displacement of the fringes from one extreme to the other, of 1.1 fringes. Disturbances due to temperature or other causes lasting for a few seconds or for a few minutes might affect the actual amount of the observed displacement and thus give less certain values for the velocity of relative motion, while at the same time the position of maximum displacement is not disturbed. Thus it is to be expected that the observations for the velocity of motion will not be as precise as the observations for the direction of motion. The two things, magnitude and azimuth of observed relative motion, are quite independent of each other.

It is desirable to have observations equally distributed over the twenty-four hours of the day; since one set requires about fifteen minutes of time, ninety-six sets, properly distributed, will suffice. The making of such a series usually occupies a period of ten days. The observations are finally reduced to one group, and the mean date is considered the date of the epoch. The observations made at Mount Wilson in 1925 correspond to the three epochs, April 1, August 1, and September 15, and are more than twice as numerous as all the other ether-drift observations made since 1881. The total number of observations made at Cleveland represents about one thousand turns of the interferometer, while all the observations made at Mount Wilson previous to 1925 correspond to 1200 turns. The 1925 observations consist of 4400 turns of the interferometer, in which over 100,000 readings were made. A group of eight readings gives a value for the magnitude and direction of the ether-drift function, so that 12,500 single measures of the drift were obtained. This required that the observer should walk, in the dark, in a small circle, for a total distance of one hundred miles, while making the readings. Throughout these observations the conditions were exceptionally good. At times there was a fog which rendered the temperature very uniform. Four precision thermometers were hung on the outside walls of the house; often the extreme variation of temperature was not more than one-tenth of a degree, and usually it was less than four-tenths of a degree. Such variations did not at all affect the periodic displacement of the fringes. It may be added that while the readings are being taken, neither the observer nor the recorder can form the slightest opinion as to whether any periodicity is present, much less as to the amount or direction of any periodic effect.

The hundred thousand readings are added in groups of twenty, are averaged, and then plotted in curves. These curves are subjected to mechanical harmonic analysis for the purpose of determining the azimuth and magnitude of the drift. In this work all the original observations have been used, without any omissions and without the assignment of weights; furthermore, there are no corrections of any kind to be applied to the observed values. The results of the analyses are finally charted in such a way as to show the variation in the azimuth of the drift throughout the day of twenty-four hours for each epoch, and the variation in magnitude is similarly charted.

[The observations of 1925 were described and the details of the results were shown by means of lantern-slide diagrams. A similar report constituted the address of the President of the American Physical Society read at Kansas City on December 29, 1925. This address is printed in full in *Science*, **63**, 433–443, April 30, 1926.]

A calculation based only on the observations of 1925 was made to determine the absolute motion of the earth. The result of this, as reported at the Kansas City meeting, indicated that the solar system is moving toward an apex in the constellation Draco with a velocity which is in excess of 200 km/sec. In order to confirm the Kansas City report, a set of observations consisting of 2020 turns of the interferometer was made at Mount Wilson, corresponding to the epoch February 10, 1926. A complete calculation has now been made, including the observations of both 1925 and 1926, which leads to the following conclusion: The ether-drift experiments at Mount Wilson show, first, that there is a systematic displacement of the interference fringes of the interferometer corresponding to a constant relative motion of the earth and the ether at this observatory of 10 km/sec., with a probable error of 0.5 km/sec.; and, second, that the variations in the direction and magnitude of the indicated motion are just such as would be produced by a constant motion of the solar system in space, with a velocity of 200 km/sec., or more, toward an apex in the constellation Draco, near the pole of the ecliptic, which has a right ascension of 255° (17 hours) and a declination of +68°; and, third, that the axis across which the observed azimuth of drift fluctuates, because of the rotation of the earth on its axis, points in a northwesterly direction, whereas the simple theory indicates that this axis should coincide with the north and south meridian.

The arguments which have led to these conclusions may be illustrated by means of Figures 6 and 7. In the lower part of Figure 6 the four light-line curves represent the average azimuths for the four epochs of observation, plotted with respect to Mount Wilson local or civil time. The curves all have the values for midnight on the ordinate for zero hours and the noon values on the ordinate for twelve hours, etc. The heavy curve represents the average of the four sets of observations and is clearly seen to be irregular and nearly zero in value. In the upper part of Figure 6, the four azimuth curves are plotted against sidereal time. The heavy-line curve representing the average is clearly a periodic curve. If the effect is due to a motion of the earth through space, the sidereal time at which

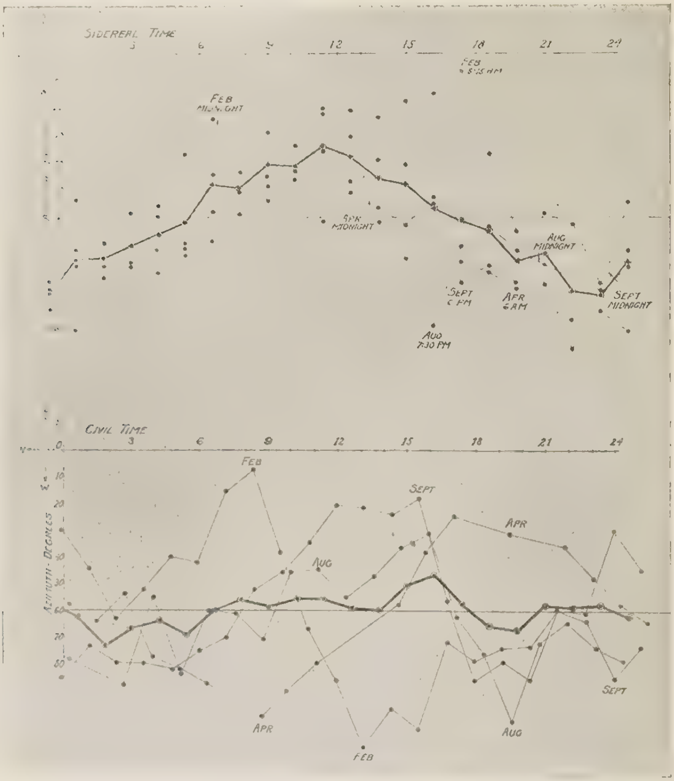

FIG. 6

this curve crosses the time axis is the right ascension of the apex of the motion. This occurs at seventeen hours. The declination of the apex is determined from the amplitude of the curve and the cosine of the latitude of the observatory, and is equal to +68°. Figure 7 shows, at the bottom, the average diurnal variation in the azimuth (the broken line) as compared with the theoretical variation shown by the smooth curve. The upper part of Figure 7 shows, in the broken line, the average diurnal variation in the observed magnitude of the effect, while the smooth curve shows the theoretical variation. If this is due to an ether drift, the sidereal time of minimum magnitude is the right ascension of the apex. This is seventeen hours, in agreement with the right ascension obtained from the azimuth curve. The declination of the apex is dependent upon the minimum and maximum values of the effect and upon the latitude of the ob-

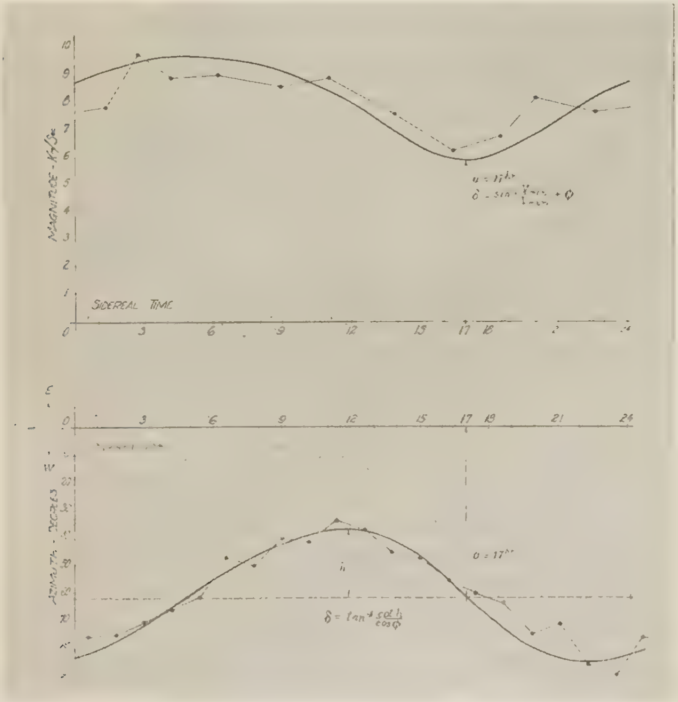

FIG. 7

servatory. The computed value is about +69°, agreeing with that obtained from the azimuth curve. As far as instrumental considerations are concerned, the azimuth and magnitude are independent of each other; it is only when they are produced by the same cause that there is any necessary connection between them. The agreement of the calculated and observed effects for both magnitude and azimuth surely points to a real, cosmical cause. The result cannot be considered as a "null" effect; neither can it be due to instrumental or local disturbances.

The fact that the direction and magnitude of the observed ether drift are independent of local time and are constant with respect to sidereal time implies that the effect of the earth's orbital motion is imperceptible in the observations. The present experiments show no effect of the orbital motion, and hence they are no more consistent with the old theory of a stagnant ether than were the experiments of Michelson and Morley. In order to account for the absence of the orbital effect, it is assumed that the constant motion of the earth in space is more than 200 km/sec., but that for some unexplained reason the relative motion of the earth and the ether in the interferometer at Mount Wilson is reduced to 10 km/sec.; under those conditions a component motion equal to the earth's orbital motion would produce an effect on the resultant which is just below the limit of the smallest quantity which can be measured by the present interferometer. It is for this reason that it is concluded that the velocity of the motion of the solar system is at least 200 km/sec., and it may be much greater.

Several critics seem to be under the impression that the earlier Cleveland observations gave a real zero effect and that it is claimed that the present positive effect is due to the greater elevation at Mount Wilson. This is not true. The numerical values of the positive effect at Cleveland and at Mount Wilson are so nearly equal that with the observations now available (those at Cleveland being relatively few in number) it is impossible to state that there is any effect due to altitude. If there is any influence of altitude, it is certainly small; further observations at Cleveland are now being made to determine this matter.

In order to account for these effects as the result of an ether drift, it seems necessary to assume that, in effect, the earth drags the ether so that the apparent relative motion at the point of observation is reduced from 200, or more, to 10 km/sec., and further that this drag also displaces the apparent azimuth of the motion about 60° to the west of north. It is possible that the westerly deflection is influenced by the trend of the Mount Wilson range of mountains from southeast to northwest. The reduction of the indicated velocity of 200 km/sec., or more, to the observed value of 10 km/sec. may be explained by the theory of the Lorentz-FitzGerald contraction without assuming a drag of the ether. This contraction may or may not depend upon the physical properties of the solid, and it may or may not be exactly proportional to the square of the relative velocities of the earth and the ether. A very slight departure of the contraction from the amount calculated by Lorentz would account for the observed effect.

The values of the quantities defining the absolute motion of the solar system as obtained from these ether-drift observations are in general agreement with the results obtained by other methods. The recent study of proper motions of stars by Ralph Wilson, of the Dudley Observatory, and of the radial motions of the stars by Campbell and Moore, of the Lick Observatory, gives the apex of the sun's way in the constellation Hercules with a right ascension of 270° and a declination of about +30°, with a velocity of about 19 km/sec. Dr. G. Strömberg, of the Mount Wilson Observatory, from a study of globular clusters and spiral nebulae, finds evidence of a motion of the solar system toward a point having a right ascension of 307° and a declination of +56°, with a velocity of 300 km/sec. Lundmark, studying the spiral nebulae, finds evidence of a motion having a velocity of 400 km/sec. The various determinations of the motion of the solar system are all in the same general direction and lie within a circle having a radius of 20°. Our assumed velocity of 200 km/sec. is simply a lower limit; it might equally well be 300 or 400 km/sec. The first assumption therefore seems to offer no difficulty. The location of the apex in the constellation Draco, at right ascension 255° and declination +68°, is within 6° of the pole of the ecliptic, that is, the indicated motion of the solar system is almost perpendicular to the plane of the ecliptic. The sun's axis of rotation points to within 12° of this apex. One cannot help wondering whether there may be some dynamic significance in these facts.

The argument now being presented can be demonstrated only by means of observations extending over the whole twenty-four hours of the day, in order to determine the exact form of the daily variation in magnitude and azimuth of the effect, and by means of observations made at different times of year, in order to prove that the effect is dependent on sidereal time. The earlier observations of 1887 and 1905 are not sufficiently numerous and are not distributed throughout the day in such a manner as to make it possible to calculate the direction of the drift. These earlier observations were made for the purpose of detecting the earth's orbital motion and consequently were made at two selected times of day, such that at one time the magnitude of this particular effect would be a maximum and at the other time it would be zero; or, two times of day were chosen in which the azimuth of the orbital component of motion would have very different values. Furthermore, until the year 1925 the experiments have never been carried out at intervals of six months. The reason that a second set of experiments following this interval has not been made before is simply that in no instance has the expected effect been found in a first set.

The observations made at Cleveland by Michelson and Morley in 1887, and later repeated by Morley and Miller, have just been recomputed on the present hypothesis; while the earlier observations are not sufficient to determine the direction of the drift, they are nevertheless shown to be entirely consistent with the conclusions drawn from the Mount Wilson experiments. Or, to state the converse, the present result wholly confirms the earlier experiments of Michelson and Morley, giving no evidence of the effect of the earth's orbital motion. In addition to this, the recent experiments, by a thorough study of the residual effects, have shown that there is a systematic cosmical effect as of a true ether drift. This conclusion introduces a new question, "Why is the magnitude of the effect less than would be expected on the classical theories and why is the direction of the effect at Mount Wilson deflected to the westward?" This question certainly is no more difficult than are many others now awaiting solution.

The interferometer is being set up again on the campus of Case School of Applied Science in Cleveland, near the place where the original Michelson-Morley experiment was performed in 1887. It is proposed to make a series of observations for four epochs of the year, comparable in every way with the Mount Wilson series. This will give information as to the possible effects of local conditions; it is hoped that it will show more definitely whether there is any effect due to altitude, and whether the orbital motion is appreciable.

IV. DR. ROY J. KENNEDY (CALIFORNIA INSTITUTE OF TECHNOLOGY)

When Professor Miller published the conclusions that he presented to us yesterday, it became necessary, or at least very desirable, that the experiment be repeated independently. It is such a performance of the experiment that I shall discuss this morning.

In this experiment the light-paths were reduced to about 4 m, and the required sensitiveness was obtained by an arrangement capable of detecting a very slight displacement of the interference pattern. The whole optical system was inclosed in a sealed metal case containing helium at atmospheric pressure. Because of its small size, the apparatus could be effectively insulated, and circulation and variations in density of the gas in the light-paths nearly eliminated. Furthermore, since the value of $\mu - 1$ for helium is only about one-tenth that for air at the same pressure, it will be seen that the disturbing effects of changes in density of the gas correspond to those in air at only a tenth of an atmosphere of pressure. Actually it was found that any wavering of the interference pattern was imperceptible, and when temperature equilibrium had been reached there was no steady shift.

The plan of the apparatus is sketched in Figure 8. The optical parts are mounted on a marble slab 122 cm square by 10.5 cm thick, which rests on an annular float in a pan of mercury 77 cm in diameter. This is simply a reduced copy of Michelson's original mounting. The mirrors M_1, M_4, and M_5 are fixed in position; such adjustments of the compensating plate C and mirror M_2 as are necessary after the cover is in place can be made from the observer's position at the telescope. The green light λ 5461 is separated by the lens and prism system from the radiation of a small mercury arc lamp

S attached to the slab, and passed through a small hole in the screen *Z*. The pencils of light are carefully limited by screens and by focusing in order to prevent stray light from reaching the eye and thereby reducing its sensitiveness. Adjustments are made so that broad fringes are formed at the surface of M_1 and M_2, on which the telescope is focused. Final adjustments are made by rotating the compensating plate *C* by means of a fine differential screw, and by placing small weights near the corner of the slab; under proper conditions a 5-g weight deflects the heavy slab just perceptibly. The adjusting screws are manipulated by means of spindles passing through short flexible tubes in such a way as to be freely rotatable but air tight. After the mirrors are given preliminary alignment, the cover is carefully lowered into place, sealed to the slab, and then filled with helium.

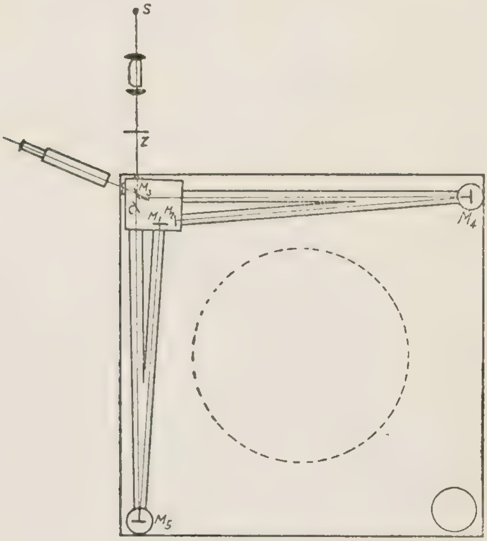

Fig. 8

Schematically, the arrangement of the interferometer is shown in Figure 9. A beam of practically plane-parallel, homogeneous light, plane-polarized so that its electric vector lies in the plane of the paper, moves to the right and falls on the mirror M_3 at the polarizing angle for the given wave-length. At the upper face the beam is split by a thin platinum film into two parts of nearly equal intensity, one passing to the mirror M_1 and the other to M_2. From there they are reflected back to M_3, where they recombine and pass to the eye through a telescope focused on M_1 and M_2. Two purposes are accomplished by the use of plane-polarized light: first, the non-interfering rays indicated by the dotted lines, which would be produced with natural light, are completely eliminated; and, second, the recombining beams can be adjusted to perfect equality of intensity by varying the relative reflecting powers of M_1 and M_2. Because there are two more glass-air interfaces to be traversed by the upper beam than by the lower, it is impossible to equalize both components of natural light in this way.

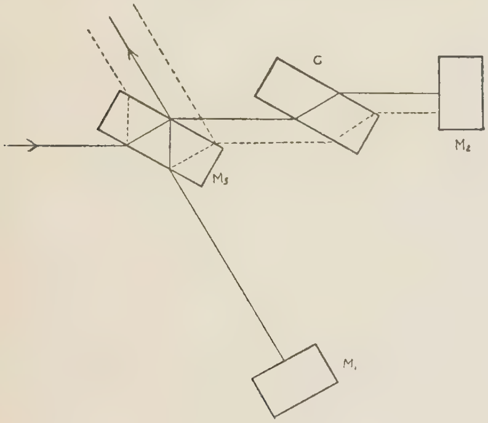

FIG. 9

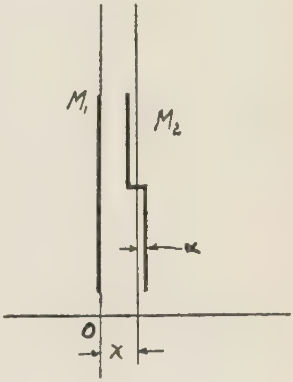

FIG. 10

The high sensibility necessary because of the short paths is secured chiefly by the simple device of raising one-half of the surface of mirror M_2 a small fraction of a wave-length above the other, the dividing line between the two levels being straight and as sharp as possible. The mirror used was made by covering part of a plane plate with a flat sharp-edged microscope cover-glass and applying the extra thickness by cathode deposition of platinum, thereafter giving the whole plate a fully reflecting coat. I ran across the suggestion of using such a divided mirror in interferometry some years ago, but am unaware to whom the credit for it belongs.

The theory of the arrangement is as follows: The interference phenomena will be the same as if the mirror M_2 were replaced by its image in M_3. Under the conditions of the experiment, where the paths are nearly equal, M_1 is perpendicular to the beam incident on it, and the reflected beams are brought nearly to parallelism, the image of M_2 will be nearly parallel and coincident with the face of M_1. Elementary theory shows that the resulting interference pattern then practically coincides with M_1. It would needlessly complicate this discussion to develop the general theory of interference for all inclinations of the mirrors; the experimentally realized case of near parallelism alone is necessary.

Let Figure 10 represent a greatly exaggerated cross-section of M_1 and the image of M_2, normal to their planes and to the dividing line in M_2. M_1 lies in the plane $x=0$, and the levels of M_2 are at equal distances on opposite sides of a parallel plane at the distance x from M_1. Let a monochromatic wave, in which the displacement is given by

$$\xi=a\cos\omega\left(t+\epsilon-\frac{x}{c}\right),$$

fall on M_1 and M_2 from the left. At the surface of M_1 the displacement in the reflected wave is then given by

$$\xi_1=a\cos\omega(t+\epsilon)$$

if we ignore the loss through imperfect reflection. The displacement in the plane of M_1 in the wave reflected from the upper part of M_2 is

$$\xi_2=a\cos\omega\left[t+\epsilon-\frac{2(x-a)}{c}\right].$$

The square of the resultant displacement is then

$$(\xi_1+\xi_2)^2=a^2\left\{\cos\omega(t+\epsilon)+\cos\omega\left[t+\epsilon-\frac{2(x-a)}{c}\right]\right\}.$$

This can be reduced to the form

$$2a^2\left[1+\cos\frac{2\omega}{c}(x-a)\right]\cos^2\omega(t-\delta).$$

Similarly, the square of the resultant displacement in the interfering beams below the dividing line is found to be

$$2a^2\left[1+\cos\frac{2\omega}{c}(x+a)\right]\cos^2\omega(t-\delta)\,.$$

The intensities, being proportional to the squares of the amplitudes, can be represented by

$$I_1=ka^2\left[1+\cos\frac{2\omega}{c}(x-a)\right]$$

and

$$I_2=ka^2\left[1+\cos\frac{2\omega}{c}(x+a)\right]\,.$$

Now $\omega=2\pi\nu$ where $\nu=$ frequency of the light. Hence $\omega/c=2\pi/\lambda$. Therefore

$$I_1=ka^2\left[1+\cos\frac{4\pi}{\lambda}(x-a)\right]$$

and

$$I_2=ka^2\left[1+\cos\frac{4\pi}{\lambda}(x+a)\right]\,.$$

For values of $x=n\lambda/4$, where n is an integer,

$$I_1=ka^2\left(1\pm\cos\frac{4\pi a}{\lambda}\right),$$

the sign being positive for even values of n and negative for odd values. The same expression holds for I_2; hence, under these conditions,

$$I_1=I_2\,.$$

To the observer, then, the field of view is equally intense on both sides of the dividing line when $x=n\lambda/4$.

We have now to determine the least change in x from this value which will produce a perceptible difference in illumination in the two sides of the field. If x is given the variation δx while a is kept constant, the difference in intensity will be

$$\delta I=\left(\frac{\partial I_1}{\partial x}-\frac{\partial I_2}{\partial x}\right)\delta x\,.$$

Now

$$\frac{\partial I_1}{\partial x} = \pm \frac{4\pi k a^2}{\lambda} \sin \frac{4\pi a}{\lambda} .$$

Similarly,

$$\frac{\partial I_2}{\partial x} = \mp \frac{4\pi k a^2}{\lambda} \sin \frac{4\pi a}{\lambda} .$$

Therefore

$$\delta I = \pm \left[\frac{8\pi k a^2}{\lambda} \sin \frac{4\pi a}{\lambda} \right] \delta x ,$$

the sign being of no importance.

The perceptibility of the variation is determined not by δI alone, but by the ratio of δI to the total intensity, I_1 or I_2. According to the Weber-Fechner law, if δI is taken to be the least perceptible variation in intensity, the foregoing ratio is nearly constant for a considerable range of intensities. With this meaning of δI, δx becomes the least detectable change of position of M_2.

If initially we have uniformity of illumination, we have from the equations above,

$$\frac{\delta I}{I} = \frac{8\pi}{\lambda} \delta x \frac{\sin \frac{4\pi a}{\lambda}}{1 \pm \cos \frac{4\pi a}{\lambda}} ,$$

or

$$\delta x = \frac{\lambda}{8\pi} \frac{\delta I}{I} \frac{1 \pm \cos \frac{4\pi a}{\lambda}}{\sin \frac{4\pi a}{\lambda}} ,$$

If now $\delta I/I$ were a true constant, we should have for the case of negative sign, which corresponds to dim illumination of the field, the sensibility of the apparatus increasing indefinitely as the factor a was made smaller. I decreases with a, however, and the Fechner "constant" soon diminishes rapidly. Nevertheless, the conditions of illumination and contrast here are similar to those in the half-shade polariscope, and from the theory of the Lippich instrument it appears that $\delta I/I$ equals about 8×10^{-3}. The lack of perfect planeness in the mirrors and of equality of intensity in the interfering beams is a further limiting factor; a little experimenting indicated that a should not be much less than 0.025 λ, which was the value finally used. Substituting these values in the last equation, we get

$$\delta x = 5 \times 10^{-5} \lambda$$

as the least detectable change in position of one of the mirrors. This corresponds to a change of optical length of path

$$\delta l = 2\delta x = 10^{-4} \lambda .$$

To take full advantage of the possibilities of the arrangement would have required perfect mirrors and an intenser and, therefore, hotter source of light than would have been desirable near the sensitive apparatus, as well as lengthening the interval between observations, thus allowing greater chance for any steady temperature shift to show itself. No attempt was made in the experiment, therefore, to go below values of δl equal to $2 \times 10^{-3} \lambda$; such variations were detectable without the least uncertainty.

With this apparatus the velocity of 10 km/sec. found by Professor Miller would produce a shift corresponding to 8×10^{-3} wavelengths of green light, which is four times the least detectable value.

The experiment was performed in a constant-temperature room in the Norman Bridge Laboratory at various times of day, but oftenest at the time when Miller's conclusions require the greatest effect. The sensitiveness of the eye was tested for each trial by the placing or removal of a small weight on the slab before and after rotating it. There being no fluctuations in the field of view, it was unnecessary to take the average of a number of readings. As has been shown, a shift as small as one-fourth that corresponding to Miller's would have been perceived. The result was perfectly definite. There was no sign of a shift depending on the orientation.

Because an ether drift might conceivably depend on altitude, the experiment was repeated on Mount Wilson, in the 100-inch telescope building. Here again the effect was null.

[*Note added April, 1928.*—Illingworth at the California Institute of Technology has continued the work with Kennedy's apparatus, using improved optical surfaces and a method of averaging. He concludes[1] that no ether drift as great as 1 km/sec. exists.]

[1] *Physical Review*, **30**, 692, 1927.

V. PROFESSOR E. R. HEDRICK (UNIVERSITY OF CALIFORNIA AT LOS ANGELES)

[Because of lack of time Professor Hedrick presented only a summary of the following contribution, prepared by himself and Professor Ingold of the University of Missouri.]

I. INTRODUCTION

The celebrated experiment by Michelson to determine the relative motion of the earth and the luminiferous ether was first made in 1881.[1] Objection to the mathematical theory was raised by H. A. Lorentz in 1886,[2] and in 1887 the theory was modified by Michelson and Morley to meet this objection.[3] It is the theory accompanying the account of their 1887 experiment that is usually given and that is now generally accepted.

Until about 1898 it does not appear that any further serious objections were raised against the theory. From that time on, however, numerous papers[4] dealing with the matter have appeared, which, in many instances, contain objections to one feature or another of the theory. The differences of opinion appear to arise mainly from different conceptions regarding the mechanism of interference phenomena.

In view of the wide diversity of opinion on the subject, it has seemed worth while to work out the theory anew, on the basis of some reasonable hypothesis that has been employed in dealing with other phases of interference phenomena.

Some portions of the present investigation appear to be closely related to part of the work of Righi as reported by Stein,[5] and confirms, by an independent calculation, some of Righi's results, which is a matter of great importance, since the accuracy of his work has been called in question.[1]

---

[1] *American Journal of Science*, **22**, 120, 1881.

[2] *Archives Néerlandaises*, **21**, 2^{me} livre, 103, 1887.

[3] *Philosophical Magazine* (5), **24**, 449, 1887.

[4] We mention the following: Sutherland, *ibid.* (5), **46**, 23, 1898; Hicks, *ibid.* (6), **3**, 9, 1902; Sutherland, *Nature*, **63**, 205, 1900; Kohl, *Annalen der Physick*, **28**, 259, 1909; Budde, *Physikalische Zeitschrift*, **12**, 979, 1911, and **13**, 825, 1912; Righi, *Sessions of the Royal Institute of Bologna*, 1919 and 1920.

For replies to some of these articles consult the following: Lodge, *Philosophical Magazine* (5), **46**, 1898; Morley and Miller, *ibid.* (6), **9**, 669, 1905; Laue, *Annalen d· Physik*, **33**, 186, 1910, and *Physikalische Zeitschrift*, **13**, 501, 1912.

[5] "Michelson's Experiment and Its Interpretation according to Righi," *Memori della Societa Astronomica Italiana*, **1**, 283, 1920.

2. REFLECTION FROM A MOVING MIRROR

We begin by obtaining certain general formulae for the reflection of light from a moving mirror. Two cases are considered: (*a*) the direction of motion of the mirror coincides with the direction of the rays of light before reflection; (*b*) the direction of motion of the mirror makes an angle Θ with the direction of the rays of light.

a) Denote the velocity of light by c and the velocity of the mirror by v. Let h represent the tangent of the angle of inclination of the mirror to the direction of motion.

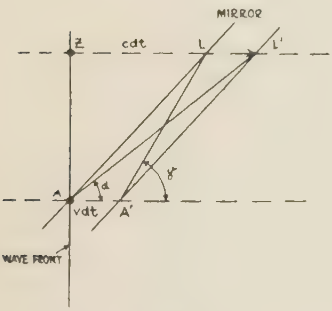

FIG. 11

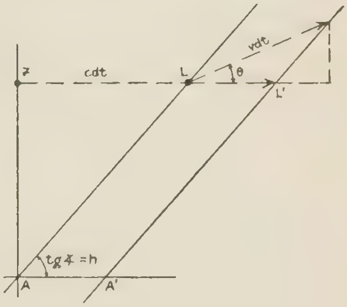

FIG. 12

In Figure 11, AZ represents the front of a wave advancing on the mirror at A. While the mirror moves from AL to $A'L'$, the portion of the wave at Z traverses the distance ZL'. Therefore, denoting the angle $A'AL'$ by α, we have

$$\tan \alpha = \frac{AZ}{ZL'} = \left(1 - \frac{v}{c}\right) h = (1-\beta) h\,,$$

which gives the position of the equivalent fixed mirror.

Similarly, $A'L$ is the position of the equivalent fixed mirror for a ray coming from the opposite direction CA; and if we denote $CA'L$ by γ, we have

$$\tan \gamma = (1+\beta) h\,.$$

---

[1] See *Observatory*, 44, 340–341, 1921.

b) If the direction of motion of the mirror makes an angle with the direction of the rays, then from Figure 12 it is clear that the mirror really advances with a velocity

$$v \cos \Theta - \frac{v \sin \Theta}{h},$$

so that the formulae for this case may be obtained from those of the previous case by putting

$$\beta\left(\cos \Theta - \frac{\sin \Theta}{h}\right)$$

in place of β.

If the mirror is inclined at an angle of 45° to the direction of the rays of light, $h = 1$ and

$$\tan \alpha = 1 - \beta(\cos \Theta - \sin \Theta),$$

while

$$\tan \gamma = 1 + \beta(\cos \Theta - \sin \Theta).$$

3. APPLICATION TO THE MICHELSON-MORLEY EXPERIMENT

In the Michelson-Morley experiment a ray of light from a source S (Fig. 13) meets a half-silvered glass plate, inclined at 45° to its path, at A. A portion is reflected to a mirror at B, parallel to SA, from which it is again reflected to pass through the plate at A' and finally into a telescope at T. Another portion is transmitted through the glass plate at A to a mirror at C, perpendicular to SA, from which it is returned to the glass plate at A' and from there a further portion is reflected into the telescope at T'. When the mirrors are set as described, with absolute accuracy, we call the experiment the "ideal Michelson-Morley experiment." We wish to compute the angle $T'A'T$.

We assume that the earth and the apparatus are moving through the ether in a direction making an angle Θ with the path of the rays SA.

It will be necessary to determine the position of the equivalent fixed mirror at B.

For convenience denote $\beta(\cos \Theta - \sin \Theta)$ by ξ. Then the angle $CAB = 2\alpha$ where $\tan \alpha = 1 - \xi$.

In Figure 14, if BE is the wave front of the ray reflected from A and if the mirror at B advances from BM to $B'M'$ (a distance r in

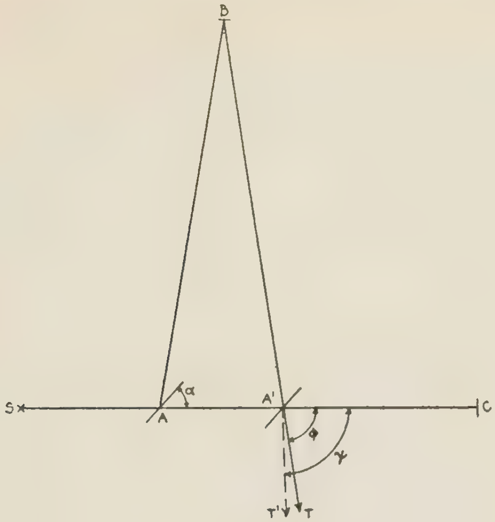

FIG. 13

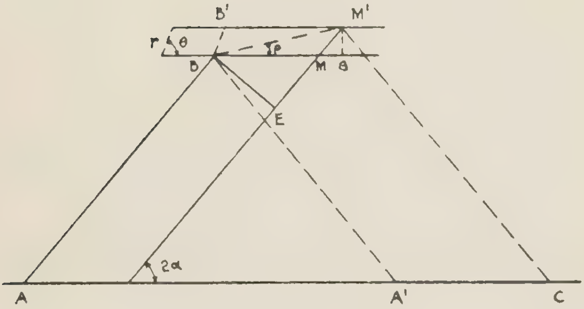

FIG. 14

the direction Θ) while the portion of the wave front at E advances to M', then BM' is the position of the equivalent fixed mirror. Denote the angle MBM' by ρ; then

$$\tan \rho = \frac{GM'}{BG}$$

where GM' is perpendicular to BM.

$$GM' = MM' \sin 2\alpha = r \sin \Theta; \qquad BG = BM + MM' \cos 2\alpha;$$

$$BM = \frac{EM}{\cos 2\alpha}; \qquad \beta = \frac{r}{EM + MM'}.$$

Therefore

$$\tan \rho = \frac{r \sin \Theta}{BM + MM' \cos 2\alpha} = \frac{r\beta \sin \Theta}{\dfrac{EM\beta}{\cos 2\alpha} + MM'\beta \cos 2\alpha}$$

$$= \frac{r\beta \sin \Theta \cos 2\alpha}{r - r\beta \sin \Theta \sin 2\alpha}.$$

But we have $\tan \alpha = 1 - \xi$; hence, to terms of the second order,

$$\sin \alpha = 1 - \frac{\xi^2}{2}, \qquad \cos 2\alpha = \xi + \frac{\xi^2}{2}.$$

Substituting these values in the expression for $\tan \rho$, we have

$$\tan \rho = \beta^2 \sin \Theta (\cos \Theta - \sin \Theta), \text{ q.p.}$$

Now if we denote the angle $CA'T$ by ϕ and the angle $CA'T'$ by ψ, we have (remembering that ϕ and ψ are negative angles)

$$\phi + \rho = 2\alpha - \rho \qquad \text{or} \qquad \phi = 2(\rho - \alpha),$$

$$\psi = 2\gamma - 180°.$$

Thus the positive angle

$$T'A'T = \phi - \psi = 2\rho - 2\alpha - 2\gamma + 180°.$$

To determine the tangent of this angle, we find

$$\tan(-2\alpha) = -\frac{2(1-\xi)}{1-(1+\xi)^2},$$

$$\tan(2\gamma - 180°) = \frac{2(1+\xi)}{1-(1+\xi)^2},$$

and therefore

$$\tan(-2\alpha - 2\gamma + 180°) = \frac{4\xi^2}{4-\xi^4} \quad \text{q.p.}$$

From this we obtain

$$\tan(\phi - \psi) = \frac{\xi^2 + 2\beta^2 \sin \Theta (\cos \Theta - \sin \Theta)}{1 - 2\beta^2\xi^2 \sin \Theta (\cos \Theta - \sin \Theta)} \quad \text{q.p.},$$

since $\tan 2\rho = 2\beta^2 \sin \Theta(\cos \Theta - \sin \Theta)$ to terms of the second order. Substituting for ξ and reducing, we have finally

$$\tan(\phi - \psi) = \beta^2 \cos 2\Theta.$$

This formula was obtained by Righi, who concluded from it that a rotation of the apparatus (in the ideal experiment) through 90° would produce absolutely no effect, since, although the distances traversed by the two rays are exchanged, yet at the same time their positions are also exchanged; that is, the ray having the longer path occupies the same relative position with respect to that one having the shorter path, after the rotation as before. It follows that the pattern of the interference fringes after the rotation cannot be distinguished from that before the rotation.[1]

4. THE USUAL THEORY

A careful computation of the difference in the length of path traversed by the two rays yields precisely the same result as is given in the usual theory, namely, $\beta^2 \cos 2\Theta$. As a matter of fact, it was also known that, under ideal conditions, there exists a second-order difference in the directions of the final rays.[2] The view has been, however, that this difference in direction could affect the difference in time up to the telescope, and therefore the difference in phase, only by an amount of the third order in β. Thus it was thought that this difference had no appreciable effect on the position of the interference fringes, although it might modify the width of the fringes.

In the next section we investigate, as far as we can, the legitimacy of this older view. As a basis for this investigation, we use a conception of the mechanism of interference phenomena which has been employed in other connections. Whether its application in the present instance is legitimate is perhaps a matter to be decided by experiment, but there does not seem to be any very evident reason why it cannot be employed with safety.

We may mention here that, quite apart from any special hypothesis concerning interference phenomena, the argument of Righi given at the conclusion of the preceding section proves absolutely that the second-order change in the angle between the final rays is by no means negligible, since in the ideal experiment the expected shift for a rotation through 90° is proportional to $2\beta^2$ if that angle is not taken into account, but is zero when it is taken into account.

---

[1] See, for example, Larmor, *Aether and Matter*, p. 53.

[2] See Michelson and Morley, *loc. cit.;* also Larmor, p. 48.

5. POSSIBLE EFFECT OF DIFFERENCE OF ANGLE ON THE POSITION OF THE INTERFERENCE BANDS

Figure 15 represents the network of wave fronts of the two interfering rays. The space between F_1 and F_2 represents the central bright fringe.

Let the ray s change its direction (relative to the ray t) by the amount $\Delta\alpha$. If the new wave front f_2 meets the old wave front f_1 near the edge of the fringe at N, the center of the fringe will be shifted to the left from M to M'. The amount of this shift, which is due wholly to the change of angle between the interfering rays, will depend on the distance of the point of intersection of the consecutive wave fronts from the edge of the fringe. As this point approaches the center of the fringe, the distance MM' becomes negligible. In

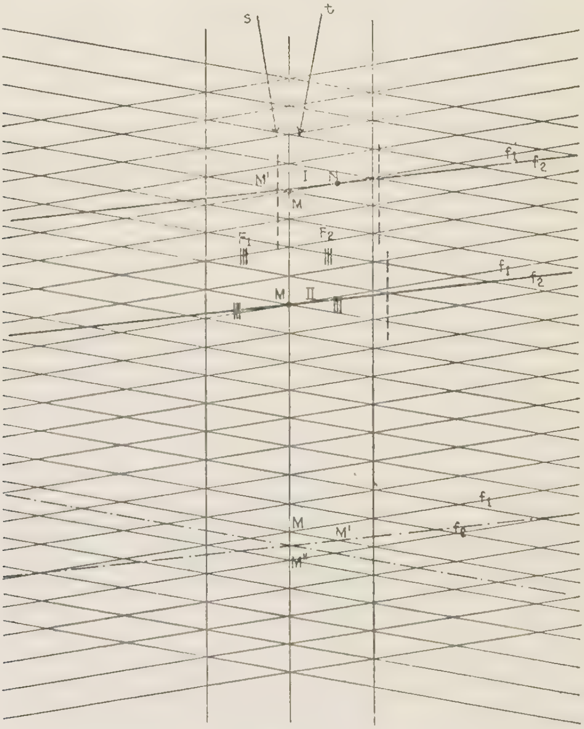

FIG. 15

this case the effect is to widen the fringe without appreciably altering the position of its center.

The foregoing is based, of course, on the hypothesis that the distances traversed by the two rays are not changing. If the distance traversed by t changes, then the wave front LM takes a new position indicated by the dotted line.

Now actually, the two changes occur simultaneously; and as both are periodic it seems inevitable that the point of intersection of f_1 and f_2 should at times come near enough to produce an appreciable displacement.

It is conceivable, of course, that the two effects might neutralize each other, as indicated at the bottom of the figure, where the point of intersection of consecutive rays is supposed to come outside of the central fringe.

6. FORMULA FOR THE SHIFT OF THE FRINGES

It seems to be impossible to obtain a formula for the amount of the shift of the fringes without making certain assumptions concerning the nature of interference phenomena.

The simplest procedure seems to be to study the network of parallelograms so drawn that each system of parallel sides represents the successive positions of some definite phase of the waves of the corresponding ray.

Let Figure 15 represent this network of parallelograms, and let a denote the distance of the middle of the central fringe to the right of some convenient origin. This distance will depend upon the initial adjustment between the distances traversed by the two rays.

If it is agreed that only the relative positions and lengths of paths of the two rays s and t are involved, we may suppose that one of the rays remains fixed in length while the other remains fixed in direction.

Let the ray t be supposed to rotate about a point in the neighborhood of its image. Then one of the lines f representing a certain phase of t may be supposed to envelop a circle. Let b denote the distance to the right of the origin of the point of contact of this circle with f in its initial position.

Use the following notations: a' equals the new value of a due to change of length of s, b' equals the new value of b due to change of direction of t, M' denotes the middle of central fringe after s has changed length, and M'' denotes the final position of the central fringe.

After the apparatus has rotated through an angle Θ, we have

$$a' = a - D\beta^2(1 - \cos 2\Theta) \, ,$$

$$b' = b + D\beta^2(1 - \cos 2\Theta) \, ,$$

$$\frac{M'M''}{1 - \cos 2\Theta} = \frac{a - b - 2D\beta^2(1 - \cos 2\Theta)}{r + \cos 2\Theta} \, .$$

Adding $M'M''$ to a', we have for the position of M'', the new middle point of the central fringe,

$$a'' = \frac{a(r+1) + b \cos 2\Theta - D\beta^2[r + 2 - (r+3) \cos 2\Theta + \cos^2 2\Theta]}{r + \cos 2\Theta} \, .$$

7. POSITION OF MAXIMUM SHIFT

The formula of the last section shows that the fringes have a periodic motion across the field of the telescope. The maximum and minimum positions of M, however, depend upon the values of the quantities a, b, and r. The values of a and r depend upon the initial adjustments, and the value of b would very likely be different for experiments performed at different times.

If, then, no effort is made to control the values of these quantities, we must suppose that the maximum and minimum positions for a series of experiments will have an entirely random distribution. It will not be legitimate, therefore, simply to average the readings of a series of observations, as was done in the Michelson-Morley experiment. In fact, there would seem to be a high degree of probability that this procedure would lead to a quite small result in case it is applied to a large number of observations.

[Professor Hedrick remarked at the end of his report that his results had been discussed by Professor Epstein from the physical point of view. This discussion has kindly been supplied for publication here.]

V. PROFESSOR PAUL S. EPSTEIN (CALIFORNIA INSTITUTE OF TECHNOLOGY)

The result of Professor Hedrick's analysis is that the two beams of light acquire a difference of phase

$$\delta-\delta'=h\beta^2\cos 2\vartheta$$

and a difference in direction

$$\Delta\alpha=\beta^2\cos 2\vartheta \qquad \left(\beta=\frac{v}{c}\right),$$

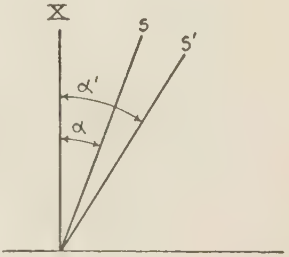

FIG. 16

in which terms of the fourth order are neglected.

Let us now choose the plane in which we observe the fringes as $x=0$ of a cartesian system (Fig. 16). We can then represent the two waves by the formulae (s = light-vector)

$$s=A\cos\left[\frac{2\pi}{\lambda}(x\cos\alpha+y\sin\alpha+ct)+\delta\right],$$

$$s'=A\cos\left[\frac{2\pi}{\lambda}(x\cos\alpha'+y\sin\alpha'+ct)+\delta'\right].$$

The illumination of the screen is then ($x=0$, $\sin\alpha=\alpha$)

$$(s+s')^2=4A^2\cos^2\left[\frac{2\pi}{\lambda}y(\alpha-\alpha')+\delta-\delta'\right]\cos^2\left[\frac{2\pi}{\lambda}y(\alpha+\alpha')+2ct+\delta+\delta'\right]$$
$$=2A^2\cos^2\left[\frac{2\pi}{\lambda}y(\alpha-\alpha')+\delta-\delta'\right].$$

We have maxima, where the argument of the cosine is a multiple of π.

The position of the central fringe is therefore given by

$$\frac{2\pi}{\lambda}y_0(\alpha-\alpha')+\delta-\delta'=0,$$

$$y_0=-\frac{\lambda}{2\pi}\frac{\delta-\delta'}{\alpha-\alpha'}. \qquad (1)$$

The distance between two maxima, or the width of the fringes, is given by the equation

$$\frac{2\pi}{\lambda}\,\Delta y(\alpha-\alpha')+\delta-\delta'=\pi\,,$$

or

$$\Delta y=\frac{\pi-(\delta-\delta')}{\alpha-\alpha'}\cdot\frac{\lambda}{2\pi}\,. \tag{2}$$

Let us first consider the interferometer at rest. We cannot take the ideal adjustment, because then we should have no fringes. Formula (2) shows that we must have a finite difference $\alpha_0-\alpha_0'$ in order to get a finite width of fringes. This width is of the order of 1 mm, so that ($\delta-\delta'=0$) we have the order of magnitude

$$\alpha_0-\alpha_0'=\frac{\lambda}{2\Delta y}=\frac{5\cdot 10^{-5}}{2\cdot 10^{-1}}=2.5\cdot 10^{-4}\,.$$

In the actual experiment, we have in addition to $\alpha_0-\alpha_0'$ the rotation $\Delta\alpha$:

$$\alpha-\alpha'=\alpha_0-\alpha_0'+\Delta\alpha\,,$$

$$y_0=-\frac{\lambda}{2\pi}\,\frac{\delta-\delta'}{\alpha_0-\alpha_0'+\Delta\alpha}\,.$$

The order of magnitude is

$$\Delta\alpha=\left(\frac{v}{c}\right)^2\cos 2\vartheta=\left(\frac{3\cdot 10^5}{3\cdot 10^{10}}\right)^2\cos 2\vartheta=10^{-8}\cos 2\vartheta\,.$$

Therefore an expansion is permissible:

$$y_0=-\frac{\lambda}{2\pi}\left(\frac{\delta-\delta'}{\alpha_0-\alpha_0'}-\frac{\delta-\delta'}{(\alpha_0-\alpha_0')^2}\,\Delta\alpha\right),$$

$$y_0=-\frac{\lambda}{2\pi}\,\frac{\delta-\delta'}{\alpha_0-\alpha_0'}\left(1-\frac{\Delta\alpha}{\alpha_0-\alpha_0'}\right).$$

The first term represents the shift due to the difference of phase, the second term is due to the rotation. We see that it is $0.4\cdot 10^{-4}$ of the first term, that is, quite outside the possibility of observation under the conditions of Michelson, Morley, and Miller's experiment.

It is interesting that in the ideal case

$$y_0 = -\frac{\lambda}{2\pi}\,\frac{\delta-\delta'}{\Delta a} = -\frac{\lambda}{2\pi}\,\frac{h\beta^2 \cos 2\vartheta}{\beta^2 \cos 2\vartheta} = -\frac{\lambda h}{2\pi}\,.$$

That is, we have a constant position, independent of the orientation of the instrument. If Michelson had devised the experiment so as to have no fringes, but light in a certain position of the ideally adjusted interferometer, expecting to have darkness in another position, because of the phase difference, the experiment would not have proved anything.

Dr. Kennedy's arrangement occupies an intermediate position. He takes fringes of considerably greater width. The width necessary to produce an appreciable error is about 250 cm, however, and it is quite certain that his fringes were not as wide as that. Professor Hedrick's theory is, however, very interesting and important in connection with Kennedy's experiment.

VI. PROFESSOR PAUL S. EPSTEIN (CALIFORNIA INSTITUTE OF TECHNOLOGY)

I cannot report to you today on anything of my own. What I intended was a short review of some recent experiments which relate to Mr. Miller's experiment, and which have been performed mainly outside of Pasadena.

I shall give you a brief account of three experiments, carried out by Tomaschek in Germany, by Chase in Pasadena, and by Piccard in Brussels.

In one of his experiments Tomaschek used the following arrangement. In the immediate neighborhood of a charged condenser *I* (Fig. 17) was suspended a magnetic needle *II*. The experiment was intended to check an old idea of Röntgen's which was as follows: The charged condenser, being in motion, represents a system of two parallel currents moving in opposite directions. These currents produce a magnetic field which should exert a force on the magnetic needle. In case the condenser is in motion relative to the ether, a deflection of the magnetic needle should be found. In reality this device cannot provide a crucial test for a decision between the old and the new theory. An exact analysis shows that both theories lead to the same result because the effect is of the first order. The explanation why no effect exists lies in the fact that it is not the condenser alone which moves, but also the indicating needle. This gives rise to a second torsional moment which just balances the first one. Moreover, Tomaschek tried the experiment with a metal cover around his needle. By this arrangement, cutting out all the magnetic actions between *I* and *II*, he eliminated any effect which might have existed without shielding. So it is not surprising that he did not obtain a positive effect. He might indeed have saved his efforts by not trying the experiment at all.

Tomaschek, and independently Mr. Chase in our laboratory, repeated the old experiment of Trouton and Noble, as they think, in a much more precise way. The underlying idea is the following:

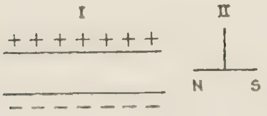

FIG. 17

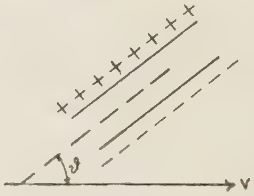

FIG. 18

Suppose *I* (Fig. 17) to be a charged condenser, suspended in such a way that it can rotate. For a condenser at rest there exists only a force of attraction between the two plates due to the charges of opposite sign. Now the apparatus being in motion with the velocity v (Fig. 18) means that the positive charge is moving in a magnetic field originated by the moving negative charge, and vice versa. Hence two additional forces are exerted on the condenser which would manifest themselves as a torque, so that a rotation of the condenser should be expected. It is easy to calculate this torque, M, which is

$$M = \frac{U}{\epsilon}\left(\frac{v}{c}\right)^2 \sin 2\vartheta \cos \varphi \,,$$

where U equals the energy content of condenser, ϵ the dielectric constant of material filling the condenser, and φ the azimuth characterizing the projection of v on the plane of the condenser in relation to the suspension.

The foregoing formula is derived on the assumption that the dielectric substance may be regarded as a continuum. The structure of ϵ has not been taken into account; but the difference would not be appreciable. Both Tomaschek and Chase used not a single condenser, but a great number of plates in order to obtain a large capacity and thus have a large value for the electric energy.

The torque is practically the same for both the classical theory and the theory of relativity, the difference arising only in some terms of the fourth order, which are of no practical importance. In spite of the existence of a torque, relativity contends that no effect can be observed at all. This follows because the torque is compensated in some way. The explanation of this peculiar fact is to be found in the tensor character of the mass in relativity. In this theory mass has a different value for accelerations in direction of the motion (m_l) and at right angles (m_{tr}) to it. The ratio of the masses is given by the expression

$$\frac{m_l}{m_{tr}}=\frac{1}{1-(v/c)^2}\,.$$

In order to analyze the effect of the torque found above, we must divide the acting forces into two components, one in direction of the motion and one at right angles to it. The first component acts against the heavier mass m_l and causes a relatively smaller acceleration than the second component. It thus happens that the two accelerations (as vectors) point to the center of gravity of the system (condenser), although the two forces do not. In this way the torque appears to be compensated in the end effect. Thus we see that the tensor character of mass is responsible for the lack of an effect. The Lorentz contraction has not to be taken into account at all. Even in case there were no Lorentz contraction, we should not obtain an effect on our condenser. If, however, an effect should really be observed, it would be a contradiction of relativity, because the ratio m_l/m_{tr} is a direct consequence of this theory. Tomaschek and Chase both claim to be able to detect an uncompensated torque corresponding to a velocity of the earth of 4 km/sec. For lower velocities no deflection could be observed with their apparatus. This limit of precision is obtained by assuming the whole torque to be in action.

Now this assumption is not quite correct even from the standpoint of the classical theory. As the nuclei are of electrical constitution, we must in the classical theory also take into account a definite relation between the mass and the velocity of the nuclei. Considering the nuclei as rigid spheres, for instance (Abraham), we should find

$$\frac{m_l}{m_{tr}}=\frac{1/(1-\beta^2)}{1/(1-\frac{4}{5}\beta^2)}\,.$$

If we use this formula, the torque will be compensated in part, but not completely as in relativity. It can easily be seen from the formula that 20 per cent of the calculated torque would manifest itself as deflection. The minimum velocity which could be observed by Chase would then be $4\sqrt{5}$ km/sec., which brings us near to Miller's value of 10 km/sec. Although interesting, these experiments cannot therefore decide either for or against Miller's results. On this account it would be of great value if they could be carried out with increased precision.

Now some remarks about the experiment of Mr. A. Piccard at Brussels: Piccard thought that the height above the earth's surface should be of influence on the effect Mr. Miller has found. (This is, in fact, a misunderstanding, because Mr. Miller does not claim any such effect.) If the ether drift may be supposed to be larger on Mount Wilson than at sea-level, it should be still larger in the free atmosphere. So Piccard tried the experiment in a balloon. His interferometer had branches with an optical path 2.8 m long. The steady temperature was controlled by a thermostat. The balloon was rotated about a vertical axis by means of a propeller. A self-recording device was used, and ninety-six rotations were registered. The curves were analyzed harmonically, but it appeared that the thermostat had not functioned as expected. For this reason the accidental errors were too large (the probable error corresponded to a velocity of 7 km/sec.). All that Piccard claims, then, is that the drift in the free atmosphere at 2300 m altitude is not larger than on Mount Wilson. No further conclusions can be drawn from this experiment.

[*Note added April, 1928.*—Both C. T. Chase and A. Piccard have continued their work during the year intervening since the foregoing report was presented. Chase,[1] working at Harvard University, increased the accuracy of his measurements about three times. Even taking into account the factor 1/5 mentioned above, his new apparatus could have detected an ether-drift velocity of 3 km/sec. Within this accuracy his results were negative, thus giving strong support to the theory of relativity. The most accurate and recent work of Piccard's was carried out by him, jointly with E. Stahel,[2] on the summit of the Rigi in Switzerland (altitude, 1800 m). The same self-recording interferometer with thermostatic temperature control was used. The results were completely negative, the ether drift being only one-fortieth part of that expected according to Miller.]

Discussion

[Dr. Walter S. Adams, director of the Observatory, opened the discussion, expressing his hope that Professor Lorentz and Professor Michelson would give their opinions in regard to the considerations of Righi and Hedrick.]

Professor H. A. Lorentz: I feel somewhat guilty in regard to the work of Righi. It was a long time ago that I read his papers, and I do not remember their contents very well, as I have been busy with quite different things these last years. I should have read them again of course for this meeting. But this good intention could not be materialized because of my being entertained so much by the people of Pasadena. After having heard Mr. Hedrick's report, I intend, however, to study these questions again very carefully in relation to Mr. Miller's experiment. Further, the considerations of Brylinski must be taken up again. Offhand, I can only say that the results of Mr. Hedrick are in contradiction with those which I presented yesterday. Until today I felt myself quite satisfied with the considerations which are based on Fermat's principle. After Mr. Hedrick's report, however, I shall have to reconsider these questions carefully. According to Mr. Hedrick's results it appears, indeed, that the result to be expected in the Michelson-Morley experiment may be numerically different from that which we ordinarily expect on the basis of the classical theory. The numerical value of the second-order effect would be different from that which Michelson calculated. My procedure seems to me still to be the easiest and most straightforward one. Still it must be found out where the discrepancy between the two ways lies. In case a method other than Fermat's is chosen, one has to do considerable work. One must distinguish, for instance, very carefully between the rays of light and the normals to the wave-trains. Another difficult point is involved in the treatment of the reflection from moving mirrors. Fermat's principle, of which I have made use, gives in any case a much simpler treatment. But as there exists a discrepancy between the results obtained by the two methods, I intend to go through the detailed calculations as soon as possible. In the meantime I still hope, of course, that my general considerations are right.

---

[1] *Physical Review*, **30**, 516, 1927.

[2] *Die Naturwissenschaften*, **16**, 25, 1928.

I should now like to make some remarks on Mr. Miller's experiment. It seems to me that there is a serious problem connected with the effect which is periodic for a full turn of the apparatus and which is discarded by Mr. Miller, who emphasizes the importance of the half-period effect (periodic with half-turns of the apparatus) in regard to the question of an ether drift. In many cases the full-period effect is much larger than the half-period effect. According to Mr. Miller, the full-period effect is dependent on the width of the fringes and would become zero for infinitely wide fringes.

Although Mr. Miller says that he was able to eliminate this effect to a great extent in his Cleveland measurements, and that it is to be explained easily by the experimental arrangement, I should like to understand its cause somewhat more clearly. Speaking now for a moment as an adherent of the relativity theory, I should contend that no such effect whatever could exist. Indeed, a rotation of the entire apparatus as a whole, the source of light included, should not give any shift at all from the standpoint of relativity. No effect would be expected were the earth and the apparatus at rest. According to Einstein, then, the same absence of an effect is to be expected for the moving earth. The full-period effect is thus in contradiction with the theory of relativity and of main importance. If then Mr. Miller has found some systematic effects whose existence cannot be denied, it is also important to know the cause for the full-period effect.

Let us discuss now the half-period effect. After having seen the different diagrams I think there can hardly exist any doubt that there is an actual displacement of the fringes with Mr. Miller's set-up. There arises, then, the question as to its possible cause. Mr. Miller himself has offered some suggestions which are very interesting. His conclusion is that the effect found corresponds to an absolute velocity of 10 km/sec. and for a definite sidereal time is the same throughout the year. It is certainly not connected with the orbital motion of the earth, but indicates a motion of the solar system relative to the stellar system of the same kind as found by Mr. Strömberg from a quite different point of view. The velocity of this motion is estimated to be at least 200 km/sec. For some reason or other, the full relative velocity between ether and earth does not come into action. Otherwise, one cannot account for the lack of an effect related to the orbital motion of the earth. There is, however, the following point to be mentioned. One could assume as Mr. Miller does that the entrainment is only partial, because the earth, for instance, is not completely impermeable to the ether. But then the following consideration would have to be taken into account. Suppose w to be the velocity of the earth relative to the ether (which is at rest at C). Then if the ether behaves as an ideal fluid, there will be a relative velocity in it at A with respect to B amounting to w/z. Miller accounts for the daily variation in amplitude of his effect, in a way which is immediately understood from Figure 20. According to the consideration given above, however, w could not be considered as a vector of constant length but would itself vary during one day. This would of course make the interpretation of the drift more complicated.

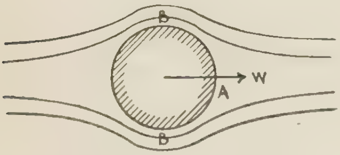

FIG. 19

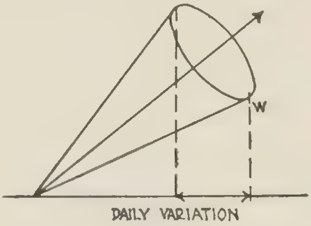

FIG. 20

As to the average displacement of the azimuth to the west (50°), it seems to be very hard to explain. Fortunately, however, it also changes about this position periodically with sidereal time. Otherwise, one could hardly escape the suspicion that the whole effect might be due to some cause in the laboratory.

Now some words about Piccard's experiment: I saw the fringes in his laboratory, and they were extremely nice indeed. As a matter of fact, Piccard considers his experiments only preliminary ones, which he hopes still to improve considerably. He worked the first time under very unfavorable conditions, as the night of his first ascent was unusually warm. I might mention, just for general interest, that such observations as Piccard's are very exhausting. Those of Mr. Miller are, too, of course. Piccard told me that he did not notice any physiological effect in the turning balloon due to centrifugal force; but motions in the vertical direction, nodding the head, for instance, were very painful, because of the effect of Corioli's force.

PROFESSOR A. A. MICHELSON: There are one or two questions which I should like to ask. Did Mr. Miller put his results together with the intention of finding an orbital effect (effect due to the motion of the earth in its orbit around the sun)?

PROFESSOR D. C. MILLER: Certainly. It was for this purpose that the observations were made at four epochs, approximately at intervals of three months; so that the direction of the orbital component of motion changes about 90° from epoch to epoch. The observations for each epoch have been reduced to determine the actual resultant motion for that epoch. The apex of the motion indicated by all the observations is near the pole of the ecliptic, and hence the orbital motion would manifest itself in a change in the position of this apex from epoch to epoch; that is, it would produce a sort of annual aberration in the apex. A comparison of the results for the four epochs fails to show conclusive evidence of this effect. I hope, however, that when several sets of observations for each epoch are available, the effect of the orbital motion may be evident. The positive effect actually obtained corresponds to a relative motion of the earth and ether of about 10 km/sec., with a probable error of $\frac{1}{2}$ km/sec. It follows that the effect of the orbital motion on the observed resultant velocity must therefore be less than $\frac{1}{2}$ km/sec.

MICHELSON: What is the probable error for this $\frac{1}{2}$ km/sec.?

MILLER: This $\frac{1}{2}$ km/sec. is itself the probable error in the measurement of the magnitude of the effect, as determined from the calculations. Since no effect has yet been detected which can positively be attributed to the orbital motion, one can only say that such an effect, if present, must be less than $\frac{1}{2}$ km/sec.

MICHELSON: Excuse me if I insist on this point. This estimation of the probable error is based on an interpretation of the experiments which does not intend to find the effect of the motion of the earth at all. Can you not find the probable error in discussing the observations from the point of view of finding the orbital motion?

MILLER: I have not calculated the error from such a point of view.

MICHELSON: It would, however, be possible to do so. I should really like to see such calculations carried out.

Had I known earlier of the beautiful and ingenious apparatus of Mr. Kennedy, I probably should not have undertaken my experiments now going on in the same form. In any case, the problem in question must be investigated further. Even a more precise repetition of experiments with older devices already used will be of great value for the reliability of the results. We have now to find out definitely what actually is the truth, without going at it with any prejudice.

I am happy in respect to Mr. Kennedy's experiment that I had the idea of this device, too. I also had intended to use the photometric comparison of the field produced by light which is reflected from a divided mirror, the two half-surfaces being at a distance of a fraction of a wave-length. But it did not occur to me that the separation could be made so nicely by sputtering. I intended to take the layer off by acids. The apparatus is indeed so beautiful that I should like to work with a similar device, in case Mr. Kennedy has no objections.

As far as Mr. Piccard's remarks are concerned (see Lorentz) I must say that every beginner thinks himself lucky if he is able to observe a shift of 1/20 of a fringe. It should be mentioned, however, that with some practice shifts of 1/100 can be measured, and that in very favorable cases even a shift of 1/1000 of a fringe may be observed. For this purpose the fringes must be extremely black. We are sufficiently advanced with our new apparatus to show such fringes [the apparatus was on view in the laboratory]. The main thing, of course, is to eliminate all stray light, which comes especially from the silver-coated plate. The ordinary plate gives rise to reflections at both surfaces. I now get rid of scattered light by this simple device illustrated in Figure 21, consisting of two prisms, with a half-silvered surface where they are in contact, oriented so that the incident light is not quite perpendicular to the face of the first prism. Very black fringes may be obtained by this combination of prisms. There are still some difficulties as to the separating surface which I hope to overcome, however, very shortly. Probably the precision will reach 1/1000 of a fringe.

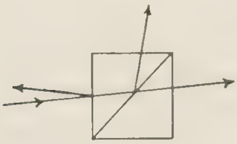

FIG. 21

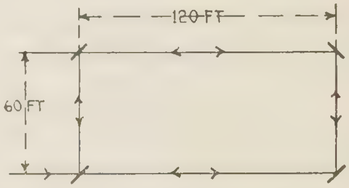

FIG. 22

I should like to make some remarks on the interpretation of Mr. Miller's experiments. It seems to me to be very hard to explain them. Indeed, why should the ether be dragged along by the earth to the extent of 19/20 and not some other fraction? If this really occurs, then we must suppose that there will be a great difference between the drag on the surface of the earth and a thousand miles above it. There the drag would probably be zero. Assuming then, for illustration, some kind of an exponential decrease of drag with altitude we should expect a large difference between the shift at sea-level and on Mount Wilson. In this case another arrangement of apparatus could be used to observe the effect. Two rays of light could be sent around a vertically mounted rectangle (Fig. 22). A shift of several hundred fringes might then be expected. No shift, however, seems to exist, according to experiments made in the Ryerson Laboratory.

To conclude, I might still mention some advantages of the new apparatus: (1) The fringes are very black. (2) The frame will be built of invar so as to make it very insensitive to changes of temperature. (3) Photographic registration will be used so as to make continuous readings possible. Thus recorded, the observations would be preserved and could be discussed later on, independently of the observer. These are the three points which represent a considerable improvement in comparison with the earlier apparatus.

It may be of some interest to mention that originally another apparatus was planned; this, however, was abandoned and the present interferometer adopted. The arms were to be 100 m long. The apparatus could not be turned, but the moving earth would have brought it into different positions relative to the ether. We now intend to try this, and the experiment is in preparation at Chicago.

LORENTZ: In regard to the theoretical details raised by Dr. Michelson, I offer the following remarks: If the ether moves freely through matter, no such difficulties arise, as far as entrainment is concerned. If, on the other hand, we should be obliged by the facts to introduce a substantial ether again, it would, of course, be a very difficult problem to find out what its properties are. What would happen, for instance, in case matter should turn out to be only partly permeable for the ether, nobody can tell. For this reason the question about the ratio 19/20 could not well be raised before the properties of the ether were better known. We can even leave open the possibility that the motion of the ether may be irrotational. In this case the ether drift would of course have a component normal to the surface of the earth, and it would be rather large. This might very well be the case, and the effect mentioned by Dr. Michelson would be null. The relative velocity of the ether drift might increase with increasing distance above the surface of the earth, and still have no rotation. This, for instance, is the case in Planck's modification of Stokes's theory. A further possibility would be a compressible ether. This would remove even the necessity of having an irrotational motion of the ether. But it is sufficient for the present moment to point out that a motion of the ether with rot $w=0$ would be sufficient to give a quantitative explanation of aberration phenomena and of Michelson's result. I tell you all this only to show how numerous the different possibilities for the theory are, if we are compelled by new experiments to go back to the notion of a substantial ether.

QUESTION TO DR. KENNEDY: Your apparatus is so sensitive that it would detect a change in the optical path equal to $\delta l = 2 \cdot 10^{-3} \lambda$.

Now this is not the sensitivity which you calculated theoretically. I should like to ask how you found this sensitivity. I do not ask this for myself, because I know how you have done it, but for the sake of the audience, because I think the method you applied is so very beautiful. Then I suggest also that you tell us if you could detect the orbital effect on the assumption of a drag of 19/20.

DR. R. J. KENNEDY: Answering first the second question, I think that the effect due to the orbital motion of the earth should be observable with my apparatus.

As to the first question, I thought that the method of determining δl was rather crude. A weight of 5–6 kg on the slab on which the apparatus was mounted produced a shift of one fringe. I determined the minimum weight (about 10 g) which produced an effect just observable. The ratio of the two weights gives, then, $\delta l/\lambda$.

I might explain also that I got rid of the surplus scattered light by using a different method from that suggested by Dr. Michelson for his new device. I used polarized light, impinging under the proper angle on the glass plate (Brewster's angle) so that no light at all was reflected. [See description in Kennedy's report. MICHELSON exclaims: "Very nice indeed."] The method I used is not my own invention. It has been suggested somewhere in *Comptes rendus* (1911), if I remember rightly.

The shift of azimuth (50° to the west) in Miller's experiment seems to indicate that some spurious effect is present, dependent only on the position of the apparatus relative to the meridian, which shifts the azimuth of the whole effect to the west. The result must then be considered as a superposition of spurious effect and ether drift. This explanation would probably require a magnitude for the effect due to ether drift smaller than anything that could have been observed with the devices used. It might also explain, as I think, the difference between the results obtained by Mr. Miller and myself.

Piccard's experiment does not seem to be of great value. As far as I can make out, he worked just at a time of the day when hardly any effect was to be expected.

LORENTZ: I do not think that Kennedy's last remark is quite right. Piccard really ascended at the time when the constellation of Hercules rose above the horizon.

KENNEDY: Piccard ascended twice. Once, when the sidereal time was right, his observations were spoiled by temperature effects. His errors were thirty times greater than the effect he was looking for. The second time he got rid of his errors, but there was no effect to be expected at the sidereal time chosen for this observation.

MILLER: I agree with Hedrick that the theory of the instrument used for the experiments should be thoroughly studied. The theory of Lorentz is exact; but it is general, and does not take into account the special conditions of the apparatus used. What actually happens to the fringes is dependent on the adjustment of the mirrors. When I became interested in the experiment in 1900, there existed no really adequate theory of the instrument. A theoretical study of the apparatus was then undertaken by W. M. Hicks, which was published in the *Philosophical Magazine* for January, 1902. We [Miller and Morley] thought it necessary to take up the question again, as Hicks had suggested that there was an additional term in the expression for the effect which had not previously been considered. This term represents an effect of appreciable magnitude, which is periodic in each full turn of the interferometer, while the ether-drift effect is periodic in each half-turn. In the *Philosophical Magazine* for May, 1905, we gave a review of the theory, showing that Hicks's calculations did not affect the conclusions previously drawn. The full-period effect is actually present in the experiments of 1887, as well as in all those that have followed. In *Comptes rendus*, **168**, 837, 1919, Righi began a series of articles, setting forth the theory in detail. He thought that our conclusions were not justified by the theory. It seems to me that Righi's theory is correct in the abstract; but it does not deal with the actual things happening in the interferometer, as Hicks's theory does. The question needs still further investigation, as suggested by Professor Hedrick. Hicks's theory takes into account the fact that in practice the image *c* (Fig. 23) of mirror *a* with regard to *a* is slightly oblique to mirror *b*. This is necessarily true when straight-line fringes of finite width are obtained. Righi's calculations are based on the assumption that *b* and *c* are exactly parallel, which would produce fringes of infinite width; thus, his criticism does not apply to the actual case. When *b* and *c* are oblique to each other, an actual ether drift will produce the additional effect predicted by Hicks, which is periodic in a full turn of the apparatus. Hicks has calculated its magnitude, showing that it depends on the angle between *b* and *c*. The effect increases with increasing angle and decreasing width of fringes. As the effect we are looking for (ether drift) must be periodic in each half-turn, we are justified in eliminating the full-period effect. This is done by plotting the single observations, turn by turn of the interferometer; these curves are analyzed by the mechanical harmonic analyzer, and the second harmonic (half-turn effect) is taken as representing the ether drift. If there is an ether-drift effect, the full-turn effect is necessarily produced, according to Hicks, and its presence may be taken as further evidence of the ether drift. The magnitude and phase of the full-period effect is variable, because it depends upon the adjustment of the mirrors as well as the ether drift. [Slides were shown representing the full-period effect.] It is evident that the magnitude is very different for different sets of observations. The half-period effect, on the other hand, is characterized by a constant magnitude. The full-period effect is small when the width of the fringes is such that five of them cover the mirror (10 cm in diameter). Under other conditions, however, it may be very large. The full-period effect is not new, but has always been present in all the experiments. It is present in Professor Michelson's original observations.

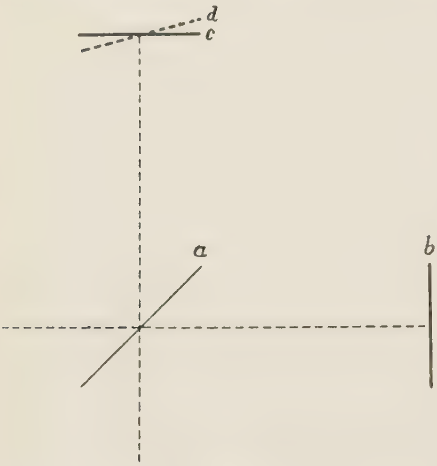

FIG. 23

KENNEDY: Are the effects the same in case you use a concrete frame instead of an iron frame?

MILLER: Yes, they are essentially the same. The concrete instrument showed smaller temperature effects than did the one with the steel frame, but its mechanical strength was also less. I have always used (as did Kennedy) the method of shifting the fringes by putting weights on the end of the frame; to produce a shift of one fringe, approximately 325 g was necessary. This is less than the corresponding weight in Dr. Kennedy's apparatus, because the arms of the frame are longer in my apparatus than in his. I should like to mention again that my experiments have been carried out under a great variety of conditions. My assistant moved around the apparatus to see if his position affected the distribution of temperature or the stability or level of the instrument. The light was placed in different positions, both inside and outside the house. At Mount Wilson, the instrument has been mounted in two different buildings, differently oriented. The effect has persisted throughout. After considering all the possible sources of error, there always remained a positive effect.

PROFESSOR E. R. HEDRICK: Mathematically speaking there cannot be any question as to the correctness of the computations which Professor Lorentz has presented to us. The result for the second-order terms seems beyond question. It is conceivable, however, that there is introduced an error when the path of the beam of light is changed by the motion of the apparatus into a new one. The instrument might not be always in the ideal position assumed in the calculations.

I should like to call your attention to a second point. We start from a certain number of assumptions. Now our aim in mathematics is always to reduce the necessary number of assumptions to a minimum. We make use in this special case of the two principles of Huyghens and Fermat. Can we trust them to terms of the third order? We do not know. Might not a combination of third-order effects eventually affect the magnitude of the second-order effect? Anyhow, if we could reduce the number of physical principles involved in our calculations to a single one, it would be very desirable. That is what Righi and also I have attempted to do.[1]

LORENTZ: I should like to defend my theory. Hedrick says we should try to reduce the number of our assumptions. Now the two principles of Huyghens and Fermat are not independent. The second may be deduced from the first. It is easy to prove that this is true. There is then no question of having two assumptions.

---

[1] It should be stated clearly that the operations of differentiation and integration, freely used in these discussions, cannot be trusted to the extent that is often assumed. The derivative of an approximation to a true formula is not necessarily an approximation to the derivative of the true formula. It is true also that the integrals to successive approximations to a true formula are not necessarily successive approximations to the integral of the true formula, unless the successive approximations are *uniform*. These conditions cannot be said to hold in such fine approximations as those of the Michelson experiment. Therefore it has seemed to us, and it still seems to us, to be necessary to proceed by direct calculations from definitely stated assumptions, rather than through an intermediate proof (e.g., Fermat's principle) that is thus questionable.

HEDRICK: Is this really generally true?

LORENTZ: Yes; the relation between Huyghens' principle and Fermat's principle is absolutely general. I might repeat more precisely some of the features of the reasoning I gave yesterday.

Suppose *P* (Fig. 5) to be a luminous point. (The difficulties might of course begin here, if we were obliged to state exactly what we mean by this.) Suppose, further, that rot $w=0$, which is Fresnel's idea. Making use of Fresnel's coefficient and entrainment, we find the influence of a motion of the apparatus on effects of the first order to be the same for each of the paths l_1 and l_2.

There is still one point to be considered which I did not mention before. If we take into account effects of the second order, the path of the rays will be changed by the motion of the apparatus, so that we should have to use in one moment l and in the next l'. Still I think that for the effects under consideration it does not make any difference which one we take. [HEDRICK remarks: "Yes, that is all right."] It can easily be seen that the difference between l and l' produces only an effect of the fourth order. We are thus justified in using the path existing without motion of the ether.

Of course the value of the light-path l must be exact to the second order. For those cases in which we are concerned with the propagation in ether only, this value follows from the expression for v (velocity of light in the moving system):

$$\frac{1}{v}=\frac{1}{c}\left[1-\frac{w}{c}\cos\vartheta+\frac{w^2}{c^2}\left(\cos^2\vartheta+\tfrac{1}{2}\sin^2\vartheta\right)\right].$$

[See expression (3) in Report II.] But the question arises, and this is what I wanted to add, what will be the form of the equation when we deal with light passing through the moving glass plates? In this case w^2/c^2 would be replaced by k^2w^2/c^2, where $1-k=(n^2-1)/n^2$ is Fresnel's coefficient. Now this value for k might not be quite rigorous in this connection. The expression $wkdt$ due to the entrainment by matter might be doubted if terms of the second order are to be considered. This indeed might necessitate a change of magnitude for these second-order effects. It is to be remarked, however, that the distances through which the light travels in glass in Michelson's experiment are comparatively so small, and that practically they cannot give rise to any difficulty at all. For all these reasons I think that the theory which I presented is general, and, at the same time of exact applicability to the actual instrument. In any case, I intend to study all the recent work such as Mr. Hedrick's.

DR. G. STRÖMBERG: It is often said that the sun's motion "in space" is 20 km/sec. toward the point $\alpha=270°$, $\delta=+30°$. This expression is quite inadequate and means that the sun's motion referred to the brighter stars is of this magnitude and direction. Referred to distant objects, this velocity is much greater. The sun's velocity relative to the system of globular star clusters is about 300 km/sec. in the direction $\alpha=320°$, $\delta=+65°$, and relative to the spiral nebulae it may be even larger, although in about the same direction.

As the bigger reference frame is, presumably, the more fundamental, the higher velocity may also be of more fundamental nature.

And this is just what has been found to be the case. The sun's motion as referred to different classes of objects in our neighborhood is quite different, and the general rule has been established that the higher the internal velocity dispersion in a group, the larger is the sun's motion relative to this group. Practically all celestial objects can be arranged in a sequence with increasing velocity dispersion, and moving with different velocity along a certain axis. This sequence terminates with the globular clusters, and a quadratic relationship exists between group motion along a certain axis and the velocity dispersion along the same axis. This phenomenon can, at least formally, be explained as the effect of a velocity restriction in a fundamental reference frame in which the globular star-clusters are statistically at rest.

Recent studies of the velocities of giant M stars have completely confirmed this hypothesis. In fact, it has been found possible to represent the velocity distribution along this fundamental axis in a much more satisfactory way by one disposable constant, in addition to this fundamental velocity vector, than by four arbitrary constants, as in the prevalent methods.

In stellar motions we have to introduce a fundamental velocity vector of 300 km/sec. in the direction mentioned in order to secure order and regularity. This implies the existence of a "fundamental" reference frame, or "medium," or "ether," whatever we prefer to call it. The introduction of such a conception has been of great value in the study of stellar motions.

PROFESSOR H. BATEMAN: The Michelson-Morley experiment may be regarded as a test of the laws of reflection by a moving mirror. For the general case in which the source of light is moving relative to the earth, the question resolves itself into two: (1) Is the image of a moving point source of light a single moving point source of light as in the classical electromagnetic theory? (2) Are the space-time co-ordinates of a point source and its image connected by the relations

$$x'=x-\frac{2c^2}{c^2-u^2}(x-ut) \qquad t'=t-\frac{2u}{c^2-u^2}(x-ut)\ ,$$

$$y'=y \qquad z'=z \qquad (u=\text{velocity of mirror})\ ,$$

of the classical electromagnetic theory and the theory of relativity?

On the assumption that the first question is to be answered in the affirmative, various modifications of the equations connecting the space-time co-ordinates of a point source and its image might be tried on the arrangements of mirrors in the Michelson-Morley experiment. The interference fringes may in each case be regarded as the fringes produced by light coming directly from certain image sources and traveling in accordance with certain assumed laws of propagation which are also under test. The general problem is still more complicated by the contraction of the apparatus. The first question of the sharpness of the image of a point source which is moving relative to the mirror is difficult to settle experimentally on account of the lack of point sources of light moving at a high speed and at some distance from the earth. The velocity of a shooting star may be forty-five miles a second, but this is probably too small for the production of lack of sharpness in the image.

Director Adams closed the conference, thanking all the speakers for their contributions.

CARNEGIE INSTITUTION OF WASHINGTON
MOUNT WILSON OBSERVATORY
April 1928

Contributions from the Mount Wilson Observatory, No. 374
Reprinted from the *Astrophysical Journal*, Vol. LXIX, pp. 43–48, 1929
Printed in the U.S.A.

REVISION OF THE VALUE OF e/m DERIVED FROM MEASUREMENTS OF THE ZEEMAN EFFECT

By HAROLD D. BABCOCK

ABSTRACT

With the aid of *recent data on the structure of the spectra of Cr and Ti* the value formerly derived for the specific *charge* of the electron has been *revised*. The previous list of 116 lines is now reduced to 48, with *only such lines* retained *as may properly be used* according to the present *theory of the Zeeman effect*. The lines now employed are those which had the greatest weight in the earlier work. *Forty-eight new values* of e/m are derived whose *weighted mean* is $e/m = (1.7606 \pm 0.0012) \times 10^7$ E.M.U./gm. This is practically the *same as the earlier result*, but somewhat more reliable.

An earlier paper[1] gives the ratio of the elementary charge, e, to the mass, m, of an electron as determined from the observed Zeeman effect produced on 116 spectral lines by a magnetic field of measured intensity. The lines were selected from the spectra of *Cr*, *Ti*, *Zn*, *Ba*, and *Cd* between the limits λ 3841 and λ 4870, and thus only part of them could be used in any single determination of e/m. Those most frequently employed have Zeeman patterns which had been found to bear fractional relations to the normal separation involving only small denominators. The modern theory of the Zeeman effect fully confirms the observational evidence which led to the selection of these lines. Examples of this are indicated by asterisks in Table I, more fully described below. The mean result for e/m, as pointed out in *Contribution* No. 263, depends chiefly on such lines.

Occasionally, however, other lines were also used for which the theoretical Zeeman effect is unknown, and still others now shown by the theory to be unsuited to precise measurement, except with resolving power much higher than that which was then available. These additional lines were included in the investigation because, with apparently reasonable assumptions, they gave results accordant with those from better lines and because at that time the spectra involved had not been sufficiently analyzed to afford a reliable criterion for excluding unsuitable lines. Although these doubtful lines played a minor rôle in the investigation, their inclusion has met with criticism, and Gerlach,[1] for example, has felt that the result could be accepted as approximate only.

---

[1] *Mt. Wilson Contr.*, No. 263; *Astrophysical Journal*, **58**, 149, 1923.

In recent years much progress has been made in systematizing the complex spectra. Thus Ti and Ti^+ have been very completely analyzed by Russell,[2] while Cr and Cr^+ have been studied by several investigators, among them Dr. C. C. Kiess, to whom I am particularly indebted for generous permission to use unpublished material. It has thus become possible to examine in detail the observations formerly made for the determination of e/m, and to derive a new value of this constant, based solely on lines whose Zeeman effects, as shown by theory, are capable of accurate measurement with the apparatus that was used.

It has been verbally suggested by Dr. W. V. Houston that a theoretical objection may be made to the use of the Zeeman effect for deriving e/m, because of a possible influence of adjacent spectral terms of different multiplicity on the magnetic levels of the terms involved in the measured lines. Thus a quintet D-term whose sublevels are widely separated might be affected by a triplet D-term whose distance, on the scale of wave-numbers, is not more than three or four times the separation of the extreme levels of the quintet term. In such a case spectral lines derived from combinations of the quintet with other terms would have slightly modified Zeeman effects.

Unfortunately, my data are too meager to afford a test of this question; but it appears that for the lines of greatest weight in this revision the terms are so compact, in comparison with their separation from other terms which might disturb the magnetic levels, that no influence is to be feared. For example, in the case most favorable to such an influence, the separation from possibly disturbing terms is seven times the range of wave-numbers in the term involved in a measured line.

Table I gives the 48 spectral lines which have been retained, together with the combination of terms for each line and the theoretical Zeeman pattern, which in every case is confirmed within the

---

[1] Geiger und Scheel, *Handbuch der Physik*, **22**, 58, Berlin, 1926.

[2] *Mt. Wilson Contr.*, Nos. 344, 345; *Astrophysical Journal*, **66**, 283, 347, 1927.

TABLE I

SPECTRAL LINES USED FOR DETERMINATION OF *a*

λ	El.	Multiplet	Separations
3852.23	*Cr*	$a^5D_1-a^3P_0$	(0) 1.50
3857.63	*Cr*	$a^5P'_1-d^5D'_1$	(1) 1.50, **2.50**
3883.30	*Cr*	$a^5D_2-a^5D'_3$	(0) 1.50
3885.22	*Cr*	$a^5D_1-a^5D'_2$	(0) 1.50
3886.80	*Cr*	$a^5D_3-a^5D'_4$	(0) 1.50
3894.05	*Cr*	$a^5D_0-a^5D'_1$	(0) 1.50
3902.95	*Cr*	$a^5D_2-a^5D'_2$	(0) 1.50
3908.76	*Cr*	$a^5D_3-a^5D'_3$	(0) 1.50
3916.25	*Cr*	$a^5D_1-a^5D'_0$	(0) 1.50
3919.17	*Cr*	$a^5D_4-a^5D'_4$	(0) 1.50
3921.03	*Cr*	$a^5D_2-a^5D'_1$	(0) 1.50
3928.65	*Cr*	$a^5D_3-a^5D'_2$	(0) 1.50
3941.50	*Cr*	$a^5D_4-a^5D'_3$	(0) 1.50
3992.85	*Cr*	$a^5P'_3-f^5P_3$	(0) 1.67
4126.52	*Cr*	$a^5G_6-b^5G'_6$	(0) 1.33
4163.63	*Cr*	$a^5G_4-b^5G'_4$	(0) 1.15
4191.27	*Cr*	$a^5G_3-b^5G'_3$	(0) 0.92
4289.72	*Cr*	$a^7S_3-a^7P_2$	(**0**, 0.33, 0.67) **1.33**, 1.67, 2.00, 2.33, 2.67
4295.79	*Cr*	$a^5P'_3-e^5P_3$	(0) 1.67
4337.57*	*Cr*	$a^5D_1-a^5F_2$	(**0**, 0.5) **0.50**, 1.00, 1.50
4339.45	*Cr*	$a^5D_2-a^5F_3$	(**0**, 0.25, 0.50) **0.75**, 1.00, 1.25, 1.50, 1.75
4351.06	*Cr*	$a^5D_1-a^5F_1$	(1.50) 0, 1.50
4359.63*	*Cr*	$a^5D_2-a^5F_2$	(0.5, **1.0**) 0.50, 1.0, 1.5, 2.0
4371.28	*Cr*	$a^5D_3-a^5F_3$	(0.25, 0.50, **0.75**) 0.75, 1.0, **1.25**, **1.50**, 1.75, 2.00
4391.76	*Cr*	$a^5D_3-a^5F_2$	(**0**, 0.5, 1.0) 0.50, 1.00, 1.5, **2.0**, **2.5**
4496.86*	*Cr*	$a^5S_2-b^5P_3$	(**0**, 0.33, 0.67) **1.0**, 1.33, 1.67, 2.0, 2.33
4526.48	*Cr*	$a^5G_6-a^5G'_6$	(0) 1.33
4533.25	*Ti*	$a^5F'_5-b^5F_5$	(0) 1.40
4554.04*	*Ba*+	$a^2S_1-a^2P_2$	(0.33) **1.0**, 1.67
4580.06*	*Cr*	$a^5S_2-b^5P_1$	(**0**, 0.5) **1.5**, 2.0, 2.5
4591.41	*Cr*	$a^5D_1-b^5P_2$	(**0**, 0.33) 1.5, 1.83, **2.16**
4613.34*	*Cr*	$a^5D_0-b^5P_1$	(0) 2.5
4616.13*	*Cr*	$a^5D_2-b^5P_2$	(0.33, **0.67**) 1.17, **1.50**, **1.83**, 2.16
4626.19*	*Cr*	$a^5D_1-b^5P_1$	(1.0) 1.50, 2.50
4651.30*	*Cr*	$a^5D_2-b^5P_1$	(**0**, 1.0) **0.50**, 1.5, 2.5
4652.16*	*Cr*	$a^5D_3-b^5P_2$	(**0**, 0.33, 0.67) **0.83**, 1.17, 1.50, 1.83, 2.16
4654.74	*Cr*	$a^7F_0-c^7D_1$	(0) 3.0
4678.15	*Cd*	$a^3P_0-a^3S_1$	(0) 2.0
4680.14*	*Zn*	$a^3P_0-a^3S_1$	(0) 2.0
4689.39	*Cr*	$a^7F_3-c^7D_2$	(**0**, 0.5, 1.0) **0.5**, 1.0, 1.5, 2.0, 2.5
4700.62	*Cr*	$a^5P'_1-b^7D'_2$	(**0**, 0.5) **1.5**, 2.0, 2.5
4722.16*	*Zn*	$a^3P_1-a^3S_1$	(0.5) **1.5**, 2.0
4758.13	*Ti*	$a^3H'_5-c^3H_5$	(0) 1.03
4759.28	*Ti*	$a^3H'_6-c^3H_6$	(0) 1.17
4799.91	*Cd*	$a^3P_1-a^3S_1$	(0.5) 1.5, 2.0
4810.53*	*Zn*	$a^3P_2-a^3S_1$	(**0**, 0.5) **1.0**, 1.5, 2.0
4824.13	*Cr*+	$a^4F'_5-a^4F_5$	(0) 1.33
4848.27	*Cr*+	$a^4F'_4-a^4F_4$	(0) 1.24

* Used on ten or more photographs.

errors of observation. Close lines like λ 4651.50 and λ 4652.16 of *Cr* were used with precautions to avoid errors of measurement caused by blending of their components. Usually the outermost components, and sometimes those of intermediate separation, were omitted, depending on circumstances such as strength of magnetic field, spectroscopic resolving power, and dispersion. Further, the inner *p*-components of lines like λ 4339.45 of *Cr* were omitted because their small separation precludes accuracy in the result.

TABLE II

Plate	*a*	*H*	*e/m*	Wt.	Plate	*a*	*H*	*e/m*	Wt.
1.....	1.352	29,030	1.7543	1	28....	1.234	26,500	1.7542	2
2.....	1.348	29,030	1.7491	1	29....	1.228	26,500	1.7457	1
3.....	1.360	29,030	1.7647	1	30....	1.225	26,500	1.7414	2
4.....	1.274	27,670	1.7344	1	31....	1.228	26,500	1.7457	2
5.....	1.287	27,670	1.7521	1	32....	1.233	26,500	1.7528	2
6.....	1.284	26,950	1.7946	1	33....	1.236	26,500	1.7571	1
7.....	1.281	26,950	1.7904	1	34....	1.241	26,500	1.7642	1
8.....	1.385	29,360	1.7769	1	35....	1.145	24,290	1.7758	2
9.....	1.423	30,300	1.7690	1	36....	1.145	24,290	1.7758	2
10.....	1.411	30,300	1.7542	1	37....	1.139	24,290	1.7664	2
11.....	1.306	27,660	1.7786	1	38....	1.238	26,500	1.7599	1
12.....	1.341	28,320	1.7837	1	39....	1.236	26,500	1.7571	2
13.....	1.485	31,810	1.7582	3	40....	1.240	26,500	1.7622	2
14.....	1.498	31,810	1.7740	3	41....	1.238	26,500	1.7599	2
15.....	1.487	31,810	1.7610	2	42....	1.231	26,500	1.7500	2
16.....	1.478	31,810	1.7502	2	43....	1.232	26,500	1.7514	2
17.....	1.490	31,810	1.7646	1	44....	1.231	26,500	1.7500	2
18.....	1.474	31,810	1.7456	3	45....	1.242	26,500	1.7656	1
19.....	1.502	31,810	1.7787	3	46....	1.242	26,500	1.7656	1
20.....	1.477	31,810	1.7491	2	47....	1.242	26,500	1.7656	1
21.....	1.486	31,810	1.7598	3	48....	1.248	26,500	1.7741	1
22.....	1.487	31,810	1.7611	3					
23.....	1.490	31,810	1.7646	2					
24.....	1.487	31,810	1.7611	3					
25.....	1.490	31,810	1.7646	1					
26.....	1.488	31,810	1.7622	2					
27.....	1.244	26,500	1.7684	2					

Table II presents the new weighted mean values of the normal separation, *a*, derived for each plate from lines contained in Table I by dividing the observed quantity $\Delta\nu$, corresponding to each pair of Zeeman components, by the number which represents the ratio of the given separation to that of the normal triplet, as listed in the last column of Table I. Weights of individual values of a depend on the magnitude of $\Delta\nu$ and on the quality of the spectral lines. The third column of Table II gives the same magnetic intensities, H, as were found in the previous investigation, while the fourth column contains the revised values of e/m.

No new measurements are given in this paper, but the new weights in the last column of Table II have been assigned to the separate determinations of e/m because of changes in the relative number of lines employed. As shown in the previous paper, however, the weights have very little effect on the final result.

The weighted mean value of e/m is found from Table II to be 1.7610×10^7, which is the same as the result derived in *Contribution* No. 263. A further slight correction is required, however, because the velocity of light in air was formerly taken to be 2.9978×10^{10} cm/sec., whereas the new result of Professor Michelson[1] is 2.99704×10^{10} cm/sec. Applying this correction, we find the final value to be

$$e/m = (1.7606 \pm 0.0012) \times 10^7 \text{ E.M.U./gm.}$$

In view of the selection of material on which this result rests, the probable error which is appended is of greater significance than in the former paper. It seems probable that the actual uncertainty in the result is not much greater than one part in one thousand.

The value of e/m found here coincides with that derived by Dr. Houston[2] from measurements of the spectra of hydrogen and helium. This coincidence is undoubtedly accidental, but the fact that the two investigations agree in giving results distinctly lower than those found by other observers is perhaps significant. Discussion of the theoretical questions involved will not be attempted here, but it may not be superfluous to recall that Birge,[3] in a thorough examination of the relations among basic constants, concludes that the most probable value of e/m is 1.760×10^7 E.M.U./gm. Furthermore, Dr. Birge, at whose suggestion this revision has been made, permits me to quote as follows from a paper which he is now preparing on the most probable values of general physical constants:

---

[1] *Annual Report of the Director, Mount Wilson Observatory*, 1927.

[2] *Physical Review*, **30**, 608, 1927.

[3] *Science*, **64**, 180, 1926.

> Summarizing the results we find
>
> $$\begin{aligned} e/m &= 1.769 \pm 0.002 \text{ from deflection experiments} \\ &= 1.761 \pm 0.002 \text{ from Zeeman effect} \\ &= 1.761 \pm 0.001 \text{ from } H \text{ and } He \text{ spectra.} \end{aligned}$$
>
> The discrepancy between the first result and the last two seems to be real.

Further details and the interesting conclusions reached must await the publication of Birge's paper.

Carnegie Institution of Washington
Mount Wilson Observatory
October 31, 1928

Contributions from the Mount Wilson Observatory, No. 375
Reprinted from the *Astrophysical Journal*, Vol. LXIX, pp. 196–208, 1929
Printed in the U.S.A.

IS THERE ARGON IN THE CORONA?

BY H. N. RUSSELL[1] AND I. S. BOWEN

ABSTRACT

Critical study of the coincidences between lines in the spectrum of the solar corona and in that of argon, which have recently been suggested by Dr. I. M. Freeman, shows: (*a*) that the number of these coincidences is little larger than might be expected from pure chance, within the very wide limits of error which have been admitted; (*b*) that the discordances for the better-measured lines greatly exceed the limits of observational error; and (*c*) that the suggested coincidences are with weak or forbidden lines, while far stronger argon lines, which should be much more persistent, are absent.

This cumulative evidence shows decisively that *the attribution of the coronal lines to argon is without foundation.*

Formulae for computing the number of chance coincidences between spectra are given and tested empirically by comparison with fictitious lines chosen at random.

Criticism of scientific work is a much less agreeable task than investigation, but it is necessary at times, for an erroneous conclusion, if not challenged, may be accepted by those without expert knowledge and may have a long life. We therefore feel under obligation to set forth the reasons which convince us that the recent attribution of most of the lines in the spectrum of the solar corona to argon[2] is without foundation.

I. THE CORONAL LINES

In the paper under consideration, Freeman lists forty-five lines as belonging to the coronal spectrum, following the list prepared in 1918 by Campbell and Moore.[3] This list, as its compilers explain, was designed to be inclusive, and contains a number of lines recorded on one occasion only, by a single observer, and regarded by him as doubtful. Davidson and Stratton,[4] after a careful discussion, reject twenty of these lines as identifiable with known radiations of the high chromosphere, and regard only sixteen as of undoubted coronal origin. St. John and his collaborators in the revision of Rowland's table[5] list seventeen lines as coronal and five more as doubtful. It may fairly be concluded that only about half the lines on the longer list really belong to the coronal spectrum.

---

[1] Research Associate of the Mount Wilson Observatory, Carnegie Institution of Washington.

[2] I. M. Freeman, *Astrophysical Journal*, 68, 177, 1928.

[3] *Lick Observatory Bulletin*, 10, 10 and 21, 1918.

[4] *Memoirs, R.A.S.*, 64, 142, 1927.

[5] *Carnegie Institution of Washington, Publication* No. 396, p. 226, 1928.

For many of the lines, as Freeman notes, the wave-lengths are very poor. The fainter ones have been observed only with the objective prism, which gives images of the corona itself, incapable of precise measurement. But the data for the stronger lines are much better. Davidson and Stratton during totality in 1926 obtained spectra of the corona (with iron comparison) with a large quartz slit-spectrograph, and of the flash at second contact with the same instrument. The latter shows hundreds of lines, which agree closely with the laboratory wave-lengths. For the first ten lines in each 100 A (blends and one questionable identification being excluded), the average residuals, regardless of sign, are as follows:

λ	Lines	Average Residuals
3100–3300	30	±0.044 A = ±0.43 wave-numbers
3400–3700	40	.045 = .35
3800–4100	40	±0.062 = ±0.40

The largest residual for these one hundred and ten lines is 0.19 A.

The published reproduction of the photographs shows that the coronal spectrum is of equally good quality. The seven coronal wave-lengths observed on this plate should therefore have probable errors of the order of ±0.04 A. Since the slit was set on the sun's eastern limb for half the exposure, and the western limb for the rest, the solar rotation was eliminated.

The measures in the visible spectrum are less satisfactory, except for the green line, for which the principal determinations with slit-spectrographs are:

		λ Rowland's Scale
Campbell	1898	5303.26
Campbell	1918	5302.98
Dyson	1905	5303.1
Furuhjelm	1914	5303.38
Adams, St. John, and Ware	1918	5303.24
Slipher	1918	5303.0
Davidson and Stratton	1926	5302.98

The simple mean is 5303.13 (Rowland) or 5302.95 (I.A.). The probable error of this mean found from the residuals for the seven determinations is ±0.04 A.

II. WAVE-LENGTHS

In comparing the observed coronal lines with the spectrum of argon, Freeman has admitted the very wide tolerance of accepting a coincidence if the wave-numbers agree within 5 units. The corresponding difference of wave-length ranges from 0.5 A at λ 3200 to 2 A at λ 6400. Within these limits he finds that twelve coronal lines coincide with lines of argon which Meissner[1] has classified as members of series in the arc spectrum, and six more with lines observed by him but not classified. Four other lines agree with lines of the "blue" (spark) spectrum of argon given in Kayser's *Handbuch;* and ten are identified as due to transitions between terms of Meissner's table, which do not lead to lines observed in the laboratory.

Two very serious objections may be made to these identifications: the limits of tolerance are far too wide, and the coincidences, such as they are, are with weak argon lines, while stronger lines, which are physically related to the lines in question, are absent.

"Coincidences" within such wide limits must often happen by chance. This is discussed in detail below (sec. iv); but all working spectroscopists will recognize that no decisive results can be obtained from comparisons with a rich spectrum like that of argon, unless greater accuracy is available. For the fainter coronal lines, the measures are so poor that no definite identification is at present possible. For the eight well-observed lines mentioned above, the agreement, if the lines are really due to argon, should be within 0.1 A. The facts are as shown in Table I. One of the eight lines has no argon line near it. For five more, the residuals are greater than for any one of one hundred and ten lines in the flash spectrum photographed with the same instrument two minutes earlier. One of the two remaining lines coincides with a very faint line in the spark spectrum of argon; the last agrees tolerably with two different predicted lines, neither of which has ever been observed.

---

[1] *Zeitschrift für Physik*, **39**, 172, 1926, and **40**, 839, 1927.

This is an extremely unfavorable showing and casts the gravest doubt upon the identification of argon in the corona.

TABLE I

WELL-OBSERVED CORONAL LINES

CORONAL LINES		ARGON LINES		Δλ	SOURCE
Intensity	λ I.A.	λ I.A.	Intensity		
20	3387.96	3388.35	5	−0.39	Meissner
5	3454.13	3454.94	5	− .81	Meissner
9	3600.97	3600.95	1	+ .02	Eder
3	3642.87	3643.09	8	− .22	Meissner
4	3800.27	3801.04	...	− .77	Predicted
10	3986.88	...	...	...	...
8	4086.29	4085.49	...	+ .80	Predicted
20	5302.95	5302.84	...	+ .13	Predicted
...	...	5302.96	...	−0.01	Predicted

III. INTENSITIES AND SERIES RELATIONS

The line-intensities lead to similar conclusions. For the six argon lines of type 1s − mp (or mx) which Freeman identifies with coronal lines, the intensities range from 4 to 10 on Meissner's scale. Within the same region (λ 3359-λ 3864) there are fifteen other lines, corresponding to transitions of the same type, and of intensities ranging from 10 to 50, which do not appear in the corona. The six lines of type 2p − ms (or md) which are supposed to appear in the corona have intensities between 0 and 10. Within the same region (λ 4586-λ 5597) there are twenty-three similar lines of intensity 10–20, and three lines of type 1s − mp with intensities 90 and 100, all of which fail in the corona. Finally, the six faint "coronal" lines recorded by Meissner, but not classified, have intensities from 0 to 5, while not one of ten lines of intensity 100 in the same region (λ 3950-λ 4300) appears! To cap the climax, two of these strong lines (λ 4044.419 and λ 4272.169; $1s_4-3p_3$ and $1s_4-3p_7$) are early members of series whose later and fainter members are supposed to be present (λ 3461.07 and λ 3388.35; $1s_4-4p_3$, $1s_4-5p_7$).

If the coronal lines were really due to argon, it would follow that a few faint members of certain series were excited, while far stronger lines of similar series, or even of the same series, failed to appear. Such erratic behavior, under solar conditions, is quite incredible. It is true that under very special conditions certain lines in a spectrum may be excited without others—for example, when the gas is stimulated to resonance by a few artificially selected wavelengths, as in Wood's experiments on mercury vapor. But, in the vicinity of the sun, excitation, whether by radiation or by collisions, must be distributed indiscriminately over a wide range of energy, and no such selective influence can occur. Even if it did, it could hardly pick out individual lines in the fashion suggested. For example, for each of the recorded lines $1s - mp$ there are two or three other lines, corresponding to transitions downward from the same excited level. However an atom of argon gets into this state, it may be expected to emit all these lines; yet the others are not recorded, though many of them are stronger than the ones which are supposed to appear.

The predicted lines remain to be discussed. Eight of them suppose transitions of the type $1s - md$ or $1s - ms'$—that is, between atomic configurations in which the excited electron is in a 4s "orbit" and a 3d—which are of the "forbidden" type. The other three transitions escape this objection; but two of them violate the inner-quantum rule, $2p_5 - 7s_1''$, involving a jump from 0 to 2, and $2p_5 - 9d_4'$ from 0 to 4 (!). Forbidden transitions may give strong lines, when the upper state involved is metastable, as in the nebulae, but such transitions from highly excited states which are not metastable have been observed only in sources where the emitting electrons are subject to strong electric fields (many thousands of volts per centimeter), and are utterly unlikely in the corona.

The only permitted line is $2p_4 - 9s_4$, which agrees fairly well with the green coronal line. But the series $2p_4 - ms_4$ is a faint one—the observed intensities for $m = 4, 5, 6, 7$ being 4, 0, 0, 0 (the last a blend with another and probably stronger line), while $m = 8$ has not been observed. There can be no chance that $m = 9$ gives a strong line.

Finally, four coronal lines (λλ 3237, 3505, 3601, 4130) are identified by Freeman with lines of the "blue" or spark spectrum of argon. These lines are faint, intensities 1–3, and their laboratory wavelengths are none too good. Many strong spark lines in the same region are absent.

It may finally be remarked that, if argon were present in the corona, it should occur in greater abundance in the chromosphere, where its lines should appear, especially the very strong ones in the red and the violet. No trace of them has been found.

In view of this cumulative evidence, there appears to be no escape from the conclusion that the coronal lines are not due to argon, and that the rough coincidences of wave-length noted by Freeman are accidental.

IV. PROBABILITY OF ACCIDENTAL COINCIDENCES

A discussion of the probability of chance agreement is next in order. Freeman states[1] that he has investigated this, and finds that there is but one chance in a thousand that the relations which he has found are accidental. He gives no details. We are unable to verify his results, and our conclusions regarding probability differ radically from his.

It is simplest to go back to first principles. Suppose that a given spectrum contains M lines within an interval of X units of frequency. What is the probability that a wave-number chosen at random within the range X shall lie within x units of one or more of the spectral lines?

Consider any one line in the real spectrum. The arbitrary "line" will meet the condition if it lies within a strip of width $2x$ units, centered on the real line. The probability that this will happen is $2x/X$, and that it will not happen, $1-2x/X$. The probability that the "coincidence" will fail for all the M lines is $(1-2x/X)^M$, and the complementary probability that it will happen is

$$p=1-\left(1-\frac{2x}{X}\right)^M . \tag{1}$$

For small values of x, this gives approximately $p=2Mx/X$; but this value is too great, since it ignores the probable overlapping of the strips centered on different spectral lines.

If now we start not with one, but with N arbitrarily chosen wave-numbers, the probability p will be the same for each. The average number C of chance coincidences within the limit x which is to be expected in a large number of trials will be given by $C=pN$.

---

[1] *Op. cit.*, p. 185.

If I is the average interval between the spectral lines, then $X = MI$, and

$$C = N\left\{1-\left(1-\frac{2x}{IM}\right)^M\right\} = N\left(1-e^{-\frac{2x}{I}}\right) . \qquad (2)$$

The latter value, which is the limit of the preceding expression when M is great, is a sufficient approximation in practice.

In the case of the coronal lines, Dr. Freeman finds the average interval between each identified line and the next adjacent argon line on each side to be 30 wave-numbers. This is then the average value of I for the part of the argon spectrum under consideration. With $N=45$, $x=5$, equation (2) gives $C=12.9$. Thirteen coincidences of coronal and argon lines, within the assigned limits of error, might be expected as a result of chance.

In individual cases deviations from the mean value are to be expected, on account of the error of random sampling. If p is the probability that a given event will happen in one trial, the probability q that it will occur r times out of N trials is given by the equation[1]

$$q = \frac{1}{\sqrt{2\pi p(1-p)N}} e^{-\frac{(r-pN)^2}{2Np(1-p)}} . \qquad (3)$$

That is, the individual values found in a large number of trials will be distributed about the mean value Np with a standard deviation given by the equation

$$\sigma^2 = Np(1-p) .$$

In the present case, $N=45$, $p=0.29$, and $\sigma = \pm 3.0$. The corresponding probable error is 2.2, so that we may state the chance expectation more precisely as 12.9 ± 2.2 coincidences. The observed number (for lines of the arc spectrum) is 18. The difference is hardly significant. The average residual in the case of accidental coincidences may readily be calculated. By (1) and (2) the probability that an arbitrarily chosen wave-number will be within the limits x and $x+dx$ from the nearest spectral line is

$$dp = \frac{2}{I} e^{-\frac{2x}{I}} dx .$$

---

[1] Burnside, *Theory of Probability*, p. 44, 1928.

The mean value of the distance, for all cases in which it is less than x, will be

$$\bar{x}=\frac{1}{p}\int_0^x x\,dp=\frac{I}{2}-\frac{xe^{-\frac{2x}{I}}}{1-e^{-\frac{2x}{I}}}=\frac{x}{2}\left(1-\frac{x}{3I}+\frac{x^3}{45I^3}\cdots\right). \qquad (4)$$

Substituting $I=30$, $x=5$, we find $x=2.36$. The observed residual, regardless of sign, is ±2.1—a good agreement.

The approximately equal numbers of positive and negative residuals, which Freeman takes as evidence that they represent the accidental errors of observation, are of course equally well explained by chance.

It appears, therefore, that the coincidences between the coronal lines and those of the arc spectrum of argon are of substantially the character which should be found if they are of accidental origin. This may be tested further by considering the numbers of coincidences within closer limits. For the eighteen arc lines in Freeman's Table II, the observed distribution of the residuals, without regard to sign, and that to be expected by chance, are as follows:

	Observed	Computed
0	4	1.3
1	4	3.0
2	3	2.7
3	2	2.5
4	3	2.2
5	2	1.2
Total	18	12.9

In computing the chance distribution from (2), it is assumed that all residuals less than 0.5 are recorded as "0," those between 0.5 and 1.5 as "1," and so on, except that "5" means residuals between 4.5 and 5.0.

On the face of this evidence, there might be some real coincidences among the lines with residuals of 0 or 1. These lines are as follows:

RESIDUAL 0

	Corona	Argon	Notes
3461	Faint	(10)	$Ti+$
5073	Faint	(8)	$Ti+$
5118	Faint	(6)	....
5597.5	Faint	(10)	....

	Residual ± 1		
3328.1	Fairly strong	(1)	*Ti*+
3455	Strong	(5)	Coronal line
4241	Faint	(0)	....
5433.4	Rather faint	(0)	....

The only strong coronal line among the eight shows an altogether inadmissible residual, according to the measures of Davidson and Stratton (Table I). Three of the others are identified by these observers as chromospheric lines of *Ti*+. The remaining four are all faint in the corona, and our physical arguments apply to them with full force.

The four lines which are identified with argon spark lines must be considered separately since this is a quite independent spectrum. They lie between wave-numbers 31,000 and 24,000. Within this region there are one hundred and twenty-three arc lines in Meissner's lists and two hundred and forty-three spark lines in Kayser's *Handbuch.* The number of chance coincidences should therefore be greater than for the arc. Within this region Freeman gives six coincidences with arc lines. There are ten coincidences with spark lines, within his limits, but when there is also agreement with an actual or predicted arc line, he prefers the latter. Here again the agreement is evidently due to chance.

In view of the importance of the conclusion that the observed agreements are accidental, we have tested the matter further in a way which takes into account the unequal density of distribution of the argon lines in different regions of the spectrum. The whole observed range has been divided into intervals of 1000 wave-numbers and formula (2) applied to each interval successively (the factor $1-2x/X$ having now the fixed value 0.99). The results are given in Table II. The sum of the resulting values of C gives the whole number of coincidences to be anticipated as 13.6, slightly greater than that of the simpler approximation.

It should be noticed that the numbers of observed coincidences rise and fall in striking parallelism with the predicted values—which is further evidence of their accidental origin.

To find the probability of coincidences between the coronal and predicted argon lines, the whole number of differences between

Meissner's terms which fall between given limits was calculated. By subtracting the number of observed series lines between these limits, the number of possible predicted lines between these limits was found. By proceeding as in Table I and considering those coronal lines which had not already been identified with arc lines of argon, the whole number of coincidences which might be expected by accident was found to be 11.17. The observed number is 10. Here less is found than should usually appear by chance.

TABLE II

CALCULATED NUMBER OF COINCIDENCES BETWEEN CORONAL AND ARGON LINES ALLOWING TOLERANCE OF 5 FREQUENCY UNITS

Frequency Range	*M* Number Argon Lines	*p* Probability of Coincidence per Line	*N* Number Coronal Lines	*C* Probable Number of Coincidences	Observed
15,000 16,000	32	0.28	1	0.28	0
17,000	57	.44	0	0.00	0
18,000	67	.49	2	0.98	1
19,000	94	.61	5	3.05	2
20,000	92	.60	2	1.20	2
21,000	77	.54	1	0.54	1
22,000	44	.36	4	1.44	2
23,000	32	.28	3	0.84	0
24,000	31	.27	4	1.08	3
25,000	7	.07	2	0.14	0
26,000	8	.08	3	0.24	1
27,000	5	.05	1	0.05	0
28,000	18	.17	6	1.02	1
29,000	20	.18	4	0.72	2
30,000	26	.23	2	0.46	2
31,000	39	.32	3	0.96	1
32,000	34	0.28	2	0.56	0
Total..	....	....	....	13.56	18

V. FURTHER TESTS OF PROBABILITY

To test still further the validity of equation (2) we have taken other sets of numbers by modifying the coronal wave-numbers in various ways—first, by adding or subtracting arbitrary amounts, and then by substituting, for the last two or three figures of the coronal data, figures obtained by putting a pencil down blindly on a table of logarithms. The latter test was repeated twenty-five times to secure statistically significant results. The results are given in Table III.

TABLE III

Coincidences of Argon Lines with 45 Arbitrarily Selected Wave-Numbers

	Number of Coincidences	Average Deviation		Number	Average Deviation	Number	Average Deviation
Corona.........	18	2.2	Corona with last three figures at random....	10	1.9	15	2.3
Corona −100...	17	2.1		11	2.4	15	1.9
Corona +100...	17	2.4		13	2.0	10	2.4
Corona −10*N*...	14	1.7		16	3.0	14	1.8
Corona +10*N*...	13	2.2		16	2.4	13	2.2
Last two figures at random.....	13	1.8		15	2.1	14	1.9
	19	2.3		14	3.3	15	2.9
	9	2.9		12	2.1	16	2.9
	15	2.5		14	2.1	10	2.5
	17	2.1		12	2.4	10	2.3

N denotes the serial number of the line in the list.

For the shifts of one hundred wave-numbers, which destroy all the physical significance of the data, the number of coincidences is only one less than for the coronal lines themselves.

TABLE IV

Number of Coincidences with Random "Lines" in 25 Trials

No. of Coincidences	Calculated Expectation	Observed in 25 Trials	No. of Coincidences	Calculated Expectation	Observed in 25 Trials
7.............	0.3	0	15.............	2.9	5
8.............	0.7	0	16.............	2.3	3
9.............	1.1	1	17.............	1.7	1
10.............	1.7	4	18.............	1.1	0
11.............	2.3	1	19.............	0.7	1
12.............	2.9	2	20.............	0.3	0
13.............	3.2	3	21.............	0.2	0
14.............	3.2	4	22.............	0.1	0

For the twenty-five cases in which the last figures are purely arbitrary, the mean number of coincidences is 13.52, as against 13.56 calculated in Table II. The average deviation of these arbitrary numbers from the argon lines, for the whole series, is ±2.34, while equation (4) gives 2.36, if applied to the data as a whole with

$2x/I=1/3$, and 2.27, if applied to successive intervals, as in Table II.

The distribution of the number of coincidences actually found in the various trials compares with that predicted by formula (3) as indicated in Table IV.

The agreement is good. The standard deviation from the mean, 13.5, is ±2.5—less than the predicted value 3.0; but the probable error of determination of the standard deviation from n observations is $0.675\sigma/\sqrt{2n}$, or ±0.40 in this case, so that the difference is not significant. This empirical test therefore confirms the theoretical formulae at all points.

VI. CONCLUSION

The result of the present investigation is definite. The number of coincidences between the coronal lines and those of argon is very little greater than would usually occur by chance, within the very wide limits of error which have been adopted, and is no greater than has been found, in a moderate number of trials, with "lines" chosen quite at random. So far as considerations of probability go, a small fraction of the apparent coincidences might be real; but the total absence of all the stronger and more characteristic lines of argon from the corona settles the question in the negative. For the well-measured coronal lines, moreover, the discordance of wave-lengths alone puts the identifications out of court. When critically considered, therefore, there is no spectroscopic evidence of the presence of argon in the corona, or, for that matter, elsewhere in the sun.

The coronal spectrum remains a mystery. A careful search by one of us (I. S. B.), to be reported elsewhere, has revealed no coincidences with forbidden lines of other elements—a fact which is probably explained by the intensity of radiative excitation as suggested by Eddington,[1] and we have at present no solution of the riddle to offer.

In conclusion we desire to impress upon observers of coming eclipses the great importance of observations for the definite discrimination between coronal and chromospheric lines, and of precise determinations of wave-length for the latter with slit-spectrographs. Without such data a positive identification of most of the coronal lines is hardly possible.

---

[1] *Monthly Notices, R.A.S.*, 88, 134, 1927.

Carnegie Institution of Washington
Mount Wilson Observatory
California Institute of Technology
December 31, 1928

Contributions from the Mount Wilson Observatory, No. 376
Reprinted from the *Astrophysical Journal*, Vol. LXIX, pp. 103–158, 1929
Printed in the U.S.A.

A SPIRAL NEBULA AS A STELLAR SYSTEM, MESSIER 31

By EDWIN HUBBLE

ABSTRACT

Material.—The present discussion of M 31 is *based on the study of about 350 photographs* taken with the 60- and 100-inch reflectors, distributed over an interval of about eighteen years. Two-thirds of the total number were obtained by the writer during the five years 1923–1928. Since the image of the nebula is much larger than the usable fields of the telescopes, *attention was concentrated on four regions centered* on (1) the nucleus, (2) 23′ north following, (3) 17′ south, (4) 48′ south preceding the nucleus. The combined *area*, with allowance for overlapping, *represents about 40 per cent of the entire nebula.*

Resolution.—The *outer regions* of the spiral arms are *partially resolved into swarms of faint stars*, while the *nuclear* region *shows no* indications of *resolution under any conditions* with the 100-inch reflector. Intermediate regions show isolated patches where resolution is pronounced or suggested.

Variables.—*Fifty variables* have been found, nearly all in the outer regions where resolution is pronounced. The *survey* is believed to be *fairly exhaustive in the four selected regions down to 19.0 photographic magnitude.*

Cepheids.—*Forty* of the *variables* are *known to be Cepheids* with periods from *48 days to 10 days* and *maxima from 18.1 to 19.3 photographic magnitude;* one exceptional star varies from 17.9 to 19.2 in a period of 175 days. The *period-luminosity relation is conspicuous*, and the slope is *approximately that* found among *Cepheids in other extra-galactic systems.*

Distance of M 31 derived from Cepheid criteria.—Comparisons of period-luminosity diagrams indicate that M 31 is about 0.1 mag. or 5 per cent more distant than M 33, and about 8.5 times more distant than the Small Magellanic Cloud. Using Shapley's value for the Cloud, we find the *distance of M 31* to be *275,000 parsecs.*

Variables other than Cepheids.—Of the 10 remaining variables, 4 are probably very faint Cepheids for which the data are insufficient to establish the characteristics, and 6 are irregular or long-period variables. The latter group includes the brightest variables in the nebula.

Novae.—*Sixty-three novae have been found by the writer*, which, together with the 22 previously observed, gives a *total of 85 observed photographically* which are now *available* for *statistical investigation*. The novae exhibit a striking similarity in their behavior, and the *mean light-curve is of the same general character as that for galactic novae.* The frequency distribution of magnitudes at maxima can be represented by an error-curve with a maximum at about 16.5 ($M=-5.7$ for the distance indicated by the Cepheids) and a probable error for a single nova of about 0.5 mag. Selective effects appear to be unimportant, and a restricted range of about 4 mag. seems to be established.

Novae are most frequent in the nuclear region, and, in a general way, their distribution follows that of the luminosity in the nebula. Position in the nebula appears to have no effect on the luminosity of novae. It is *estimated* that *novae appear at the rate of about 30 per year.*

Brighter non-variable stars.—Preliminary surveys suggest that few stars in M 31 are brighter than $M=-6$ (distance, that indicated by the Cepheids) and that large numbers are to be found only for M fainter than -5. A study of the open cluster N.G.C. 206, involved in M 31, indicates that the average color-index of the brighter stars is of the order $+0.3$ or $+0.4$ mag.

Mass and luminosity densities in M 31.—The mass density of M 31 appears to be of the order of one sun per 20 cubic parsecs, and the luminosity density, about 9.0 mag. per

cubic parsec. With the sun as unit, $Mass = 5.5L$. These values are of the *same order as those for the galactic system* in the neighborhood of the sun. As the nucleus is approached, the coefficient of the mass-luminosity relation decreases until, for the nucleus itself (diameter about 4 parsecs), it falls below 0.001.

Relative dimensions of M 31 and the galactic system.—A tentative comparison of sizes, masses, luminosities, and densities suggests that the *galactic system is much larger than M 31* but that the ratio is not greater than that between M 31 and other known extra-galactic systems.

Messier 31, the great nebula in Andromeda, is the most conspicuous of all the spirals and the only one which can be seen easily with the naked eye. It appears as a hazy patch about 30′ by 15′, somewhat brighter in the center, with a total luminosity variously estimated as from the fourth to the fifth magnitude. The object is listed as a nebula in the tenth-century star catalogue of Al-Sufi, and appears on some of the pre-telescopic star charts. It was first examined with a telescope in 1612 by Marius, who gave the famous description, "like a candle seen through a horn." Of the many subsequent drawings and descriptions that were based on visual observations, the most notable are those by Bond and by Trouvelot.

In 1885 interest in the nebula was stimulated by the appearance very close to the nucleus, of a nova, which reached the eighth magnitude. Two years later the photographs made by Isaac Roberts with his 20-inch reflector showed for the first time the main pattern of the spiral structure. Ranyard reproduced one of Roberts' photographs in *Knowledge* for February, 1889, and the article which accompanied it was the best discussion of a spiral nebula which had appeared up to that date.[1] Among other things he mentioned the numerous stars in the outer regions of the nebula, the significance of which was not fully appreciated until many years later.

Early visual observers of the spectrum reported bright lines on a continuous background. In 1899, however, Scheiner[2] photographed the now familiar solar-type absorption spectrum and announced emphatically that the nebula must be a system of stars. Radial velocities of the order of -300 km/sec. have since been measured by several observers. The inclination of the lines which appears when the slit is oriented along the major axis, first reported by Slipher, was measured by Pease[1] in 1917. The linear velocity of rotation as indicated by the measures is of the order of 0.48x km/sec., where x is the distance from the nucleus in seconds of arc. The measures extend to about 150″ from the nucleus, and the rotation is in the sense that the south preceding end of the nebula is approaching us relative to the nucleus.

---

[1] This first reproduction was from a drawing copied from the negative. The same volume, however, contains two photographic reproductions, the later of which, in the August number, is exceptionally good.

[2] *Astrophysical Journal*, **9**, 149, 1899.

Ritchey,[2] in 1917, discovered two faint novae on his earlier photographs of M 31, and since then the observers at Mount Wilson, following the nebula for the purpose, have found eighty-three others. In the course of this work the writer, in 1923, found two faint variable stars which further investigation proved to be Cepheids with periods of twenty and thirty-one days, respectively. About the same time, photographs centered along the outer arms of the spiral revealed a high degree of resolution into individual stars (Plate I), which was entirely lacking in the nuclear region where previous plates had been centered. This opened a new field for investigation—the study of individual stars involved in a spiral nebula—which has been developed primarily by means of the 100-inch reflector.

Thus far some fifty variables have been found in M 31, and forty of them are known to be Cepheids. The period-luminosity relation is conspicuous among the Cepheids, hence the distance of the spiral is determined with considerable accuracy in terms of the distance of the Magellanic Clouds. Shapley's value for the zero point of the period-luminosity relation leads to a provisional value for the absolute distance.

The stars in M 31, including the novae and the Cepheids, are so closely comparable with those in the neighboring spiral, M 33, that the two systems may be combined for a general discussion. The considerable numerical data resulting from this combination, together with the consistency of the various independent criteria, confirm the general order of the distances derived from the Cepheids and suggest no revision of Shapley's value for the zero point of the period-luminosity relation. The data for M 33 have already been published,[3] and will be used freely in the present discussion of M 31.

---

[1] *Proceedings of the National Academy of Sciences*, **4**, 21, 1918.

[2] *Publications of the Astronomical Society of the Pacific*, **29**, 210, 1917.

[3] *Mt. Wilson Contr.*, No. 310; *Astrophysical Journal*, **63**, 236, 1926.

VARIABLE STARS

M 31 is an intermediate-type spiral, Sb in the writer's classification,[1] with its equatorial plane inclined about 15° to the line of sight. The unresolved nuclear region is about $30' \times 10'$, and the maximum extension of the arms, on long exposures, is about $160' \times 40'$. The arms exhibit considerable resolution, and there are patches, especially in the south preceding end, where the stars fairly swarm on the photographic plates.

Fifty variables have been found among the stars scattered over the image of the spiral, and most of these undoubtedly belong to the nebula. The search is believed to be fairly exhaustive, down to 19.0 photographic magnitude, in four regions of the nebula, centered as follows:

Region 1. The nucleus
2. 23′ north following the nucleus
3. 17′ south of the nucleus
4. 48′ south preceding the nucleus

The usable fields around these centers have radii of from 12′ to 15′, and the combined area, with allowance for overlap in Regions 1–3, represents about 40 per cent of the entire nebula.

For the central region and for the brighter stars in the adjacent regions as well, some two hundred and seventy plates covering a period of eighteen years are available. A series of ten photographs by Ritchey in the autumn of 1909 is followed by a gap of eight years during which only three usable plates were obtained, but from 1917 on the material is fairly well distributed. Previous to 1920 the plates were all obtained with the 60-inch reflector; since then the 60- and the 100-inch have been used indiscriminately. The exposures and seeing conditions vary widely since many of the plates were obtained in the search for the relatively bright novae. The better photographs represent average exposures of about sixty minutes with the 60-inch reflector and thirty to forty minutes with the 100-inch, although occasional plates were exposed up to five hours or more. In general, fast plates were used throughout.

The photographs centered on Regions 2, 3, and 4 represent exposures of seventy-five to ninety minutes with the 100-inch reflector and, in general, are of a rather better quality. The variables in Regions 2 and 3 have been followed consistently only since 1924, but some of them are found on the larger and longer-exposed plates of the earlier series. The season 1924–1925 is especially well represented. Two series of fifteen and ten consecutive nights, respectively, during which the observing conditions were uniformly excellent, indicated immediately the general nature of the light-curves of many of the variables, and suggested periods which were confirmed by reference to earlier plates. Variables Nos. 5 and 10, with about sixty-five observations each, are the least well observed.

---

[1] *Mt. Wilson Contr.*, No. 324; *Astrophysical Journal*, **64**, 321, 1926.

Some seventy-five plates of Region 4 have been assembled, representing exposures on about sixty different nights. The material appears to be rather scanty, but, in this region as well as in the others, each variable for which a period has been determined has been followed for at least one complete season after the determination, and in no case has this test led to a radical revision. Periods close to an even day, or submultiple of a day, have been definitely eliminated by sets of plates obtained on single nights. In all, about twenty such sets were made, often on successive nights, representing intervals ranging from two to nine hours.

Sequences of comparison stars with steps averaging about 0.2 mag. were selected for each variable and were calibrated by some sixteen comparisons with Selected Areas 20, 21, 44, and 45. The magnitudes are all photographic. The unpublished magnitudes of stars in the Selected Areas, available through the kindness of Mr. Seares, extend to about 18.5. Fainter magnitudes are extrapolations; but to 19.0 they are believed to be of the same accuracy as the fainter stars of the Selected Areas. From 19.0 to 20.0 the extrapolations must be considered as increasingly unreliable, although the results from the various plates are in substantial agreement. In the case of a few variables, notably Nos. 3 and 4, the background of nebulosity is so dense that the measures are very uncertain even for the brighter stars.

The magnitudes of the variables, estimated to the nearest tenth by comparison with the sequences, are believed to be fairly trustworthy (except where the plates were exposed under poor conditions) over the brighter portion of the light-curves. The minima, however,

TABLE I

VARIABLES IN M 31, CENTRAL REGION

J.D.*	Plate†	Qy.	1‖	2	3	4	5§	6	7	8	9
8562.7‡	R18	F	19.0	19.1+	18.6	19.3+	18.8+	......	18.9	19.5	......
8563.5‡	20	G	19.15	19.2	18.85	19.7	18.9+	18.7	18.9	19.6	......
8565.5	26	G	19.15	18.6	18.9	19.7	19.1+	18.9	19.0	19.7	19.3
8566.6	27	F	19.0+	18.6	18.9	19.4+	18.8+	18.7	18.9	19.7	......
8591.5	34	G	19.05	19.3	18.9	19.6	18.9	18.6	18.4	19.5	19.4
8593.4	39	G	19.1	19.2	19.3	19.1	18.7	18.9	18.4	19.2	19.4
8885.6	108	G	19.3	19.0	18.4	19.1	......	19.5	18.95	19.7	......
0720.5	121	E	18.35	19.1	18.4	19.1	......	19.0	18.85	20.0	......
0781.5	122	E	18.25	19.1	19.3	19.0	......	19.6	18.2	19.3	......
1462.6	P300	F	19.2+	18.8	19.2+	19.1	......	......	18.2	19.5	......
1483.5	Sh3991	P	18.7+	19.0+	......	......	......	19.0	18.7	......	......
1489.5	R146	G	19.3	19.1+	19.2+	19.4+	......	19.4+	18.8	19.0	......
1518.5	147	F	19.3	18.6	......	......	......	......	18.7	......	......
1547.5	151	G	19.2	19.1+	19.3+	19.4	......	18.7	18.1	19.5	......
1575.4	154	G	19.1	19.1+	19.2+	19.5+	......	19.5	19.0	19.5	......
1576.4	156	G	19.2	19.15	19.4	19.5+	......	19.5	18.8	19.3	......
1609.3	161	G	19.3	19.4	19.4	19.2	......	18.9	18.7	19.6	......
1634.3	162	P	18.8+	19.1+	19.2+	19.3+	......	18.6	18.5	19.4	......
1635.3	163	P	18.8+	......	19.2+	......	......	18.7	18.4	19.4	......
1781.6	D2	P	18.6+	18.9	19.1	......	......	......	18.3	......	......
1782.6	5	P	18.2	18.8	......	......	......	......	......	......	......
1783.6	9	P	18.2	18.9	......	......	......	......	......	......	......
1811.3‡	11	P	19.0+	19.0+	......	19.0	......	18.65	18.85	19.3	......
2104.7	Sh4934	P	18.6	18.8	......	......	......	......	......	......	......
2161.6	4978	F	18.25	18.7	......	19.1	......	......	18.8	......	......
2163.6	5025	F	18.6	18.5	......	19.3	......	......	18.8	19.0	......
2168.6	D24	P	18.85	19.2+	......	......	......	18.7	......	......	......
2169.6	27	F	19.0	19.1	19.4+	19.5+	......	18.8	18.9	19.5+	......
2195.5	30	F	18.6	19.1+	19.3+	19.5+	......	18.8	18.6	19.3+	......
2223.5	Sh5054	P	18.3	18.7	......	19.0	......	......	......	......	......
2263.4	5117	G	19.0	18.8	19.1	19.3	......	......	18.7	19.6	18.9
2311.3	5149	F	19.0+	19.2	......	......	......	......	18.4	19.4	......
2314.3	5160	G	19.0	19.2+	18.4	......	......	19.5	18.1	19.6	19.2+
2317.3	Hg2	G	18.25	19.3+	......	......	......	......	18.2	......	18.2
2521.6	D37	P	18.8+	19.2+	19.2+	19.4+	......	18.6	19.0	19.2	......
2545.6	Sh5189	F	18.9	19.0	......	......	......	18.6	18.2	......	18.2
2547.6‡	D42	F	19.1	19.2	19.4+	19.7	18.55	18.6	18.3	......	18.4
2548.6	44	E	19.15	19.2	19.7	19.7	18.5	18.7	18.3	19.8	18.4
2580.5	62	F	19.15	19.1+	19.3+	19.4	......	19.6	18.6	19.5	......
2581.6	65	P	......	18.8+	19.2+	......	......	......	18.4	19.4+	......
2584.4	70	F	19.2	18.7	18.4	19.5+	19.0+	19.6	18.1	......	18.8
2585.0‡	71	G	19.4	18.7	18.4	19.6+	19.3+	19.6	18.1	19.7	18.8
2585.3	72	P	19.2	18.8	......	......	19.0+	......	18.1	......	18.9
2608.5	76	F	18.9	19.2	19.2+	19.4+	......	19.3+	18.9	19.0	......
2609.6	80	P	18.8+	18.9+	19.4	......	......	18.7	18.9	19.2	......
2612.3	S68	F	19.1	19.1+	18.3	19.3+	......	18.7	18.8	19.3	......
2641.6	75	F	19.1	19.2+	19.1	......	......	......	18.6	19.2	......
2642.5	77	G	19.1	19.0	18.6	19.6	......	......	......	19.1	......
2669.3‡	D106	F	18.8	18.9+	18.9	19.4+	......	......	18.6	19.5	......
2694.3‡	118	G	18.2	19.2+	18.65	19.5+	......	......	18.6	19.4	......
2695.3	122	F	18.3	19.1+	18.9	19.5	......	......	18.9	19.1	......
2698.4‡	131	F	18.5	19.1+	19.1	19.2	......	19.2+	18.85	19.05	......
2903.4‡	200	P	18.8+	18.8+	......	19.0	......	18.8	18.2	......	......
2935.5	H150	E	......	......	......	......	18.8	......	......	......	......
3029.4	A10	F	19.3	19.1	19.5	19.2	......	......	18.8	19.4+	......
3256.6	29	P	19.1	19.1+	19.4	19.2	......	18.7	18.7	19.6+	......
3258.7	B51	F	18.2	19.0+	......	......	......	18.8	......	......	......
3259.6	56	P	18.2	19.0+	18.6	......	......	18.8	......	......	......
3260.7	S156	P	18.25	18.7+	18.4	......	......	......	18.1	......	......
3264.6	D222	P	18.6	19.0+	......	......	......	......	18.3	19.0	......

TABLE I

Variables in M 31, Central Region

J.D.	10§	11	12	13	14	15	16	17	18	19
8562.7‡	......	......	......	......	......	17.5	......	......	......	16.0
8563.5‡	19.0+	......	......	......	......	17.5	......	19.35	......	16.0
8565.5	19.3	19.5+	19.5+	19.3	......	17.5	......	19.0	......	16.0
8566.6	......	......	19.3+	19.3	......	17.5	19.5+	18.8	19.7+	16.0
8591.5	19.2+	19.5	19.5	19.5	19.8	17.6	19.3	19.9	19.9	16.0
8593.4	19.2+	......	......	19.8	......	17.6	19.3	19.9	19.2	15.9
8885.6	......	19.5+	19.1	19.7+	......	17.5	19.3	19.1	19.7+	15.85
0720.5	......	19.5	19.8+	19.5	19.7	17.4	18.8	19.7	19.9+	15.3
0781.5	......	19.3	......	19.1	18.9	17.3	18.5	18.9	19.2	15.3
1462.6	......	18.9	19.0	......	......	17.0	18.8	......	19.5+	15.8
1483.5	......	18.6	......	......	......	17.1	......	......	......	15.6
1489.5	......	18.5	19.2	......	......	17.0	......	......	......	15.6
1518.5	......	18.7	19.4+	19.4	19.6+	17.0	19.4	19.5	19.6+	15.5
1547.5	......	18.6	19.4+	19.5	......	16.9	......	......	19.6+	15.55
1575.4	......	18.6	19.15	19.6+	19.1	16.9	......	......	19.6+	15.6
1576.4	......	18.7	19.4	19.6+	19.0	16.9	......	19.9	19.6+	15.6
1609.3	......	19.0	......	19.4	19.3	16.9	19.5+	19.1	19.6+	15.7
1634.3	......	19.2	......	......	......	16.8	19.1	......	19.3	15.7
1635.3	......	19.1	......	......	......	17.0	18.9	......	19.2	15.8
1781.6	......	......	......	......	......	......	......	......	......	16.15
1782.6	......	......	......	......	......	17.1	......	......	......	16.2
1783.6	......	......	......	......	......	16.9	......	......	......	16.1
1811.3‡	......	19.2	......	......	......	17.0	......	......	......	16.15
2104.7	......	......	......	......	......	17.1	......	......	......	16.2
2161.6	......	......	......	19.5+	19.5	17.2	18.9	......	......	16.3
2163.6	......	......	......	......	......	17.1	18.8	19.6+	......	16.3
2168.6	......	......	......	......	......	16.8	......	......	......	16.2
2169.6	......	19.3	......	......	......	......	19.4	18.9	19.6	16.2
2195.5	......	19.2	19.1	19.6+	19.3	16.9	19.4+	......	19.5+	16.3
2223.5	......	......	......	......	......	17.1	......	......	......	16.4
2263.4	......	19.4	19.1	19.6+	19.0	17.0	19.4	18.9	19.3	16.2
2311.3	......	19.5	......	19.5+	......	17.1	......	......	......	16.2
2314.3	......	19.3	19.4+	19.5+	19.2	16.8	19.5+	19.6+	19.5+	16.2
2317.3	......	......	19.4+	19.6+	19.3	......	......	......	......	16.1
2521.6	......	19.2	......	19.5	......	16.8	......	......	......	15.6
2545.6	......	......	......	......	18.9	16.8	......	......	19.5	15.7
2547.6‡	18.8	19.3+	19.5+	19.7	19.3	16.9	19.45	19.15	19.7	15.7
2548.6	18.9	19.3	19.5	19.7	19.4	16.9	19.3	19.0	19.7	15.6
2580.5	......	......	......	......	18.9	......	19.3	19.3	19.3	15.5
2581.6	......	......	......	......	......	17.0	......	19.1	......	15.5
2584.4	10.2+	19.4+	19.5+	19.2	19.5	16.9	19.5	19.1	19.5	......
2585.0‡	19.4	19.3	19.8+	19.2	19.5	17.0	19.3	19.1	19.8	......
2585.3	19.2+	......	......	......	......	......	......	......	......	......
2608.5	......	......	......	19.4	......	......	19.3+	......	......	15.5
2609.6	......	......	......	......	......	16.9	......	......	......	15.4
2612.3	......	19.4	......	......	......	17.1	18.9	......	......	15.4
2641.6	......	......	......	......	......	17.0	......	......	......	15.4
2642.5	......	......	......	......	19.4+	17.1	......	......	19.6+	15.3
2669.3‡	......	......	......	......	18.9	17.0	......	......	......	15.4
2694.3‡	......	19.5+	19.3	19.5+	19.4+	16.8	19.1	19.1	19.4	15.4
2695.3	......	......	......	19.5+	19.4+	17.0	18.8	18.75	19.5	15.5
2698.4‡	......	......	19.2+	......	......	16.9	18.8	......	19.6	15.6
2903.4‡	......	......	......	......	......	16.8	......	......	......	15.3
2935.5	18.8	......	......	......	......	......	19.8+	19.8	19.7	15.3
3029.4	......	19.2+	......	......	19.6	......	18.9	......	19.5	15.3
3256.6	......	......	......	......	19.6	......	......	......	......	15.9
3258.7	......	......	......	......	......	......	......	18.7	......	16.0
3259.6	......	......	......	......	......	......	......	18.75	......	15.9
3260.7	......	......	......	......	......	16.8	......	......	......	15.85
3264.6	......	......	......	......	......	16.8	......	......	......	15.9

TABLE I—*Continued*

J.D.*	Plate†	Qy.	1‖	2	3	4	5§	6	7	8	9
3287.6........	B58	P	18.6+	18.6	18.6	......	......	......	......	19.2	......
3289.6........	62	P	18.25	18.9+	18.6	......	......	......	18.9	......	......
3317.7........	S172	F	18.9+	19.1+	18.7	......	......	......	18.4	18.9	......
3350.3........	A42	P	18.8+	18.7	......	......	......	......	......	......	......
3433.3........	B100	F	19.1	19.1	19.5	......	......	18.7	18.8	19.5+	......
3610.6........	126	F	18.5	19.0	18.6	......	......	......	18.9	19.3	......
3612.6........	131	P	19.0	19.2	......	......	......	......	19.0	......	......
3615.7........	A58	P	19.15	19.1+	......	......	......	......	18.8	......	......
3617.7........	S254	P	19.1	18.7+	18.9	......	......	......	18.5	19.4+	......
3639.7........	267	F	18.3	18.8+	......	......	......	19.1	18.6	18.9	......
3641.5........	S278	P	18.5	18.8+	18.5	......	......	......	......	19.2+	......
3698.6........	H335	G	18.3	19.4	19.4	19.7	......	......	......	19.7	......
3737.6........	339	G	18.85	19.2	19.5	19.7	......	19.6+	18.9	19.6	......
3765.45.......	348	F	18.5	19.2+	19.5	19.7	......	19.5	18.3	19.2	......
3768.4........	351	P	18.7	18.55	......	......	......	18.7	18.5	19.5	......
3789.3........	353	P	18.8+	18.6	......	......	......	18.6	......	19.3+	
3790.4........	S285	F	18.8	18.8	19.4+	19.1	......	18.6	......	19.5+	18.8
3791.4........	292	F	18.3	18.8	19.3+	19.0	......	18.5	......	19.6	18.9
3818.3........	301	F	19.3	19.1+	19.0	19.3+	......	......	18.55	19.2	18.4
3819.3........	310	F	19.1+	19.1+	19.1+	19.3+	......	......	18.65	19.3	18.5
3820.3........	320	F	19.1+	19.3	......	......	......	......	18.7	......	18.6
3821.3........	H355	G	19.1	19.1+	19.5	19.7	......	19.3	18.65	19.5	......
3822.3........	357	F	18.6	19.2+	19.6+	19.6	......	19.5	18.7	19.7	......
3823.3........	363	F	18.3	19.2+	19.6+	19.6+	......	19.5+	18.7	19.6	......
3843.3......	A73	P	......	......	......	......	......	......	......	......	......
3969.6‡.......	H376	P	......	18.7	18.8	......	18.9	......	......	......	......
3970.6........	381	F	......	......	......	19.3+	......	18.9	19.2	19.3+	19.4+
3971.6........	S329	P	19.2+	18.5	......	......	......	......	......	......	......
3990.6‡.......	336	P	......	18.6	18.4	......	......	......	......	......	......
3991.6........	338	G	19.3	18.85	18.7	......	19.4+	18.6	......	19.3	......
3993.6........	S339	G	19.3	18.95	18.9	......	19.4+	18.6	......	19.1	......
3994.6‡.......	343,4	F	19.4	19.0	19.1	19.3+	19.6	18.9	18.6	19.0	19.4
3995.6‡.......	348,9	G	19.4	19.2	18.9	19.2	19.5	18.8	18.6	19.15	19.3
3996.6‡.......	H384,5	E	19.4	19.4	19.3	19.0	19.3	18.9	18.7	19.3	19.4
3997.6‡.......	389,0	G	19.4	19.4	19.5	19.0	19.1	19.0	18.5	19.4+	19.4
3998.6‡.......	394,5	E	19.4	19.4	19.5	19.2	18.9	19.3	18.5	19.3+	19.4
3999.6‡.......	S350,1	G	19.4	19.4	19.5	......	18.6	19.1	18.7	......	19.4+
4000.6‡.......	H397	F	19.4	19.3	19.6	......	18.7	......	18.7	19.3+	19.4
4001.6‡.......	398	F	19.3	19.5	19.5	......	18.6	......	18.8	19.3+	19.4
4002.6‡.......	403,4	E	19.4	19.3+	19.55	19.4+	18.55	19.5	18.9	19.4+	......
4003.6‡.......	409,0	E	19.4	19.5	......	......	18.5	19.6	18.8	19.3+	19.4
4004.5‡.......	414,5	E	19.4	19.5	19.5	......	18.6	......	19.0	19.5+	19.5
4023.4........	B182	F	19.3	19.4+	19.4	......	19.3+	......	......	......	......
4024.5‡.......	D238,1	F	19.2	19.4+	19.25	19.3+	19.3	19.5	18.2	19.7	19.4
4025.5‡.......	243,6	F	19.4	19.4	19.3	19.7	19.3	19.5	18.1	19.5	19.3
4026.5‡.......	S353,6	F	19.3	19.5	19.3+	......	19.3	19.5	18.2	19.4+	19.3
4027.6‡.......	359,0	F	19.4	19.35	19.5	......	19.2+	19.7	18.2	18.9	19.4
4028.5........	H418	G	......	19.1	19.5+	19.6+	......	19.8	18.1	19.0	......
4029.4........	S361	F	19.1+	18.75	......	......	19.1+	......	......	......	......
4030.5........	362	F	......	18.6	......	......	......	19.7	18.25	19.1	19.4
4031.5‡.......	H420,1	G	19.1+	18.6	19.4	......	19.4	19.5	18.2	19.3	19.4
4032.5‡.......	424,6	G	19.3	18.9	19.6	19.7	19.2+	18.6	18.35	19.3	19.4+
4033.6‡.......	427,0	G	19.3+	19.05	19.7+	19.3+	19.3	18.75	18.3	19.5	19.4
4049.5‡.......	S366,0	F	18.8	18.6	18.7	......	18.6	19.4+	18.8	......	18.75
4050.5‡.......	372,4	F	18.9	18.55	19.1	......	18.6	19.7	18.8	19.4+	18.8
4054.6‡.......	H434	F	......	......	......	19.4+	......	......	18.9	19.4+	18.9
4055.6........	S376	G	19.2	19.15	19.3+	......	18.6	18.7	......	......	......
4056.6........	385	G	......	19.2	......	......	18.75	18.6	19.0	19.5+	19.1
4057.4........	388	G	19.3	19.3	19.7	19.0	18.7	18.6	19.1	19.6+	19.3
4059.4‡.......	H443,4	G	......	......	......	19.0	18.7	18.6	19.0	19.5+	19.3

TABLE I—*Continued*

J.D.	10§	11	12	13	14	15	16	17	18	19
3287.6	......	......	......	......	......	......	......	......	......	16.0
3289.6	......	......	19.3	......	......	16.7	......	......	......	16.0
3317.7	......	19.1	......	......	......	16.8	......	18.75	19.4+	16.2
3350.3	......	......	19.1	......	......	......	......	......	......	16.0
3433.3	......	......	......	......	......	......	19.3	19.4	......	16.2
3610.6	......	......	......	......	......	16.9	19.2	19.4+	......	16.0
3612.6	......	......	19.1	......	......	......	19.3	......	......	16.1
3615.7	......	......	......	......	......	......	......	18.85	......	......
3617.7	......	......	......	......	......	16.8	......	......	......	16.0
3639.7	......	......	......	......	19.3	16.8	18.9	......	......	16.2
3641.5	......	......	......	......	......	16.9	......	......	......	16.1
3698.6	......	19.4	......	......	19.5+	......	......	......	......	16.2
3737.6	......	19.3	......	19.5	19.5+	16.9	......	......	19.6+	16.3
3765.45	......	19.1	19.3+	19.5	19.6	17.0	18.85	......	19.1	16.3
3768.4	......	......	......	......	......	......	......	......	......	16.2
3780.3	......	......	......	......	......	17.0	19.5	......	19.6	16.1
3790.4	......	19.1	......	19.5	19.5+	17.0	19.5+	19.6	19.6	16.2
3701.4	......	19.1	19.4+	19.6+	19.6+	17.1	......	......	19.8	16.1
3818.3	......	......	19.0	19.3+	19.4+	17.2	19.2	......	19.3	16.2
3819.3	......	19.3+	19.3	19.4+	19.6	17.2	19.3	19.6+	19.4+	16.2
3820.3	......	......	19.1	19.3+	19.3+	17.1	19.4	19.3	19.25	16.3
3821.3	......	19.4+	19.2	19.2	19.6+	17.0	......	......	19.2	16.3
3822.3	......	19.3+	19.2+	19.2	19.5+	17.1	......	......	19.3	16.3
3823.3	......	......	19.3+	19.2+	19.4+	17.0	......	......	19.3	16.3
3843.3	......	......	......	......	......	......	......	18.8	......	16.3
3969.6‡	19.1+	......	......	......	......	......	18.85	19.4	19.0	16.1
3970.6	......	......	19.6+	19.7+	19.7+	16.9	......	......	......	16.2
3971.6	......	......	......	......	......	......	19.1	......	......	......
3990.6‡	......	......	......	......	......	16.7	......	18.7	......	16.3
3991.6	18.9	19.4	......	......	......	16.8	19.5	18.75	19.4	16.3
3993.6	19.0	19.3	......	......	......	......	19.5	19.1	19.6	16.2
3994.6‡	19.2	19.3	19.2	19.7	19.4	17.0	19.7	19.25	19.7	16.3
3995.6‡	19.2	......	19.2	19.2	19.5	16.8	19.8	19.3	19.7	16.3
3996.6‡	19.2	......	19.0	19.2	19.8	16.8	19.8	19.35	19.7+	16.2
3997.6‡	19.3	......	19.2	19.3	19.8	16.8	19.6	19.6	19.9	16.2
3998.6‡	19.4	......	19.2	19.4	19.8+	16.9	19.8	19.6	19.9	16.1
3999.6‡	19.4+	19.3	19.35	19.4	19.8+	17.0	19.7	19.7	19.8+	16.0
4000.6‡	......	......	19.4	19.4	19.8+	17.0	19.9	19.7	19.9	16.2
4001.6‡	19.3	......	19.4	19.4	19.8+	16.8	19.8+	19.7	19.9	16.1
4002.6‡	......	19.1	19.4	19.5	19.8+	16.7	19.7+	19.7	19.8+	16.2
4003.6‡	19.5	19.3	19.6	19.6	19.9	16.7	19.8	19.7	19.9	16.2
4004.5‡	19.4	......	19.6	19.6	......	16.9	19.9	19.7	......	16.2
4023.4	19.4+	......	......	......	19.6+	......	19.15	19.8+	19.7+	......
4024.5‡	19.4+	19.2	19.7	19.7	19.8	16.6	19.2	19.9	19.2	16.0
4025.5‡	19.5+	19.3	19.7	19.8	19.2	16.7	19.35	19.9	19.2	16.1
4026.5‡	19.4+	19.1	19.7	19.8	19.0	16.8	19.4	19.4	19.2	16.2
4027.6‡	19.2	19.1	19.7	19.8	19.05	16.8	19.4	18.75	19.3	16.1
4028.5	......	19.3	19.7+	19.8+	19.2	16.7	......	......	......	15.9
4029.4	18.8	......	......	19.4+	19.2	16.8	19.5	19.1	19.5+	16.0
4030.5	......	19.1	19.8+	19.8+	19.3	16.9	......	......	......	16.1
4031.5‡	18.9	19.1	19.8	19.8+	19.7	16.7	19.4	19.1	19.7+	16.1
4032.5‡	18.95	......	19.7+	19.8+	19.7	16.8	19.5	19.4	19.7+	16.1
4033.6‡	......	19.15	19.7+	19.8+	19.9	16.7	19.6	19.35	19.7	16.2
4049.5‡	19.3+	19.0	19.8+	19.8+	......	16.7	19.2	19.0	19.7+	16.3
4050.5‡	19.1	18.9	19.8+	19.9	19.8	16.7	19.1	18.9	19.7	16.3
4054.6‡	......	......	19.8	19.8	19.8	16.8	......	......	......	16.2
4055.6	18.8	19.0	......	......	19.8	......	18.85	19.4	19.7+	16.2
4056.6	18.95	18.9	19.8	19.9	19.9+	16.9	......	......	......	16.2
4057.4	18.95	19.0	19.8	20.0	20.0	16.7	18.8	19.6	......	16.2
4059.4‡	19.0	18.8	19.7	19.8	19.8+	16.7	18.9	19.7	19.7+	16.2

TABLE I—*Continued*

J.D.*	Plate†	Qy.	1‖	2	3	4	5§	6	7	8	9
4085.4	451	G	......	......	19.4	......	19.2+	......	......	......	......
4086.4‡	S394,5	F	19.1	19.3+	19.3+	......	19.1+	......	18.5	......	19.05
4089.4‡	400,1	G	19.2	18.8	19.4+	......	19.5+	19.15	18.7	19.6	19.3
4090.4	H457	G	......	......	......	......	......	......	18.7	19.7	19.4
4092.3	464	F	......	18.6	......	......	......	19.5	18.8	......	19.4
4108.4‡	H469,0	F	18.45	19.2	19.5+	......	18.85	......	18.8	19.5+	18.2
4109.3	471	F	......	......	......	19.7	......	19.5	18.8	19.7+	18.3
4114.4	S411	G	19.0	19.0	19.4	19.7	19.05	19.6	18.2	19.4+	18.7
4150.3	H510	P	19.1+	18.55	18.4	......	......	19.3+	18.9+	......	......
4168.3	S417	P	18.2	18.8+	......	......	......	18.6	18.4	......	19.2+
4177.4	424	F	19.0	19.2+	18.7	......	......	19.1	18.6	19.6	......
4178.3	433	F	19.1	19.2+	18.4	19.5+	......	......	18.8	19.6+	18.8
4181.3	H531	P	19.1	19.4	18.7	19.0	......	......	18.9	......	......
4197.3	S434	P	19.1	19.4	......	......	......	......	19.2	......	19.2+
4207.3	446	P	......	......	......	......	......	......	18.15	......	......
4319.6	H571	F	19.4	19.3	19.3	19.7	......	19.6	18.7	19.6+	......
4321.6	S483	G	19.4	19.3+	19.1	......	19.2+	18.8	......	......	......
4339.5	H580	F	......	19.1	19.3+	19.0	......	19.0	18.4	19.1	......
4351.6	D251	F	19.4	18.5	19.5	19.2	......	19.3	18.6	19.2	19.1
4356.6	268	G	18.2	19.2	19.5	19.5	......	19.5	18.7	19.6+	18.9+
4358.5	S496	G	18.2	19.3	19.4+	19.6	......	19.7	18.7	19.5+	19.3+
4377.4	H586	F	19.3+	19.3	19.3	19.6+	......	19.3	18.9	19.7+	......
4379.7	598	P	19.2+	19.2	19.3+	......	......	19.3	18.9	19.7	......
4406.6	607	P	......	......	......	......	......	......	18.9	19.3+	18.8
4414.7	609	F	......	18.9	19.5+	19.2	......	18.6	19.0	19.8	18.9
4433.3	615	P	......	18.6	19.4	......	......	......	18.0	19.3+	......
4441.5	S505	F	19.3+	19.2	......	......	......	19.0	18.3	19.5	18.9
4444.4	H617	F	......	......	......	19.6	......	19.6	18.5	19.7	18.9
4475.3	621	P	......	......	18.6	......	......	19.3+	18.1	19.5	......
4476.5	Sr6276	P	19.2+	19.1	18.4	......	......	......	18.2	......	......
4493.4	H624	F	19.1	18.85	19.5	19.1	......	19.6	18.7	19.2	......
4495.3	626	P	19.3	19.0	......	......	18.95	......	......	......	......
4522.3	627	P	......	......	......	......	......	18.6	18.2	......	......
4530.3	SS45	P	19.2+	19.3	18.4	19.3+	......	19.1	18.4	19.5	......
4531.3	H629	P	19.2+	18.65	18.6	19.3	......	19.3	18.4	......	......
4671.6	S533	P	18.4	19.0	......	......	......	......	18.65	......	......
4680.6	D304	P	19.0	19.2+	......	......	......	18.6	18.9	......	......
4700.6	315	G	18.7	19.4	19.5	19.2	......	18.6	18.0	19.7	......
4709.6	H668	F	18.9	19.4	19.5	19.6	......	19.5	18.4	19.5	......
4711.6	S539	F	19.1	19.3	......	......	......	......	18.3	......	......
4739.5	540	P	18.6	19.15	......	19.0	......	19.6	19.0	19.0	......
4762.4	H675	G	19.3	19.4	19.6	19.2	......	19.6	18.55	19.5	......
4764.4‡	686	E	18.25	19.5	19.4	19.3	......	19.6	18.6	19.6	......
4770.4	690	E	18.9	19.4	19.1	19.6	......	18.6	18.8	19.6	......
4772.4‡	703	E	18.8	18.75	18.4	19.6	......	18.9	18.9	19.5+	......
4793.3	S545	F	19.2	18.45	19.5	19.5+	......	18.6	18.1	19.2	18.6
4800.3	H708	E	18.5	19.2	18.4	19.0	......	19.6	18.3	19.6	......
4801.3	S547	P	18.6	19.3	18.7	19.1	......	......	18.5	......	......
4822.5	BB104	F	19.3+	19.5	......	19.2	......	19.6	18.8	......	......
4823.5	117	F	19.4	19.3+	19.3+	19.3	......	......	18.9	19.5	......
4882.3	166	F	19.4+	19.4+	18.5	18.9	......	18.7	18.2	19.0	......
4883.3	180	P	19.1+	19.1+	18.7	19.1	......	18.8	18.0	......	......
4908.3	H715	G	19.4	19.6	18.4	19.4	......	19.3	19.0	19.6+	......
4918.3	720	F	19.2+	19.05	19.3+	19.4+	......	......	19.0	19.2	......
4938.3	732	P	19.2	19.0	18.6	......	......	......	18.5	19.2	......
5035.6	780	P	19.3	18.5	......	......	......	18.7	18.8	19.6	......
5036.6	785	F	19.3	18.7	19.6	19.6+	......	18.8	18.8	19.7	......
5063.6	798	F	19.1	19.5	19.6+	19.5	......	19.4	18.2	19.5	......
5083.5	812	F	18.6	19.5	19.8	19.8	......	19.2	18.7	19.6	......
5091.5	815	P	......	......	19.3+	19.2	......	......	19.0	......	......

TABLE I—*Continued*

J.D.	10§	11	12	13	14	15	16	17	18	19
4085.4	19.1+	....	....	....	....	....	19.8	18.85	19.4	....
4086.4‡	19.1+	19.0	19.35	19.4	19.6+	16.7	....	19.1	19.5	16.2
4089.4‡	19.3+	19.2	19.6	19.7	19.8	16.7	19.4	19.4	19.8	16.1
4090.4	....	18.9	19.7	19.8	19.6+	....	....	....	....	16.15
4092.3	....	19.1	19.6+	19.6+	19.7	16.7	....	....	....	....
4108.4‡	19.1	19.0	19.1	....	....	16.8	19.3	19.2	19.5	16.2
4109.3	....	19.1	19.2	19.5	19.8	16.9	....	....	....	16.3
4114.4	19.4+	19.0	19.4	19.5	19.1	16.9	19.5	19.4	19.7+	16.1
4150.3	....	19.2	18.9	....	19.0	16.9	....	....	....	16.2
4168.3	....	....	....	....	19.2	....	....	....	....	16.0
4177.4	....	....	19.5	....	19.6+	16.8	18.85	19.0	19.7+	16.2
4178.3	....	19.3	....	....	19.6+	16.8	18.9	18.75	....	16.2
4181.3	....	....	19.6	....	....	16.8	....	....	....	16.3
4197.3	....	19.2	19.3	....	....	....	19.3	18.8	19.7+	16.2
4207.3	....	....	....	....	....	....	....	....	....	16.1
4319.6	....	19.0	19.3+	19.6+	19.6+	16.9	....	....	19.5	15.9
4321.6	19.3+	19.2	....	....	....	16.8	19.4	19.6	19.0	16.0
4340.5	....	....	19.2+	....	....	16.7	....	....	....	16.0
4351.6	....	19.2	18.8	....	19.7	....	19.3	19.35	19.8+	16.0
4356.6	....	19.3	19.2+	....	....	16.7	19.5	19.7	19.7	15.9
4358.5	....	19.4	19.4	19.6+	19.7+	16.8	19.4	19.7+	19.1	15.8
4377.4	....	19.3+	19.0	19.6+	19.4	16.7	....	....	....	15.9
4379.7	....	....	....	....	18.9	16.8	....	....	....	15.8
4406.6	....	....	....	....	....	16.8	....	....	....	15.7
4414.7	....	19.5+	19.6+	19.6	19.0	16.7	....	....	....	15.7
4433.3	....	....	....	....	19.2	16.7	....	....	....	15.7
4441.5	....	19.4+	18.9	19.5+	19.4+	16.7	19.6	18.7	19.7+	15.6
4444.4	....	19.4+	19.3	....	....	16.8	....	....	....	15.6
4475.3	....	19.4+	....	19.0	....	16.8	....	....	....	15.3
4476.5	....	....	....	19.1	....	16.8	....	....	....	15.4
4493.4	....	19.6	....	....	....	16.9	....	....	....	15.3
4495.3	19.2	....	....	....	....	....	19.7	19.7	19.7+	15.4
4522.3	....	....	....	....	....	....	....	....	....	15.3
4530.3	....	....	....	....	....	17.0	....	....	....	15.4
4531.3	....	....	....	....	....	16.9	....	....	....	15.4
4671.6	....	....	....	....	....	17.3	....	....	....	15.55
4680.6	....	....	....	....	19.3	17.3	19.3	19.4+	19.5+	15.55
4700.6	....	....	....	....	....	17.2	....	....	19.7	15.4
4709.6	....	....	....	....	....	17.3	....	....	19.3	15.5
4711.6	....	....	....	....	....	17.3	18.7	18.9	19.1	15.4
4739.5	....	....	....	19.2	....	17.2	19.5+	19.2	19.6+	15.5
4762.4	....	19.6	19.6+	19.6+	19.7	17.2	18.9	....	19.8+	15.55
4764.4‡	....	....	....	....	19.7	17.1	....	....	19.8+	15.6
4770.4	....	19.6	19.4	....	19.4	17.2	....	....	....	15.7
4772.4‡	....	19.6	....	....	19.7	17.1	19.4	19.7	19.7	15.6
4793.3	....	....	....	....	....	17.2	18.9	19.7	19.7+	15.6
4800.3	....	19.6+	19.3	19.0	19.7+	17.3	19.05	....	....	15.6
4801.3	....	....	19.3+	19.1	19.0	17.3	19.2	18.9	....	15.7
4822.5	....	....	19.4+	18.9	19.1	17.2	19.5+	19.2	19.1	15.6
4823.5	....	19.4	19.3+	19.2	19.4	17.2	19.5+	19.2	19.2	15.6
4882.3	....	....	....	....	....	17.2	19.1	19.4	....	15.4
4883.3	....	....	....	....	....	17.2	18.85	19.3+	....	15.5
4908.3	....	19.5+	18.0	19.1	19.2	17.2	....	....	....	15.4
4918.3	....	....	19.2+	19.3+	19.4+	17.1	18.75	19.5	19.25	15.4
4938.3	....	....	....	....	....	17.2	....	....	....	15.45
5035.6	....	....	19.2+	....	....	17.2	....	....	....	15.8
5036.6	....	19.6+	....	19.8	19.8+	17.1	....	....	19.4+	15.9
5063.6	....	....	19.1	19.5	19.8+	17.2	19.5	....	19.15	16.0
5083.5	....	....	....	19.1	19.5	....	18.8	....	19.35	16.0
5091.5	....	....	....	....	19.7	17.1	19.1	....	19.7	16.0

TABLE I—*Continued*

J.D.*	Plate†	Qy.	1‖	2	3	4	5§	6	7	8	9
5115.4........	H824	F	18.7	18.6	19.6	19.3	......	19.6	18.2	19.4	......
5116.4........	828	F	18.8	18.8	19.6	19.4	......	19.7	18.3	19.4	......
5124.4........	H832	P	19.2	19.6	18.7	19.7	......	18.9	18.5	19.7	......
5145.4........	S577	F	18.3	19.5+	19.4+	19.5+	......	18.8	18.9	19.5	......
5147.6........	H848	P	18.6	......	19.2	......	......	19.0	18.8	19.1	......
5149.6........	H855	F	18.9	19.6+	18.7	19.5	......	19.1	18.4	19.1	......

are often below the limits of the plates, and generally below the limits of accuracy. For this reason statistical discussions must be confined largely to the magnitudes at maxima.

Magnitudes for the variables in Regions 1, 2, and 3 are listed in Table I, and for those in Region 4, in Table II. Values for different plates exposed during a single night are generally combined, as they seldom differ by more than the errors of observation.

TABLE I—*Continued*

J.D.	10§	11	12	13	14	15	16	17	18	19
5115.4	....	19.6	19.3+	19.7	19.8	17.0	....	....	....	16.0
5116.4	....	19.6	19.4+	19.5+	19.8	17.0	....	....	19.4+	16.0
5124.4	....	19.8	....	19.4	19.6	17.0	....	....	19.4+	16.0
5145.4	....	....	....	....	....	17.2	....	....	....	16.0
5147.6	....	....	....	19.0	....	17.1	....	....	....	16.0
5149.6	....	19.6	19.1	19.3	....	17.0	....	....	19.7	16.0

* Add 2,410,000 to the first seven dates and 2,420,000 to the remainder.

† Letters preceding the plate numbers refer to the following observers: R = Ritchey, P = Pease, Sh = Shapley, D = Duncan, Hg = Hoge, S and H = Hubble, A and B = Humason, Sr = Seares, SS = Schilt, BB = Brown.

‡ Nights on which more than one plate were obtained.

‖ A plus sign following magnitude indicates that the variable was invisible, but certainly fainter than the tabulated value.

§ See Table I*a* for additional observations.

TABLE I*a*

ADDITIONAL OBSERVATIONS, VARIABLES IN M 31, CENTRAL REGION; VARIABLES NOS. 5 AND 10

J.D.	Plate	Qy.	5	10
4054.4	H432	P	....	18.8
4056.4	S379	G	18.65	....
4113.4	408	P	18.9	19.2+
4168.3	416	P	19.1+	18.85
4323.6	494	F	19.2+	19.2+
4384.5	D276	E	18.65	19.2+
4387.5	287	E	18.5	19.2+
4731.5	323	F	....	19.4+
4739.5	S541	F	19.0	18.9

TABLE II

Variables in M 31, Region 4

J.D.*	Plate†	Qy.	21‖	22	23	24	25	26	27	28
4032.4	H424	F	19.9	20.1	19.5	19.4	19.7	19.05	19.0	19.1
4054.4	432	P	19.2	19.5+	19.6	19.6	19.8+	19.7	19.4	19.3
4056.4	S379	G	19.0	19.3	18.7	19.8	19.8	19.1	19.3	19.25
4058.55	H438	F	19.2	18.95	19.0	19.8	20.0	19.1	18.7	19.2
4085.6	454	E	19.9	19.7	19.8	19.2	19.2	19.2	19.0	19.4
4090.55	461	P	19.1	19.5	18.7	19.7	19.8	19.6	19.5	19.2
4108.35	468	F	19.1	19.5	18.8	19.7	18.95	19.45	18.8	19.2
4113.4	S408	P	19.35	....	19.2	....	....	19.2	....	19.3
4115.5	H478	F	19.8	19.4	19.4	19.9	19.9	19.5	19.4	19.4
4117.5	497	F	19.8	19.7	....	19.8+	19.7	19.45	19.5	19.3
4147.4	504	P	19.5	19.1	19.3	19.7+	19.55	19.7+	19.5	18.3
4151.4	512	F	19.9	19.5	19.7	19.9	19.7+	19.8	19.5	18.8
4168.3	S416	P	....	....	....	....	....	....	....	....
4171.3	H516	G	20.0	19.7	19.6	20.0	19.7	19.6	19.5	19.3
4180.3	525	F	19.35	18.9	18.8	19.7	19.4	19.9	18.9	18.7
4198.3	S439	P	....	....	....	....	....	....	....	....
4320.6	H573	F	19.8	19.1	18.8	19.8	19.6	19.0	19.5	19.15
4323.6	S494	F	....	....	19.2	19.7+	19.5	19.2	18.7	19.1
4349.6	H581	G	19.3	19.7	19.8	19.25	19.9	19.35	18.95	19.2
4353.6	D257	P	19.6	....	18.8	19.55	19.8+	19.6	18.9	19.2
4357.5	H583	G	20.1	19.0	19.1	19.8	19.05	19.6	19.4	19.3
4377.5	587	E	20.1	19.1	19.4	20.0+	19.7	19.4	19.2	19.3
4379.5	599	P	....	....	....	....	....	19.4+	19.3	....
4384.5	D276	E	19.3	19.8	19.6	19.2	19.7	20.0	19.5	19.35
4387.45	287	E	19.5	19.8	19.6	19.55	20.1	19.9	19.4	18.8
4405.4	H605	G	19.6	19.7	19.45	19.5	19.4	19.5	19.4	19.3
4414.4	610	F	19.6	19.5	19.5	20.0	19.5	19.9	19.5	18.5
4444.3	616	F	19.9	18.9	19.1	19.9	19.9+	19.8	18.8	18.5
4493.4	625	F	19.7	19.7	19.4	19.55	20.0	20.0	18.7	19.35
4709.6	669	F	19.0	19.15	19.1	19.8	19.7	19.8	18.75	18.2
4731.5	D323	F	19.7	19.7	19.7+	19.9	19.9	19.8	19.3	19.3
4739.5	S541	F	19.8	19.6+	18.9	19.5	19.7	19.0	19.15	18.25
4762.5	H676	G	19.3	19.0	19.2	19.7	19.8	19.7	19.15	18.5
4770.5‡	691	F	19.8	19.6	19.6	19.8	19.2	19.5	19.5	18.8
4771.5‡	697	F	19.9	19.7	19.6	19.45	19.4	19.6	19.5	18.9
4772.5	707	P	....	....	....	....	....	19.5	....	19.1
4800.4	709	G	19.6	19.4	19.55	19.8	19.8	19.8	19.5	19.2
4907.3	714	F	19.8	19.3	19.6	19.8+	20.0	19.9	19.15	19.2
4947.3	S556	P	....	....	....	....	....	18.9	....	....
5035.63	H781	VP	....	....	....	....	....	....	....	....
5053.60	794	P	....	....	19.5	19.4	19.2	19.0	....	19.3
5063.61	799	G	20.0	19.3	19.5	19.9	19.7	19.6	19.4	18.6
5065.68	810	G	19.8	19.4	19.6	20.0	19.2	19.8	19.5	18.7
5083.55	813	P	19.3	19.4	19.5+	19.6+	....	19.45	19.4	18.9
5091.6	816	F	19.7	19.6	18.7	19.55	19.5	19.9	19.5	18.8
5115.5	825	F	20.0	19.3	19.5	20.0	19.5	19.6	19.4	18.4
5116.48‡	829	E	19.75	19.4	19.6	20.0	19.7	19.8	19.4	18.5
5124.45	H833	F	19.7	19.7	19.6	19.4	19.4	20.0	19.2	19.2
5145.52	S578	P	....	....	19.1	....	....	....	19.0	18.9
5147.5‡	H843	F	20.0	18.8	19.1	19.7	19.6	19.8	19.1	18.9
5148.3	850	P	....	18.8	19.2	....	....	....	....	18.9
5149.5‡	851	F	20.0	19.05	19.3	19.8	19.15	19.8	19.3	19.1
5150.5‡	858	F	19.8	19.15	19.45	19.9	19.3	20.0	19.4	19.2
5266.3	899	P	19.8	....	18.7	19.5	....	19.2	18.8	19.4
5475.5	920	G	19.9	19.6	19.45	19.9	20.1	19.4	19.4	19.2

TABLE II

Variables in M 31, Region 4

J.D.	29	30	31	32	33	34	35	36	37	38
4032.4	19.7	19.9+	19.2	19.4+	18.7	18.8	19.6	19.6	19.9	19.6
4054.4	19.2	19.5	19.2	19.6	18.9	19.8+	19.6	19.3	19.35	19.5
4056.4	19.8	18.9	19.5	19.5	18.95	19.8+	19.6	19.1	19.65	19.8
4058.55	19.6+	18.8	19.7	19.4	19.1	19.6+	19.4+	19.3	19.8+	19.9
4085.6	19.9+	19.8	19.8	19.5	19.0	19.9	19.6	19.7	20.0	19.7
4090.55	19.6+	19.4+	19.9	18.7	18.9	19.5+	19.6	19.1	19.8	19.7+
4108.35	19.7+	19.4	20.0	19.5	18.75	19.55	19.5+	19.1	19.5	19.8
4113.4	19.5	19.05	19.4+	19.3	19.1	19.6+	19.0	19.4	19.6+	....
4115.5	19.5	19.2	20.0	18.7	19.3	19.6	19.3	19.5	19.9	19.6
4117.5	19.6+	19.6+	19.8+	19.0	19.4	....	....	19.6	19.8+	19.8+
4147.4	19.6+	18.75	19.4	19.2	18.9	19.6+	18.9	19.2	19.4	....
4151.4	19.5	19.3	19.8	19.4	19.1	19.6+	19.4	19.6	19.9	19.9
4168.3	....	18.8	....	19.0	19.0	19.4+	19.3	....	....	....
4171.3	19.4	19.3	19.65	19.1	19.2	19.5	19.5	19.6	19.8	20.0+
4180.3	19.8+	19.4	19.8+	19.4	19.0	19.7+	19.5+	19.1	19.9	19.9
4198.3	....	....	....	....	19.2	....	....	....	....	....
4320.6	19.8+	19.8	19.9	18.9	19.1	19.6	....	19.6	19.4	19.9
4323.6	....	19.8	19.8	19.2	19.2	18.7	19.0	19.0	19.6	19.7+
4349.6	19.7	18.75	19.1	19.3	18.95	19.8	19.6+	19.5	19.8	19.8
4353.6	....	19.1	19.5	19.4	18.75	19.3	19.4+	19.7	19.8+	19.7+
4357.5	19.9+	19.6	19.8	19.6	18.9	18.9	18.95	19.6	19.9	19.3
4377.5	19.9+	19.9	19.6	19.3	19.1	19.9	19.2	19.2	19.9	19.3
4379.5	....	....	....	....	19.2	....	....	....	....	....
4384.5	19.4	18.7	20.0	....	19.4	19.6	19.6	19.6	19.8	19.9
4387.45	19.8	18.8	20.0	19.6	19.0	18.7	19.7	19.7	19.4	19.4
4405.4	19.3	18.9	19.8	19.5	19.2	19.8+	19.6	19.6	19.8	19.8
4414.4	19.9+	19.8	19.9	19.4	19.0	19.8	19.4	19.2	19.4	20.1
4444.3	19.2	19.2	19.5	18.9	19.1	19.8	19.2	19.7	19.9	19.9+
4493.4	19.9	19.4	19.9	19.4	19.3	19.4	19.6	19.6	19.35	19.8
4709.6	19.9+	19.9	20.0	19.4	18.6	18.9	19.15	19.6	19.55	19.8
4731.5	19.9+	19.1	20.0	19.1	18.9	19.9	19.5	19.6	19.7	19.5
4739.5	19.6+	19.2	19.3	19.4	19.3	19.6+	19.6	19.4	19.9	19.8
4762.5	20.0+	19.9+	19.3	19.5	19.3	19.9	19.2	19.6	19.55	19.35
4770.5‡	20.0+	18.8	20.0	19.6	19.1	19.8	19.6	19.5	19.7	19.8
4771.5‡	19.8+	19.0	19.9	19.5	19.0	19.55	19.6	19.0	19.7	19.6
4772.5	....	19.15	19.5+	19.4	19.1	....	....	19.0	19.3	19.5
4800.4	19.9+	19.8	19.9	18.8	19.3	19.8	19.4	19.7	19.5	19.9
4907.3	19.9+	19.7+	19.9	19.2	19.3	19.2	19.5	19.6	19.4	19.8
4947.3	....	....	....	....	....	....	....	....	....	....
5035.63	....	....	....	....	19.1	....	....	....	....	....
5053.60	....	19.3+	19.2	18.75	19.1	....	....	....	....	....
5063.61	20.0+	18.95	19.9	19.4	19.3	19.05	19.4	19.65	19.9	19.7
5065.58	20.0+	19.1	19.9	19.4	19.2	19.05	19.6	19.65	19.6	19.4
5083.55	19.4+	19.1	19.6	19.0	19.3	19.4+	....	19.6+	19.7	19.8
5091.6	19.5	19.6	19.9	19.5	18.95	19.7	19.6	19.6	19.9	19.9+
5115.5	19.8+	19.2	20.0	19.5	19.4	19.7	19.5	19.5	20.0	19.6
5116.48‡	19.9+	18.65	19.9	19.6	19.4	19.8	19.6	19.6	20.0	19.4
5124.45	19.6	19.7	19.3	19.5	18.6	19.8	19.6	19.8	19.9	19.7
5145.52	19.5	19.6+	....	....	18.9	....	18.9	19.5	19.6	....
5147.5‡	19.4	19.7	19.3	19.5	18.95	19.7	19.3	19.1	19.4	19.3
5148.3	....	....	....	....	18.9	....	....	19.2	....	....
5149.5‡	19.6	19.65	19.5	19.5	19.15	19.8	19.4	19.4	19.6	19.75
5150.5‡	19.7	19.55	19.6	19.5	19.2	19.8	19.5	19.5	19.7	19.9
5206.3	....	18.8	....	19.2	19.4	....	....	19.5+	19.4	....
5475.5	19.8	19.7	19.8	19.7	19.4	19.8	19.6	19.5	19.8	19.8

TABLE II—*Continued*

J.D.*	Plate†	Qy.	39	40	41	42§	43	44	45	46
4032.4	H424	F	19.7	19.0	19.6	19.0	19.8	19.2	19.6	19.7
4054.4	432	P	19.8+	19.0	19.3	18.5	19.7	19.1	20.0	19.6
4056.4	S379	G	19.9+	19.1	19.6	18.4	19.8+	18.7	19.7	19.7
4068.55	H438	F	....	18.9	19.6	18.2	19.7	19.1	19.3	19.8
4085.6	454	E	19.3	19.0	19.7	17.9	19.7	19.3	19.35	19.7
4090.55	461	P	....	18.8+	19.6+	17.9	19.7	19.2	19.7+	19.4
4108.35	468	F	19.1	18.6	19.4	18.4	19.7+	19.1	19.9	19.8
4113.4	S408	P	....	....	19.4+	18.4	....	19.0	19.7	19.6
4115.5	H478	F	19.7	19.0	19.7	18.5	19.8+	19.2	19.9	19.4
4117.5	497	F	19.5+	19.0	19.5+	18.4	19.7	19.2	19.7+	19.5
4147.4	504	P	19.5+	18.9	19.4	19.0	19.6	18.7	19.7	19.7
4151.4	512	F	19.8	19.15	18.9	19.1	19.7	18.7	19.7	19.7
4168.3	S416	P	....	....	....	19.0	....	....	....	....
4171.3	H516	G	19.8	18.4	19.6	19.0	19.9	18.7	19.9	19.7
4180.3	525	F	19.2	18.75	19.0	19.0	19.7+	19.0	19.9	19.2
4198.3	S439	P	....	....	....	19.1	....	....	....	....
4320.6	H573	F	19.6	19.1	19.6	18.8	19.5	18.7	19.7	19.45
4323.6	S494	F	19.2	19.1	19.5	18.9	....	18.7	19.9+	19.35
4349.6	H581	G	19.45	18.9	19.7	19.0	19.4	18.7	20.0	19.4
4353.6	D257	P	....	18.8+	18.9	19.0	19.3	18.8	19.9	19.7
4357.5	H583	G	19.9	19.2	18.95	18.9	19.3	18.8	19.7	19.6
4377.5	587	E	19.7	18.7	19.2	18.9	19.35	18.8	19.95	19.6
4379.5	599	P	....	18.75	18.7	19.0	....	....	....	....
4384.5	D276	E	20.1	18.9	19.1	18.9	19.4	18.8	19.8	19.6
4387.45	287	E	20.0	19.2	19.4	18.85	19.4	18.9	20.0	19.3
4405.4	H605	G	20.0	18.4	18.8	18.3	19.5	18.7	19.8	19.8
4414.4	610	F	20.0	18.8	19.4	17.9	19.45	18.8	20.0	19.3
4444.3	616	F	19.3	18.75	19.7	18.1	19.6	18.7	19.8	19.7
4493.4	625	F	19.45	19.1	19.5	19.0	19.7	18.8	19.9	19.5
4709.6	669	F	19.5	18.6	19.2	19.1	19.3	19.3	20.0	19.3
4731.5	D323	F	19.15	19.2	19.7	19.0	19.1	19.4	19.5	19.8
4739.5	S541	F	19.8	18.5	19.0	19.2	19.2	19.3	19.8+	19.5
4762.5	H676	G	19.9	19.15	18.95	18.3	18.9	19.3	20.0	19.2
4770.5‡	691	F	19.8+	18.8	19.6	18.1	19.1	19.1	19.45	19.7
4771.5‡	697	F	20.0	18.5	19.6	18.0	18.9	19.1	19.6	19.6
4772.5	707	P	....	18.3	19.6	18.0	....	19.1	....	....
4800.4	709	G	19.5	19.2	19.7	18.3	19.0	19.1	19.9	19.25
4907.3	714	F	19.7	18.4	19.6	19.0	19.7	19.2	20.0	19.5
4947.3	S556	P	....	....	....	18.2	....	....	....	....
5035.63	H781	VP	....	....	....	19.0	....	....	....	....
5053.60	794	P	....	18.9	....	19.1	....	....	....	....
5063.61	799	G	19.6	19.1	19.6	19.2	19.75	19.25	19.7	19.6
5065.58	810	G	19.0	19.1	19.5	19.2	19.75	19.2	19.3	19.8
5083.55	813	P	19.5+	18.75	19.5+	19.1	....	....	19.9	19.5
5091.6	816	F	19.35	19.1	19.3	18.8	19.5	19.3	19.5	19.8
5115.5	825	F	19.4	18.7	19.7	18.2	19.4	19.2	19.7	19.7
5116.48‡	829	E	19.5	18.75	19.5	18.2	19.3	19.1	19.2	19.9
5124.45	H833	F	19.8	19.2	19.15	17.8	19.25	19.2	20.0	19.35
5145.52	S578	P	....	18.6	18.8	17.9	19.2	19.2	....	....
5147.5‡	H843	F	19.8+	18.7	19.0	18.1	19.0	19.2	19.9	19.55
5148.3	850	P	....	18.8	19.1	18.1	....	....	....	....
5149.5‡	851	F	19.9	18.8	19.25	18.2	18.9	19.1	19.9	19.25
5150.5‡	858	F	19.9	18.85	19.4	18.25	18.9	19.1	20.0	19.25
5266.3	899	P	....	19.1	19.5	18.8	19.5	19.2	19.5+	19.2
5475.5	920	G	19.7	18.4	18.8	18.0	19.8	19.4	19.9	19.5

* Add 2,420,000.

† D plates were obtained by Duncan; S and H plates, by Hubble.

‡ Two or more plates in one night.

‖ The plus sign following a magnitude indicates that the variable was invisible, but certainly fainter than the tabulated magnitude.

§ Additional observation of Variable No. 42, H916, J.D. 5291.3, 17.9.

Cepheids.—Data for the normal light-curves of the forty variables recognized as Cepheids are given in Table III. Magnitudes at minima and ranges are included, but in most cases they are very uncer-

TABLE III

CEPHEIDS IN M 31

VAR. NO.	PERIOD IN DAYS	LOG *P*	PHOTOGRAPHIC MAGNITUDES				EPOCH J.D.*	POSITION†	
			Max.	Min.	Range	Med.		*X*	*Y*
1.......	31.390	1.497	18.2	19.4	1.2	18.8	3823.0	+13.7	+ 8.1
2.......	20.090	.303	18.6	(19.6)‡	(1.0)	(19.1)	4029.5	− 1.6	−13.9
3.......	27.00	.431	18.4	19.7	1.3	19.05	4771.0	+ 8.0	− 4.3
4.......	20.60	.314	19.0	(19.8)	(0.8)	(19.4)	3995.5	− 1.4	+ 5.0
5.......	48.36	.684	18.5	(19.7)	(1.2)	(19.1)	3990.0	+21.6	−10.6
6.......	22.23	.347	18.6	19.7	1.1	19.15	3788.0	−10.7	− 9.7
7.......	45.05	.654	18.1	19.1	1.0	18.6	2583.0	−16.9	− 3.2
8.......	17.764	.249	19.0	(19.8)	(0.8)	(19.4)	3992.5	− 4.2	+ 2.0
9.......	32.56	.513	18.2	19.4	1.2	18.8	4108.0	−23.1	+ 1.4
10.......	22.823	.358	18.8	(19.6)	(0.8)	(19.2)	4029.0	+24.2	−15.3
12.......	22.225	.347	18.9	(20.0)	(1.1)	(19.45)	3994.5	−18.3	− 3.2
13.......	21.726	.337	19.05	(19.95)	(0.9)	(19.5)	3822.0	−16.7	− 6.8
14.......	17.632	.246	18.9	(20.0)	(1.1)	(19.45)	4026.0	− 9.8	− 7.3
16.......	41.157	.614	18.8	19.8	1.0	19.3	4011.0	+11.9	−10.5
17.......	18.773	.274	18.75	19.9	1.15	19.3	3990.0	+14.3	− 8.0
18.......	18.538	.268	19.1	(19.9)	(0.8)	(19.5)	4025.0	+11.5	− 7.3
21.......	17.15	.234	19.0	20.0	1.0	19.5	4055.0	+51.0	− 0.9
22.......	17.60	.246	18.95	(19.85)	(0.9)	(19.4)	4181.0	46.7	+ 0.5
23.......	17.54	.244	18.7	19.7	1.0	19.2	4319.0	54.5	− 4.1
24.......	17.61	.246	19.25	(20.0)	(0.75)	(19.6)	4349.0	49.7	− 3.2
25.......	11.82	.073	19.1	19.9	0.8	19.5	4511.0	49.2	3.6
26.......	26.18	.418	19.0	19.9	0.9	19.45	4319.0	46.6	3.6
27.......	24.07	.381	18.75	19.45	0.7	19.1	4324.0	49.4	5.8
28.......	26.78	.428	18.25	19.35	1.1	18.8	4147.0	51.7	6.9
29.......	19.524	.290	19.1	(20.0)	(0.9)	(19.55)	4444.0	49.4	6.7
30.......	18.28	.262	18.75	19.85	1.1	19.3	4383.0	44.5	4.9
31.......	22.73	.357	19.1	20.0	0.9	19.55	4349.0	48.0	2.1
32.......	25.32	.403	18.7	19.6	0.9	19.15	4318.0	61.9	6.0
33.......	18.82	.275	18.7	19.3	0.6	19.0	4031.0	54.0	1.9
34.......	32.25	.508	18.8	19.9	1.1	19.35	4708.0	42.0	9.4
35.......	17.49	.243	18.95	(19.6)	(0.65)	(19.3)	4356.0	34.3	4.2
36.......	17.90	.253	19.05	(19.75)	(0.7)	(19.4)	4325.0	53.0	8.4
37.......	13.328	.125	19.3	(19.9)	(0.6)	(19.6)	4319.5	52.6	2.6
38.......	10.128	.005	19.3	(20.0)	(0.7)	(19.65)	4357.0	51.2	5.1
39.......	23.92	.379	19.1	(20.1)	(1.0)	(19.6)	4730.0	46.5	7.4
40.......	33.455	.524	18.4	19.2	0.8	18.8	4373.0	48.0	3.5
41.......	25.458	1.406	18.8	19.7	0.9	19.25	4379.0	56.7	5.1
42.......	175.	2.243	17.9	19.2	1.3	18.55	4425.0	58.1	2.4
45.......	12.90	1.111	19.3	(20.0)	(0.7)	(19.65)	4084.0	51.9	8.0
46.......	12.93	1.112	19.2	(19.8)	(0.6)	(19.6)	4321.5	+52.4	−1.4
Mean..	....	1.350	18.81	....	....	....	....	....	....
Mean, omitting No. 42	....	1.327	18.83	....	....	....	....	....	....

* Add 2,420,000 to tabular values.

† Positions are referred to the nucleus, *X* along the major axis, + to the south preceding; *Y* along the minor axis, + to the north preceding.

‡ Magnitudes in parentheses are uncertain.

tain and are bracketed in order to indicate this fact. Positions are given to the nearest 0.′1 with respect to a system of co-ordinates determined by the major and minor axes of the nebula, and the stars themselves are marked on the various plates used as illustrations. The same system is used for the novae and will be described more fully in connection with the distribution of those objects. For the present it is sufficient to mention that Cepheids are rare in the unresolved nuclear region and that position in the nebula appears to have no effect on the period-luminosity relation.

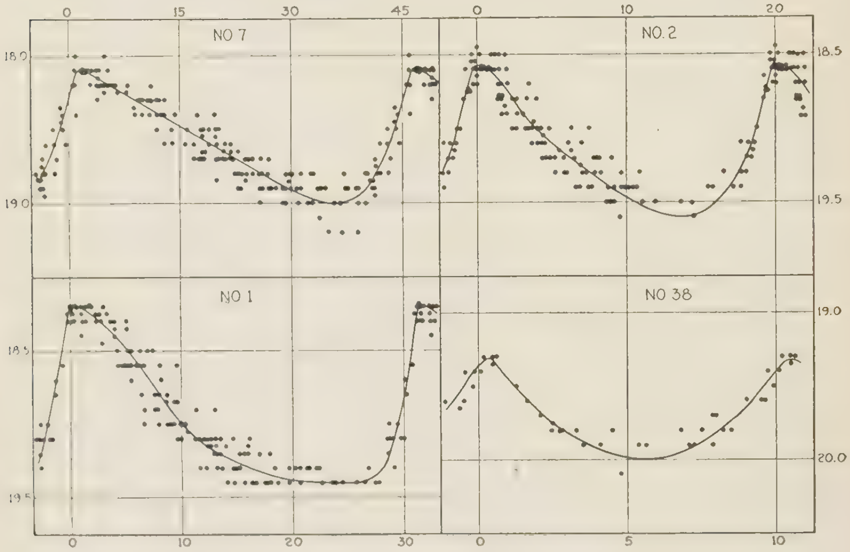

Fig. 1.—Light-curves of four Cepheids in M 31; ordinates, photographic magnitudes; abscissae, days.

The periods of the Cepheids range from forty-eight to ten days, and the magnitudes at maxima, from 18.1 to 19.3, with the exception of No. 42, which varies from 17.9 to 19.2 in a period of one hundred and seventy-five days. The Cepheid characteristics are obvious in the normal curves illustrated in Figure 1, and the forms of the curves tend to harmonize with Hertzsprung's relation between shape and period.[1]

The numbers of Cepheids increase steadily as the periods shorten, with a limit at about seventeen days. This appears to represent the general limit of the data, and the five variables with shorter periods may be regarded as chance catches. Other very faint variables have been found, but the very exacting conditions required for determining periods have not as yet been realized. There are indications, however, that the periods of some at least are less than ten days.

---

[1] *Bulletin of the Astronomical Institute of the Netherlands*, **3**, 115 (No. 96), 1926.

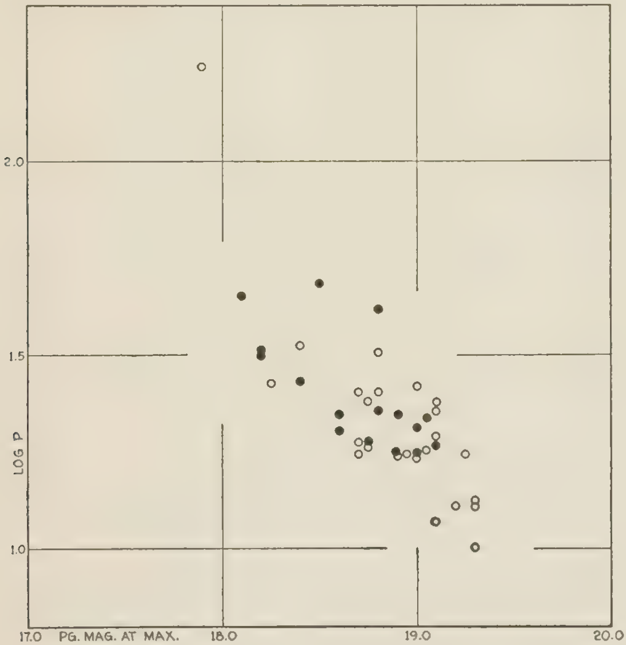

FIG. 2.—Period-luminosity relation among Cepheids in M 31. Photographic magnitude at maximum plotted against logarithm of period expressed in days. Cepheids in Region 4 are designated by circles in order to emphasize the absence of any selective effect due to position in the nebula.

In Figure 2, the logarithms of the periods have been plotted against magnitudes at maxima. The variables in Region 4 have been distinguished by circles in order to emphasize the absence of any effect that can be attributed to location in the nebula. The relatively larger number of very faint variables in the outer region is probably due to the longer exposures used in studying that field.

The period-luminosity relation is clearly shown, although the range is limited and the data for the fainter magnitudes are incomplete. The slope is approximately that of the curve published by Shapley for Cepheids in the Small Magellanic Cloud.[1] The residuals, which average about 0.2 mag., are slightly smaller than those found by Shapley, but the difference can be attributed largely to the incompleteness of the data for the fainter variables. Number 42, the outstanding exception, deviates from the curve by 0.75 mag., but the next largest residual, that for No. 16, is less than 0.5 mag.

The distance of M 31 has been derived by comparing Figure 2 with corresponding diagrams for Cepheids in M 33 and in the Small Magellanic Cloud. The latter diagrams, drawn on transparent paper, were superposed on Figure 2 and shifted along the axis of magnitudes until the best fit was obtained. Some personal judgment was involved in allowing for the effects of selection in favor of brighter stars among the shorter periods, but the limits of the probable errors are small.

In the case of the two spirals, where the scales of magnitudes are strictly comparable, since they are based largely upon the same Selected Areas, the shift in m, the apparent magnitude, was determined as 0.1 mag., in the sense that the stars in M 31 are the fainter. A shift of 0.1 mag. in either direction from this adopted value appreciably unbalanced the fit, hence the probable error of the determination was estimated to be of the order of 0.05 mag.

M 33 had already been compared with the Small Magellanic Cloud in order to determine the relative distance, hence the comparison of M 31 with the cloud was largely a check on the previous comparison. The result for the new comparison, $\Delta m = 4.7 \pm 0.1$, agrees, within the probable errors, with the value for M 33 when corrected for the difference between the two spirals.

The data for the two spirals are so nearly comparable—thirty-five Cepheids being known in M 33 and forty in M 31—that they may be combined into a single diagram for a final comparison with the diagram for the Small Magellanic Cloud. The result is shown in Figure 3. The magnitudes for the Cepheids in M 33 have been increased by 0.1 mag. in order to reduce them to the distance of M 31. These seventy-five variables form a period-luminosity diagram of considerable weight, in which the internal relations are reasonably consistent.

---

[1] *Harvard Circular*, No. 280, 1925.

To obtain the best fit, the superposed diagram for the Small Cloud was shifted 4.65 mag., with an estimated probable error of 0.1 mag. The magnitudes at maximum of the Cepheids in the Small Cloud, increased by 4.65 mag., are included in Figure 3 in order to show the appearance of the diagram for what was judged to be the best agreement. For the sake of completeness, nine Cepheids in N.G.C. 6822 have also been included, their magnitudes increased by 0.55 mag.[1] Figure 3, therefore, includes all extra-galactic Cepheids for which data have been published.

No corrections to the distances of N.G.C. 6822 and M 33 as previously determined are indicated. The distance of M 31 is about 0.1 mag., or 5 per cent, greater than that of M 33, and 8.5 times the distance of the Small Magellanic Cloud. Using Shapley's value for the cloud ($m-M=17.55$), we find for M 31

$$\begin{aligned} m-M &= 22.2 \\ \pi &= 0''.00000363 \\ \text{Distance} &= 275{,}000 \text{ parsecs} \\ &= 900{,}000 \text{ light-years} \end{aligned}$$

---

[1] The periods of the Cepheids in N.G.C. 6822, as published in *Mt. Wilson Contr.*, No. 304; *Astrophysical Journal*, 62, 409, 1925, were derived from rather limited material. Additional data collected in the last two years have led to some revision. The revised periods, which are believed to be reliable, are as follows:

No. 7	65.05 days	No. 4	17.36 days
2	37.50	9	16.84
1	30.47	5	13.864
3	29.24	13	122.
6	20.00		

The possibility of periods close to an even day or submultiple thereof has definitely been eliminated in the case of variables Nos. 2, 4, 5, and 6 by series of morning and evening plates on successive nights. Numbers 10 and 12 appear bright and faint in alternate seasons and probably have periods of the order of six hundred days. Their color-indices are estimated as moderately large, but the stars are not red. No revisions have been found necessary for Nos. 8 and 11, but the data in these cases are very uncertain. Two new variables have been found, both of which appear to be irregular. One of these stars is very red.

Continued observation of M 33 has led to the discovery of two additional novae, making four in all, and of two new variables, but to no revision in the periods of the Cepheids. Dr. W. Baade, of the Hamburg Observatory, has communicated by letter his discovery of an additional variable in the extreme northern region of M 33. This star appears near the edge of several of the Mount Wilson plates, where the variation, although small, is quite definite. It is one of the brightest variables in the region, being surpassed only by Nos. 1 and 2.

The accuracy of the relative distances is very satisfactory. In the case of the two spirals, the probable error is of the order of 2.5 per cent; for the spirals and the Cloud, it is of the order of 5 per cent. The accuracy of the distances in parsecs or light-years, however, depends largely upon the accuracy of the zero point of the period-luminosity curve. Accumulating evidence indicates that Shapley's value is certainly of the right general order of magnitude, but there still remains the possibility of a considerable correction when more data on galactic Cepheids become available.

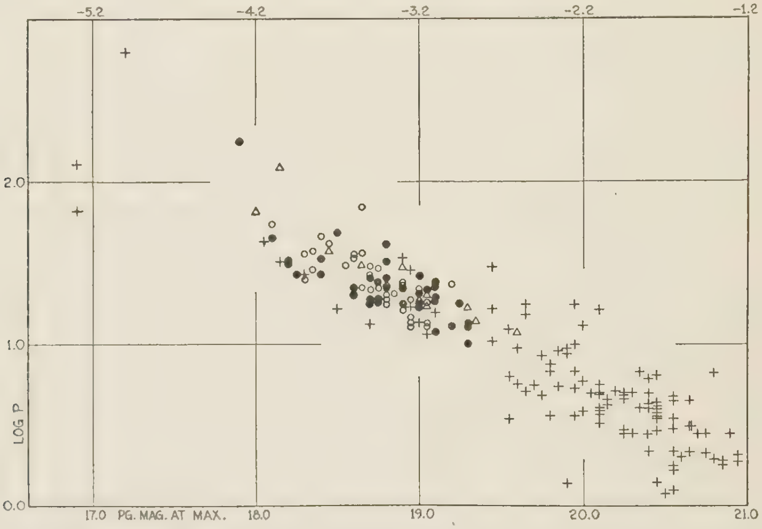

FIG. 3.—Period-luminosity relation among the extra-galactic Cepheids. The crosses refer to 106 Cepheids observed by Shapley in the Small Magellanic Cloud; the black discs, to 40 Cepheids in M 31; the open circles, to 35 in M 33; the triangles, to 9 in N.G.C. 6822. The apparent magnitudes at maxima have been reduced to the distance of M 31 by adding 4.65 to those in the Small Magellanic Cloud, 0.1 to those in M 33, and 0.55 to those in N.G.C. 6822. The absolute photographic magnitudes at the top of the diagram are based upon Shapley's zero point ($m-M=17.55$ for the Small Magellanic Cloud).

Variables other than Cepheids.—Of the ten variables other than recognized Cepheids, four are probably Cepheids for which the data are insufficient to establish the characteristics, while six are irregular or have long periods. To the first class belong the following stars:

Variable No.	Max.	Min.	X	Y
47.......	19.7	20.3	+55.5	−3.9
48.......	19.6	20.3	48.8	4.0
49.......	19.6	20.3	49.7	4.4
50.......	19.2	(19.5)	+50.0	−6.2

Number 50 is involved in a group or cluster, and is especially difficult to observe. These stars can be followed, in general, only on plates exposed under exceptionally good conditions. Short periods, however, may be inferred from the short duration of maxima. In the case of No. 47, two maxima have been observed with an interval of five days.

The irregular or long-period variables are Nos. 11, 15, 19, 20, 43, and 44.

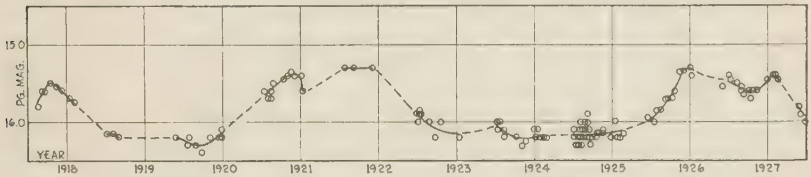

FIG. 4.—Light-curve of variable No. 19

Number 11 ($X=-7'.5$; $Y=-8'.3$) has varied from 18.6 to about 19.6. The brightest maximum occurred in the autumn of 1917, and seven years later it again rose above 19.0.

Number 15 ($X=-16'.1$; $Y=-10'.4$), the second brightest variable in the nebula, rose gradually from 17.5 in 1909 to 16.8 in 1924. In 1926 it faded to 17.3, but rose again to 17.0 in 1927, and in 1928, to about 16.7. The absolute magnitude at maximum, calculated with the distance indicated by the Cepheids, is about −5.5. The color-index appears to be less than 0.2 mag.

Number 19 ($X=-2'.3$; $Y=-9'.8$) is the brightest of all the variables that have been observed. Its color-index is uncertainly estimated as of the same order as that of No. 15—less than 0.2 mag. The variation is from about 15.3 to 16.3, and there are some indications of a period of the order of five years. The light-curve, however, which is shown in Figure 4, does not repeat itself very faithfully, and further observations will be required to settle the question. If the star actually belongs to the nebula, the absolute magnitude varies from −6.9 to −5.9. Numbers 15 and 19 show some analogies with variables Nos. 1 and 2 in M 33. Number 19 was found independently by W. J. Luyten on plates made with the 24-inch Bruce camera.[1]

Number 20 ($X = +4'.6$; $Y = +11'.5$) was recorded on several plates from 1909 to 1910 as about 18.6. By 1915, however, it had risen to about 18.0, where it has remained up to the present. For this reason the individual observations are not listed in Table I. The star may be similar to those listed as novae Nos. 36 and 39, which appeared suddenly but have remained constant since their appearance. It may be significant that these are among the faintest novae that have been observed.

Numbers 43 ($X = +51'.3$; $Y = -4'.8$) and 44 ($X = +43'.5$; $Y = -8'.1$) are in Region 4 and hence have been observed only since 1924. The former appears to be red, while the latter has a color-index considerably less than the color-indices of the Cepheids. Number 43 averaged about 19.8 in 1924–1925 and about 19.4 in 1925–1926. From 19.2 in August, 1926, it rose to 18.9 in September, only to fade again until by January, 1927, it was 19.6. In July it was still faint, about 19.7, but rose rapidly to 18.9 in October. By January, 1928, however, it had faded to 19.5, and by August had reached 19.8.

Number 44 has varied from 18.7 to about 19.4. It was active during the first season, 1924–1925, rising, fading, and rising again to the maximum observed luminosity. During 1925–1926 it averaged about 18.8, and since then, about 19.2.

The significant feature of these stars appears to be their restricted ranges in luminosities. They are giant stars and might well be classed as "super-giants." One, No. 43, is clearly red, but three at least appear to be early-type stars. The red star may be analogous to Betelgeuse, but stars similar to the other three variables are not known in our own system. It is not improbable, however, that the variables found in M 81 and N.G.C. 2403, and some at least of those in M 101, are similar to the bright irregular variables in M 31 and 33, and may eventually be used as rough criteria of distances.

---

[1] *Harvard College Observatory Bulletin*, No. 851, 1927, in which Luyten announces another variable, about 13.5 at maximum, on the extreme edge of M 31, north following the nucleus. Color and type of variation are uncertain, but in view of the relative luminosity, further data will be required to determine a connection with the spiral.

NOVAE

S Andromedae, the first nova found in the spiral, was discovered visually in August, 1885. It was announced by Hartwig, although, as subsequently disclosed, it had been seen previously by several other observers. The position of this nova, about 16″ preceding and 4″ south of the nucleus, is unique. No other has been found within 1′.5 of the nucleus, although it should be remembered that only exceptionally bright novae could be detected on the dense background of unresolved nebulosity in this region. The photometric measures of the first nova are rather discordant, but a general review of the published results indicates that the visual magnitude at maximum was about 8.0. This places it at once in that mysterious class of exceptional novae which attain luminosities that are respectable fractions of the total luminosities of the systems in which they appear.

Photographic observations of novae in M 31 began in 1917. Ritchey had found a nova in N.G.C. 6946 and, following up the suggestion, examined all the negatives of spirals in his collection. Indications of changes, novae or variables, were reported in M 81, M 101, and N.G.C. 2403, but no further investigations were made of these objects.[1] In M 31, however, two novae were found on the first plates of the nebula obtained with the 60-inch reflector in the autumn of 1909, and sufficient data were available to establish the character of the variation. Other plates of the spiral were immediately obtained, and these led to the discovery of six additional novae during the season 1917–1918, by Ritchey, Shapley, and Duncan. During the next five years the spiral was photographed more or less sporadically, and thirteen novae were discovered by Sanford, Humason, Duncan, Shapley, and Miss Ritchie.

---

[1] *Publications of the Astronomical Society of the Pacific*, **29**, 210, 1917. Ritchey's remarks refer to the following objects: (*a*) The star in M 81 is 4′.5 from the nucleus in a direction S 27° W. On two plates taken in February, 1910, it was about 19.0; on three plates in March, 1916, and March and December, 1917, it was about 18.6; in April, 1921, and from 1924 to 1927 it was normal again at 19.0. Six additional variables have since been found, and all appear to be analogous to the brighter irregular variables in M 31. (*b*) The object in N.G.C. 2403 appears to be a defect. Under a microscope the edges are sharper and the color more brownish than the ordinary star-images. Five variables are now known in this nebula, but the nature of the variations is uncertain. (*c*) In M 101, two stars were marked. One, 2′.85 due south of the nucleus, was about 18.8 in March, 1910, and about 19.5 in May, 1915. On a few subsequent long exposures it appears about the latter luminosity. The other star, 4′.13 from the nucleus in the direction S 4° E, was about 19.2 in 1910 and 19.6 in 1915. From 1922 onward it has remained constant at about 18.5. Eight other variables have since been found.

The 1910 plate of M 101 shows a star of 16.8 mag., some 12′.3 from the nucleus in the direction W 35° N, which does not appear on any of the later plates. It was not mentioned by Ritchey, although the image shares the distortion, due to coma, of the other images and there seems to be no reason for doubting that it represents an actual star. It might well be an unusually bright nova.

In the autumn of 1923 the writer began to photograph the nebula more systematically in order to accumulate data for the statistical study of novae. Since that time sixty-three additional novae have been found, and the material is now sufficient for a preliminary general discussion.[1] The nova of 1885 is clearly an exceptional case, and the eighty-five photographic novae must be considered as normal.

Although more than three hundred plates are now available, the material is not strictly homogeneous with respect either to effective exposure or to spacing in time. The 60- and 100-inch reflectors have been used indiscriminately under all conditions of seeing and with exposures ranging from twenty minutes to upward of two hours. The limiting magnitudes on the various plates are usually 19.0 or fainter, although occasionally they may be brighter than this by 0.5 mag. or more. A hundred plates, however, show stars fainter than 20.0. The observing seasons ran from June to February. The exposures were all made during the dark of the moon. From first quarter to third quarter both reflectors are always used in the Cassegrain form with the spectrographs attached, and hence are not available for direct photography. As a result, at least half of each lunation was unobserved, and generally the remaining half was not fully covered. For the years before 1923, the gaps are considerably greater. Following Ritchey's excellent series in the autumn of 1909, only four plates were exposed during an interval of eight years.

In general, the plates were centered on the nucleus and, as regards limiting magnitudes, the distortion of the images in the outer regions is roughly balanced by the background of unresolved nebulosity near the nucleus. Since the plane of the spiral is but little inclined to the line of sight, a strip nearly 30′ wide, extending entirely across the nebula at right angles to the major axis, has been observed in a fairly homogeneous manner. In addition, Region 4, with its center some 48′ south preceding the nucleus along the major axis, has been under observation since 1924; Regions 2 and 3 were well observed during the season 1924–1925; about thirty plates were centered on other regions or covered large areas with long exposures. These furnish information concerning the outer regions of the spiral supplementary to that contained in the main series centered on the nucleus.

---

[1] The four novae, Nos. 87–90, discovered by Duncan in August, 1928, are not included in the present discussion. The announcement is in *Publications of the Astronomical Society of the Pacific*, **40**, 347, 1928.

Following the procedure established in 1917, the novae have been numbered serially according to the date of discovery. Number 1 is therefore the great nova of 1885, S Andromedae; Nos. 2–22, inclusive, are the photographic novae found at Mount Wilson from 1917 to 1922; Nos. 23 and upward are the novae found by the writer from 1923 to 1927. Data on Nos. 2-21 have been published from time to time in *Publications of the Astronomical Society of the Pacific*.[1] The magnitudes were generally estimated by comparison with a sequence of stars measured by Shapley with the 60-inch telescope. These measures have not been published, but are on file at Mount Wilson.

New measures by the writer with the 100-inch are in fair agreement down to about 17.0, but beyond this point they diverge somewhat, probably because of the greater efficiency of the larger telescope in registering star-images free from the nebulous background. For the sake of homogeneity, the plates of the older novae have been re-examined and the magnitudes have been re-estimated by comparison with the new sequence. These data, together with those for the more recent novae, are given in full in Table IV. The date of the plate immediately preceding that on which a nova first appeared and the date of the plate next following that on which it was last

---

[1] The references are as follows:

Novae 2, 3	**29**, 210, 1917	Novae 12, 13	**31**, 109, 1919
4	**29**, 213, 1917	14, 15, 16	**31**, 280, 1919
5	**29**, 257, 1917	17	**32**, 63, 1920
6, 7, 8	**30**, 162, 1918	18, 19, 20	**33**, 56, 1921
9	**30**, 255, 1918	21	**34**, 222, 1922
10, 11	**30**, 341, 1918		

TABLE IV

MAGNITUDES OF NOVAE IN M 31

1909	J.D.	Plate	Qy.	2‡	3	38				
Sept. 12	8562.5*	R17	G	18.3+	18.2+					
12	8562.7	18	F	17.6	17.5	18.7				
13	8563.45	19	G	16.9	17.7	18.7				
13	8563.65	20	G	17.4	17.7	18.7				
15	8565.45	26	E	16.7	17.4	18.9				
16	8566.65	27	F	16.8	17.1	18.8				
Oct. 11	8591.45	34	E	17.4	17.6	18.8				
13	8593.35	39	G	17.5	17.7	19.4				
Nov. 7	8618.3	47	P	17.9	17.5	19.4+				
7	8618.5	48	P	18.0	17.6	18.3+				
1917–18	**J.D.**	**Plate**	**Qy.**	**4**	**5**	**6**	**7**	**8**	**9**	**85**
Aug. 12	1462.65†	P300	G	18.6+						
Sept. 11	1483.45	Sh3991	P	17.5						
17	1489.5	R146	G	17.7	18.5+					
Oct. 13	1515.5	Sh4091	VP	18.2+	17.3					
16	1518.5	R147	F	18.6	17.4	18.3+				
Nov. 14	1547.5	151	G	18.5+	18.2	16.5	....	....	....	19.0+
Dec. 12	1575.4	154	G	....	18.5+	17.5	....	....	....	17.4
13	1576.4	156	G	....	....	17.6	18.6+	....	....	17.4
Jan. 15	1609.3	161	G	....	....	18.3	17.1	18.5+	18.5+	19.0+
17	1611.3	Sh4333	VP	....	....	17.6+	17.1	17.6+	17.6+	
Feb. 9	1634.3	R162	F	....	....	18.5+	18.5+	17.5	17.5	
10	1635.3	163	F	....	....	....	....	17.4	17.5	
1918–19	**J.D.**	**Plate**	**Qy.**	**10**	**11**	**12**	**13**			
Aug. 30	1836.6	Sh4663	P	18.0+	18.0+					
Oct. 7	1874.4	Sa10	F	17.4	17.6					
8	1875.36	Sa12	F	17.5	17.6					
8	1875.38	13	F	17.5	17.7					
Nov. 2	1900.4	17	G	17.8	18.8+					
2	1900.4	18	F	17.8	....	18.5+	18.5+			
Jan. 4	1963.23	21	P	18.0+	....	17.0	17.2			
4	1963.24	22	P	....	....	17.1	17.2			
5	1964.3	23	P	....	....	17.0	17.3			
Feb. 3	1993.25	27	G	....	....	17.5	18.5			
3	1993.3	28	G	....	....	17.5	18.5			
1919	**J.D.**	**Plate**	**Qy.**	**14**	**15**	**16**	**17**	**86**		
June 28	2138.7	Sa36	P	....	17.7					
29	2139.7	37	G	....	17.8					
30	2140.6	38	G	....	17.9					
30	2140.7	39	F	18.8+	18.0					
July 21	2161.6	Sh4978	F	16.1	17.4					
23	2163.6	5025	F	16.1	17.5					
28	2168.6	D24	P	16.2	17.4					
29	2169.6	27	G	16.3	17.6	17.8+				
Aug 24	2195.5	30	F	18.8+	17.9	17.1				
28	2199.5	Sa41	G	....	18.2	17.1				
29	2200.5	42	G	....	18.0	17.1				
Sept. 1	2203.5	46	P	....	18.0	17.2				
21	2223.5	Sh5054	P	....	17.9	17.4	....	16.7		
Oct. 16	2248.4	Sa49	P	....	18.0	17.8+	18.5+			
30	2262.4	Sh5105	VP	....	....	....	15.8			
31	2263.4	5107	G	....	18.0	....	16.6			
Nov. 30	2293.4	Sa50	F	....	18.2	....	18.5+			
Dec. 21	2314.3	Sh5160	G	....	18.2					
1920	**J.D.**	**Plate**	**Qy.**	**18**	**19**	**20**	**80**	**81**		
July 22	2528.6	Sh5479	P	....	....	....	17.8+			
Aug. 8	2545.6	5489	G	....	....	....	18.0			
10	2547.63	D42	F	....	....	....	17.9			
11	2548.56	44	E	....	....	....	18.0			
Sept. 12	2580.5	62	F	....	....	....	17.5			
13	2581.6	65	P	....	....	....	17.5			

TABLE IV—*Continued*

1920–21	J.D.	Plate	Qy.	18	19	20	80	81		
Sept. 16, 17	2585.0	71	G	18.5+	......	......	17.8			
17	2585.3	72	P	......	......	......	17.8			
Oct. 10	2608.5	76	F	17.2	......	......	18.1			
11	2609.6	80	P	17.3	......	......	18.2			
14	2612.3	S68	F	17.4	......	......	18.1			
Nov. 12	2641.6	75	F	18.3+	......	......	18.5			
13	2642.5	77	G	18.5+	18.5+	18.5+	18.5	19.0+		
Dec. 10	2669.3	D106	F	......	16.0	17.7	18.6	16.7		
10	2669.35	107	F	......	15.9	17.7	18.6	16.7		
12	2671.3	112	P	......	16.6	17.6	18.2+	17.1		
12	2671.33	113	P	......	16.7	17.6	......	17.2		
17	2676.4	B2	P	......	17.2	17.8	......	18.0		
Jan. 4	2694.3	D118	G	......	18.2	18.0	......	19.0+		
5	2695.3	122	F	......	18.3	18.0				
8	2698.4	132	F	......	18.5	17.8				
Feb. 6	2727.3	136	P	......	18.0+	18.0+				
1921	J.D.	Plate	Qy.	26§	83	20				
July 3	2874.6	B5	P	......	18.0+	18.0				
Aug. 1	2903.4	D200	P	......	17.6	18.0				
1	2903.45	201	P	......	17.6	18.0				
Oct. 4	2967.5	A6	P	19.0	18.5					
Dec. 5	3029.4	10	F	18.6	18.5+	18.3+				
1922–23	J.D.	Plate	Qy.	26	21	22	84	82		
May 29	3204.6	B40	P	18.6	18.0					
June 23	3229.6	A22	P	......	17.5					
28	3234.6	S150	F	......	17.8	......	19.0+			
July 20	3256.6	A29	P	18.6	18.5+	......	17.5			
22	3258.7	B51	F	......	......	......	17.5			
23	3259.6	56	F	......	......	......	17.6			
24	3260.7	S156	P	......	......	......	17.6			
25	3261.6	163	F	18.6	......	......	17.6			
27	3263.6	D220	P	......	......	......	17.6			
28	3264.65	222	P	18.6	......	......	17.6			
Aug. 20	3287.6	B58	P	......	......	......	17.7			
22	3289.6	62	P	......	......	......	17.8			
28	3295.6	S171	F	18.5	......	......	18.0			
Sept. 19	3317.7	172	F	18.5	......	......	19.0+			
24	3322.6	B67	F	......	......	......	......	18.5+		
Oct. 16	3344.4	70	G	......	......	......	......	17.9		
22	3350.3	A42	P	......	......	......	......	18.4		
Jan. 13	3433.3	B100	F	......	......	18.0+	......	18.5+		
Feb. 15	3466.3	A47	P	18.5	......	16.9				
1923–24	J.D.	Plate	Qy.	23	24	25	27	28	29	30
July 16	3617.8	S254	F	18.0+						
Aug. 7	3639.8	267	F	17.0						
9	3641.5	278	P	17.1	18.0+	18.3+				
Oct. 4	3697.55	H331	VP	17.5+	17.2	17.3				
5	3698.55	335	G	18.5+	17.3	17.4				
6	3699.4	S282	VP	......	17.3	17.4				
8	3701.35	B142	F	......	17.4	17.3				
9	3702.5	A61	G	......	17.2	17.3				
Nov. 13	3737.55	H339	G	......	18.5	18.4	18.5+	19.0+	19.0+	
Dec. 11	3765.45	348	G	......	18.5+	19.0	17.2	16.2	17.5	
14	3768.4	351	P	......	......	18.5+	17.5	16.2	18.0	
30	3784.3	B158	P	......	......	......	18.2	18.2+	18.0	
Jan. 4	3789.35	H353	P		......	......	18.0			
5	3790.4	S285	G	31	......	......	18.2			
6	3791.4	292	G		......	......	18.8	19.0+	19.0	
9	3794.3	H354	P	18.2+	......	......	18.5+	......	......	18.5+
31	3816.3	A69	P	16.8	......	......	......	......	......	17.3
Feb. 2	3818.3	S301	F	17.1	......	......	19.0+	......	19.0+	17.2
3	3819.3	310	F	17.1	......	......	......	......	......	17.2
4	3820.3	320	F	17.2	......	......	......	......	......	17.3
5	3821.3	H355	G	17.2	......	......	......	......	......	17.2
6	3822.3	357	F	17.2	......	......	......	......	......	17.3
7	3823.3	363	F	17.3	......	......	......	......	......	17.2
27	3843.3	A73	P	18.2+	......	......	......	......	......	18.5+

TABLE IV—*Continued*

1924–25	J.D.	Plate	Qy.	32	33	34	35¶	37	40	41	42
July 2	3969.55	H375	P	17.4							
2	3969.65	376	F	17.2							
4	3971.6	S329	P	16.4							
23	3990.5	336	P	17.5							
24	3991.6	338	G	18.0							
26	3993.6	339	G	18.0							
27	3994.6	344	G	18.0							
28	3995.5	348	G	17.5							
29	3996.55	H384	G	17.6							
30	3997.6	390	G	17.7							
31	3998.6	395	G	18.0							
Aug. 1	3999.6	S351	G	18.0							
2	4000.5	H397	F	18.0							
3	4001.6	398	P	18.3							
4	4002.6	404	E	18.0							
5	4003.5	405	E	18.2							
6	4004.45	414	E	18.2	18.5+	......	18.5+				
25	4023.4	B182	F	18.2	17.6	......	17.0				
26	4024.65	D241	F	18.4	17.4	......	16.8				
27	4025.63	246	G	18.8+	17.3	18.8+	16.9				
28	4026.5	S356	G	......	17.4	......	16.9				
29	4027.65	360	F	......	17.1	18.5+	17.1				
30	4028.5	H418	G	......	17.2	17.0	17.0				
31	4029.45	S361	F	......	17.3	16.2	17.1				
Sept. 1	4030.45	362	F	......	17.3	16.2	17.0				
2	4031.5	H421	G	......	17.4	16.8	17.0				
3	4032.5	426	G	......	17.3	17.1	17.2				
4	4033.5	430	G	......	17.4	16.4	17.0				
20	4049.4	S360	F	......	17.5	17.2	17.6				
21	4050.5	374	F	......	17.7	17.3	17.7	18.6+			
25	4054.5	H434	P	......	18.0	17.3	17.8	16.6			
26	4055.5	S376	G	......	......	17.5	17.8				
27	4056.5	385	G	......	18.0	17.6	......	16.6			
28	4057.5	388	G	......	18.0	17.8	18.0	17.2	19.5+		
30	4059.4	H444	G	......	18.0	18.0	18.2	17.5	19.0		
Oct. 26	4085.35	451	G	......	18.5+	18.6	18.5	......	19.0		
27	4086.4	S394	F	......	......	18.5	......	18.5	18.7		
30	4089.4	401	G	......	......	18.6+	18.7+	18.6	18.5		
31	4090.4	H457	G	......	......	......	......	18.6			
Nov. 2	4092.3	464	F	......	......	......	......	......	18.5		
18	4108.4	469	F	......	......	......	......	......	18.1		
19	4109.4	471	G	......	......	18.8	......	18.6			
22	4112.4	S406	P	......	......	......	......	......	18.0		
24	4114.4	411	G			18.8+		18.8	17.5		
Dec. 28	4148.35	H507	P	43	44	......	45	......	18.4		
30	4150.35	510	P			......		......	18.4	18.5+	18.3+
Jan. 17	4168.35	S417	P	......	18.2+	......	18.3+	......	18.1	17.1	16.4
19	4170.3	H514	P	18.2+	16.5	......	18.2+	......	18.2	17.4	16.7
26	4177.35	S424	F	16.8	17.8	......	17.7	......	18.3	17.5	17.1
27	4178.3	433	G	17.0	18.0	......	17.5	......	18.4	17.8	17.2
30	4181.35	H531	P	17.4	18.0	......	18.0	......	18.2	18.0	17.4
Feb. 15	4197.3	S434	P	18.2	18.5+	......	18.0	......	18.2	18.2+	18.2+

1925	J.D.	Plate	Qy.	47	48	49	50	51	52	53	54
June 17	4319.6	H571	F	17.7	17.0	19.0+	19.0+	19.0+	......	18.6	
19	4321.6	S483	G	17.5	17.0	......	......	......	......		
July 16	4348.55	H576	P	18.5+	18.2+	17.3	17.6	18.2	......	18.4	
17	4349.5	580	F	......	......	17.2	18.0	18.1	......	18.4	
19	4351.6	D251	F	19.0	19.0+	17.2	18.0	18.0	......		
24	4356.6	268	G	19.2	19.0+	17.8	17.6	18.3	......	18.8	
26	4358.5	S496	G	19.0+	......	18.0	18.0	18.7+	18.6+		
Aug. 14	4377.45	H586	F	18.3	......	19.0	19.0	......	17.3	18.6	
16	4379.7	598	P	18.0	......	19.2	19.0+	......	17.1	18.6	18.8+
Sept. 11	4405.7	604	VP	18.2	......	19.0	......	......	18.0	......	17.3
12	4406.6	607	VP	18.6	......	18.8+	......	......	18.5	18.5	15.3
19	4413.6	S499	P	......	......	......	......	......	18.5	18.5	15.7
20	4414.7	H609	F	19.0	......	19.2	......	......	18.5	18.8	15.7
Oct. 9	4433.3	615	P	......	......	......	......	......	18.8+	18.8	18.8+
17	4441.45	S505	F	19.0+	......	19.0+	......	......	......	......	19.0
20	4444.35	H617	F	......	......	......	......	......	19.0	18.2	19.0+
Nov. 10	4465.35	620	P	......	......	......	......	......	......	18.2	
20	4475.3	621	P	......	......	......	......	......	......	18.2	
Dec. 8	4493.35	H624	G	......	......	......	......	......	......	18.8	

TABLE IV—*Continued*

1925–26	J.D.	Plate	Qy.	55	56	57	58	59	60	61
June 17	4319.6	H571	F							
19	4321.6	S483	G	19.0+						
July 16	4348.55	H576	P	17.3						
17	4349.5	580	F	17.3						
19	4351.6	D251	F	17.6						
24	4356.6	268	G	18.0						
26	4358.5	S496	G	18.1						
Aug. 14	4377.45	H586	F	18.8						
16	4379.7	598	P	18.8	19.0+	......	19.0+			
Sept. 11	4405.7	604	VP	18.5+	......	......	18.5			
12	4406.6	607	VP	......	18.5+	......	18.5			
19	4413.6	S499	P	......	17.8					
20	4414.7	H609	F	......	17.7	18.5+	18.4			
Oct. 9	4433.3	615	P	......	18.8	17.4	18.6			
17	4441.45	S505	F	......	19.0	17.8	18.6	19.0+		
20	4444.35	H617	F	......	19.0+	17.7	17.5			
Nov. 10	4465.35	620	P	......	......	18.5	18.5	16.5	18.8+	
20	4475.3	621	P	......	......	18.5+	18.6	17.5	16.6	
21	4476.5	Se6276	F	......	......	......	......	17.5	16.5	
Dec. 8	4493.35	H624	G	......	......	......	18.6	18.3	17.8	18.6+
10	4495.35	626	P	......	......	......	......	18.4		
Jan. 6	4522.3	627	P	......	......	......	......	18.8+	18.8+	16.8
14	4530.3	SS 45	F	......	......	......	......	......	......	17.3
15	4531.3	H629	P	......	......	......	......	......	......	17.5
Feb. 16	4563.3	634	P	......	......	......	......	......	......	18.0+

1926–27	J.D.	Plate	Qy.	62	63	64	65	66	67	68	69
June 4	4671.65	S533	P	17.7							
13	4680.6	D304	VP	17.4	......	......	......	......	18.3+		
14	4681.6	309	VP	17.4	18.0+	18.0+	......	......	18.0+		
July 3	4700.6	315	G	17.8	17.3	17.5	18.8+	......	18.2		
12	4709.55	H668	F	18.2	17.4	18.0	18.2	19.0+	18.2		
14	4711.6	S539	G	18.4	17.4	18.0	18.3	......	18.3		
Aug. 11	4739.5	540	F	19.0+	17.7	18.0	18.2+	18.2	18.3		
Sept. 3	4762.4	H675	E	......	18.8	18.5	......	19.0	17.5		
5	4764.35	686	E	......	18.8	18.8	......	19.2	17.4		
11	4770.4	690	E	......	18.8	18.8	......	19.2	17.4		
13	4772.4	703	E	......	19.0+	19.0+	......	19.2	18.2	19.2+	
Oct. 4	4793.3	S545	G	......	......	......	......	19.2	18.2	17.7	
11	4800.3	H708	E	......	......	......	......	19.3+	18.5	18.0	
12	4801.3	S547	F	......	......	......	......	......	18.4	18.1	19.0+
Nov. 2	4822.5	BB104	G	......	......	......	......	......	18.5	18.4	17.4
3	4823.5	117	G				......	......	18.5	18.6	17.4
Dec. 1	4851.5	150	P	70	71	72	......	......	18.2	18.5	18.2
Jan. 1	4882.3	166	F				......	......	18.3	19.0+	18.6
2	4883.3	180	F	19.0+	......	......	......	......	18.4+	......	18.7
6	4887.3	197	P	18.5	......	......	......	......	17.7+		
27	4908.35	H715	G	18.1	19.0+	......	......	......	17.7	......	19.0
Feb. 6	4918.35	720	F	18.6	16.6	19.0+	......	......	17.5	......	19.3
25	4937.3	730	P	18.6	18.1	17.0	......	......	18.3	......	19.2+
26	4938.3	732	P	18.6+	18.4	17.3	......	......	18.3		

TABLE IV—*Continued*

1927	J.D.	Plate	Qy.	73	74	75	76	77	78	79	
May 23....	5024.65	H770	P	17.4	17.6+						
June 3....	5035.6	780	F	17.6	18.0						
4....	5036.6	785	G	17.7	17.7	18.5+					
20....	5052.6	789	P	17.7	17.8	18.0+					
July 1....	5063.6	798	G	18.0	17.8	18.4					
21....	5083.5	812	F	18.8	18.4	18.2					
29....	5091.5	815	P	18.2+	18.5+	18.0	18.0+				
Aug. 22....	5115.45	824	G	18.6+	......	18.5	17.1				
23....	5116.45	828	G	......	......	18.3	17.2				
31....	5124.4	832	F	......	......	18.3	17.5	19.0+	19.0+		
Sept. 11....	5145.35	S577	F	......	......	18.8	18.0	17.7	18.2		
23....	5147.6	H848	F	......	......	19.0	18.5	17.8	18.2		
25....	5149.6	855	F	......	......	19.0	18.5	17.8	18.3		
Oct. 22....	5176.35	S591	F	......	......	18.8+	18.5+	19.0	19.0+		
Nov. 1....	5186.3	H866	P	......	......	......	......	18.8	......	18.5+	
23....	5208.5	S603	G	......	......	......	......	19.0+	......	16.7	
26....	5211.3	H867	G	......	......	......	......	......	......	16.8	
28....	5213.45	885	F	......	......	......	......	......	......	16.6	
Dec. 19....	5234.4	888	F	......	......	......	......	......	......	17.5	

* Add 2,410,000.

† Add 2,420,000.

‡ A plus sign following the magnitude indicates limiting magnitudes of plates on which the novae did not appear. Novae are tabulated according to observing seasons, but numbered serially according to dates of discovery. High serial numbers in the earlier seasons represent novae found on re-examining the older plates.

§ Number 26 appeared in October, 1921, and by December had risen to 18.6. During the season 1922–1923 it remained about constant at 18.6, and from July, 1923, to December, 1925, at about 18.0. In January, 1925, it began to fade, but declined so slowly that it did not reach 19.5 until January, 1927. In 1928 it did not appear even on the best plates.

¶ Numbers 36, 39, and 46 are not listed. Number 36 first appeared in August, 1917, after an unobserved interval of two years, and has since remained constant at about 18.2. Number 39 first appeared in February, 1924, and is still visible, varying in an apparently irregular manner between 19.0 and 19.5. Number 46 appeared in Region 4, about 42′ from the nucleus, on the first plate of the season 1926–1927. The data are as follows:

J.D. 2,424,709.6	18.7
2,424,731.5	18.8
2,424,739.5	19.2
2,424,762.5	19.4
2,424,800.4	19.7+

On three plates between the last two dates, with limiting magnitudes about 19.4, the nova was invisible.

seen are included in the table. Magnitudes of stars in the immediate region of the nucleus fainter than about 18.0 are uncertain because of the nebulous background, but outside that region they should be fairly reliable down to about 19.0.

The significant data are collected in Table V. These include the observed duration of a nova; the unobserved intervals immediately preceding and following the observations; the magnitudes at the first observation, at maximum, and at the last observation; the intervals between the first observation and maximum, and between maximum and the next following observation; the number of observations; the approximate co-ordinates measured from the nucleus along the major axis (plus to the south preceding) and the minor axis (plus to the north preceding); and, finally, the latter co-ordinates multiplied

TABLE V

NOVAE IN M 31

Nova	Duration*			Magnitude				Interval between Observations		No. Obs.	Position†		
	Prec.	Obs.	Fol.	First Obs.	Last Obs.	Max. Obs.	Max. Cal.	1st — Max.	Max. — N'xt		X	Y	4Y
2.....	4hr	56d	....	17.6	18.0	16.7	16.7	2.8d	1d	9	+ 4′.0	+ 1′.0	+ 4′.0
3.....	4hr	56	....	17.6	17.6	17.1	17.1	3.8	25	9	+ 2.5	+ 2.2	+ 8.8
4.....	21d	35	29	17.5	18.6	17.5	16.7	0	6	3	−10.1	− 0.0	− 0.1
5.....	26	32	28	17.3	18.2	17.3	16.4	0	3	3	+ 3.9	− 2.2	− 8.8
6.....	29	62	25	16.5	18.3	16.5	15.5	0	28	4	− 5.2	+ 0.6	+ 2.4
7.....	33	2	23	17.1	17.1	17.1	15.9	0	2	2	+ 1.5	+ 1.95	+ 7.8
8.....	25	1	....	17.5	17.4	17.4	16.6	1	....	2	+ 1.8	+ 1.1	+ 4.4
9.....	25	1	....	17.5	17.5	17.5	16.7	0	1	2	− 8.8	− 2.7	−10.8
10.....	38	26	63	17.4	17.8	17.4	16.1	0	1	5	− 7.0	+ 2.9	+11.6
11.....	38	1	25	17.6	17.7	17.6	16.3	0	1	3	+ 4.9	− 3.5	−14.0
12.....	63	30	....	17.0	17.5	17.0	......	0	1	5	− 2.2	+ 3.3	+13.2
13.....	63	30	....	17.2	18.5	17.2	......	0	1	5	+ 5.7	+ 0.1	+ 0.4
14.....	21	8	26	16.1	16.3	16.1	15.3	0	2	4	− 0.1	− 5.3	−21.2
15.....	......	176	....	17.7	18.2	17.4	......	23	2	17	− 0.8	+ 3.7	+14.8
16.....	26	28	25	17.1	17.4	17.1	16.2	0	4	5	+ 4.15	+ 0.6	+ 2.4
17.....	14	1	30	15.8	16.6	15.8	15.2	0	1	2	− 2.2	+ 1.4	+ 5.6
18.....	25	4	29	17.2	17.4	17.2	16.3	0	1	3	− 0.2	+ 1.3	+ 5.2
19.....	27	29	29	16.0	18.5	15.9	15.0	1hr	2	8	+ 2.3	− 1.9	− 7.6
20	27	29	....	17.7	17.8	17.6	16.7	2	5	9	− 2.6	− 0.8	− 3.2
21.....	......	29	22	18.0	17.8	17.5	16.7	24	5	3	− 4.65	− 1.5	− 6.0
22.....	33	....	....	16.9	16.9	16.9	15.8	....	....	1	− 1.6	− 0.1	− 0.4
23.....	22	2	56	17.0	17.1	17.0	16.2	0	2	2	+ 1.8	+ 2.65	+10.6
24.....	56	40	28	17.2	18.5	17.2	......	0	1	6	+ 9.6	+ 1.25	+ 5.0
25 ...	56	68	3	17.3	19.0	17.3	......	0	1	7	+12.35	+ 0.5	+ 2.0
26	64	5.5yr	....	19.0	19.5	18.0	......	3yr	....	....	+ 3.2	− 5.4	−21.6
27.....	28	26	27	17.2	18.8	17.2	16.3	0	3	6	− 0.5	+11.7	+46.8
28.....	28	3	16	16.2	16.2	16.2	15.3	0	3	2	− 5.45	− 4.05	−16.2
29.....	28	26	27	17.5	19.0	17.5	16.6	0	3	4	+ 6.8	− 3.5	−14.0
30.....	22	7	20	17.3	17.2	17.2	16.4	2	1	7	+11.0	− 6.25	−25.0
31.....	22	7	20	16.8	17.3	16.8	16.0	0	2	7	0.0	− 2.7	−10.8
32.....	......	55	1	17.4	18.4	16.4	16.4	2	19	19	+ 6.8	− 0.6	− 2.4
33.....	19	36	26	17.6	18.0	17.1	16.4	4	1	17	+ 0.75	−2.95	−11.8
34.....	1	58	3	17.0	18.5	16.2	16.2	1	1	15	− 0.45	− 3.6	−14.4
35.....	19	62	4	17.0	18.5	16.8	16.3	1	1	18	+ 2.1	+ 1.5	+ 6.0
36‡....	......	11yr	....	18.2	18.2	......	......	....	....	....	−10.25	+ 2.6	+10.4
37.....	4	60	34	16.6	18.8	16.6	16.4	0	2	9	−32.4	−14.3	−57.2
38.....	......	31	25	18.7	19.4	18.7	......	0	1	8	+16.3	− 9.9	−39.6
39§...	25	4.5yr	....	19.0	19.5	......	......	....	....	....	+ 0.7	+ 6.65	+26.0
40.....	2	138	....	19.0	18.2	17.5	17.5	55	34	16	+ 4.35	−10.3	−41.2
41.....	18	13	16	17.1	18.0	17.1	16.4	0	2	5	− 5.0	+ 1.3	+ 5.2
42	18	13	16	16.4	17.4	16.4	15.7	0	2	5	+ 3.8	+ 1.3	+ 5.2
43.....	7	20	....	16.8	18.2	16.8	16.5	0	1	4	+ 4.4	− 0.15	− 0.6
44	2	11	16	16.5	18.0	16.5	16.4	0	7	4	+ 7.9	−11.9	−47.6
45	7	20	....	17.7	18.0	17.5	17.3	1	3	4	+ 3.05	−12.25	−49.0
46.....	......	53	8	18.7	19.4	18.7	......	0	22	4	+41.5	+ 3.7	+14.8
47.....	......	95	27	17.7	19.0	17.5	......	2	27	11	− 8.2	− 0.1	− 0.4
48.....	......	2	27	17.0	17.0	17.0	......	0	2	2	+18.4	+ 2.7	+10.8
49.....	29	66	27	17.3	19.2	17.2	16.2	1	2	9	− 9.6	− 7.5	−30.0
50.....	29	29	2	17.6	19.0	17.6	16.6	0	1	6	−13.65	+ 1.1	+ 4.4
51.....	29	8	2	18.2	18.3	18.0	17.1	3	5	4	+10.2	− 0.5	− 2.0

TABLE V—*Continued*

Nova	Duration*			Magnitude				Interval Between Observations		No. Obs.	Position†		
	Prec.	Obs.	Fol.	First Obs.	Last Obs.	Max. Obs.	Max. Cal.	1st—Max.	Max.—N'xt		*X*	*Y*	4*Y*
52.....	19d	67d	19d	17.3	19.0	17.1	16.4	2	26	8	+ 3.15	− 0.9	− 3.6
53.....	......	174	....	18.6	18.8	18.2	......	126	21	15	− 2.8	+ 0.2	+ 0.8
54.....	26	36	3	17.3	19.0	15.3	15.3	0.8	7	6	−18.6	+ 1.65	+ 6.6
55.....	27	31	26	17.3	18.8	17.3	16.4	0	1	7	+ 5.2	− 0.65	− 2.6
56.....	7	28	3	17.8	19.0	17.0	16.4	1	19	4	− 1.1	+14.5	+58.0
57.....	19	32	10	17.4	18.5	17.4	16.7	0	8	4	+ 4.6	+ 0.7	+ 2.8
58.....	26	88	....	18.5	18.6	17.5	17.5	39	21	9	− 1.6	− 1.8	− 7.2
59.....	24	30	27	16.5	18.4	16.5	15.7	0	10	5	+11.4	− 1.6	− 6.4
60.....	10	18	29	16.6	17.8	16.5	16.1	1	17	3	−24.3	− 7.5	−30.0
61.....	29	9	32	16.8	17.5	16.8	15.8	0	8	3	+ 1.9	− 0.3	− 1.2
62.....	......	40	28	17.7	18.4	17.4	16.7	9	1	6	+17.5	+ 2.2	+ 8.8
63.....	19	70	2	17.3	18.8	17.3	16.6	0	9	7	+ 1.75	− 1.1	− 4.4
64.....	19	70	2	17.5	18.8	17.5	16.8	0	9	7	+ 0.8	+ 1.75	+ 7.0
65.....	9	2	28	18.2	18.3	18.2	17.8	0	2	2	− 0.9	− 1.2	− 4.8
66.....	30	54	7	18.2	19.2	18.2	17.2	0	23	6	+ 2.9	− 6.0	−24.0
67.....	19	238	....	18.2	18.3	17.4	16.6	64	6	21	+ 4.1	+ 1.5	+ 6.0
68.....	21	58	31	17.7	18.5	17.7	16.9	0	7	6	−10.9	+ 2.4	+ 9.6
69.....	21	96	19	17.4	19.3	17.4	16.6	0	1	7	+ 7.8	− 3.5	−14.0
70.....	4	50	1	18.5	18.6	18.1	16.8	21	10	4	−18.1	+ 0.1	+ 0.4
71.....	10	20	....	16.6	18.4	16.6	16.1	0	19	3	−16.9	− 0.5	− 2.0
72.....	19	1	....	17.0	17.3	17.0	16.2	0	1	2	+ 2.5	− 1.3	− 5.2
73.....	......	59	8	17.4	18.8	17.4	......	0	11	6	+ 4.3	− 0.35	− 1.4
74.....	11	48	8	18.0	18.4	17.7	17.7	1	16	5	+16.1	− 2.6	−10.4
75.....	11	86	27	18.4	19.0	18.0	16.9	28	24	9	− 5.95	− 2.6	−10.4
76.....	24	34	27	17.1	18.5	17.1	16.3	0	1	6	+ 3.45	− 0.6	− 2.4
77.....	21	41	22	17.7	18.2	17.7	16.9	0	2	5	+ 6.05	+ 7.55	+30.2
78.....	21	4	27	18.8	18.3	18.2	17.4	0	2	3	+14.5	+ 0.5	+ 2.0
79.....	22	26	....	16.7	17.5	16.7	15.9	0	3	4	+ 1.5	+ 2.0	+ 8.0
80.....	17	124	2	18.0	18.6	17.5	17.3	35	1	14	+ 3.0	+ 2.8	+11.2
81.....	27	7	18	16.7	18.0	16.7	15.8	0	2	5	− 7.4	−11.7	−46.8
82.....	22	6	....	17.9	18.4	17.9	17.1	0	6	2	− 7.1	+ 1.8	+ 7.2
83.....	27	64	62	17.6	18.5	17.6	16.7	0	64	3	+ 3.0	− 2.35	− 9.4
84.....	22	39	22	17.5	18.0	17.5	16.7	0	2	10	+12.2	− 1.15	− 4.6
85.....	28	1	33	17.4	17.4	17.4	16.5	0	1	2	−11.5	− 8.3	−25.2
86.....	20	0	25	16.7	......	16.7	16.0	....	....	1	− 9.4	− 3.3	−13.2
Mean ¶	......	....	....	......	......	17.20	16.43	....	....	....	....	....	......

---

* Under "Duration" are listed the length of the unobserved interval preceding the first observation, the interval between the first and the last plates on which the nova appeared, and the unobserved interval following the last observation. When no preceding interval is given, the nova appeared on the first plate of an observing season. The intervals are expressed in days unless otherwise designated.

† Positions are given with respect to the nucleus, *X* along the major axis (plus to the south preceding), *Y* along the minor axis (plus to the north preceding). The last column gives the *Y* co-ordinate corrected for foreshortening due to the inclination of the nebula to the line of sight.

‡ Number 36 first appeared in August, 1917, following an unobserved interval of two years, and has maintained a constant luminosity, 18.2, up to the present time.

§ Number 39 first appeared in February, 1924, and has remained visible up to the present, varying between 19.0 and 19.5.

¶ The mean observed maximum represents 82 novae; Nos. 26, 36, and 39 are rejected. The mean calculated maximum represents 71 novae. In addition to Nos. 26, 36, and 39, the following are omitted on the grounds that the preceding unobserved intervals are excessive—Nos. 12, 13, 15, 24, 25, 38, 46, 47, 48, 53, and 73.

by 4 in order to correct for the inclination of the plane of the spiral to the line of sight. The position of the major axis was estimated on several plates of long exposures on different scales. The line selected was then drawn on a print of the nebula and the orientation was measured with reference to stars whose positions were accurately known. The position angle of the major axis as thus determined is N 36°7 E. The ratio of the axes was estimated on long exposures as about 4 to 1, hence the inclination of the spiral to the line of sight is of the order of 15°. The nuclear region, by analogy with other spirals of the same type which are seen edge on, is probably much less flattened than the nebula as a whole—a circumstance to be considered in reconstructing the image as it would appear were the plane perpendicular to the line of sight.

An inspection of Table V indicates the necessity of some culling before entering upon a general discussion. The most conspicuous abnormalities occur in Nos. 26, 36, and 39. Number 26 was first observed in October, 1921, at about 19.0. It brightened slowly until by July, 1924, it was about 18.0. By December of the same year it had begun to fade and now, four years later, it has vanished. The description appears to be that of a long-period or an irregular variable rather than of a nova, and analogies may possibly be found in variables Nos. 15 and 19 in M 31 and Nos. 1 and 2 in M 33. Numbers 36 and 39 appeared, the former between 1915 and 1917, the latter in February, 1924, at about 18.6 and 19.0, respectively, and have maintained constant luminosities up to the present date. These stars may be of the same general type as No. 26, or possibly they may be ordinary stars which have drifted out from behind clouds of dark nebulosity. Variable No. 20 in M 31 may be a similar object. At any rate, the three stars clearly are not normal novae and can be discarded in statistical discussions. It is significant also that they are among the faintest which were originally observed as novae.

Number 22, discovered by Humason in February, 1923, appeared on only one plate. The image, however, shares the distortion, due to astigmatism in the mirror, which the other stars exhibit, hence there is no doubt as to the reality of the nova. Number 86 is a similar case, but no other object is included which has not appeared on more than one plate. For the following sixteen, however, the observations are very meager: Nos. 7, 8, 9, 11, 17, 18, 23, 28, 48, 51, 61, 65, 71, 72, 82, and 85. In these cases there are either but two observations or three or four covering a short interval of time.

Numbers 15, 38, 46, 47, 48, 53, 62, and 73 appeared on the first plates obtained after unobserved intervals of more than a hundred days. The maximum observed magnitudes of some of these are probably much fainter than the real maxima, which may have occurred some weeks earlier. This offers a ready explanation of the faintest two maxima listed in Table V, 18.7 for Nos. 38 and 46. In eight other cases, the first observations follow unobserved intervals of more than thirty days.

In five cases, Nos. 40, 58, 67, 75, and 80, observed maxima occurred several weeks after the first observations, although it is uncertain whether these represent primary or secondary maxima. In the discussions which follow, all novae are included excepting Nos. 1, 26, 36, and 39. The twenty-three novae listed in the two preceding paragraphs, however, and, to a lesser degree, the six mentioned at the beginning of the present paragraph are entitled to smaller weight than the remaining novae.

These stars have been called novae because they flare up very suddenly, fade slowly, and vanish completely. In the eighty-five cases listed, none has reappeared during the eighteen years covered by the observations at Mount Wilson. Occasional plates at other observatories extend the period less certainly over an additional ten years. Novae are the only galactic objects which exhibit such characteristics.

These stars at maxima, moreover, are about the brightest objects in the spiral, and average more than 2 mag. brighter than the Cepheids. In the case of No. 54, a small-scale slitless spectrogram was obtained by Humason, at the Newtonian focus of the 100-inch reflector, some six days after maximum. The continuous spectrum extended well into the violet, and faint patches of emission could be seen in the region of the Balmer lines of hydrogen. The color-index was less than the errors of the determination, which were estimated as about 0.2 mag. These indications, while by no means conclusive, strengthen the analogy with galactic novae.

LIGHT-CURVES OF NOVAE

The data on individual stars are usually fragmentary, but in a few cases they are sufficient to indicate the general form of the light-curves. The sharp initial rise, familiar in galactic novae, appears to be certainly present. The most conspicuous examples are novae Nos. 2 and 3, which Ritchey found on a plate exposed on the morning of September 13, 1909, although they were not visible on a plate exposed four hours earlier. Both novae had brightened at least 0.7 mag. within that interval. By the next exposure, on the late evening of the same day, No. 2 had brightened another 0.7 mag. Nova No. 34 rose 1.5 mag. above the limits of the plates during an unobserved interval of about twenty hours, and on the next plate, a day later, was 0.8 mag. brighter yet. Other instances are Nos. 37 and 44, which appeared about 2 mag. above the limits of the plates after unobserved intervals of four and two days, respectively. Number 54 first appeared at 17.3 after a long unobserved interval, but on the next plate, twenty-two hours later, it was 15.3. Since these data set lower limits only, the actual rates of brightening may be considered comparable with those of galactic novae.

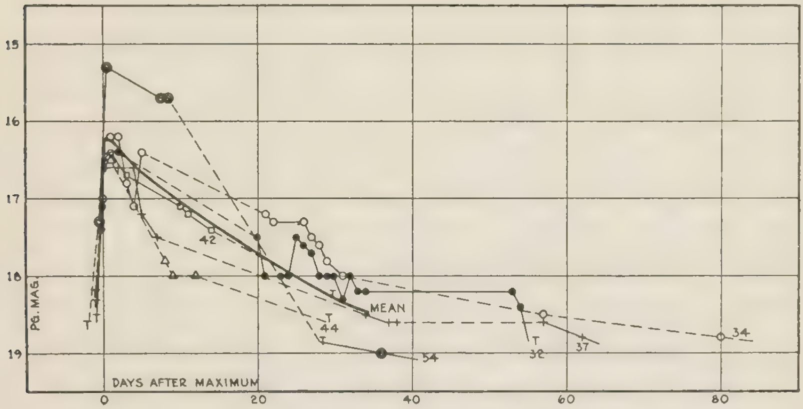

FIG. 5.—Light-curves of six novae in M 31 observed near maximum

Data for six novae well observed near maximum, Nos. 32, 34, 37, 42, 44, and 54, furnish a mean light-curve, shown in Figure 5, in which the rapid rise, the minor fluctuations, and the slow decline are conspicuous. A composite light-curve, incorporating most of the data in Table IV, has also been constructed on the assumption that the actual maxima of the various novae occurred in the middle of the unobserved interval preceding the first observation. Novae for which this unobserved interval exceeds thirty days were excluded, and, in addition, those for which the observed maxima occurred long after the first observations, and Nos. 21 and 70, for which the data were so poorly distributed that the curves could not be reconstructed with any certainty. This selection reduced the number of available novae to fifty-seven.

Mean magnitudes were computed for various dates after maximum, and the mean curve thus indicated is approximately linear with a slope of about 0.05 mag. per day. The region of greatest weight, however, is between ten and twenty days after maximum, the earlier and later portions depending largely on linear extrapolations or interpolations from rather meager data. A comparison of the mean magnitudes on the two curves, the composite curve, and that for the six well-observed novae indicates that the latter is somewhat steeper, but that in the region where the former has greatest weight, the two agree very closely. This suggests that the six selected novae are representative cases, and that their behavior near maximum is probably typical.

The composite curve indicates a mean maximum of about 16.6 as against 16.2 for the selected curves. The discrepancy is due to two factors—the inclusion of fainter novae in the composite curve and the linear extrapolations backward from the first observations. The latter is the more serious since it ignores the humps at maxima which are indicated by the well-observed novae. The point is rather important in connection with the frequency distribution of maxima; hence some form of the mean curve in this region must be adopted, even though it be somewhat arbitrary. Fortunately, the limits of the selection are not widely separated, and a simple mean between the two curves will not be grossly in error. With this procedure, the hypothetical mean maximum is 16.4 and the mean magnitudes at three, five, seven, and ten days after maximum are 16.7, 16.8, 16.9, and 17.1, respectively. At ten days after maximum the two curves are in agreement, and from then on the composite curve may be used with its linear slope of about 0.05 mag. per day.

FREQUENCY DISTRIBUTION OF MAXIMA

The maxima of the various novae can be determined with the aid of this standard light-curve by extrapolating backward from the first observations, on the assumption that the maxima occurred midway in the unobserved intervals preceding these observations and that the various individual curves are approximately parallel. In a few cases, departures from the formal procedure, clearly indicated by the data, have led to more probable values for the maxima. The maxima, observed or hypothetical, are listed in the eighth column of Table V, and exceptional cases are given in the footnotes.

TABLE VI

Mean Magnitudes on the Composite Light-Curve and the Light-Curve for Six Well-observed Novae

Interval in Days after Max.	Composite	Six Novae	Mean
0	(16.6)	16.23	(16.4)
1	....	16.25	(16.5)
3	16.8	16.5	(16.7)
5	16.95	16.65	(16.8)
7	17.0	16.8	(16.9)
10	17.14	17.05	(17.1)
14	17.33	17.3	....
15	17.37	17.4	....
20	17.63	17.7	....
25	17.88	18.0	....
30	18.1	(18.3)	....
40	18.6	(18.6)	....

A frequency-curve of seventy-one maxima[1] is shown in Figure 6. In order to smooth the curve somewhat, the numbers of novae have also been summed over intervals of 0.3 mag., centered upon successive tenths. The restricted range, the symmetrical form, and the narrow maximum are unexpected features; but they appear to be definite characteristics, independent of the particular method of analysis. Any reasonable treatment of the data would lead to results of the same general character. The mean magnitude is 16.43, and the most frequent magnitude, about 16.5.

---

[1] In addition to Nos. 26, 36, and 39, novae Nos. 12, 13, 15, 24, 25, 38, 46, 47, 48, 53, and 73 are omitted because the unobserved intervals preceding the first observations exceed forty days.

Although the general character of the frequency-curve appears to be established, the details depend upon extrapolations of a somewhat arbitrary nature. For this reason a similar curve has been constructed, showing the frequencies of magnitudes fourteen days after maximum, where the extrapolations and interpolations are reduced to a minimum. This curve (see Fig. 7) is of the same general character as that in Figure 6. The mean magnitude is 17.37, and the most frequent magnitude is about 17.35. The mean magnitude, extrapolated according to the standard curve, gives a maximum of 16.44, in agreement with Figure 6, hence the adopted maximum, 16.5, appears to be a conservative estimate.

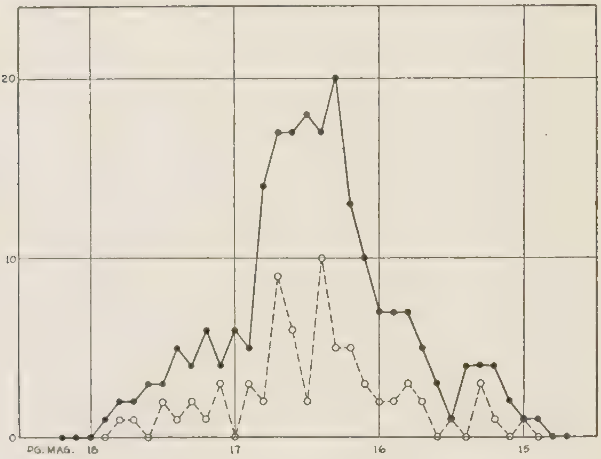

Fig. 6.—Frequency distribution of magnitudes at maximum among 71 novae in M 31. Open circles indicate numbers for each 0.1 mag.; black disks indicate sums over intervals of 0.3 mag., centered on successive tenths. The maxima, in general, have been derived from the mean light-curve of novae in M 31, on the assumption that maxima occurred at the middle of the unobserved intervals preceding the first actual observations of the novae.

These frequency-curves indicate that the novae observed in M 31 are very similar objects. Their maxima, for instance, can be predicted with a probable error of the order of 0.5 mag., and the total range is of the order of 3 or 4 mag. The data indicate only two maxima fainter than 17.5, although the limits of the observations are from 1.0 to 2.5 mag. fainter. It is probable that some faint novae have been missed, especially in the very dense nuclear region; but the wealth of material covering other regions clearly indicates that the number is relatively small. Variables were frequently found whose maxima were around 19.0 and were followed to 20.0 and fainter, but no very faint novae were found except on plates following long unobserved intervals. The relative distribution of maximum magnitudes actually observed among novae and variables is shown in Figure 8.

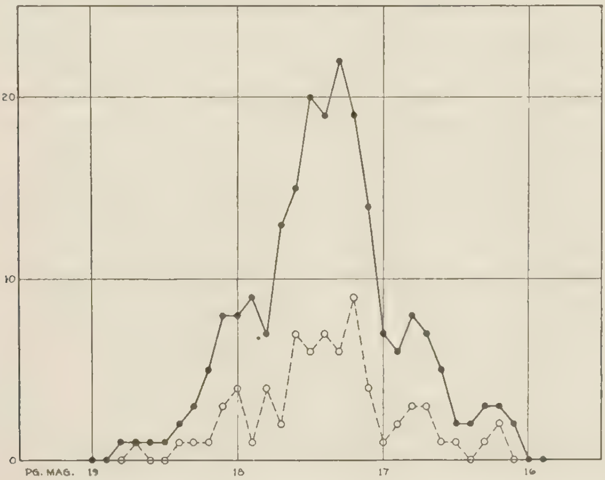

FIG. 7.—Frequency distribution of magnitudes of novae 14 days after maximum. Open circles indicate numbers for each 0.1 mag; black disks indicate sums over intervals of 0.3 mag., centered on successive tenths.

At the distance indicated by the Cepheids, the most frequent magnitude at maximum, 16.5, corresponds to an absolute photographic magnitude of −5.7. Since the color-indices of novae at maximum are negligible, the visual magnitude is about the same. Absolute magnitudes at maximum are reliably determined for only two galactic novae—Nova Persei (1901) at −5.0 and Nova Aquilae (1918) at −9.2. The various discussions of the mean magnitude of galactic novae at maxima, mainly by Lundmark, have led to values ranging from −3 to −9, the last published value[1] being −6.1. This

[1] "Studies of Anagalactic Nebulae," *Meddelanden från Astronomiska Observatorium, Upsala,* No. 30, 1927.

agrees as closely as can be expected with the value for novae in M 31 and suggests no considerable revision of Shapley's zero point in the period-luminosity curve for Cepheids.

Aside from the possible uncertainty in this zero point, the absolute magnitudes of novae in M 31 are determined with a much greater precision than those in the galactic system. Hence, if the novae in the two systems are objects of the same sort, the frequency-curves for those in M 31 may be used to advantage in studying the distribution of novae in the galactic system. The approximate agreement in the mean magnitudes at maximum, the characteristics of the light-curves, and the fragmentary evidence of color and spectrum suggest very strongly that the two groups actually are similar. The range in magnitude at maximum among galactic novae is unknown at present, and no definite conclusion can be formulated as to its value until the number of reliable individual distances is sufficient to permit a statistical treatment of the data. If the use of the frequency distribution of maxima in M 31 should lead to wholly inconsistent results for the distances of galactic novae, the question of similarity would be definitely settled in the negative.

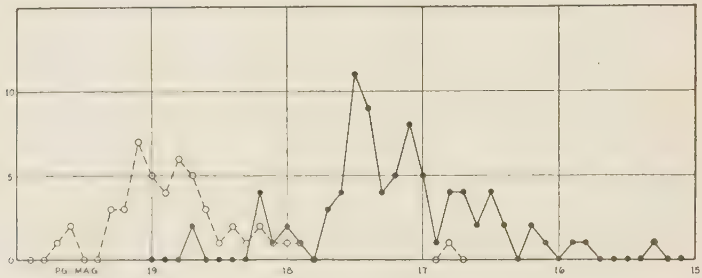

FIG. 8.—Frequency distribution of observed maxima of novae and variable stars in M 31. Black disks refer to novae; open circles, to variable stars. The points indicate numbers for each 0.1 mag. The diagram emphasizes the *completeness* of the data for novae, and hence the reality of the restricted range in magnitudes at maxima indicated by Figures 6 and 7.

Four novae have been found thus far in M 33, but each has first appeared on plates following unobserved intervals of several months. Two of these are discussed in an earlier paper, and data for the two later objects are given in the footnote below.[1] All four were obviously on the descending branch of their light-curves when first observed, hence no certain information is available concerning their maxima. The first observations give 17.2, 17.9, 18.1, and 17.9 mag. The mean, 17.7, is about the same as the mean of the ten similar cases in M 31, namely, 17.6, and leaves little doubt that the novae in the two spirals are similar objects. This evidence, weak as it is, materially strengthens the analogy between the spirals and the galactic system based upon the observations of Cepheids.

The one nova thus far observed in the Magellanic Clouds[2] reached an absolute magnitude of at least −5.0, but, as far as can be judged from the records, probably did not exceed −7.0.

The occasional novae which have appeared in the smaller extragalactic nebulae and which have attained luminosities that are respectable fractions of the total luminosities of the nebulae themselves are clearly a different sort of object from the normal novae in M 31 and 33. They are generally classed with S Andromedae, the nova of 1885 in M 31, as a rare and peculiar type.

FREQUENCY OF NOVAE

The numbers of novae for the various observing seasons are given in Table VII. The more systematic spacing of the plates accounts for the larger numbers of novae discovered during the last five seasons,

---

[1] *Mt. Wilson Contr.*, No. 310; *Astrophysical Journal*, **63**, 236, 1926. Nova No. 3 appeared 6.′6 south following the nucleus of M 33; No. 4 appeared 1.′9 south and 0.′4 following variable No. 34. The magnitudes are as follows:

Plate	J.D.	No. 3	No. 4
H619	2,424,444.5	....	....
623	2,424,493.3	18.1	
673	2,424,610.6	18.6	
621	2,424,918.3		
817	2,425,091.6	....	17.7
834	2,425,124.5	....	18.1
847	2,425,147.6	....	19.2
868	2,425,211.3		

After the present paper was prepared for publication, W. Baade announced the discovery on October 15, 1928, of a nova in M 33, which was observed at the sixteenth magnitude. This fifth nova strengthens the analogy with M 31 in a very evident manner.

[2] *Harvard College Observatory Bulletin*, Nos. 847 and 851, 1927.

hence these data may be regarded as representative. Comparison of the numbers of novae with the months covered by the observations indicates a frequency of sixteen or seventeen novae per year. This, however, neglects the very considerable gaps in the observations. By assuming that each plate shows all novae which appeared during the preceding ten days, the average number per year is found to be about thirty. If the preceding interval is put at fifteen days, the annual average is 21.5; for an interval of twenty days, the average is 18.5. Since the ten-day interval is almost certainly too short and the twenty-day interval is probably too long, the intermediate value may be accepted as a reasonable approximation.

TABLE VII

FREQUENCY OF OBSERVED NOVAE

Season	Novae	Interval	Season	Novae	Interval
1909–1910	3	3.0 mo.	1923–1924	8	7.5 mo.
1917–1918	7	6.0	1924–1925	11	8.0
1918–1919	4	7.0	1925–1926	15	8.0
1919–1920	5	7.0	1926–1927	12	8.5
1920–1921	5	7.0	1927——	7	7.0
1921–1922	1	7.0			
1922–1923	4	8.5			
Total	29	45.5	Total	53	39.0

The resulting annual average of 21.5 must be increased to include novae which have been missed in the study of the plates, those which have been below the limits of plates made under exceptionally poor conditions, and still others which have appeared in regions not covered by the plates. The first and last of these sources of error are believed to be of minor importance. Thus, during the re-examination of the entire series, eight additional novae were found on plates prior to the season 1923–1924, but none on the more recent plates. In the outer region of the nebula, novae appear to be very rare; in Region 4, 48′ from the nucleus, only one example has been found on the sixty-five plates covering four observing seasons. Allowance for losses arising from these two sources might perhaps increase the annual average to twenty-five.

Loss from the second cause is believed to be more important, especially during the winter months when the observing conditions are frequently bad, but the amount is difficult to evaluate. It suggests, however, that thirty per year is a reasonable estimate of the frequency of novae in M 31.

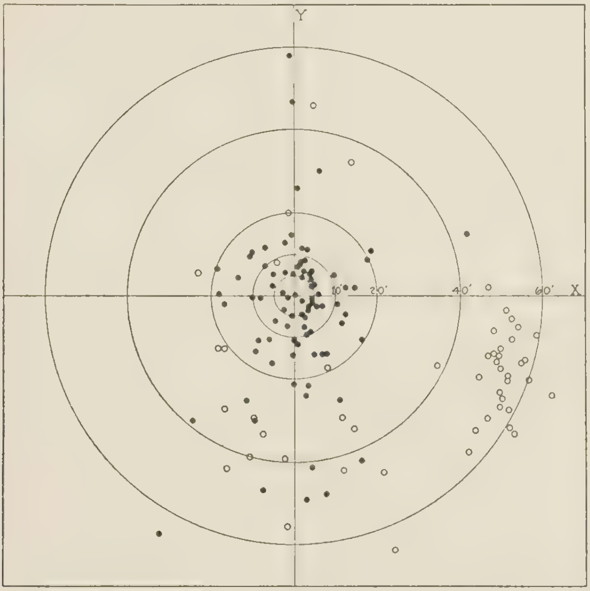

FIG. 9.—Distribution of novae and variables observed in M 31. Black discs refer to novae; open circles, to variable stars. *X* and *Y* are the major and minor axes of the nebula. The *Y* co-ordinates have been corrected to represent the plane of the spiral as perpendicular to the line of sight. The blank region to the left of $X = -30'$ is accounted for by lack of observations. The preponderance of negative signs among the larger numerical values of *Y* appears to be significant.

DISTRIBUTION OF NOVAE

The distribution of novae over the image of the nebula is shown on Plates II, III, IV, where positions are marked. The positions are given diagrammatically in Figure 9, the *Y* co-ordinates being corrected to represent the spiral as perpendicular to the line of sight. Few novae have been found in the great rifts between the spiral arms, nor do they show any conspicuous relation to the numerous small dark markings. In general, the distribution of novae follows the distribution of luminosity in the nebula. The concentration in the nuclear region is conspicuous, although it is noteworthy that only three novae besides S Andromedae have been found less than 4′ from the center. This does not appear to be wholly a result of limitations set by the dense nebulous background. The zone from 4′ to 8′ from the center is the most prolific, having produced twenty-eight novae, or about one-third of the total number observed. From 4′ outward, the total numbers in 5′ zones diminish steadily, and the numbers per unit area diminish even more rapidly, as may be seen in Table VIII.

Beyond the nuclear region there is an apparent asymmetry in the distribution in the sense that the observed novae are more numerous in the half of the nebula south following the major axis than in the north-preceding half. For $4Y > 15'$, there are only three novae in addition to the doubtful No. 39 in the north-preceding half, while in the south-following half there are eighteen besides the doubtful No. 26. When other variable stars are considered, the discrepancy is even greater—six objects as against thirty-one. In the north-preceding half, the nebula is less luminous, the rifts between the arms more pronounced, and, in general, the mottling due to dark markings is more conspicuous. This suggests a correlation with some form of obscuration, but the relation is not definitely indicated. The mean magnitude of the three novae in the north-preceding half, Nos. 27, 56, and 77, is 17.6 for the observed, and 16.95 for the computed maxima. These are somewhat fainter than the corresponding values for the novae in general, but the data are too limited for the differences to be regarded as significant.

Among the novae, as among the Cepheids, there is no definite relation between luminosity and distance from the nucleus. The data are shown in Table VIII.

These results indicate the absence of any considerable absorption by the unresolved luminous portions of the nebula, although obscuration by well-defined dark markings is conspicuous. The fact that the nucleus is sharply visible, although buried to a depth of many hundreds of parsecs of nebular material, points in the same direction.

The observational data bearing on the composition of the nuclear region are (1) the lack of absorption, (2) the infrequency of very bright giants ($M < -3.2$), (3) the appearance of novae, and (4) the characteristic dwarf solar-type spectrum with broad fuzzy lines. A superficial interpretation of these data suggests a star cloud in which bright giants are rare, in contrast with the outer arms of the spiral, where giants are abundant. The Cepheids would then follow the distribution of the giants, while the novae would follow that of the fainter stars, or possibly that of the stars in general.

From the observed shapes of nebulae, however, Sir James Jeans has concluded that the nuclear regions of spirals, as well as the elliptical nebulae, must be gaseous.[1] The lack of resolution is thus accounted for, and since the densities are low—of the order of 10^{-21}, the lack of appreciable absorption is also explained. The novae and the spectrum raise difficulties, but these, according to Jeans, are not unsurmountable. The novae, for instance, might possibly be explained as due to the penetration into the gaseous region of stars from the outer portions. This would also account for the lower frequency of novae in highly resolved nebulae (e.g., M 33, N.G.C. 6822, and the Magellanic Clouds), where the unresolved regions are relatively small.

TABLE VIII

FREQUENCY OF NOVAE AT DIFFERENT DISTANCES FROM THE NUCLEUS

Zone	Novae	Mean Distance	Mean Maximum	
			Obs.	Cal.
0′– 5′	12	4′.0	17.32	16.51
5 –10	25	7.2	17.04	16.31
10 –15	19	12.9	17.35	16.59
15 –30	13	19.5	17.03	16.34
30	13	44.5	17.38	16.69

THE BRIGHT NON-VARIABLE STARS

No general investigation of the luminosity function of the giant stars in M 31 has been undertaken, but measures have been made of stars in the cluster N.G.C. 206, which appears to belong to the spiral. This is an open cluster in Region 4, about 41′ south preceding the nucleus along the major axis ($X=40'.8$; $Y=+4'.4$). Its dimensions are about $6'\times 2'$, and the elongation is roughly north-south. About ninety stars are brighter than photographic magnitude 18.5, twelve of which may be attributed to the galactic foreground. At the distance indicated by the Cepheids, the dimensions of the cluster would be of the order of 480×160 parsecs, and apparent magnitude 18.5 would correspond to absolute magnitude -3.7. There are no definite indications of stars brighter than -5.5, but at -5.0 they begin to be fairly numerous. Preliminary inspection of other fields in the nebula suggests the possibility of a few stars brighter than -6.0, but that large numbers do not appear until -5.0 is passed.

---

[1] *Astronomy and Cosmogony*, p. 336, 1928.

Very bright stars appear to be relatively more numerous in M 33, where, in general, they seem to be white or blue. In M 31 the brightest stars appear to have a slightly larger color-index, averaging perhaps $+0.3$ or $+0.4$ mag. The stars in N.G.C. 206 have been measured on Cramer Iso plates, exposed with the 100-inch reflector for two hours through a visual color-filter, the scale being established by three comparisons with the North Polar Sequence made with the 60-inch reflector. The various plates are not of the best quality; but the internal agreement is rather good, and the results probably indicate the order of the colors. The faintest photovisual magnitudes represent an extrapolation of about 1.5 mag. beyond the standard stars.

A plot of the color-indices against the photographic magnitudes is shown in Figure 10. The galactic latitude of the cluster, $+22°$, is only 6° less than that of the North Pole, hence the distribution of the colors among the foreground stars should approximate that among stars in the Polar Sequence, although the polar stars may be expected to average slightly redder. A probable lower limit to the color-indices of the foreground stars, similar to that used in discussing the color-indices in M 33,[1] may be derived from these data. This limit has been indicated in the figure by a dotted line, and the numbers of stars above the line are roughly the numbers of foreground stars to be expected within the area. The area is too small to inspire any confidence in statistical conclusions, but the results suggest that red stars are not frequent among the brighter stars in the cluster and that the average color-index of the latter is about 0.35 mag.

Photovisual plates of other regions, notably Region 4, about 10′ south of N.G.C. 206, appear to be consistent with these conclusions, but the scales have not been sufficiently well established to permit

[1] *Mt. Wilson Contr.*, No. 310; *Astrophysical Journal*, **63**, 236, 1926.

numerical comparisons. The Cepheids, however, clearly have larger color-indices than the general average of the other stars in this region of the nebula, and appear to be approximately of the solar type. Great clouds of dark material occur in these outer regions, but the normal residuals from the period-luminosity curve of the Cepheids suggest that absorption, either general or selective, is not appreciable beyond the observed limits of these clouds.

No patches of luminous diffuse nebulosity have been found in M 31, although they appear, along with blue giants, in several of the most conspicuous of the late-type spiral and irregular nebulae. Diffuse nebulosities with emission spectra are the most easily identified, and these seem normally to accompany the characteristic of high apparent resolution. In general, such resolution implies an abundance of super-giant stars, and it is possible that the presence of emission nebulosities may indicate the relative frequencies of blue stars among these super-giants. The argument is rather speculative, but, since emission nebulosity is found only in highly resolved nebulae, it encourages the idea of a progressive tendency toward blueness among the brightest stars along the normal sequence of nebular types, such as is suggested by the comparison of color-indices in M 31 and 33.

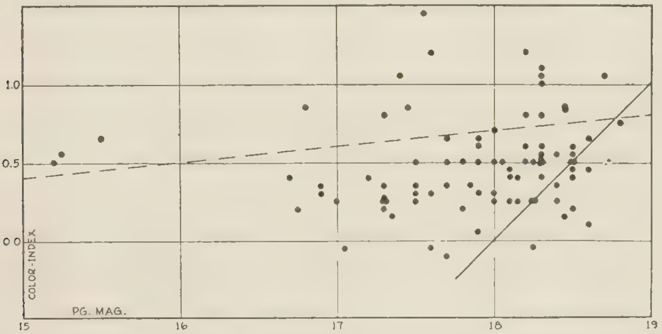

FIG. 10.—Color-indices of the brighter stars in N.G.C. 206, an open cluster in M 31. The diagram includes all stars down to 18.5 pg. mag. The dotted line indicates the probable lower limit of color-index among the foreground stars. The number of stars above this line is about the number of foreground stars to be expected. The data on color-indices are complete to the full line with a slope of 45°; below this line, the photovisual magnitudes are incomplete.

Another suggestion arising from the comparison, namely, that brighter absolute photographic magnitudes are attained in the late-type spiral M 33 than in that of the intermediate type M 31, seems also to be an example of a more general relation. The evidence, scanty and rather ambiguous, is found in the slight systematic decrease along the sequence of nebular types, in the difference between the luminosities of the brightest stars and the total luminosities of the nebulae in which they are involved. In an earlier discussion of such differences, a mean value was derived for all available nebulae, of whatever type, in which stars could be detected. A closer inspection of these data, supplemented by additional material, suggests the systematic effect above mentioned.[1]

MASS AND LUMINOSITY DENSITIES IN M 31

Some notion of the conditions within the nebula may be derived from rough estimates of the density both of mass and of luminosity. At a distance of 275,000 parsecs, the scale is $1' = 80$ parsecs, and the radius of the spiral, 80′, is 6400 parsecs. By analogy with spirals of the same type seen edge on,[2] the semi-minor axis is assumed to be one-eighth of the radius, or 800 parsecs. The order of the volume can be approximated by supposing the figure to be generated by an isosceles triangle with an altitude four times the base, rotated around the base. This gives

$$V = \tfrac{2}{3}\pi \frac{(6400)^3}{8} = 6.9 \times 10^{10} \text{ cubic parsecs .}$$

The mass of the inner region, out to $2\overset{'}{.}5$ from the nucleus, can be estimated on the assumption that the spectrographic rotation represents motions in circular orbits in a gravitational field. Then,[3] since the velocity of rotation at $2'.5$, or 200 parsecs, from the nucleus is about 72 km/sec.,

---

[1] *Mt. Wilson Contr.*, No. 324; *Astrophysical Journal*, **64**, 321, 1926. No stars have been found in any of the Sa spirals, or in any of the elliptical nebulae except M 87 (N.G.C. 4486), where the difference between the nebula and the brightest stars is about 10 mag. For 14 Sb spirals, the average difference is about 9.6 mag., and for 12 Sc spirals, about 9.0.

[2] *Mt. Wilson Contr.*, No. 324; *Astrophysical Journal*, **64**, 321, 1926.

[3] The formula $\text{Mass } \odot = 235 a v^2$, where a is the distance from the center in parsecs and v is the velocity of rotation in km/sec., is derived from the familiar formula for circular orbits in the solar system, $\text{Mass} = v^2 r k^{-2}$.

$$\text{Mass}=235\times 200\times 72^2\odot=2.4\times 10^8\odot\ .$$

The total mass of the nebula follows from the arbitrary assumption that it is ten or twelve times that of the inner region. A value previously used, $3.5\times 10^9\odot$, is probably of the right general order.[1]

The absolute visual magnitude, -17.2, which follows from Holetschek's value for the apparent magnitude, 5.0, is probably a lower limit, but may be used for the rough calculations.

With these values, the mean luminosity density, in absolute visual magnitudes, is 9.9 per cubic parsec, and the mean mass density is about one sun per 20 cubic parsecs. Both densities are of the same order as those for the galactic system in the vicinity of the sun. In M 33,[2] the luminosity density is slightly brighter, 9.3 per cubic parsec, but the estimated mass density, $3\ \odot$ per cubic parsec, is about sixty times greater, and the discrepancy suggests the inadequacy of the methods used in determining the masses, especially in the case of M 33.

In terms of the sun's mass and luminosity, the relation

$$\text{Mass}=5.5\,L\ ,$$

which holds in M 31, has a coefficient about twice that for the relation in the vicinity of the sun. The inaccuracy of the data, however, justifies only the conclusion that the coefficients are of the same order in two cases. The coefficient for the relation in M 33, 160, again suggests the inadequacy of the estimated mass of that spiral.

The central sphere, with a radius of $2'.5=200$ parsecs, which appears to rotate like a rigid body, has a mass, as previously computed, of $2.4\times 10^8\odot$ and a volume of 3.4×10^7 cubic parsecs. The mean mass density is about $7\odot$ per cubic parsec, or 5×10^{-22} in c.g.s. units. If the central sphere is assumed to be 2 mag. fainter than the entire nebula, the absolute visual magnitude is -15.2 and the mean luminosity density is 3.6 M per cubic parsec. The relation between mass and luminosity,

---

[1] *Mt. Wilson Contr.*, No. 324; *Astrophysical Journal*, **64**, 321, 1926.

[2] *Mt. Wilson Contr.*, No. 310; *Astrophysical Journal*, **63**, 236, 1926. The radial component of the velocity of rotation of M 33 is derived from the difference between the radial velocities of the nucleus and of a patch of emission nebulosity in one of the arms. The velocity of the nucleus depends upon one spectrogram on a very small scale and is very uncertain.

$$\text{Mass} = 2.3\,L\,,$$

is of the same order as for the nebula as a whole, but this result follows from the tacit assumption involved in estimating the whole mass, namely, that in the outer regions, the distribution of mass tends to follow the distribution of luminosity.

As the nucleus is approached, however, the mass density remains constant (according to the assumption of uniform angular rotation), while the luminosity density is observed to increase rapidly. The nucleus itself, on the shortest exposures, is sensibly round, with a diameter of about 3″, or 4 parsecs, and an apparent photographic magnitude about 14.0, or −9.2 on the absolute visual scale. Since the volume of the sphere is about 34 cubic parsecs, the mean luminosity density is of the order of −5.4 M per cubic parsec. The mass density, on the assumption of uniform angular rotation, is 5×10^{-22}, or 7 ⊙ per cubic parsec as given above.

The relation between mass and luminosity is now of the order

$$\text{Mass} = 0.001L\,,$$

which clearly does not represent the relation to be expected in a star or a cluster of stars giving a dwarf spectrum. Inaccuracies in the data will not seriously affect the order of the luminosity density, hence the uncertainties must be referred to the estimation of mass. If the latter approximates the proper order of magnitude, the mass-luminosity relation becomes significant and suggests that the nuclear material is in a gaseous state.

The nucleus of M 33 is very similar to that of M 31. The two show about the same spectral type, diameter, and absolute magnitude. The mean luminosity densities are not very different from those in the central regions of the more compact globular clusters. M 3, for instance, has a total absolute magnitude of −9.1, and the central sphere, with a diameter of 4 parsecs, is possibly 2 mag. fainter. The mean luminosity density of this inner region is therefore about −3.3 M per cubic parsec, or about one-seventh as bright as in the nuclei of the spirals. Nothing definite is known concerning the masses of globular clusters, hence comparisons of mass densities cannot be made. The similarity in the luminosity densities suggests an analogy which is not encouraged by the mass-luminosity relation in the nuclei of the spirals.

A comparison of M 31 with the galactic system involves even greater uncertainties than those encountered above. Seares's[1] recent discussion of the galactic system, based upon star counts in the Selected Areas, suggests that it resembles a very late-type spiral, from 60,000 to 90,000 parsecs in diameter, in which the nucleus, 15,000–20,000 parsecs distant according to Shapley, is hidden from the earth by the obscuring clouds which form the great rift in the Milky Way. The sun is perhaps halfway out from the nucleus to the border, in one of the condensations represented by the local cluster, hence the density in our vicinity would be of the same general order as, or perhaps somewhat greater than, the mean density of the system. This lends some significance to the comparison of mass and luminosity densities in the vicinity of the sun with those for M 31.

If a diameter of 80,000 parsecs is assigned to the galactic system and a ratio of diameters of 1 to 10, the volume is of the order of 1.3×10^{13} cubic parsecs. The most plausible estimate of the mass is perhaps that suggested tentatively by Eddington,[2] based on the assumption that the observed motion of the system of the globular clusters is in reality a reflection of the rotation of the galaxy. Using Shapley's minimum value of the distance of the sun from the center of the system, he finds a mass of $2.7 \times 10^{11} \odot$. These figures lead to a mean mass density of one sun per 50 cubic parsecs as compared with one sun per 20 cubic parsecs in M 31.

Some notion of the order of magnitude of the total luminosity of the system can be derived by estimating the luminosity of the visible region and applying a reasonable correction for the invisible. Kapteyn's very generalized representation of stellar distribution out to star densities one one-hundredth that in the vicinity of the sun provides about the only data available. The numbers of stars to this limit (out to a distance of 8465 parsecs in the galactic plane) are equivalent to the numbers in a volume of 1.45×10^{10} cubic parsecs of unit density.[1] Since the unit density corresponds to $8.16M$ per cubic parsec, the absolute magnitude of Kapteyn's system is

---

[1] *Mt. Wilson Contr.*, No. 347; *Astrophysical Journal*, **67**, 123, 1928.

[2] *Monthly Notices, R.A.S.*, **88**, 331, 1928.

$$8.16-2.5 \log 1.45\times 10^{10}=-17.24 .$$

The larger system, with an assigned diameter of 80,000 parsecs, has a volume about twenty-seven times that of Kapteyn's, hence, if the latter were representative, it would be about 3.6 mag. fainter than the former. The great amount of obscuration along the galactic plane, especially between us and the central region, probably more than balances the influence of the local cluster and suggests that the magnitude difference should be materially increased. Possibly the round number $-22\,M$ may represent the luminosity of the galactic system within 2 or 3 mag. This leads to a mean luminosity density of $10.8\,M$ per cubic parsec as compared with $9.9\,M$ in M 31. The relation between mass and luminosity, $\text{Mass}=5.2\,L$, is also about the same as in the spiral.

These comparisons indicate a general similarity which further data are not likely to disprove. The outstanding discrepancy between the two systems is in their dimensions. According to the present figures, the galactic system is five or six times the diameter of the spiral, although the latter is the largest of the extra-galactic systems whose distances are reliably known. M 31, however, is in an intermediate state of concentration in the observed sequence of spiral forms, and could be spread through a much greater volume without losing the characteristics of an extra-galactic system.

Moreover, while the galactic system is very large, the outer regions, as viewed from a distant source, are very faint. Seares,[2] using a method independent of the spatial distribution of stars, finds that the surface brightness of our region, as viewed from a direction perpendicular to the galactic plane, is about 22.93 in visual magnitudes per square second of arc. Beyond a certain lower limit, this, of course, is independent of distance. Photographic magnitude 23.5 per square second of arc represents about the limiting faintness that can be registered by long exposures with reflectors of focal ratio 1 to 5, and this, corrected by a reasonable color-index, is of the same order as Seares's result. Viewed from a direction in the galactic plane, the surface brightness would be considerably greater, but it is improbable that photographs from a distant point would show the full dimensions suggested by the investigations of Seares and Shapley. This, together with the greater concentration in M 31, tends to reduce the apparent disparity in size between the two systems very materially. The galactic system must be considered as much larger than M 31, but the ratio is not greater than that between M 31 and other known extra-galactic systems.

---

[1] *Mt. Wilson Contr.*, No. 230; *Astrophysical Journal*, **55**, 302, 1922. See also Sir James Jeans, *Astronomy and Cosmogony*, p. 15, 1928, where Kapteyn's data are given in fuller detail.

[2] *Mt. Wilson Contr.*, No. 191; *Astrophysical Journal*, **52**, 162, 1920.

Carnegie Institution of Washington
Mount Wilson Observatory
December 1928

DESCRIPTION OF PLATES

PLATE I

South Preceding End of Messier 31

Plate by Duncan, August 24, 1925; 100-inch reflector, exposure 2 hrs. on Eastman 40 plate. Scale 1 mm=15″.1. Top is north. The bright patch 34 mm to the right of the brightest star (B.D.+39°158) is a defect.

PLATE II

Messier 31

Plate by Ritchey, 24-inch reflector at Yerkes Observatory, September 18, 1901. Scale 1 mm=39″.1. Novae are indicated by crosses; variables, by lines and a V preceding the number. V1, 15, and 19 can be seen on the plate. The open cluster N.G.C. 206 is 3 mm below nova No. 46. Variables in Region 4, centered 13 mm to the right of N.G.C. 206, and novae near the nucleus are not marked.

PLATE III

Central Region of Messier 31

Plate by Duncan, 100-inch reflector, 9 hrs. exposure, September 16–17, 1920. Scale 1 mm=16″.4. Novae are indicated by crosses, excepting Nos. 36 and 80, which are visible and enclosed in circles; variables, by a V preceding the number. V2, 3, 7, 9, and 13 are near maxima.

PLATE IV

Variables in Messier 31

Plates with 100-inch reflector; scale 1 mm=8″.0. *Top.*—V1 near minimum, August 4, 1924. At maximum it equals the brighter of the two stars above and to the left. *Middle.*—V5 near maximum; V10 near minimum, August 5, 1924. The large object is M 32. *Bottom.*—V12 near maximum; V7 and 9 near minimum, July 30, 1924. The bright star is B.D.+40°151.

PLATE V

Messier 31, Region 4

From same negative as Plate I. Scale 1 mm=14″.2. The patch 36 mm to the right of the brightest star, B.D.+39° 158, is a defect. The cross marked 40, a mistake for 46, indicates the only nova observed in this region. All other numbers refer to variables. V48 to the left of V25 should read V47. V40 is on the edge of a small compact cluster, of the same order of dimensions as a globular cluster. V23, 24, 28, 30, 34, 37, 38, 39, and 46 are near maxima.

PLATE VI

Variables in Region No. 4

Plates with 100-inch reflector. Scale 1 mm=6″.5. Right-hand plate, October 26, 1924; left-hand plate, August 24, 1925. Variation is conspicuous in V25, 26, 30, and 39.

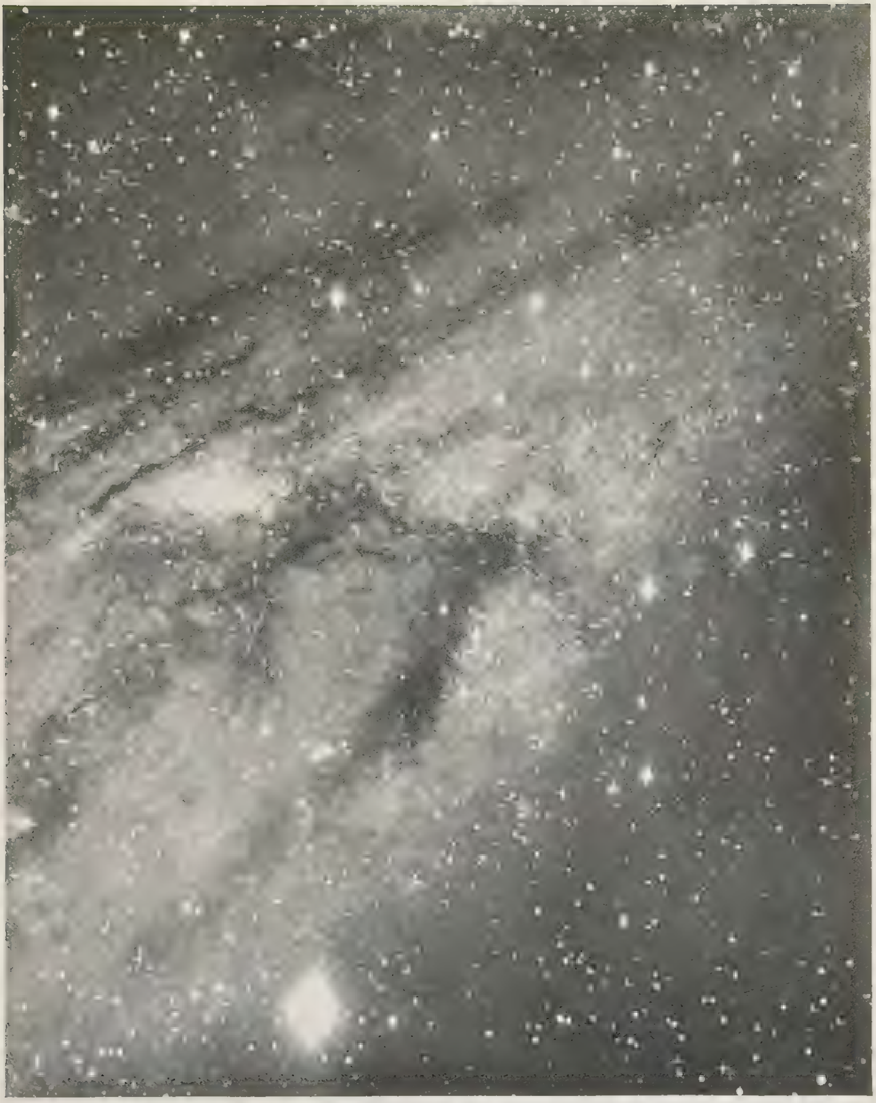

N

PLATE II

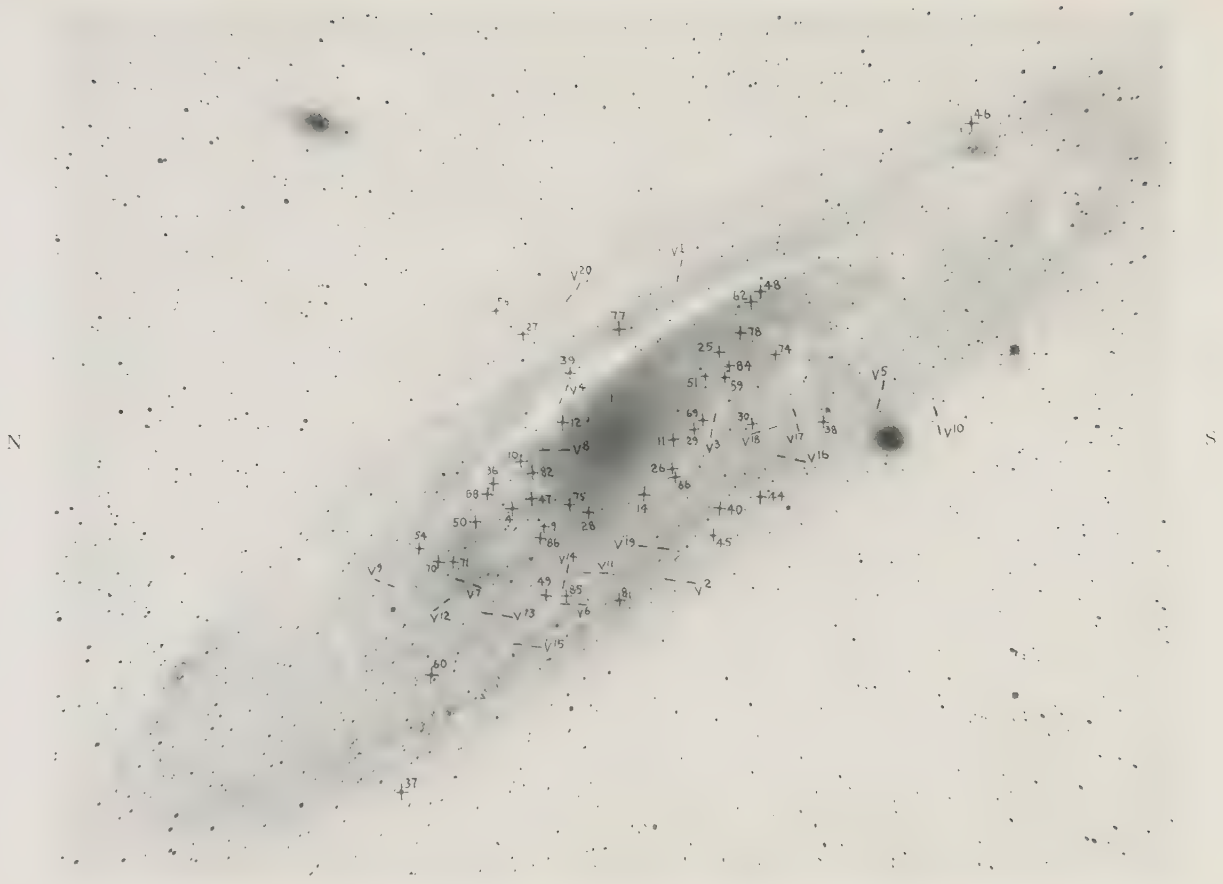

N
S
46
V1
V20
62
48
77
27
78
74
25
84
51
59
39
V4
V5
12
69
30
38
V10
11
29
V3
V18
V17
V8
V16
10
82
26
66
36
68
47
75
14
44
40
50
4
9
28
86
54
45
V19
V9
70
71
V14
V11
49
85
V7
81
V2
V12
V13
V6
V15
60
37

PLATE III

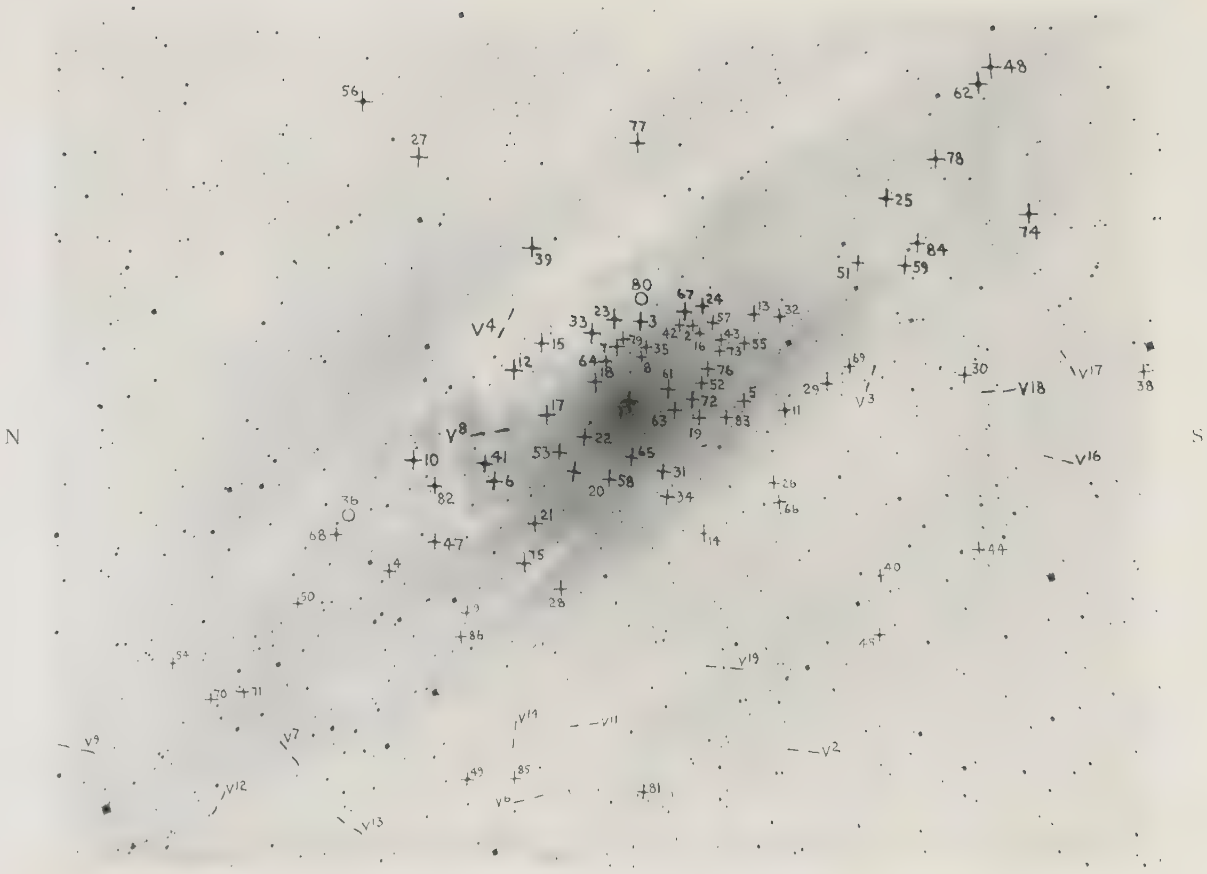

N
S
48
62
56
27
77
78
25
74
39
84
59
51
80
67
24
13
32
V4
33
23
3
57
42
2
43
55
16
73
7
79
35
15
12
64
18
8
61
76
52
69
29
V3
30
V18
V17
38
17
72
5
63
83
19
11
V8
22
10
41
53
65
31
6
20
58
82
34
26
66
V16
36
68
21
47
14
44
4
75
40
28
50
9
86
45
54
V19
70
71
V14
V11
V9
V7
V2
49
85
V12
V6
81
V13

PLATE IV

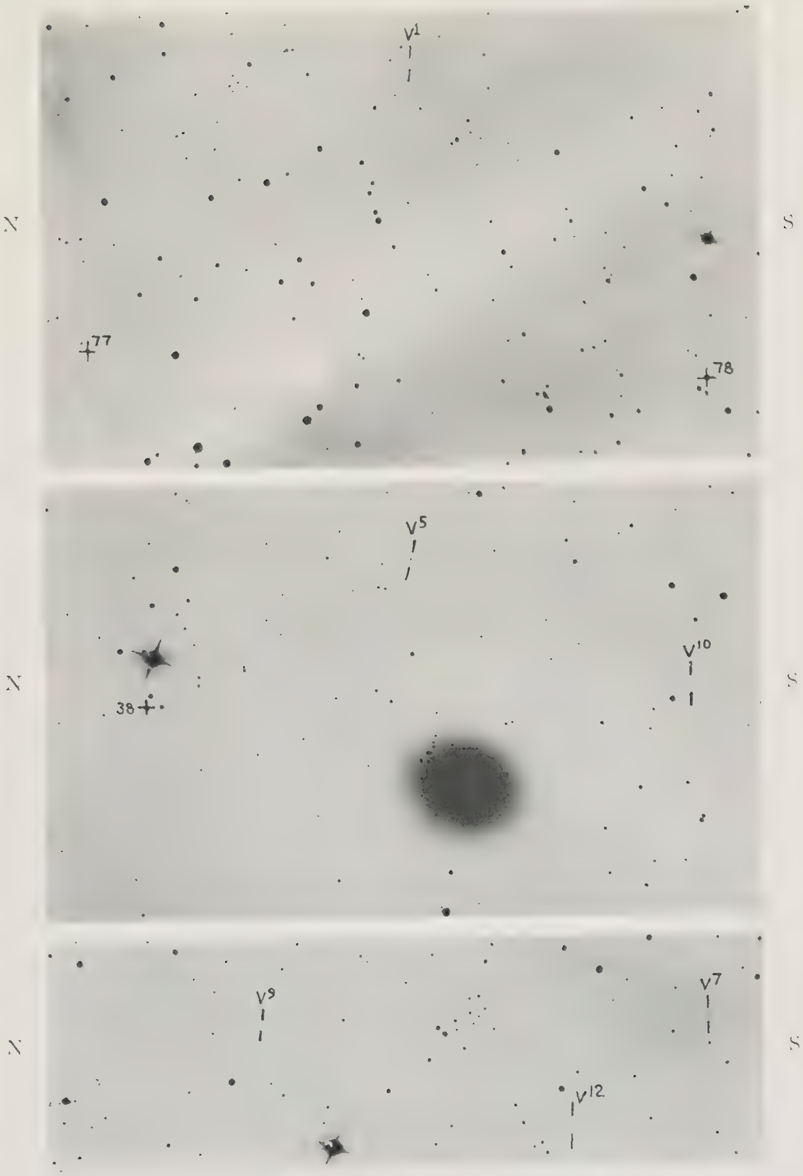

PLATE V

N

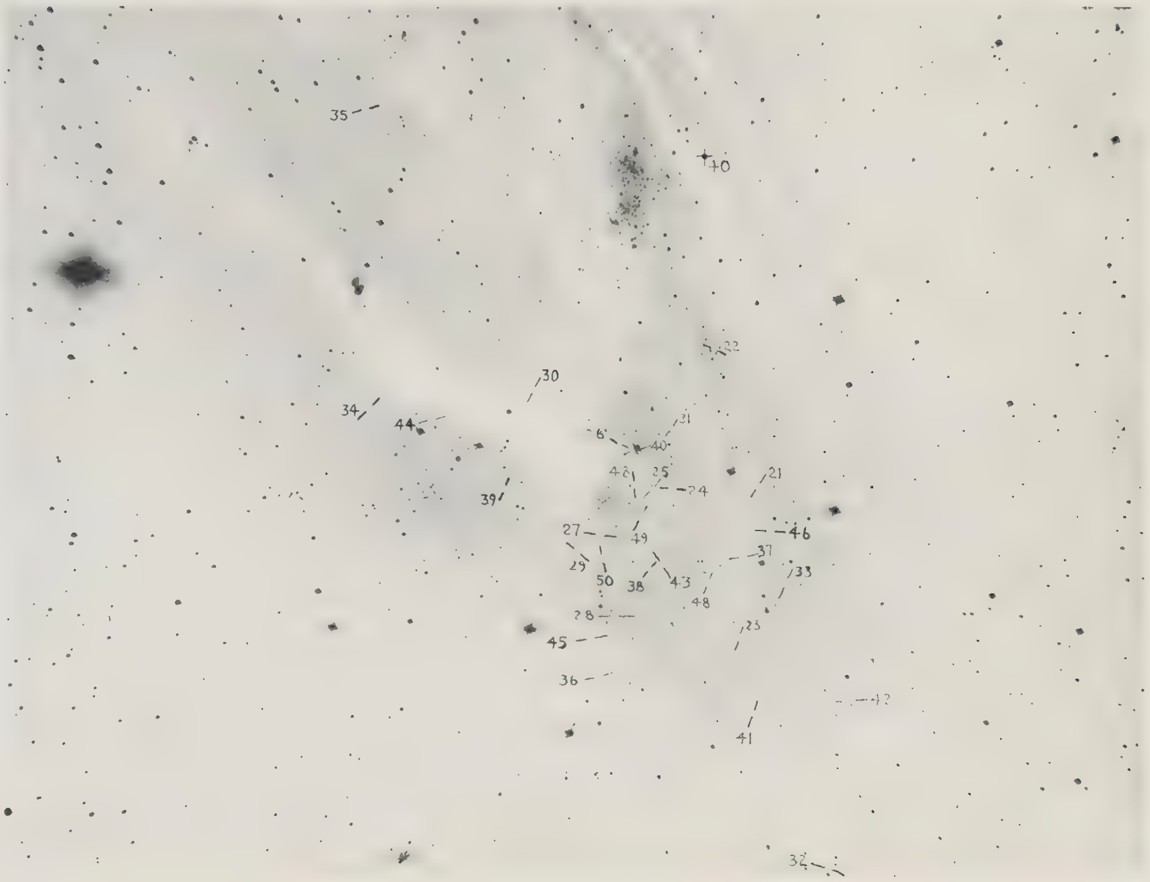
35
40
22
30
34
44
31
6
40
42
25
24
21
39
27
49
46
37
33
29
50
38
43
48
28
23
45
36
42
41
32

PLATE VI

Contributions from the Mount Wilson Observatory, No. 377
Reprinted from the *Astrophysical Journal*, Vol. LXIX, pp. 209–226, 1929
Printed in the U.S.A.

A SPECTROSCOPIC DETERMINATION OF THE PRESSURE IN THE CALCIUM CHROMOSPHERE

AN EXPERIMENTAL TEST OF MILNE'S THEORY

By ALBRECHT UNSÖLD[1]

ABSTRACT

1 and 2. *Application of the theory of radiative equilibrium* to the emission and absorption spectrum of the calcium chromosphere.

3. *The coefficient of scattering.*—The dependence on wave-length is largely the result of Doppler effect which is produced by a kind of turbulent motion in the chromosphere.

4. *Observations of the* H *and* K *emission and absorption lines* with the 150-foot tower telescope.

5. *Comparison of the observations with the theory* developed in sections 1 and 2. By determining the numerical values involved in this theory the Ca^{+} pressures in the chromosphere can be measured.

6. *Comparison with Milne's theory.*—Deviations from thermodynamic equilibrium in the chromosphere.

7. *Dynamics* and *stability* of the chromosphere.

8. Theoretical remarks concerning the *distribution of pressure* in the chromosphere and the theory of Milne.

INTRODUCTION

In a previous paper the author[2] has given an explanation of the self-reversals[3] observed in the emission spectrum of the limb of the sun. It appeared that the structure of these emission lines is not determined, as in the case of absorption lines, solely by the total optical depth of the solar atmosphere for the corresponding wave-length, but depends on the pressure of the chromosphere itself. In the present paper the theory will first be extended for the case of the Ca^{+} resonance lines, H and K. It will then appear that the spectral distribution of the coefficient of scattering of the upper layers of the chromosphere does not depend primarily on resonance scattering as in the reversing layer, but is essentially the result of Doppler effect of the Ca^+ atoms. The observations indicate velocities of about 15 km/sec.

---

[1] Fellow of the International Education Board.

[2] *Zeitschrift für Physik*, **46**, 782, 1928.

[3] These were previously observed by G. E. Hale and F. Ellerman, *Yerkes Observatory Publications*, **3**, Part 1, 1903, and by H. Deslandres, *Annales de l'Observatoire de Paris-Meudon*, **4**, Part 1, 1910.

With the aid of this coefficient of scattering, the pressure and even the variation of pressure with height in the chromosphere may be deduced, as regards order of magnitude, from the observations. Pressures of $\sim 10^{-15}$ atm. are obtained.

If the chromosphere is really supported by radiation pressure, the radiation which is removed by the chromospheric absorption lines, H_3 and K_3, must exactly suffice to support the mass of Ca^+ corresponding to the foregoing pressure. We shall see that this fundamental requirement of Milne's theory is actually fulfilled. Finally, we shall add some further considerations about the dynamics of the chromosphere. In particular, we shall show that theoretically there may be a continuous transition between the ordinary chromosphere and the prominences.

1. APPLICATION OF THE THEORY OF RADIATIVE EQUILIBRIUM TO THE EMISSION SPECTRUM OF THE SOLAR LIMB

Before we can calculate the distribution of intensity of the emission spectrum we must find the emissivity, J, of the solar atmosphere as a function of the optical depth. For this purpose the curvature of the layers may be neglected, since the height H of the chromosphere is small in comparison with the radius R of the sun.

The solar chromosphere does not receive its radiation directly from the photosphere, but through the reversing layer, which produces the broad H_1 and K_1 lines. In these deep layers the pressures are still comparatively high (10^{-4} to 10^{-7} atm.). Therefore, in addition to pure resonance-scattering, collisions between Ca^+ atoms and other particles will play an important part. Consequently, as the author has shown elsewhere,[1] there remains in the middle of these lines a residual intensity which must be equal for H and K. We take its numerical value from the observations as $\frac{1}{r} \sim \frac{1}{10}$ of the intensity of the undisturbed continuous spectrum of the center of the sun. The dependence of this residual intensity on direction is given, theoretically, as well as by observations, for $r \gg 1$, by $1+\frac{3}{2}\cos\vartheta$, where ϑ is the angle between the direction of the radiation and the normal to the solar surface. Thus, at the lower limit of the chromosphere, the outward radiation is

---

[1] *Probleme der modernen Physik: Festschrift zum 60. Geburtstag von A. Sommerfeld,* Leipzig, 1928.

$$I_0=\frac{2}{5}\cdot\frac{1}{r}\,I_1\left(1+\frac{3}{2}\cos\vartheta\right) . \tag{1}$$

In the outer chromosphere we can surely neglect the effect of collisions and so concern ourselves with pure scattering. We denote by $\bar{s}$ the mean value per centimeter of the coefficient of scattering for the whole chromosphere. The mean value for all layers whose distance from the outer boundary of the chromosphere is $\leqq y$ is denoted by s. We have designated the total height of the calcium chromosphere by H. If we neglect the reaction of the chromosphere on the reversing layer, then, according to Milne,[1] the emissivity of the chromosphere is

$$J=\frac{2}{5}\cdot\frac{1}{r}\,I_1\,\frac{1+\frac{3}{2}\,sh}{1+\bar{s}H} . \tag{2}$$

Evidently $\bar{s}=s(H)$; the dependence on the wave-length is the same for both $\bar{s}$ and s. If we take into account the backward radiation of the chromosphere and solve the Schwarzschild differential equations for an atmosphere which, in its lower part (reversing layer), exerts both scattering and absorption, but in its upper part (chromosphere), scattering only,[2] we obtain, instead of (2), the equation

$$J=\frac{2}{5}\cdot\frac{1}{r}\,I_1\,\frac{1+\frac{3}{2}\,sh}{1+\frac{2\omega}{1+\omega}\,\bar{s}H} . \tag{2$'$}$$

The coefficient ω is determined[3] from $\omega^2/1-\omega^2$, the ratio of the coefficient of absorption κ to coefficient of scattering σ for the reversing layer. As was shown in a former paper already cited, $\frac{\kappa}{\sigma}=0.044$ for the H and K lines, and, therefore, $\frac{2\omega}{1+\omega}\approx\frac{1}{3}$.

---

[1] *Philosophical Transactions of the Royal Society of London*, A, **223**, 201, 1922; A. Unsöld, *Zeitschrift für Physik*, **46**, 765, 1928, esp. pp. 767 ff.

[2] Cf. *Mt. Wilson Contr.*, No. 378; *Astrophysical Journal*, **69**, 278, 1929.

[3] We adopt here the designation of the above-mentioned paper.

The observable brightness I of the spectrum of the limb is now determined exactly in the manner previously described[1] by integrating along the line of vision over the emissivity multiplied by the corresponding absorption factor. If we designate by y the distance of the line of vision from the outer boundary of the chromosphere, we obtain by the method already described

$$I=\frac{\frac{2}{5}\cdot\frac{I_1}{r}}{1+\frac{2\omega}{1+\omega}\bar{s}H}\left\{\left(1-\frac{3}{2Rs}+3\sqrt{\frac{y}{2R}}\right)-e^{-2s\sqrt{2Ry}}\left(1-\frac{3}{2Rs}-3\sqrt{\frac{y}{2R}}\right)\right\}. \quad (3)$$

2. THE ABSORPTION SPECTRUM OF THE CHROMOSPHERE

To the Ca^+ emissions observed at the solar limb there correspond in the absorption spectrum of the solar disk two narrow depressions in the middle of the H and K lines, the so-called H_3 and K_3 lines, whose distribution of intensity F_a is determined by the total optical depth $\bar{s}H$ of the chromosphere alone. If we confine ourselves for the sake of simplicity to the integrated solar radiation[2] and make use of the circumstance that for all wave-lengths $\frac{2\omega}{1+\omega}\bar{s}H<1$, the formulae derived in the former paper[3] give

$$F_a=\frac{F_0}{1+\frac{2\omega}{1+\omega}\bar{s}H}, \quad (4)$$

where F_0 is the intensity in the middle of the H and K lines for the integrated solar spectrum. This formula allows us to determine from the observed structure of the H_3 and K_3 lines the total optical thickness of the chromosphere as a function of wave-length. The rough picture thus obtained can afterward be refined with the help of equation (3) by observations of the corresponding emission spectrum. As we shall see, these confirm, first, the belief that the H_3 and K_3 lines originate in the outer chromosphere, and allow, moreover, a rough estimation of the pressure gradient in the chromosphere. Before we start with the description and evaluation of the observations, however, it is desirable to make some remarks concerning the coefficient of scattering s or $\bar{s}$.

---

[1] A. Unsöld, *op. cit.*, p. 782.

[2] For pure scattering it is known that the dependence of the form of lines on direction is very small.

[3] A. Unsöld, *op. cit.;* esp. p. 768.

3. THE COEFFICIENT OF SCATTERING

In previous papers concerning the structure of solar lines we have shown that the coefficient of scattering in the neighborhood of a resonance line is determined by radiative damping. The broadening of lines by Doppler effect could be neglected. The broadening corresponding to the thermal motion of atoms in the solar atmosphere is of the order of 1/100 A, which can be neglected, and there are no other motions which could have any considerable effect on the broader lines. There is a temptation to apply also to the chromosphere the well-known formula[1]

$$s=\frac{2\pi e^4\lambda_0^2 Nf}{3\, m^2c^4\Delta\lambda^2}. \tag{5}$$

Great difficulties are met in doing this, however. The middle of the H_3 and K_3 absorptions and emissions should show practically complete darkness, as the factor $\bar{s}H$ in the denominator of formulae (3) and (4) becomes enormously great. As we shall see, this is not in accordance with the observations; moreover, such an atmosphere could not be supported by the light-pressure. An explanation of the residual intensity in the middle of the lines by the assumption of collisions, as in the case of the reversing layer, would scarcely be possible on account of the very low pressures of the chromosphere.

---

[1] Cf., for instance, *ibid.*, p. 768. The designations are:
e,m = electronic charge and mass
c = Velocity of light
λ_0 = Wave-length of the spectral line
$\Delta\lambda$ = Distance of the place observed (λ) from the spectral line (λ_0)
N = Number of atoms per cubic centimeter
f = Oscillatory power ($f=\frac{1}{3}$ and $\frac{2}{3}$ for H and K)

A possibility of avoiding these difficulties and, as far as I see, the only one, is indicated by a consideration of the geometrical structure of the chromosphere. As the spectroheliograms show, the outer chromosphere is not a quiet gaseous layer, as was assumed in deriving (5), but resembles more a burning prairie. These observations suggest the assumption that the whole chromosphere is in a kind of turbulent motion with an average velocity v. For the sake of simplicity we consider the distribution of velocities as Maxwellian, although naturally this is quite unimportant. As an approximate calculation easily shows, it is sufficient for what follows to compute the coefficient of scattering for the case of Doppler width $\gg$ damping width. Because of the Maxwellian distribution of velocity, its dependence on the wave-length is given by

$$s=C\cdot e^{-\left(\frac{\Delta\lambda}{\Delta\lambda_0}\right)^2}, \tag{6}$$

where $\Delta\lambda_0=\lambda_0\frac{v}{c}$ is the Doppler shift corresponding to the most probable velocity. The constant C is most easily determined by means of Tolman's "relation between the "total absorption" and the Einstein transition probability B_{12}. We thus have

$$\frac{1}{N}\int s d\nu=\frac{h\nu}{c}B_{12}, \tag{7}$$

the integral being extended over the H and K lines. But, on the other hand, B_{12} is determined by the sum rule of Kuhn, Thomas, and Reiche,[1] which gives

$$B_{12}=\frac{\pi e^2}{mh\nu}. \tag{8}$$

We thus obtain directly:[2]

$$s=\frac{\sqrt{\pi}\,e^2\lambda_0^2\,Nf}{mc^2\,\Delta\lambda_0}\,e^{-\left(\frac{\Delta\lambda}{\Delta\lambda_0}\right)^2}. \tag{9}$$

---

[1] *Zeitschrift für Physik*, **34**, 510, 1925.

[2] First derived in a somewhat different way by W. Voigt, *Sitzungsberichte der Akademie der Wissenschaften zu München*, p. 603, 1912; esp. p. 617. The earlier literature on the subject is given there.

PLATE VII

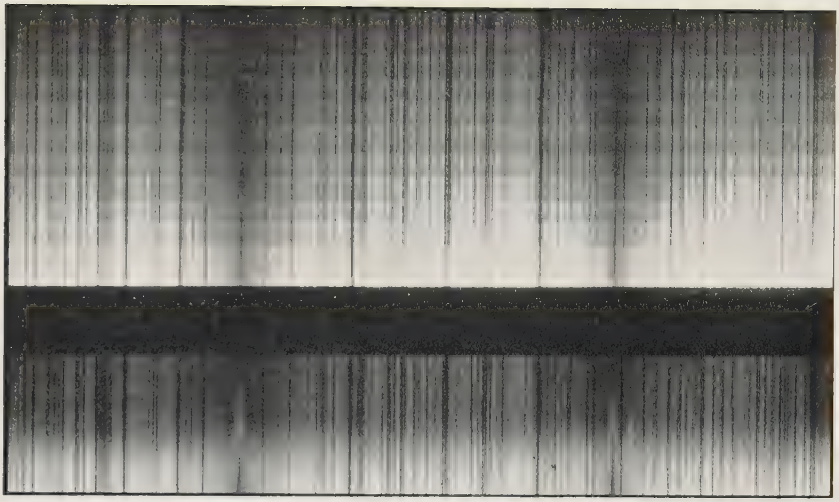

Chromospheric Spectrum with Intensity Marks

Having prepared the necessary foundation, we may now begin in a following section the description and evaluation of the observations.

4. OBSERVATIONS OF THE EMISSION AND ABSORPTION SPECTRA OF THE CALCIUM CHROMOSPHERE

By means of the 150-foot tower telescope, a solar image 42.6 cm in diameter was projected on the slit of the 75-foot grating spectrograph. In order to obtain the emission spectrum of the chromosphere, the solar limb was so placed that it formed an angle of about 20° with the slit. The spectrum was photographed in the first order (1 mm = 0.7 A). The photometric scale was obtained in the manner previously described.[1] By means of a rotating sector with stair-shaped sections, spectra of the center of the solar disk having graded intensities were photographed on the same plate. As very great intervals of intensity were to be covered, Eastman 40 plates were used. The photographs of the narrow H_3 and K_3 absorptions in the spectrum of the solar disk were taken with the third order of the same spectrograph. For the photometric measures the thermoelectric registering photometer of the Mount Wilson Observatory was used. A superficial survey of the material showed at once that the emission and especially the absorption spectrum of the chromosphere is subject to considerable variation in different parts of the sun. The numerical values can therefore claim no very great accuracy. They are, however, as may easily be seen, fully sufficient for our purposes.

Plate VII shows one of the chromospheric spectra thus obtained. Figures 1–4 give photometric traces of the H and K lines (besides H, the hydrogen line H_ϵ appears in emission) at altitudes of 2500 and 5600 km above the photosphere. On Plate VII, 1 mm corresponds to about 1000 km.

5. NUMERICAL EVALUATION OF THE OBSERVATIONS AND COMPARISON WITH THE THEORY

We come now to the most important part of the present investigation, the measurement of the pressure in the chromosphere. As already mentioned, the attempt to account for the observations was first made under the assumption of a quiescent chromosphere. The coefficient of scattering would then be determined by equation (5) of section 3. According to this formula, however, as can be seen by means of (3) and (4), the middle of the absorption and emission

---

[1] A. Unsöld, *op. cit.*, p. 769.

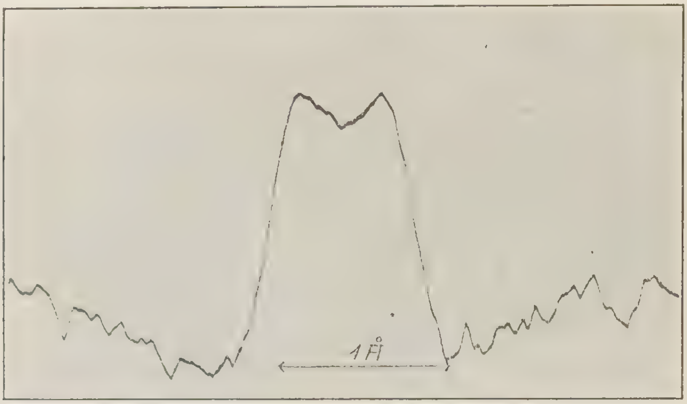

FIG. 1.—K emission 2500 km above the photosphere

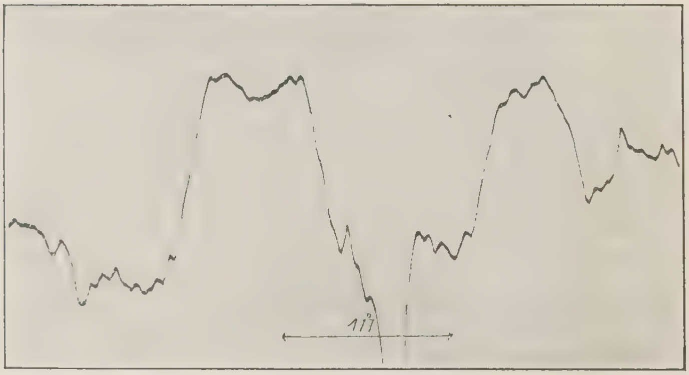

FIG. 2.—H and H_ϵ emission 2500 km above the photosphere

lines ought to be perfectly dark. Furthermore, since in (5) the distance from the center of the line, $\Delta\lambda$, occurs only in the combination $f/(\Delta\lambda)^2$, the widths of the H and K emission (and absorption) lines should have the ratio of $1:\sqrt{2}$. None of these predictions is fulfilled, for the middle portions of the lines show considerable central intensity, and the ratio of the widths of the emission lines is about 1:1.1 instead of 1:1.4. Equation (5) cannot therefore be applied to the chromosphere. As was shown in section 3, the only way out of this dilemma is the assumption that the chromosphere is permanently in a kind of turbulent motion. This hypothesis gives formula (9) for the coefficient of scattering. We will now show that this assumption gives a satisfactory representation of the observations and furnishes reasonable values for the pressures in the chromosphere. Here and in what follows we are, naturally, dealing always with the Ca^+ partial pressure.

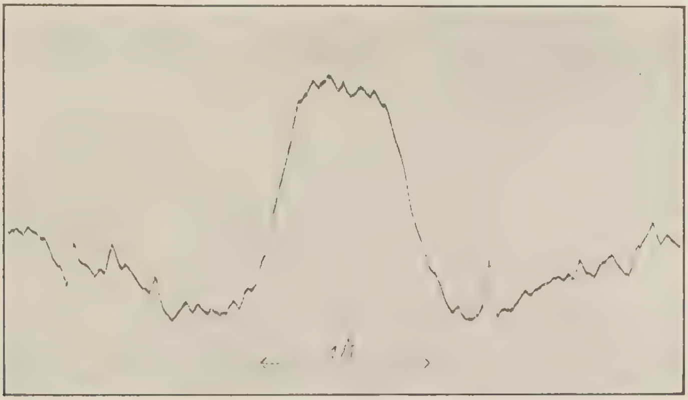

FIG. 3.—K emission 5600 km above the photosphere

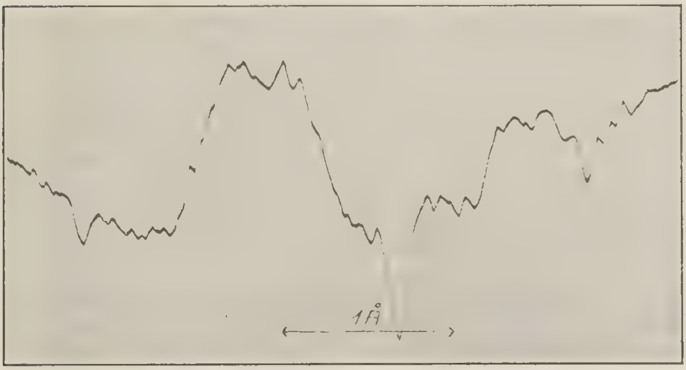

FIG. 4.—H and H_ϵ emission 5600 km above the photosphere

Numerical values must now be introduced into equations (9), (4), and (3). The solar radius is $\sim 7\times10^{10}$ cm. The height of the Ca^+ chromosphere, according to S. A. Mitchell,[1] is 14,000 km $=14\times10^8$ cm. Since the photometric traces refer to heights of 2.5×10^8 and 5.6×10^8 cm, the values for y, the distance of the line of vision from the outer boundary of the chromosphere, are 11.5×10^8 and 8.4×10^8 cm. For a first approximation, consider the pressure in the upper chromosphere as constant, an assumption that will be dropped later, and write in (3), for trial, $s=\frac{1}{3}\bar{s}$.

The depth of the absorption lines, measured from the bottom F_0 of the ordinary H and K lines, is $\sim$ 25–30 per cent;[2] hence, for $\Delta\lambda=0$ we put in (4) $F_a \approx 0.75\ F_0$. Thus we can calculate first $\bar{s}H$, then $\bar{s}$, and finally, by means of (9), the value of $N/\Delta\lambda_0$ where N is the number of atoms per cubic centimeter and $\Delta\lambda_0$ is the Doppler width corresponding to the average velocity of the Ca^+ atoms. Either the width of the absorption lines or the value of $F_a:F_0$ for any $\Delta\lambda\neq0$ makes it possible by means of equation (9) to determine $\Delta\lambda_0$ itself and therefore also the value of N. At the same time, the intensity of the emission lines is fixed throughout the chromosphere by the values of N and $\Delta\lambda$. By successive trials the numerical values were improved somewhat further, and then the calculations were carried through for $\Delta\lambda_0=0.2$ A, corresponding to a velocity of $\frac{0.2}{3950}\times3\cdot10^5$ km/sec. $=15$ km/sec., and for $N=5700$ atoms per cubic centimeter (the average over the whole chromosphere). For $\bar{s}$ we then obtain the following formulae in which $\Delta\lambda$ is measured in A,

$$\left.\begin{aligned} K_3\text{ line:}\quad \bar{s}_K &= 15\times10^{-10}e^{-\left(\frac{\Delta\lambda}{0.2}\right)^2}\,, \\ H_3\text{ line:}\quad \bar{s}_H &= 7.5\times10^{-10}e^{-\left(\frac{\Delta\lambda}{0.2}\right)^2}\,. \end{aligned}\right\} \qquad (10)$$

Figure 5 gives a graphical representation of these formulae. Here and in what follows the full curve refers to the K line; the dotted curve, to H. All the curves are drawn for only one side of the lines. By equation (4) the whole distribution of intensity of the absorption lines can now be calculated. Figure 6 shows the curves thus obtained.

---

[1] *Astrophysical Journal*, **38**, 407, 1913.

[2] The difference of this value for H_3 and K_3 can scarcely be measured.

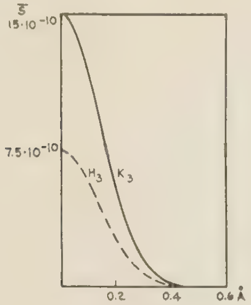

FIG. 5

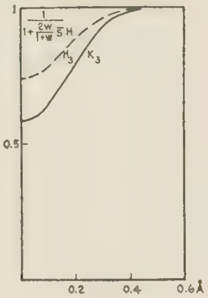

FIG. 6

FIG. 5.—Scattering coefficient for H_3 and K_3
FIG. 6.—Contours of H_3 and K_3 absorption lines

Let us now consider the emission lines. In Figure 7, again under the assumption $s=\frac{1}{3}\bar{s}$, we have plotted by means of equation (3) the intensity I of the emission, in units of $\frac{2}{5}\frac{I_1}{r}$, as function of $\bar{s}$

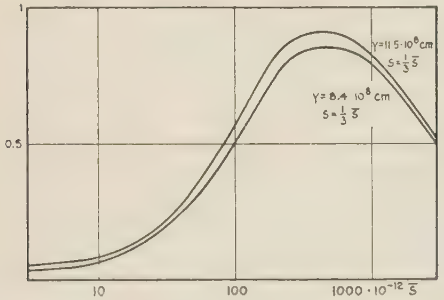

FIG. 7

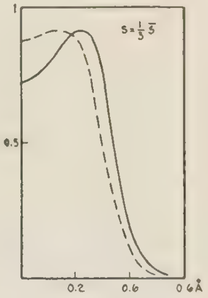

FIG. 8

FIG. 7.—Intensity of emission as function of $\bar{s}$
FIG. 8.—Emission lines for $y=11.5\times10^8$ cm

(abcissae in logarithmic scale) for the two values of y corresponding to our observations. With the help of the curves in Figure 5 we can now draw the profiles of the corresponding emission lines. Figures 8 and 9 show the curves obtained in this way. The general agreement with observation is fairly satisfactory. The ratio of the line widths is really 1 : 1.1, as the observations require.[1] In the same way the characteristic dip in the center of the lines results directly from our formulae. The agreement of the calculated absorption lines with observation is also satisfactory. Only in one respect is there still a discrepancy between theory and observation. The intensity in the middle of the emission line decreases much more rapidly with increasing altitude above the photosphere, that is, with values of $H-y$, than our calculations require. Furthermore, the intensity in the middle of the emission lines ($I_{\Delta\lambda=0}$) is smaller in comparison with the continuous spectrum of the center of the sun, I_1, than our present theory demands. As seen from Figure 8, this gives, for $y=11.5\times10^8$ cm, the value $I_{\Delta\lambda=0}\sim0.8\times\frac{2}{5}\frac{I_1}{r}$, or, with $r\approx11$ (Schwarzschild), $I_{\Delta\lambda=0}\approx0.03\ I_1$. The observations give about $I_{\Delta\lambda=0}\approx0.01\ I_1$, but this numerical value has a considerable uncertainty.

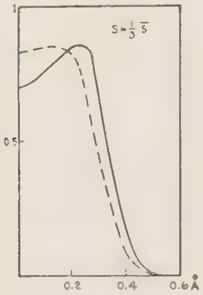

FIG. 9

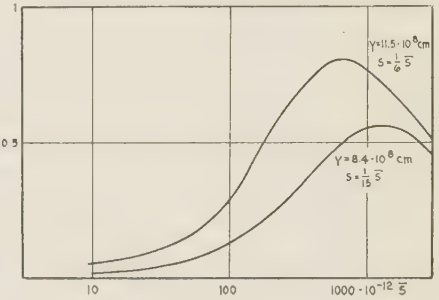

FIG. 10

FIG. 9.—Emission lines for $y=8.4\times10^8$ cm
FIG. 10.—Intensity of emission as function of $\bar{s}$

These differences between the observations and our calculations indicate clearly that the assumption of a constant value for s over the whole outer chromosphere is only a very rough approximation. We must therefore use in equation (3) different numerical values of s for different heights. The dependence on the wave-length, in other words, the average velocity of the Ca^+ atoms, we shall assume to be constant. The value of $\bar{s}$ naturally cannot be changed, as it is fixed by the absorption lines. After some trials it was seen that the observations can be represented best by putting $s=\frac{1}{6}\,\bar{s}$ for $y<11.5\times 10^8$ cm and $s=1/15\,\bar{s}$ for $y<8.4\times 10^8$ cm. Figure 10 shows for these cases I (in the former unit) as a function of $\bar{s}$. It will be noted that the maximum of the emission, especially for the higher layers, has shifted toward increasing $\bar{s}$, that is, toward the center of the line, and becomes lower at the same time.

---

[1] Also the ratio of intensities of the Ca^+ lines, K : H = 1 : 0.8, measured by C. R. Davidson, *Monthly Notices, R.A.S.*, 88, 30, 1927, agrees well with our results. The measures by C. R. Davidson, M. Minnaert, L. S. Ornstein, and F. J. M. Stratton, *ibid.*, p. 536, which give an intensity ratio of 1 : 0.57, refer apparently to a prominence, to which our calculations naturally cannot be applied.

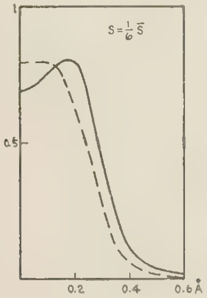

FIG. 11

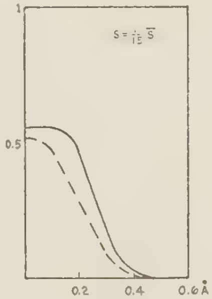

FIG. 12

FIG. 11 —Emission lines for $y=11.5\times 10^8$ cm
FIG. 12.—Emission lines for $y=8.4\times 10^8$ cm

The distributions of intensity for the H and K lines calculated for $y=11.5\times 10^8$ cm ($s=1/6\,\bar{s}$) and for $y=8.4\times 10^8$ cm ($s=1/15\,\bar{s}$) are shown in Figures 11 and 12.

The agreement with the observations is now a great deal better, but the calculated total intensity is still too great, and the observed decrease of $I_{\Delta\lambda=0}$ with elevation above the photosphere which is expressed by

$$\frac{I_{y=11.5\times 10^8}}{I_{y=8.4\times 10^8}}\sim 3$$

is also greater than our calculations indicate. A much greater decrease of the pressures toward higher layers cannot well be assumed, because a comparison of curves 7 and 10 shows that the characteristic minimum of intensity in the middle of the emission lines would then disappear. This remaining disagreement cannot, however, be considered a serious objection to the theory, since the assumption that $\Delta\lambda_0$ is independent of y and that s can be considered as constant for $y >$ some given value furnishes at best only a rough picture of the reality.[1]

All things considered, the uncertainty of the pressures derived in the following paragraph should not be much greater than a factor of 10.

Assuming a temperature of $T=4800^\circ K$, the exact numerical value of which is not very essential, we obtain for the average pressure of the chromosphere

$$p=NkT=4\times 10^{-9} \text{ dynes/cm}^2=4\times 10^{-15} \text{ atm.}\,, \qquad (11)$$

where $N=5700$ atoms/cm³; $k=$ Boltzmann's constant. The mean pressures for the higher layers are correspondingly:
for

$$y<11.5\times 10^8 \text{ cm}; \quad 0.6\times 10^{-15} \text{ atm.}\,,$$

and for

$$y<\ 8.4\times 10^8 \text{ cm}; \quad 0.3\times 10^{-15} \text{ atm.}$$

If we further consider the pressures in the three layers into which the chromosphere is divided by our points of observation to be constant, the individual values, which may be regarded as the average pressure for these layers, can be estimated by means of the foregoing figures. Let us designate the thickness of these arbitrarily chosen layers by a, b, c, and the corresponding pressures by P_a, P_b, P_c. We then have the equations

$$\left.\begin{aligned} aP_a+bP_b+cP_c &= (a+b+c)\ p\,, \\ aP_a+bP_b &= (a+b)\ \tfrac{1}{6}\ p\,, \\ aP_a &= a\ \tfrac{1}{15}\ p\,. \end{aligned}\right\} \qquad (12)$$

By solving these equations and inserting the numerical values we find the following stratification of pressure which is still affected with considerable uncertainty, but surely gives the right order of magnitude:

---

[1] The assumption of a smaller height of the chromosphere H would also improve the agreement between theory and observation. We shall not, however, make an attempt to press the data.

Layer	Thickness	Pressure	
a	$\updownarrow$ 8.4×10^8 cm	$P_a \sim 0.3\times10^{-15}$ atm.	Total height $=14\times10^8$ cm Average pressure $=4\times10^{-15}$ atm.
b	$\updownarrow$ 3.1×10^8 cm	$P_b \sim 2\times10^{-15}$ atm.	
c	$\updownarrow$ 2.5×10^8 cm	$P_c \sim 19\times10^{-15}$ atm.	

Height above the Photosphere	$Ca+$ Pressure
0–2500 km	19×10^{-15} atm.
2500–5600	2×10^{-15}
5600–14,000 (?)	0.3×10^{-15}

In order to summarize all the results at this point it may be worth while to state once more that the average velocity obtained for the Ca^+ atoms is 15 km/sec. The thermal velocity of Ca^+ at $T=4800^\circ K$ is

$$v_{th}=\sqrt{\frac{3kT}{M}}\,,$$

where $M=6.60\times10^{-23}$ is the mass of the Ca^+ atom. Hence $v_{th}=1.7$ km/sec.

6. COMPARISON WITH MILNE'S THEORY

Since a nearly isothermal atmosphere with a pressure of only a fraction of an atmosphere would immediately be compressed to a thickness of a few hundred kilometers under the action of the solar gravitation, E. A. Milne has worked out in a series of papers the hypothesis that the chromosphere is supported essentially by light-pressure. If this assumption is right, the radiation absorbed, or better, scattered away by the H_3 and K_3 lines, must be just sufficient to support the spectroscopically determined mass of the Ca^+ chromosphere. Measurement of the areas under the curves in Figure 6 leads to the result that the quantity of light scattered away by the H_3 and K_3 lines corresponds to the complete absorption of a band 0.3 A wide having the intensity in the middle of the broad H and K lines. As this residual intensity, produced by the influence of collisions of Ca^+ atoms with other particles, is about 1/10 of the intensity of the continuous spectrum of the same spectral region, the H_3 and K_3 lines correspond to the complete absorption of a zone of the continuous spectrum 0.03 A wide.

According to Milne[1] the number of atoms which can be supported by a band of the breadth $\Delta\nu$ is given by

$$N_m = \frac{4\pi h\nu^3}{gMc^3} e^{-\frac{h\nu}{kT}} \Delta v \,, \tag{13}$$

where $g = 2.74 \times 10^4$ is the gravitation at the solar surface; $M = 6.6 \times 10^{-23}$ is the mass of Ca^+ atoms; and ν is the frequency of the Ca^+ lines. Substitution of the numerical values gives

$$N_m = 7 \times 10^{12} \text{ atoms.}$$

On the other hand, our spectroscopic determination gives

$$N_{sp} = NH = 5700 \times 1.4 \times 10^9 = 8 \times 10^{12} \text{ atoms.}$$

The two values agree therefore far within the accuracy of measurement. Milne himself has given in his publications pressures of $\sim 10^{-13}$ atm. for the chromosphere, while we find $\sim 10^{-15}$ atm. The origin of this difference is that he has overestimated the total absorption corresponding to the chromosphere.[2]

Our result has a further important consequence: It indicates that calcium cannot be doubly ionized to an appreciable degree in the chromosphere. For if it were, the light-pressure calculated from the total absorption of the H_3 and K_3 lines would not be sufficient to support the spectroscopically determined quantity of Ca^+ and at the same time the corresponding quantity of Ca^{++}.

On the other hand, according to Saha's formula, the ratio of Ca^{++}/Ca^+ at a temperature of $T = 4830°\ K$ and a partial pressure of 10^{-15} atm. for the Ca^+ atoms is given by

$$\begin{aligned} \log_{10} \frac{Ca^{++}}{Ca^+} (Ca^+ + 2Ca^{++}) &= \log_{10} Ca^+ \left[\frac{Ca^{++}}{Ca^+} + 2\left(\frac{Ca^{++}}{Ca^+}\right)^2 \right] \\ &= -\frac{5036\ I}{T} + 2.5 \log_{10} T - 6.5 \,, \end{aligned} \tag{14}$$

where the chemical symbols are put for the pressures in atmospheres, and $I = 11.82$ volts represents the ionization potential of Ca^+. One obtains, thus,

$$\frac{Ca^{++}}{Ca^+} \approx 350 \,.$$

---

[1] See *Monthly Notices, R.A.S.*, 88, 188, 1928; esp. p. 192.

[2] Milne himself has remarked, however, that smaller figures would probably correspond more closely to reality. Cf. *op. cit.*, p. 193 n.

It follows that the degree of ionization is much lower than the calculation made on the assumption of thermal equilibrium would indicate.

7. DYNAMICS AND STABILITY OF THE CHROMOSPHERE[1]

We have still to discuss why the average velocity of the Ca^+ atoms in the chromosphere (15 km/sec.) is considerably higher than the thermal velocity corresponding to the solar temperature. This discussion will lead us to considerations of stability.[2]

The lower boundary of the chromosphere should be determined by the fact that at a certain pressure collisions between the different particles begin to play an important part (condition I).[3] On the other hand, however, according to Milne, the chromosphere can be supported only if the residual intensity in the middle of the Ca^+ lines[4] has a certain value. Because of this, according to equations (9) and (4), the numerical value of $NH/\Delta\lambda_0$ is fixed (condition II). Conditions I and II permit a separation of the values of NH and $\Delta\lambda_0$, and these lead to a knowledge of the whole chromosphere. At the present time, however, it is not quite possible to carry through these ideas quantitatively.

The necessity for a "turbulent" motion of the chromosphere of an average velocity corresponding to the Doppler width has another interesting consequence. Since the entropy of the chromosphere cannot increase, in course of time these motions will tend to become equal and approach the value ~ 1.7 km/sec., the thermal motion at the solar temperature. If, however, $\Delta\lambda_0$ becomes smaller than the assumed value, the total absorption will no longer be sufficient to support the chromosphere, which will therefore collapse. Then, however, the light-pressure will again expel atoms until the "normal state" is regained, when the play begins anew. In appearance, the chromosphere can never reach a stationary state, but will always be going up and down; in fact, spectroheliographic observations show that the chromosphere often looks like a "burning prairie." The single flames seem to change rather rapidly. Our explanation thus leads to a steady transition between the normal chromosphere and the prominences which is very satisfactory from the viewpoint of spectroheliographic observations. The changes of brightness of the photosphere through changes in light-pressure will naturally also give rise to motions.

---

[1] These considerations are merely a first attempt to explain the observations. Our very schematic ideas are evidently still too rough for giving a complete theory.

[2] Cf. esp. Milne, *Monthly Notices, R.A.S.*, 86, 459, 1927.

[3] Cf. A. Unsöld, *loc. cit.*

[4] The reference here and in the following is to a mean value for H_3 and K_3.

8. THE DISTRIBUTION OF PRESSURE IN THE CHROMOSPHERE

In a former paper[1] the author has proposed a theory of the chromosphere different from Milne's. However, as Milne[2] and Anderson[3] have shown, the assumption of constant light-pressure which was made in that paper was not justified. Moreover, as Milne has already assumed (and as was demonstrated in section 6), Saha's formula cannot be applied to the chromosphere, since the conditions deviate very much from thermal equilibrium.

Milne, on the other hand, has neglected in his theory the action of ionization. The dynamic equilibrium is regulated by changing the number of excited atoms. This assumption is justified, as may easily be seen, as long as the free path for recombination of Ca^{++} atoms with electrons is greater than the height of the chromosphere. According to an estimate by Milne,[4] this requirement is in general likely to be fulfilled. At very great heights it is possible that Ca^{++} atoms, a very small degree of ionization being sufficient, produce an apparent diminution of the coefficient $1-\mu=$light-pressure: gravitation, and hence a rather definite boundary for the chromosphere. The decrease of pressure with increasing height as derived in section 5 of the present paper, in so far as order of magnitude is concerned, is in agreement with Milne's theory. More cannot very well be expected in the present state of affairs.

In conclusion, I should like to express my heartiest thanks to Dr. St. John, Dr. Dunham, and Dr. Nicholson for much help and advice; and to Miss Louise Ware for her help in the photometric measurements. I am indebted furthermore to the International Education Board for giving me the opportunity to work at the Mount Wilson Observatory.

Carnegie Institution of Washington
Mount Wilson Observatory
January 1929

---

[1] *Zeitschrift für Physik*, **44**, 793, sec. 7, 1927.

[2] *Op. cit.*, **88**, 188, 1928.

[3] *Zeitschrift für Physik*, **46**, 445, 1927.

[4] *Loc. cit.*, **88**, 188, sec. 7, 1928.

Contributions from the Mount Wilson Observatory, No. 378
Reprinted from the *Astrophysical Journal*, Vol. LXIX, pp. 275-286, 1929
Printed in the U.S.A.

ON THE PHYSICAL INTERPRETATION OF SPECTROHELIOGRAMS

By ALBRECHT UNSÖLD[1]

ABSTRACT

Introduction.—Short recapitulation of the observations.

1. *Radiative equilibrium in a stratified atmosphere with scattering and absorption.*—The intensity of radiation emerging from such an atmosphere is calculated as a function of the coefficients of scattering and of absorption and of the temperatures of the different layers.

2. *Application of these theoretical considerations to calcium spectroheliograms.*—It is shown how different parts of the lines are co-ordinated with different levels. Photometric measures of the distribution of intensity in the inner parts of the H and K lines are described.

3. *Hydrogen spectroheliograms.*—A comparison of calcium and hydrogen spectroheliograms shows that in disturbed regions of the sun the hydrogen atoms are probably affected through electric disturbances by other particles.

4. *In the Evershed effect* and *similar phenomena* lines of the *same multiplet* seem to indicate *different velocities.* This observation can be explained on the basis of the theory developed in sections 1 and 2, supplemented by considerations on contrast effect. Experiments with artificial lines confirm this explanation.

INTRODUCTION

The spectroheliographic researches of G. E. Hale[2] and of H. Deslandres[3] led to the important result that spectroheliograms taken with the center of a Ca^+ line correspond to the highest calcium levels of the solar atmosphere, while pictures in the light of the wings of these lines represent layers whose depth increases with increasing distance from the center of the line. This interpretation was based on the general appearance of the pictures and has been confirmed by the observations of Adams[4] on the differences in the rotational velocities of the outer solar layers, and of St. John[5] on the Evershed effect. The physical interpretation of these relations, however, remained in an unsatisfactory state. As long as pressures of several atmospheres were ascribed to the reversing layer, direct effects of pressure could be assumed, and in this way the wings of the lines could be attributed to the most "quenched" atoms of the deeper layers. Since the pressures in solar and stellar atmospheres have been shown by both observation[1] and general astrophysical considerations to be very low, this explanation is generally discarded today. After it was realized[2] that the H and K lines are produced mainly by resonance scattering, the following explanation might have been substituted: As the coefficient of scattering is considerably greater for the light of the middle of the line than for that of the wings, it might have been assumed that the spectroheliograph penetrates deeper into the solar atmosphere with the light of the wings than with the light of the center of the line, just as a photographic camera penetrates farther into a hazy atmosphere with a red filter than without. This comparison, however, cannot be applied directly to the sun, for the exchange of radiation in the solar atmosphere is regulated in a manner wholly different from that in the terrestrial atmosphere. Furthermore, on the earth the objects to be seen are small compared with the dimensions of the atmosphere, while on the sun this is usually not the case. Moreover, it can easily be shown from known formulae that an increase of the density in a certain layer influences (in the case of pure resonance scattering) the different parts of a line in exactly the same manner. As the changes in the form of spectral lines important for us concern especially the middle of these lines, it is reasonable to assume that in the present problem atomic collisions play a decisive rôle. To clarify the matter, we shall therefore (sec. 1) first apply the theory of radiative equilibrium to a stratified atmosphere in which occur resonance scattering and collisions, the collisions producing absorption in the sense in which the term was used by Schwarzschild. These considerations lead to a satisfactory theory of spectroheliograms (sec. 2). In sections 3 and 4 we shall briefly treat the differences between calcium and hydrogen spectroheliograms, and, finally, discuss a curious observation concerning currents in different solar layers which is connected with the considerations of section 1.

---

[1] Fellow of the International Education Board.

[2] *Yerkes Observatory Publications*, **3**, 1903, and *The Study of Stellar Evolution*, Chicago, 1908.

[3] *Annales de l'Observatoire de Paris-Meudon*, **4**, 1910.

[4] *Mt. Wilson Contr.*, No. 33; *Astrophysical Journal*, **29**, 110, 1909.

[5] *Mt. Wilson Contr.*, No. 69; *Astrophysical Journal*, **37**, 322, 1913.

---

[1] C. E. St. John and H. D. Babcock, *Mt. Wilson Contr.*, No. 278; *Astrophysical Journal*, 60, 32, 1924.

[2] Cf., for instance, A. Unsöld, *Zeitschrift für Physik*, 46, 765, 1928.

1. RADIATIVE EQUILIBRIUM OF A STRATIFIED ATMOSPHERE WITH SCATTERING AND ABSORPTION[1]

We consider the following schematic solar atmosphere:

Above the photosphere let there be, first, the layer I (reversing layer), with the scattering and absorption coefficients σ_1, and κ_1 and the Kirchhoff-Planck function B_1, all of which are assumed to be constant throughout this layer. For the sake of simplicity we consider the emission of the photosphere, I_0, as independent of direction. Above this assume a second layer II, in which these quantities have the values σ_2, κ_2, and B_2. We shall later on identify this layer with the upper part of the reversing layer, or the chromosphere.

In order to simplify the calculations, we assume furthermore the inward radiations, I_1' and I_2', for layers I and II, respectively, and the outward, I_1 and I_2, to be independent of direction. The differential equations of radiative equilibrium have then the well-known Schwarzschild-Schuster form. Their solutions for layers I and II may therefore be taken from my earlier paper.[2]

We have for layer I:

$$\left.\begin{aligned} 2I_1 &= R_1(1-\omega_1)e^{-u_1}+S_1\left(\frac{e^{u_1}-e^{-u_1}}{a_1}+\omega_1\,\frac{e^{u_1}+e^{-u_1}}{a_1}\right) \\ &\qquad +2B_1\left(1-\omega_1\,\frac{e^{u_1}-e^{-u_1}}{2}-\frac{e^{u_1}+e^{-u_1}}{2}\right), \\ 2I_1' &= R_1(1+\omega_1)e^{-u_1}+S_1\left(\frac{e^{u_1}-e^{-u_1}}{a_1}-\omega_1\,\frac{e^{u_1}+e^{-u_1}}{a_1}\right) \\ &\qquad +2B_1\left(1+\omega_1\,\frac{e^{u_1}-e^{-u_1}}{2}-\frac{e^{u_1}+e^{-u_1}}{2}\right), \end{aligned}\right\} \quad (1)$$

---

[1] The following calculations are very closely connected with the former paper: "Über den Einfluss von Stössen auf die Struktur der Fraunhoferschen Linien," *Probleme der modernen Physik: Festschrift zum 60. Geburtstag von A. Sommerfeld*, Leipzig, 1928. The notations are essentially the same. Here we shall repeat only the most important principles.

[2] *Op. cit.*, equation (7).

and correspondingly for layer II:

$$\left.\begin{aligned} 2I_2 &= R_2(1-\omega_2)e^{-u_2}+S_2\left(\frac{e^{u_2}-e^{-u_2}}{a_2}+\omega_2\frac{e^{u_2}+e^{-u_2}}{a_2}\right) \\ &\qquad +2B_2\left(1-\omega_2\frac{e^{u_2}-e^{-u_2}}{2}-\frac{e^{u_2}+e^{-u_2}}{2}\right), \\ 2I_2' &= R_2(1+\omega_2)e^{-u_2}+S_2\left(\frac{e^{u_2}-e^{-u_2}}{a_2}-\omega_2\frac{e^{u_2}+e^{-u_2}}{a_2}\right) \\ &\qquad +2B_2\left(1+\omega_2\frac{e^{u_2}-e^{-u_2}}{2}-\frac{e^{u_2}+e^{-u_2}}{2}\right). \end{aligned}\right\} \quad (2)$$

The notation is the same as in the former paper. In formulae which are equally valid for layers I and II, the subscripts 1 and 2 will be omitted. R and S are constants of integration, which will subsequently be determined. If we set $\frac{2\kappa}{\sigma}=\lambda$ and $t=\frac{3}{4}\sigma\times$depth, we have, as in the previous paper, $u=\sqrt{\lambda(2+\lambda)}\,t$, $a=\sqrt{\lambda(2+\lambda)}$, and $\omega=\sqrt{\frac{\lambda}{2+\lambda}}$.

The boundary conditions which are necessary for the determination of the four constants of integration can now be formulated as follows:

A. At the outer boundary of the atmosphere the inward radiation disappears.

B. At its inner boundary, layer I receives the radiation of the photosphere; that is, for $u_1=u_{10}$, a given large value (compare, however, condition C), we have $I_1=I_0$.

C. At the boundary between layers I and II, $I_1=I_2$ and $I_1'=I_2'$. The depth $u_1=u_{12}$ corresponding to the upper boundary of layer I remains undetermined, since in the final equations u_{12} occurs in such relation to the constants of integration that only the difference $u_{12}-u_{10}$ has a physical meaning.

Condition A, by means of equation (2), gives at once:

$$R_2(1+\omega_2)-S_2\frac{2\omega_2}{a_2}=0\,. \qquad (3)$$

To obtain the second boundary condition in a convenient form and to simplify the following calculations, we assume that the optical depth of layer I is always >1, which means that we confine ourselves to following the changes of the broad H and K lines in the neighborhood of their centers. Then we obtain, with the aid of (1):

$$S_1 = a_1 B_1 \, . \tag{4}$$

The boundary conditions (C), by means of (1) to (4), may now be written, the lower boundary of layer II being determined by u_2:

$$\left.\begin{aligned}(1-\omega_1)(R_1-2B_1)e^{-u_{12}}+2B_1 &= R_2\left\{2\cosh u_2+\left(\omega_2+\frac{1}{\omega_2}\right)\sinh u_2\right\}\\ &\quad +2B_2\{1-\omega_2\sinh u_2-\cosh u_2\}\, ,\\ (1+\omega_1)(R_1-2B_1)e^{-u_{12}}+2B_1 &= -R_2\left(\omega_2-\frac{1}{\omega_2}\right)\sinh u_2\\ &\quad +2B_2\{1+\omega_2\sinh u_2-\cosh u_2\}\, .\end{aligned}\right\} \tag{5}$$

By elimination of R_1, the constant R_2 can be calculated. We find:

$$\left.\begin{aligned}R_2\left\{(1+\omega_1)\cosh u_2+\left(\omega_2+\frac{\omega_1}{\omega_2}\right)\sinh u_2\right\}&\\ =2(B_1-B_2)\omega_1+2B_2(\omega_1\cosh u_2+\omega_2\sinh u_2)&\, .\end{aligned}\right\} \tag{6}$$

Now we are already at our goal, since by means of (2) we see that at the outer boundary of the atmosphere

$$I_2 = R_2 \, . \tag{7}$$

In other words, the constant of integration, R_2, itself gives directly the average intensity of the observed radiation. Its distribution in direction we shall not treat.

2. INTERPRETATION OF CALCIUM SPECTROHELIOGRAMS

In order to obtain a physical interpretation of the calcium spectroheliograms, we must discuss in what way the shape of the line depends upon the constants ω_1, B_1 and ω_2, B_2.

If we leave layer II out of consideration for the moment ($u_2=0$), equation (6) gives for the residual intensity of the primary absorption line the value (for integrated radiation)

$$R_2 = R_1 = \frac{2B_1\omega_1}{1+\omega_1}\, , \tag{8}$$

which was contained implicitly in the above-mentioned paper. If, however, $u_2 \gg 1$, that is, if the optical depth corresponding to the middle of our "secondary" line is still considerable, we have

$$R_2 = \frac{2B_2\omega_2}{1+\omega_2}, \tag{9}$$

which shows that the residual intensity then depends only on the uppermost layer. This means that, roughly speaking, the radiation of deeper layers cannot in an appreciable degree penetrate through this layer. However, if $u_2 \ll 1$, we can develop equation (6) in increasing powers of u_2 and obtain[1]

$$R_2 = \frac{2(B_1\omega_1 + B_2\omega_2 u_2)}{1+\omega_1+\left(\omega_2+\dfrac{\omega_1}{\omega_2}\right)u_2} = R_1\left\{1-\left(\frac{\omega_2+\dfrac{\omega_1}{\omega_2}}{1+\omega_1}-\frac{B_2\omega_2}{B_1\omega_1}\right)u_2\right\}. \tag{10}$$

In this case the two lines are superposed and the upper layer gives only a comparatively small modification of the center of the line.

For the Ca^+ lines our second assumption ($u_2 < 1$) should come nearer to the truth.

Let us assume now that, through deviations from equilibrium conditions in the lower layer I, the constant B_1, or ω_1, or both together, rise above their average values. Then R_1 will increase according to (8). The more we approach the center of the line, the greater will be the increase in brightness indicated by the spectroheliograph. In the very schematic Figure 1 let the line *a* correspond to undisturbed conditions. Then line *b* will result from the described changes. For, as shown in the earlier paper, the intensity of the outermost part of the wings does not depend at all upon B_1 and ω_1, while the intensity of the intermediate and inner parts is determined by these very factors. This effect is modified, however, as soon as the zone of the secondary line, originating in layer II, is entered. If the u_2 corresponding to the middle of this line is $\gg 1$, we shall, according to (9), have there no change at all. If $u_2 \ll 1$, then according to (10) the effect will not increase in any case (cf. again Fig. 1, curve *b*).

---

[1] For $B_2 = 0$ and $\lambda_2 \rightarrow 0$ we get from this formula at once the one (equation 2′) used in the preceding paper (*Mt. Wilson Contr.*, No. 377; *Astrophysical Journal*, 69, 209, 1929).

Just the reverse happens if we change the constants B_2 and ω_2 of the upper layer, but leave unchanged those of the lower one. Then R_1, and therefore the principal lines, naturally remain unmodified, while the secondary line changes according to (10). In Figure 1 these modifications are represented in various degrees by curves *c* and *c′*.

We observe that the behavior of the whole line corresponds throughout to the spectroheliographic observations. The bright parts correspond therefore to an increase either of the (approximate) Kirchhoff function B_2 or of the activity of the collisions, ω_2.

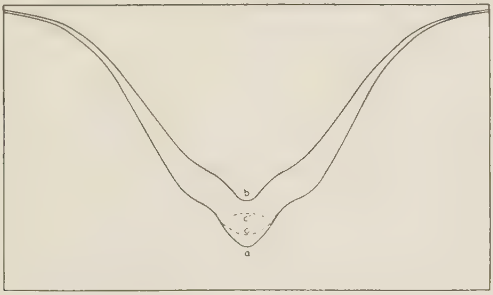

FIG. 1.—Schematic Contours

Since the optical depth of the higher Ca^+ layers is rather small, we must have $u_2 < 1$. It follows from this, in accordance with the preceding considerations, that all the flocculi which are visible in the light of the wings appear also in the spectroheliograms taken with the center of the line.

We have still to write down the theoretical conditions corresponding to real emission (H_2, K_2) in the middle of the Ca^+ absorption lines. Equation (10) shows that if the intensity in the line is to increase with the optical depth (toward the line-center),

$$\frac{\omega_2 + \frac{\omega_1}{\omega_2}}{1+\omega_1} - \frac{B_2\omega_2}{B_1\omega_1} < 0 \,. \tag{11}$$

That is, either $\omega_2 > \omega_1$, $B_2 > B_1$, or both. The presence of emission lines is therefore connected with a reversal of the temperature- or pressure-gradient (ω increases with pressure).

From our discussion it appears that the preceding considerations on the relations of the different parts of the calcium lines are applicable to both absorption and emission lines.

To summarize, the theory of radiative equilibrium therefore leads to the following picture of the solar calcium atmosphere: The broad H_1 and K_1 lines originate at a depth where collisions play a part not to be neglected (as was shown previously, $\lambda_1 = 0.088$ and $\omega_1 = 0.2$). Above this comes a transition layer, in which, apparently, abnormally strong excitation by collisions takes place very easily. This excitation seems to be connected[1] with the very rapid change in density between reversing layer and chromosphere; besides this, the "aerodynamic" perturbations in the neighborhood of spots and faculae surely play an important rôle. In the outer chromosphere, finally, collisions cannot be of any importance. A strong absorption (H_3, K_3) therefore corresponds to this layer. Quite generally, the innermost parts of a line correspond to the highest layers, the outer parts to deeper layers. The form of the outermost wings, in which, as previously shown, collisions are not of importance, is determined only by the number of atoms in the whole atmosphere.

In order to get an idea of the quantitative side of the phenomena, two spectrograms of the integrated solar radiation taken November 9, 1928, with the 75-foot spectrograph of the 150-foot tower telescope, without the objective, were measured photometrically. It was found that the maxima of the H_2 and K_2 lines rise only about 6 per cent above the brightness of the surrounding minima. The strong visual impression produced by these lines is much exaggerated by contrast effect. For the sun as a whole the average deviations from the state of equilibrium are therefore rather small; in the neighborhood of disturbed regions they are naturally much greater. The intensity in the middle of the H_3 and K_3 lines came out about 23 per cent smaller than the intensity of the H_2 and K_2 maxima, in close agreement with measures in the light from the center of the solar disk.

---

[1] Cf. R. W. Gurney, *Monthly Notices, R.A.S.*, 88, 377, 1928.

3. HYDROGEN SPECTROHELIOGRAMS

As the well-known work of Hale and of Deslandres has shown, spectroheliograms taken with the hydrogen lines, especially $H\alpha$, give pictures which are essentially different from the calcium pictures.[1] Photographs with the border of the $H\alpha$ line usually show dark hydrogen flocculi, instead of bright flocculi. Photographs taken with the middle of the line show similarity to those obtained in H_3 or K_3 light, but the pictures are simpler. This anomalous behavior of the hydrogen lines is not astonishing, as the contours of the undisturbed Balmer lines are very different from those of other lines and are therefore likely to have a different physical cause. As has already been assumed by various authors, electrical disturbances by neighboring particles—a kind of Stark effect—are likely to play the decisive rôle.

On the other hand, as Hale and Deslandres have pointed out, the difference between calcium and hydrogen flocculi arises from the fact that to an enhancement of the H_2 and K_2 emissions there always corresponds a broadening of the hydrogen lines, which in many cases is apparently connected with an increase of the central intensity. A series of $H\alpha$ and $H+K$ spectra taken in immediate succession in November, 1928, confirms the correlation between the width of $H\alpha$ and the brightness of H_2 and K_2. Photometric measures show, moreover, that $H\alpha$ never becomes narrower than it is normally, but only broader (in disturbed regions). The change in central intensity does not seem to be uniquely connected with the change of line width; but the spectroheliographic results do favor a rather strong correlation between the two phenomena.

An explanation of the phenomena just described is as follows: As we have seen, the brightening of the H_2 and K_2 lines is caused by increased excitation by collisions. If we assume now, as is very plausible, that the active particles are charged electrically—in other words, that they are ions or free electrons—we can understand at once that, as in a condensed discharge, the hydrogen lines may be broadened by their electrical fields. In the inner part of the line, however, according to our general theory, the dependence of the coefficients of scattering and absorption on wave-length is rather unimportant; the middle of the line will therefore behave nearly in a normal way, as the observations indicate. The assumption that perturbed parts of the solar surface contain a considerable number of free charges is strongly favored by the existence of strong magnetic fields in the neighborhood of spots.

---

[1] Cf. the extremely interesting reproductions in the paper by H. Deslandres, already cited, especially Plate 36*bis*.

4. EVERSHED EFFECT AND LIMB-CENTER DISPLACEMENTS

After having cleared up theoretically the relations of the various zones of a spectral line to the stratification of the solar atmosphere, some remarks concerning a curious phenomenon connected with the currents of the solar atmosphere may be in order.

According to the well-known observations of Evershed and of St. John, the velocity of the currents in the solar atmosphere in the neighborhood of spots (Evershed effect) and also the general currents (limb-center displacements)[1] show a marked dependence on the height above the photosphere.

It seems, however, a perfect riddle that not only various atoms, but also lines of the same multiplet and other groups of lines, which originate in the same atomic level, indicate different velocities, so that strong (broad) lines may correspond to a higher level than weak (narrow) lines. This observation seems at first sight to contradict all atomic physics. We shall show, however, that the general results of section 2, connected with some elementary facts from physiological optics,[2] which naturally influence all such measurements, give at once an explanation.

As we have seen, the core of a line corresponds, roughly speaking, to high layers, the outer parts to deep layers.

On the other hand, the visual impression of a line, whether observed directly or on the photographic plate, depends not only on the true distribution of intensity, but is also strongly influenced by the effect of contrast. This in our case is approximately proportional to the second derivative of the intensity with respect to the longitudinal extension of the spectrum, as measured on the retina of the observing eye.[2] From this it follows that, other things being equal, the contrast effect for similar lines, that is, lines whose widths for every value of intensity are in a constant ratio, is inversely proportional to the square of line width. The contrast effect for a broad line will therefore be rather unimportant, and in setting the cross-wire one will be likely to put it on the real minimum of the line.

---

[1] Our further considerations would still remain valid, even if these displacements are to be explained by something else than Doppler effect.

[2] For the following cf. the paper by A. Kühl, *Physikalische Zeitschrift*, **29**, 1, 1928, which is extremely important for all such questions. Further references are given there.

In the case of a narrow line, however, the "center" is determined primarily by the contrast effect, which is connected with the rapid change in the slope of the intensity-curve; the real intensity-distribution plays a subordinate part. In this case the cross-wire will be set not on the real minimum but about halfway between the points of the most rapid change in intensity.

If the various layers of the solar atmosphere have different velocities, the Fraunhofer lines will be somewhat asymmetrical,[1] because the minimum indicates the velocity of the highest layers, while the displacement of the outer parts of a line corresponds to deeper layers. From the previous considerations concerning physiological optics it is now apparent why measures of narrow lines give the velocity of deep layers, but broad lines the velocity of high layers, although the real displacements of the various parts of both lines are the same.

In order to test this theory experiments with artificial asymmetrical lines were made as follows: Profiles of the lines, with a certain displacement of the minimum with respect to the middle of the wings, were drawn on paper. The areas within the lines were then blackened and fixed around a cylinder which could be rapidly rotated. This device affords a means of producing lines having any given distribution of intensity. Besides the lines themselves, reference marks were also made on the drawing. In order to approach the circumstances of ordinary measurement as closely as possible, the whole arrangement was photographed. The pictures of the rotating cylinder seem to show a real spectral line. Two lines were made having the same displacement of the center relative to the wings, but with widths in the ratio of 3:1, about 0.6 and 0.2 mm, respectively, on the plate. For measurements with a microscope of the usual magnifying power (about 15), the result in both cases was that the settings were made on the real minimum. With low magnifying power, however, it was apparent that in the case of the broad line the eye still selected the real minimum, but in the case of the narrow line, the settings were nearer to the middle between the wings. While in the first case the shifts, on an arbitrary scale, were 1.6 for both broad and narrow lines, they were in the second case 1.7 for the broad, but only 1.05 for the narrow line. Under the conditions of dispersion and magnifying power which occur in the measures of the solar spectrum here considered, it is likely that the limit between the two kinds of setting, which naturally is not sharply defined, falls within the range of line widths appearing on the spectrograms. The quantitative side of the phenomenon is likely to depend largely on the character of the plate and the kind of development used. For the conditions which prevailed in the experiments described and for the usual measuring microscope, the limiting line width on the plate would be of the order of 0.05–0.10 mm. Since, however, real spectral lines on plates taken for measurement for various reasons often look considerably blacker than those of the experiments, the limit may be shifted toward broader lines. The discrepancy between solar observations and the requirements of atomic physics, which at first sight appears so strange, thus finds a satisfactory explanation.[1] Further observations concerning the problems here considered are naturally very desirable.

---

[1] Cf. also K. Burns and W. F. Meggers, *Publications of the Allegheny Observatory*, **2**, 105, 1910.

The writer wishes to express his thanks to Dr. Charles E. St. John for much help and advice, and to the International Education Board for the opportunity of working at the Mount Wilson Observatory.

Carnegie Institution of Washington
Mount Wilson Observatory
January 1929

---

[1] As J. W. Nicholson and T. R. Merton, *Proceedings of the Royal Society*, A, **98**, 261, 1920, have pointed out, the finite resolving power of the spectrograph acts in the same direction.

Contributions from the Mount Wilson Observatory, No. 379
Reprinted from the *Astrophysical Journal*, Vol. LXIX, pp. 322-329, 1929
Printed in the U.S.A.

ON THE THERMAL EXCITATION OF ATOMS IN THE REVERSING LAYER OF THE SUN

By ALBRECHT UNSÖLD

ABSTRACT

1. Adams and Russell have shown that the distribution of atoms in higher quantum states does not in general agree with Boltzmann's law.

2. In order to test Boltzmann's relation for a *single* star, the number of atoms multiplied by the corresponding oscillatory power, f, for two states of the same atom may be determined by the *line-contour method.* The unknown f's can be eliminated by using *two similar atoms*, for instance, $Ca+$ and $Ba+$, which may be assumed to have practically the same transition probabilities.

3. *Photometric measures* of the *infra-red* 3^2D-4^2P *lines* of $Ca+$ and of the *corresponding* $Ba+$ *lines* are described. The effect of the finite resolving power of the grating is investigated.

4. Discussion of the observations indicates that *for excitation potentials up to 1.7 volts Boltzmann's relation holds* within the accuracy of measurement. For the *ratio of the oscillatory powers* f_{DP}/f_{SP} the value 0.2–0.25 is obtained.

5. An upper limit for the *transition probability* of the forbidden $Ca+$ lines 4^2S-3^2D is derived. The *lifetime* of the *metastable* 3^2D *state* must be $>10^{-2}$ sec.

I. INTRODUCTION

Former investigations of thermal excitation and ionization[1] have mostly assumed tacitly that the formulae of Boltzmann and Saha, derived on the assumption of thermal equilibrium, could be applied with sufficient accuracy to a stellar atmosphere.

A closer investigation by Adams and Russell[2] showed, however, that the percentage of highly excited atomic states is much greater in cool stars, compared with that in hotter stars, than would be expected from Boltzmann's formula. In order to derive stellar temperatures in a purely spectroscopic way, Adams and Russell made the assumption that the above mentioned deviations are due to the highly excited atoms alone, while in the limiting case of very low excitation potentials the Boltzmann formula should remain valid.

In the present paper the thermal excitation of atoms will be investigated for one definite star, namely, the sun, by the method of quantitative spectral analysis developed in an earlier paper.[1] It will be shown that for excitation potentials below 1.7 volts the observations agree with Boltzmann's formula within the accuracy of measurement and that the assumption of Adams and Russell is therefore justified. As a by-product it is found that the transition probability of the infra-red lines of Ca^+ and of the corresponding Ba^+ lines agrees in order of magnitude with a calculation made by A. Zwaan[2] on the basis of quantum mechanics.

---

[1] Cf. the report of Cecilia H. Payne, *Stellar Atmospheres, Harvard Observatory Monographs*, No. 1, Cambridge, 1925.

[2] *Mt. Wilson Contr.*, No. 359; *Astrophysical Journal*, 68, 9, 1928; also M. Minnaert, *Observatory*, 51, 347, 1928.

2. THEORETICAL RELATIONS

By photometric measures of the contours of a Fraunhofer line it is possible to determine N, the number of atoms in the state of excitation under consideration which lie above 1 sq. cm of the photosphere,[3] multiplied by the "oscillatory power" of this line. As it has been possible thus far to apply this method only to resonance lines, we choose for investigation groups of lines which approach the resonance character as closely as possible, namely, the H and K lines (4^2S-4^2P) and the infra-red group (3^2D-4^2P) of Ca^+, on the one hand, and, on the other, the corresponding lines of the Ba^+ spectrum (cf. Fig. 1). By photometric measures we can determine the "effective numbers of atoms," $N_S f_{SP}$ and $N_D f_{DP}$, for Ca^+ and Ba^+, where f_{SP} and f_{DP} refer to the whole multiplet.

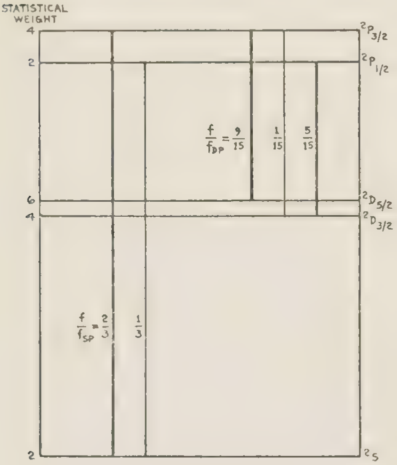

Fig. 1

---

[1] *Zeitschrift für Physik*, **46**, 765, 1928.

[2] *Die Naturwissenschaften*, **17**, 121, 1929.

[3] In terms of E. A. Milne's new model of a stellar atmosphere (*Monthly Notices, R.A.S.*, **89**, 3, 1928), we should say "above an optical depth $\tau_0 \backsim 0.5$."

Further, by assuming thermal equilibrium, the ratio of these numbers is given by the Boltzmann relation:

$$\frac{N_D f_{DP}}{N_S f_{SP}} = \frac{q_D f_{DP}}{q_S f_{SP}} e^{-\frac{11,600}{T} E} , \tag{1}$$

where $q_S = 2$ and $q_D = 10$ are the statistical weights of the S and D terms, T the solar temperature, and E the excitation potential, ${}^2S - {}^2D$, measured in volts.

If the ratio of the f's were known a priori with sufficient accuracy, this relation could be subjected directly to an experimental test. However, as this is not the case, it seems best to compare two atoms having a similar term system but different values of E. We can then assume that the ratio of the f's is the same for both. For this reason we use the Ba^+ lines which are perfectly analogous to the Ca^+ lines mentioned. If now we apply equation (1) to the Ca^+ and Ba^+ atoms and take the ratio of the left-hand members, the q's and f's on the right side drop out (the q's exactly, the f's only approximately), and we obtain

$$\left(\frac{N_D f_{DP}}{N_S f_{SP}}\right)_{Ca^+} : \left(\frac{N_D f_{DP}}{N_S f_{SP}}\right)_{Ba^+} = e^{-\frac{11,600}{T}(E_{Ca^+} - E_{Ba^+})} \tag{2}$$

This equation may now be compared directly with the observations, as all the quantities on the left-hand side can be determined spectrophotometrically. Having verified equation (2), we may use equation (1) to derive the ratio f_{SP}/f_{DP} from astrophysical observations.

3. OBSERVATIONS OF THE ${}^2D - {}^2P$ MULTIPLETS OF Ca^+ AND Ba^+

As observations of the ${}^2S - {}^2P$ doublets are already available,[1] we need not treat these in detail. For convenience the results are repeated in Table I. The observations of the ${}^2D - {}^2P$ lines were made by exactly the same method[2] with the 75-foot spectrograph of the 150-foot tower-telescope.

a) *The infra-red Ca^+ lines.*—For the spectra of the infra-red

---

[1] A. Unsöld, *loc. cit.*

[2] *Ibid.* and *Mt. Wilson Contr.*, No. 377; *Astrophysical Journal*, **69**, 209, 1929.

Ca^+ lines near 8500 A, Eastman neocyanine plates were used which had been hypersensitized with ammonia. In order to avoid prohibitively long exposures and to compensate to some extent for the steep gradation of the sensitized plates, they were developed with "Eastman Threshold" developer. All plates were taken in the first order of the grating. In order to exclude the superposed violet second order and stray light, a Wratten filter No. 87 was used. The exposure times were of the order of five hours.

TABLE I

El.	λ in I.A.U.	Classification	f/f_{SP}	$N_{S\ SP}$
$Ca+$	3933.684	$4^2S-4^2P_{3/2}$	2/3	$23.3\cdot10^{18}$
	3968.494	$4^2S-4^2P_{1/2}$	1/3	
$Ba+$	4554.038	$6^2S-6^2P_{3/2}$	2/3	$4\cdot10^{15}$
	4934.040	$6^2S-6^2P_{1/2}$	1/3	

To get some idea of the accuracy of the measures, the three lines were evaluated separately. The numbers of atoms thus determined should agree. Table II gives in the first three columns the data concerning the lines, and in the fourth column, the value of f determined from the Burger-Dorgelo summation rules, referred to f_{DP} as unit.

TABLE II

El.	λ in I.A.U.	Classification	f/f_{DP}	Nf_{DP}
$Ca+$	8498.060	$3^2D_{3/2}-4^2P_{3/2}$	0.0667	$0.465\cdot10^{18}$
	8542.132	$3^2D_{5/2}-4^2D_{3/2}$	0.600	$0.425\cdot10^{18}$
	8662.170	$3^2D_{3/2}-4^2P_{1/2}$	0.333	$0.462\cdot10^{18}$
Mean	....	....	....	$0.45\cdot10^{18}$

The last column, finally, gives the individual and the mean results for Nf_{DP}. The mutual agreement is quite satisfactory.

b) The Ba^+ 5^2D-6^2P *lines,* λλ *5853, 6141, 6496.*—As these lines are rather narrow, spectra were taken in the first and third orders of the 75-foot spectrograph. Ilford Special Rapid Panchromatic plates were used. To obtain a favorable blackening curve, developing was done with Agfa Rodinal 1:20. Nf_{DP} was again evaluated separately for each line and for the two orders of the grating.

In calculating the f's it was necessary to take into account the fact that this multiplet can no longer be considered as "narrow." The well-known rules apply strictly to the values of $f\lambda$.[1] The results are given in Table III. The table shows that the weakest line always gives too great a value for Nf_{DP}; moreover, this effect is more pronounced on the first-order plates than it is on those of the third order. This indicates that instrumental influences produce a considerable broadening in the case of the line λ 5853. An elementary consideration shows that the resolving power of the Michelson grating used is not sufficient to give the true contour of this line. The resolving power in the first order is ∾77,500. Near λ 5853 this corresponds to a "separating power" of 0.075 A. On the other hand, the width of the line on the third-order plates, measured at an intensity equal to 80 per cent of the continuous spectrum, is only 0.093 A. It is therefore not astonishing that this line is considerably distorted. In forming the mean value in Table III the line λ 5853 has accordingly been ignored. The other two lines, which are considerably wider, should be little affected by instrumental influences. J. A. Carroll[2] has shown recently how the disturbing influence of the grating may be allowed for theoretically. It seems doubtful, however, how far these calculations can be applied to an actual grating.

TABLE III

El.	λ in I.A.U.	Classification	f/f_{DP}	Nf_{DP}	
				First Order	Third Order
$Ba+$..........	5853.691	$5^2D_{3/2}-6^2P_{3/2}$	0.071	$3.6\cdot10^{15}$	$2.0\cdot10^{15}$
	6141.733	$5^2D_{5/2}-6^2P_{3/2}$	0.609	$1.0\cdot10^{15}$	$0.97\cdot10^{15}$
	6496.916	$5^2D_{3/2}-6^2P_{1/2}$	0.320	$1.2\cdot10^{15}$	$0.88\cdot10^{15}$
Mean.....	....	....	....	$1.0\cdot10^{15}$	

---

[1] Cf. the paper of L. S. Ornstein, M. Coelingh, and J. G. Eymers, *Zeitschrift für Physik*, **44**, 653, 1927, which verifies this generalized rule for some $Ba+$ multiplets.

[2] *Monthly Notices, R.A.S.*, **88**, 154, 1927.

4. DISCUSSION OF THE OBSERVATIONS

According to the measures described in section 3,

$$\left(\frac{N_D f_{DP}}{N_S f_{SP}}\right)_{Ca^+}=\frac{0.45\cdot 10^{18}}{23.3\cdot 10^{18}}=0.0193\ ,$$

$$\left(\frac{N_D f_{DP}}{N_S f_{SP}}\right)_{Ba^+}=\frac{1.0\cdot 10^{15}}{4\cdot 10^{15}}=0.25\ .$$

The corresponding excitation potentials are 1.69 volts for Ca^+, 4^2S-3^2D, and 0.65 volts for Ba^+, 6^2S-5^2D. If now we assume that the ratio f_{DP}/f_{SP} is the same for Ca^+ and Ba^+, we find from equation (1)

$$\left.\begin{aligned}\log_{10}\left(\frac{N_D f_{DP}}{N_S f_{SP}}\right)&=\log_{10}\frac{q_D}{q_S}+\log_{10}\frac{f_{DP}}{f_{SP}}-\frac{11{,}600}{T}E\log_{10}e\ ,\\&=0.699+\log_{10}\frac{f_{DP}}{f_{SP}}-\frac{5040}{T}E\ .\end{aligned}\right\}\qquad(3)$$

In Figure 2, $\log_{10}(N_D f_{DP}/N_S f_{SP})$ is plotted as a function of E. The inclination of the dotted line is drawn on the basis of a solar temperature of 5040°. As may be seen, the agreement with the experimental values is within the accuracy of measurement. On the other hand, we may use the inclination of the line connecting the two experimental points (full line in Fig. 2) in order to derive, with the aid of equation (2), the solar temperature. The result is $T=4700°$. As a comparison of the two straight lines in Figure 2 indicates, the uncertainty of this value is considerable. It may be seen at once, however, that deviations from Boltzmann's formula must be much smaller in the cases investigated here than Adams and Russell found them to be in the case of high-excitation potentials. Unfortunately, the solar spectrum shows no high-excitation lines to which our present method can be applied. The points at which the straight lines in Figure 2 intersect the axis of ordinates give, according to equation (3), the ratio of the oscillatory powers f_{DP}/f_{SP}. The line drawn on the assumption of a temperature of 5040° gives

$f_{DP}/f_{SP}=0.2$; the purely empirical line ($T=4700°$) gives $f_{DP}/f_{SP}=0.25$. On the other hand, A. Zwaan[1] has recently calculated the transition probabilities of Ca^+ lines according to quantum mechanics, using a simplified atomic model with a suitably chosen potential field of spherical symmetry. He finds $f_{DP}=0.09$ and $f_{SP}=1.08$, whence $f_{DP}/f_{SP}=0.083$. The agreement of the theoretical and experimental values must be considered satisfactory in view of the simplifying assumptions which are necessary in order to carry through the very long quantum-mechanical calculation of transition probabilities. It would be very interesting to test the value deduced from astrophysical observations by laboratory measures, for instance, by the method of anomalous dispersion.

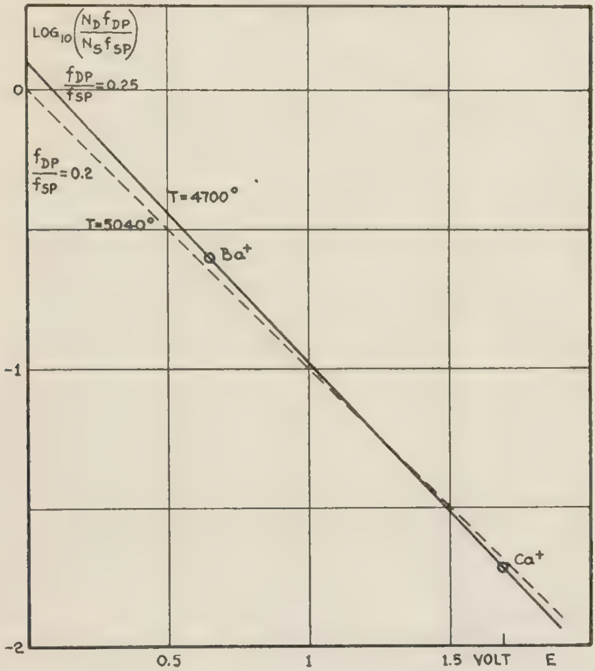

FIG. 2

---

[1] *Loc. cit.*

5. ESTIMATION OF THE TRANSITION PROBABILITY FOR THE FORBIDDEN LINES[1] $4^2S-3^2D_{3/2,\,5/2}$ OF THE Ca^+ ATOM (λλ 7291.40 AND 7323.89)

The results obtained in this and in a preceding paper[2] on the effective numbers of atoms Nf necessary for the production of various lines allow us to estimate an upper limit for the transition probabilities of these forbidden Ca^+ lines.

As may be seen from the revision of Rowland's table,[3] no absorption lines corresponding closely to the forbidden transitions are visible in the solar spectrum. For these forbidden lines, therefore, we must have $Nf<10^{13}$, since the Ba^+ line λ 5853 with $Nf \backsim 7\cdot 10^{13}$, for example, is still quite strong. On the other hand, Table I shows that for the Ca^+ resonance lines, which originate from the same term, $Nf=2.3\cdot 10^{19}$. The oscillatory power of the forbidden lines must therefore be $<10^{-6}$, and the "lifetime" of the metastable ^2D term at least $>10^{-2}$ sec., a value which agrees well with other estimates.[4]

I desire to express my heartiest thanks to Professor Russell for his kind interest in this paper. The work in the infra-red could not have been carried through without help and advice from Mr. Babcock, to whom I am deeply indebted. Finally, I am greatly obliged to the International Education Board for giving me the opportunity to work at the Mount Wilson Observatory.

Carnegie Institution of Washington
Mount Wilson Observatory
March 1929

---

[1] I. S. Bowen and D. H. Menzel, *Publications of the Astronomical Society of the Pacific*, **40**, 332, 1928.

[2] *Loc. cit.*

[3] *Revision of Rowland's Preliminary Table of Solar Spectrum Wave-Lengths, Carnegie Institution of Washington Publication*, No. 396, 1928.

[4] I. S. Bowen and D. H. Menzel, *loc. cit.*

Contributions from the Mount Wilson Observatory, No. 380
Reprinted from the *Astrophysical Journal*, Vol. LXIX, pp. 293–311, 1929
Printed in the U.S.A.

ENERGY SPECTRA OF THE STARS

By C. G. ABBOT

ABSTRACT

A sensitive radiometer.—Fragments of *flies' wings* are used as *vanes*, and the exceptionally light *suspension* is sealed into a *fused-quartz tube*, optically figured opposite the vanes and mirror and *filled with hydrogen* at 0.23-mm pressure. The description includes various data regarding the weights, moments of inertia, advantages of hydrogen as compared with air, and sensitiveness of the apparatus.

Radiometric observations of stars.—The instrument was used to measure the distribution of energy in stellar spectra formed by a 60° flint-glass prism at the coudé focus of the Mount Wilson 100-inch telescope. The deflections were observed at a scale distance of 6 m by a special reading device, with a probable error of 2″.8 in the rotation of the suspension. This figure includes errors of reading and those due to all other accidental causes. *Spectral energy-curves for eighteen stars and two planets were observed*, sometimes on two or three nights. The faintest star measured is of mag. 3.8. A comparison of the results with those obtained by the author in 1923 with a larger radiometer shows, in general, an agreement as good as could be expected from the accuracy of the observations.

In the year 1923, with a radiometer prepared for me by the late Dr. E. F. Nichols and his colleague, Dr. J. D. Tear, I measured relatively the intensities in spectra of the sun and nine very bright stars of various types, whose radiation was collected by the 100-inch telescope of the Mount Wilson Observatory.[1] Obviously it is desirable to measure a considerable number of specimens of each type of stellar spectrum, but, in order to do so, it appeared necessary to secure either greater sensitiveness or less accidental disturbance of the record.

The radiometer system employed in 1923 had vanes of mica, 0.5 mm wide by 1.5 mm high, separated 2.5 mm between centers, and the stem carried a mirror of fair dimensions, suitable to telescope and scale observation. It occurred to me that a very much lighter system might show increased sensitiveness. In 1926, I therefore constructed a system with vanes consisting of houseflies' wings separated by only 1 mm, and with a mirror of microscope cover-glass only 1 mm square. On trial, this system showed very high sensitiveness, but was so excessively damped at the air pressure best suited to the radiometer effect as to be quite useless. Dr. Anderson suggested that hydrogen might be an advantageous substitute for air.

---

[1] *Mt. Wilson Contr.*, No. 280; *Astrophysical Journal*, **60**, 87, 1924.

Accordingly, in 1927, I made up two very light systems, one with 1.2 mm, the other with 2.0 mm between vane centers, each with vanes approximately 0.4 mm wide and 1.0 mm high. I made, also, bolometric strips which were used with them in the following manner. Three parallel test-tubes were joined by tubes, so that all three could be evacuated and filled together to any desired pressure with air or gas. In two tubes were sealed the radiometer systems, suspended on fine quartz fibers, and in the third were sealed the bolometer strips. Having been charged to a desired gas pressure, the instruments were exposed to a beam of light of nearly constant intensity. The deflection and the time of swing of each radiometer were observed when one of its vanes was illuminated. Also the deflection of a connected galvanometer was observed when one bolometer strip was exposed to the beam. By changing the pressure and the kind of gas, two series of measures were obtained in this manner, one for hydrogen, the other for air. These showed two kinds of results: from the bolometric deflections, the relative rise of temperature of blackened surfaces within the competing gases; and from the deflections of the suspended vanes, the comparative behavior of the two gases as regards radiometer effect and damping effect. Table I shows some of the results near optimum pressures.

TABLE I

COMPARATIVE RESULTS, AUGUST 5, 1927

INSTRUMENT		SMALLER SYSTEM				LARGER SYSTEM				BOLOMETER
Pressure mm Hg	Gas	Time of First Swing, Seconds	Deflections of Successive Swings, mm			Time of First Swing, Seconds	Deflections of Successive Swings, mm			Deflection, mm
			1st	2d	3d		1st	2d	3d	
0.19	H_2	1.25	92	52	38	3.0	165	50	18	46.5
0.19	Air	1.6	82	22	8	4.0	110	0	0	61.3
0.26	H_2	1.3	98	45	31	3.1	125	35	7	36.8
0.26	Air	2.0	93	21	7	4.2(?)	110	0	0	60.4

For these light systems it thus appears that, although hydrogen is somewhat less efficient than air as regards rise of temperature of the blackened surface, the loss of efficiency is not so great as to offset the advantage of the very decided decrease in damping. It seemed evident that if the quartz fiber of a hydrogen-surrounded radiometer should be thinned until the time of swing matched that of a similar air-surrounded radiometer of 10-second single swing, the deflection of the hydrogen-surrounded instrument would be much the greater. Subsequent experiments demonstrated that for a system of the same dimensions as the smaller one, the deflections in hydrogen at 0.23-mm pressure for single swings between 0.5-2.5 seconds were almost exactly proportional to the square of the time of swing. At 2.5 seconds, the vane was far from critical damping. This leads to the expectation that such a system would show a decided gain in deflections from 2.5 up to 10 seconds single swing – probably not sixteen fold, corresponding to the square of the time of swing, but perhaps tenfold.

Anticipating the success of hydrogen as a substitute for air, I had obtained, by the kindness of Director Burgess, of the Bureau of Standards, and the skill of Mr. Sperling, of the Bureau, a special pyrex glass tube with optically figured windows. In this tube Mr. A. Kramer, instrument-maker of the Smithsonian Astrophysical Observatory, had arranged a mechanism operated by a magnetic device from without. It was expected that when the tube had been filled to the proper hydrogen pressure and hermetically sealed, the vanes and mirror could be turned by magnetic influence to a proper orientation with respect to the windows. On trial, however, this device failed, because the rotation of the mechanism set up currents in the gas which so irregularly displaced the radiometer system that it was quite impossible to set it at a proper angle for observing.

In 1928, at the suggestion of Director W. S. Adams, of the Mount Wilson Observatory, a simpler plan was adopted. A fused-quartz tube, about 4 cm in diameter, was made to my order by the General Electric Company. In its middle section it was figured within and without to concentric circular curvature by Mr. Kinney, of the optical shop of the Observatory. This tube was exhausted to 0.0001-mm pressure through a liquid-air trap, washed out repeatedly with electrolytic hydrogen, filled to 0.23-mm pressure therewith, and sealed up with the suspended radiometer inclosed. In this work, which had to be done on Mount Wilson, I was greatly assisted by Mr. Pompeo, whose skill in working quartz and glass is very great.

Since the quartz tube was optically figured and of excellent clearness, it made no difference how the mirror and vanes were oriented. It was only necessary to support the tube from a ground-joint in a brass case in order that the whole tube containing the radiometer system might be rotated until the mirror looked out through the window of the brass case toward any desired part of the reading scale. A quartz window was employed opposite the vanes, so that, if desired, the experiments might be made with very short wave ultra-violet, or very long wave infra-red stellar radiation. In the experiments of 1928, however, a flint-glass prism was employed, and generally the spectral range was only from about 0.5 to about 2.5 microns.

A quartz fiber, so fine as to be handled with extreme difficulty, was used as a suspension. The vanes of the radiometer system were 0.4 mm wide and 1.0 mm tall, and but 1.2 mm between centers. Each vane had three parallel laminae of houseflies' wings, of which the front one was painted dead black, the two rear ones being unpainted. The laminae were separated by spaces of about 0.1 mm, in order that the communication of heat from front to back would be greatly impeded. The mirror, 0.9 by 1.0 mm and situated about 3 cm above the vanes, was made of microscope cover-glass which had been ground and polished to about half the usual thickness and platinized on both sides by sputtering. The whole system, including vanes, glass stem, and mirror, weighed 0.94 mg.

Some notion of the excessive fineness of the quartz fiber, 10 cm long, may be had from the fact that when suspended in full atmospheric air pressure, forty-four complete turns of the top support were made before the suspended system began to rotate in response. The air, in other words, acted as if viscous, like tar, although the vanes were so small and near together that very slight force must suffice to rotate them.

The following are details relating to weights and moments of inertia of the radiometer parts. The weight of 22 flies' wings, approximating 200 sq. mm in area, was 1.7 mg. After blackening, 8 flies' wings having an area of approximately 70 sq. mm weighed 3.1 mg. Hence the weights of the four fragments of unblackened flies' wings which were used were negligible compared to the two fragments of blackened wings. The moment of inertia of the fly-wing vanes as actually cut and mounted is 132×10^{-9} g. cm².

After grinding, polishing, and platinizing, the mirror glass weighed 0.20 mg per square millimeter. The moment of inertia of the mirror used, 0.9×1.0 mm, is 121×10^{-9} g. cm². The glass cross-rod weighs 0.023 mg, and its moment of inertia is 37×10^{-9} g. cm². Compared to these, the moments of inertia of the vertical glass stem and wax used are negligible.

Hence, the total amount of inertia is 290×10^{-9} g. cm², nearly equally divided between the vanes and the non-deflective parts.

The total weights are as follows:

Vanes	0.035 mg
Mirror	.180
Cross-rod	.023
Vertical	0.700
Total	0.938

The glass parts were cemented together with minute quantities of shellac from which all alcohol had been evaporated by heat and reduced pressure. The vanes and mirror were cemented on with minute quantities of beeswax. Since there was some doubt as to whether beeswax would evaporate sufficiently to contaminate the hydrogen within a moderate time, an area of 1400 sq. mm of mica was coated with beeswax on August 24, 1926, and weighed after standing a half-hour under a bell-jar with phosphorus pentoxide. After a similar drying on October 30, the weight appeared unchanged, and on June 21, 1927, there appeared to be a loss of weight of 0.2 mg. Throughout this period the temperature of the beeswax considerably exceeded that to which it would be subjected on Mount Wilson. When the times, areas, and temperatures involved are taken into consideration, the evaporation appears to be negligible, even compared to the weight of hydrogen in the containing case.

During the exhaustion and filling of the quartz tube, rough tests indicated that the system would have a single swing of about 12 seconds. But when the tube was inserted in its brass case it was astonishing to find that the time of single swing was only 0.5 second. When the apparatus was left over night, the time of swing increased to nearly 2 seconds. After a week's rest it appeared again to be above 10 seconds. It was then found necessary, however, to remove the tube to clean finger-marks from the quartz surfaces. On reassembling, it was found that the time of single swing had diminished to 1 second. On the assumption that electrical charge, due to friction, was the cause of the controlling field, sufficient water was introduced to saturate the air of the outer case. The apparatus was untouched for more than a week afterward before trying it for the first time on stellar spectra. But the time of swing rose only to 1.5 seconds. After a further interval of nearly three weeks before a second trial, the time of swing remained 1.5 seconds. I still think, however, that the cause of this unduly quick action is electrostatic, and hope that before another trial is made the instrument will recover its longer time of swing and high sensitiveness.

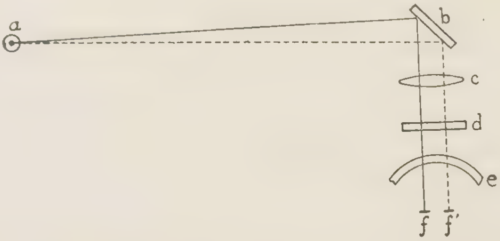

Fig. 1.—Set-up for test of sensitiveness: *a*, candle; *b*, silvered mirror; *c*, glass lens; *d*, quartz plate; *e*, quartz tube; *ff'*, radiometric vanes.

The following test, with the set-up shown in Figure 1, was made to measure the sensitiveness of the radiometer as actually used with a single swing of 1.5 seconds. The radiometer was exposed to rays from a candle, *a*, at 2.4 m distance, reflected at 45° by a silvered glass mirror, *b*, through a crown-glass lens, *c*, of 3-mm thickness and 3.7-sq. mm aperture, and thence through two quartz plates, *d*, each of 3-mm thickness, to focus on a radiometer vane, *ff'*. Since this was only about two-thirds as tall as the candle-flame image, there was a large loss of radiation. Under these circumstances a deflection of 80 mm was produced on a scale at 40 cm distance when the image of the flame was shifted from one vane to the other, just as in actual practice with stellar spectra. During observations on stars, the scale distance was 6 m instead of 40 cm, thus giving fifteen fold greater sensitiveness than during the tests. Had the desired time of single swing of 10 seconds or more been available, the sensitiveness would, I believe, have been further increased nearly twenty fold. A rough test made with the candle source on the only day when the time of swing exceeded 10 seconds showed a deflection on the scale at 40 cm which was evidently several times as great as the entire length of the 200-mm scale. Whether this increased sensitiveness would have produced a very great gain in accuracy of the results I am not prepared to say, for no doubt the accidental errors of reading would have increased with a longer time of swing and greater sensitiveness.

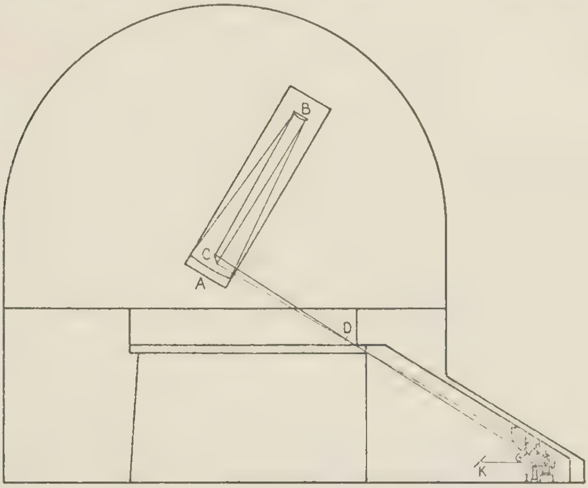

FIG. 2.—Diagram of stellar spectral set-up

The optical system employed is shown diagrammatically in Figures 2 and 3. Rays reflected by the 100-inch telescope mirror *A* came nearly to a focus at the top of the telescope tube. Thence they were reflected down the tube by a convex mirror *B*, and thence by a plane mirror *C*, southward down the hollow telescope axis converging toward the coudé focus at *D*. At that focus was placed a circular variable aperture, about 3 mm in diameter at maximum, through which the rays diverged for a distance of about 16 m to fill a concave mirror *E*, of 50-cm aperture and 1-m principal focus, situated near the floor of the constant-temperature room. Thence they were reflected back to a 10-cm convex mirror *F*, near the conjugate focus. By this small mirror the rays were rendered parallel and reflected southward and downward through a hole in the center of the 50-cm mirror to pass, at approximately minimum deviation, through a 60° flint-glass prism *G*, with faces 13 cm wide and 17 cm long, whose refracting edge lay horizontally. Beyond this and attached to the prism, was a plane mirror *H*, which reflected the rays nearly vertically downward to a concave mirror *I* of 45-cm focus. From this mirror they were reflected vertically upward to a small plane mirror near the focus, and thence horizontally southward to the focus of the spectrum on the vane of the radiometer at *J*.

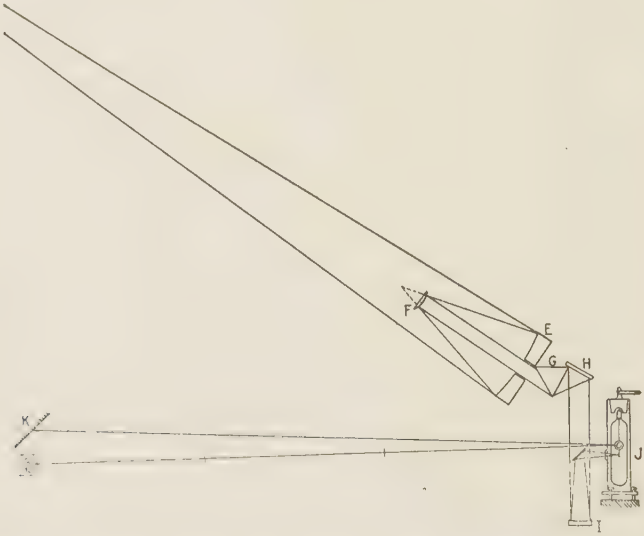

Fig. 3.—Means of forming the spectrum and of observing deflections

With the arrangement described, the spectrum was vertical. In order to make readings at different points in the spectrum, means were provided for rotating the prism and its attached plane mirror about a horizontal axis. Whenever the 3-mm circular diaphragm at the coudé focus of the great telescope was filled with light, the width of the spectrum at the radiometer was about 0.4 mm and equal to the width of the radiometer vanes. For many of the stellar observations, the diameters of the star images were so small that the spectral width observed hardly exceeded half the width of the radiometer vanes. With Mars and Jupiter, the images were so large that only a small central part of their rays passed through the diaphragm. The vertical extension of the spectrum was about 30 mm, between wave-lengths 0.48 and 2.00 microns. Thus, for any single setting, the radiometer vanes 1 mm high subtended about one-thirtieth of the average extension of the observed spectrum. Means were provided for horizontally displacing the spectrum at pleasure, from one vane to the other, and the deflections observed in the stellar spectra all corresponded to such displacements.

It is unfortunate that the rays suffered losses of intensity at so many reflecting surfaces, including eight silvered mirrors, two prism faces, and the four faces of the two quartz plates traversed by the beam. These losses differed, of course, for different wave-lengths. For the yellow rays the total loss may have been approximately 75 per cent, and for green or blue rays was still more. Owing to the impossibility of making these delicate stellar-spectrum energy observations with the radiometer, except under conditions of great freedom from vibration and of nearly constant temperature, it is difficult to see how these large losses of energy could have been much reduced. Were it possible to observe the energy of stellar spectra with the thermopile near the direct focus of the telescope mirror, as Pettit and Nicholson observe total stellar radiation, about half of these losses could be avoided.

The success of the experiments depended on the means used for observing the deflections. These are indicated by Figures 3 and 4. A 100-watt incandescent lamp with ring-shaped filament sent a tiny ray through several diaphragms and through a long-focus lens to illuminate the mirror of the radiometer, about 5 m distant. Owing to the shape of the constant-temperature room, the beam, both in approaching and receding from the radiometer, had to be turned through 90° by small mirrors. The spot of light fell upon a long horizontal cylindric lens, 6 m distant from the radiometer, and beyond it, upon a ground glass, not marked in any way. A fairly bright blur of light, nearly circular in form and about 1 cm in diameter, was thus produced. Behind the ground glass was a little movable frame, operated at pleasure by a screw or by hand displacement, which carried opposite the spot of light a bit of cork cut so that when placed centrally it obscured all but a thin halo of light. Below the ground glass was a scale of equal parts ruled on the ground-glass base-side of a long 45° prism of glass, which could be illuminated from beneath by total reflection at the hypotenuse of the prism. A cross-wire, carried by the movable frame, indicated on the illuminated scale the number of whole turns of the screw corresponding to a given setting. A divided head of ground glass which could also be illuminated indicated the hundredths of a turn of the screw. As the pitch of the screw was 3 mm, the settings could readily be observed to 0.03 mm, and by estimation of tenths, to 0.003 mm, if desired.

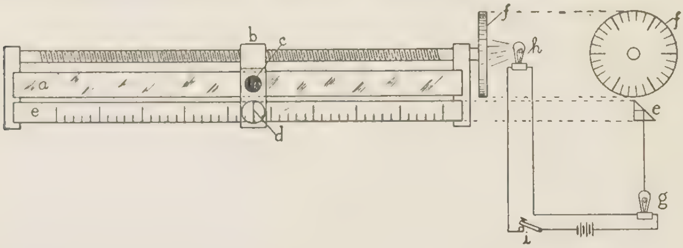

FIG. 4.—Special scale for reading deflections: *a*, plain ground glass; *b*, sliding frame; *c*, cork occulter; *d*, cross-hair; *e*, triangular glass scale of screw divisions; *f*, ground-glass divided screw-head; *g*, *h*, lamps for scales; *i*, switch.

The method of reading deflections will now be apparent. By a photometric comparison of the total light on the right and left of the occulting cork, the observer, working in almost total darkness, made the setting. Then by pressing a button the scales were momentarily illuminated and the accurate readings were made. As will appear from the tabular values, the average probable error of a single reading was only 0.06 mm, including not only the errors of a single setting but also those displacements produced by changes of transparency of the air, "boiling" of the star image, and unsteadiness of the radiometer.

Director W. S. Adams very greatly aided me on all three nights of observation by finding the stars at the coudé focus and recording all observations. Night assistants Bebee and Nelson kept the stars accurately in the field, and to them also my thanks are due.

Table II gives a list of the objects, in order of their spectral type, observed in the year 1928, and notes on the conditions of observation. Figure 5 shows curves representing the energy distributions found in the prismatic spectrum. For convenience in plotting, a somewhat different order of arrangement from that of the table is used in the figure.

TABLE II

Celestial Objects Observed in 1928

Object	Mag.	Sp.	Dates Obsd.*			Spectral Range	Results
						microns	
β Orionis	0.3	B8p	....	....	13	0.423–0.905	Good
α Lyrae	0.1	A0	25	26	13	.437–1.751	Unsatisfactory
α Cygni	1.3	A2p	25	....	13	.472–1.316	Good
α Aquilae	0.9	A5	....	26	....	.437–1.316	Good
α Canis Min.	0.5	F5	....	....	13	.472–1.316	Excellent
α Persei	1.9	F5p	....	26	13	.520–1.751	Good
γ Cygni	2.3	F8p	....	....	13	.472–2.224	Fair
α Aurigae	0.2	G0	25	....	....	.472–2.224	Good
Mars	....	....	....	....	13	.520–1.751	Good
Jupiter	....	....	....	26	....	.520–1.751	Good
β Ceti	2.2	K0	25	26	....	.589–1.751	Good
γ Aquilae	2.8	K0	....	26	....	.589–2.224	Excellent
α Boötis	0.2	K0	25	....	....	.589–2.224	Good
α Tauri	1.1	K5	25	....	....	.589–2.224	Good
α Orionis	0.9	Ma	25	....	....	.589–2.224	Excellent
β Andromedae	2.4	Ma	25	26	....	.589–2.224	Good
β Pegasi	2.6	Ma	25	....	....	.589–2.224	Excellent
δ Sagittae	3.8	Map	25	26	....	.589–2.224	Unsatisfactory
α Herculis	Var.	Mbp	25	26	....	.589–2.224	Excellent
o Ceti	Var.	Md	25	26	13	0.589–2.224	Good

* The entries refer to August 25, 26, and September 13, respectively.

As an example of the direct observations, Table III shows the complete set of measurements made on β Orionis, September 13, 1928. The places in the spectrum are recorded in turns of the tangent screw which rotates the prism from the position of the yellow sodium lines. The readings of the radiometer (marked R) are given in turns and hundredths of a turn of the screw of the observing device. The corresponding deflections (marked Δ), which, when positive, produced smaller scale readings, are computed by subtracting the intermediate reading of each successive triad from the mean of the values preceding and following it.

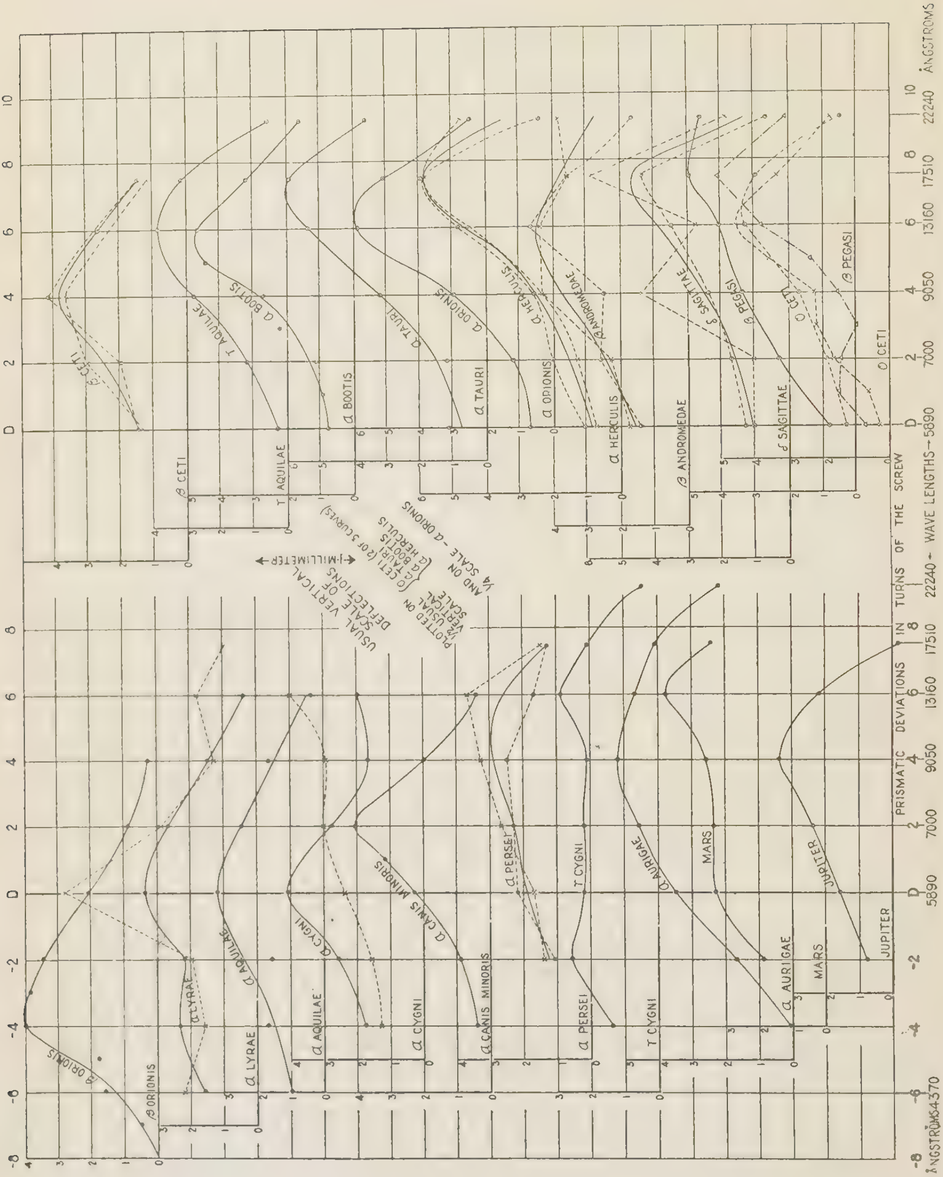
PRISMATIC DEVIATIONS IN TURNS OF THE SCREW
22240 - WAVE LENGTHS - 5890
ÅNGSTROMS
ÅNGSTROMS 4370
USUAL VERTICAL SCALE OF DEFLECTIONS
←1 MILLIMETER→
PLOTTED ON USUAL VERTICAL SCALE
(β CETI (2 of 3 curves)
(α TAURI
(α BOOTIS
(α HERCULIS
AND ON 1/4 SCALE - α ORIONIS
β CETI
τ AQUILAE
α BOOTIS
α TAURI
α ORIONIS
α HERCULIS
β ANDROMEDAE
δ SAGITTAE
β PEGASI
ο CETI
β ORIONIS
α LYRAE
α AQUILAE
α CYGNI
α CANIS MINORIS
α PERSEI
τ CYGNI
α AURIGAE
MARS
JUPITER

Fig. 5

From Table III, which is in no respect exceptional, it appears that the drift, as usual, was toward smaller readings, but amounted to only about 0.3 division, or 1 mm, in approximately 20 minutes.

TABLE III

OBSERVATIONS OF β ORIONIS, SEPTEMBER 13, 1928

Time of Start, P.S.T. Place in Spectrum . . . Wave-Length, Microns	15^h48^m −7 0.423		15^h32^m −6 0.437		15^h52^m −5 0.454		15^h34^m −4 0.472		15^h54^m −3 0.494	
Reading, Deflection . .	*R*	Δ	*R*	Δ	*R*	Δ	*R*	Δ	*R*	Δ
Energy readings in 60° glass prismatic spectrum, expressed in scale division of 3 mm and fractions thereof	20.00		20.35		19.91		20.34		19.99	
	19.88	0.08	.23	0.11	.71	0.20	19.91	0.39	.65	0.30
	.92		.34		.91		20.26		.91	
	.86	.00	.17	.14	.74	.16	19.92	.42	.46	.42
	.80		.28		.90		20.42		.85	
	.80	0.06	.00	0.22	.69	0.19	19.93	0.43	.44	0.44
	19.91		20.16		19.86		20.29		19.92	
Mean	. . . . . .	0.05	. . . . .	0.16	. . . .	0.18	. . . . .	0.41	. . . . .	0.39
Probable error . . .	. . . . . .	0.018	. . . . .	0.026	. . . . .	0.010	. . . . .	0.010	. . . . .	0.035

Time of start, P.S.T. Place in Spectrum . . . Wave-Length, Microns	15^h37^m −2 0.520		15^h40^m 0 0.589		15^h42^m +2 0.700		15^h44^m +4 0.905	
Reading, Deflection . .	*R*	Δ	*R*	Δ	*R*	Δ	*R*	Δ
Energy readings in 60° glass prismatic spectrum, expressed in scale division of 3 mm and fractions thereof	20.30		20.11		20.17		20.30	
	20.00	0.28	19.91	0.20	.17	0.07	.31	−0.03
	20.25		20.11		.31		.25	
	19.90	.38	20.00	.16	.24	.10	.13	+0.08
	20.30		20.20		.37		.17	
	19.86	0.40	19.94	0.27	.23	0.11	.10	+0.04
	20.21		20.22		20.30		20.12	
Mean	. . . .	0.35	. . . . . .	0.21	. . . . . .	0.09	. . . . . .	0.03
Probable error . . .	. . . .	0.038	. . . . . .	0.025	. . . . . .	0.010	. . . . . .	0.025

Also, since the mean probable error of a determination (the mean of three complete measurements) is 0.021 divisions, or 0.063 mm, and, since this rests on seven readings of the scales, the mean probable error of a single reading is $0.063\sqrt{7}=0.17$ mm. This figure of demerit is swelled by all the causes which tend to produce accidental deflections, as well as by the errors of reading itself. It corresponds to a rotation of the radiometer mirror through 2″.8.

The maximum deflection in the spectrum on this occasion was only 0.41 division, or 1.23 mm, yet the energy-curve is rather well delineated and smoothly indicated.

With Rigel omitted, which has already been given in detail, Table IV includes a summary of the observations made in 1928.

Times and air masses are not given more exactly in Table IV because, when corrections to a mean air mass of 1.30 were computed, corresponding to the mean atmospheric transmission coefficients for Mount Wilson, it proved that only in the case of Procyon were they large enough to affect the results.

In the stellar radiometer observations of 1923, the selective transmissions of the apparatus and the atmosphere were allowed for in order to give the spectral distribution as in free space. For this purpose the energy-curve of the sun's spectrum, as observed with the stellar set-up of telescope and radiometer, was compared with that determined by bolometric work in 1920 and 1922 on Mount Wilson.[1] As time did not permit a repetition of this comparison in 1928, the coefficients of transmission adopted in 1923 were made available by comparing prismatic energy-curves of 1928 with those of 1923 for all stars observed in both years. From this comparison it appeared that the infra-red portion of the spectrum, compared to the visible, was less intense as observed in 1928 than in 1923. This difference may have been due to an increased infra-red transparency of the lamp-black-coated fly-wing vanes used in 1928, as compared to the lamp-black-coated purled mica vanes, prepared by Dr. Tear and used in 1923. The results of the comparison are, on the whole, very accordant. (The curious infra-red observations of Rigel made in 1923 were omitted.) Unfortunately, data for rays of wave-length less than 0.589 microns are almost lacking. In extrapolating the curve, it seemed reasonable to assume only a slight change in that region. Table V gives the mean observed reduction factors; the adopted smoothed factors employed to reduce prismatic observations of 1928 to the conditions as of 1923; the factors determined in 1923 to reduce to the wave-length scale outside the

---

[1] *Smithsonian Miscellaneous Collections,* 74, No. 7, 1923.

TABLE IV

THE MEAN PRISMATIC DEFLECTIONS AND PROBABLE ERRORS, OBSERVATIONS OF 1928

Object	Date P.S.T.*	Air Mass	Places in Prismatic Spectrum and Wave-Lengths, Microns																	
			−6 0.437		−4 0.472		−2 0.520		0 0.589		+2 0.700		+4 0.905		+6 1.316		+7½ 1.751		+9½ 2.224	
			Mean	P.E.	Mean	P.E.	Mean	P.E.	Mean	P.E.	Mean	P.E.	Mean	P.E.	Mean	P.E.	Mean	P.E.	Mean	P.E.
α Lyrae	26^d 8^{h}45^m	1.01	0.22	0.03	0.16	0.03	0.20	0.02	0.58	0.03	0.29	0.07	0.13	0.09	0.18	0.02	0.10	0.01	.....	.....
	13 10 04	1.25	.16	.03	.23	.04	.22	.02	.34	.01	.27	.01	.15	.02	.04	.01	.....	.....	.....	.....
α Cygni	25 10 36	1.02	.....	.....	.18	.04	.26	.08	.41	.03	.28	.05	.17	.04	.20	.04	.....	.....	.....	.....
	13 13 27	1.56	.....	.....	.13	.02	.16	.04	.24	.01	.30	.02	.29	.00	.40	.01	.....	.....	.....	.....
α Aquilae	26 10 56	1.20	0.10	0.03	.17	.05	.16	.04	.32	.03	.25	.02	.17	.01	.04	.02	.....	.....	.....	.....
α Canis Min.†	13 16 16	2.44	.....	.....	.04	.04	.09	.01	.23	.03	.41	.04	.20	.05	.04	.05	.....	.....	.....	.....
	....	.....	.....	.....	(.05)	.....	(.10)	.....	(.25)	.....	(.44)	.....	(.21)	.....	(.04)	.....	.....	.....	.....	.....
α Persei	26 15 44	1.07	.....	.....	.....	.....	.14	.02	.17	.04	.27	.05	.33	.01	.37	.01	.15	.02	.....	.....
	13 14 42	1.06	.....	.....	.....	.....	.11	.01	.22	.02	.23	.02	.25	.01	.17	.03	.13	.05	.....	.....
γ Cygni	13 12 00	1.21	.....	.....	.14	.04	.26	.02	.22	.03	.22	.03	.21	.03	.29	.05	.21	.04	0.05	0.02
α Aurigae	25 15 47	1.16	.....	.....	0.01	0.02	.17	.01	.35	.07	.46	.02	.52	.01	.47	.01	.41	.08	.22	.06
Mars	13 15 12	1.46	.....	.....	.....	.....	.19	.03	.33	.01	.34	.03	.36	.01	.48	.01	.14	.02	.....	.....
Jupiter	26 14 20	1.18	.....	.....	.....	.....	0.08	0.05	.16	.01	.24	.01	.34	.02	.22	.01	−.02	.04	.....	.....
β Ceti	25 13 26	1.71	.....	.....	.....	.....	.....	.....	.14	.02	.30	.05	.37	.05	.....	.....	.12	.04	.....	.....
	26 13 45	1.67	.....	.....	.....	.....	.....	.....	.15	.05	.20	.04	.42	.04	.27	.04	.15	.02	.....	.....
γ Aquilae	26 9 36	1.09	.....	.....	.....	.....	.....	.....	.03	.02	.11	.05	.28	.02	.39	.07	.32	.04	.06	.02
α Boötis	25 7 40	1.40	.....	.....	.....	.....	.....	.....	.18	.04	.23	.02	.53	.00	0.94	.08	0.63	.01	.33	.01
α Tauri	25 15 16	1.45	.....	.....	.....	.....	.....	.....	.23	.04	.24	.04	0.65	.03	1.06	.02	1.19	.03	0.73	.05
α Orionis	25 16 17	1.71	.....	.....	.....	.....	.....	.....	.28	.05	.49	.02	1.19	.05	2.35	.09	2.06	.09	1.01	.03
β Andromedae	25 13 58	1.02	.....	.....	.....	.....	.....	.....	.17	.06	.23	.07	0.44	.06	0.44	.10	0.36	.04	0.38	.02
	26 13 05	1.06	.....	.....	.....	.....	.....	.....	.14	.08	.26	.02	.25	.06	.47	.06	.36	.05	.17	.01
β Pegasi	25 12 53	1.01	.....	.....	.....	.....	.....	.....	.08	.13	.22	.14	.34	.14	.41	.07	.50	.03	.47	.05
δ Sagittae	25 9 53	1.05	.....	.....	.....	.....	.....	.....	.10	.06	.10	.05	.44	.02	.28	.02	.59	.07	.19	.10
	26 10 20	1.07	.....	.....	.....	.....	.....	.....	.13	.05	.17	.02	.24	.02	.35	.03	0.44	.03	.07	.03
α Herculis	25 8 28	1.15	.....	.....	.....	.....	.....	.....	.21	.02	.41	.05	.52	.05	.97	.02	1.20	.07	.49	.02
	26 7 56	1.10	.....	.....	.....	.....	.....	.....	.15	.02	.26	.02	.47	.05	.90	.07	1.18	.06	.96	.03
o Ceti	25 14 37	1.35	.....	.....	.....	.....	.....	.....	.15	.05	.29	.01	.31	.04	.77	.05	1.03	.01	.63	.04
	26 14 59	1.30	.....	.....	.....	.....	.....	.....	.06	.01	.34	.02	.45	.02	.92	.03	0.67	.04	.36	.02
	13 14 06	1.28	.....	.....	.....	.....	.....	.....	.13	0.03	.19	0.01	.27	0.06	.43	0.02	.40	0.02	.15	0.01
	13‡14 06	1.28	.....	.....	.....	.....	.....	.....	0.26	.....	0.38	.....	0.54	.....	0.86	.....	0.80	.....	0.50	.....

* The days refer to August 25, 26, and September 13, 1928, respectively.

† Values given for α Canis Minoris in parentheses are corrected to air mass 1.3.

‡ o Ceti appears to have been only half as bright on September 13 as on August 25 and 26. For easy comparison, the September values are doubled and are thus plotted in Figs. 5 and 6.

apparatus and the atmosphere; and the combined values of both factors.

Multiplying the values in Table IV by the combined factor in Table V, we obtain values for points on the normal scale outside the earth's atmosphere as given in Table VI.

The results given in Table VI are plotted in Figure 6. Most of the curves are fairly smooth and reasonable. As for individual discrepancies, it is obvious that the first three points on the curves for Rigel are too small, and that the observations of Vega, Deneb, and δ Sagittae are too irregular to give a fair indication of the march of their spectral energy-curves. A low value occurs at 0.589 microns in the spectrum of Capella, and surprisingly high values are found on all three nights at 0.700 microns in the spectrum of Mira.

TABLE V

REDUCING FACTORS

PLACE	FACTOR OF 1928		FACTOR OF 1923	COMBINED
	Obs.	Used		
−7		0.44	2300	1010
−6		.44	1400	616
−5		.45	910	410
−4	0.45	.45	620	279
−3	.42	.46	460	212
−2		.50	335	167
−1		.53	253	134
0	0.59	0.59	188	111
2	1.03	1.03	96	99
4	1.71	1.71	41	70
6	1.74	1.74	25	43
7½	1.37	1.37	21	29
9¼	0.69	0.69	25	17

It is interesting to compare the results with those of the year 1923. For this purpose the results of 1928 were reduced by applying appropriate factors, as nearly as possible, to the scale of those given in Table V of *Mount Wilson Contr.*, No. 280.[1] When this had been done, 43 places in the spectra of 8 stars were found for which ratios of intensities could be computed. Of these, 7 are so wild as to be rejected. The remaining 36 show an average deviation, 1928 from 1923, of 19.8 per cent. Assuming that the observations of 1923 and 1928 are of equal accuracy, we find the probable error of a single average observation to be (0.84×19.8)/1.41 = 11.8 per cent,

---

[1] *Astrophysical Journal*, **60**, 87, 1924.

TABLE VI

STELLAR ENERGY SPECTRUM DISTRIBUTION; NORMAL SCALE, OUTSIDE THE ATMOSPHERE

OBJECT	DATE	PLACE ON PRISMATIC SCALE AND WAVE-LENGTHS, MICRONS								
		−6 0.437	−4 0.472	−2 0.520	0 0.589	+2 0.700	+4 0.905	+6 1.316	+7½ 1.751	+9½ 2.224
β [illegible]nis*	13†	990	1140	584	233	89	21	......	.....	.....
α Lyrae	26	1355	446	334	644	287	91	77	29	.....
	13	990	642	367	377	267	105	17	.....	.....
α Cygni	25	......	502	434	455	277	121	86	.....	.....
	13	......	363	267	266	297	206	172	.....	.....
α Aquilae	26	616	474	267	355	247	121	17	.....	.....
α Canis Min.	13	......	139	167	277	436	149	17	.....	.....
α Persei	26	......	......	234	189	267	231	159	43	.....
	13	......	......	184	244	228	177	73	38	.....
γ Cygni	13	......	390	434	244	208	149	125	60	8
α Aurigae	25	......	28	284	388	455	369	202	119	37
Mars	13	......	......	317	366	337	256	206	41	.....
Jupiter	26	......	......	134	178	238	241	95	6	.....
β Ceti	25	......	......	.....	155	297	263	......	35	.....
	26	......	......	.....	166	198	298	116	43	.....
γ Aquilae	26	......	......	.....	33	109	199	168	93	10
α Boötis	25	......	......	.....	200	228	376	404	183	56
α Tauri	25	......	......	.....	255	238	461	456	345	124
α Orionis	25	......	......	.....	311	485	844	1010	597	172
β Andromedae	25	......	......	.....	189	228	312	189	104	65
	26	......	......	.....	155	257	177	202	104	29
β Pegasi	25	......	......	.....	89	218	241	176	145	80
δ Sagittae	25	......	......	.....	111	99	312	120	171	32
	26	......	......	.....	144	168	170	150	128	12
α Herculis	25	......	......	.....	233	406	369	417	348	83
	26	......	......	.....	166	257	334	387	342	163
o Ceti	25	......	......	.....	166	287	220	331	299	107
	26	......	......	.....	67	337	319	396	194	61
	13	......	......	.....	144	188	192	185	116	26
	13‡	......	......	.....	288	376	383	370	232	51

* Additional observations for β Orionis: −7, 0.423 μ, 505; −5, 0.454 μ, 738; −3, 0.494 μ, 827.

† The dates refer to August 25, 26, and September 13, 1928, respectively.

‡ Values of preceding line doubled.

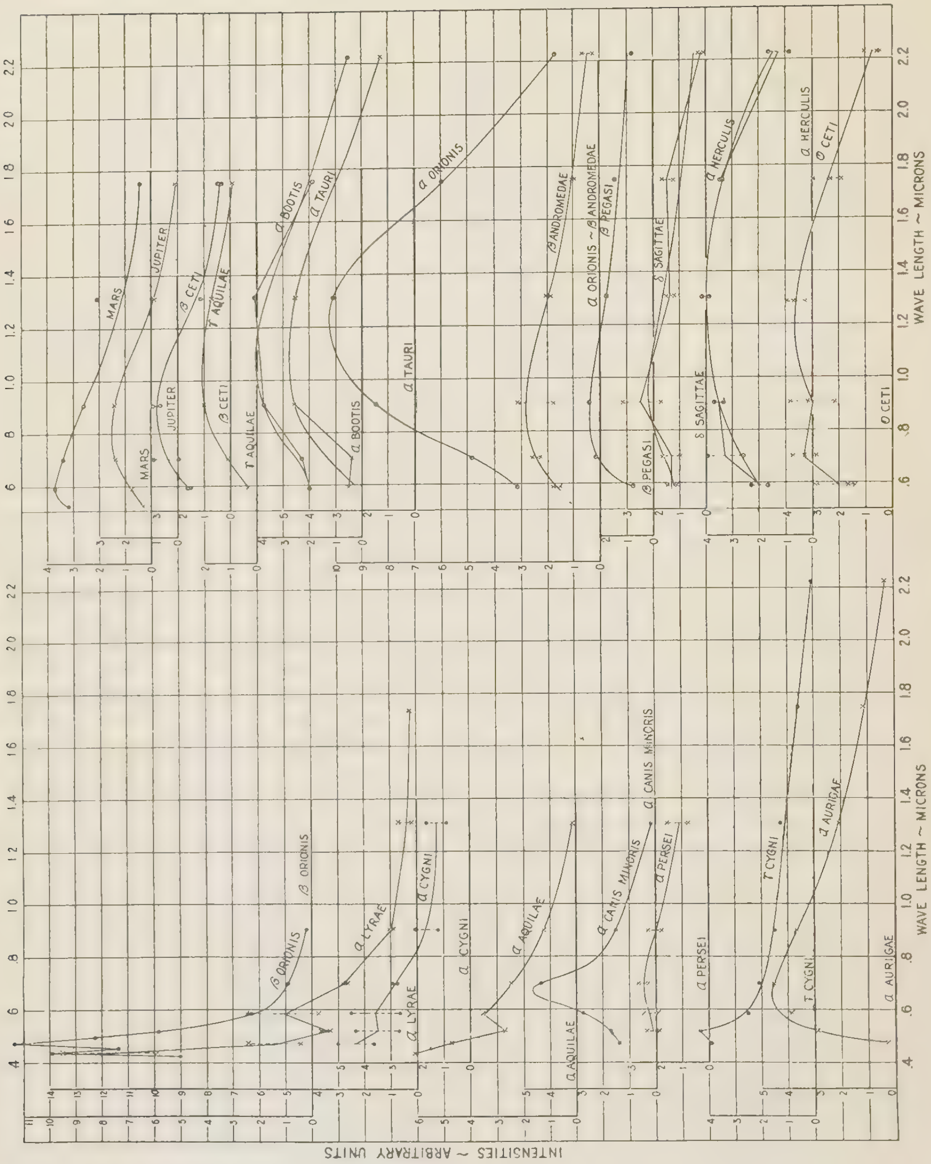
MARS
JUPITER
β CETI
τ AQUILAE
α BOOTIS
α TAURI
α ORIONIS
β ANDROMEDAE
α ORIONIS ~ β ANDROMEDAE
β PEGASI
δ SAGITTAE
α HERCULIS
o CETI
β ORIONIS
α LYRAE
α CYGNI
α AQUILAE
α CANIS MINORIS
α PERSEI
τ CYGNI
α AURIGAE
.4
.6
.8
1.0
1.2
1.4
1.6
1.8
2.0
2.2
WAVE LENGTH ~ MICRONS
INTENSITIES ~ ARBITRARY UNITS

FIG. 6

which agrees fairly well with what is shown by Table III; for the average deflection in Table III is 0.21 divisions, and the average probable error is 0.021 divisions, or 10 per cent of the average deflection.

As a more concrete illustration of the degree of consonance between the observations of 1923 and 1928, consider the following table, where the results for α Orionis and β Pegasi for the two years are reduced to approximately the same scale.

TABLE VII

VALUES OF 1923 AND 1928 COMPARED

Place		0	+2	+4	+6	+7½	+9¼
Wave-length, μ		0.589	0.700	0.905	1.316	1.751	2.224
α Orionis	1923	378	614	1132	1202	918	407
	1928	407	635	1105	1440	782	225
	Δ	+29	+21	−27	+238	−136	−182
β Pegasi	1923	75	144	205	167	132	72
	1928	76	185	205	150	123	68
	Δ	+1	+41	0	−17	−9	−4

Although the agreement between the observations of 1923 and 1928 is as good as the accuracy of the results warrants us to expect, much improvement is needed before the spectral energy-curves of any of the stars can be regarded as well determined. If possible, continuous registration should be introduced in order that special features occurring within narrow ranges of wave-length may be detected. The measurements should be extended toward both shorter and longer wave-lengths than can penetrate the great glass prism used for these observations. More exact standardization of the observations in terms of radiation of known spectral energy distribution must be sought. It is highly desirable to obtain as much as tenfold greater sensitiveness than was available in 1928, without increased accidental disturbance, so that stars of the third magnitude may easily be observed. With such improvements a long campaign of observations of stellar spectral distribution would be justified.

CARNEGIE INSTITUTION OF WASHINGTON
MOUNT WILSON OBSERVATORY
SMITHSONIAN INSTITUTION
February 1929

Contributions from the Mount Wilson Observatory, No. 381
Reprinted from the *Astrophysical Journal*, Vol. LXIX, pp. 330–378, 1929
Printed in the U.S.A.

THE SPECTRUM OF B.D.+11°4673

By PAUL W. MERRILL

ABSTRACT

Previous spectroscopic observations of this peculiar Be star by Fleming, Campbell, Cannon, and Merrill showed the bright lines to have characteristics of special interest. Collected *photometric data* make it probable that the light has not been constant, but do not indicate the exact nature of the variations.

Mount Wilson observations.—Forty-six spectrograms were obtained from 1919 to 1928. *More than 160 bright lines* have been observed, of which *nearly all are variable in intensity and position*, and *some are variable in structure*. The elements whose lines were studied in some detail are *H*, *He*, *Fe*, *Al*, *N*, and *Si*; other elements represented by bright lines are *Ti*, *Cr*, *Mg*, *C*, and *Sc*.

Hydrogen (p. 219).—The bright lines are always outstanding but vary in intensity. At times they are accompanied by *dark companions on their violet edges*. The distances between the centers of the bright and dark lines are different in various years, the values falling in two distinct groups. In passing from one line to another in the same spectrogram the variation is approximately as the cube of the wave-length. On two or three plates weak bright components are visible on the violet side of the strong bright lines.

The *displacements* of the various bright hydrogen lines give fairly consistent results, the small systematic differences yielding no evidence that the dark borders are directly effective in displacing the bright lines toward the red. The *displacements vary in* a cycle of *800 days* with a semi-amplitude of about 20 km/sec. There is some indication that the amplitude increased from 1915 to 1928.

Helium (p. 230).—Prior to 1920 *the lines were dark;* since then they have been *bright with dark borders on their violet side*. In a given series the distance between the centers of bright and dark lines varies as the cube of the wave-length. The *displacements* exhibit an 800-day period with a semi-amplitude of 16 km/sec. The *difference in phase* between the oscillations of hydrogen and helium lines is 160 days.

Iron (p. 235).—Lines of the ionized atom only are present. An interesting feature is the presence of *numerous forbidden lines*. *Intensities* of both allowed and forbidden lines are *variable*. The *displacements* probably vary in the 800-day period, but with a *smaller semi-amplitude* (about 8 km/sec.) and a lower mean axis than for hydrogen or helium, and with a *different phase*.

Aluminum (p. 240).—λλ 4512 and 4529 of doubly ionized aluminum are well marked in emission, and several other lines of singly and doubly ionized aluminum are probably present. The variation of the displacement resembles that of the helium lines, but the whole curve is about 26 km/sec. lower.

Nitrogen (p. 243).—Numerous bright lines of ionized nitrogen, several of which are accompanied by a dark border, are present. The variation of the displacements is similar to that of the helium lines. The *forbidden nitrogen lines* recently identified by Bowen in the *spectra of nebulae*, λλ 5755, 6548 and 6583, are *present in emission*.

Silicon (p. 247).—Neutral atoms (probably) and the *first three stages of ionization* are represented by bright or dark lines as follows: *Si* I bright, *Si* II bright, *Si* III bright and dark, *Si* IV dark only.

Various elements.—The lines of *Ti* II resemble in behavior those of *Fe* II, except that they are much weaker. Lines of *C* II, *Mg* II, *Sc* II, and *Cr* II are faintly present in emission. A complete list of lines is given in Table XXII.

Detached lines.—K(*Ca*) and D_1, D_2 (*Na*) are weak dark lines.

Discussion.—The *maximum ionization* is apparently slightly in excess of 33 volts.

Elements whose *bright lines* increased in *intensity* in 1921 are *H*, *He* I, *Fe* II, *N* II, *Al* III, while lines of [*Fe* II] (forbidden lines) and *Si* III did not increase. Since 1922 the intensity-curves for *H* and *Fe* II have more in common than those for *H* and *He*.

The distance of the centers of the bright lines from the centers of their accompanying *dark borders* is approximately the same for *H*, *He* I, *N* II, and *Si* III. The dark lines of *He* I, *N* II, and *Si* III shifted toward the violet upon the appearance of bright components.

The *oscillations of the bright lines* of seven elements are concisely compared in Table XXVI. They exhibit extraordinary differences, suggesting a tenuous atmosphere in which the elements are sorted by light pressure and gravitation.

I. Previous Spectroscopic Observations

Harvard observations.—Attention was first called to this remarkable star[1] in 1894 by Mrs. Fleming's announcement[2] of the presence in its spectrum of the bright hydrogen lines $H\beta$, $H\gamma$, and $H\delta$. These lines appeared on objective-prism spectrograms taken at the Harvard College Observatory during the course of the spectroscopic survey of the sky inaugurated by Professor E. C. Pickering. Seven photographs of the spectrum were obtained between 1893 and 1912 with the 8-inch Draper telescope, giving a dispersion of approximately 160 A per millimeter. According to a recent examination by Miss Cannon, these seem to show, between $H\beta$ and $H\gamma$, several narrow bright lines which cannot be identified with certainty on account of the small dispersion. She found no appreciable change in the spectrum during this interval.

The star was included by Miss Cannon in a list of "Spectra of the P Cygni Type,"[3] and the meaning of this designation was explained in the following words:

> On plates of small dispersion, P Cygni shows a strong continuous spectrum, with $H\beta$, $H\gamma$, and $H\delta$ very bright, and other bright lines are clearly seen. Ten other spectra have been found which resemble that of P Cygni, taken with small dispersion. As these stars are rather faint, it is not possible to decide, with the photographs now available, whether they resemble the spectrum of P Cygni as regards the fainter lines.

Observations at Lick Observatory.—In 1894 Campbell, observing visually with a spectroscope attached to the 36-inch refractor at Lick Observatory, found $H\alpha$ to be bright.[4]

Ann Arbor observations.—In order to make a detailed comparison with P Cygni, the spectrum of B.D.+11°4673 was photographed in 1915 by the writer with a one-prism slit spectrograph attached to the $37\frac{1}{2}$-inch reflector of the Detroit Observatory.[1] The main results of this investigation may be summarized as follows:

---

[1] H.D. 207757, R.A. $21^{h}46^{m}.2$; Dec. +12°9′, 1900; mag. 7.6; spectrum pec. Remark in the Henry Draper Catalogue, "The lines $H\beta$, $H\gamma$, $H\delta$, and $H\epsilon$ are bright. $H\beta$ is the strongest and the spectrum is of the P Cygni type."

[2] *Astronomy and Astrophysics*, **13**, 502, 1894.

[3] *Harvard Annals*, **76**, 31, 1916.

[4] *Astrophysical Journal*, **2**, 180, 1895.

1. The *hydrogen lines* were bright, with weak dark components on their more refrangible edges. The bright hydrogen lines agreed in giving a radial velocity of +16.0 km/sec.
2. Numerous *enhanced metallic lines, chiefly iron*, appeared bright, some of them being accompanied by weak dark borders. These bright lines were displaced toward the violet by about 0.6 A with respect to the bright hydrogen lines.
3. Several *bright lines of unknown origin* were present, the most notable being λλ 4244.0, 4287.0, 4358.6.
4. A number of weak *absorption lines* without visible bright portions were measured. Most of those identified were due to helium and silicon. Five helium lines and one silicon line gave a velocity of −12 km/sec.
5. *The similarity to P Cygni* did not extend to the fainter bright lines.

II. VARIATIONS IN LIGHT

The estimates of magnitude in Table I have been collected from various sources by Lundmark.[2] From an examination of fifty-one Harvard photographs covering an interval of fifteen years, Miss Wells found[3] that the star was apparently slowly decreasing in brightness. In January, 1922, it was about 0.3 mag. fainter than in 1906. Additional information is contained in a letter from Dr. Shapley, dated March 18, 1929: "Miss Wells has now looked up plates since 1922 and finds no evidence of variation. The decrease in brightness throughout an interval of fifteen years seems to be definite."

TABLE I

MAGNITUDE ESTIMATES OF B.D.+11°4673

Source	Epoch	Magnitude
$W_1 21^h 1043$	1821.8	9
$Mü_1 29674$	1841.9	9
B.D.+11°4673	1855±	7.7
Sj 8881	1861.9	7
Lpz I 8693	1870.8	6.3
Harvard map	1905.6	6.7
Lundmark	1920.8	6.8 photographic 7.0 visual

---

[1] *Publications of the Observatory, University of Michigan*, **2**, 71, 1916.

[2] *Astronomische Nachrichten*, **213**, 93, 1920.

[3] *Harvard College Observatory Bulletin*, No. 762, 1922.

III. MOUNT WILSON OBSERVATIONS

A. THE SPECTROGRAMS

Spectroscopic observations of this star were resumed by the writer at Mount Wilson in 1919 in order to extend our knowledge of its intricate and interesting spectrum, as well as to ascertain whether any changes had occurred since the Ann Arbor observations in 1915.

On the first Mount Wilson plates the spectrum appeared essentially the same as in 1915, although certain lines did not have exactly the same relative intensities. In 1920 and 1921, however, a striking new feature developed, and numerous minor changes have occurred since that time. The presence of several features of special physical interest and the fact that they are subject to curious changes make this spectrum a fascinating one to follow. A few spectrograms have been obtained each year since 1919.

Table II gives a list of spectrograms upon which the present study is based. The first five, obtained at Ann Arbor in 1915, have been previously described,[1] but are included here for convenience. The remainder were obtained at Mount Wilson with the 100-inch reflector, except two marked γ, taken with the 60-inch reflector. The C plates were taken with one prism and an 18-inch camera; the dispersion at various points in the spectrum is as follows: $H\alpha$, 170 A per millimeter; $H\beta$, 57; $H\gamma$, 36; $H\delta$, 28. Most of these plates were taken on the fine-grained Seed 23 or Eastman 33 emulsion, and were widened by allowing the star to drift the length of the slit during the exposure. These circumstances, together with the high purity[2] obtained by use of a narrow slit (about 0.03 mm), made it possible to measure numerous narrow bright lines having small contrast with the background of continuous spectrum. The G plates were taken with a plane-grating spectrograph and have a dispersion of 67 A per millimeter. The H plates were taken with a small-dispersion ultraviolet spectrograph. The observation of April 27, 1921, was made with a three-prism spectrograph belonging to the Lowell Observatory, which was being used in connection with the 100-inch telescope for a special investigation by Dr. V. M. Slipher; the dispersion at

---

[1] *Publications of the Observatory, University of Michigan*, **2**, 71, 1916.

[2] The focal length of the collimator lens is 40 inches (102 cm).

TABLE II

Journal of Observations

Plate	Date	J.D.	Emulsion*	Remarks
		2420000		
3228 A	1915 May 21	+0639	S 30	Ann Arbor
3259 B	June 13	0662	S 30	Ann Arbor
3332 A	July 23	0702	S 30	Ann Arbor
3340 B	Aug. 6	0716	S 30	Ann Arbor
3368 A	Nov. 12	0814	S 30	Ann Arbor
C 36 . . .	1919 Sept. 3	2205	S 30	
37 . . .	Sept. 3	2205	S 23	Strong exposure
40 . . .	Sept. 4	2206	S 23	Strong exposure
45 . . .	Sept. 5	2207	S 23	
46 . . .	Sept. 5	2207	S 23	
49 . . .	Sept. 6	2208	S 23	
50 . . .	Sept. 6	2208	S 23	
51 . . .	Sept. 6	2208	S 23	Focused for $H\beta$ region only
52 . . .	Sept. 6	2208	S 23	Focused for $H\beta$ region only
181 . . .	Nov. 7	2270	C.I.I.	
183 . . .	Nov. 8	2271	S 23+Pcl.	Weak exposure in red
529 . . .	1920 July 7	2513	S 23	
642 . . .	Sept. 3	2571	S 23	
γ 9570 . . .	Sept. 25	2593	Ilf.	40″ camera; bright $H\alpha$ and $H\beta$ only
. . . .	1921 Apr. 27	2807	S 30	Slipher's three-prism; bright $H\beta$ and $H\gamma$ only
C 1060 . . .	June 20	2861	S 23	
1193 . . .	Aug. 11	2913	S 23	
1399 . . .	Oct. 13	2976	S 23	
1400 . . .	Oct. 13	2976	Ilf.	For region from $H\beta$ to $H\alpha$ only
1405 . . .	Oct. 14	2977	Ilf.	For region from $H\beta$ to $H\alpha$ only
1666 . . .	1922 Apr. 13	3158	S 30	
1704 . . .	May 15	3190	A.G.S.	Very weak exposure
1745 . . .	June 11	3217	S 23	
1822 . . .	Aug. 9	3276	S 23	
1942 . . .	Oct. 8	3336	Ilf.	For region from $H\beta$ to $H\alpha$ only
2222 . . .	1923 Apr. 30	3540	S 23+Pcl.	Includes red region; weak exposure
2342 . . .	July 3	3604	S 23	
2415 . . .	Aug. 31	3663	S 30	Strong exposure
2467 . . .	Sept. 30	3693	S 23	Very weak exposure
2470 . . .	Oct. 1	3694	S 23	
γ 12175 . . .	Oct. 3	3696	S 30	Spectrum narrow
C 2750 . . .	1924 Apr. 17	3893	S 30	Weak exposure
2892 . . .	July 19	3986	S 23	Weak exposure
G 20 . . .	Oct. 3	4062	S 23+Pcl.	Plate fogged
C 3073 . . .	Nov. 8	4098	S 23	
3383 . . .	1925 July 6	4338	S 23	
H 37 . . .	Aug. 19	4382	E 40	
42 . . .	Aug. 20	4383	E 33	Very strong exposure
C 3541 . . .	Oct. 1	4425	S 23	

TABLE II—*Continued*

Plate	Date	J.D.	Emulsion*	Remarks
		2420000		
C 3811...	1926 May 30	+4656	E 33	Weak exposure
3935...	Aug. 12	4740	E 33	
4321...	1927 June 22	5054	E 33	Weak exposure
4418...	Sept. 9	5133	E 33	
4867...	1928 June 28	5426	E 33	
G 194...	Aug. 2	5461	E Sl. P.	
C 5026...	Oct. 5	5525	E 33	

* S = Seed; E = Eastman.
C.I.I. = Cramer Instantaneous Iso.
Ilf. = Ilford Special Rapid Panchromatic, hypersensitized by an ammonia bath.
A.G.S. = Astronomical Green Sensitive, prepared by the Research Laboratory of the Eastman Kodak Co.
+Pcl. = sensitized to red light by bathing in a solution of pinacyanol.
Sl.P. = "Slow Panchromatic," a special red-sensitive emulsion made by the Research Laboratory of the Eastman Kodak Co., hypersensitized by an ammonia bath.

$H\beta$ is 26 A per millimeter; at $H\gamma$, 12.5. γ 9570 was taken with one prism and a 40-inch camera; γ 12175 with one prism and an 18-inch camera.

B. GENERAL DESCRIPTION OF THE SPECTRUM AND ITS PRINCIPAL CHANGES

Before proceeding to a detailed description of the spectrograms it may be well to mention the chief features of the spectrum and the principal changes which have recently occurred.

The most conspicuous features are the bright *hydrogen lines*, which vary in intensity but are always strong. At times they are accompanied by relatively weak absorption borders on their more refrangible edges, but at other times these dark borders disappear.

The *helium lines* have behaved in a striking manner. In 1915 they were dark; in 1919, nearly neutral; in 1920 they were emerging in emission; and since June, 1921, they have been present on all the spectrograms as strong bright lines, accompanied by dark borders of shorter wave-length.

Numerous well-known *iron spark lines* are conspicuous in emission on many spectrograms, but on other plates of equal quality are scarcely visible. Forbidden lines of the ionized iron atom, re-

PLATE VIII

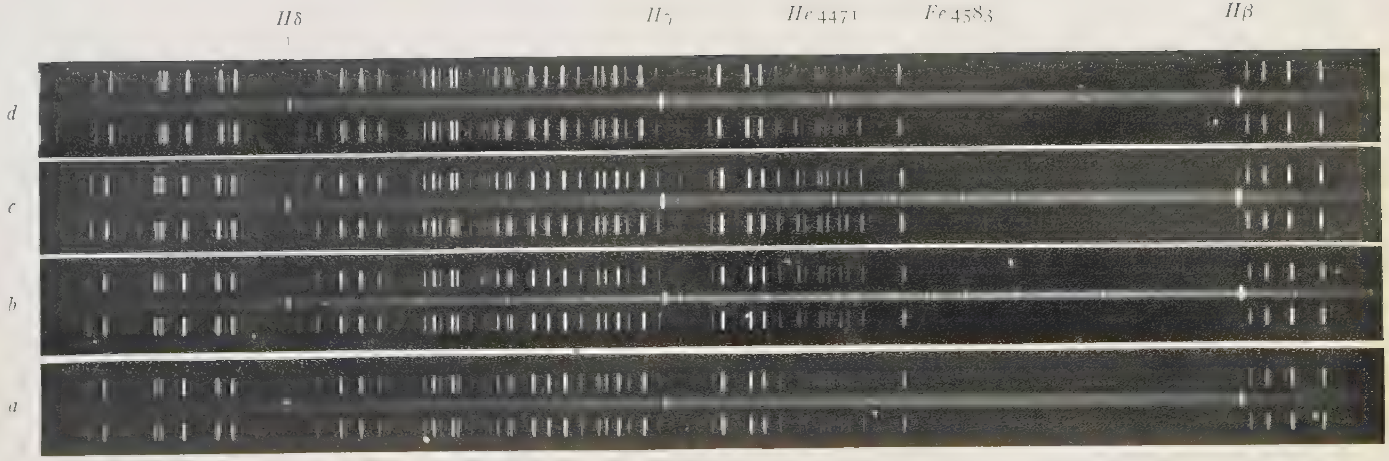

SPECTROGRAMS OF B.D.+11°4673

(*a*) C529, 1920 July 7
(*b*) C1399, 1921 Oct. 13
(*c*) C1745, 1922 June 11
(*d*) C3383, 1925 July 6

cently identified in the spectrum of η Carinae,[1] are present in emission on many plates. They vary in intensity with respect to the continuous spectrum and also with respect to the ordinary lines of the *Fe* II spectrum.

Other elements, represented chiefly by emission lines, with their respective degrees of ionization, are as follows: *Al* II, III; *N* II, including the forbidden (nebular) lines λλ 6548, 6583; *Si* I?, II, III, IV; *Ti* II; *Cr* II; *Mg* II; *C* II?; *Sc* II?.

A continuous spectrum having about the usual energy distribution for a B-type star is quite strong at all times, forming a background against which the numerous bright lines appear with various and varying degrees of contrast.

The variations in the intensities of the bright lines are on the whole rather gradual; that is to say, plates taken within an interval of a few weeks do not exhibit a wide range of behavior. From one year to another, however, large differences may appear. The course of the variations is too complicated to permit a brief description, but some idea of it may be gained from Figure 13. One notable phenomenon was the simultaneous strengthening of the hydrogen, helium, and enhanced iron lines, beginning in 1920. A strict periodicity in the various changes is lacking, but the recurrence of certain features at intervals of about eight hundred days is of considerable interest.

In addition to their variations in intensity, the lines are subject to variations in position which differ for the various elements in a most extraordinary fashion. The eight-hundred-day cycle is a common feature, but, aside from this, each element seems to be a law unto itself. One especially curious phenomenon is the apparent increase in the amplitude of the oscillations of the hydrogen lines (see Figs. 1 and 4).

C. HYDROGEN LINES

The bright hydrogen lines are the outstanding features of the spectrum. $H\alpha$ is an extraordinarily intense line, badly overexposed on plates that show the continuous spectrum on either side. The intensities of the bright lines diminish along the Balmer series toward the ultra-violet as usual in spectra of class Be. $H\beta$, $H\gamma$, and $H\delta$ are

---

[1] *Mt. Wilson Contr.*, No. 354; *Astrophysical Journal*, **67**, 391, 1928.

TABLE III

INTENSITIES OF LINES

PLATE	J.D.	HYDROGEN		HELIUM		IONIZED IRON		λ 4359 [*Fe* II] / λ 4352 *Fe* II
		Em.	Abs.	Em.	Abs.	Lab.	Forb.	
	2420000							
3228 A....	+0639	5	3	0	....	(2)	(2)	0.9
3259 B....	0662	5	4	0	1	3.5	2.5	1.1
3332 A....	0702	7	2.5	0	1	3.5	3	0.9
3340 B....	0716	7	2.5	0	2	3.5	2.5	1.15
3368 A....	0814	6.5	3	0	1	2.5	3.5	1.35
Mean .	0707	6.1	3.0	0	1.2	3.2	2.9	1.08
C 36....	2205	4	4	0	0.5	4.5	2	0.6
37....	2205	5	6	0	1	6.5	2.5	0.5
40....	2206	5.5	6	0	1	6.5	2.5	0.55
45....	2207	5.5	6	0	1	6.5	3	0.45
46....	2207	5	6	0	1	6.5	3.5	0.35
49....	2208	5.5	5	0	0.5	7	3	0.35
50....	2208	5.5	6	0	0.5	7	3.5	0.4
51....	2208	4	....	0	....	(6)	....	....
52....	2208	5	....	0	(1)	(6)	....	....
Mean .	2207	5.0	5.6	0	0.8	6.3	2.9	0.46
C 181....	2270	(5)	....	0	2	6	3.5	0.4
183....	2271	(5)	....	0	3	(5)	(3)	0.6
Mean .	2270	5	....	0	2.5	5.7	3.3	0.5
C 529....	2513	4.5	5.5	0	2	2	4	1.5
642....	2571	6	6.5	1.5	1	2.5	5	2.0
1060....	2861	11	5.5	8.5	5	7	5	0.7
1193....	2913	12	7	10.5	6	9	5	0.6
1399....	2976	12.5	7	9	6	10	4.5	0.45
1666....	3158	12.5	0	5.5	4	6	1.5	0.3
1745....	3217	12.5	0.5	8	5	6	2.5	0.6
1822....	3276	11	1	8	5	6	4	0.7
2342....	3604	10	5	10	5	5	5	(2.0)
2415....	3663	10	5	8	5	5	5	1.2
2470....	3694	10	3.5	7.5	5	5	4.5	0.85
2750....	3893	12	1	5	5	5.5	1.5	0.3
2892....	3986	12	(1)	5	5.5	6	1.5	0.4
3073....	4098	14.5	0.5	8.5	5	4.5	3	0.8
3383....	4338	10	2	9	4.5	1.5	2	(1.5)
3541....	4425	9.5	?	8.5	6.5	4.5	1	0.2
3811....	4656	11.5	0	5.5	5	4.5	1	0.25
3935....	4740	15	0	8	5	6	1	0.35
4321....	5054	(9)	5.5	6.5	6	3	0	<1
4418....	5133	8.5	3	7	6.5	1	0	....
4867....	5426	14.5	1	8	6.5	5	0	<0.3
5026....	5525	11.5	1	7	5.5	4.5	1	0.3

very conspicuous; the lines of shorter wave-length less so. With low dispersion (plates H 37 and H 42), a few of the ultra-violet lines are seen in absorption without recognizable bright portions.

The bright hydrogen lines are sharp and well defined on most of the spectrograms. A noticeable widening accompanied by a slight diffuseness of the edges may be observed, however, on the following plates: C 1666, C 1745, C 1822, C 2892, C 3073, C 3811, C 3935, C 4867. These were taken at times when the bright lines had their greatest intensities.

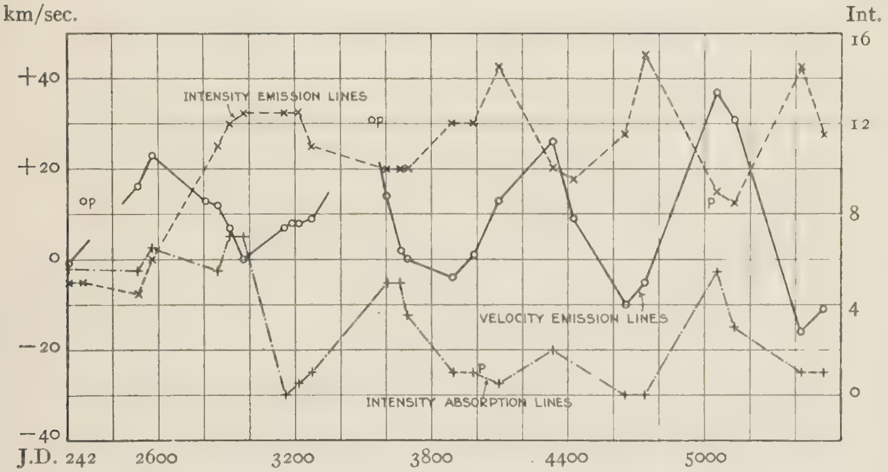

FIG. 1.—Behavior of hydrogen lines

Examination of the spectrograms reveals a considerable variation in the intensities of the bright hydrogen lines. The relative intensities on different plates have been estimated by comparing them with plate C 2342, on which the intensity was arbitrarily called 10. The estimates refer to the lines $H\beta$, $H\gamma$, and $H\delta$, and were made when viewing each spectrum alongside the standard spectrum in the Hartmann comparator. Additional intercomparisons of various plates were made later, but the resulting changes were inconsequential. The estimates are given in Table III and are plotted in Figure 1.

The first feature of interest in connection with the bright hydrogen lines is the rapid increase in intensity which began in 1920 and continued for about a year. After a broad maximum lasting from 1921 to 1922, there was a slight decrease in intensity, followed by narrower and higher maxima in 1924, 1926, and 1928. The intensities in 1915 and 1919 were about the same as in 1920, but since 1920 the average intensity has been much higher. Even the minima of the recent fluctuations have been above the 1919–1920 level.

On many plates dark borders occur on the violet side of the emission lines. They are seen only at $H\gamma$ and lines of shorter wave-length. Their increase in intensity toward the ultra-violet follows the usual behavior of the dark portions of the Balmer lines in spectra of class Be. The intensities of the dark portions of $H\gamma$ and $H\delta$ have been estimated in the same way as those of the bright lines except that the intensity on the standard plate, C 2342, was assumed to be 5 instead of 10. This was because the absorption lines at their best are relatively weak features. The data are in Table III, and are plotted in Figure 1.

In general, the behavior of the dark borders is opposite that of the bright portions; that is, relatively strong dark lines accompany relatively weak bright lines, and vice versa. Thus the average intensity of the dark lines has decreased since 1920, while that of the bright lines has increased; moreover, the maxima of the dark lines correspond to minima of the bright lines, and vice versa. Interesting exceptions to these rules occurred, however, in the years preceding 1922. The rapid increase of the intensity of the bright lines from 1920 to 1921 was accompanied, not by a weakening of the dark borders, but by a slight strengthening. Between the observations in 1921 and those in 1922, moreover, the dark borders practically disappeared, while the bright lines retained their high intensities.

Another relationship between the bright and dark lines is evident upon inspection of the plates. When the absorption borders are strong, the bright lines are narrow and their violet edges very sharp; when the absorption borders are weak or absent, the bright lines are slightly wider and their violet edges are not so well defined. The effects on the violet edge of the bright lines seem to have some correlation with the measurements of position; when the dark borders are strong, the apparent centers of the bright lines are displaced toward longer wave-lengths. This does not prove, however, that the presence of the absorption borders is the cause of the apparent displacement of the bright lines, as discussion on another page will show.

TABLE IV

HYDROGEN LINES, EMISSION *minus* ABSORPTION
(Angstrom Units)

Plate or Year	$H\gamma$	$H\delta$	$H\epsilon$	$H\zeta$	$H\eta$
1915	1.59	1.23	1.26	1.12	1.0
C 36	0.96	0.74	0.71	....	....
37	1.08	.82	.72	0.78	0.78
40	1.00	.82	.76	0.78	....
45	0.96	.76	.68	....	....
46	.96	.80	.67	....	....
49	0.92	.67	....	....	....
50	1.02	0.72	0.68	....	....
Mean (1919)	0.99	0.76	0.70	0.78	0.78
C 529	0.94	0.92	....	....	....
642	1.08	0.94	....	....	....
Mean (1920)	1.01	0.93	....	....	....
C 1060	1.53	1.30	....	....	....
1193	1.51	1.38	1.22	....	....
1399	1.54	1.20	....	....	....
Mean (1921)	1.53	1.29	1.22	....	....
C 2342	1.61	1.32	....	....	....
2415	1.84	1.38	1.15	....	....
2470	1.51	....	....	....	....
γ 12175	....	1.29	....	....	....
Mean (1923)	1.66	1.33	1.15	....	....
C 3383	1.26	0.90	0.77	....	....
3541	1.08	0.96	0.79	....	....
Mean (1925)	1.17	0.93	0.78	....	....
C 4321	1.58	....	....	....	....
4418	1.52	....	....	....	....
Mean (1927)	1.56	....	....	....	....

The distances between the effective centers of the bright lines and their dark companions were measured for those lines whose dark portions were clearly visible. The difference in wave-length increases with increasing wave-length, and for a given line varies considerably from year to year. For $H\gamma$, for example, it ranges from 1.0 A to 1.7 A. The measures are collected in Table IV, and the annual means are plotted in Figure 2. The data fall in two groups: the values for the years 1915, 1921, 1923, and 1927 ($H\gamma$ only) are much alike, while those for the years 1919, 1920, and 1925 resemble each other. In both groups the displacements are approximately proportional to the cube of the wave-length, but in one group the constant factor is about 50 per cent larger than in the other. Expressing λ and $\Delta\lambda$ in angstroms, we have approximately

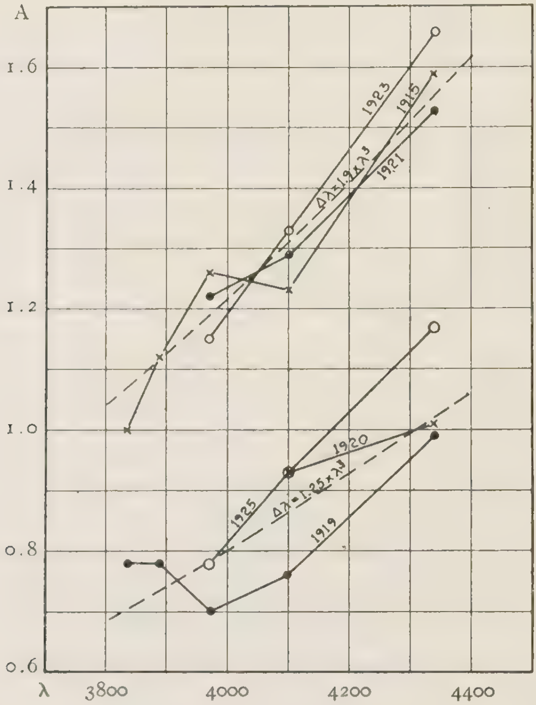

FIG. 2.—Hydrogen: relative displacements of emission and absorption lines

$$\Delta\lambda = a\lambda^3,$$

where $a = 1.25 \times 10^{-11}$ for the lower group, and 1.9×10^{-11} for the upper.

On plates C 3383 and C 3541 the bright hydrogen lines have weak *bright* companions toward shorter wave-lengths. These components are visible also on the three-prism plate taken on April 27, 1921. Table V gives the measured distances of these weak components from the centers of the main bright components.

Data concerning the intensity and structure of the hydrogen lines have been set forth in some detail in the preceding paragraphs. During recent years the characteristics of these lines seem to have been subject to a fairly regular succession of variations which suggests a periodicity of some kind in the star's atmosphere. In this connection it is interesting to note that a similar type of variation is shown by the positions (apparent radial velocities) of the lines, as the data which follow indicate.

TABLE V

RELATIVE DISPLACEMENTS OF WEAK BRIGHT COMPONENTS OF HYDROGEN LINES

Plate	$H\beta$	$H\gamma$	$H\delta$
3-prism.......	−1.92 A	−1.51 A	....
C 3383........	....	−1.58	....
3541........	....	−1.62	−1.48 A

The bright hydrogen lines are favorable for measurement as they are narrow and stand out prominently from the continuous spectrum. On many plates they are practically monochromatic;[1] on others, slightly widened. They appear symmetrical except when a dark companion makes the violet edge sharper than the red edge. The bright components to the violet, seen on two or three plates, are feeble, and, as in most cases they are slightly separated from the principal line, offer little interference with the measurements.[2] The measured displacements of the bright hydrogen lines are tabulated in Table VI. They are given for convenience in units of radial velocity, but other phenomena may of course be involved.

The agreement of the various Balmer lines is reasonably good, as is shown by a tabulation of the differences of successive lines (Table

---

[1] This refers, of course, only to the dispersion actually employed, about 36 A per millimeter at $H\gamma$.

[2] See, however, remarks in the following paragraph concerning the $H\beta$ line on two plates.

VII). For the purpose of this tabulation the Ann Arbor plates were counted as one observation, as were also plates C 36–C 50; all other

TABLE VI

DISPLACEMENTS OF BRIGHT HYDROGEN LINES

(Kilometers per Second)

Plate	$H\beta$	$H\gamma$	$H\delta$	$H\epsilon$	$H\zeta$	$H\eta$	Mean	Remarks
Ann Arbor	+16	+12	+16	+20	+20	+19	+16	
C 36	......	+ 5	− 6	0	......	......	0	
37	......	+ 3	− 4	− 5	− 3	− 6	− 3	
40	......	0	− 5	− 6	− 5	− 4	− 4	
45	......	+ 7	− 1	− 2	......	......	+ 1	
46	......	+ 2	− 1	− 4	......	......	− 1	
49	......	+ 1	− 4	0	......	......	− 1	
50	......	+ 6	− 1	0	......	......	+ 2	
Mean	......	+ 3	− 3	− 2	− 4	− 5	− 0.9	
C 51	+13	......	......	......	......	......	......	
52	+13	......	......	......	......	......	......	
181	+16	+10	......	......	......	......	+13	Poor
183	......	+15	......	......	......	......	......	Poor
529	+18	+14	+16	......	......	......	+16	
642	+25	+22	+23	......	......	......	+23	
γ 9570	+20	......	......	......	......	......	......	
3-prism	+14	+11	......	......	......	......	+13	
C 1060	+10	+12	+12	+13	......	......	+12	
1193	+17	+ 2	+ 6	+ 4	......	......	+ 7	
1399	+13	+ 2	− 8	− 7	......	......	0	
1400	+ 8	......	......	......	......	......	......	
1405	+16	......	......	......	......	......	......	
1666	+10	+ 1	+10	......	......	......	+ 7	
1704	+14	+ 6	+ 4	......	......	......	+ 8	
1745	+ 8	+ 5	+ 8	+ 8	......	......	+ 8	
1822	+13	+ 7	+ 6	......	......	......	+ 9	
1942	+29	......	......	......	......	......	......	
2222	+35	+28	......	......	......	......	+31	Fogged
2342	+21	+18	+14	+ 3	......	......	+14	
2415	......	+ 7	+ 6	− 2	− 2	......	+ 2	
2467	+ 6	− 2	− 3	......	......	......	0	
2470	+ 9	+ 8	0	− 4	......	......	+ 3	
γ 12175	− 8	− 3	− 8	......	......	......	− 6	Small weight
C 2750	+ 5	− 3	− 6	− 9	......	......	− 4	
2892	+ 4	− 1	+ 2	− 2	......	......	+ 1	
3073	+13	+ 8	+16	+15	......	......	+13	
3383	+14	+32	+31	+25	+26	......	+26	Vi. comp.
3541	− 3	+20	+16	+ 8	+ 3	......	+ 9	Vi. comp.
3811	− 8	−10	−10	−13	......	......	−10	
3935	−13	− 5	− 2	− 4	......	......	− 5	
4321	+42	+38	+36	+31	......	......	+37	
4418	+30	+28	+29	+35	......	......	+31	
4867	−11	−18	−19	−22	− 8	......	−16	
5026	−20	− 9	−10	− 4	......	......	−11	

plates were counted separately. Two plates, C 3383 and C 3541, give large negative values for the difference $H\beta-H\gamma$. On these plates the hydrogen lines have weak bright components toward the violet, which, in the case of $H\beta$, are blended with the principal line. These components are very weak and apparently have little effect upon the measurement of $H\gamma$ and lines of shorter wave-length, but they may build up the violet edge of the overexposed $H\beta$ line sufficiently to account for the measured shift of the center. The mean differences, $H\beta-H\gamma$, with and without these two plates, are +2.1 and +4.0 km/sec., respectively. The differences between other pairs of lines are small but positive in all cases. This is of interest because *negative* values would be expected if the dark borders had an appreciable effect in shifting the bright line toward the red. This is because the dark borders grow rapidly weaker in passing along the Balmer series from the ultra-violet lines to $H\beta$. These data therefore suggest that the dark borders have no strong influence on the positions of the bright lines. A few measures of the displacement of $H\alpha$ (Table VIII) show that it agrees approximately with those derived from the other hydrogen lines. Because of low dis-

TABLE VII

RELATIVE DISPLACEMENTS OF HYDROGEN LINES

Lines	Difference	No. Obs.
$H\beta-H\gamma$	+2.1 km/sec.	27
$H\beta-H\gamma$	4.0	25
$H\gamma-H\delta$	0.6	26
$H\delta-H\epsilon$	2.0	20
$H\epsilon-H\zeta$	+3	6

TABLE VIII

DISPLACEMENTS OF THE BRIGHT $H\alpha$ LINE

Plate	$H\alpha$	Other Hydrogen Lines at Same Epoch
γ 9570	+31 km/sec.	+27 km/sec.
C 1405	−14±	0
1942	+19±	+20±
G 20	+ 8	+ 9
194	+ 4	−14

persion or overexposure, the errors of measurement of all plates except the first are rather large.

The measured displacements of the bright hydrogen lines are plotted in Figure 1, along with the intensities of both the bright and the dark portions of the lines. It is obvious that the displacement is not constant, but rises and falls at intervals of about eight hundred days. To ascertain whether or not the curve is repeated with unchanging period and amplitude, the observations have been reduced to a single cycle by assuming the period to be eight hundred days (Fig. 3). The sine curve in the diagram corresponds to the equation

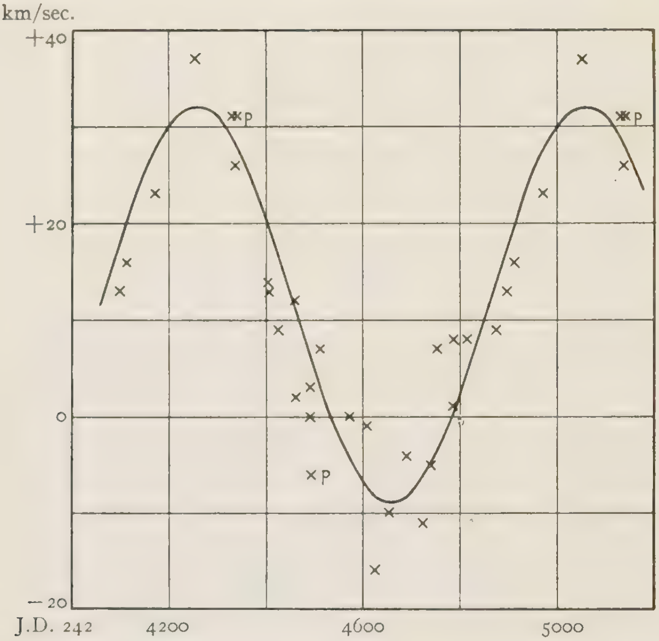

FIG. 3.—Hydrogen: velocities from emission lines, reduced to one cycle

$$V = 20.5 \sin 360° \frac{(t-4860)}{800} + 11.5 ,$$

where V is the velocity in km/sec., and t is the time in Julian days. Only two observations (not plotted) disagree badly, and these depend on poor plates (C 181, C 183) and have little weight. A well-determined normal place but two months before lies fairly near the mean curve. The Ann Arbor observations of 1915, however, taken at a time when the curve calls for minimum velocity, lie slightly above the mean velocity, and cannot well be reconciled with the others, even by changing the assumed period. This fact, together with the configuration of the Mount Wilson observations, suggests that the amplitude of the oscillations may have increased from 1915 to 1928. In Figure 4 the equation

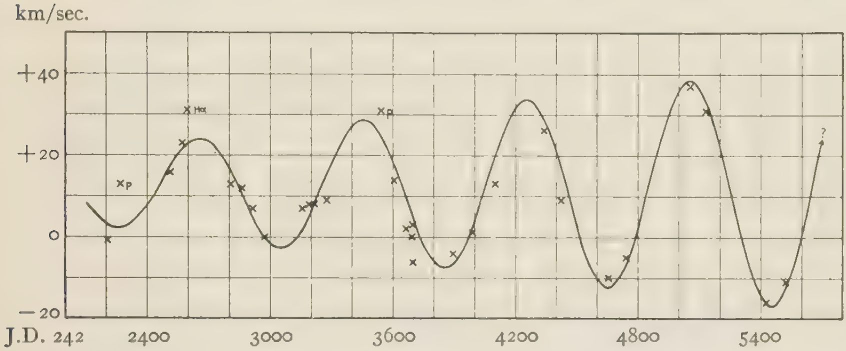

FIG. 4.—Velocities from hydrogen emission lines with the curve $V=0.006\,(t-0640)\times\sin 360°\frac{(t-1650)}{800}+12.0.$

$$V=0.006\,(t-0640)\,\sin 360°\,\frac{(t-1650)}{800}+12.0$$

is plotted together with the measured displacements. This formula represents a sinusoidal fluctuation in a period of eight hundred days, whose semi-amplitude increases 2.2 km/sec. per year. For the Ann Arbor observations, the formula gives a mean residual (O−C) of +4 km/sec.

It is of course a question to what extent the displacements of the hydrogen lines correspond to line-of-sight motions. The effect of the varying intensity of the absorption borders deserves investigation in this connection. Inspection of Figure 1 shows that in general the bright lines are displaced to the red when the dark lines are strong, but a detailed comparison of the data[1] does not establish the hypothesis that one phenomenon is the cause of the other; it leads rather to the conviction that such a hypothesis is either partly or wholly incorrect, and that the positions of the bright lines are to a considerable degree independent of the intensities of their dark borders. This conclusion is in harmony with that drawn from the relative displacements of the various Balmer lines on the same spectrograms.[1]

---

[1] E.g., a plot of the measured displacements of the bright lines against the intensity of the absorption components.

The displacements of the bright lines show a certain degree of correlation with the intensities of the bright lines themselves, the higher intensities corresponding to algebraically smaller velocities (see Fig. 1). This relationship, however, still leaves open the question of the cause of the displacements and the changes in intensity.

D. HELIUM LINES

In 1915, 1919, and on July 7, 1920, helium was represented by faint dark lines without recognizable bright portions. The first plate to show definite helium emission was C 642, taken September 3, 1920. By the following year the bright helium lines had become conspicuous and have remained so since that time, although with some fluctuations in intensity. The development of λ 4471 in emission is particularly striking because, next to the lines of hydrogen, it has become the most conspicuous line in the blue-violet portion of the spectrum, exceeding in intensity dozens of bright lines of other elements. D_3 likewise is outstanding in the yellow region. The lines of ionized helium have not been observed.

The bright helium lines are accompanied by dark borders on their violet side, forming lines of the P Cygni type. These dark borders are conspicuous for λ 4471 and several other lines, and are decidedly stronger than the dark lines prior to 1920. Within a particular series the lines of shorter wave-length have the relatively stronger absorption borders, as is the case with the hydrogen lines. One series may differ systematically, however, from another series. For example, the lines in the diffuse singlet series, particularly λλ 4388 and 4143, seem to have especially strong dark borders.

The intensities of the helium lines, estimated in the same manner as those of the hydrogen lines, are shown in Table III and Figure 5. The intensities of the bright lines have fluctuated somewhat since their remarkable rise in 1920–1921, but the dark borders have remained at nearly the same intensity.

---

[1] See p. 227.

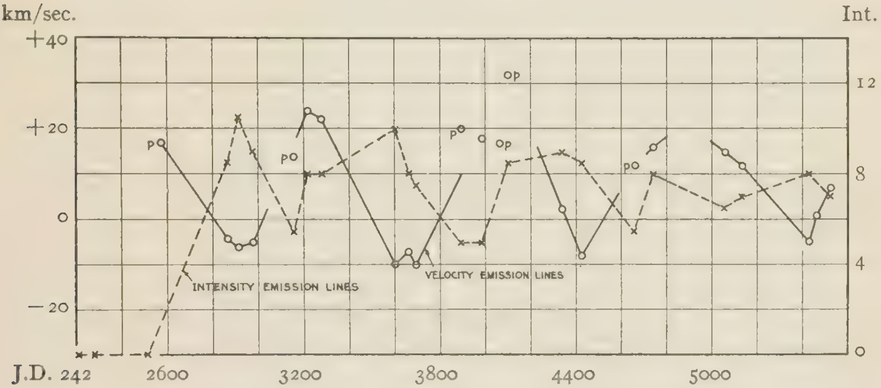

FIG. 5.—Helium emission lines: intensity and radial velocity

TABLE IX

HELIUM LINES, EMISSION *minus* ABSORPTION
(Angstrom Units)

Year	Plate	λ 3965	λ 4009	λ 4026	λ 4120	λ 4143	λ 4388	λ 4437	λ 4471	λ 4712
1920	C 642	......	......	......	......	......	......	......	1.31	......
1921	1060	......	......	0.99	......	0.96	1.46	......	1.55	1.41
	1193	1.17	......	1.19	0.91	1.16	1.20	......	1.68	......
	1399	......	......	0.95	.78	0.82	1.32	1.23	1.48	1.44
1922	1666	......	......	......	......	......	......	......	1.48	1.50
	1745	......	......	......	.92	1.14	1.53	......	1.30	1.39
	1822	......	......	......	......	0.91	1.32	......	1.45	1.50
1923	2342	......	......	1.15	.92	1.10	1.17	......	1.51	1.54
	2415	1.10	1.22	1.19	.82	1.14	......	......	1.89	......
	2470	......	......	......	......	0.97	1.22	......	1.48	1.63
	γ 12175	......	......	......	......	0.90	......	......	......	......
1924	C 2750	......	......	......	......	......	......	......	1.73	......
	2892	......	......	......	......	......	......	......	1.87	......
	3073	......	1.01	1.15	......	1.34	1.42	......	1.66	1.74
1925	3383	0.93	0.93	1.05	.96	1.10	1.11	......	1.48	......
	3541	1.17	......	1.19	......	1.33	1.38	......	1.51	1.65
1926	3811	......	......	......	......	......	......	......	1.64	......
	3935	1.19	......	1.08	......	0.92	1.32	......	1.64	1.90
1927	4321	......	......	......	......	......	1.50	......	1.60	1.53
	4418	......	......	1.17	......	1.28	1.28	......	1.56	1.87
1928	4867	......	......	1.29	0.77	1.17	1.52	1.61	1.69	1.55
	5026	......	......	......	......	......	1.62	......	1.69	......
Mean........		1.11	1.05	1.13	0.87	1.08	1.36	1.4	1.58	1.59

The measured intervals between the centers of the bright lines and the accompanying dark components are collected in Table IX, and the mean values are plotted in Figure 6. The behavior of lines in the same series (connected by straight lines in Fig. 6) resembles that of the Balmer series, as may be seen by comparing Figure 2. The variation from one line to another of the same series is approximately as the cube of the wave-length, and a mean value for the constant coefficient lies between the values for the two groups of the hydrogen series.

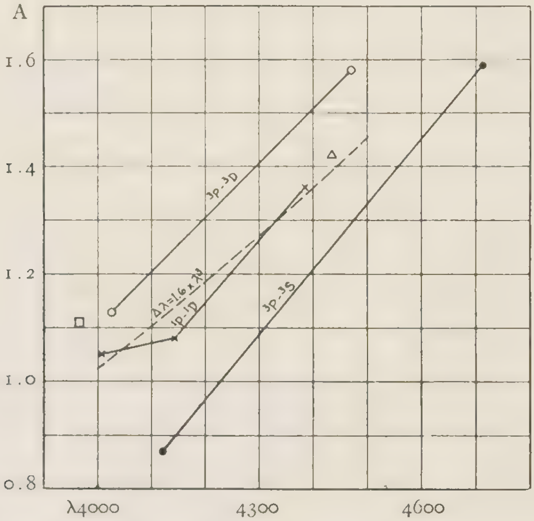

Fig. 6.—Helium: relative displacements of emission and absorption lines

The measured displacements of the bright helium lines, expressed in terms of radial velocity, are found in Table X. The lines most frequently used are λλ 3965, 4026, 4120, 4143, 4388, 4471, and 4712. All these except the first give consistent mean velocities. λ 3965, measured on ten plates, is displaced toward the violet by 0.13 A or 10 km/sec. compared with the mean of the other lines, but this may be due to error of measurement as this line is usually underexposed and on some plates is slightly out of focus. The lines with the stronger dark components do not appear to be displaced toward the red relatively to the other lines. Thus, as in the case of the hydrogen

TABLE X

VELOCITIES FROM EMISSION LINES
(Kilometers per Second)

Plate	J.D.	*He*	*Fe* II	[*Fe* II]
Ann Arbor	2420000 +0707	...	−24	−24
C 36	2205	...	−18	...
37	2205	...	−17.9	−11
40	2206	...	−18	−25
45	2207	...	−10.0	−21
46	2207	...	−13.0	−23
49	2208	...	−13.9	−19
50	2208	...	−15.7	−16
51	2208	...	(−21)	...
52	2208	...	−12	−12
Mean	2207	...	−14.8	−18.6
C 181	2270	...	−16	...
183	2271	...	(− 6)	...
Mean	2270	...	−13	...
C 529	2513	...	−24	−23
642	2571	(+17)	−24	−16
1060	2861	− 4	−25.8	−11
1193	2913	− 6	−26.3	−18
1399	2976	− 4	−18.9	−18
1400	2976	(− 3)	−10	...
1405	2977	(− 9)	−22	(−15)
Mean	2976	− 5	−17	−17
C 1666	3158	(+14)	−14.2	(−13)
1745	3217	+24	−13.9	(−15)
1822	3276	+22	−15.9	(− 5)
1942	3336	...	(−28)	...
2342	3604	−10	−28.5	− 6
2415	3663	− 7	−20	− 8
2470	3694	− 6	−24	−21
γ 12175	3696	(−19)	(−27)	(−26)
Mean	3695	−10	−25	−23
C 2750	3893	(+20)	−11.7	...
2892	3986	+18	−18.1	(−19)
G 20	4062	+17	(−10)	...
C 3073	4098	(+32)	−12.7	− 8
3383	4338	+ 2	−30	−27
3541	4425	− 8	−27.1	...
3811	4656	(+12)	−11	...
3935	4740	+16	−19.2	(+ 2)
4321	5054	+15	−12	...
4418	5133	+12	(−18)	...
4867	5426	− 5	−11.5	...
G 194	5461	+ 1	(− 4)	...
C 5026	5525	+ 7	−19.6	−16

lines, the dark border apparently has little direct influence on the position of the bright line.

The velocities from the bright lines are plotted in Figure 5. They are evidently subject to more or less regular fluctuations in a period of about eight hundred days. Figure 7 shows the velocities brought to one cycle by applying this period. The sine curve in the diagram corresponds to the equation

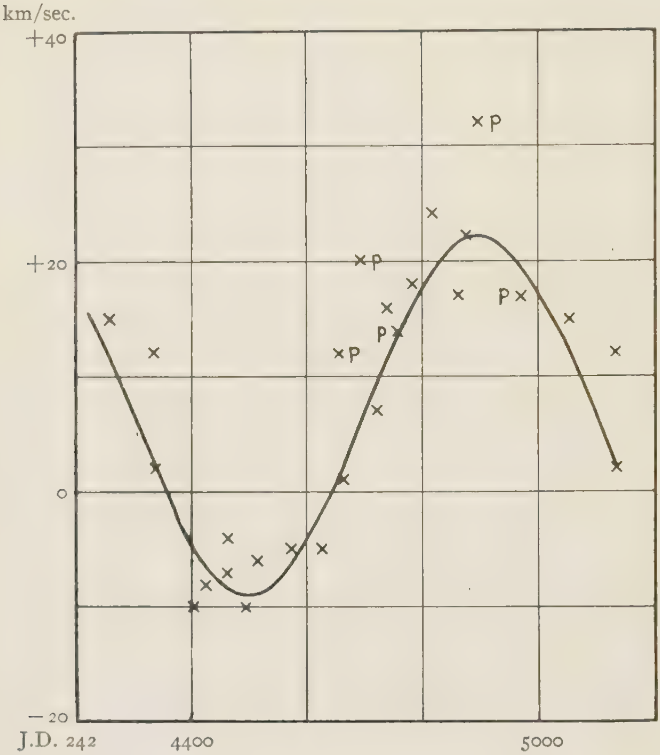

FIG. 7.—Helium: velocities from emission lines, reduced to one cycle

$$V=15.5 \sin 360° \frac{(t-4700)}{800}+6.5 \, .$$

In spite of considerable scattering, the periodicity seems to be real. A surprising feature is the phase difference of about one hundred and sixty days, or one-fifth of the period, between the curves for hydrogen and helium. As with hydrogen, high intensities tend to accompany low velocities, and vice versa.

The displacements of the dark lines are decidedly less consistent than those of the bright lines. Their mean values, however, exhibit an interesting phenomenon. The average displacement since the development of the bright lines has been about −85 km/sec. In prior years it was much less: in 1915, −11 km/sec.; in 1919, −47; in 1920, −40±. In 1919 and 1920 the conditions which later led to the appearance of strong bright lines were evidently already causing negative displacements of the dark lines.

E. IRON LINES

Iron is represented in the spectrum of B.D.+11°4673 by numerous emission lines of the ionized atom. Many of these are well known in the laboratory, while others (the "forbidden" lines) have been observed only in the spectra of certain peculiar stars. Lines of the neutral atom have not been detected. The observed lines, with their series designations, are listed in Table XI. The wave-lengths and intensities are given in the first two columns. An asterisk in the second column indicates that the line has not been observed in the laboratory, the wave-length having been obtained from the solar spectrum.[1] The third column gives the inner-quantum number transitions. The usual convention of placing the lower term first has been followed in the multiplet designations and the inner-quantum numbers. The actual atomic transitions which produce the emission lines are, of course, in the reverse direction. The atomic relationships of these lines are shown by a Grotrian diagram in Figure 1, *Mt. Wilson Contr.*, No. 354.[2]

The estimated intensities of the normal lines, *Fe* II, and the forbidden lines, [*Fe* II], are given in Table III. It is obvious from the plot of these intensities in Figure 8 that both groups of lines are variable and that they do not vary together. The relative behavior of the two types of lines may be found by taking the ratios of the estimated intensities. These agree well with the estimates of the relative intensities of λ 4359 [*Fe* II] and 4352 *Fe* II, made directly from the spectrograms (last column of Table III). These lines were

---

[1] *Mt. Wilson Contr.*, No. 318; *Astrophysical Journal*, **64**, 194, 1926.

[2] *Astrophysical Journal*, **67**, 397, 1928.

TABLE XI

IRON LINES, *Fe* II, OBSERVED

I.A.	Int.	I.Q. Nos.	Int. in Star	Remarks
		Permitted Lines		
		$b^4P'-a^4F$		
4122.67	*	3−3	2	
4178.87	8	3−4	4	
4258.16	*	2−2	1	
4296.56	3	2−3	2	
4369.41	*	1−2	0	
		$b^4P'-a^4D'$		
4128.74	*	3−2	0	1 measure
4173.48	5	3−3	3	
4233.16	10	3−4	6	
4273.31	1	2−1	0	
4303.18	4	2−2	2	
4351.77	10	2−3	3	
4385.39	5	1−1	2	
4416.81	8	1−2	2	Blend with [*Fe* II]
		$b^4F'-a^4F$		
4489.21	10	4−3	2	Blend with [*Fe* II]
4491.41	8	2−2	2	
4515.34	15	3−3	2	
4520.24	8	5−4	2	
4534.17	*	2−3	1	
4555.90	15	4−4	3	
4582.84	*	3−4	....	Too near 4583.84
4666.75	*	4−5	1	
		$b^4F'-a^4D'$		
4508.29	15	2−1	2	
4522.64	10	3−2	2	
4541.52	*	2−2	1	
4549.48	20	4−3	4	
4583.84	30	5−4	4	
4595.70	*	2−3	0	1 measure
		a^6S-a^4D'		
4601.38	*	3−2	....	Too near *N* II
4656.98	*	3−3	....	Blend with neb. line
4731.49	1	3−4	1	
		a^6S-a^6P		
4923.92	20	3−2	4	
5018.44	20	3−3	4	
5169.03	20	3−4	2	
		a^4G-a^4F		
5197.56	4	3−2	2	
5234.62	4	4−3	2	
5276.01	5	5−4	2	
5316.62	8	6−5	3	
5325.56	0	4−4	0	1 measure

TABLE XI—*Continued*

I.A.	Int.	I.Q. Nos.	Int. in Star	Remarks
Permitted Lines—*Continued*				
		a^6S-a^6F		
5284.11	*	3−4	....	Doubtful
		a^4G-a^4D'		
5316.78	*	4−3	....	Blend with $a^4G_6-a^4F_5$
5362.87	*	5−4	1	
		b^4D-a^4P		
6147.85	0	2−1	0	
6247.56	1	3−2	0	1 measure
6407.30	*	2−3	0	Doubtful
6416.92	0	3−3	0	1 measure
6456.39	3	4−3	1	
		a^6S-a^6D'		
6369.48	*	3−2	0	1 measure doubtful
6432.69	*	3−3	0	
6516.08	0	3−4	1	1 measure
Forbidden Lines				
		a^6D-a^6S		
4287.40	....	5−3	3	
4359.34	....	4−3	2	
4413.79	....	3−3	2	
4452.09	....	2−3	1	
4474.90	....	1−3	....	Not observed
		a^6D-b^4P'		
4728.09	....	3−2	0	
4889.66	....	4−3	0	
		a^6D-b^4F'		
4416.28	....	5−5	....	Blend with *Fe* II
4457.96	....	4−4	0	
4488.77	....	3−3	....	Blend with *Fe* II
		$a^4F'-b^4F'$		
4774.74	....	5−4	0	
4814.55	....	5−5	1	
		$a^4F'-a^4G$		
4177.22	....	5−5	1	Blend
4243.97	....	5−6	1	
4244.85	....	4−4	0	Blend with 4243.97
4276.87	....	4−5	1	
4319.64	....	3−4	0	Blend with *Sc* II?
4358.38	....	2−3	0	

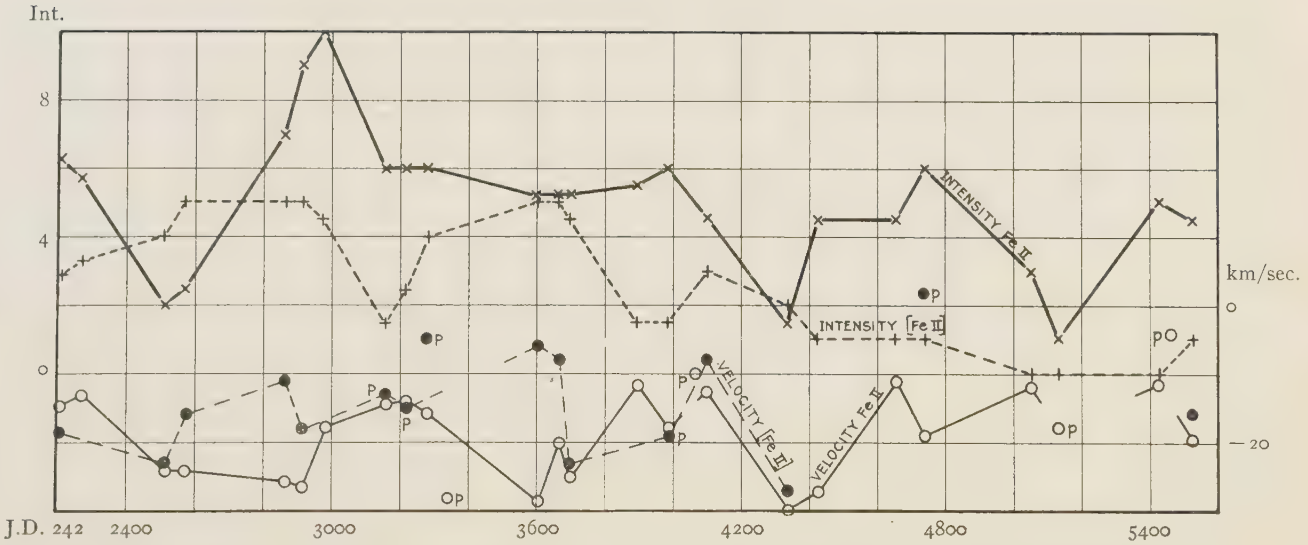

FIG. 8.—Iron emission lines: intensity and radial velocity. *Fe* II, laboratory lines; [*Fe* II], forbidden lines

chosen because they lie near together in a favorable region and have easily comparable intensities. The curve plotted in Figure 13 is the mean of the two determinations. The changes shown by the curve are decidedly greater than the errors of the estimates.

The bright iron lines are narrow, fairly well defined, and without accompanying dark companions. The forbidden lines appear, in general, somewhat hazier than the laboratory lines.

The measured displacements of the bright lines are given in Table X. The most accurate observations, depending on twelve to thirty lines in reasonable agreement, are given to the tenth of a kilometer; those less accurate, to the whole kilometer; while poor observations are inclosed in parentheses. The relative weights are about 4, 2, and 1, respectively. The results for forbidden transitions, [*Fe* II], depend in most cases on three to ten lines and are considerably less accurate than those for the normal lines. The general agreement between the displacements of the normal and the forbidden lines, however, is good. For most of the individual plates the difference, normal *minus* forbidden, does not exceed the errors of measurement, although this is doubtful in the case of C 1060, C 2342, and C 2415.

The displacements of the iron lines are plotted in Figure 8. The curve for the ordinary lines, *Fe* II, shows maxima near J.D. 3200 and 4000, and minima near 2800, 3600, and 4400, which have the appearance of reality. The eight-hundred-day period exhibited by hydrogen and helium is thus indicated by iron for several cycles, but ceases or becomes poorly marked toward the end of the interval under observation. Speaking broadly, however, the disagreement of the iron lines with those of hydrogen and helium is very striking. The mean displacement of the iron lines is algebraically less by the equivalent of nearly 30 km/sec., and the large fluctuations of hydrogen and helium are not duplicated. Further reference to these facts will be made in the discussion. The curve for the forbidden lines, [*Fe* II], is poorly determined but shows nearly the same mean value and range as that for the ordinary lines. Figure 9 shows the measurements of the iron lines reduced to one cycle with the period of eight hundred days. The sine curve corresponds to the equation

$$V=8.5 \sin 360^\circ \frac{(t-4540)}{800}-21.5 \, .$$

F. ALUMINUM LINES

The lines of neutral aluminum, particularly the low-temperature pair, λλ 3944, 3961, are well known in the spectra of the sun and the cooler stars. A few weak lines in the solar spectrum are doubtfully attributed to singly ionized aluminum, but aside from this, no lines of the ionized atoms have been recognized in astronomical spectra. It is of interest, therefore, to find lines of doubly ionized aluminum,

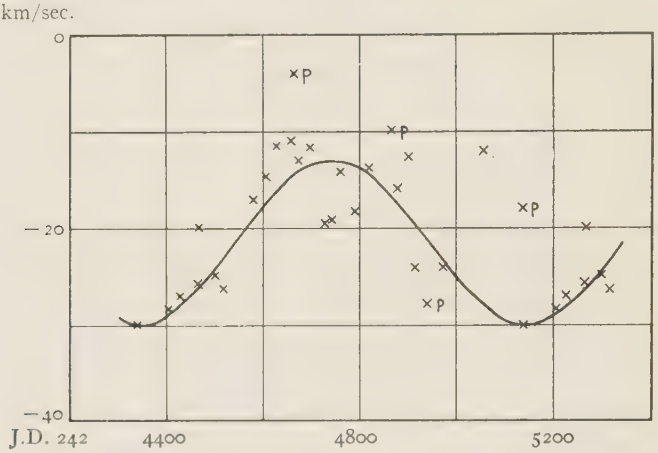

FIG. 9.—Iron: velocities from emission lines, reduced to one cycle

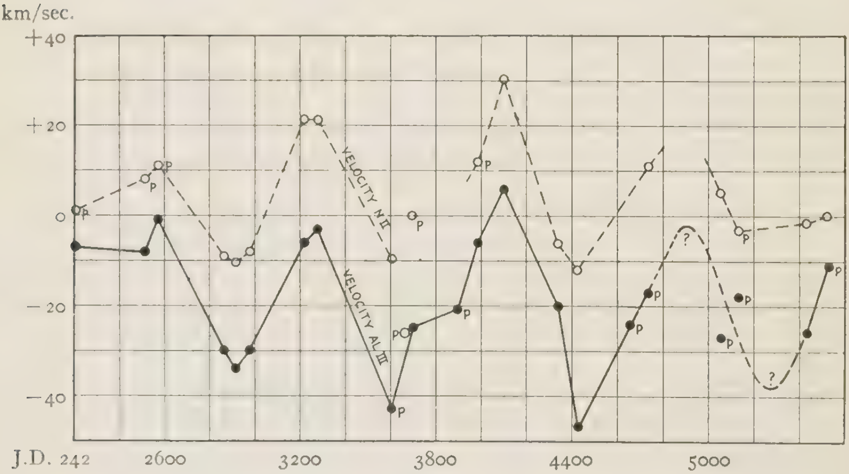

FIG. 10.—Aluminum and nitrogen: velocities from emission lines

Al III, well marked in B.D.+11°4673. Lines of the singly ionized atom, *Al* II, also are probably present.

The first three columns of Table XII give the laboratory data[1] for the stronger lines of *Al* III, while the remaining columns record the observations of the lines in the stellar spectrum, where they appear as narrow bright lines without absorption components. For the computation of the stellar wave-lengths the radial velocity of the star was assumed to be −18.0 km/sec. This value, derived from measurements of the bright iron lines, has been similarly employed for all the following tabulations of mean stellar wave-lengths.

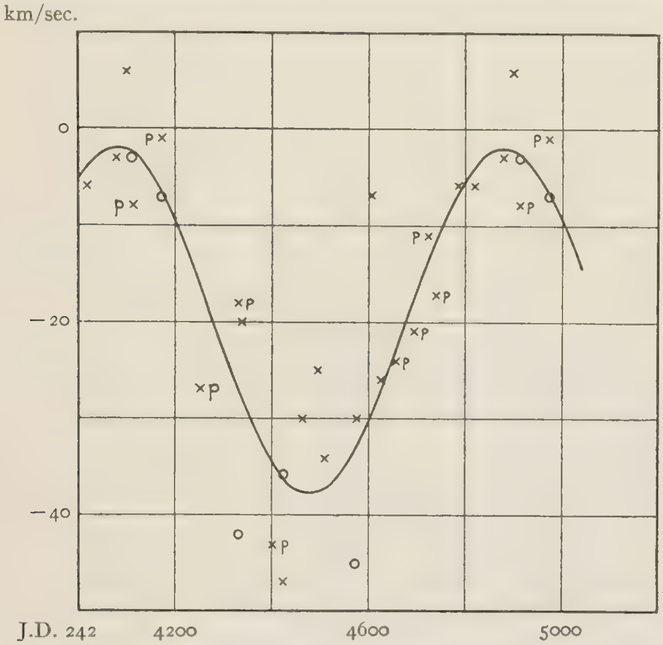

FIG. 11.—Aluminum: velocities from emission lines, reduced to one cycle

The *Al* III lines λλ 4512 and 4529 are accurately measurable and yield accordant displacements, whose mean values are found in Table XIII, and are plotted in Figure 10. The first portion of the plot shows large fluctuations in the eight-hundred-day period. They seem to cease after J.D. 2424800, but this appearance may be an effect of the distribution of the observations. When the measured velocities are reduced to one cycle by using the eight-hundred-day period, a fairly definite curve is obtained (see Fig. 11). The sine curve corresponds to the equation

---

[1] Paschen, *Annalen der Physik*, 71, 142, 1923.

$$V = 18.0 \sin 360^\circ \frac{(t-4680)}{800} - 20.0 \, .$$

The only badly discordant observation is that depending on three plates in 1919. The lines are poor on these plates, but the mean value has a probable error of about 4.5 km/sec., which is small compared to the divergence from the curve determined by the other observations.

The stronger lines of *Al* II[1] are listed in Table XII, together with the stellar lines which lie near their positions. The lines are weak

TABLE XII

LINES OF ALUMINUM

LABORATORY			B.D. +11°4673	
I.A.	Int.	Combination	I.A.	No. of Plates
		Al III		
4149.90	3	$4D_1-5F_1$	49.98	4
4149.92	2	$4D_1-5F_2$		
4150.14	1	$4D_2-5F_2$		
4479.89	3	$4F_2-5F'$	...	...
4479.97	4	$4F_1-5F'$	...	...
4512.54	4	$4P_2-4D_2$	12.45	14
4528.91	1	$4P_1-4D_2$	...	...
4529.18	6	$4P_1-4D_1$	29.18	23
4701.65	6	$4F-5D$	01.7	1
5150.86	6	$5F-7F'$	...	...
5163.90	7	$5F'-7F''$	...	...
5696.47	8	$4S-4P_1$	§	...
5722.65	6	$4S-4P_2$	§	...
		Al II		
3900.68*	10	3^1P-3^1D	00.56	2
3995–96†‡	...	4^3D-10^3F	...	...
4226–27‡	...	4^3D-9^3F	27.46	1
4585.82	6	$4^3D_3-8^3F_3$	...	...
4588–89‡	...	4^3D-8^3F	88.5 ±	3
4663.05	11	3^1D-4^1P	63.08	8
5280.21	6	$5^3P_1-8^3D$	81.6?	1
5283.77	8	$5^3P_2-8^3D$		
5285.85	6	5^1P-9^1D	...	...
5593.23	10	4^1P-5^1D	...	...
6243.35	10	$4^3P_2-4^3D_3$	...	...

* Near 3900.53 *Ti* II. † Near strong *N* II line. ‡ Close multiplet.

§ These lines are in a region of the spectrum which is poorly observed. Perhaps faintly present on grating plates.

---

[1] Sawyer and Paschen, *Annalen der Physik*, 84, 1, 1927.

in the star and the correspondence is incomplete, but the line λ 4663 seems fairly conclusive evidence of the presence of singly ionized aluminum in the star's atmosphere. A few satisfactory measures of this line are available, and these give displacements agreeing with those of *Al* III (see Table XIII and Fig. 11).

TABLE XIII

Displacements of Aluminum Lines

Plate	J.D.	*Al* III λ 4512 λ 4529	*Al* II λ 4663
	2420000	km/sec.	km/sec.
C 37, 45, 50	+2207	− 7	....
529	2513	(− 8)	− 3
642	2571	(− 1)	− 7
1060	2861	−30	....
1193	2913	−34	....
1399	2976	−30	−45
1745	3217	− 6	....
1822	3276	− 3	....
2342	3604	(−43)	....
2470	3694	−25	....
2750	3893	(−21)	....
2892	3986	− 6	....
3073	4098	+ 6	....
3383	4338	−20	−42
3541	4425	−47	−36
3811	4656	(−24)	....
3935	4740	(−17)	....
4321	5054	(−27)	....
4418	5133	(−18)	....
4867	5426	−26	....
5026	5525	(−11)	....

G. NITROGEN LINES

The ionized nitrogen lines, although not very intense in this spectrum, are of special interest because, as with iron, both ordinary and forbidden transitions are represented. The laboratory lines, including λ 3995 and the group near λ 4600, although not uncommon in absorption in class B, are of infrequent occurrence in emission in stellar spectra. The forbidden lines λλ 5755, 6548, and 6583, have, I believe, not heretofore been observed except in nebulae. It is possible, of course, that a very small peculiar nebula surrounds this star.

The correspondence between the spectrum of *N* II[1] and the stellar lines is indicated in Table XIV. An asterisk after a stellar wave-

---

[1] Fowler and Freeman, *Proceedings of the Royal Society*, 114, 662, 1927.

TABLE XIV

LINES OF NITROGEN, *N* II

LABORATORY			B.D.+11°4673	
I.A.	Int.	Combination	I.A.	Remarks
Triplet System				
3855.08	2	$2^3P_1 - 2^3P_0$	....	Weak if present
3856.07	3	$2^3P_2 - 2^3P_1$	....	Near 3856.02 *Si* II
4601.49	8	$1^3P_1' - 2^3P_2$	01.87*	
4607.17	7	$1^3P_0' - 2^3P_1$	07.97*	
4613.88	6	$1^3P_1' - 2^3P_1$	14.43*	
4621.40	7	$1^3P_1' - 2^3P_0$	21.46*	
4630.55	10	$1^3P_2' - 2^3P_2$	31.04	
4643.11	8	$1^3P_2' - 2^3P_1$	43.73*	
4779.71	4	$1^3D_1' - 1^3D_1$	80.3	1 plate
4788.13	5	$1^3D_2' - 1^3D_2$	88.04	
4803.27	6	$1^3D_3' - 1^3D_3$	03.10	
4987.38	4	$1^3S_1' - 1^3P_0'''$	....	
4994.36	6	$1^3S_1' - 1^3P_1'''$	94.2	1 plate
5007.32	7	$1^3S_1' - 1^3P_2'''$	?	
5535.39	5	$a^3P_2' - a^3D_3'$	34.9	1 plate
Singlet System				
3995.00	10	$1^1P_1' - 1^1P_1$	95.20*	
4447.04	10	$2D_2' - 1^1D_2?$	47.29	
6482.07	8	$1^1P_1' - 2^1D_2'$	83.0	1 plate
Intercombination				
3955.85	6	$1^3P_1' - 1^1P_1$	55.95	
Forbidden Lines				
(5754.8)	....	$a^1D_2 - a^1S_0$	54	A real line but measures poor
(6548.1)	....	$a^3P_1' - a^1D_2$	47.8	
(6583.6)	....	$a^3P_2' - a^1D_2$	83.4	
Unclassified Lines				
4236.98	6n	....	36.71	
4241.80	8n	....	42.03	
4426.05	0	....	26.2?	1 plate
4427.21	2	....	27.68	
4427.97	2	....		
4432.71	6n	....	32.60	
4441.99	3n	....	41.96	
4609.60	0	....	10.3	1 plate
4895.20	4	....	95.0	1 plate
6610.58	6	....	11.9	1 plate

* Both bright and dark components.

length means that both bright and dark components are present; for the remaining lines bright components only have been observed. The line λ 4631.04 probably deserves an asterisk, but the presence of the strong iron line λ 4629.33 prevents a definite observation of the dark companion to the violet of the nitrogen line. In addition to the lines listed, the stronger members of the $3D'-3F'$ multiplet are perhaps faintly present in the star.

TABLE XV

N II, Emission *minus* Absorption

(Angstrom Units)

Plate	λ 3995	λ 4601	λ 4607	λ 4643
C 642	....	....	1.44	....
1060	0.68	1.08	1.47	2.56
1193	.95	1.10	1.42	2.36
1399	....	1.38	1.46	1.89
1745	....	....	2.02	1.93
1822	....	....	1.91	2.28
2342	....	1.59	1.22	....
2415	0.83	....	....	....
2892	....	1.34	....	....
3073	1.03	2.48	1.89	2.01
3383	0.89	0.96	1.16	2.00
3935	0.94	....	1.74	....
4321	....	....	....	2.39
4867	....	2.52	2.51	2.89
5026	....	1.88	....	....
Mean	0.89	1.59	1.66	2.26

Most of the nitrogen lines are weak at best, and it is accordingly difficult to trace their variations in detail. Inspection of the plates shows, however, that, like the helium lines, they have been stronger since 1921 than before. The behavior of the strongest nitrogen line, λ 3995, clearly parallels that of the helium lines. In 1915, 1919, and probably 1920[1] it was an absorption line, while from 1921 on it has been a well-marked bright line with a dark border on the violet side.

The measured distances between the centers of the bright and dark components of four lines are found in Table XV. With the exception of λ 4643 the relative displacements of the dark components are about the same as for hydrogen and helium (see Tables IV and

---

[1] The region of this line is poorly shown on the 1920 plates, but the line does not appear bright.

IX). λ 4643 is in a somewhat confused region and may be interfered with by other lines.

Apparent radial velocities derived from nitrogen emission lines are found in Table XVI and are plotted in Figure 10. While the accuracy is not high, it is sufficient to show that the behavior resembles closely that of helium (see Fig. 14). The velocities reduced to one cycle are plotted in Figure 12. The sine curve corresponds to the equation

TABLE XVI

Radial Velocities from Emission Lines

Plate	J.D.	*N*	*Si*	*Ti*
	2420000	km/sec.	km/sec.	km/sec.
C 37	+2205	...	−28.5	−17.1
40	2206	...	−21	−28
45	2207	...	...	−16.7
46	2207	...	...	−16
49	2208	+ 1±	...	−25.0
50	2208	...	...	−17.9
529	2513	+ 8±	...	...
642	2571	+11±	...	...
1060	2861	− 9	...	−30±
1193	2913	−10.2	+17±	−31.4
1399	2976	− 8.1	+11	−18.1
1745	3217	+21.4	...	−24±
1822	3276	+21.1	...	...
2342	3604	− 9.7	+10±	− 7±±
2415	3663	−26	...	...
2470	3694	0±	...	−10±±
2892	3986	+12±	+41±	...
G 20	4062	...	− 7	...
C 3073	4098	+30.4	...	...
3383	4338	− 6.4	...	...
3541	4425	−12	...	...
3935	4740	+11	+28±	...
4321	5054	+ 5	...	...
4418	5133	− 3±	+14	...
4867	5426	− 1.4	...	−11±
G 194	5461	...	−44±±	...
C 5026	5525	0	...	...

$$V = 17.0 \sin 360° \frac{(t-4660)}{800} + 6.0 \; .$$

The apparent displacements of the dark portion of λ 3995 exhibit a decided progression of the same character as that of the dark lines of helium (see p. 235). Mean values are as follows: 1915, +4 km/sec.; 1919, −37; since 1921, −62.

H. SILICON LINES

Silicon is certainly present in the atmosphere of this star, and the behavior of its spectral lines is very interesting. Neutral atoms (probably), as well as those in the first three stages of ionization, are represented by bright or dark lines or both. As the lines are not strong and the observations of most of them are therefore scattering and somewhat unsatisfactory, a number of interesting questions, particularly concerning changes, must remain unanswered.

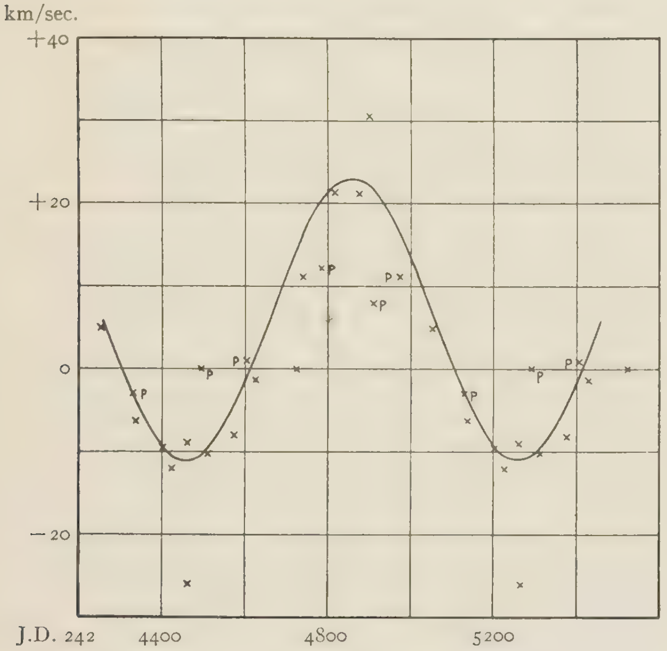

FIG. 12.—Nitrogen: velocities from emission lines, reduced to one cycle

Table XVII contains a list of the stronger silicon lines taken from Fowler's convenient tabulation,[1] with notes on their presence in the star. The evidence for the first three stages of ionization seems quite convincing; that for the neutral atom less so because it depends on one line, λ 3905. Among the lines of *Si* II, λλ 4128, 4130 are surprisingly weak. It is interesting to note that this is true also in the spectrum of another peculiar bright-line star, Z Andromedae.[1]

---

[1] *Philosophical Transactions of the Royal Society*, A, **225**, 1, 1925.

Both bright and dark components of the *Si* III lines λλ 4552, 4567 have been measured on a number of plates. The mean values of the distance between the centers of the bright and dark portions are slightly less than those for hydrogen, helium, and nitrogen (see Table XVIII).

TABLE XVII

SILICON LINES

I.A.	Int.	Spect.	Series	Star	Remarks*
3856.02....	8	II	$X_1-2^2P_1$	55.90	
3862.59....	6	II	$X_2-2^2P_2$	62.5	1 plate
3905.52....	10	I	$a^1S_0-a^1P_1$	05.58	
4088.86....	10	IV	$2^2S-2^2P_1$	....	Absorption only
4102.94....	5	I	....	....	Too near *Hδ*
4116.10....	8	IV	$2^2S-2^2P_2$	....	Absorption only
4128.05....	8	II	$2^2D_2-3^2F$	....	Very weak or absent†
4130.88....	10	II	$2^2D_1-3^2F$	....	
4552.65....	9	III	$2^3S-2^3P_1$	53.21	Absorption with weak bright fringe on red
4567.87....	7	III	$2^3S-2^3P_2$	68.37	Absorption with weak bright fringe on red
4574.78....	4	III	$2^3S-2^3P_3$	....	Absorption only? Near 4576 *Fe*
4716.66....	5	III	....	16.9	1 plate
5041.06....	8	II	$2^2P_2-3^2D_2$	....	
5056.02....	10	II	$2^2P_2-3^2D_1$	57.7	1 plate
5202.51....	3	II	....	02.7	1 plate
5669.50....	4	II	....	....	In poorly observed region
5739.62....	8	III	....	....	In poorly observed region
5957.61....	5	II	$2^2P_2-3^2S$	57.4	
5978.97....	7	II	$2^2P_1-3^2S$	79.01	
6347.09....	10	II	$2^2S-2^2P_1$	47.2	
6371.36....	8	II	$2^2S-2^2P_2$	70.3	1 plate. Blend ?

* Lines in the stellar spectrum are bright unless otherwise noted.

† On a few plates there are barely perceptible traces of emission.

A few measurements of the displacements of the bright silicon lines are collected in Table XVI. The lines are weak and the measurements scattering and inaccurate. The apparent velocities seem in the mean to be algebraically larger than those of iron and aluminum, and to correspond more nearly to those of hydrogen, helium, and nitrogen. This is doubtless connected with the presence of the dark border on the violet side of several silicon lines.

---

[1] H. H. Plaskett, *Publications of the Dominion Astrophysical Observatory*, **4**, 119, 1928.

The absorption lines are measurable on more plates than the emission lines, and are accordingly tabulated by themselves in Table XIX.

TABLE XVIII

Emission *minus* Absorption, Silicon Lines

Plate	λ 4552	λ 4567
C 1193	1.2 A	1.6 A
1399	1.1	....
2342	....	1.2
3073	....	1.8
3383	1.5	1.2
3935	1.6	....
4418	1.2	1.2
Mean	1.3	1.4

TABLE XIX

Displacements of Silicon Absorption Lines

Plate	*Si* III λλ 4552, 4567, 4574	*Si* IV λλ 4088, 4116
	km/sec.	km/sec.
C 37–50	− 19	−30
529	− 16	....
642	− 21	....
1060	− 71	....
1193	− 79	−54
1399	− 68	....
1745	− 49	....
1822	− 62	....
2342	− 74	−39
2415	....	−40
2470	− 73	....
2750	− 68	....
2892	− 44	....
3073	− 34	− 9
3383	− 78	−30
3541	− 77	−52
3811	− 83	....
3935	− 77	−33
4321	− 59	....
4418	− 64	....
4867	− 77	−58
5026	−108	....

I. OTHER ELEMENTS

Titanium.—A few emission lines of ionized titanium (*Ti* II) are faintly visible on a number of plates. These are indicated in Table

XX. Concerning changes in intensity, about all that can be said is that these lines were probably stronger in 1919 than in later years.

Displacements measured on a few plates are recorded in Table XVI. The mean displacement is nearly the same as for iron, the behavior thus differing from that of η Carinae, whose titanium lines are displaced about half an angstrom toward the violet with respect to those of iron.

TABLE XX

Lines of Ionized Titanium, *Ti* II

Laboratory			B.D.+11°4673	
I.A.	Int. Spark	Classification*	I.A.	Remarks
3900.53	70	$a^{2}G_{5}-a^{2}G'_{5}$	00.56	Blend with *Al* II?
4290.23	50	$a^{4}P'_{2}-a^{4}D'_{3}$	90.09	
4294.10	40	$a^{2}D_{3}-a^{2}D'_{3}$	94.01	
4300.05	60	$a^{4}P'_{3}-a^{4}D'_{4}$	00.08	
4301.93	15	$a^{4}P'_{1}-a^{4}D'_{2}$	01.78	
4307.89	40	$a^{4}P'_{2}-a^{4}D'_{2}$	07.87	
4312.88	35	$a^{4}P'_{3}-a^{4}D'_{3}$	12.79	
4314.98	40	$a^{4}P'_{1}-a^{4}D'_{1}$	14.36	Blend with *Sc* II?
4337.92	50	$a^{2}D_{2}-a^{2}D'_{2}$	....	Too near $H\gamma$
4367.67	15	$b^{2}F'_{4}-b^{2}G'_{5}$	67.93	
4395.04	60	$a^{2}D_{3}-a^{2}F_{4}$	96.00	Blend?
4399.77	35	$a^{2}P'_{2}-a^{4}D'_{3}$	99.77	
4443.80	50	$a^{2}D_{2}-a^{2}F_{3}$	43.4?	
4468.49	50	$a^{2}G_{5}-a^{2}F_{4}$	....	Too near *He* 4471
4501.27	40	$a^{2}G_{4}-a^{2}F_{3}$	01.2	1 plate
4533.97	30	$a^{2}P'_{2}-a^{2}D'_{3}$	34.08	Blend with *Fe* II
4549.64	60n	$a^{2}H'_{6}-a^{2}G'_{5}$	49.62	Blend with *Fe* II
4571.98	50n	$a^{2}H'_{5}-a^{2}G'_{4}$	71.8	1 plate

* Russell, *Mt. Wilson Contr.*, No. 344; *Astrophysical Journal*, **66**, 283, 1927.

TABLE XXI

Lines of Ionized Chromium, *Cr* II

I.A.	Int. Spark	B.D.+11°4673
4555.09	10	Near strong *Fe* II line
4558.66	20	58.67
4588.21	20	88.5
4618.82	10	18.4
4634.09	10	34.7 1 plate; blend?

Chromium.—Ionized chromium is barely recognizable by means of the strongest lines in the $b^{4}F'-a^{4}D'$ multiplet. The laboratory and stellar measurements are given in Table XXI.

Magnesium.—The ionized magnesium line λ 4481 was measured as a narrow and very weak bright line on five plates. It is probably variable.

Carbon.—A faint emission line measured on two plates at λ 4267.0 may be the *C* II line near this wave-length.

Scandium.—Weak emission lines measured at λ 4246.84 and λ 4214.36 are probably due to ionized scandium, although the second one may be blended with *Ti* II 4314.98. Several other strong *Sc* II lines are doubtfully present in the stellar spectrum.

Nebular lines.—The chief nebular lines have not been observed, but the red pair λλ 6548 and 6583 and the fainter line λ 5755, ascribed by Bowen[1] to *N* II, are present. This accords with the fact that numerous laboratory lines of nitrogen have been measured in the stellar spectrum, while no lines of oxygen have certainly been identified. The line measured on ten plates at λ 4658.06 probably corresponds to the line whose wave-length in RY Scuti[2] was found to be λ 4658.08. Two plates, C 1193 and C 1399, on which lines of *Fe* II are especially strong, give λ 4657.30. This is probably a blend with λ 4656.98 *Fe* II.

Detached lines.—Faint absorption lines are visible on a few plates in the positions of *Ca* II, λ 3933 (K) and *Na* I, λλ 5890, 5896 (D_2, D_1). Approximate velocities yielded by these lines are: K (2 plates), −17 km/sec.; D_2, D_1 (2 plates), −27 km/sec. The correction for solar motion is +11.4 km/sec.

Complete list of lines.—Practically all the lines measured in the stellar spectrum, with their intensities and probable identifications, are collected in Table XXII. For the computation of the wave-lengths a radial velocity of −18.0 km/sec., derived from the bright iron lines, has been assumed. Certain lines, such as those of hydrogen and helium, to which the application of this velocity would clearly be inappropriate, are inclosed in parentheses. Special discussions of the positions of these lines may be found in the preceding pages. The intensities are visual estimates with the measuring microscope and make no pretense to high accuracy. Nearly all the lines vary in intensity, but it was not considered feasible to indicate

---

[1] *Astrophysical Journal*, **67**, 1, 1928.

[2] *Mt. Wilson Contr.*, No. 349; *Astrophysical Journal*, **67**, 179, 1928.

TABLE XXII

Complete List of Lines

I.A.	Int.	Identification	Excitation Potential
(3835)*	2	35.90 *Hη*	13.4
3855.90	1	56.02 *Si* II	10.1
3862.5	1	62.59 *Si* II	10.1
(3889)*	3	89.05 *Hζ*	13.3
3900.56	1	00.53 *Ti* II, 00.68 *Al* II	4.3
3905.58	1	05.52 *Si* I	5.1
(3933)**	1	33.66 *Ca* II	0.0 lower term
3938.29	1	...	...
3955.95	0	55.85 *N* II	21.5
(3964)*	2	64.73 *He* I	23.6
(3970)*	5	70.08 *Hε*	13.3
3995.20*	2	95.00 *N* II	21.5
(4009)*	1	09.27 *He* I	24.2
(4026)*	4	26.19 *He* I	24.0
4067.07	0	...	...
(4088)**	2	88.86 *Si* IV	24.0 lower term
(4101)*	10	01.74 *Hδ*	13.2
(4116)**	2	16.10 *Si* IV	24.0 lower term
(4120)*	2	20.81 *He* I	23.9
4122.64	2	22.67 *Fe* II	5.6
(4143)*	2	43.77 *He* I	24.1
4149.98	0	Trip. *Al* III	23.5
4173.46	3	73.48 *Fe* II	5.5
4177.59	1	77.22 [*Fe* II], —?	3.2
4178.87	4	78.87 *Fe* II	5.5
4202.1	0	...	...
4233.17	6	33.16 *Fe* II	5.5
4236.71	0	36.98 *N* II	?
4238.6	0	...	...
4242.0	0	41.80 *N* II	?
4244.11	1	43.97 [*Fe* II], 44.85 [*Fe* II]	3.1, 3.2
4246.84	0	46.83 *Sc* II	3.2
4254.1	0	...	...
4258.18	1	58.16 *Fe* II	5.6
4267.0	0	67.27 *C* II, 67.02 *C* II	20.9
4273.21	0	73.31 *Fe* II	5.6
4277.00	1	76.87 [*Fe* II]	3.2
4277.9	0	...	...
4282.1	0	...	...
4287.44	3	87.40 [*Fe* II]	2.9
4290.09	0	90.23 *Ti* II	4.0
4294.01	0	94.10 *Ti* II	4.0
4296.57	2	96.56 *Fe* II	5.6
4300.08	0	00.05 *Ti* II	4.0
4301.78	0	01.93 *Ti* II	4.0
4303.18	2	03.18 *Fe* II	5.6
4307.87	0	07.89 *Ti* II	4.0
4312.8	0	12.88 *Ti* II	4.0
4314.36	0	14.09 *Sc* II, 14.98 *Ti* II	3.5, 4.0
4317.52	0	...	...
4319.89	0	19.64 [*Fe* II], 20.73 *Sc* II?	3.2, 3.5
(4340)*	18	40.47 *Hγ*	13.0
4345**	0	...	...

TABLE XXII—*Continued*

I.A.	Int.	Identification	Excitation Potential
4349.96	0	...	...
4351.84	3	51.77 *Fe* II	5.5
4352.7	0	52.80 [*Fe* II]	3.2
4358.3	0	58.38 [*Fe* II]	3.2
4359.35	2	59.34 [*Fe* II]	2.9
4367.93	1	67.67 *Ti* II, —?	5.4
4369.22	0	69.41 *Fe* II, —?	5.6
4372.1	0	72.46 [*Fe* II]?	3.2
4374.7	0	74.46 *Sc* II?	3.4
4384.6	1	...	...
4385.26	2	85.39 *Fe* II	5.6
(4387)*	2	87.93 *He* I	24.0
4396.0	0	...	...
4399.77	0	99.78 *Ti* II	3.0
4413.73	2	13.79 [*Fe* II]	2.9
4416.68	2	16.81 *Fe* II, 16.28 [*Fe* II]	5.6, 2.8
4419.80*	0	...	...
4426.2	0	26.05 *N* II?	?
4427.68	0	27.21 *N* II, 27.97 *N* II	? ?
4430.94*	0	...	...
4432.60	1	32.71 *N* II	?
(4437)*	0	37.55 *He* I	23.9
4438.7	0	...	...
4441.96	0	41.99 *N* II	?
4443.4	0	43.80 *Ti* II ?	3.9
4447.29	1	47.04 *N* II	23.1
4452.08	1	52.09 [*Fe* II]	2.9
4458.09	0	57.96 [*Fe* II]	2.7
4461.5	0	...	...
4464.4	0	64.46 *Ti* II ?	3.9
(4471)*	9	71.48 *He* I	23.6
4481.40	0	81.33 *Mg* II	11.6
4489.09	2	89.21 *Fe* II, 88.77 [*Fe* II]	5.6, 2.8
4491.40	2	91.41 *Fe* II	5.6
4501.2	0	01.27 *Ti* II	3.8
4508.37	2	08.29 *Fe* II	5.6
4512.45	1	12.54 *Al* III	20.6
4515.41	2	15.34 *Fe* II	5.6
4520.26	2	20.24 *Fe* II	5.5
4522.68	2	22.64 *Fe* II	5.6
4529.18	2	29.18 *Al* III, 28.91 *Al* III	20.6
4532.5	1	...	...
4534.08	1	34.17 *Fe* II, 33.97 *Ti* II	5.6
4538.5	0	...	...
4541.58	1	41.52 *Fe* II	5.6
4549.62	4	49.48 *Fe* II, 49.64 *Ti* II	5.5
4553.21*	0	52.65 *Si* III	22.2
4555.85	3	55.90 *Fe* II	5.5
4558.67	0	58.66 *Cr* II	6.8
4568.37*	0	67.87 *Si* III	22.2
4571.8	0	71.98 *Ti* II	5.8
(4574)**	1	74.78 *Si* III	19.5 lower term
4576 24	2	76.31 *Fe* II	5.5
4583.73	4	83.84 *Fe* II	5.5

TABLE XXII—*Continued*

I.A.	Int.	Identification	Excitation Potential
4595.8.	0	95.70 *Fe* II	5.5
4601.87*.	1	01.49 *N* II	21.0
4607.97*.	0	07.17 *N* II	21.0
4610.3.	0	09.60 *N* II	?
4614.43*.	0	13.88 *N* II	21.0
4618.4.	0	18.84 *Cr* II?	6.7
4621.46*.	0	21.40 *N* II	21.0
4629.27.	4	29.33 *Fe* II	5.5
4631.04.	1	30.55 *N* II	21.0
4643.73*.	1	43.11 *N* II	21.0
4649.3*.	0	. . . .	. . . .
4651.1.	0	. . . .	. . . .
4658.06.	1	58.08 *Neb.* (56.98 *Fe* II)	—, 5.5
4663.08.	1	63.05 *Al* II	13.1
4666.70.	1	66.75 *Fe* II	5.5
4670.0.	0	. . . .	. . . .
(4713)*.	4	13.14 *He* I	23.5
4728.3.	0	28.09 [*Fe* II]	2.7
4731.46.	1	31.49 *Fe* II	5.5
4735.0.	0	. . . .	. . . .
4774.6.	0	74.74 [*Fe* II]	2.8
4788.04.	0	88.13 *N* II	23.2
4803.10.	1	03.27 *N* II	23.2
4814.49.	1	14.55 [*Fe* II]	2.8
(4861)*.	30	61.33 *H*β	12.7
4889.2.	0	89.66 [*Fe* II] ?	2.6
4895.0.	0	95.20 *N* II	?
(4921)*.	4	21.93 *He* I	23.6
4923.98.	4	23.92 *Fe* II	5.4
4994.2.	0	94.36 *N* II	23.4
5000.8.	0	01.13 *N* II, 01.47 *N* II	23.0, 23.0
5005.6.	0	05.14 *N* II, 07.31 *N* II	23.0, 23.4
(5015)*.	4	15.68 *He* I	23.0
5018.46.	4	18.44 *Fe* II	5.3
5055.7.	1	56.02 *Si* II	12.4
5158.1.	0	58.05 [*Fe* II]?	2.7
5169.3.	2	69.03 *Fe* II	5.3
5197.6.	2	97.56 *Fe* II	5.6
5202.7.	0	02.51 *Si* II	?
5234.5.	2	34.62 *Fe* II	5.6
5276.0.	2	76.01 *Fe* II	5.5
5316.8.	3	16.62 *Fe* II	5.5
5325.3.	0	25.56 *Fe* II	5.5
5363.0.	1	62.87 *Fe* II	5.5
5534.9.	1	34.84 *Fe* II ?	?
5754.	0	[*N* II]	4.0
(5875).	8	75.62 *He* I	23.0
(5890)**.	1	89.96 *Na* I	0.0 lower term
(5896)**.	1	95.93 *Na* I	0.0 lower term
5957.4.	1	57.61 *Si* II	12.1
5979.0.	2	78.97 *Si* II	12.1
6147.6.	0	47.85 *Fe* II	5.9
6247.3.	0	47.56 *Fe* II	5.9
6318.0.	2	. . . .	. . . .

TABLE XXII—*Continued*

I.A.	Int.	Identification	Excitation Potential
6347.2	2	47.09 *Si* II	10.1
6370.3	1	71.36 *Si* II, —	10.1
6384.2	1	83.82 *Fe* II ?	?
6407.3	0	07.32 *Fe* II	5.8
6417.4	0	16.92 *Fe* II ?	5.8
6432.8	0	32.69 *Fe* II	4.8
6442.8	1	....	....
6456.7	1	56.39 *Fe* II	5.8
6492.8	0	....	....
6516.3	1	16.08 *Fe* II	4.8
6547.8	3	[*N* II]	1.9
(6562)	100	62.79 *Hα*	12.0
6583.4	4	[*N* II]	1.9
(6678)	4	78.15 *He* I	23.0

Most of the lines are in emission; those which have an absorption component on the violet side are marked with an asterisk. The wave-lengths and intensities for compound lines refer to the bright portions. Absorption lines are marked with a double asterisk.

in this table either the mean values or the variations. Instead, two plates, C 1193 and C 1399, taken when the iron lines were especially strong, were chosen as a basis for the recorded intensities. The excitation potential in the last column is that corresponding to the upper of the two terms involved in the production of the line. It represents the energy required to change the atom or ion from its lowest state to one in which it can emit the line under consideration. For absorption lines the excitation potential is that of the lower term.

IV. DISCUSSION

Detailed data concerning numerous spectral lines having been recorded in the preceding pages, it now becomes of interest to compare the behavior of lines of the various chemical elements.

Table XXIII shows the various ionization potentials of several elements in the stellar atmosphere. The columns headed I, II, III, and IV give the energy required to detach from the atom the first, second, third, and fourth electrons, respectively. The stages of ionization whose lines have been observed in the spectrum of B.D.+11°4673 are marked either by X for emission lines, or X* for emission lines with absorption borders, or X** for absorption lines.

That the maximum excitation exceeds 33.4 volts (the ionization potential of *Si* III) is shown by the presence of lines of *Si* IV; and that it exceeds it but slightly is suggested by the fact that these lines are in absorption and of moderate intensity. The absence of λ 4686 of *He* II indicates that the excitation required for its production, about 50 volts, is not available.

From Tables XXII and XXIII we note that elements appearing in emission only are *Mg* I, *Al* II, *Al* III, *Si* I, *Si* II, *Ti* II, *Cr* II, *Fe* II (including forbidden lines); those whose lines have both bright and dark components are *H*, *He* I, *N* II, *Si* III, while *Si* IV has only dark lines. Dark lines of *Na* I and *Ca* II were observed, but they originate presumably outside the star's atmosphere. The behavior of silicon indicates that it is very abundant.

TABLE XXIII

IONIZATION POTENTIALS
(Volts)

	I	II	III	IV
H	X* 13.5	....	....	....
He	X* 24.1	....	....	....
N	— 14.5	X* 29.5	....	....
Mg	— 7.6	X 14.0	....	....
Al	— 6.0	X 18.2	X 28.3	....
Si	X 8.2	X 16.2	X* 33.4	X** 45.0
Ti	— 6.8	X 13.6	....	....
Cr	— 6.7	X 16.6	....	....
Fe	— 7.8	X 16.5	....	....

The most remarkable event in the recent spectroscopic history of this star was the outburst of helium emission in 1921. This was accompanied by a notable increase in the intensities of the bright lines of *H*, *Fe* II, *N* II, and *Al* III. Lines of [*Fe* II] and *Si* III did not take part in this increase, while the behavior of numerous weak lines is uncertain. Curiously enough the enhancement of the iron lines was preceded by a decrease in intensity from 1919 to 1920 (see Fig. 13). The behavior from 1915 to 1919 is unknown.

Since 1922 the curves for hydrogen and helium have little in common. Hydrogen and iron (laboratory lines), however, exhibit a general similarity throughout the whole observed interval. These circumstances remind one of the fact that in normal Be stars, bright iron lines are of much more frequent occurrence than those of helium.[1] The conditions required for the appearance of bright iron lines in stellar spectra seem intermediate between those for hydrogen and those for helium.

The forbidden iron lines behave quite differently from those due to the permitted transitions, as shown clearly by Figure 13. The curves for helium and forbidden iron have certain similar features but disagree radically at times.

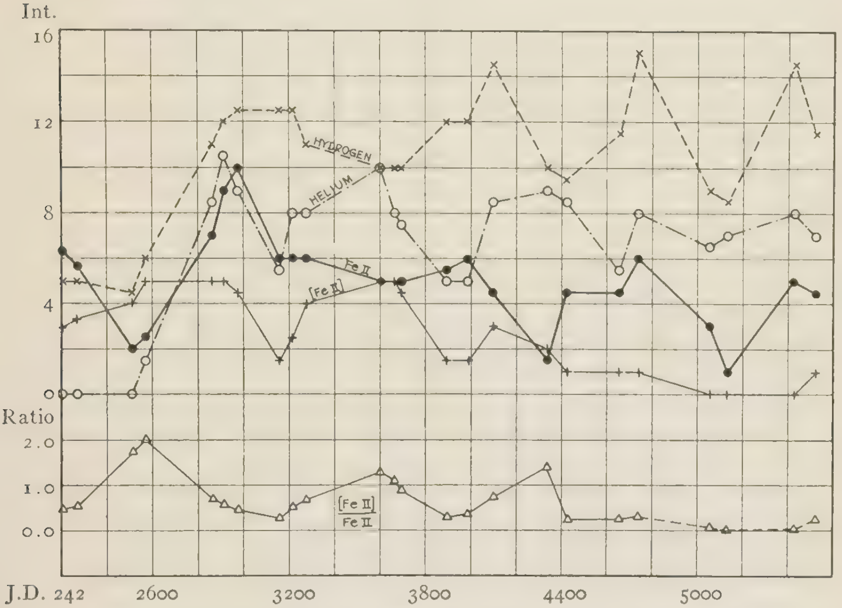

FIG. 13.—Intensities of emission lines. The lower curve shows the relative intensity of the forbidden iron lines, [*Fe* II], and the laboratory lines, *Fe* II.

The relative displacements of the bright and dark components of compound lines of four elements are compared in Table XXIV. The first value for nitrogen is for the line λ 3995, the second (4604) is the mean for the lines λλ 4601, 4607; that for silicon (4560) is the mean for the lines λλ 4552, 4567. To compare with these, the hypothetical displacements of hydrogen and helium at 4580 were taken from the curves passing through the observed lines of these elements (see Figs. 2 and 6). This procedure is necessary because of the rapid variation of displacement with wave-length—approximately as the cube. As noted on an earlier page, the values for hydrogen fall into two groups. The displacements for the four elements are not greatly different in spite of the fact that the hydrogen and helium lines are much stronger than those of nitrogen and silicon. Whatever the cause of the phenomenon, it evidently has about the same effect on the atoms of at least four elements.

---

[1] *Mt. Wilson Contr.*, No. 334; *Astrophysical Journal*, **65**, 286, 1927.

TABLE XXIV

EMISSION *minus* ABSORPTION

H	(4580)	1.2 A 1.8
He I	(4580)	1.6
N II	λ3995	0.89
	(4604)	1.63
Si III	(4560)	1.36

Measurements of the dark helium lines show that their effective centers moved toward the violet with the development of the bright components. Even in 1919–1920, before the appearance of definite bright lines, the dark lines were somewhat displaced, as indicated in Table XXV. Similar behavior was exhibited by the *N* II line λ 3995, and by the *Si* III lines λλ 4552, 4567, 4574, although the change in the silicon lines apparently took place somewhat later.

TABLE XXV

DISPLACEMENTS OF ABSORPTION LINES

	1915	1919–1920	1921–1928
	km/sec.	km/sec.	km/sec.
He	−11	−45	−85
N II 3995	+ 4	−37	−62
Si III 4552, 4567, 4574	−13	−19	−69

To facilitate comparison the measured displacements of the bright lines of several elements are plotted in Figure 14. All these curves have been given separately on previous pages. The interpretation of the displacements is a difficult problem. They may not be caused wholly by radial motions, but other plausible explanations are lacking.

Preceding discussions of individual elements have brought out the fact that the oscillations are fairly well represented by sine curves having a common period of eight hundred days but different amplitudes and phases. Table XXVI brings together the con-

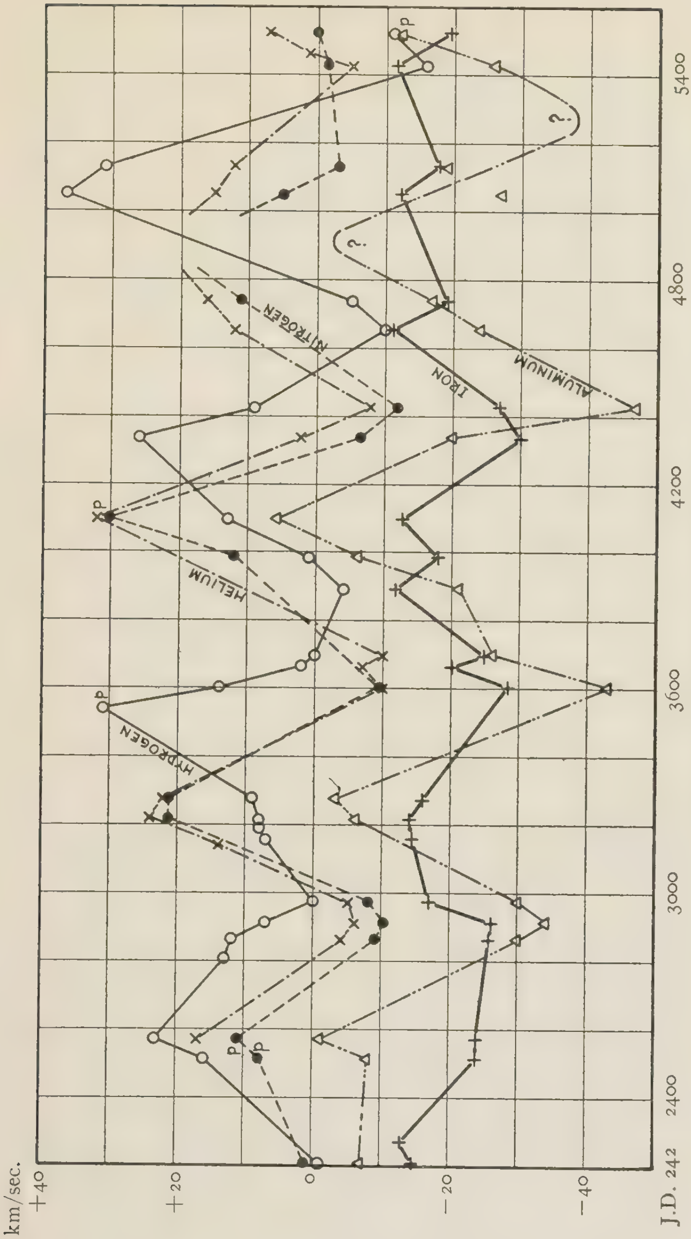

FIG. 14.—Velocities from emission lines

stants of such curves for seven elements. The third column gives the semi-amplitude of the oscillation; the fourth and fifth columns, the velocity and the Julian day when the phase angle is zero; while the last column indicates whether or not the lines are accompanied by a dark border on the violet edge.

In terms of a spectroscopic binary orbit the meaning of the various columns is as follows: "Amp.," the orbital velocity (assuming the orbital plane to contain the line of sight); V_0, the velocity of the center of mass; "Phase," the time when the source of light is in that part of its orbit nearest the earth. On the hypothesis of volume pulsation, "Amp." is the maximum integrated velocity outward or inward; V_0, the velocity of the star as a whole; "Phase," the time when the star is the largest.

TABLE XXVI

Data from Bright Lines

Element	At. Wt.	Amp.	V_0	Phase J.D.	Dark Comps.
		km/sec.	km/sec.	2420000	
H............	1.0	20.5*	+11.5	+4860	Yes
He I..........	4.0	15.5	+ 6.5	4700	Yes
N II..........	14.0	17.0	+ 6.0	4660	Yes
Al III.........	27.0	18.0	−20.0	4680	No
Ti II..........	48.1	7??	−20	....	No
Fe II..........	55.8	8.5	−21.5	4540	No
[*Fe* II].........	55.8	7	−16	....	No

* Increasing?

It is astonishing to find large differences between the data for various elements. Those for helium and nitrogen agree within errors of determination; the data for titanium and forbidden iron lines are uncertain, but resemble those for permitted iron lines. This leaves four groups which apparently cannot be reconciled: namely, (1) *H;* (2) *He* I and *N* II; (3) *Al* III; (4) *Ti* II, *Fe* II, and [*Fe* II]. The first four elements in order of atomic weight have amplitudes of about 18 km/sec., while the remaining three elements have amplitudes of about 8 km/sec. Hydrogen has phase J.D. 4860; three elements with atomic weights 4.0-27.0, phase about 4680; while iron with atomic weight 55.8 has phase 4540. Compared with iron, the lag of the three elements is 140 days (0.18 period), that of hydrogen 320 days (0.40 period). The V_0's fall into two groups, being about +8 km/sec. for elements whose lines have dark companions, and −20 km/

sec. for elements whose lines are wholly bright. It seems probable that the latter value more nearly represents the actual motion of the star. That the relative displacement toward the red of those bright lines which have absorption borders is a true stellar effect and not merely one introduced at the photographic plate by the lack of symmetry is indicated by several facts previously mentioned. Moreover, the displacement of the bright lines seems more or less independent of the intensity of the dark border. Apparently, displacements are found in those series of bright lines which are subject to dark borders even when those borders are weak or absent.

Instances of anomalous displacements are known in the spectra of other peculiar bright-line stars, including η Carinae and Z Andromedae. In η Carinae, measurements showed the titanium lines to be displaced about half an angstrom toward the violet with respect to those of iron and chromium.[1] In addition, a general displacement of about 0.2 A seems to have taken place between the years 1912 and 1913.[2] In Z Andromedae the difference in apparent velocity between high- and low-excitation lines seems to have changed from +18 to −7 km/sec.[3]

The immediate outcome of this investigation is an example of what a stellar atmosphere can do. A complete interpretation of the observations in terms of physical conditions in the star will not be made at once—at least by the writer. The general hypothesis which comes to mind is that of a star with an extensive, tenuous atmosphere in which the chemical elements are well sorted by light pressure and gravitation. Neither the double-star hypothesis nor that of a strict volume pulsation explains the facts, although both may be involved in some measure. For example, a dark companion with a period of eight hundred days may cause complex tidal phenomena in an atmosphere which is on the verge of instability. Or there may be a special, temporary type of pulsation with pronounced effects in an unusually extensive chromosphere.

Carnegie Institution of Washington
Mount Wilson Observatory
March 1929

---

[1] *Mt. Wilson Contr.*, No. 354; *Astrophysical Journal*, **67**, 391, 1928.

[2] *Lick Observatory Bulletins*, **8**, 55 and 134, 1916.

[3] H. H. Plaskett, *Publications of the Dominion Astrophysical Observatory*, 4, 133, 1928.

Contributions from the Mount Wilson Observatory, No. 382
Reprinted from the *Astrophysical Journal*, Vol. LXIX, pp. 379–385, 1929
Printed in the U.S.A.

SPECTROSCOPIC OBSERVATIONS OF R VIRGINIS

By PAUL W. MERRILL and ALFRED H. JOY

ABSTRACT

A *mean light-curve* for the interval 1920–1928 is shown in Fig. 1. The spectral type is M4e at maximum and M8 near minimum. The spectroscopic absolute magnitude at maximum is −0.6. The curve of *velocities* derived from the *absorption lines* resembles the light-curve, but that from the *emission lines* is entirely different (see Fig. 1). The bright hydrogen lines have their greatest intensity near maximum light, and their displacements behave in the same general manner as in *o* Ceti, but there are interesting differences between the two stars. The low-temperature lines of iron, magnesium, and other elements, observed in emission in *o* Ceti, are weak or absent in R Virginis.

This variable star[1] has the large range of magnitude and the Me spectrum regularly associated with variables of long period. The variability was discovered by Harding in 1809. The following data are taken from the recent "Harvard Catalogue of Long-Period Variable Stars," by Townley, Cannon, and Campbell:[2] maximum magnitude, 6.9; minimum magnitude, 11.4; period, 145.4 days; interval from minimum to maximum, 77 days; spectrum, M3e to M6e. The period is unusually short for variables having spectra of type Me. The mean period for 390 variables with this type of spectrum is 298 days,[3] while less than 5 per cent have periods shorter than that of R Virginis.

A mean light-curve (Fig. 1) for the interval covered by the Mount Wilson spectroscopic observations, 1920–1928 (J.D. 2422400–2425450), has been constructed from data supplied through the kindness of Dr. Shapley and Mr. Campbell, of the Harvard College Observatory. The curve is nearly symmetrical about maximum. Minimum is slightly narrower than maximum. The magnitudes at maximum and minimum agree closely with those found previously.

Previous spectroscopic observations, while not extensive, have revealed the outstanding phenomena. The Harvard objective-prism photographs showed a spectrum of class M with bands of varying intensity.[1] Bright hydrogen lines were visible on nearly all the plates. A short series of radial-velocity observations at Ann Arbor[2] in 1915 and another at Mount Wilson[3] in 1922 showed the apparent velocity of approach, measured from the bright lines, to be rapidly increasing at the time of maximum light. The same general phenomenon has been observed for several other long-period variables[4] and seems to be characteristic. In R Virginis the effect appeared to be especially marked, and for this reason among others a more complete series of observations was undertaken.

---

[1] H.D. 109914, 1900, R.A. $12^{h}33^{m}.4$; Dec. +7°32′; variable, class II.

[2] *Harvard Annals*, **79**, 157, 1928.

[3] *Harvard College Observatory Bulletin*, No. 862, 1928.

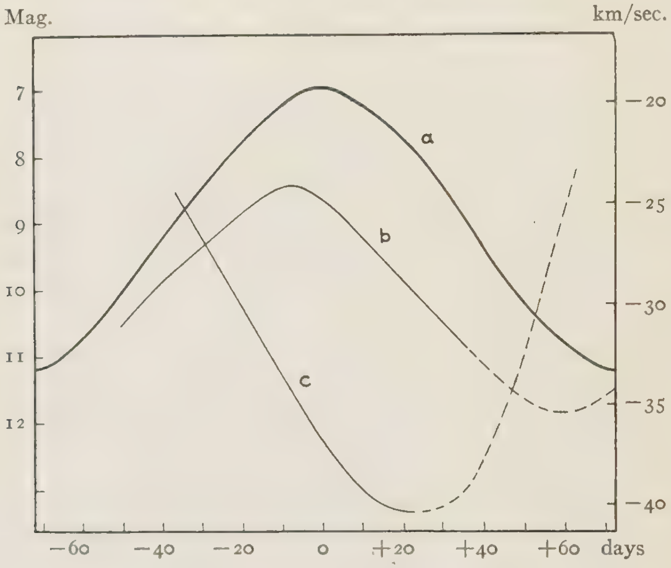

Fig. 1.—(*a*) Mean light-curve
(*b*) Velocity from dark lines (see Fig. 2)
(*c*) Velocity from bright lines (see Fig. 3)

---

[1] *Harvard Annals*, **79**, 199, 1928.

[2] *Publications of the Astronomical Observatory, University of Michigan*, **2**, 54, 1916.

[3] *Mt. Wilson Contr.*, No. 264; *Astrophysical Journal*, **58**, 235, 1923.

[4] R Leonis, X Ophiuchi, χ Cygni, T Cephei: *Mt. Wilson Contr.*, No. 264; *Astrophysical Journal*, **58**, 237, 1923: o Ceti, *Mt. Wilson Contr.*, No. 311; *Astrophysical Journal*, **63**, 298, 1926.

The journal of observations, including, for convenience, the earlier ones, is found in Table I.

TABLE I

JOURNAL OF OBSERVATIONS

PLATE	DATE	J.D. 242	MAG.	PHASE	SPECT.	ABS. LINES		EM. VEL.
						Vel.	Wt.	
				days		km/sec.		
A.A.	1915 Mar. 28	0585	7.9	−21	......	......	......	−32
A.A.	Apr. 16	0604	7.9	− 2	......	......	......	27
A.A.	May 7	0625	8.1	+19	......	......	......	44
C 397	1920 May 1	2446	9.1	−39	M6.5e	......	......	27
C 1558	1922 Feb. 12	3098	8.5	+32	6.5e	−32	2	43
C 1700	May 15	3190	9.0	−31	5.5e	......	......	24
C 3614*	1925 Dec. 23	4508	9.3	−27	6.5e	23	0.5	22
γ 13941	Dec. 26	4511	9.0	−24	5.5e	......	......	34
C 3625	Dec. 26	4511	9.0	−24	6e	30	2	34
γ 13989	1926 Jan. 30	4536	6.7	+ 1	4.8e	26	1	42
γ 14022	Feb. 3	4550	7.4	+15	5.5e	32	1	43
γ 14025	Feb. 18	4565	9.0	+30	7e	......	......	39
C 4101*	Nov. 14	4834	6.8	+ 6	3.8e	27	0.5	41
C 4123	Nov. 24	4844	7.5	+16	4e	34	2	42
γ 14841	1927 Mar. 10	4950	8.3	−20	......	......	......	33
γ 14849	Mar. 12	4952	8.2	−18	6e	26	1	33
C 4203	Mar. 17	4957	7.8	−13	5e	23	3	30
γ 14871	Mar. 19	4959	7.7	−11	5.5e	24	1	36
γ 14912†	Apr. 12	4983	7.5	+13	5.5e	......	......	......
γ 14926	Apr. 17	4988	7.8	+18	6e	27	2	40
C 4246*	May 8	5009	9.2	+39	8e	42	0.5	38
C 4271*	May 14	5015	9.6	+45	8e	30	0.2	39
C 4589	Dec. 22	5237	7.9	−23	6e	26	3	30
C 4613	1928 Jan. 4	5250	7.3	−10	5.5e	28	1	31
C 4617	Jan. 5	5251	7.2	− 9	4.5e	23	3	36
C 4622	Jan. 6	5252	7.2	− 8	4.5e	......	......	31
C 4661*	Jan. 30	5276	7.2	+16	5e	23	1	29
C 4668	Feb. 1	5278	7.3	+18	5e	27	2	43
C 4679	Feb. 10	5287	8.1	+27	6.5e	......	......	37
C 4682	Feb. 11	5288	8.2	+28	7e	31	2	36
C 4708*	Mar. 16	5322	11.0	+62	8ep	23	0.5	23
C 4735*	Apr. 8	5345	10.6	−60	8	35	1	......
C 4763*	Apr. 24	5361	8.8	−44	7.5e	29	0.2	28
C 4794*	May 2	5369	8.4	−36	6.5e	24	0.5	17
C 4801*	May 12	5379	8.1	−26	6.2e	28	1	25
γ 15843	June 4	5402	6.9	− 3	4e	22	2	36
γ 15897	June 21	5419	7.1	+14	4e	28	2	36
C 4861	June 27	5425	7.4	+20	4.8e	26	2	37
γ 15946	July 5	5433	7.9	+28	6.5e	23	1	44
C 4892	July 10	5438	8.5	+33	M6.5e	−35	1	−43

* 10-inch camera. † Comparison spectrum displaced.

The spectral type changes with the brightness of the star, ranging from M4e at maximum to M8 near minimum. The most conspicuous variations of the absorption spectrum are in the titanium bands, *Ca* λ 4226, and the chromium triplet λλ 4254, 4274, 4289. All these features are considerably more intense when the star is faint. Similar behavior is well known in *o* Ceti[1] and other long-period variables. The mean spectral types estimated from our plates and those derived from the Harvard data are shown in Table II.

TABLE II

PHASE AND SPECTRAL TYPE

Phase from Maximum	Spectral Type	
	Mt. Wilson	Harvard
−60 days	M8	....
−40	M7e	M5e
−20	M5.5e	M4e
0	M4e	M3e
+20	M5.5e	M4e
+40	M7.5e	M6(e)
+60	M8(e)	....

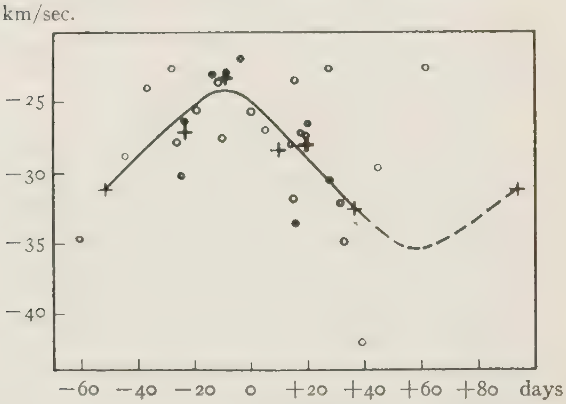

FIG. 2.—Velocities from dark lines. Individual observations are represented by circles, normal places by crosses. Heavy symbols indicate high weights.

The absolute magnitude at maximum determined from the intensities of λλ 4077, 4215, 4258, 4388, and 4490 in the same manner as for non-variable M-type stars is −0.6.

The radial velocities derived from the absorption lines are recorded in Table I and are plotted in Figure 2. Normal places formed

[1] *Loc. cit.*

by dividing the observed portion of the period into intervals of 15 days are shown in Table III.

As in the case of *o* Ceti,[1] the velocity-curve resembles the light-curve, the greatest velocity of recession occurring near the time of greatest light (see Fig. 1). The maximum of the velocity-curve seems to precede light-maximum by about 9 days, but further observations are required to establish this beyond doubt.

According to our observations, the chief emission lines in the spectrum, $H\gamma$ and $H\delta$, appear about 50 days before maximum light and increase in intensity toward maximum, after which they become weaker until at phase +60 days they are barely perceptible. The average intensity of $H\gamma$ is slightly greater than that of $H\delta$, but the relative intensity $H\gamma:H\delta$ ranges from about ½ to more than 2. This ratio does not show a consistent correlation with phase, as the lines behave differently in different cycles. Bright $H\beta$ is not distinctly seen until about 10 days before maximum. It then remains visible until about 35 days after maximum. It is usually less than half as intense as $H\gamma$, but on a few plates it approaches equality with $H\gamma$. $H\zeta$ is visible on a few plates on which $H\delta$ is strong. Traces of $H\epsilon$ are seen on two or three plates taken 6–20 days after maximum. Bright λ 4202 *Fe* makes its appearance about 30 days after maximum and remains as a feeble emission line until near minimum. λλ 4308 *Fe* and 4571 *Mg* are present as weak emission lines on plate C 4708, phase +62 days. These three bright lines are conspicuous in the spectrum of *o* Ceti and other typical Me variables, where

TABLE III

VELOCITIES FROM ABSORPTION LINES

Normal Places

Phase	Velocity	Weight
−51 days	−31.1 km/sec.	1.7
−23	27.1	7.5
− 9	23.4	10.0
+10	28.6	4.5
+20	28.0	12.0
+37	−32.7	4.2

---

[1] *Loc. cit.*

they are accompanied by numerous additional low-temperature lines not observed in R Virginis.

Radial velocities derived from the emission lines are tabulated in Table I and are plotted in Figure 3. They depend very largely on $H\gamma$ and $H\delta$, although measurements of $H\beta$, $H\epsilon$, and $H\zeta$ have been included in a few cases. In forming the normal places in Table IV, plates with the 10-inch camera were given weight one-half.

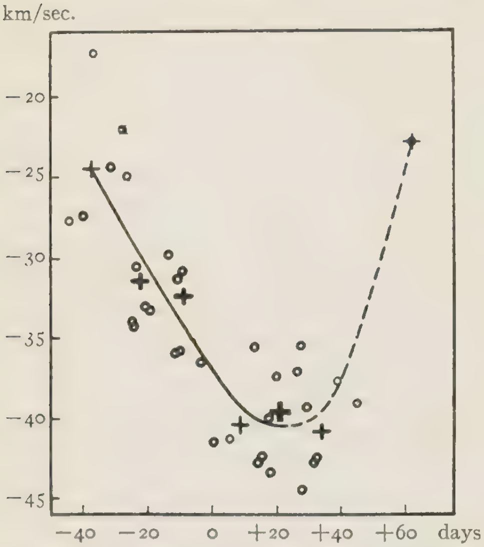

FIG. 3.—Velocities from bright lines. Individual observations are represented by circles, normal places by crosses. Heavy symbols indicate high weights.

The velocity-curve derived from the emission lines is decidedly different from that derived from the absorption lines and from the light-curve. The earlier measurements showing a rapid decrease in velocity at time of maximum light are confirmed. Compared with other stars,[1] the acceleration is exceptionally great. This suggests that,

TABLE IV

VELOCITIES FROM EMISSION LINES

Normal Places

Phase	Velocity	Weight
−37 days	−24.5 km/sec.	3
−22	31.4	7
− 8	32.4	7
+ 9	40.4	3.5
+21	39.7	8.5
+34	40.9	4
+62	−23	0.5

---

[1] See footnote on p. 264.

other things being equal, the acceleration is inversely correlated with the period of light-variation. Present data are insufficient to bring out the exact relationship.

On plate C 4708, phase +62 days, the hydrogen lines are barely distinguishable from the continuous spectrum, and measurements of their positions are not reliable. $H\gamma$, λ 4308, and λ 4571 give fairly accordant values, however, with a mean about 17 km/sec. above the value for phase +34 days. This may indicate a sudden rise in the curve similar to that found by Joy in *o* Ceti.[1]

It must be remembered, of course, that the curves are called velocity-curves for convenience; the quantities actually measured are the effective displacements of the lines. These may or may not be caused by line-of-sight motions. If we ascribe them to motion, we should perhaps distinguish between atomic motions and gross motions (of a whole stratum bodily).

From this brief study of R Virginis we infer that its period, 145.4 days, is near the lower limit of those stars that have the special spectroscopic features typical of long-period variables. The absorption spectrum is of earlier type and the bright lines are less intense than in variables with longer periods. Published investigations[2] and others now in progress at Mount Wilson show that variables with period or light-range less than that of R Virginis conform less closely to the typical star, *o* Ceti. They form a miscellaneous group with many different varieties of spectroscopic behavior. For example, the bright lines may appear at some phase other than maximum, or they may be irregular in behavior. Whether any of these stars are actually intermediate between long-period variables and Cepheids or RV Tauri stars is an important question for further investigation.

Carnegie Institution of Washington
Mount Wilson Observatory
April 1929

---

[1] See Fig. 4, *Mt. Wilson Contr.*, No. 311; *Astrophysical Journal*, **63**, 298, 1926.

[2] E.g., that by Miss Allen on T Centauri, period 91 days, *Lick Observatory Bulletins*, **12**, 73, 1925.

Contributions from the Mount Wilson Observatory, No. 38
Reprinted from the *Astrophysical Journal*, Vol. LXX, pp. 11–82, 1929
Printed in the U.S.A.

UNIV. OF ARIZONA
STEWARD
OBSERVATORY
TUCSON, ARIZONA

ON THE COMPOSITION OF THE SUN'S ATMOSPHERE

By HENRY NORRIS RUSSELL[1]

ABSTRACT

The *energy of binding* of an electron in different quantum states by *neutral* and *singly ionized* atoms is discussed with the aid of tables of the data at present available. The *structure of the spectra* is next considered, and *tables* of the *ionization potentials* and *the most persistent lines* are given. The *presence* and *absence* of the lines of different elements in the solar spectrum are then simply explained. The *excitation potential, E,* for the strongest lines in the observable part of the spectrum is the main factor. Almost all the elements for which this is small show in the sun. There are *very few solar lines* for which *E exceeds 5 volts;* the only strong ones are those of hydrogen.

The *abundance* of the various elements in the solar atmosphere is calculated with the aid of the calibration of Rowland's scale developed last year and of Unsöld's studies of certain important lines. The *numbers of atoms* in the more important energy states for each element are thus determined and found to decrease with increasing excitation, but a little more slowly than demanded by thermodynamic considerations.

The *level of ionization* in the solar atmosphere is such that atoms of *ionization potential 8.3 volts are 50 per cent ionized.*

Tables are given of the *relative abundance* of *fifty-six elements* and *six compounds.* These show that six of *the metallic elements, Na, Mg, Si, K, Ca,* and *Fe,* contribute 95 per cent of the whole mass. The whole number of metallic atoms above a square centimeter of the surface is 8×10^{20}. Eighty per cent of these are ionized. Their mean atomic weight is 32 and their total mass 42 mg/cm^2. The well-known difference between elements of *even* and *odd* atomic number is conspicuous—the former averaging *ten times as abundant* as the latter. The *heavy metals*, from *Ba* onward, are but little less abundant than those which follow *Sr*, and the hypothesis that the heaviest atoms sink below the photosphere is not confirmed. *The metals from Na to Zn, inclusive,* are *far more common* than the rest. The *compounds* are present in but small amounts, cyanogen being rarer than scandium. Most of those elements which *do not appear* in the solar spectrum should not show observable lines unless their abundance is much greater than is at all probable. There is a chance of finding faint lines of some additional rare earths and heavy metals, and perhaps of boron and phosphorus.

The *abundance of the non-metals*, and especially of hydrogen, is difficult to estimate from the few lines which are available. *Oxygen* appears to be about as abundant by weight as all the metals together. The abundance of *hydrogen* may be found with the aid of Menzel's observations of the flash spectrum. It is finally estimated that the *solar atmosphere contains 60 parts of hydrogen (by volume), 2 of helium, 2 of oxygen, 1 of metallic vapors, and 0.8 of free electrons*, practically all of which come from ionization of the metals. This great abundance of hydrogen helps to explain a number of previously puzzling astrophysical facts. The temperature of the reversing layer is finally estimated at 5600° and the pressure at its base as 0.005 atm.

A *letter from Professor Eddington* suggesting that the *departure from the thermodynamic equilibrium* noticed by Adams and the writer is due to a *deficiency* of the number of atoms in the higher excited states is quoted and discussed.

The hope that from the familiar qualitative spectrum analysis of the solar atmosphere a quantitative analysis might be developed is of long standing. Recent developments in spectroscopy and astrophysics have turned the hope into a rational anticipation. The most precise method of investigation—the study of the detailed contours of individual lines—promises the most, but it will be some time before it can be applied to the multitude of lines available. In the meantime, a survey of the problem and a discussion of the existing evidence regarding the relative abundance of those elements which show lines in the solar spectrum, and of the significance of the "absence" of those which do not, may be in order.

---

[1] Research Associate of the Mount Wilson Observatory, Carnegie Institution of Washington.

I. THE IONIZATION POTENTIALS AND SPECTRA OF THE ELEMENTS

The manner in which the appearance of the arc and spark lines of a given element in earlier and later types of the sequence of stellar spectra is governed by the condition of ionization and excitation in the atmosphere of the stars is now familiar. The way in which the spectra and related properties of the atoms themselves vary with the atomic number is less widely known, and our discussion may well begin with a summary of the facts as at present understood.

The electrons in an atom, whether neutral or ionized, are bound in different states—a term now preferable to the old "orbits." The more firmly bound inner electrons which form parts of the completed groups or "shells" are of concern in the spectroscopy of X-rays, but not of ordinary light. The latter deals with the outer electrons and with the complex set of excited states into which one or more of them may be raised from their normal positions. When there is but one outer electron, the various energy-levels, or spectroscopic terms, in which the atom itself can exist are intimately correlated with the state of this electron and are not very numerous, and the spectrum is then simple. When there are several outer electrons, however, a single configuration of electronic states may give rise (by space quantization) to an almost bewildering number of different spectroscopic terms, and the spectra are very complicated. As the number of outer electrons approaches that required to form a complete "shell," Pauli's restriction principle comes into play and the spectra are again simpler. The brilliant and detailed success of Hund's theory in predicting the characteristics of the spectrum from the electronic configurations is well known.

The transitions between spectroscopic terms, which give rise to the various spectral lines, are of great variety, but the transitions in the electronic states within the atom which accompany them are much simpler and afford the clue to what would otherwise be a hopeless maze.[1]

1. *Observed energy of binding of electrons.*—We may therefore best approach the subject by a study of the energy of binding of an electron, in different atoms, into the same state—that is, into the state characterized by the same total and azimuthal quantum numbers, and denoted, in Bohr's notation, by the symbols 1_1, 2_1, 3_1,—; 2_2, 3_2, 4_2,—; 3_3, 4_3,—; 4_4,—, or more commonly at present by the equivalent notation 1s, 2s, 3s,—; 2p, 3p, 4p,—; 3d, 4d,—; 4f,—.

This energy of binding is given, so far as data are available,[2] in Table I for neutral, and in Table II for singly ionized atoms. The first column gives the atomic number; the next, the chemical symbol. The remaining columns give the energy in volts required to remove an electron in the given state from the atom, or liberated when it returns. Among the numerous energy-levels resulting from different space quantizations of the same electronic configuration, that with the greatest energy of binding is given, regardless of the multiplicity involved.

The lines across each column mark the completion of the shell of electrons in the state in question. For heavier elements, electrons of this sort belong to the interior of the atom. Their energy of binding increases rapidly but does not concern us here.

Most of the tabular values are derived from series in the spectra and are fully reliable. The rest have been estimated in different ways. Those in parentheses and given to two decimals are extrapolated by series formulae and should be substantially correct. Those in parentheses and with one decimal are interpolated between the corresponding entries for neighboring elements and may be in error by one- or two-tenths of a volt. Those in square brackets have been derived from these last with the aid of known lines and should be equally accurate. The numerous gaps represent terms

---

[1] Cf., for example, "Related Lines in the Spectra of the Elements of the Iron Group," *Mt. Wilson Contr.*, No. 341; *Astrophysical Journal*, **66**, 184, 1927.

[2] References to the spectroscopic and other data are to be found at the end of the paper in Table XXI and in the list following this table.

TABLE I

Energy of Binding of an Electron—Neutral Atoms

Z	El.	1s	2s	2p	3s	3p	3d	4s	4p	4d	5s	5p	5d
1	*H*	13.54	3.38	3.38	1.50	1.50	1.50	0.81	0.81	0.81	0.54	0.54	0.54
2	*He*	24.48	4.75	3.61	1.86	1.57	1.51	0.99	.87	.85	.61	.56	.54
3	*Li*		5.36	3.40	2.01	1.55	1.51	1.05	0.87	.85	.64	.55	.54
4	*Be*		9.29	6.57	2.86		1.62	1.32		.90	.76		.57
5	*B*			8.28	3.34		1.52	1.49		.87			.57
6	*C*			11.22	3.78	2.42	1.57		1.19				
7	*N*			14.50	4.20	2.78	1.55	1.69		.87	.93		.56
8	*O*			13.56	4.45	2.86	1.52	1.77	1.32	.86	0.95		.55
9	*F*			[17.3]	(4.7)	(3.0)							
10	*Ne*			21.47	4.93	3.17	1.53	1.86	1.41	.86	1.00	.80	.55
11	*Na*				5.11	3.02	1.51	1.94	1.38	0.85	1.02	.79	.54
12	*Mg*				7.61	4.92	1.88	2.52	1.70	1.05	1.21	.92	.66
13	*Al*					5.95	1.95	2.83	1.89	1.15	1.31	0.99	.75
14	*Si*					8.14		3.08		1.16	1.37		
15	*P*					[10.5]		(3.5)					
16	*S*					10.31	(1.98)	3.82	2.48	1.06	(1.59)	1.19	.65
17	*Cl*					[12.9]		(3.9)	[2.6]				
18	*A*					15.69	(1.93)	4.19	2.84	1.06	1.69	1.29	.65
19	*K*						1.65	4.33	2.72	0.94	1.72	1.27	.59
20	*Ca*						3.57	6.09	4.21	1.42	2.19	1.57	.81
21	*Sc*						5.13	6.57	4.59	1.66	2.40		
22	*Ti*						5.95	6.80	4.76	1.60	2.32		
23	*V*						6.68	7.04	4.92		2.35		
24	*Cr*						8.24	7.28	5.05		2.43		
25	*Mn*						5.76	7.40	5.09	1.64	2.54		
26	*Fe*						6.98	7.83	5.45	1.63	2.55		
27	*Co*						7.82	8.25	5.33		2.62		
28	*Ni*						8.63	8.65	5.25	1.65	2.55		
29	*Cu*						10.41	9.02	5.58	1.65	2.69		
30	*Zn*							9.36	5.30	1.66	2.72	1.80	.89
31	*Ga*								5.98	1.68	2.92	1.89	0.94
32	*Ge*								7.89	1.87	3.26		1.04
33	*As*								[9.6]		(3.4)		
34	*Se*								[9.4]	(1.9)	(3.4)		(0.8)
35	*Br*								[11.4]		(3.6)		
36	*Kr*								[13.9]		(3.9)		
37	*Rb*									1.76	4.13	2.60	0.88
38	*Sr*									3.42	5.65	3.82	1.34
	Yt									5.04	6.40	4.55	1.61

TABLE II

Energy of Binding of an Electron—Singly Ionized Atoms

Z	El.	1s	2s	2p	3s	3p	3d	4s	4p	4d	5s	5p	5d
2........	He^+	54.16	13.54	13.54	6.02	6.02	6.02	3.38	3.38	3.38	2.16	2.16	2.16
3........	Li^+	(80)	16.58	14.70	6.83	6.24	6.03	3.72	3.48	3.39	2.33	2.22	2.17
4........	Be^+	....	18.13	14.18	7.25	6.27	6.03	3.88	3.47	3.40	2.41	2.21	2.17
5........	B^+	....	23	20.41	9.00	7.27	6.43	4.52	....	3.56	....	....	....
6........	C^+	....	....	24.28	9.90	8.01	6.31	4.87	4.22	3.52	2.85	....	2.24
7........	N^+	....	....	29.50	11.10	8.93	6.45	5.22	....	3.54	3.04	....	....
8........	O^+	....	....	34.94	12.09	9.76	6.37	5.44	....	....	3.10	....	....
9........	F^+	....	....	[34.9]	(13.1)	....	....	....	....	....	....	....	....
10........	Ne^+	....	....	40.89	13.74	10.40	6.33	5.98	....	....	....	....	....
11........	Na^+	....	....	47.02	14.31	10.83	6.20	6.18	....	....	....	....	....
12........	Mg^+	....	....	....	14.97	10.56	6.13	6.33	5.01	3.34	3.51	2.94	2.20
13........	Al^+	....	....	....	18.74	14.12	8.19	7.48	5.73	5.15	3.92	3.22	3.34
14........	Si^+	....	....	....	....	16.27	6.46	8.24	6.25	3.80	4.18	3.44	2.40
15........	P^+	....	....	....	....	19.81	6.95	9.11	7.08	4.07	4.58	....	....
16........	S^+	....	....	....	....	23.32	9.70	9.80	7.51	4.54	4.75	....	....
17........	Cl^+	....	....	....	....	[23.9]	10.25	10.56	7.98	4.79	5.08	....	....
18........	A^+	....	....	....	....	27.62	11.23	11.00	8.42	4.90	5.16	....	....
19........	K^+	....	....	....	....	31.68	11.50	11.62	9.07	5.43	5.08	....	....
20........	Ca^+	....	....	....	....	....	10.14	11.82	8.72	4.80	5.37	4.35	2.84
21........	Sc^+	....	....	....	....	....	12.19	12.80	9.58	5.40	5.68	....	....
22........	Ti^+	....	....	....	....	....	13.45	13.60	9.98	5.55	5.90	....	....
23........	V^+	....	....	....	....	....	(14.7)	(14.4)	(10.3)	....	....	....	....
24........	Cr^+	....	....	....	....	....	(16.6)	(15.1)	(10.7)	....	....	....	....
25........	Mn^+	....	....	....	....	....	13.93	15.70	10.91	5.85	6.50	....	....
26........	Fe^+	....	....	....	....	....	(16.3)	(16.5)	(11.7)	....	....	....	....
27........	Co^+	....	....	....	....	....	(17.2)	(16.8)	(11.7)	....	....	....	....
28........	Ni^+	....	....	....	....	....	18.19	17.15	11.75	....	7.20	....	....
29........	Cu^+	....	....	....	....	....	20.34	17.62	12.13	....	6.99	....	....
30........	Zn^+	....	....	....	....	....	....	17.89	11.79	5.92	6.97	5.40	3.35
31........	Ga^+	....	....	....	....	....	....	(18.8)	14.00	5.68	7.14	....	....
32........	Ge^+	....	....	....	....	....	....	....	15.98	6.00	8.28	6.21	3.62

which have not yet been identified spectroscopically—often because they would give lines in the infra-red. For the elements beyond yttrium the data are too fragmentary to tabulate.

The 4f state is not included in the table because it gives few terms of spectroscopic importance for the elements here considered.

It will be noticed that the rows in the table are filled out to the end only for the elements in which a shell of electrons is completed and for those immediately following. In these cases the spectra are relatively simple, and long series have been observed. For elements in which a group is about half complete (such as iron), the recognizable electronic configurations are few, although the number of spectroscopic states and of spectral lines is very great.

Table II is arranged the same as Table I. It stops at Ge^+ for lack of data. A number of the entries have been derived by interpolation or extrapolation in different ways. Some of them may be in error by half a volt; that for Li^+, by 3 or 4 volts.

The data of these tables are plotted in Figures 1 and 2, which illustrate many important atomic properties. The most firmly bound states are represented by the lowest points. The s, p, and d states are plotted as circles, crosses, and dots, respectively, and corresponding states in different atoms are connected by lines to guide the eye. These lines terminate abruptly at the points corresponding to the filling of a complete shell of electrons in the state considered. For larger atomic numbers these electrons pass into the inner structure, and those corresponding to the next lowest line on the diagram take their place as outer electrons. Thus a shell of six 2p electrons is filled up from *B* to *Ne* (or from C^+ to Na^+ among the ions). A shell of two 3s electrons is then filled in *Na* and *Mg*, followed by one of six 3p electrons (*Al* to *A*). Two 4s electrons go on in *K* and *Ca*, followed by ten 3d's from *Sc* to *Zn*. In this case, the 4s and 3d electrons are bound with about equal firmness and both groups are to be considered as outer electrons until the two shells are completely filled. Similar conditions are met from *Yt* to *Cd* (just beyond the limits of the diagram), where 5s and 4d electrons are going on, and among the rare earths (6s, 5d, and 4f). All this is, of course, merely a graphical representation of Bohr's theory of atomic structure.

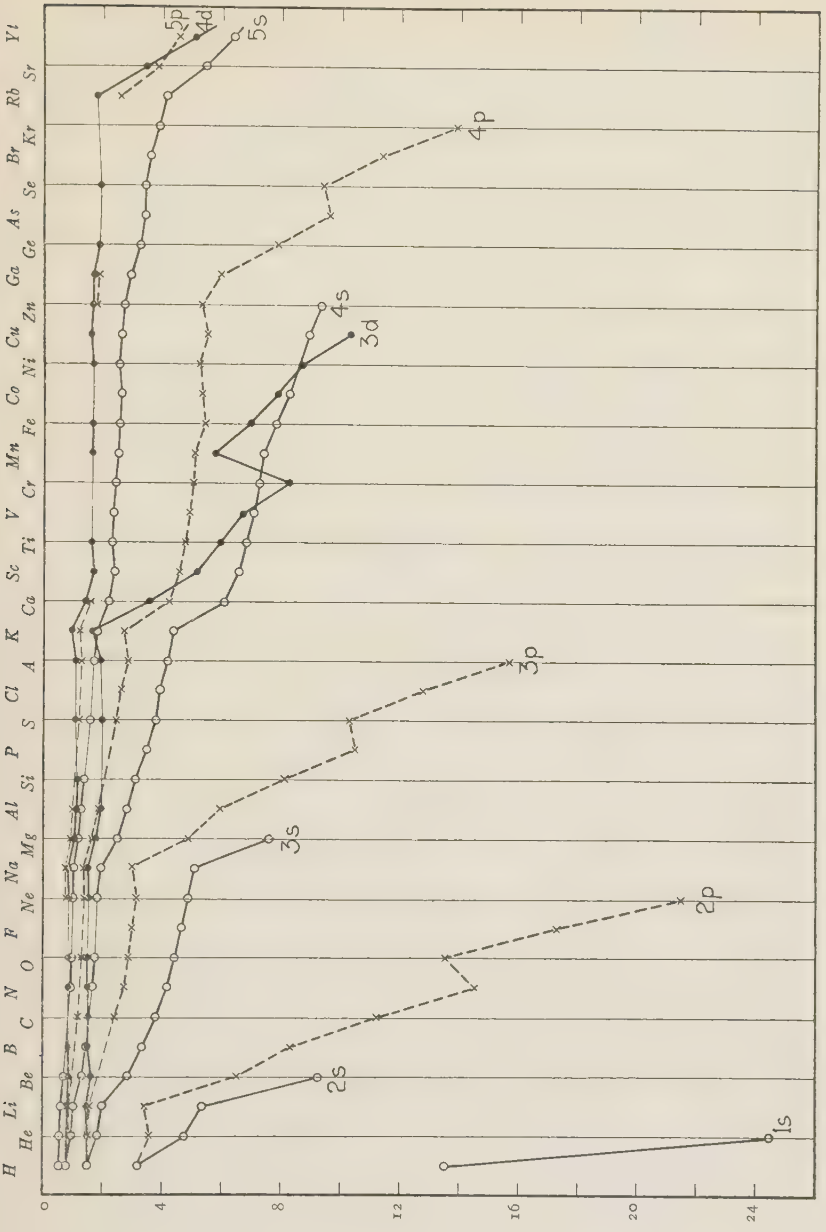

FIG. 1.—Energy of binding of electrons: neutral atoms

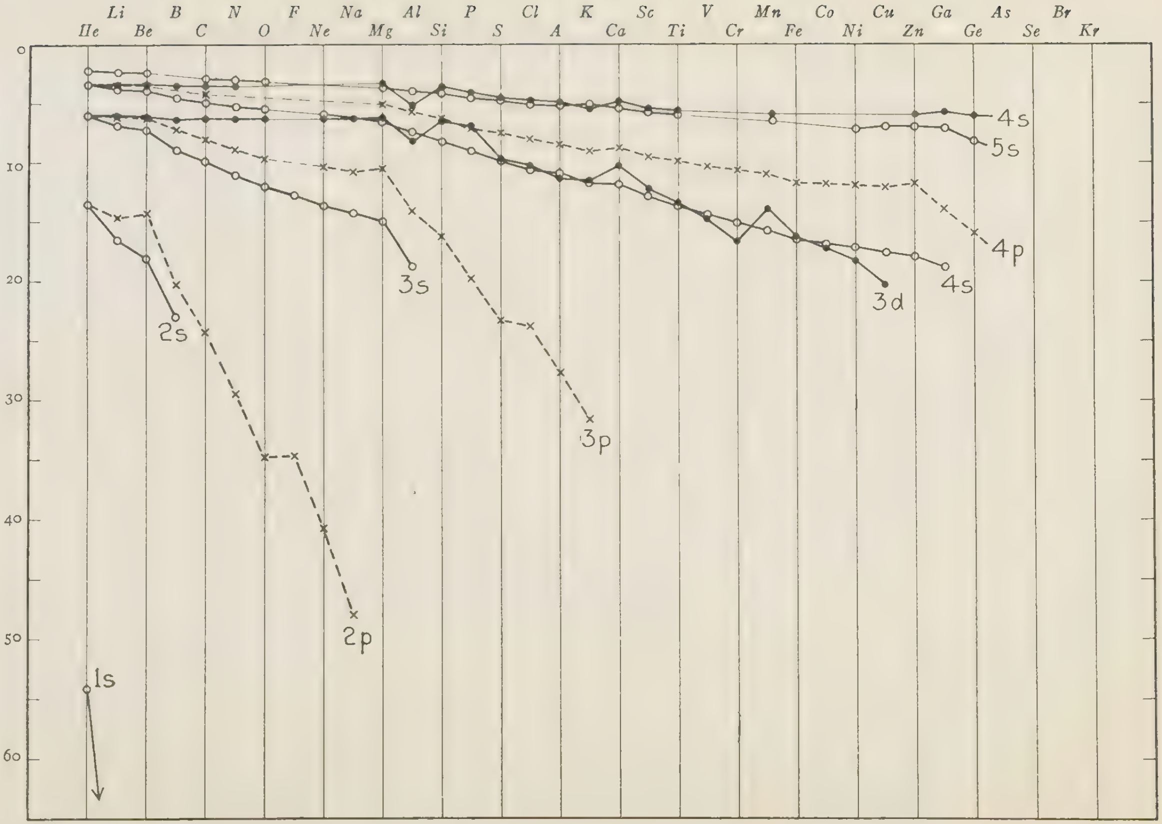

FIG. 2.—Energy of binding of electrons: singly ionized atoms. The designation 4s for the top curve should read 4d

Among the relations which are illustrated by these figures we may note:

a) The diagrams for the neutral and ionized atoms are strikingly similar, not only in their general outlines, but also in detail. In other words, the familiar "displacement law" applies not only to the multiplicities present in a spectrum, but also to the energy relations —the spark spectrum of any element resembling in both respects that of the arc spectrum of the preceding element. The further remarks apply therefore to both arc and spark spectra.

b) The energy of binding, for an electron in a given state, increases with the atomic number. For the s states the increase is steady; for the p and d states it is interrupted by fluctuations, which are remarkably similar in the neutral and ionized atoms.

c) The increase of energy is most rapid (1) when electrons of the type considered are being added to build up a complete shell; (2) when s electrons are being added. The most conspicuous fluctuations occur when a shell is half completed (half of the 6p electrons in N, P, As, O^+, S^+, and of the 10d electrons in Cr, Mn^+).

The explanation of these regularities by the older orbit theory is very pretty. For an outer excited orbit the increase in nuclear charge with atomic number is nearly compensated by the screening action of the electrons circulating in smaller orbits near the nucleus, and the effective attraction and energy of binding increase but slowly until electrons in orbits of the same type begin to be added, when the screening becomes very imperfect and the binding energy rapidly rises. The s orbits come nearer the nucleus than the others; hence they are less screened, and have greater binding energy than p orbits of the same total quantum number—and these again less than d orbits. Moreover, they go farther from the center; hence screening by an s electron is less effective and the binding energies of all outer orbits increase when they are being built in. Finally, the irregularities in the p and d curves can be explained as effects of space quantization. The conspicuous breaks which occur when a shell is half built are interpreted as due to the change from magnetic attraction to repulsion, when Pauli's restriction first compels the added electron to have a direction of spin opposite to that of the electrons which are already present.

The wave theory, when developed to include these complicated cases, will doubtless give a still better, though less picturesque, account of the facts. But we must return to spectroscopic considerations.

2. *Characteristics of the spectra of different elements.*—It may now be recalled that spectral lines are emitted, or absorbed, when an atom changes from one energy-level to another. Since the standpoint of the present paper is astrophysical, we may think of lines primarily as arising from transitions from lower to higher energy-levels, with absorption of radiation.

Whether such a transition will ordinarily occur, or is "forbidden," depends on the nature of the electronic transition involved. In permissible transitions one electron must jump between an even state (s or d) and an odd one (p or f). Another may jump at the same time between two even or two odd states, but this need not concern us for the moment.

Actual lines will therefore be represented in our diagrams by transitions between a point on a continuous line and one on a dotted line, while those between points on lines of the same sort are forbidden. When it is further recalled that the wave number of the line is proportional to the energy change involved, i.e., to the vertical shift on the diagram, some of the most important properties of the spectra and their variation with atomic number may be read from the figures. The wave-length of any line and the corresponding energy change in volts are related by the equation $\lambda = 12{,}336/V$. Taking sodium as an example, we see from Figure 1, or Table I, that an atom in the lowest energy state 3s can undergo transitions to 3p, 4p, 5p, etc., absorbing energy equivalent to 2.09, 3.73, and 4.32 volts, and giving lines at λλ 5900, 3310, and 2860 which agree, within the errors imposed by neglected decimals, with the lines of the principal series at λλ 5896, 3303, and 2853. An atom in the 3p state may change to 4s, 5s, absorbing 1.08, 2.00 volts (λλ 11404, 6160), or to 3d, 4d (1.51, 2.17 volts, λλ 8194, 5688). Changes between the higher states give lines in the infra-red.

The spectrum of sodium therefore shows strong lines in the easily accessible region. It is evident from inspection of Figure 1 that the same will be true of magnesium. For aluminium the 3s configuration has gone inside the atom, and the principal jumps between the remaining states, 3p to 4s and 3d, are longer, so that the lines are in the violet and ultra-violet. For the following elements, from silicon to argon, these transitions increase in energy and the lines move into the far ultra-violet and the Schumann region, while the transitions next in importance, 4s to 4p, are still of small energy, and give lines in the infra-red, or beyond sulphur, in the deep red. Those from 4s to 5p give accessible lines which shift from the yellow for silicon to the violet for argon; but these lines, as is true in general for the later members of series, are relatively faint. In the case of phosphorus, indeed, they have not yet been recognized, nor have the infra-red lines arising from the transition 4s−4p been observed. The arc spectrum of phosphorus, then, contains no known lines except in the ultra-violet beyond λ 2500, and it is obvious why it has not been recognized in the sun.

Similar conditions are encountered for all the non-metallic elements, which, with the exception of hydrogen and helium, belong where an outer shell of p electrons is being built up. The transition from the lowest configuration, mp, to the next, (m+1)s, gives lines in the far ultra-violet; the next, from (m+1)s to (m+1)p, lines in the deep red or infra-red, and only the weak lines, (m+1)s to (m+2)p, are accessible. For hydrogen and helium the energy relations are similar, except that *Hα* is visible.

It must further be borne in mind that even at solar temperatures the great majority of the atoms of any given kind, whether ionized or neutral, will be in the state of lowest energy. The number in higher states decreases rapidly as the energy of excitation increases. The fraction of the atoms of a non-metal which are in the excited s state and capable of absorbing the infra-red or visible lines, is, therefore, small. This imposes an additional handicap upon the non-metals, and it is no wonder that they show so feebly in the sun.

Silicon is an exception. To understand its case we must remember that Figure 1 is a mere skeleton. Except when the formation of a new shell is just beginning, as in *Na* or *Al*, there are a number (often a great number) of additional atomic states, which correspond to the same electron configuration, with different space quantization. Such states would be represented on the figure by a swarm of other points, lying above those which have been plotted by amounts ranging from a fraction of a volt to 2 volts or more. Those which belong to the same electronic configuration as the lowest state are metastable. In silicon there are two metastable states belonging to the configuration here called 3p. One of them is 0.78 volt above the bottom, and its combination with the 4s levels gives only wave-lengths shorter than λ 3000. The other, which is 1.12 volts higher, combines with the same levels to give the lines at λλ 3905 and 4102, which are strong in the sun. From phosphorus to argon, however, the corresponding lines are beyond λ 3000 and inaccessible astrophysically.

One non-metal, however, presents a real and glaring exception to the general rule. The hydrogen lines of the Balmer series, and, as Babcock has recently shown,[1] of the Paschen series as well, are very strong in the sun, though the energy required to put an atom into condition to absorb these series is, respectively, 10.16 and 12.04 volts—higher than for any other solar absorption lines. The obvious explanation—that hydrogen is far more abundant than the other elements—appears to be the only one.

Among the metals of the first long period, from scandium to zinc, the number of these additional energy states is great. The metastable states are numerous, since both 4s and 3d electrons may take part in forming them, and there are many higher states which are not represented at all in Table I or Figure 1. The tabular data give the energy released when an electron in the various states is added to ionized atoms which are in the states tabulated under 4s in Table II and described in a more generalized notation by $d^{n-2}s$. Addition of similar electrons to the ions in the states tabulated under 3d (in the general notation d^{n-1}) gives an entirely different set of higher energy-levels. Combinations between terms belonging to the two families, although usually involving a double electron jump, are very common, and add much to the complexity of the observed spectra. The tabular data, though referring to only a single family, give, however, a very good idea of the positions of the stronger lines. For each of the metastable spectroscopic terms there is a certain family of higher terms which arise from the addition of an electron to the same metastable state of the ion, and have this state as their series limit. Combinations between terms of the same family give, in general, much stronger lines than those between terms of different families. Hence these strong lines, when arising from the same electronic transition, lie usually in much the same part of the spectrum for all the families.[1]

---

[1] *Revision of Rowland's Preliminary Table of Solar Wave-Lengths*, p. 223.

A glance at Figure 1 shows that among the elements considered the transition from 4s to 4p involves an energy change which increases slowly and rather steadily from 1.8 volts for *Ca* to 4.1 for *Zn*. The corresponding lines work from the red into the near ultraviolet as the atomic number increases. The energy of transition from 4p to 5s increases, though more slowly, from 2.0 to 2.4 volts, giving lines in the visible spectrum. The spectra of the metals of the "iron group" contain therefore strong lines (usually very numerous), which correspond to electron transitions from the low to the middle terms (4s − 4p or 3d − 4p). These lie mainly in the visible spectrum for the smaller atomic numbers, but shift into the ultraviolet toward the end of the group, until, in *Cu* and *Zn*, very few are left on the red side of λ 3000. They are low-temperature lines in the furnace. The transitions from the middle to the higher levels, 4p − 5s or 4p − 4d, give high-temperature lines in the laboratory which remain in the visible spectrum throughout the group. They overlap the low-temperature lines widely, but, on the whole, have shorter wave-lengths—which explains the well-known fact that arc lines in the red are in general harder to produce by temperature excitation than those in the violet.

The next six elements, in which 4p electrons are successively added, are very like the 3p group. Germanium, like silicon, has a few low-temperature lines in the visible region; arsenic, like phosphorus, has none at all so far as present observations go; and the rest could be detected only by faint lines demanding high excitation. The spark spectra behave very similarly, except that the energy steps are much greater and the lines much farther to the violet. The transitions from the low terms to middle terms belonging to the same family give the strongest enhanced lines, which are prominent in the arc spectrum also. These lines lie in the violet for the metals at the beginning of a group, Ca^+ and Sr^+, but shift rather fast toward shorter wave-lengths, so that, beyond V^+ and Cb^+, they pass into the closed region beyond λ 3000. Weaker lines, produced by transitions between the upper levels of the "low" group and the lower levels of the middle group, belonging to different families, are observable as far as Fe^+, and a few for Co^+ and Ni^+, after which they, too, are lost in atmospheric absorption. Such lines are usually faint in arc spectra. Transitions from the middle to the upper terms give lines which, in the laboratory, are practically confined to the spark. Among the metals these transitions involve more energy than those previously considered, and the corresponding lines are observable only at the beginning of a group (Ca^+ to Ti^+, and homologous elements). An especially interesting case is that of Mg^+, where 3s − 3p, 3p − 4s, and 3p − 3d give lines lying near together (λλ 2795, 2936, 2798) and all just out of reach, so that the observable lines correspond to high excitations, such as 3d − 4f (λ 4481). For Be^+, however, the principal pair is just accessible at λ 3131.

---

[1] For an example in *Ti* II, see *Mt. Wilson Contr.*, No. 344; *Astrophysical Journal*, **66**, 323, 1927.

For the non-metals, the principal enhanced lines are hopelessly far out, and only a few transitions between highly excited states are accessible. The only enhanced lines of a non-metal which have been observed in the sun are a few of Si^+; and for these, as Figure 2 shows, the excitation potential is less than in almost any other case. The enhanced lines of the alkali metals present the same situation in its most extreme form.

3. *Ionization potentials.*—In discussing the relative strength of arc and enhanced lines in any source, knowledge of the ionization potentials involved is essential. These are given in Tables III and IV. Their values, for the first thirty-nine elements, are implicitly contained in Tables I and II—but not quite obviously. What is required in most cases is the energy difference between the normal states of the neutral atom and the ion, and complications arise in the iron group. Table I gives the energy difference between the 4s state of the ion ($d^{n-2}s$) and the various states of the neutral atom, of which we must evidently choose the lowest, whether it be 4s ($d^{n-2}s^2$) or 3d($d^{n-1}s$). But sometimes, as Table II shows, the 3d (d^{n-1}) state

of the ion is the lowest, and the values of Table I must be corrected accordingly. This is taken into account in Table III. For the second ionization potentials (Table IV) no such complication occurs. Both tables have been extended to include those heavier elements for which data are available. They are divided into two sections, corresponding to the "building on" of shells of s and d, or of p electrons. *He*, *Be*, *Mg* are put on the line with *Zn*, *Cd*, *Hg* because their spectra resemble those of the latter much more closely than those of *Ca*, *Sr*, and *Ba*. The line below *La* marks the position of the rare earths, where fourteen 4f electrons are added. These elements are listed separately.

The changes in ionization potential from element to element are immediately comprehensible by reference to Figures 1 and 2. While each shell of outer electrons is being completed, it increases, although with minor irregularities due to space quantization or to the interchange of s and d configurations. It reaches a maximum whenever a shell is completed. The drop after completion of an s shell in *Be* and *Mg* is between 1 and 2 volts; after completion of the combined s and d shells in *Zn*, *Cd*, *Hg*, it is 3 or 4 volts, while that following the completion of a p shell in the inert gases is much greater—8 to 16 volts. For the second ionization, these discontinuities are greater in absolute value, but are a smaller fraction of the potentials themselves. The ratio of the first and second ionization potentials for similar electronic structures—that is, for the neutral atom of one and the ion of the next following—ranges from 2.9 to 2.5 when a group of electrons begins to be formed, while for atoms with completed groups it runs from 2.4 to 2.0. For the first few elements, it has higher values, culminating with 4.0 for H and He^+.

The general character of the spectra of most of the heavier elements can be deduced from Tables III and IV. For the second long period (*Rb* to *Xe*) the ionization potentials are nearly the same as for homologous elements in the first, but average a little lower. The same is true, in general, regarding the other energy-levels, so that the arc and spark spectra of these elements show high- and low-excitation lines in the same regions of the spectrum as for those of the first long period, but, on the whole, a little farther to the red.

At the beginning of the next period, we find the lowest known

TABLE III

First Ionization Potentials of the Elements

H	13.59	*Li*	5.36	*Na*	5.11	*K*	4.33	*Rb*	4.13	*Cs*	3.86	*Ce*	6.9
						Ca	6.09	*Sr*	5.65	*Ba*	5.19	*Pr*	5.8
						Sc	6.57	*Yt*	6.5	*La*	5.5	*Nd*	6.3
						Ti	6.80	*Zr*	....	*Hf*	....	*Il*	....
						V	6.76	*Cb*	....	*Ta*	....	*Sa*	6.6
						Cr	6.74	*Mo*	7.35	*W*	8.1	*Eu*	....
						Mn	7.40	*Ma*	....	*Re*	....	*Gd*	6.7
						Fe	7.83	*Ru*	7.7	*Os*	....	*Tb*	6.7
						Co	7.81	*Rh*	7.7	*Ir*	....	*Dy*	6.8
						Ni	7.64	*Pd*	8.28	*Pt*	9.2	*Ho*	....
						Cu	7.69	*Ag*	7.33	*Au*	9.20	*Er*	....
He	24.48	*Be*	9.29	*Mg*	7.61	*Zn*	9.36	*Cd*	8.95	*Hg*	10.39	*Tu*	....
		B	8.28	*Al*	5.95	*Ga*	5.98	*In*	5.76	*Tl*	6.08	*Yb*	7.1
		C	11.22	*Si*	8.14	*Ge*	7.89	*Sn*	7.37	*Pb*	7.38	*Lu*	....
		N	14.50	*P*	[10.5]	*As*	[9.6]	*Sb*	8.35	*Bi*	7.25		
		O	13.56	*S*	10.31	*Se*	[9.4]	*Te*	[8.7]	*Po*	....		
		F	[17.3]	*Cl*	[12.8]	*Br*	[11.4]	*I*	[10.2]	......	....		
		Ne	21.47	*A*	15.69	*Kr*	[13.9]	*Xe*	[12.1]	*Rn*	....		

TABLE IV

Second Ionization Potentials

He^+	54.16	Be^+	18.13	Mg^+	14.97	Ca^+	11.82	Sr^+	10.98	Ba^+	9.96	Ra^+	10.2
						Sc^+	12.80	Yt^+	12.3	La^+	....	Ac^+	....
						Ti^+	13.60	Zr^+	....	Hf^+	....	Th^+	....
						V^+	(14.7)	Cb^+	....	Ta^+	....	Pa^+	....
						Cr^+	(16.6)	Mo^+	....	W^+	....	U^+	....
						Mn^+	15.70	Ma^+	....	Re^+	....		
						Fe^+	(16.5)	Ru^+	....	Os^+	....		
						Co^+	(17.2)	Rh^+	....	Ir^+	....		
						Ni^+	18.19	Pd^+	19.8	Pt^+	....		
						Cu^+	20.34	Ag^+	21.9	Au^+	....		
						Zn^+	17.89	Cd^+	16.82	Hg^+	18.9		
Li^+	(80)	B^+	(23)	Al^+	18.74	Ga^+	(18.8)	In^+	....	Tl^+	20.0		
		C^+	24.28	Si^+	16.27	Ge^+	15.98	Sn^+	14.5	Pb^+	14.96		
		N^+	29.50	P^+	19.81	As^+	....	Sb^+	....	Bi^+	....		
		O^+	34.94	S^+	23.32	Se^+	....	Te^+	....	Po^+	....		
		F^+	[34.9]	Cl^+	[23.9]	Br^+	....	I^+	....	.....	....		
		Ne^+	40.89	A^+	27.62	Kr^+	26.4	Xe^+	....	Rn^+	....		
		Na^+	47.02	K^+	31.68	Rb^+	....	Cs^+	....	.....	....		

ionization potentials (*Cs*, and Ba^+ for the second stage), which remain lower than in other periods until the rare-earth group begins. In these elements the outer electrons consist of two 6s, one 5d, and from one to fourteen 4f electrons, and the ionization potential slowly rises as the 4f group is built up. For the earlier members of the group, the lines of the ionized atom are the main features of the arc spectrum and those of the neutral atom are best brought out in the furnace, thus showing that the first ionization potentials are very low.[1] The strong lines of the first spark spectrum shift toward the violet with increasing atomic numbers, which practically proves that the second ionization potential also increases. The number of atomic energy states should be much greater among the rare earths than for any other elements, and their spectra are actually very intricate.

Upon the completion of the shell of 4f electrons the ionization potential ceases to have any important effect on the properties of the elements, as is shown by their chemical behavior and what little is known of their spectra (Hf^+, *W*). We should therefore expect a considerable fall in the ionization potential between the last rare earth, *Lu*, and *Hf*, and then a gradual rise to *Au* and *Hg*. For the last-named elements ionization is more difficult than for the homologous elements in the preceding periods. Whether this is also true for *Hf* cannot be determined from the existing data.[2]

4. *Raies ultimes.*—The strongest lines of any element, which are the last to disappear when the quantity present is diminished, usually arise from transitions from the lowest energy-level to middle levels of the same multiplicity and belonging to the same family. Among the various lines in a multiplet, that involving the highest inner quantum numbers is the most persistent; among transitions to terms of the same family the term of greatest azimuthal quantum number has the advantage; and the larger multiplicities are pre-

---

[1] The measures of Rolla and Piccardi indicate that it reaches about 7.5 volts at the end of the group.

[2] A table of ionization potentials, with discussion, has been given by Rolla and Piccardi (*Philosophical Magazine*, **7**, 286, 1929).

ferred to the smaller.[1] In a few cases, the combination of these influences causes a line originating from a level a little above the lowest to be the most persistent of all.

Lists of these lines, in the various arc spectra, are given in Table V. The lines marked with an asterisk have been recorded by De Gramont[2] or Meggers and Kiess[3] as *raies ultimes*, which actually persist in the manner described. Most of the rest are of too short wave-length to have been observed by them, but are undoubtedly of the same nature. Table VI gives similar data for spark spectra. The arrangement for the short periods differs slightly in order to bring spectroscopically similar terms into the same line.

These tables confirm the conclusions which were drawn from the general structure of the spectra. The most persistent arc lines of almost all the metals lie within the region accessible in the sun, while those of the non-metals are without exception out of range. Conditions for detecting the spark lines astrophysically are favorable only for the metals in the earlier parts of the successive periods—for *Be*, *Ca* to *V*, *Sr* to *Cb*, *Ba*, *La*, and probably several of the rare earths, and finally for *Ra*.

It may be remarked that the persistent lines and their spectroscopic notation are known for a number of elements for which the ionization potential and energy levels have not yet been determined. Indeed, the values given in square brackets in Tables I–IV have all been determined by utilizing persistent lines (not always the ones given in Tables V and VI), as explained in §1.

5. *Molecular spectra.*—No detailed discussion of the energy relations for the various band spectra which have been recognized in the sun is attempted here. It may be said, however, that, so far as the present evidence goes, all the bands which have been observed correspond to electronic transitions from the normal energy state of the molecule to higher states, and hence are comparable in nature to the persistent lines. Most of these bands are known to arise from molecules which are unsaturated chemically, and the others are probably

---

[1] Laporte and Meggers, *Journal of the Optical Society of America*, **11**, 459, 1925.

[2] *Comptes rendus*, **171**, 1105, 1920.

[3] *Journal of the Optical Society of America*, **12**, 417, 1926.

TABLE V

PERSISTENT LINES—ARC SPECTRA

WAVE-LENGTHS IN I.A.

H	1215.7	*Li*	*6707.85	*Na*	*5895.93	*K*	7699.01	*Rb*	7947.64	*Cs*	8943.46	.....	....	$^2S_1-^2P_2$
						Ca	*4226.73	*Sr*	*4607.34	*Ba*	*5535.53	*Ra*	4825.9	$^1S_0-^1P_1$
						Sc	3911.81	*Yt*	4102.38	*La*	....	*Ac*	....	$^2D_3-^2F_4$
						Ti	*3653.49	*Zr*	*3601.18	*Hf*	*4093.17†	*Th*	....	$^3F'_4-^3G'_5$
						V	*4379.24	*Cb*	*4058.99	*Ta*	....	*Pa*	....	$^6D_5-^6F_6$
						Cr	*4254.34	*Mo*	*3798.26	*W*	5053.30‡	*U*	....	$^7S_3-^7P_4$
						Mn	*4030.76	*Ma*	....	*Re*	....	.....	....	$^6S_3-^6P_4$
						Fe	3581.20	*Ru*	*3498.95	*Os*	....	.....	....	$^5F'_5-^5G'_6$
						Co	*3465.80	*Rh*	*3434.90	*Ir*	*3220.79§	.....	....	$^4F'_5-^4G'_6$
						Ni	*3524.54	*Pd*	*3634.69	*Pt*	*3064.69	.....	....	$^3D_3-^3P_2$
						Cu	*3247.55	*Ag*	*3280.66	*Au*	*2427.98	.....	....	$^2S_1-^2P_2$
He	584.4	*Be*	2348.63	*Mg*	*2852.11	*Zn*	*2138.61	*Cd*	*2288.02	*Hg*	1849.57	.....	....	$^1S_0-^1P_1$
					4571.10		3075.88		*3261.04		*2536.52	.....	....	$^1S_0-^3P_1$
		B	*2497.7	*Al*	*3961.54	*Ga*	*4172.06	*In*	*4511.27	*Tl*	*5350.46	.....	....	$^2P_2-^2S_1$
		C	1657.01	*Si*	2524.12	*Ge*	2709.63	*Sn*	*2863.32	*Pb*	2833.07	.....	....	$^3P_1-^3P'_1$
			1658.13		*2528.52		2754.59		3175.04		*4057.83	.....	....	$^3P_2-^3P'_1$
		N	1200.7	*P*	1787.5	*As*	1972.0	*Sb*	*2311.50	*Bi*	*3067.69	.....	....	$^4S'_2-^4P'_1$
		O	1302.25	*S*	1807.4	*Se*	1960.2	*Te*	2142.7	*Po*	....	.....	....	$^3P_2-^3S_1$
		F	954.7	*Cl*	1347.2	*Br*	1488.6	*I*	1642.5	.....	....	.....	....	$^2P_2-^2P'_2$
		Ne	735.8	*A*	1048.3	*Kr*	1164.9	*Xe*	1295.7	*Rn*	....	.....	....	$^1S_0-^1P_1$

† Spectroscopic classification unknown (Meggers, *Bureau of Standards Journal of Research*, 1, 187, 1928).

‡ $^5D_1-^5P_1$. Excitation potential, 0.206 volts.

§ Spectroscopic classification unknown.

TABLE VI

Persistent Lines — Spark Spectra

WAVE-LENGTHS IN I.A.

He^+	303.8	Be^+	*3130.42	Mg^+	*2795.52	Ca^+	*3933.66	Sr^+	*4077.71	Ba^+	*4554.04	Ra^+	3814 43	$^2S_1-^2P_2$
						Sc^+	*3613.84	Yt^+	*3710.30	La^+	*3949.10	Ac^+	....	$^3D_3-^3F_4$
						Ti^+	*3383.76	Zr^+	*3391.96	Hf^+	*2773.37†	Th^+	....	$^4F_5-^4G_6$
						V^+	*3093.10	Cb^+	*3094.20	Ta^+	....	Pa^+	....	$^5F_5-^5G_6$
						Cr^+	*2835.64	Mo^+	*2816.16	W^+	....	U^+	....	$^6D_5-^6F_6$
						Mn^+	*2576.12	Ma^+	....	Re^+	....		....	$^7S_3-^7P_4$
						Fe^+	*2382.04	Ru^+	....	Os^+	....		....	$^6D_5-^6F_6$
						Co^+	*2378.62	Rh^+	....	Ir^+	....		....	$^5F_5-^5G_6$
						Ni^+	2216.47	Pd^+	2296.53	Pt^+	....		....	$^4F_5-^4G_6$
						Cu^+	2247.00	Ag^+	*2437.81	Au^+	2082.06		....	$^3D_3-^3P_2$
						Zn^+	2061.96	Cd^+	*2265.04	Hg^+	1942.3		....	$^2S_1-^2P_2$
Li^+	(192)‡	B^+	1362.46	Al^+	1670.98	Ga^+	1414.4	In^+	1586.4	Tl^+	1321.8		....	$^1S_0-^1P_1$
		C^+	858.56	Si^+	1533.55	Ge^+	1649.27	Sn^+	1900.05	Pb^+	*2203.5		....	$^2P_2-^2S_1$
		N^+	1085.70	P^+	1542.29	As^+	....	Sb^+	....	Bi^+	....		....	$^3P'_2-^3D'_3$
		O^+	834.46	S^+	1259.53	Se^+	....	Te^+	....	Po^+	....		....	$^4S'_2-^4P'_3$
		F^+	606.81	Cl^+	1071.03	Br^+	....	I^+	....	.....	....		....	$^3P'_2-^3P_3$
		Ne^+	460.72	A^+	919.69	Kr^+	886.29	Xe^+	....	Rn^+	....		....	$^2P_2-^2P'_2$
		Na^+	376.34	K^+	612.61	Rb^+	....	Cs^+	....	.....	....		....	$^1S_0-^1P_1$

† See note for *Hf* in Table V.

‡ Not yet observed; estimated by extrapolation of series.

of the same sort. For molecules which are stable enough to endure ordinary chemical manipulation, the normal energy state appears to be so far below the others that the bands absorbed by the unexcited molecules lie in the extreme ultra-violet and are inaccessible.

This is certainly true of the hydrogen molecules, and the presence of lines of the "secondary" hydrogen spectrum in sun-spots[1] which has just been reported would be as striking an exception to the general rule as is the great strength of the Balmer lines.

The sources from which the data regarding the spectra and ionization potentials of the elements have been taken are summarized in Table XXI at the end of the paper. It is hoped that the list of references following the table is fairly complete; but no attempt has been made at a general bibliography of the subject. In the cases marked by square brackets in the tables (and in a few others) this material has been further worked over by the writer.

II. THE PRESENCE AND ABSENCE OF THE ELEMENTS IN THE SOLAR SPECTRUM

6. *Summary of the data.*—We are now in a position to understand the significance of the absence of recognizable lines of many of the elements from the solar spectrum. The present state of knowledge on this subject is summarized in Table VII, which is taken from the *Revision of Rowland's Table*,[2] with slight modifications, as explained below. The intensity of the strongest solar line which is believed to be due mainly, if not entirely, to the given elements is tabulated, thus indicating some idea of the prominence of the element in the spectrum, as well as its mere presence. The arc and spark spectra are tabulated separately under the headings *El* and El^+. An intensity given in parentheses signifies that the lines of the elements appear in spots, or in the disturbed regions near them, but not on the rest of the disk. A question mark shows that the identification of the element in the sun is uncertain. The table is arranged in fashion

---

[1] G. Piccardi, *Nature*, **122**, 880, 1928.

[2] *Carnegie Institution of Washington, Publication*, No. 396, 1928. Table A, p. xv. This will hereafter be referred to as R R. Since the publication of this work evidence has appeared that lines of *Pt* are probably, and *As* and *Ir* are possibly, present in the solar spectrum. This will be discussed in a forthcoming *Contribution* by Dr. St. John.

TABLE VII

Intensities of Strongest Absorption Lines of Each Element in the Solar Spectrum

Z		El	El+	*Z*		El	El+	*Z*		El	El+	*Z*		El	El+	*Z*		El	El+	*Z*		El	El+	*Z*		El	El+	*Z*		El	El+
1	*H*	40	—	3	*Li*	(4)	.....	11	*Na*	30	.....	19	*K*	5	.....	37	*Rb*	(1)	.....	55	*Cs*	....	.....	87	....	—	—	58	*Ce*	....	0
												20	*Ca*	20	200	38	*Sr*	1	8	56	*Ba*	....	8	88	*Ra*	....	....	59	*Pr*	....	−1?
												21	*Sc*	2	7	39	*Yt*	0	3	57	*La*	....	1	89	*Ac*	—	—	60	*Nd*	....	0
												22	*Ti*	7	12	40	*Zr*	−1	2	72	*Hf*	....	−1	90	*Th*	....	....	61	*Il*	—	—
												23	*V*	4	5	41	*Cb*	−2?	−1	73	*Ta*	....	.....	91	*Pa*	—	—	62	*Sa*	....	−1
												24	*Cr*	8	5	42	*Mo*	−2	0	74	*W*	−2	.....	92	*U*	....	....	63	*Eu*	....	1?
												25	*Mn*	10	6	43	*Ma*	—	—	75	*Re*	—	—					64	*Gd*	....	0?
												26	*Fe*	40	6	44	*Ru*	0	.....	76	*Os*	....	.....					65	*Tb*	—	—
												27	*Co*	6	0	45	*Rh*	−2	.....	77	*Ir*	−2?	.....					66	*Dy*	....	0?
												28	*Ni*	20	2	46	*Pd*	0	.....	78	*Pt*	1	.....					67	*Ho*	—	—
												29	*Cu*	10	.....	47	*Ag*	0	.....	79	*Au*	....	.....					68	*Er*	....	−1?
2	*He*	(0)	....	4	*Be*	−3	1	12	*Mg*	30	0	30	*Zn*	3	.....	48	*Cd*	−1	.....	80	*Hg*	....	.....					69	*Tu*	—	—
				5	*B*	....	.....	13	*Al*	20	−2?	31	*Ga*	−1	.....	49	*In*	(−1)	.....	81	*Tl*	−2?	.....					70	*Yb*	....	−1?
				6	*C*	0	.....	14	*Si*	12	2	32	*Ge*	0	.....	50	*Sn*	−2?	.....	82	*Pb*	−2	.....					71	*Lu*	—	—
				7	*N*	−2?	.....	15	*P*	....	.....	33	*As*	−3?	.....	51	*Sb*	−3	.....	83	*Bi*	....	.....								
				8	*O*	2	.....	16	*S*	−1	.....	34	*Se*	....	.....	52	*Te*	....	.....	84	*Po*	—	—								
				9	*F*	....	.....	17	*Cl*	....	.....	35	*Br*	....	.....	53	*I*	....	.....	85	....	—	—								
				10	*Ne*	....	.....	18	*A*	....	.....	36	*Kr*	....	.....	54	*Xe*	....	.....	86	*Rn*	—	—								

similar to the others, except that the rare earths are added in a separate column.

The presence in the spectrum of the disk of band lines due to the molecules C_2, CH, CN, NH, and OH, and, in addition, of BO, MgH, CaH, TiO, and probably H_2, in the spot spectrum, should be mentioned for completeness and as affording the principal evidence for the presence of B, C, and N in the sun. The strength of the emission lines of He in the chromosphere and the presence of a faint line of He^+ (λ 4685.808) are noteworthy.

It should further be borne in mind that some of the gaps in the table represent a lack of adequate data. The spectra of the recently discovered elements *Ma* and *Re*, and of the short-lived radioactive products, *Po*, *Ac*, and *Pa*, are still wholly or substantially unknown, and that of the "emanation" *Rn* is very incompletely observed. For several of the rare earths, *Il*, *Tb*, *Ho*, *Tu*, and *Lu*, the existing spectroscopic data "are not adequate either to establish the probability of their presence or to eliminate them from further consideration."[1] For these 11 elements, dashes have been inserted in the table to indicate the impossibility of a decision from existing data—as has also been done for the unknown elements of atomic numbers 85 and 87 and for the non-existent spark spectrum of hydrogen. This leaves 79 elements whose presence or absence in the spectrum can be discussed on the basis of existing data. Of these, 49 appear certainly to be present, 9 are doubtful, and 21 absent. Eighteen of the 49 reveal their presence by both their arc and spark spectra, 22 by the arc spectrum alone, 7 by the spark alone, and 2 (*B* and *N*) primarily by band spectra of compounds. Four of the doubtful identifications have to do with arc lines; the other 5 probably with spark lines (of the rare earths).

7. *Importance of excitation potential.*—In discussing this material, we may first consider the enhanced lines. Thirteen elements (Table VI) have their most persistent spark lines in the region accessible to observation. These are *Be*, *Ca*, *Sc*, *Ti*, *V*, *Sr*, *Yt*, *Zr*, *Cb*, *Ba*, *La*, *Hf*, and *Ra*. All but the last appear in the list of elements showing enhanced lines in the sun. Most of the other elements which do

---

[1] St. John and Moore, *Mt. Wilson Contr.*, No. 364; *Astrophysical Journal*, **68**, 106, 1928.

so (*Cr*, *Mn*, *Fe*, *Co*, *Ni*, *Mo*) come near the middle of the first two long periods. In their cases, the most persistent enhanced lines lie beyond λ 3000, but others, arising from low energy-levels, though not the lowest, are accessible. The rare earths should undoubtedly be divided between these two groups—just how cannot be said until the analysis of their spectra has been begun. The statement that enhanced lines are found in the sun for those elements which have lines of low excitation potential in the accessible region has therefore few exceptions. On the one hand, lines of *Ra*, and perhaps of some of the rarer of the rare earths, are absent. On the other, a very few enhanced lines, demanding high excitation, appear for *Mg* and *Si* and doubtfully for *Al*. It is obvious that considerations of abundance may explain both sets of exceptions. For the remaining elements which fail to show enhanced lines in the sun, the excitation potentials for the accessible lines are high in every case for which they have been determined.

The case of the arc spectra is not quite so simple. There are 37 elements, excluding the rare earths, whose arc spectra are little known, for which the most persistent lines are accessible. Arc lines of 25 of these are present in the solar spectrum. For 3 others (*Li*, *In*, *Rb*), the most persistent lines appear in sun-spots, though not on the disk. Three more (*Cb*, *Ir*, *Tl*) are doubtful, leaving 6 which fail to appear—*Cs*, *Ba*, *La*, *Hf*, *Bi*, and *Ra*. It is well known that most of these absences are explicable by ionization in the solar atmosphere.[1]

Among the elements whose most persistent lines are inaccessible, the majority of those which appear in the sun have accessible lines of low or moderate excitation potential (*Be*, *Mg*, *Si*, *Zn*, *Ge*, *Cd*, *Sb*, and the doubtful *As* and *Sn*). For the non-metals, *H*, *He*, *C*, *N*, *O*, and *S*, the excitation potentials are high and the lines weak, except for hydrogen.

It appears, therefore, that the principal factor which is unfavorable to the appearance of a spectral line in the sun is a high excitation potential. How important it is, is shown by Table VIII, which includes all the Fraunhofer lines which are known to have excitation potentials above 5 volts. There are 46 such lines out of nearly 6000 for which the excitation potentials are known. Twenty-eight of them have intensity 0 or fainter, and only 1 exceeds intensity 2, except the hydrogen lines, whose altogether exceptional behavior is well illustrated.

---

[1] M. N. Saha, *Philosophical Magazine* (6), **40**, 472 and 809, 1920.

Of the elements whose persistent lines appear in the sun, only a few (*Fe*, *Cu*, *Co*, *Mn*, Ca^+) show lines of high excitation, and the latter are all faint. The reason is simple: for such lines the lower level involved must be more than 5 volts above the bottom, and the upper level, even for a line at λ 8000, must be at a height of at least 6.5 volts. Aside from the case of a few exceptional states of low statistical probability, this level, again, will be well below ionization. Hence the ionization potential must be fairly high, as it is for the elements whose arc lines appear.

TABLE VIII

Solar Absorption Lines of High Excitation Potential

E.P.	El.	I.A.	Int.	E.P.	El.	I.A.	Int.
5.011....	*Fe*	8945.20	−1	7.455....	*C?*	9095.02	1
5.042....	*Fe*	8920.027	0		*C?*	9111.93	0
	Fe	9148.02	−1	7.473....	Ca^+?	5001.479	−2
5.064....	*Fe*	7086.729	−1	7.483....	Ca^+?	5021.153	−3
5.050....	*Cu*	4651.118	−1	7.591....	*C*	4932.020	−2
5.080....	*Cu?*	3319.689	−3		*C*	5039.006	−3
	Cu?	4586.998	−1	8.085....	Si^+	6347.104	2N
5.060....	*Si*	5948.552	6		Si^+	6371.362	1N
5.086....	*Mg*	7657.605	2	8.825....	Mg^+	4481.142	0
5.183....	*Co?*	6864.958	−3	8.826....	Mg^+	4481.340	0
5.467....	*Mn*	7680.267	1	9.106....	*O*	7771.954	2
5.771....	*Zn*	4629.806	−1		*O*	7774.177	2
	Zn	6362.357	1		*O*	7775.394	1
6.496....	*S?*	9228.19	−1	9.479....	*O*	8446.350	0
	S?	9237.49	0		*O*	8446.728	−1
6.827....	Si^+	3853.672	−1	10.155....	*H*	3970.078	5N
	Si^+	3862.595	1		*H*	4101.750	40N
6.829....	Si^+	3856.028	1		*H*	4340.477	20N
7.140....	*Mg?*	3892.017	−2		*H*	4861.344	30
7.388....	Al^+ ?	3900.662	−2		*H*	6562.816	40
7.450....	*C*	4770.001	−2	10.302....	*N?*	8680.403	−2
	C	4775.886	−2	12.035....	*H*	10049.5	25
	C?	9061.50	−1	20.871....	*He*	5875.62	*
	C?	9078.34	−1				

* Appears only in disturbed regions.

For spark spectra, the explanation is different. In order that the persistent lines may be accessible, the energy differences between the low and middle states (e.g., 4s, 3d, and 4p) must be rather small compared with the energy of ionization. The differences between the levels next in series (e.g., 5s, 4d, and 5p) will then be so small that the corresponding lines are in the infra-red, and the only accessible lines of high excitation will be later members of series, which are inherently faint. An example is found in Ca^+, where the observed lines correspond to the electron transition 5p − 6d.

8. *Significance of the "absences."*—The excitation potentials for the accessible lines of those elements which have not been identified in the solar spectrum are given in Table IX, those for which no reliable spectroscopic data exist being omitted as usual. The last column contains the elements whose presence is doubtful.

TABLE IX

EXCITATION POTENTIALS FOR ACCESSIBLE LINES OF ELEMENTS WHICH ARE MISSING OR DOUBTFUL IN THE SOLAR SPECTRUM

El.	E.P.	El.	E.P.	El.	E.P.	El.	E.P.
B.........	4.94	*Kr*.......	9.9	*Au*......	4.60	*N*.......	10.30
F.........	12.62	*Te*.......	5.45	*Hg*......	4.65	*S*........	6.50
Ne........	16.54	*I*........	6.73	*Bi*.......	0.00	*As*.......	2.30
P.........	6.90	*Xe*.......	8.2	Bi^+......	>6	*Sn*.......	0.21
Cl........	8.88	*Cs*.......	0.00	*Ra*.......	0.00	*Ir*.......	0.35
A.........	11.50	Cs^+	15.	Ra^+.....	0.00	*Tl*.......	0.00
Se........	5.94	*Ta*.......	0. ?	*Th*.......	0. ?		
Br........	7.81	*Os*.......	0.00?	*U*.......	0. ?		

The values given to two decimal places are derived from known resonance lines and are accurate. Those given to one decimal involve estimates of the positions of levels near those given by resonance lines, but slightly lower, and should be correct to 0.1 volt. The remaining values require explanation. For *Os*, lines from the lowest level revealed by the present incomplete analysis are accessible; there may, however, be unrecognized levels which are still lower, but by no great amount.

The spectra of *Ta*, *Th*, and *U* have not been analyzed, but comparison with homologous elements makes it very probable that their persistent lines lie in the observable region. For Bi^+ all that can be said is that the resonance lines are pretty certainly of shorter wave-length than for Pb^+ (for which the E.P. is 6 volts). In the case of Cs^+, which has a spectrum similar to that of *Xe*, the energy of binding of the 5p electron—the lowest state—may be estimated from the run of similar ratios for other elements, as 1.8 times the value for *Kr* I, that is, about 22 volts. The next level above this involves a 6s electron, which has a binding energy of 7.45 volts in Ba^+ and should have slightly less in Cs^+. The difference gives the tabular value of 15 volts. This may be wrong by a volt or two, but must be of the right order. For *B*, *P*, *Te*, *Br*, and *I*, lines of the given excitation potentials ought theoretically to exist in the infra-red, with fainter ones in the visible region; but none of these has yet been identified.

The elements which fail to appear in the sun fall sharply into two groups. The first contains all those with atomic numbers up to 54, *Xe*. Here the excitation potentials are so high that there is no chance of the lines appearing unless the elements are abundant. The same is true, to a somewhat less degree, of *Au* and *Hg;* and *Cs* may be added to the list for the reason that its first ionization potential is so low that no neutral atoms remain, even above the spots, and its second is so high that the observable lines demand a prohibitive degree of excitation. The absence of lines of these elements from the sun is consistent with their presence in fairly considerable amounts in the solar atmosphere.

The case of most of the heavier elements is quite different. For three of them—*Os*, *Bi*, and *Ra*—persistent lines lie in accessible regions and are definitely absent from the solar spectrum. Though *Ra* is probably easily ionized, the persistent lines of Ra^+ are also absent. There seems to be no escape, therefore, from the conclusion that these elements are present in the sun's atmosphere in negligible quantities, if at all.

For *Ta*, *Th*, and *U*, the spectra are complex, with numerous lines of moderate intensity and few very strong ones, and have not yet been analyzed. A definite decision upon their presence in the sun demands laboratory observations with the under-water spark, or some similar source, which will pick out the persistent lines among the swarms which fill the spectrum.

The weakness or absence of solar lines of the heavy metals is an old story. The present discussion indicates that this is not to be accounted for by the structure of their spectra (except for *Au* and

Hg) and supports the conclusion that these elements are present in the reversing layer in small proportions.

III. THE ABUNDANCE OF THE ELEMENTS IN THE SUN

9. *Absolute calibration of Rowland's intensity scale.*—There is reason to hope that within a few years the quantitative analysis of the solar atmosphere will be put on a solid basis by the accurate measurement of the contours of large numbers of lines and the interpretation of these by physical theory. An admirable beginning has already been made by Unsöld[1] and others; but a general investigation will be a heavy piece of work observationally, and perhaps theoretically too, and will take a long time to finish.

In the meantime a reconnaissance of the field may be made with the aid of the calibration of Rowland's intensity scale.[2] As derived last year, this gives only the relative numbers of atoms engaged in the production of different lines. More precisely, the numbers are those of the "fictitious oscillators," acting independently for each wave-length, which would produce lines of the observed intensity. For each spectral region the number of such resonators required to produce a line of intensity 0 was taken as the unit, irrespective of its absolute value or its possible variation in different regions.

Both these last questions may be approximately answered by comparison with Unsöld's results. From the observed contours of a number of typical resonance lines he determines theoretically the number of atoms, NH, above 1 sq.cm of the sun's surface, which are concerned in their production. When multiplied by a factor f, depending on quantum numbers, these give the number of "oscillators" for each line. The calibration of Rowland's table gives a quantity N, defined by the equation

$$\log N = B \log A \,, \qquad (1)$$

where B and $\log A$ are taken from empirical tables, which should be proportional to the number of oscillators. We may therefore write

$$\log (NHf) = \log N_0 + B \log A \,, \qquad (2)$$

---

[1] *Zeitschrift für Physik*, **46**, 765, 1928.

[2] Russell, Adams, and Moore, *Mt. Wilson Contr.*, No. 358; *Astrophysical Journal*, **68**, 1, 1928.

where N_0 is the number of oscillators for a line of intensity 0. Each of Unsöld's lines then gives a determination of N_0. The results are as shown in Table X, in which R denotes Rowland's intensity, "Res." the differences of the individual determinations of N_0 from the mean, and R_c the Rowland intensity computed from Unsöld's data by working the equations backward with the mean value of $\log N_0$. The H and K lines are too strong to calibrate, and the values of R_c were derived by extrapolating the relation

$$\Delta \log R = \tfrac{2}{3} \Delta \log A ,$$

which holds good from $R=15$ to $R=40$.

TABLE X

ABSOLUTE CALIBRATION OF ROWLAND'S INTENSITY SCALE

El.	λ	R	$B \log A$	$\log NHf$	$\log N_0$	Res.	R_c
Na	5889	30	3.58	16.24	12.66	−0.10	25
	5896	20	3.35	15.94	12.59	−0.17	15
Al	3961	20	4.28	16.67	12.39	−0.37	13
	3944	15	4.10	16.37	12.27	−0.49	9
Ca	4226	20	4.13	16.83	12.70	−0.06	18
Sr	4607	1	0.54	14.34	13.80	+1.04	3
Sr^+	4077	8	3.39	16.15	12.76	0.00	8
	4215	5d?	2.65	15.85	13.19	+0.43	6
Ba^+	4554	8	3.15	15.43	12.28	−0.48	6
	4934	3 and 4*	2.12	15.13	13.01	+0.25	5
Ca^+	3933	1000	....	19.19	....	....	340
	3968	700	....	18.89	....	....	230
Mean	....	....	....	....	12.76	....	....

* Given by Rowland as double; component intensities 3 and 4; see §10.

The average residual for one determination of $\log N_0$ is ±0.35. The value previously found in another way[1] for the determination of $\log N$ from a single line was ±0.37.

The residuals show a systematic trend such as would be produced if the calibration of Rowland's scale gave differences in $\log N$ that are too great. A plot of the data suggests a reduction of the calibrated values by about 25 per cent; but so large a correction appears to be inconsistent with the much more extensive data obtained from a study of the solar multiplets. Moreover, the residuals are already as small, on the average, as was to be anticipated. It may be that the calibration gives values too low for the numbers of atoms which produce the weaker lines; but the existing evidence is insufficient to determine what correction, if any, is required. The largest residual, for λ 4607, would be reduced to +0.50 if R were taken as 2 instead of 1, which would be in better agreement with Rowland's estimates for neighboring lines of equal strength; this would, however, give a smaller average residual than was to be expected. Taking the observations as they stand, we have $\log N_0 = 12.76 \pm 0.10$, so that it requires 6×10^{12} "atoms" per square centimeter to produce a line of intensity 0. The residuals show no definite evidence of a change of this quantity with the wave-length, although of course only a large change could be detected by so few observations, and the result may be adopted as generally applicable.

---

[1] *Op. cit.*, p. 7.

The mass of 6×10^{12} atoms of atomic weight m is $1.0 \times 10^{-11}\ m$ grams. To produce a line of intensity 0 requires therefore 0.1 m grams of matter per square kilometer of the sun's surface, or 0.6 m millions of tons for the whole surface, 6×10^{12} km². The amount of an element which must exist in the sun's atmosphere to permit its spectroscopic detection is very great when measured by ordinary standards. For example, the platinum line at λ 3064.696 ($R = 1$) indicates the existence of some five hundred million tons of the metal in the reversing layer. This is of course very small compared with the whole mass of the reversing layer, which, as we shall see later, probably exceeds 10^{15} tons.

10. *Numbers of atoms effective in different energy-levels.*—Accepting, then, for the present purpose, the calibration tables determined last year, we proceed to determine the "effective numbers" of atoms of the elements in their various energy-levels. The most direct way to do this is to calculate N by equation (1) for every solar line arising from the given level and add the results. This has two disadvantages: first, some lines are obscured in the sun by blends; second, on account of the approximately logarithmic character of Rowland's intensity scale, accidental errors of the estimates which make R too great increase the sum far more than errors in the opposite direction diminish it. When no theoretical information is available regarding

the relative intensities of the lines, as is the case for lines of a singlet system, or for inter-system combinations, these sources of error are unavoidable. Fortunately they affect the final sum in opposite directions. In normal multiplets, however, both may be avoided. If N' represents the sum of the number of atoms effective in producing the whole multiplet, and N that for a given line, one may write $N = N'F$, where F is a factor depending only on the quantum numbers. The values of these factors have been determined by several investigators.[1] Each line then gives an equation of the form

$$\log N' = B \log A - \log F \ . \tag{3}$$

By taking the mean of the values then found for all the lines of a given multiplet, the systematic effect of the errors of Rowland's estimates is eliminated, and the loss of some of the lines by blending is no longer serious. Errors may arise in multiplets when the actual intensities differ seriously from the theoretical. These will be serious only when some lines are abnormally faint. Such lines can almost always be recognized on the basis of laboratory intensities, and omitted from the mean.

One further complication sometimes arises. A good many of the stronger solar lines are given by Rowland as double, though all other evidence indicates that they are single. To add his intensities for the "components" gives much too high an intensity for the line, as is shown by comparison with other lines in the multiplet; but the assumption that the actual value of N is the sum of the values computed for the components as if they were separate lines gives results for N' in fair accordance with the others. As an example of the method, the strong multiplet $a^4F' - a^4G'$ of *Ti* II (λ 3349, etc.) gives the results in Table XI.

No theoretical formulae for the relative intensities of different multiplets arising from the same lower level are yet available, except for a few very simple cases, and our best recourse is to add the individual values of N'. Their sum, which may be called M, expresses the whole number of atoms effectively at work for the given spectroscopic term. In a few cases, where the term separations are very wide (as in *Tl* and *Pb*), the separate components have been treated independently, but this is rarely necessary.

---

[1] For numerical data see Russell, *Proceedings of the National Academy of Sciences*, 11, 314, 1925.

In practice, it is usually found that much the greater part of *M* is contributed by a few multiplets, which correspond to transitions within the same family of terms (§2).[1] When these multiplets lie in the observable part of the solar spectrum, the values of *M* derived from the solar lines should be nearly correct. When, however, these strong groups are inaccessible, *M* will be too small. Present knowledge of spectra is sufficient to permit the recognition of these cases, except for a few complex spectra, notably the rare earths.

TABLE XI

Inner Quantum Number	R	log N	$-\log F$	log N'
5–6	7+2	3.8	0.48	4.3
4–5	8	3.9	0.59	4.5
3–4	5+5	3.5	0.72	4.2
2–3	3	2.0	0.84	2.8
5–5	3+3	2.4	1.64	4.0
4–4	5	3.1	1.52	4.6
3–3	3	2.0	1.64	3.6
4–3	2	1.3	3.20	4.5
3–2	2	1.3	3.10	4.4
Mean	....	....	....	4.10

The results deduced in this way from the *Revision of Rowland's Table* are given in Table XII. The first two columns give the element and the spectroscopic term. The notation 4s, 3d, etc., has the significance described in §1. The designations of a few configurations which do not fit into this simplified scheme will be understood by those familiar with the subject. The third column gives the excitation potentials, measured from the lowest known energy-level, and the fourth, the number of lines, arising from the given term, which have been taken into account. For *Ti* and *Fe* all the lines of any strength were tabulated. For most of the rest, the lines which would obviously make but an insignificant contribution to the final sum were ignored, and the numbers are much smaller. The fifth column contains the value of log *M*, obtained from Rowland's in-

---

[1] Many of these are listed in "Related Lines," *Mt. Wilson Contr.*, No. 341; *Astrophysical Journal*, 66, 184, 1927.

TABLE XII

NUMBERS OF EFFECTIVE ATOMS

El.	Term		*E*	Lines	log *M*	log *M* Comp.
H..........	1	^2S	0.00	....	....	11.5
	2	^2S, P	10.15	1	3.5:	3.5
Li..........	2s	^2S	0.00	1	1.7*	1.7
Be..........	2s	^1S	0.00	....	....	1.8
	2p	^3P	2.72	2	>−2.0	0.1
Be$^+$........	2s	^2S	0.00	2	1.1	0.8
C..........	2p	$^3P'$	0.00	....	....	7.4
	3s	^3P	7.45	6	>0.9	1.1
	3s	^1P	7.59	1	>>−1	0.6
N..........	2p	$^4S'$	0.00	....	....	7.6
	3s	$^4P'$	10.30	1	>−0.7?	−0.7
O..........	2p	^3P	0.00	....	....	9.0
	3s	^5S	9.11	3	1.3:	1.0
	3s	^3S	9.48	2	0.0:	0.5
Na.........	3s	^2S	0.00	4	4.0	4.0
	3p	^2P	2.09	15	>2.7	2.7
Mg.........	3s	^1S	0.00	1	>>2.5	7.0
	3p	^3P	2.70	11	4.8	5.3
	3p	^1P	4.33	10	>4.0	3.5
	4s	^3S	5.09	1	>>0.8	2.9
	$(3p)^2$	$^3P'$	7.14	1	>−0.7	1.6
Mg$^+$........	3s	^2S	0.00	....	....	7.7
	3d	^2D	8.83	2	0.3	0.9
Al..........	3p	^2P	0.00	5	4.6	4.6
	4s	^2S	3.13	2	>>0.6	1.4
Al$^+$........	3s	^1S	0.00	....	....	6.4
	3p	^1P	7.39	1	>−1.3	0.3
Si..........	3p	$^3P'$	0.00	....	....	7.0
	3p	^1D	0.77	....	....	6.0
	3p	^1S	1.90	2	3.9	4.4
	4s	^3P	4.91	10	>>2.2	2.8
	4s	^1P	5.06	1	>>2.4	2.2
Si$^+$.........	3p	^2P	0.00	....	....	7.0
	$(3p)^2$	^2D	6.83	3	>>0.9	1.4
	4s	^2S	8.09	2	1.0	−0.4
S..........	3p	$^3P'$	0.00	....	....	5.7
	4s	$^5S'$	6.50	1	0.0:	0.0
K..........	4s	^2S	0.00	5	2.8:	2.8

* Line appears only in sun-spots.

TABLE XII—*Continued*

El.	Term		E	Lines	log M	log M Comp.
Ca.........	4s	^1S	0.00	3	4.1	4.5
	4p	^3P	1.88	35	>3.6	3.6
	3d	^3D	2.51	33	3.4	3.2
	3d	^1D	2.70	11	2.5	2.6
	4p	^1P	2.92	7	>2.8	2.2
Ca^+........	4s	^2S	0.00	2	6.7	6.7
	3d	^2D	1.69	3	>4.1:	6.0
	4p	^2P	3.12	5	3.5	4.5
	5p	^2P	7.48	2	>>−0.7	0.8
Sc..........	4s	^2D	0.00	15	1.6	1.9
	3d	$^4F'$	1.43	12	>0.3	0.8
	3d	$^2F'$	1.85	5	>−0.7	0.2
Sc^+.........	4s	^3D	0.01	15	3.7	3.5
	4s	^1D	0.31	3	3.0	2.8
	3d	$^3F'$	0.61	11	>2.5	3.1
	3d	^1D	1.35	3	1.7	1.8
	3d	$^3P'$	1.49	10	1.4	2.0
	(4s)^2	^1S	1.45	1	>0.5	1.3
	3d	^1G	1.76	1	1.4	1.7
Ti..........	4s	$^3F'$	0.02	37	3.6	3.5
	3d	$^5F'$	0.82	28	3.0	2.7
	4s	^1D	0.90	6	2.0	2.1
	4s	$^3P'$	1.05	26	>2.0	2.3
	3d	$^3F'$	1.44	17	2.2	2.0
	4s	^1G	1.50	6	>1.4	1.8
	3d	$^5P'$	1.73	17	1.9	1.6
	3d	^3G	1.87	20	1.8	1.7
	4p	$^5G'$	2.00	15	>1.3	1.8
	4p	^5F	2.09	10	>1.3	1.7
	3d	^3D	2.15	24	>1.1	1.2
	3d	$^3P'$	2.23	5	>0.4	1.0
	3d	$^3H'$	2.24	10	>1.5	1.5
	3d	^1G	2.26	6	>0.5	0.9
	4p	$^5D'$	2.29	9	>0.6	1.4
	3d	$^3P'$	2.32	7	>0.6	0.9
	3d	^1D	2.50	2	>−0.2	0.5
	3d	$^1H'$	2.57	6	>0.6	0.8
Ti^+........	4s	$^4F'$	0.02	22	4.5	4.8
	3d	$^4F'$	0.13	19	>4.1	4.7
	4s	$^2F'$	0.58	6	4.2	4.1
	4s	^2D	1.08	16	3.0	3.5
	3d	^2G	1.12	8	>3.2	3.7
	3d	$^4P'$	1.16	16	3.2	3.5
	3d	$^2P'$	1.22	8	3.2	3.1
	4s	$^4P'$	1.23	13	3.3	3.4
	3d	^2D	1.56	20	3.3	3.1
	3d	$^2H'$	1.57	7	3.0	3.4
	4s	^2G	1.88	9	3.2	3.1
	4s	$^2P'$	2.04	9	2.4	2.4
	3d	$^2F'$	2.58	4	>1.9	2.3

TABLE XII—*Continued*

El.	Term		E	Lines	log M	log M Comp.
V..........	4s	$^4F'$	0.03	46	>2.3	3.5
	3d	^6D	0.28	49	2.9	3.0
	3d	^4D	1.05	29	>1.5	2.2
V^+.........	3d	^5D	0.00	....	....	4.8
	4s	$^5F'$	0.36	8	>3.9	4.6
	4s	$^3F'$	1.09	17	3.9	3.8
		$^3P'$	1.43	7	>1.8	3.1
		^3G	1.80	11	>2.3	3.3
		$^3H'$	2.50	15	>2.5	2.8
Cr..........	3d	^7S	0.00	8	4.3	4.0
	3d	^5S	0.94	8	>2.9	3.1
	4s	^5D	0.98	51	>3.6	4.1
	3d	^5G	2.53	46	2.4	2.7
Cr^+........	3d	^6S	0.00	....	....	5.6
	4s	^6D	1.51	....	....	5.0
	4s	^4D	2.43	21	>3.4	4.0
		^2D	2.69	18	>>2.3	3.5
		^4D	3.09	9	>>2.7	3.5
Mn.........	4s	^6S	0.00	7	>3.6	5.1
	3d	^6D	2.14	41	3.6	3.7
	4p	^8P	2.29	14	3.5	3.4
	3d	^4D	2.91	26	>2.7	2.8
	4p	^6P	3.06	14	2.9	2.7
Mn^+........	4s	^7S	0.00	....	....	5.7
	4s	^5S	1.17	....	....	4.6
	3d	^5D	1.83	9	>>3.2	4.7
Fe..........	4s	^5D	0.07	86	>6.1	6.6
	3d	$^5F'$	0.99	133	5.7	5.7
	3d	$^3F'$	1.54	61	5.4	5.0
	3d	$^5P'$	2.19	86	4.3	4.3
	4s	$^3P'$	2.38	56	>3.4	4.2
	4p	$^7D'$	2.41	56	4.2	4.5
		$^3H'$	2.42	38	>3.7	4.5
		$^3F'$	2.57	36	>2.8	4.2
		^3G	2.71	38	4.1	4.1
	3d	$^3P'$	2.83	31	3.4	3.5
	4p	^7F	2.84	53	4.2	4.3
	4p	^7P	2.98	27	3.9	3.8
	4p	^3P	4.23	5	>2.4	2.4
Fe^+........	4s	^6D	0.06	....	....	6.9
	3d	$^4F'$	0.33	....	....	6.7
	4s	^4D	1.04	11	>>4.0	5.9
	3d	$^4P'$	1.69	11	>>2.7	5.2
	4s	$^4P'$	2.68	12	>>2.6	4.3
	4s	$^4F'$	2.82	18	>>2.6	4.6
	$(4s)^2$	^6S	2.88	12	>>2.7	4.1
	4s	^4G	3.18	13	>>2.2	4.4
	4s	^4D	3.88	8	>>1.6	3.5

TABLE XII—*Continued*

El.	Term		E	Lines	log M	log M Comp.
Co..........	4s	$^{4}F'$	0.12	34	>3.6	5.0
	3d	$^{4}F'$	0.54	38	4.2	4.4
	3d	$^{2}F'$	0.98	15	3.9	3.7
Ni.........	3d	^{3}D	0.12	25	5.1	5.1
	4s	$^{3}F'$	0.14	42	>4.4	5.5
	3d	^{1}D	0.42	17	4.5	4.3
	4s	^{1}D	1.67	14	2.8	3.6
	d^{10}	^{1}S	1.82	5	2.9	2.4
Cu.........	3d	^{2}S	0.00	2	4.5	4.3
	4s	^{2}D	1.51	3	>>1.8	4.0
	(4p)	^{2}P	3.79	7	>1.1	1.5
	4p	^{4}P	4.82	1	>>−0.2	1.0
	4p	^{4}F	5.07	3	>>0.0	1.2
Zn.........	4s	^{1}S	0.00	1	>>0.7	4.9
	4p	^{3}P	4.02	7	1.9	2.1
	4p	^{1}P	5.77	2	0.5	0.2
Ga.........	4p	^{2}P	0.00	1	>−0.1	0.2
Ge.........	4p	$^{3}P'$	0.05	....	....	2.5
	4p	^{1}D	0.88	3	1.4	1.5
	4p	^{1}S	2.02	2	0.1	−0.1
As.........	4p	$^{4}S'$	0.00	....	....	0.6
	4p	$^{2}D'$	1.33	....	....	0.1
	4p	^{2}P	2.27	1?	>>−2.5?	−1.2
Rb.........	5s	^{2}S	0.00	2	0.1:*	0.1
Sr.........	5s	^{1}S	0.00	1	0.6	0.6
	5p	^{3}P	1.80	4	>−0.4	−0.3
Sr^{+}.........	5s	^{2}S	0.00	2	3.4	3.3
	5p	^{2}P	2.97	4	1.2	1.3
Yt..........	5s	^{2}D	0.03	9	0.8	0.8
	4d	$^{4}F'$	1.36	4	0.0	−0.2
Yt^{+}........	$(5s)^{2}$	^{1}S	0.00	3	1.4	1.6
	5s	^{3}D	0.10	18	2.5	2.4
	5s	^{1}D	0.40	4	1.6	1.7
	4d	$^{3}F'$	1.00	11	1.5	1.8
	4d	$^{3}P'$	1.71	6	0.1:	0.8
Zr..........	5s	$^{3}F'$	0.07	18	0.3	0.8
	4d	$^{5}F'$	0.66	9	0.0	0.3
Zr^{+}........	4s	$^{4}F'$	0.08	19	2.4	2.2
	3d	$^{4}F'$	0.34	12	>1.5	2.0
	4s	^{2}D	0.54	5	1.1	1.3
	4s	$^{2}F'$	0.75	7	1.8	1.3
	3d	$^{2}P'$	0.73	4	>1.1	1.0

TABLE XII—*Continued*

El.	Term	E	Lines	log M	log M Comp.
Cb$^+$	4d ^5D	0.00	....	....	0.8
	5s $^5F'$	0.40	4	>0.3	0.6
Mo	4d ^7S	0.00	....	....	0.3
	4d ^5S	1.33	1	−0.6	−0.9
	5s ^5D	1.35	5	>−1.2	0.0
Mo$^+$	4d ^6S	0.00	....	....	1.3
	5s ^6D	1.5?	....	....	0.7?
	5s ^4D	2.4?	2	>−1.7	−0.2?
Ru	4d $^5F'$	0.16	5	>0.0	0.9
	4d $^3F'$	0.97	3	0.0	0.0
Rh	4d $^4F'$	0.27	8	−0.6	−0.3
	4d $^2F'$	0.88	1	>−0.9	−1.1
Pd	d^{10} ^1S	0.00	....	....	0.1
	4d ^3D	1.00	5	0.4	0.4
	4d ^1D	1.45	2	>−0.6	−0.4
Ag	4d ^2S	0.00	2	0.0	0.0
Cd	5s ^1S	0.00	1	>>−0.7	2.1
In	5p ^2P	0.00	1	−0.4*	−0.1
Sn	5p $^3P'$	0.21	....	....	0.3
	5p ^1D	1.06	2?	−1.0?	−0.7
Sb	5p $^4S'$	0.00	....	....	0.3
	5p $^2D'$	1.14	....	....	−0.3
	5p ^2P	2.15	2	>−2.0	−1.3
Ba$^+$	6s ^2S	0.00	2	3.0	2.9
	5d ^2D	0.65	3	>2.7	3.0
	6p ^2P	2.60	4	1.2	1.2
La$^+$	5d $^3F'$	0.12	12	1.4	1.5
	^1D	0.17	9	0.9	0.9
	6s ^3D	0.32	13	1.3	1.2
	^1S	0.91	1	>−0.5	−0.5
	5d ^1G	0.92	1	0.0	0.5
Ce$^+$	....	0.4:	249	2.1	2.1
Pr$^+$	....	0.4:	18	0.3:	0.3
Nd$^+$	....	0.4?	107	1.6	1.6
Sa$^+$	....	0.4?	67	1.1	1.1
Eu$^+$	....	0.4:	5	1.0:	1.0
Gd$^+$	....	0.5:	15	0.7:	0.7:

TABLE XII—*Continued*

El.	Term		*E*	Lines	log *M*	log *M* Comp.
Dy$^+$	....		0.5:	12	1.2:	1.2
Er$^+$	....		0.5:	2	−0.3:	−0.3
Hf$^+$	....		0.7	28	−0.1	−0.1
W	6s	^5D	0.44	5	>−0.6	−0.6
Ir		^2D	0.18	1?	−1.5?	−0.5
Pt		^3D...	0.04	3	1.0	1.5
Tl	6p	$^2P_1$ $^2P_2$	0.00 0.96	1? 1?	−0.9:? −1.5:?	−0.9 −1.4
Pb	6p	$^3P'_0$ $^3P'_1$ $^3P'_2$ $^1D_2$	0.00 0.97 1.32 2.65	.... 1 1 1	.... >−1.7 −0.7 >−1.3	0.0 −0.3 −0.4 −1.6
CN	....		0 ?	872	3.2	....
C$_2$	....		0 ?	422	1.3	....
CH	....		0 ?	155	3.0	....
NH	....		0 ?	157	2.1	....
OH	....		0 ?	185	3.0	....
BO	....		0 ?	28	1.4*	....

tensities as described above, and represents the "absorbing power" of the term. For the H and K lines Unsöld's measures (§ 9) are used.

The sign > preceding an entry signifies that important multiplets arising from the term are known to be out of reach in the infra-red or ultra-violet, and >> that such multiplets are much stronger than those observed. Lines which appear only in sun-spots are denoted by an asterisk. A colon means, as usual, that the results are uncertain, and a question mark, that the attribution to the given element is doubtful. For *C*, *N*, *O*, *S*, *K*, and *Rb*, most or all of the lines are in the deep red, beyond the limit of Rowland's original work, where the scale of intensities may differ considerably from Rowland's and has not been independently calibrated. These values of log *M* may be too low. For hydrogen, the situation is peculiar.

We should expect the widths and intensities of $H\beta, H\gamma, H\delta$ to diminish rapidly, since the transition probabilities fall off. Unsöld's measures,[1] however, show that this is not the case, and some exceptional influence must be at work—perhaps the Stark effect. The $H\alpha$ line must also be affected, though to a less degree. The tabular value is derived from Rowland's intensity for this line alone, without correction for the factor 0.64, which expresses the theoretical value for $H\alpha$ relative to the sum of the whole Balmer series. It may nevertheless be too great. Unsöld's measures of the width of this line, treated similarly, give $\log M = 4.1$. This is probably considerably too great, for the reasons stated. For the rare earths, whose spectra have not been analyzed, the sum of the values of N for all the unblended lines has been taken, and increased pro rata in proportion to the number of blended lines recorded. The values of the average excitation potential for these elements are rough estimates based on the data for La^+ and Hf^+. Many of the lines of the latter are unclassified, and the same method has been applied to them.

The band spectra due to compounds, which appear at the end of the table, have been treated in the same way. These bands are all absorbed by unexcited molecules, but, owing to the vibrational and rotational energy, the excitation potentials may be somewhat above the zero values entered in the table. The fifth column of the table contains values of $\log M$ calculated in the way described below (§13). These values have been included, for completeness, in a number of cases where no observations can be made.

11. *Discussion of these data.*—Much has been written on the theoretical distribution of the energy states of the atoms in a stellar atmosphere. An exact discussion would be very complicated, but, fortunately, there is good reason to believe that the most simple and obvious approximations should give results close to the truth.

The temperature of the reversing layer doubtless increases toward its base, but it is probable that the change is relatively small. According to Eddington,[2] it increases from 0.81 to 0.88 times the effective temperature T_e between the outer boundary and the depth corresponding to the optical thickness $\tau = 0.25$. These values hold

[1] *Zeitschrift für Physik*, **46**, 778, 1928.

[2] *The Internal Constitution of the Stars*, pp. 332 and 335.

for the integrated light. For the center of the disk the range is from the same lower limit to 0.91 T_e. Since most of the material is in the deeper layers, the assumption $T = 0.87\ T_e$ would appear to be reasonable. For the sun, $T_e = 5730°$ and $T = 4980°$.

The pressures in the upper and lower parts of the reversing layer must differ very greatly. Milne[1] has just shown, however, that the assumption of a uniform pressure gives surprisingly good results. Although the opacity actually increases gradually with the depth, the line contours should be very similar to those produced by an atmosphere devoid of general opacity and overlying a solid photosphere, provided that the amount of matter in this fictitious atmosphere were equal to that which is actually above the optical depth $\tau = 1/3$. The "number of atoms above the photosphere" then takes on a definite meaning. He shows also that the total numbers of neutral and ionized atoms above any depth will be very nearly the same as those calculated from the elementary formula of Saha, with an electronic pressure one-half of the value at the given depth. The effects of a chromosphere supported by radiation pressure are excluded from consideration.

In what follows, we shall therefore consider the sun's atmosphere as having a definite temperature T, and a definite electronic pressure P. In thermodynamic equilibrium, the number M_0 of neutral atoms in any energy state is then given by the equation

$$\log M = \log A_0 + \log W - \frac{5040\ E}{T}\,, \tag{4}$$

where A_0 is a constant depending on the abundance of the element considered, W is the total quantum weight of the state or the corresponding spectroscopic term, and E the excitation potential in volts. The value of W is the product of the multiplicity of the term (1, 2, 3, for singlets, doublets, triplets) by 1, 3, 5, 7, for S, P, D, F terms. For terms arising from electron configurations involving two equivalent s electrons, these values should be doubled.[2] Such terms occur in *Be*, *Mg*, *Ca* to *Zn*, *Sr* to *Cd*, and *Ba* to *W* for the terms denoted by 2s, 3s, etc., in Table XII. A few similar cases in ionized atoms are denoted by $(4s)^2$ and the like. For an energy state of an ionized atom we have

---

[1] *Monthly Notices, R.A.S.*, **89**, 3 and 17, 1928.

[2] W. Heisenberg, *Zeitschrift für Physik*, **38**, 411, 1926. For the application to more complex spectra, the writer is indebted to a conversation with Professor Sommerfeld.

$$\log M_1 = \log A_1 + \log W_1 - \frac{5040E}{T}\,, \tag{5}$$

where A_1 is the abundance factor for ionized atoms. This is connected with A_0 by Saha's equation

$$\log A_1 - \log A_0 = -\frac{5040I}{T} + \tfrac{5}{2}\log T - 6.5 - \log P\,. \tag{6}$$

If we set

$$\tfrac{5}{2}\log T - 6.5 - \log P = \frac{5040I_0}{T}\,, \tag{7}$$

this means

$$\log A_1 = \log A_0 + \frac{5040}{T}(I_0 - I)\,. \tag{8}$$

The constant I_0 is the ionization potential of an element which would be just half ionized under the conditions. It may be taken as defining the "level of ionization" in the star's atmosphere.

We have finally to take into consideration the fact that the atmosphere may not be in thermodynamic equilibrium. The comparison of solar and stellar spectra affords evidence that this is the case.[1] The lines arising from excited states are stronger in the cooler stars than the elementary theory expressed by equation (4) predicts. The degree of ionization appears to be unaffected. We may take account of this by writing

$$\log M = \log A_0 + \log W - \frac{5040}{T}(E - C)\,, \tag{9}$$

and similarly for ionized atoms. It is assumed that C is a function of E, which must be determined empirically. The evidence from the stars indicates that C is small at first, but increases rapidly when E exceeds 2 or 3 volts. Were it not for the limitation of the solar record, the determination of this correction would be simple, especially since for the sun's atmosphere $5040/T = 1$ within the uncertainty of estimation. Each value of log M in Table XII leads by (9) to one of log $A-C$ for the same element, and a plot of these for elements such as Fe and Ti would give values of C up to $E=4.5$. But so many of the lines arising from these higher levels are in the infra-red that this is impracticable.[1] The data are, however, sufficient to show that C is small if E is less than 2 volts, and to give reliable values of log A_0 for the neutral atoms of many elements, and of log A_1 for a smaller number of ionized atoms. When we know A_0 and A_1 for the same element, we can find I_0 by (8). The determinations of this quantity from different elements are in good agreement (see below). Taking the mean, we can then find A_1 for any element, if we know A_0 and I.

---

[1] Adams and Russell, *Mt. Wilson Contr.*, No. 359; *Astrophysical Journal*, **68**, 11, 1928.

Now there are a few solar lines of Si^+, Mg^+, and Al^+, for which E is between 7 and 9 volts. Having found A_1 for these elements, as just described, we may use these lines to obtain the values of C corresponding to these large values of E. The results are discordant. The Si^+ lines λλ 6347, 6371 give $C=2.6$ for $E=8.09$; Mg^+ λ 4481, $C=0.7$, $E=8.83$; and Al^+ λ 3900, $C=-0.5$, $E=7.39$. In all these cases the lines are the strongest which arise from atoms in the given state, and the correction on this account is small.

The Al^+ line is very faint and deserves half weight. We therefore adopt as a mean $C=+1.2$ for $E=8.2$ volts. In default of further information, we will assume that $C=0.15E$ for all values of E.

A more satisfactory determination of the important correction is much to be desired; but no further solar data are available. In a star of earlier spectral type, such as Procyon, a larger number of enhanced lines would be available, and determinations of the correction, made for dwarf stars, might perhaps be extended to apply to the sun. To use giant stars for this purpose would be unsafe.

As matters stand, the determination of the solar abundance factors A_0 and A_1 is little influenced by this uncertainty for the metals, while the values for the non-metals, especially those of low atomic weight, remain considerably uncertain.

12. *Level of ionization in the sun.*—There are five elements for which the principal lines of both the neutral and ionized atoms are

---

[1] This difficulty does not affect the comparison of the intensity of the same lines in the sun and a star, on which last year's results were based.

accessible. Each of them may be used to determine the level of ionization I_0 by the equation

$$I_0 = I + \frac{T}{5040}(\log A_1 - \log A_0) . \tag{10}$$

The results are shown in Table XIII. The five values agree remarkably well, when we consider that they have been determined in some cases (*Ca*) from extremely strong lines, and in others (*Sc*, *Yt*) from very weak ones. Giving double weight to the values for *Ca* and *Ti*, we find the mean value $I_0 = 8.26 \pm 0.08$ volts. This probable error, which is derived from the residuals, should be taken only as an indication of the consistency of the determinations. The value $I_0 =$ 8.3 volts will be adopted in the present discussion.

TABLE XIII

IONIZATION IN THE SUN

	ELEMENT				
	Ca	*Sc*	*Ti*	*Sr*	*Yt*
$\log A_0$	4.2	0.3	2.1	0.3	−0.4
$\log A_1$	6.4	2.5	3.3	3.0	1.2
$\log A_1 - \log A_0$	2.2	2.2	1.2	2.7	1.6
I	6.1	6.6	6.8	5.6	6.5
I_0	8.3	8.8	8.0	8.3	8.1

By equation (7) this corresponds to the electron pressure $P = 3.1 \times 10^{-6}$ atm. = 3.1 dynes/cm². These values of I_0 and P depend on the assumed temperature of the solar atmosphere. If, for example, we had taken $T = 5740°$, as Milne does in his latest paper,[1] we would have found $I_0 = 8.53$ volts and $P = 2.5 \times 10^{-5}$ atm. The computed pressure is much more sensitive to changes in the assumed temperature than is the value of I_0. The latter appears, therefore, to have considerable advantage for the specification of the state of a stellar atmosphere. If only the farther ultra-violet were accessible, the enhanced lines of the more difficultly ionizable elements could be observed, and the value of I_0 found almost as a direct result of observation, independent of any theory except that involved in the calibration of the lines. The pressure here derived is in fair agreement with the values found by the same method from the calcium lines in stars by Miss Payne and Mr. Hogg[1] ($P=2.54\times10^{-6}$ atm. in class G0) and by Unsöld[2] from the strontium lines (3.3×10^{-6}). From the calcium lines Unsöld finds 3.4×10^{-7}. The difference arises mainly from the fact that the other calcium lines used in the present work give a greater value for A_0 than does λ 4226. Unsöld's value, which rests on precise measurements, is doubtless more accurate, but the mean value resulting from the calibration of Rowland should clearly be used in the present work.

---

[1] *Monthly Notices, R.A.S.*, **89**, 35, 1928.

13. *Abundance of the elements in the sun's atmosphere.*—With the constants thus determined, we may now compute the number, M, of atoms which are in any given energy state, neutral or ionized, by the equations

$$\left.\begin{aligned}\log M&=\log A_0+\log W-0.85E\ \text{(neutral atom)}\,,\\ \log M&=\log A_1+\log W-0.85E\ \text{(ionized atom)}\,,\\ \log A_1&=\log A_0+I_0-I\,.\end{aligned}\right\}\qquad(11)$$

Each observational value of log M gives one of log A_0 or log A_1. Mean values of these for each element are given in Table XIV and the values of log M calculated from these in Table XII, under the heading "Log M Comp." In adopting these values and adjusting those of A_0 and A_1 to satisfy the ionization equation, the accuracy of the individual values of log M has been kept in mind. Examination of Table XII shows that, for the more abundant metals, a change in log A_0 and log A_1, by 0.1 or 0.2 at most, is all that is permissible. For some elements, such as *Si*, the data are discordant, and the uncertainty greater. There are many elements, however, for which the determination rests only on a few faint lines, and in these cases the tabular values are only an indication of the order of magnitude of the results. Such cases are denoted in the table by a colon, while a question mark indicates that the origin of the lines is doubtful. The remaining columns of Table XIV give quantities related to the abundance of the atoms in the solar atmosphere. S_0 is the whole number of neutral atoms per unit area, derived from the sum of the values of M for the different energy levels, and S_1, the

---

[1] *Harvard Circular*, No. 334, 1928.

[2] *Zeitschrift für Physik*, **46**, 778, 1928.

TABLE XIV

ABUNDANCE OF ELEMENTS AND COMPOUNDS IN THE SUN

El.	log A_0	log A_1	log S_0	log S_1	log T	log Q
H	11.2::	5.7::	11.5::	5.7::	11.5::	11.5::
Li	− 1.2:	1.7:	− 0.9:	2.0:	2.0:	2.8:
Be	1.5	0.5	1.8	0.8	1.8	2.8
C	6.5:	3.6:	7.4:	4.4:	7.4:	8.5:
N	7.0?	0.8?	7.6?	1.8?	7.6?	8.7?
O	8.0:	2.7:	9.0:	3.3:	9.0:	10.2:
Na	3.7	6.9	4.0	7.2	7.2	8.6
Mg	6.7	7.4	7.0	7.7	7.8	9.2
Al	3.8	6.1	4.6	6.4	6.4	7.8
Si	6.0	6.2	7.0	7.0	7.3	8.8
S	4.8:	2.8:	5.7:	3.4:	5.7:	7.2:
K	2.5:	6.5:	2.8:	6.8:	6.8:	8.4:
Ca	4.2	6.4	4.6	6.7	6.7	8.3
Sc	0.6	2.3	1.9	3.6	3.6	5.3
Ti	1.9	3.4	3.6	5.2	5.2	6.9
V	1.8	3.4	1.9	5.0	5.0	6.7
Cr	3.2	4.8	4.4	5.7	5.7	7.4
Mn	4.0	4.9	5.1	5.8	5.9	7.6
Fe	5.0	5.5	6.7	7.1	7.2	9.0
Co	3.4	3.9	5.1	5.4	5.6	7.4
Ni	4.0	4.7	5.7	5.7	6.0	7.8
Cu	4.0	4.6	4.3	4.9	5.0	6.8
Zn	4.6	3.5	4.9	3.8	4.9	6.7
Ga	− 0.6:	1.7:	0.2:	2.0:	2.0:	3.8:
Ge	1.6	2.0	2.5	2.8	3.0	4.9
As	0.0?	− 1.3?	0.6?	− 0.7?	0.6?	2.5?
Rb	− 2.8:	1.4:	− 2.5:	1.7:	1.7:	3.6:
Sr	0.3	3.0	0.6	3.3	3.3	5.2
Yt	− 0.5	1.3	0.8	2.6	2.6	4.5
Zr	− 0.7	0.8	0.9	2.5	2.5	4.5
Cb	− 1.8:	− 0.6:	− 0.2:	1.0:	1.0:	3.0:
Mo	− 0.5	0.5	0.5	1.4	1.4	3.4
Ru	− 0.5	0.1	1.0	1.6	1.7	3.7
Rh	− 1.5	− 0.9	− 0.3	0.5	0.5	2.5
Pd	0.1	0.1	0.6	0.9	1.1	3.1
Ag	− 0.3	0.7	0.0	1.0	1.0	3.0
Cd	1.8:	1.3:	2.1:	1.6:	2.2:	4.2:
In	− 2.8:	− 0.3:	− 2.0:	0.0:	0.0:	2.1:
Sn	− 0.5?	0.4?	0.3?	1.2?	1.2?	3.3?
Sb	− 0.3:	− 0.3	0.4:	0.7:	0.8:	2.9:
Ba	− 0.5	2.6	− 0.2	3.3	3.3	5.4
La	− 2. :	0.3	− 0.7:	1.8	1.8	3.9
Ce	....	....	....	2.4	2.4	4.6
Pr	....	....	....	0.6:	0.6:	2.8:
Nd	....	....	....	2.0	2.0	4.2

TABLE XIV—*Continued*

El.	log A_0	log A_1	log S_0	log S_1	log T	log Q
Sa				1.5	1.5	3.7
Eu				1.4:	1.4:	3.6:
Gd				1.1:	1.1:	3.3:
Dy				1.6:	1.6:	3.8:
Er				0.1:	0.1:	2.3:
Hf				0.4	0.4	2.6
W	−1.5	−1.5	−0.1	−0.1	0.2	2.5
Ir	−1.5?	−1.5?	−0.5?	−0.5?	−0.2?	2.1?
Pt	0.4	0.0	1.5	1.0	1.6	3.9
Tl	−1.2?	1.1?	−0.8?	1.4?	1.4?	3.7?
Pb	0.0	0.9	0.2	1.2	1.2	3.5
CN			3.2		3.2	4.6
C_2			1.3		1.3	2.7
CH			3.0		3.0	4.1
NH			2.1		2.1	3.3
OH			3.0		3.0	4.2
BO			1.4		1.4	2.8

number of ionized atoms. In a few cases such as *Ru* II and *Rh* II, the calculation of S_1 involves assumptions regarding the nature of the lowest terms in spectra which have not yet been analyzed; but the uncertainty thus arising is much less than that of the observational data for these elements. The next column gives log T, where T is the total number of atoms of the element considered in both stages of ionization. Doubly ionized atoms may safely be neglected. They should be relatively most numerous for *Ba*, for which log $S_2 = 1.3$, but this is only 1 per cent of the number of singly ionized atoms. For the rare earths the values of S_1 have been directly calculated by the approximate process described in §10. The ionization potentials are unknown, and S_0 cannot be given; there is no doubt, however, that it is small, and that no serious error is committed by neglecting it, as has been done here. For the band spectra, S_0 gives the number of neutral molecules. Finally, Q represents the total mass of the atoms or molecules of the substance per unit area of the sun's surface. The tabular values are obtained by multiplying T by the atomic or molecular weight. We have already found that the unit of T represents 6×10^{12} atoms per square centimeter. That of Q corresponds, therefore, to 1.0×10^{-11} gm/cm².

In a number of cases special considerations have been applied in deriving A_0 or A_1 from the observations. For several elements, many or most of the lines arising from the best observable level are out of reach in the ultra-violet, and the observed value of log M must be corrected from the probable intensity. The corrections which have been applied are +1.3 for As, +0.3 for Cb^+, +0.7 for Sb, +0.5 for W and Pt, and +1.0 for Ir. Though rough estimates, they probably improve the tabular values. For Cd, only a single inter-system combination, ${}^1S_0-{}^3P_1$, is observed (λ 3261). For this line Prokofjev[1] has found that the number of effective resonators is 1/600 that for the resonance line ${}^1S-{}^1P$. The values of the corresponding ratios for lines of Ca and Zn, derived from the solar data, agree with his formula as well as could be expected. The correction +2.8 for the Cd line may therefore be adopted. For Mo^+ the analysis of the spectrum is fragmentary, and the relative energy-levels of the terms have been assumed to be the same as in Cr^+, a permissible assumption, as very rough values will suffice.

Finally, there are three elements, Li, In, and Rb, whose lines appear only in sun-spots. To attempt to correct for the change of ionization theoretically would lead us too far. It may suffice to take the observed intensities of a number of faint lines of other metals of easy ionization in the same part of the spectrum and thus find ratios of the change in log N from the spot to the disk. Thirty-seven lines between λ 4350 and λ 4650 give a mean change of −1.9, which has been adopted for In λ 4511; thirty between λ 6100 and λ 6600 give +2.6, which has been adopted for Li λ 6708, and in default of other data, for Rb λλ 7947, 7800.

Table XIV contains the principal conclusions of the present paper. The main source of uncertainty which affects them is the magnitude of the correction for departure from thermodynamic equilibrium. For the metals, this is always small, and the tabular data may be accepted with confidence. For the non-metals it is much greater (except for Si). For C, N, O, and S, the value of E averages 8.4 volts, while for H it is 10.2. The uncertainty of the correction is at least 10 per cent of these values. To increase this correction would diminish the very large values for the abundance of these elements. For hydrogen the uncertainty is increased, since it is unknown how much of the width of the lines, which was clearly the main criterion in Rowland's estimates of intensity, arises from special causes. Anything short of an extreme correction for both these factors would still leave hydrogen the most abundant element by weight, and more abundant, by number of atoms, than all the rest together. Even with a liberal correction, oxygen and its neighbors remain among the most abundant elements by weight, and still more by number.

---

[1] *Ibid.*, **50**, 708, 1928.

The values of log Q are plotted in Figure 3—the more reliable ones by solid dots and the less trustworthy by open circles. Two features of the distribution are conspicuous. First is the general downward trend toward the right, corresponding to a diminution in the abundance with increasing atomic number. The fact is familiar; its interpretation, less certain. The faintness of the lines of the heavy elements in the sun is commonly attributed to the tendency of the heavy atom to diffuse downward, below the photosphere. If this were the main explanation we should expect the heavy elements following *Ba* to be considerably less abundant than those which succeed *Sr;* but the figure shows that this is not the case and suggests a relatively rapid fall for the lighter elements from *H* about as far as *Zr* and a very slow decrease for the heavier ones.

Stirring of the solar atmosphere by currents and other forms of turbulence favors a uniform mixture. This process occurs on an enormous scale in sun-spots, where the material must ascend from a considerable depth.[1] The fact that the lines of La^+ and other heavy elements, which are completely ionized even in the spots, are not perceptibly strengthened in the spot spectrum indicates that the difference in composition is small at the depth from which the ascending vortex comes. It does not appear necessary, therefore, to assume that downward diffusion depletes the sun's atmosphere of the heavier elements, though the possibility of such an influence remains.

Second, there is a conspicuous zigzag arrangement of the points, which represents the well-known fact that the elements of even atomic number are more abundant than those whose numbers are odd. The generality of this rule is well illustrated by the diagram. Every

---

[1] Russell, *Astrophysical Journal*, 54, 293, 1921.

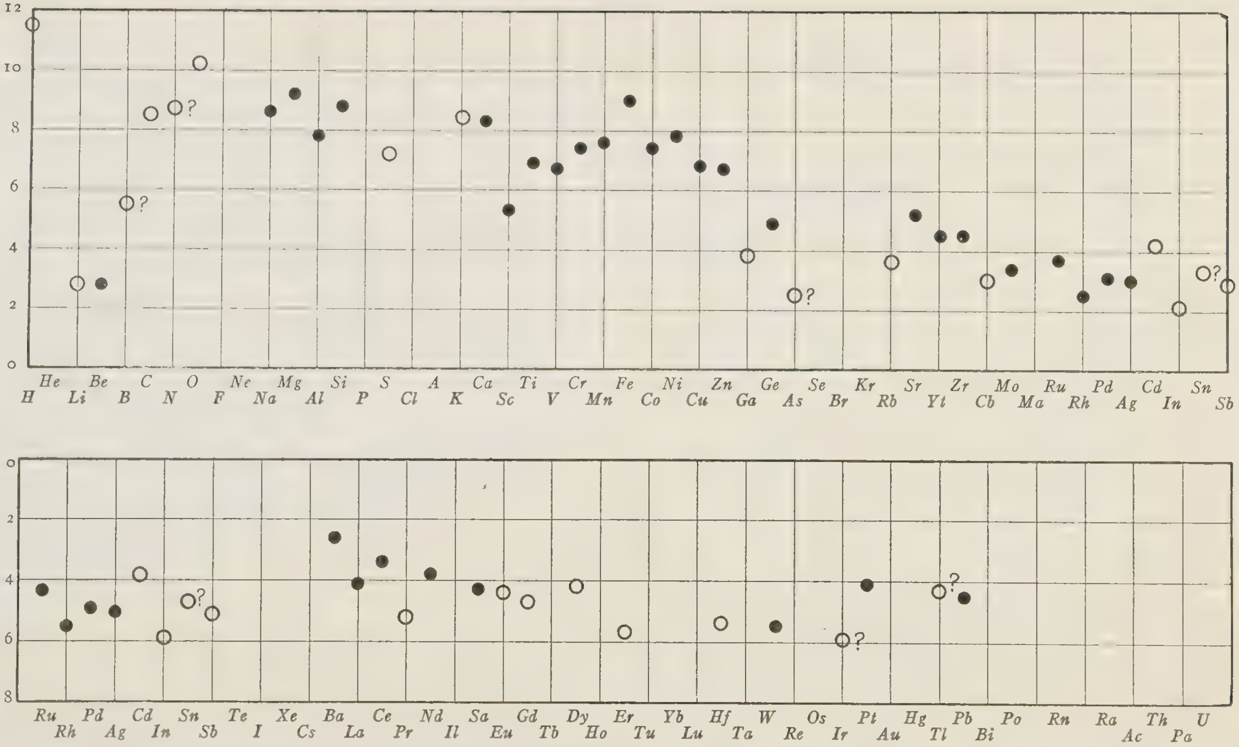

FIG. 3.—Values of log Q, where Q represents the total mass of the atoms or molecules of an element per unit area of the sun's surface.

element of even number except *Be* is more abundant than the mean of the adjacent elements, when both these are known, and every odd element less abundant, with the exception of *Eu*, for which the data are uncertain. For *Tl*, which also looks like an exception, they are still more doubtful. There is little doubt, however, that *Na* and *K* are real exceptions, for if *Ne* and *A*, which precede them, were anything like as abundant, we might expect them to show in the flash spectrum. The average difference between log *Q* for an even element and the mean for the two adjacent odd ones is +1.03 (14 cases), while for an odd element and the adjacent even ones it is −1.05 (15 cases). If the weaker determinations are excluded, these values become +0.86 for six even elements and −0.93 for ten odd ones. This indicates that the even elements are, on the average, about ten times as abundant as the odd. Among the rare earths and the heavier elements, only those with even atomic numbers have been conclusively identified in the sun. Certain elements stand out as rare in comparison with their neighbors—notably *Sc*, *Ga*, and *In*. These are well-known chemical rarities; it is surprising, however, to find *As* behaving in the same way. It may be that the estimated correction, which allows for the fact that all but weak lines of this element are inaccessible, was too small. The most striking examples of all are *Be* and *Li*. The latter is not ordinarily considered a rare element, but it is evidently present only in small proportions in the sun. The most abundant elements, compared with the mean of their neighbors, are *Fe* (and probably *Na* and *K*). If these individual differences are corrected for the general tenfold difference between odd and even elements, what remains is surprisingly small. *Sc* and *Ga* are one-twentieth and one-tenth as abundant as might be expected on this basis, and *Fe* only three times more abundant.

The abundance of an element is probably a function of yet unknown properties of the structure of the atomic nucleus. The results here obtained suggest that, in general, these properties change slowly and rather regularly with the nuclear charge. The very low abundance for *Li* and *Be* suggests that nuclei containing so few component parts may be hard to keep together. The amounts of the compounds which are present in the sun's atmosphere are surprisingly small. No one would have guessed, for example, that *CN* was but one-fifth as abundant as *Sc*. A moment's consideration, however, shows that molecules have a great advantage in the banded nature of their spectra. A single electron transition, which in an atom gives rise to at best but a very few multiplets, will, in a molecule, produce a whole system of bands, containing perhaps thousands of lines. The width of a line and the amount of light which it cuts out of the spectrum vary approximately as the square root of the number of atoms which are acting. To break up one strong line into a hundred faint ones increases tenfold the total effect on the spectrum—as much as a hundred fold increase in the number of atoms would do, if the original lines were unaltered.

For any atom which enters into one of these compounds, there are great numbers of the same kind in the free state. The values of log S for the combined atoms are, in fact, found to be 4.5 for C, 4.4 for N, 4.2 for O, and 3.3 for H. Those given in Table XIV for the free atoms exceed these by 2.9, 3.3, 4.8, and 8.2, respectively. On the face of the record, then, only one atom in a thousand, at most, enters into combination. This accords with the fact that the band spectra are at the point of disappearance in class G0. From the BO bands, which appear only in the spots, the amount of combined boron corresponds to log $S = 2.4$. For the free atoms it is probable that log $S = 5.5$ or perhaps more. This value has been plotted with a question mark in Figure 3. There is but one element known to exist in the sun for which no estimate of abundance has now been made—and this is He. The intensity of its lines in the chromosphere shows that it must be present in considerable amount, but no quantitative estimate seems possible.

The total quantity of the metallic elements (among which Si should be included for astrophysical purposes) in the solar atmosphere can be determined with considerable confidence from the spectrum. That of the non-metals is much less certain. It is fortunate, however, that the metals provide almost all of the ions and electrons. The values of S_1 in Table XIV indicate that the non-metals provide only 1/200 of the free electrons. If the correction for departure from thermodynamic equilibrium should be wholly disregarded, the calculated abundance of hydrogen—already very great—would be increased thirty fold; but even then the non-metals would provide only 13 per cent of the electrons. The table should therefore give a practically complete census of the charged particles in the atmosphere. Summing the values of S_1, we find, for the whole number of ions or electrons, 1.05×10^8 of our arbitrary units, or actually 6.3×10^{20} per square centimeter of the sun's surface. Six elements, *Na*, *Mg*, *Si*, *K*, *Ca*, and *Fe*, contribute 95 per cent of these. *Mg* alone accounts for nearly half the total; *Ca* for 5 per cent. The number of neutral atoms of the metals comes out 2.6×10^7 units, or 1.6×10^{20} atoms/cm². *Mg*, *Si*, and *Fe* contribute 96 per cent of the total. The whole number of metallic atoms in the solar atmosphere may therefore be taken as 8×10^{20} per square centimeter, of which 20 per cent are neutral and 80 per cent ionized.

The total mass of the metals is found to be 4.2×10^9 in our units, or 42 mg/cm². The mean atomic weight is 32. The six most abundant elements account for 94 per cent of the whole mass. The amounts of these elements in the solar atmosphere, as determined in the present work, are given for reference in Table XV. Those of the compounds are added at the bottom. This table brings out very clearly the extraordinary preponderance of the metals in the second short and the first long period. The only rare metal among these, *Sc*, is more abundant than any one of the heavier metals except *Ba*. For all these metals together the total mass is only 0.7 unit—much less than that of any metal in the favored region, except *Sc*. The "heavy metals," from *Ba* onward, appear to be somewhat less abundant than those from *Ge* to *Sb*, but this difference is relatively small. The extreme rarity of *Li* and *Be* is conspicuous. The correction factors for the non-metallic elements are too uncertain to justify their inclusion in the table. With the data as they stand, the number of atoms of *C*, *N*, and *S* together is 7.5×10^7 of our units—about half that for all the metals; that of oxygen is 10^9, and of hydrogen 3×10^{11}. By weight the abundances are 10^9 for *C*, *N*, and *S;* 1.6×10^{10} for *O;* and 3×10^{11} for *H*. It appears to be a safe conclusion that *C*, *N*, and *S* are not more abundant, either by number or by weight, than the commoner metals. The conclusion from the "face of the returns" is that *O* is four times, and *H* eighty times, as abundant by weight as all the metals together. These numerical values should not be stressed; but the great abundance of *H* can hardly be doubted. It is, however, very difficult to estimate it from the intensity of the Balmer lines. The great width of these may be partly due to Stark effect caused by the fields of neighboring ions or electrons.[1] This would make the lines stronger as well as wider; for the separate components into which the line is divided, if acting independently, would produce a greater total "absorption" than a single line. This should still happen even though the fields differ from atom to atom, so that the components are smeared into a diffuse line.[2] The tabular value, which is one-fifth of that calculated by Unsöld from the width of $H\alpha$, is already partially corrected.

TABLE XV

AMOUNTS OF THE METALS IN THE SOLAR ATMOSPHERE, BY WEIGHT
(Unit 100 mg per Square Meter)

Li	0.0006	*Zn*	5.	*Sb*	0.001:
Be	0.0006	*Ga*	0.006:	*Ba*	.25
Na	400.	*Ge*	.08	*La*	.008
Mg	1500.	*As*	.0003?	*Ce*	.04
Al	60.	*Rb*	.004:	*Pr*	.001:
Si	600.	*Sr*	.15	*Nd*	.015
K	250.:	*Yt*	.03	*Sa*	.005
Ca	200.	*Zr*	.03	*Eu*	.004:
Sc	0.2	*Cb*	.001:	*Gd*	.002:
Ti	8.	*Mo*	.003	*Dy*	.006:
V	5.	*Ru*	.005	*Er*	.0002:
Cr	25.	*Rh*	.0003	*Hf*	.0004
Mn	40.	*Pd*	.0012	*W*	.0003
Fe	1000.	*Ag*	.001	*Ir*	.0001:
Co	25.	*Cd*	.015:	*Pt*	.008
Ni	60.	*In*	*.0001:	*Tl*	.005?
Cu	6.	*Sn*	0.002?	*Pb*	0.003
CN	0.04	*CH*	0.012	*OH*	0.015
C_2	0.0005	*NH*	0.002	*BO*	0.0006

* Occurs in sun-spot spectrum only.

14. *Comparison with the results of other investigations.*—The most important previous determination of the abundance of the elements by astrophysical means is that by Miss Payne,[3] who determined, by Milne's method of marginal appearances, the relative abundance of

---

[1] Russell and Stewart, *Astrophysical Journal*, **59**, 197, 1924; Eddington, *Internal Constitution of the Stars*, p. 354, 1926.

[2] It may be noticed, in passing, that the effect should contribute toward the strengthening, in sun-spots, of lines which have complicated Zeeman patterns.

[3] *Stellar Atmospheres* ("Harvard Observatory Monographs," No. 1), Cambridge, Mass., p. 184, 1925; also *Harvard Observatory Bulletin*, No. 835, 1926.

eighteen of the most important elements. The arbitrary zero point to which they are referred differs from that adopted here, and comparison shows that this may be allowed for by adding 1.9 to Miss Payne's values of log a_r and 6.3 to those of her later paper. Taking the mean of her values when she has determined them for two or more stages of ionization, except that for He^+, which is uncertain, and comparing with log T from Table XIV, we find the results given in Table XVI. The value given for H in Table XIV is uncertain, while Miss Payne's value for K depends on the faint lines λλ 4044, 4047, and is therefore likely to be too low. If these two are rejected, the average difference, regardless of sign, for the other sixteen elements is ±0.44. This is a very gratifying agreement, especially when it is considered that Miss Payne's results were determined by a different theoretical method, with instruments of a quite different type (Harvard objective prisms), and even on different bodies—a long list of stars, almost all of which are giants. About the only common features are the observations of spectral lines and the use of the ionization theory.

TABLE XVI

COMPARISON WITH MISS PAYNE'S RESULTS

El.	Miss Payne	Table XIV	Diff.	El.	Miss Payne	Table XIV	Diff.
H........	12.9	[11.5]	(+1.4)	*Ca*......	6.7	6.7	0.0
He.......	10.2	....	....	*Ti*......	6.0	5.2	+0.8
Li.......	1.9	2.0	−0.1	*V*......	4.9	5.0	−0.1
C........	6.4	7.4:	−1.0	*Cr*......	5.8	5.7	+0.1
O........	8.0	9.0:	−1.0	*Mn*.....	6.5	5.9	+0.6
Na.......	7.1	7.2	−0.1	*Fe*......	6.7	7.2	−0.5
Mg......	7.5	7.8	−0.3	*Zn*......	6.1	4.9	+1.2
Al.......	6.9	6.4	+0.5	*Sr*......	3.5	3.3	+0.2
Si.......	7.5	7.3	+0.2	*Ba*......	3.0	3.3	−0.3
K........	5.3	6.8:	−1.5				

We may next compare the results with the abundance of the elements in the outer ten miles of the earth's crust,[1] including the ocean and atmosphere, and in stony meteorites.[2] The results are exhibited in Table XVII. Here 8.3 has been added to the logarithm of the percentage abundance in the earth's crust, and 8.0 to those for the meteorites, to reduce them approximately to the scale of log *Q*. For the more prominent metallic elements, the relative abundance in the sun resembles that in meteorites more closely than that in the earth's outer layers. The latter show an excess of *Al*, *Si*, and *Ti*, and a deficiency of *Mg*, which is probably due to the prevalence of granitic rocks. A deeper sample would be composed mainly of the heavy ferromagnesian rocks, and would show proportions more like those in the sun. The deficiency of the alkali metals in the meteorites is conspicuous, but unexplained.

---

[1] F. W. Clarke and H. S. Washington, *Proceedings of the National Academy of Sciences*, **8**, 114, 1922.

[2] G. P. Merrill, *ibid.*, **1**, 429, 1915.

TABLE XVII

ABUNDANCE OF ELEMENTS IN SUN, EARTH, AND METEORITES

El.	Sun	Earth	E−S	Meteorites	M−S	El.	Sun	Earth	E−S	Meteorites	M−S
Na.....	8.6	8.7	+0.1	7.8	−0.8	*Ni*.....	7.8	6.8	−1.0	8.2	+0.4
Mg....	9.2	8.6	−0.6	9.1	−0.1	*Cu*.....	6.8	6.3	−0.5	6.2	−0.6
Al.....	7.8	9.2	+1.4	8.2	+0.4	*Zn*.....	6.7	5.9	−0.8	....	......
Si.....	8.8	9.7	+0.9	9.3	+0.5						
K......	8.4:	8.7	+0.3	7.2	−1.2	*H*.....	11.5:	8.3	−3.2:	6.9	−4.6
Ca.....	8.3	8.8	+0.5	8.1	−0.2	*C*......	8.5:	7.4	−1.1:	7.2	−1.3
Sc.....	5.3	3. :	−2. :	....	......	*N*.....	8.7?	6.8	−1.9?	....	......
Ti.....	6.9	8.1	+1.2	7.0	+0.1	*O*......	10.2:	9.7	−0.5:	9.6	−0.6
V......	6.7	6.9	+0.2	....	......	*F*......	......	6.8	....	....	......
Cr.....	7.4	7.1	−0.3	7.5	+0.1	*P*......	......	7.4	....	7.0	......
Mn....	7.6	7.3	−0.3	7.3	−0.3	*S*......	7.2:	7.3	+0.1:	8.3	+1.1
Fe.....	9.0	9.0	0.0	9.4	+0.4	*Cl*.....	......	7.7	....	6.9	......
Co.....	7.4	5.8	−1.6	7.1	−0.3						

Among the non-metals, the figures for *N* are too uncertain to be of value. Those for *C*, *O*, and *S* indicate a considerable excess in the sun, or deficiency in the earth, while the difference for *H* is enormous. How much of this is real, and how much due to the uncertainties of the calculation, which are here greater than for any other element, is discussed in §16. It is noteworthy, however, that a discrepancy in this sense, and perhaps a very large one, might be anticipated in just this case. It is probable that the earth and the meteorites were formed by condensation from matter ejected from the sun, as first suggested by Chamberlin and Moulton. The ejected material must have been intensely hot, and would be likely to lose constituents of low atomic weight, hydrogen most of all. Moulton long ago suggested that the low density of the major planets might be explained by the hypothesis that such losses were less important for the larger bodies. In the outer parts of the sun, on the other hand, there are certain diffusional and electrostatic effects which tend to concentrate the hydrogen at the surface. Thus, for divers reasons, we might expect to find hydrogen much more abundant in the sun's atmosphere than on earth.

Table XVIII gives a comparison of the abundance of the less common elements in the sun and the earth arranged in order of their terrestrial abundance. For those in the first column, Clarke and Washington[1] give specific estimates of percentage. These all appear to be much more abundant on the earth than in the sun. It may be that *Ba*, *Sr*, and some of the others tend to segregate in the granitic surface rocks, as *Ra* is known to do. For the rest, the terrestrial data are rough estimates of the order of magnitude, which agree tolerably with the solar observations, except for the last few elements. It is likely that these, especially *Ga*, *In*, and *Ge*, are widely disseminated in quantities too minute to be detected by ordinary quantitative analysis, and the same is probably true of *Sc*.

TABLE XVIII

ABUNDANCE OF ELEMENTS IN SUN AND EARTH

El.	Sun	Earth	El.	Sun	Earth	El.	Sun	Earth
Ba........	5.4	7.2	*Rb*........	3.6:	4.5:	*Ag*........	3.0	2.5:
Zr........	4.5	7.0	*As*........	2.5:	4.5:	*Pt*........	3.9	1.5:
Sr........	5.2	6.8	*Mo*........	3.4	4.5:	*Tl*........	3.7?	0.5:
Ce, Yt.....	4.9	6.6	*Sn*........	3.3:	4.5:	*In*........	2.1:	−0.5:
Li........	2.8:	6.0	*Sb*........	2.9:	3.5:	*Ga*........	3.8:	−0.5:
Pb........	3.5	5.6	*Cd*........	3.6:	3.5:	*Ge*........	4.7	−1.5:
B.........	5.5?	5.3	*W*........	2.5	2.5:			
Be........	2.8	5.3	*Cb, Ta*....	3.0:	2.5:			

15. *Limits of abundance for elements absent from the solar spectrum.*—We are now in a position to compute superior limits, below which the abundance of the elements not represented in the solar spectrum must lie in order to account for their absence. It appears from Table XII that there are very few instances in which spectral lines are recorded as arising from a term for which the computed

---

[1] *Loc. cit.*

value of log M is less, algebraically, than -1. Adopting this as the limit of "visibility," we may find by (11) the numbers M_0 and M_1 of neutral and ionized atoms in the normal state (which, in the cases we have here to consider, are usually far greater than any others). If W_0 and W_1 are the weights of the normal states, we have, by (11), setting $M=-1$ for the state which fails to give observable lines:

$$\left.\begin{aligned}\log M_0&=\log W_0-\log W+0.85E-1\ ,\\ \log M_1&=\log M_0-\log W_0+\log W_1+I_0-I\ .\end{aligned}\right\}\qquad(12)$$

The limits thus calculated are given in Table XIX. The column headed λ gives the wave-length of the line most likely to appear. When a question mark appears in this column, the most persistent lines from the level under consideration are known to be in the deep red or infra-red, but have either not been analyzed or not observed at all. In these cases, lines in the visible spectrum should also be available, though they are often still unknown. Since these are second members of a series, the tabular values of log Q should be increased for them, probably by about 1. For B, P, and Cs the most promising lines of both the neutral and ionized atoms are included. In calculating log Q, account has been taken, when required, of the relative number of neutral and ionized atoms (log $M_1/M=-1.4$ for B, -2.2 for P, $+4.4$ for Cs, and $+0.5$ for Bi). For Os, which has many low energy-levels, it has been assumed that S_1+S_0 is five times the value of M_0 for the lowest level.

The reason for the absence of most of these elements from the solar spectrum is now perfectly clear. The lowest abundance necessary for the appearance of even their most favorable lines is usually far above the values indicated by their abundance on earth, or by that of elements of similar atomic number in the sun. Only a few cases need special mention.

Boron.—The infra-red lines 3s−3p should appear, but these are so far out as to be accessible only with the bolometer. The pair 3s−4p should be in the yellow and may perhaps be found in the sun, after it has been observed in the arc.

Phosphorus.—The infra-red lines should be near λ 10,000, and the same remark applies to them.

Caesium.—The tabular data refer to the sun's disk. According to our reckoning, the ultimate lines should appear in the spot spectrum, unless $\log Q < 3$. It may be noted, however, that the arc lines of *Ba* do not appear in the spots, although, for its normal state, $\log M = -0.2$. For Cs^+, the excitation potential is so high that there is no possibility of its lines appearing in the sun. The lines attributed to this element in the *New Rowland* must be accidental coincidences. For *Os* and *Bi* the limit is low, but not so much lower than the observed abundance of the other heavy elements as to cause any serious difficulty. The atomic number of *Os* is even, which makes its rarity somewhat surprising. For *Ra*, in fine, there is ample reason why the actual abundance should be far below the limit here computed.

TABLE XIX

LIMITS OF ABUNDANCE OF ELEMENTS NOT OBSERVED IN THE SUN

El.	λ	*E*	log *W*	log W_0	log *M*	log *Q*
He	5875	20.8	0.95	0.30	< 17.1	<17.7
B	?	4.9	0.30	.78	< 3.6	< 4.6
B^+	3541	9.1	0.48	.30	< 6.6	< 6.2
F	6856	12.6	1.08	.78	< 9.4	<10.7
Ne	6402	16.5	0.95	.30	< 12.3	<13.6
P	?	7.0	1.08	.60	< 4.5	< 6.0
P^+	5427	10.7	0.95	.95	< 10.0	< 9.3
Cl	8375	8.9	1.08	.78	< 7.2	< 8.8
A	8115	11.6	0.95	.30	< 9.1	<10.7
Se	?	6.0	0.70	.95	< 5.8	< 7.7
Br	?	8.0	1.08	.78	< 6.5	< 8.4
Kr	?	10.0	0.95	.30	< 7.8	< 9.7
Te	?	5.4	0.70	.95	< 4.9	< 7.0
I	?	6.7	1.08	.78	< 5.4	< 7.5
Xe	?	8.4	0.95	.30	< 6.4	< 8.5
Cs	8521	0.0	0.30	.30	<− 1.0	< 5.5
Cs^+	4603	15.	0.95	.30	< 11.1	<13.2
Os	3058	0.0	....	....	<− 1.0	< 1.7
Au	5837	4.6	0.30	.30	< 2.9	< 5.2
Hg	4046	4.6	0.00	.30	< 3.2	< 5.5
Bi	3067	0.0	0.60	.60	<− 1.0	< 1.9
Ra^+	3814	0.0	0.30	0.30	<− 1.0	< 1.3

The result of this survey is, therefore, that the absence of elements from the solar spectrum is completely explicable, quantitatively as well as qualitatively, by the structure of their spectra. In a few cases it is probable that the atoms under consideration are less abundant than others of similar atomic weight; but in no case is a great discrepancy necessary to explain the facts. For only two elements—boron and phosphorus—does there appear to be any chance of finding lines in the sun. In both cases, the anticipated lines must first be observed in the laboratory.

There are several additional elements whose presence or absence in the sun cannot at present be definitely determined for lack of laboratory data. These are *Ma*, *Il*, *Tb*, *Ho*, *Tm*, *Yb*, *Lu*, *Ta*, *Re*, *Th*, and *U*. All but *Yb*, *Th*, and *U* have odd atomic numbers. Progress for *Ta*, *Th*, and *U* demands the identification of the persistent lines, preferably by the under-water spark; for the rare earths, better wave-lengths are required; while for *Ma* and *Re* material for spectroscopic study is not yet available. Some of these metals may yet be found in the sun, but their lines are likely to be very faint.

IV. ASTROPHYSICAL CONSIDERATIONS

16. *The abundance of hydrogen and its consequences.*—The results of the present investigations leave some puzzles to be solved.

a) The calculated abundance of hydrogen in the sun's atmosphere is almost incredibly great.

b) The electron pressures calculated from the degree of ionization and from the numbers of metallic atoms and ions are discordant.

The former method (§11) gave a mean electron pressure $\bar{P}$ of 3.1 dynes/cm². Milne has shown that the pressure P at the bottom of the effective atmosphere should be twice this, or 6.2 dynes/cm². At the end of §13 we found that the total mass of metallic elements above this level is 42 mg/cm²; that the mean atomic weight is 32; and that 80 per cent of the atoms are ionized. At the sun's surface $g = 2.74 \times 10^4$ cm/sec.², so that the pressure due to the metallic constituents of the atmosphere is 1160 dynes/cm². If no other constituents were present, the electron pressure should be 4/9 of this, or 510 dynes/cm². One of these values is eighty times the other. A similar discrepancy occurs between Unsöld's value determined from the ionization of *Ca* and that calculated from his figures for its abundance,[1] and has also been detected in the redder stars by Miss Payne and Mr. Hogg.[2]

The assumption of a higher temperature for the solar atmosphere would diminish this discordance, but by no means remove it. The rather extreme assumption $T=5740°$ (the effective temperature of the photosphere) gives from ionization $P=50$ dynes/cm^2. A discordance by a factor of ten still remains.

c) We may add a difficulty arising from other solar observations. The calculated rate of increase of density with depth in the reversing layer is much more rapid than that indicated by observations of the flash spectrum.

It does not seem to have been noticed that the theoretical difficulties (*b*) and (*c*) can be greatly alleviated, if not removed, by the assumption that the difficulty (*a*) does not exist—in other words, the solar atmosphere really does consist mainly of hydrogen. The solution of (*c*) is obvious. The depth for which the density in an isothermal atmosphere is doubled varies inversely as the mean molecular weight $\bar{m}$. At the sun's surface (with $T=5000°$) it is $105/\bar{m}$ km. A small molecular weight accords much better with the eclipse observations. Menzel, for example, has made a brief report[3] on a determination of the law of decrease of density in the reversing layer by a study of lines in multiplets, which ought to give reliable values.

The writer is greatly indebted to Professor Menzel for permission to state that his unpublished reduction of the Lick Observatory eclipse spectra shows that, in the lower part of the reversing layer, the logarithmic decrement of density, if a temperature of 5000° is assumed, corresponds to a mean molecular weight of about 2.

If only hydrogen and the metals were present, this would determine the abundance of the former. Take the number of metallic atoms per square centimeter as unit, and let H be the number of hydrogen atoms. Since the hydrogen is not appreciably ionized, the whole number of atoms and electrons is then $H+1.8$, and we have $\bar{m}=(H+32)/(H+1.8)$, or for $\bar{m}=2$, $H=28.4$; hydrogen would therefore constitute more than 96 per cent of the atmosphere by volume, and nearly one-half by weight. Now let O and He be the numbers of the corresponding atoms. We have then

---

[1] Milne, *Nature*, **121**, 1017, 1928.

[2] *Harvard Circular*, No. 334, 7, 1928. It may be remarked in passing that the criticism which these authors pass (p. 8) on the method of calibration used by Dr. Adams and the writer appears to be needlessly severe, in view of the fact that lines of different elements were used in the two investigations and that there is no theoretical evidence that the effect in question ought to be the same for atoms of different kinds, and good observational evidence that it is not.

[3] *Popular Astronomy*, **36**, 603, 1928.

$$\bar{m}=(H+4He+16O+32)/(H+He+O+1.8)\ ,$$

and if $\bar{m}=2$,

$$H=28.4+2He+14O\ .$$

According to Table XIV, oxygen is four times as abundant by weight and eight times by volume as all the metals together. Miss Payne (Table XVI) makes it 1.5 times as abundant by volume as all the metals. This determination is probably better than ours, which suffers from difficulties in calibration, and we will assume $O=2$, whence $H=56+2He$. The abundance of helium is very hard to estimate, even in the stars, for its lines appear to be abnormally strong like those of hydrogen, though to a less degree. It is probably conservative to guess that it is at least as abundant as oxygen. Setting $He=2$, we have the results shown in Table XX. Here log T and log Q are on the scale of Table XIV. The other non-metals, C, N, S, etc., would probably add but little to the total. These estimates are provisional and will require revision when the density gradient in the flash spectrum is more accurately determined, when the oxygen lines in the deep red are better calibrated, and when—or if—the correction C for departure from thermodynamic equilibrium can be found with less uncertainty.

As they stand, these estimates go a long way toward resolving difficulty (b). The whole pressure due to the solar atmosphere as here contemplated is 4.1 times that due to the metals alone, or 4800 dynes/cm², which is almost 1/200 of an atmosphere, or 3.6 "mm" on the familiar barometric scale; but the electronic pressure is only 0.8/65.8 of this, or 58 dynes/cm². To obtain this value from the observed ionization we must assume $T=5800°$, which seems im-probably high; but none of the factors involved is determined with any great accuracy, and a tolerable adjustment could be made with a lower assumed temperature. It appears probable, however, that the temperature so far assumed for the reversing layer (5040°) is too low and should be increased to about 5600°. This would raise the computed level of ionization I_0 to 8.5 volts. The calculated ratio of the numbers of neutral and ionized atoms would be the same as before for $I=6.3$, the average for the elements used in finding I_0. For larger values of I (Mg, Fe, Si), the computed degree of ionization would be slightly increased, but as the changes would affect log A by 0.2 at most, there is no need to revise Table XIV. With the higher assumed temperature, the correction C for departure from thermodynamic equilibrium, determined from the enhanced lines as before, would be diminished from 1.2 to 0.4 when $E=8.2$, that is, from $0.15E$ to $0.05E$, and the computed abundances for the nonmetals would be practically the same as before. With regard to the intensity of the hydrogen lines, with log $T=9.9$, and $T=5600°$, equation (4) gives, for the two-quantum state, log $M=1.4$, and theoretically for $H\alpha$, $H\beta$, $H\gamma$, and $H\delta$, log $N=1.2$, 0.5, 0.0, and -0.3. The values of log N derived from Unsöld's line contours are 4.1, 3.9, 4.0, and 4.1. To obtain these contours the theoretical number of atoms must be increased by factors ranging from 800 for $H\alpha$ to 25,000 for $H\delta$. Effects peculiar to the hydrogen lines and increasing with the serial number evidently account for a great part of this discrepancy, but a good deal may remain to be set to the account of some more general departure from thermodynamic equilibrium.

TABLE XX

PROBABLE COMPOSITION OF THE SUN'S ATMOSPHERE

Element	By Volume	By Weight	log T	log Q
Hydrogen............	60 parts	60	9.9	9.9
Helium.............	2 ?	8?	8.4?	9.0?
Oxygen.............	2	32	8.4	9.6
Metals..............	1	32	8.1	9.6
Free electrons........	0.8	0	8.0	....
Total...........	65.8	132	....	....

17. *Note on the departure from thermodynamic equilibrium.*—Professor Eddington, in a letter which he has generously given permission to quote, makes a very important suggestion regarding the excess of intensity of lines of high excitation potential. This phenomenon, which is especially conspicuous when the redder giant stars are compared with the sun, was attributed by the writer[1] to a progressive increase in the number of excited atoms, compared with the number for thermodynamic equilibrium. Eddington writes:

> I am convinced that the right interpretation is exactly the opposite—that there are too few highly excited atoms. The argument is very simple, and the reason you differ is that you considered the formation of the line as a matter of absorption only without considering the emission. Suppose e.g. that the number of atoms in states
>
> 1, 2, 3, 4 . . . .
>
> were 1, 2, 4, 8 . . . . times the proper equilibrium numbers. Then considering the absorption line 3→4 you evidently have 4 times the equilibrium amount of absorption but 8 times the equilibrium amount of emission in this line. Naturally the excessive emission will tend to wash out the line and perhaps even make it a bright line. On the other hand if the numbers were
>
> 1, $\frac{1}{2}$, $\frac{1}{4}$, $\frac{1}{8}$ of the equilibrium numbers there is an actual loss of the 4→3 radiation (absorbed and not re-emitted in the same wave-length). This is much more effective in producing dark lines than the ordinary process of turning radiation backwards, which produces the line as a sort of second order effect.

Modifying the investigation in §§ 234–235 of *The Internal Constitution of the Stars*, he writes:

> Omitting ϵ for simplicity, but inserting a factor $\gamma(<1)$ representing reduced emission due to defect of atoms in the upper of the two states, I find instead of (235.4)
>
> $$H'=\alpha H\left(\frac{k}{k'}+\frac{p\left(1-\frac{k}{k'}\right)}{p+\frac{3}{2}}\,e^{-p\tau'}\right)$$
>
> where $$\alpha=\frac{k}{k'(1-\gamma)+\gamma k}\qquad p^2=\frac{3(k'(1-\gamma)+\gamma k)}{k'}\,.$$

---

[1] Adams and Russell, *Mt. Wilson Contr.*, No. 359; *Astrophysical Journal*, **68**, 20, 1928.

Retaining only the largest terms this gives at the boundary

$$H'/H = \tfrac{2}{3}\alpha p \qquad \text{(cf. [238.1])}$$

$$= \frac{2}{\sqrt{3}} \frac{k}{\sqrt{k'(k'(1-\gamma)+\gamma k)}} .$$

Thus for $\gamma = 1$

$$H'/H = \frac{2}{\sqrt{3}} \sqrt{\frac{k}{k'}}$$

for $\gamma = \frac{1}{2}$

$$H'/H = \frac{2}{\sqrt{3}} \sqrt{2} \frac{k}{\sqrt{k'(k'+k)}} = \frac{2}{\sqrt{3}} \sqrt{2} \frac{k}{k'}, \text{ approximately.}$$

Since $k' : k$ is large (ratio of absorption coefficients inside and outside the line) the latter gives much deeper blackening than the former.

I do not think you will need large deviations from the equilibrium proportions to account for your results, remembering that the introduction of differential emission and absorption is much more potent than a mere increase of both.

It seems much more easy to account for a defect of highly excited atoms than an excess—perhaps due to removal of the extreme ultra-violet radiation by continuous absorption which I expected would be shown in the sun's spectral energy curve though apparently the later determinations do not seem to bear it out. Again a spectrum of the principal lines of the element is being formed in the ordinary way and this, of course, means there is less radiation available to bring the atoms to the highly excited states. (It is, however, not obvious that this would give a *progressively decreasing* number in the higher states.) However, whether easily explicable or not, I think this is the immediate deduction from the results you have reached.

The importance of distortion of the sun's energy-curve has recently been pointed out by Gerasimovič,[1] who has shown that local weakening of the spectrum in the near ultra-violet, leaving the remoter part little affected, would lead to an excess of atoms in the highly excited states.

Such a distortion of the energy-curve seems improbable; but a progressive weakening in the remoter ultra-violet, beyond the region accessible to our observation, is more likely. The lines of the principal series beyond which general absorption might be expected to set in are at λ 2850 for *K*, λ 2420 for *Na*, and λ 2030 for *Ca*, and so on, and beyond these one would expect depression in the energy-curve similar to that which exists beyond the Balmer limit in A stars.

---

[1] *Monthly Notices, R.A.S.*, **89**, 272, 1929.

Another possibility deserves discussion. Compare a solar atmosphere composed solely of metallic atoms (neutral and ionized) and electrons with another which contains the same numbers of each of these constituents in each unit of volume diluted with an excess of hydrogen. The hydrogen atoms will be practically all neutral and almost inert, except that collisions between them and the excited metallic atoms will tend to bring the latter back to states of lower energy. In thermodynamic equilibrium, the effect would be balanced by excitation by collisions with fast-moving hydrogen atoms. In the reversing layer, however, the number of excitations by photospheric radiation exceeds that in an atmosphere in thermodynamic equilibrium, and it would appear that the intensity of a dark spectral line should be greater when most of these additional excited atoms are discharged by collisions of the second kind, than when they unload their energy by radiation. It is well known that the effective collision radii of excited atoms are large, and, if they increase, as is probable, for the more highly excited states, the differential effect which is observed might be accounted for.

This qualitative argument is not presented as conclusive, but in the hope that the problem will be attacked in detail by some competent investigator.

18. *A new case in Milne's ionization equations.*—Milne, in a very important paper,[1] has proved that under very varied conditions the ratio of the total numbers of neutral and ionized atoms of a given element above any specified level in a stellar atmosphere will be very nearly equal to that computed from a simple Saha formula, on the assumption of a mean pressure one-half of that at the base-level. The principal simplifications are that the atmosphere is treated as isothermal and radiation pressure is neglected. His Problem IV, in which the atoms considered are in presence of an excess of atoms of a different ionization potential, is similar to our present case, but in his solution, he assumes that practically all the electrons come from the ionization of the abundant element, which is not the case in a solar atmosphere rich in hydrogen. The general formulae

---

[1] *Ibid.*, p. 17, 1928.

are simple and may be given here. If N_0, N_1 are the numbers of neutral and singly ionized atoms of the first element per square centimeter above the given level, and $N = N_0 + N_1$, $x = N_1/N$, we have

$$\frac{N_1}{N_0} = \frac{x}{1-x} = \frac{K}{P} , \qquad x = \frac{K}{P+K} , \tag{13}$$

where K is the ionization factor, which is given in our notation by

$$\log_{10} K = -\frac{5040 I}{T} + \tfrac{5}{2} \log T - 6.5 , \tag{14}$$

and is constant, since the atmosphere is isothermal. Now let N', X', K', etc., refer to the atoms of the second element and let ϵ and $\epsilon' = 1 - \epsilon$ be the relative *numbers* of atoms of the two kinds and m the mean atomic weight. We have, then, for the total pressure, $p = (N+N')mg$, whence

$$N = \frac{\epsilon}{mg} p . \tag{15}$$

Milne has shown that

$$N_1 = \frac{\epsilon}{mg} \int_0^p x \, dp . \tag{16}$$

Now

$$\frac{p}{P} = 1 + \frac{1}{\epsilon x + \epsilon' x'} = 1 + \frac{(P+K)(P+K')}{P(\epsilon K + \epsilon' K') + KK'} = 1 + \frac{(P+K)(P+K')}{Q(P+R)}$$

where

$$Q = \epsilon K + \epsilon' K' , \qquad R = KK'/Q .$$

Hence

$$dp = dP + (P+K) d \, \frac{P(P+K')}{Q(P+R)} + \frac{P(P+K')}{Q(P+R)} \, dP .$$

Introducing this into (16), we find

$$N_1 = \frac{K\epsilon}{mg} \left\{ \log \left(1 + \frac{P}{K} \right) + \frac{P(P+K')}{Q(P+R)} + \frac{P}{Q} + \frac{1}{Q} \int_0^p \frac{P(K'-K-R) - KR}{(P+K)(P+R)} \, dP \right\} \tag{17}$$

$$= \frac{K\epsilon}{mg} \left\{ \frac{P(2P+K'+R)}{Q(P+R)} + \frac{K(Q-K)}{Q(K-R)} \log \left(1 + \frac{P}{K} \right) - \frac{R(K'-R)}{Q(K-R)} \log \left(1 + \frac{P}{R} \right) \right\} ,$$

$$N_1 = \frac{K\epsilon}{mg} \left\{ \frac{P(2P+K'+R)}{Q(P+R)} + \frac{\epsilon'}{\epsilon} \left[\log \left(1 + \frac{P}{K} \right) - \frac{R^2}{K^2} \log \left(1 + \frac{P}{R} \right) \right] \right\} . \tag{18}$$

With this and

$$N=\frac{\epsilon}{mg}\,P\left\{1+\frac{(P+K)(P+K')}{Q(P+R)}\right\}\,, \tag{19}$$

the general problem is solved.

We are concerned at present, however, with the case in which K' is negligibly small. Setting $K'=0$, we have $Q=\epsilon K$, $R=0$. Equation (17) still holds good, but the integral takes a different and much simpler form, giving

$$\left.\begin{aligned}
N_1&=\frac{1}{mg}\left\{2P-(1-\epsilon)K\log\left(1+\frac{P}{K}\right)\right\}\,,\\
N&=\frac{1}{mgK}\left\{\frac{P^2}{K}+(1+\epsilon)P\right\}\,,\\
N_0&=\frac{1}{mg}\left\{\frac{P^2}{K}-(1-\epsilon)P+(1-\epsilon)K\log\left(1+\frac{P}{K}\right)\right\}\,.
\end{aligned}\right\} \tag{20}$$

If we write $P/K=z$, the effective electronic pressure is given by

$$\overline{P}=\frac{KN_0}{N_1}=P\,\frac{z^2-(1-\epsilon)\{z-\log(1+z)\}}{2z^2-(1-\epsilon)z\log(1+z)}\,. \tag{21}$$

Whenever $\epsilon=1$, $P/P=\frac{1}{2}$. The greatest deviation from this ratio occurs when $\epsilon=0$ and z is about 3, when $P=0.535P$. The approximation $P=P/2$ is remarkably good under all circumstances.

19. *Applications to the stars.*—The assumption of an atmosphere composed mainly of hydrogen serves also to resolve some difficulties which appeared in the study of stellar spectra made last year by Adams and the writer.[1] The electronic pressures, computed from the relative strength of the arc and enhanced lines, came out about 10 times greater in Procyon and 60 times greater in Sirius than in the sun, while the amounts of metallic vapor above equal areas of surface were 0.6 and 0.05 times as great. Allowance for double ionization in Sirius would increase the last figure, but could hardly double it. It was then suggested that a great abundance of hydrogen in Sirius might explain these facts, but the full effect was not realized. At the temperature of an A star, hydrogen must be heavily ionized. If the hydrogen atoms are as abundant as has been sug-

---

[1] *Mt. Wilson Contr.*, No. 359; *Astrophysical Journal*, **68**, 9, 1928.

gested for the sun, there are dozens of them for every metallic atom, and, when a considerable fraction of these are ionized, the electronic pressure may be many times that which would arise from the ionization of the metallic atoms alone. At the same time, these electrons and the hydrogen ions contribute to the general opacity, so that the photosphere is raised and the total quantity of gas above it is much diminished, and the metallic lines are thus weakened.

Hydrogen must be extremely abundant in the atmosphere of the red giants, for its lines are stronger in their spectra than in that of the sun. With any reasonable allowance for the effect of the lower temperature in diminishing the proportion of excited atoms, the relative abundance of hydrogen, compared with the metals, comes out hundreds of times greater than in the sun. If this is true, the outer portions of these stars must be almost pure hydrogen, with hardly more than a smell of metallic vapors in it.

The theory of such an atmosphere presents an interesting problem, for quantities which are ordinarily neglected may have to be considered—for example, scattering by the unexcited neutral atoms. The effect of hydrogen in reducing the electronic pressure in the sun appears to be already near its limiting value, and it cannot be invoked further to account for the extraordinary discrepancy in these stars between the degree of ionization indicated by the enhanced lines and the pressure calculated from the extent of the atmospheres and the surface gravity. Discussion of these matters, however, cannot be undertaken in the present paper.

In conclusion, it should be emphasized that the present work, like that of Dr. Adams and the writer last year, is of the nature of a reconnaissance of new territory. It is to be hoped that the determinations made here by approximate methods will be replaced within a few years by others of much greater precision, based on accurate measures of the contours and intensities of as many lines as possible. An extensive field of work is open, and it is hoped that much more may be done at this Observatory.

It is a pleasure to express the writer's indebtedness for the use of the great mass of manuscript dealing with solar lines, multiplets, and the like, which has been collected by Dr. St. John and Miss

Moore; to Messrs. E. F. Adams and Theodore Dunham, Jr., for friendly aid in the tabulation of some of the material; and especially to Professor Eddington for the suggestion quoted in §17, and to Professor D. H. Menzel for the unpublished data mentioned in §16.

Carnegie Institution of Washington
Mount Wilson Observatory
February 14, 1929

TABLE XXI

References for Spectroscopic Data

Element	I	II	Element	I	II	Element	I	II
H......	1	....	*Fe*.....	4, 65, 95	4, 69	*Te*.....	55	....
He.....	1	1	*Co*.....	4, 21	4, 63	*I*......	93	....
Li.....	1	80, 96	*Ni*.....	4, 7, 75	4, 50, 83	*Xe*.....	6, 41	....
Be.....	10, 68	10	*Cu*.....	1, 81	4, 50, 82	*Cs*.....	1	....
B......	11, 78	9, 17	*Zn*.....	1	4, 94	*Ba*.....	1	1
C......	31	27, 32	*Ga*.....	1	49	*La*.....	5, 60	61
N......	23, 46	28, 30	*Ge*.....	34	51	*Ce*.....	5	....
O......	1, 43	73	*As*.....	56	....	*Pr*.....	5	....
F......	26	12	*Se*.....	1, 55	....	*Nd*....	5	....
Ne.....	3	74	*Br*.....	93	....	*Sa*.....	5	....
Na.....	1	16	*Kr*.....	6	....	*Gd*.....	5	....
Mg....	1	1	*Rb*.....	1	....	*Tb*.....	5	....
Al.....	1	66, 79	*Sr*.....	1	1	*Dy*....	5	....
Si.....	29, 33	29	*Yt*.....	62	62	*Yb*.....	5	....
P......	56	13	*Zr*.....	2, 48	2, 48	*W*.....	52, 53	....
S......	1, 18, 42	44	*Cb*.....	2	2	*Os*.....	59	....
Cl.....	24	14, 67	*Mo*....	45	2	*Ir*.....	59	....
A......	64, 77	22, 25	*Ru*....	88	....	*Pt*.....	40, 59	....
K......	1	15	*Rh*.....	89	....	*Au*....	91	....
Ca.....	1	4, 76	*Pd*.....	8, 84	86	*Hg*....	1	19
Sc.....	4, 70	4, 70	*Ag*.....	1	85	*Tl*.....	1	87
Ti.....	4, 72	4, 71	*Cd*.....	1	94	*Pb*.....	35	36
V......	4, 57, 63	4, 58	*In*.....	1	....	*Bi*.....	92	....
Cr.....	4, 48	4, 47, 48	*Sn*.....	37, 90	38	*Ra*.....	....	1
Mn....	4, 20	4	*Sb*.....	39, 54	....			

1. Fowler, *Report on Series in Line Spectra*, London, 1922.
2. Meggers and Kiess, *Journal of the Optical Society of America*, **12**, 417, 1926.
3. Paschen-Götze, *Seriengesetze der Linienspektren*, Berlin, 1922.
4. Russell, *Mt. Wilson Contr.*, Nos. 341 and 342; *Astrophysical Journal*, **66**, 184, 233, 1927.
5. Rolla and Piccardi, *Philosophical Magazine*, **7**, 296, 1929.
6. Abbink and Dorgelo, *Zeitschrift für Physik*, **47**, 221, 1928.
7. Bechert and Sommer, *Annalen der Physik*, **77**, 351, 1925; Bechert, *ibid.*, p. 537, 1925.
8. Bechert and Catalan, *Zeitschrift für Physik*, **35**, 449, 1925.
9. Bowen and Millikan, *Physical Review*, **26**, 310, 1925.
10. *Ibid.*, **28**, 256, 1926.

11. Bowen, *Physical Review*, **29**, 231, 1927.
12. *Ibid.*, p. 246, 1927.
13. *Ibid.*, p. 510, 1927.
14. *Ibid.*, **31**, 34, 1928.
15. *Ibid.*, p. 497, 1928.
16. *Ibid.*, p. 967, 1928.
17. Bowen, personal communication.
18. Bungartz, *Annalen der Physik*, **76**, 709, 1925.
19. Carroll, *Philosophical Transactions of the Royal Society*, A, **225**, 365, 1925.
20. Catalan, *ibid.*, **223**, 127, 1922.
21. Catalan und Bechert, *Zeitschrift für Physik*, **32**, 336, 1925; Catalan, *ibid.*, **47**, 89, 1928.
22. Compton, Boyce, and Russell, *Physical Review*, **32**, 179, 1928.
23. Compton and Boyce, *ibid.*, **33**, 145, 1929.
24. De Bruin and Kiess, *Science*, **68**, 356, 1928, and unpublished material.
25. De Bruin, *Zeitschrift für Physik*, **48**, 62, 1928; *Proceedings of the Amsterdam Academy*, **31**, 771, 1928.
26. Dingle, *Proceedings of the Royal Society*, A, **113**, 323, 1926; **117**, 407, 1928.
27. Fowler, *ibid.*, **105**, 299, 1924.
28. *Ibid.*, **107**, 31, 1925.
29. Fowler, *Philosophical Transactions of the Royal Society*, A, **225**, 1, 1925.
30. Fowler and Freeman, *Proceedings of the Royal Society*, A, **114**, 662, 1927.
31. Fowler and Selwyn, *ibid.*, **118**, 34, 1928.
32. *Ibid.*, **120**, 312, 1928.
33. Fowler, personal letter.
34. Gartlein, *Physical Review*, **31**, 782, 1928.
35. Gieseler and Grotrian, *Zeitschrift für Physik*, **39**, 377, 1926.
36. Gieseler, *ibid.*, **42**, 265, 1927.
37. Green and Loring, *Physical Review*, **30**, 574, 1927.
38. *Ibid.*, **31**, 151, 1928.
39. Green, *ibid.*, p. 707, 1928.
40. Haussmann, *Astrophysical Journal*, **66**, 333, 1927; discussed by A. G. Shenstone and J. J. Livingood, *Physical Review*, **34**, 185, 1929.
41. Hertz and Abbink, *Die Naturwissenschaften*, **14**, 648, 1926.
42. Hopfield, *Nature*, **112**, 437, 1923.
43. Hopfield, *Astrophysical Journal*, **59**, 114, 1924.
44. Ingram, *Physical Review*, **32**, 172, 1928.
45. Kiess, *Scientific Papers of the Bureau of Standards*, **19**, 113 (No. 474), 1923.
46. Kiess, *Journal of the Optical Society of America*, **11**, 1, 1925.
47. Kiess and Laporte, *Science*, **63**, 234, 1926.
48. Kiess, unpublished material.
49. Lang, *Physical Review*, **30**, 762, 1927.
50. *Ibid.*, **31**, 773, 1928.
51. Lang, *Proceedings of the National Academy of Sciences*, **14**, 32, 1928.
52. Laporte, *Die Naturwissenschaften*, **13**, 627, 1925.
53. O. Laporte and J. E. Mack, unpublished material (provisional value).
54. Malurkar, *Proceedings of the Cambridge Philosophical Society*, **24**, 85, 1927.
55. McLennan, McLay, and McLeod, *Philosophical Magazine*, **4**, 486, 1927.

56. McLennan and McLay, *Transactions of the Royal Society of Canada* (sec. 3), **21,** 63, 1927.
57. Meggers, *Journal of the Washington Academy of Sciences,* **13,** 317, 1923.
58. Meggers, *Zeitschrift für Physik,* **33,** 509, 1925; **39,** 114, 1926.
59. Meggers and Laporte, *Physical Review,* **28,** 642, 1926.
60. Meggers, *Journal of the Washington Academy of Sciences,* **17,** 25, 1927.
61. Meggers, *Journal of the Optical Society of America,* **14,** 191, 1927.
62. Meggers and Russell, *Bureau of Standards Journal of Research,* **2,** 733 (No. 55), 1929.
63. Meggers, unpublished material.
64. Meissner, *Zeitschrift für Physik,* **39,** 172, 1926; **40,** 839, 1926.
65. Moore and Russell, *Mt. Wilson Contr.,* No. 365; *Astrophysical Journal,* **68,** 151, 1928.
66. Paschen, *Annalen der Physik,* **71,** 142, 537, 1923.
67. *Ibid.,* p. 559, 1923.
68. Paton and Rassweiler, *Physical Review,* **33,** 16, 1929.
69. Russell, *Mt. Wilson Contr.,* No. 318; *Astrophysical Journal,* **64,** 194, 1926.
70. Russell and Meggers, *Scientific Papers of the Bureau of Standards,* **22,** 329 (No. 558), 1927.
71. Russell, *Mt. Wilson Contr.,* No. 344; *Astrophysical Journal,* **66,** 283, 1927.
72. Russell, *Mt. Wilson Contr.,* No. 345; *Astrophysical Journal,* **66,** 347, 1927.
73. Russell, *Physical Review,* **31,** 27, 1928.
74. Russell, Compton, and Boyce, *Proceedings of the National Academy of Sciences,* **14,** 280, 1928.
75. Russell, unpublished material.
76. Saunders and Russell, *Astrophysical Journal,* **62,** 1, 1925.
77. Saunders, *Proceedings of the National Academy of Sciences,* **12,** 556, 1926.
78. Sawyer, *Die Naturwissenschaften,* **15,** 765, 1927.
79. Sawyer and Paschen, *Annalen der Physik,* **84,** 1, 1927.
80. Schüler, *Zeitschrift für Physik,* **37,** 568, 1926.
81. Shenstone, *Physical Review,* **28,** 449, 1926.
82. *Ibid.,* **29,** 380, 1927.
83. *Ibid.,* **30,** 255, 1927.
84. Shenstone, *Nature,* **121,** 619, 1928, and personal communication.
85. Shenstone, *Physical Review,* **31,** 317, 1928.
86. Shenstone, *ibid.,* **32,** 30, 1928.
87. Smith, *Proceedings of the National Academy of Sciences,* **14,** 951, 1928.
88. Sommer, *Zeitschrift für Physik,* **37,** 1, 1926.
89. *Ibid.,* **45,** 147, 1927.
90. Sponer, *ibid.,* **32,** 19, 1925.
91. Thorsen, *Die Naturwissenschaften,* **11,** 501, 1923.
92. Thorsen, *Zeitschrift für Physik,* **40,** 642, 1926.
93. Turner, *Physical Review,* **27,** 397, 1926.
94. von Salis, *Annalen der Physik,* **76,** 145, 1925.
95. Walters, *Journal of the Optical Society of America,* **8,** 245, 1924, and unpublished material.
96. Werner, *Nature,* **115,** 191, 1925.

Contributions from the Mount Wilson Observatory, No. 384
Reprinted from the *Astrophysical Journal*, Vol. LXX, pp. 105–113, 1929
Printed in the U.S.A.

STEWARD
OBSERVATORY
TUCSON, ARIZONA

THE ELECTRIC-FURNACE SPECTRUM OF HAFNIUM

By ARTHUR S. KING

ABSTRACT

The spectrum of metallic hafnium has been examined from λ 2640 to λ 6500 in the carbon-tube *furnace* and compared with the spectra of the *arc* and *spark*. A list of *338 lines* includes the stronger neutral and ionized lines in this range. The usual *temperature classification* is given for the lines of the *neutral spectrum*, based on their relative intensities at 2900° and 2600° C. The lines which, judged by their relative intensities in arc and spark, belong to the *ionized atom* are *absent* from the furnace spectrum. The ionized lines are selected on the basis of their behavior in the three sources.

Attention is called to a *band spectrum* appearing in the arc in air and presumably due to the *oxide*. *Wave-lengths* are given for the *first head* in each of *nine groups* between λ 3200 and λ 5700.

The discovery of the element hafnium, by means of its Röntgen-ray spectrum, was announced by D. Coster and G. v. Hevesy[1] in January, 1923. During the same year, measurements of wave-lengths from λ 2254 to λ 7241 were published by H. N. Hansen and S. Werner.[2] A recent paper by W. F. Meggers[3] gave extended data on this spectrum, consisting of wave-lengths of nearly 1500 lines between λ 2155.72 and λ 9250.27, with their intensities in arc and spark. Regularities among the singly ionized lines were also found by Meggers and Scribner.[4] It was obviously desirable that the next investigation be made with the electric furnace in order to show the relative response of the lines to various excitations, and to render more definite the division of the spectrum into lines of the neutral and of the ionized atom.

It has been recognized since its discovery that hafnium is likely to be associated with zirconium to the extent of a fraction of 1 per cent, but the separation is difficult, and hafnium in any sort of purified form is still extremely scarce. The writer is greatly indebted to Dr. G. Holst, director of the Research Laboratory of the Philips

---

[1] *Nature*, **111**, 79, 1923.

[2] *Ibid.*, p. 322, 1923; **112**, 618, 900, 1923.

[3] *Bureau of Standards Journal of Research*, **1**, 151, 1928.

[4] *Journal of the Optical Society of America*, **17**, 83, 1928.

Lamp Works in Eindhoven, Holland, for his kindness in furnishing a small rod of highly purified hafnium for this work. No troublesome impurities were present in this sample, even the prominent lines of zirconium being quite faint.

EXPERIMENTAL METHOD

In these experiments, the furnace, arc, and spark spectra of hafnium were photographed within the range λ 2640 to λ 6500. A comparison of my results with those of Meggers shows that the neutral lines outside this interval are so faint that it is doubtful if the furnace can give useful data farther toward either the ultraviolet or the infra-red. The spectrograms from the ultra-violet to λ 4900 were made in the second order of the 15-foot concave grating (scale 1.86 A per millimeter), and beyond this in the first order.

In charging the furnace a thin graphite combustion boat containing fragments of hafnium was placed in the resistor tube. The metal was changed into a dark powder by the operation of the furnace, and the boat with its contents was used in successive tubes during the experiments. The melting point of hafnium has been measured in the Philips Laboratory as near 2400° C., and I found a temperature of 2600° necessary to bring out any considerable number of lines. Temperatures of 2900°–3000° were required to do justice to the neutral spectrum. Although at the highest of these temperatures some of the weaker arc lines were still absent from the furnace spectrum, 2600° and 2900° were taken as the two stages for the classification of furnace lines. Because of the high temperatures required, the Swan bands of carbon were always strong in the furnace spectrum, and occasionally masked the hafnium lines which would be expected to appear.

The electrodes used for the arc and spark were silver rods 6 mm in diameter, the lower having in its end a small piece of hafnium. A comparison of the arc of 4 amp at 220 volts with a very disruptive transformer spark served to distinguish clearly between the neutral and ionized lines, the former being very faint in the spark spectrum. As the lines enhanced in the spark, even when of considerable strength in the arc, were quite absent from the furnace spectrum, it was not possible to employ the usual test for enhanced lines of quenching them by a mixture of the substance in the furnace with one of lower ionization potential.[1] The selection of enhanced lines must therefore rest on their absence from the furnace and their strengthening in the spark; in nearly all cases, however, this effect was so definite that there is no likelihood of error in distinguishing them.

EXPLANATION OF THE TABLE

The first column contains Meggers' wave-lengths on the international system and also a few measurements by the writer of lines probably unresolved on Meggers' plates or disturbed by foreign lines. The neutral lines listed are those present in the furnace spectrum, or, if absent, are those of sufficient strength in the arc to make their absence at the furnace temperatures significant. Enhanced lines are included only when of considerable strength in the arc. Estimated intensities for the arc spectrum are in the second column. It must be remembered that the relative intensities of neutral and ionized lines, as groups, vary greatly in different spectrograms according to the arc conditions. On this account consistent relative intensities can be given only between the lines of each group. The columns of furnace intensities for 2900° and 2600°, respectively, show the relative response of the neutral lines to temperature change. In the fifth column, the usual temperature classification is held to as closely as possible, although it must be taken into account that hafnium lines are in general faint in the furnace spectrum, and that only two temperature stages were used. The data do not justify placing any lines in class I. Those emitted with fair strength at 2600° are put in class II, while lines appearing only at high temperature are in class III or class IV according to their relative strength in furnace and arc. Neutral lines absent from the furnace are placed in class V, while all enhanced lines are classed as V E.

An asterisk adjacent to a wave-length indicates that an explanatory note concerning this line is given at the end of the table. Disturbance by the band spectrum of carbon, which frequently conceals hafnium lines in the furnace spectrum, is denoted by a dagger.

---

[1] *Mt. Wilson Contr.*, No. 233; *Astrophysical Journal*, 55, 380, 1922.

TABLE I

Temperature Classification for Hafnium

λ (I.A.) (Meggers)	Arc Int.	Furnace Intensity		Class	λ (I.A.) (Meggers)	Arc Int.	Furnace Intensity		Class
		2900°	2600°				2900°	2600°	
2641.42....	100	......	......	V E	2866.38....	150	4	3	II
2642.07....	3	......	......	V	2876.33....	20	......	......	V E
2642.76....	5	......	......	V	2887.13....	15	......	......	V
2647.31....	60	......	......	V E	2887.54....	15	......	......	V
2657.85....	12	......	......	V E	2889.62....	80	4	2	II
2661.89....	20	......	......	V E	2898.26....	125	6	4	II
2668.28....	5	......	......	V	2898.71....	20	......	......	V E
2683.36....	30	......	......	V E	2904.42....	80	4	1	III
2696.18....	4	......	......	V	2904.76....	80	4	2	II
2699.63....	3	......	......	V	2909.91*...	20	......	......	V E
2705.62....	30	......	......	V	2916.49....	300	6	4	II
2712.43*...	40	......	......	V E	2918.58....	80	3	1	III
2713.84....	6	......	......	V	2919.59....	100	......	......	V E
2718.57....	8	......	......	V	2924.61*...	8	1	......	IV
2726.69....	2	......	......	V	2928.98....	2	......	......	V
2730.71....	2	......	......	V	2929.63*...	100	......	......	V E
2730.84....	4	......	......	V	2929.90....	40	......	......	V
2738.76....	100	......	......	V E	2937.80....	80	......	......	V E
2743.63....	6	......	......	V	2940.77....	200	10	8	II
2751.81*...	30	......	......	V E	2944.71....	15	2	......	III
2758.76*...	6	......	......	V	2950.68....	125	8	4	II
2761.62....	30	......	......	V	2954.21....	100	5	2	II
2766.96....	8	......	......	V	2958.02....	40	2	......	III
2773.01....	8	......	......	V	2964.88....	150	10	5	II
2773.37*...	150	......	......	V E	2966.95....	40	2	......	III
2774.02....	15	......	......	V E	2967.24....	20	......	......	V E
2779.36....	20	1	......	IV	2968.83*...	100	......	......	V E
2783.68....	2	......	......	V	2973.38....	6	......	......	V
2789.51....	3	......	......	V E	2975.90....	100	......	......	V E
2789.74*...	6	......	......	V E	2979.28....	8	......	......	V
2808.00....	20	......	......	V E	2980.82....	100	12	7	II
2813.86....	20	......	......	V E	2982.73....	8	......	......	V
2814.47....	15	......	......	V E	2984.06....	2	......	......	V
2817.68....	5	......	......	V	3000.10....	80	......	......	V E
2818.93....	3	......	......	V	3005.56....	100	3	......	III
2819.75....	8	......	......	V	3012.90....	200	......	......	V E
2820.23....	150	......	......	V E	3016.71*...	30	4	1	III
2822.67....	80	......	......	V E	3016.83*...	80	12	6	II
2833.29....	20	1	......	IV	3016.93*...	2	......	......	V E
2834.12....	3	......	......	V	3018.32....	80	15	8	II
2841.49...	2	......	......	V	3020.54....	100	10	5	II
2845.83....	20	......	......	V	3024.61....	4	......	......	V
2849.21....	30	......	......	V E	3025.29....	10	......	......	V E
2850.96....	25	......	......	V	3031.17....	100	......	......	V E
2851.21....	30	......	......	V E	3049.30....	2	......	......	V
2852.03....	8	......	......	V E	3050.76....	60	3	2	II
2860.56....	10	......	......	V	3054.52*...	6	......	......	V E
2861.01....	80	......	......	V E	3055.43....	3	......	......	V E
2861.69....	100	......	......	V E	3057.02....	100	12	4	II

TABLE I—*Continued*

λ (I.A.) (Meggers)	Arc Int.	Furnace Intensity		Class
		2900°	2600°	
3063.77*	6	—?	......	V ?
3064.68	8	......	......	V E
3067.41	80	10	4	II
3069.21	2	......	......	V
3072.88	300	20	15	II
3074.09	10	1	......	IV
3074.78	30	2	1	II
3080.63	60	......	......	V E
3080.84	80	8	3	II
3091.37	2	......	......	V
3092.25	8	......	......	V E
3096.76	15	2	1	II
3100.78*	2	......	......	V
3101.38	100	......	......	V E
3109.11	200	......	......	V E
3110.88*	20	......	......	V E
3119.97	10	1	......	IV
3126.65	4	......	......	V
3128.75	6	1	tr	III
3129.59	4	1	tr	III
3131.81	150	3	1	III
3134.72	300	......	......	V E
3137.52	8	......	......	V
3138.67*	8	......	......	V
3139.67	20	......	......	V E
3140.77	10	......	......	V E
3145.33	40	......	......	V E
3148.41	15	1	......	IV
3151.63	6	......	......	V
3152.96	2	......	......	V
3156.68	50	5	3	II
3159.83	30	8	4	II
3162.57*	80	15	10	II
3162.62*	15?	......	......	V E
3164.39*	12	3	1	III
3165.73	3	......	......	V
3168.39	20	1	......	IV
3172.94	100	10	5	II
3176.86	75	......	......	V E
3178.43	2	......	......	V
3179.63	2	......	......	V
3181.02	15	2	1	II
3181.13	8	1	......	III
3189.63	8	3	2	II
3193.53	75	......	......	V E
3194.20	200	......	......	V E
3196.92	10	1	tr	III
3200.00	12	......	......	V E
3206.11	25	3	2	II
3210.97	8	1	......	III
3217.30*	20	......	......	V E
3220.66	20	......	......	V E
3227.87	2	......	......	V
3230.07	4	......	......	V
3236.77*	8	......	......	V
3239.41	3	......	......	V
3243.36	4	......	......	V
3247.66*	20?	5	4	II
3249.53*	12	4?	2	II
3253.70	100	......	......	V E
3254.86	3	......	......	V
3255.29*	30	......	......	V E
3261.90	3	......	......	V
3262.47	5	......	......	V
3265.29	4	......	......	V
3267.01	3	......	......	V
3267.17	5	......	......	V
3273.66	8	......	......	V E
3291.04*	8	......	......	V E ?
3298.94	2	......	......	V
3306.12	10	2	2	II
3309.20	3	......	......	V
3310.27	25	4	3	II
3312.87	100	12	12	II
3316.18	2	......	......	V
3317.99*	6	......	......	V E
3328.21*	4	......	......	V E
3331.87	2	......	......	V
3332.73	200	20	20	II
3352.06	50	......	......	V E
3356.78	2	......	......	V
3358.95*	{2 5}	1	tr	III
3360.06	6	2	2	II
3366.68	3	......	......	V
3378.93*	{3 5}	1	1	II
3384.70*	3	......	......	V E
3386.21*	5	......	......	V
3389.83	80	......	......	V E
3392.81	4	......	......	V
3394.58*	10	......	......	V E
3394.99	3	......	......	V E
3397.26	8	2	1	II
3397.60	6	......	......	V
3399.80	300	......	......	V E
3400.21	8	5	3	II
3402.51	6	1	tr	III
3407.13	2	......	......	V
3407.76	3	......	......	V E
3410.18	6	......	......	V E
3412.38	2	......	......	V

TABLE I—*Continued*

λ (I.A.) (Meggers)	Arc Int.	Furnace Intensity		Class	λ (I.A.) (Meggers)	Arc Int.	Furnace Intensity		Class
		2900°	2600°				2900°	2600°	
3417.35	6	3	2	II	3849.52	5	......	......	V E
3419.18	12	4	2	II	3858.30	20	......	......	V
3428.36*	7	......	......	V E	3872.54	3	......	......	V E
3438.43	5	1	......	IV	3880.81	10	......	......	V E
3440.88	2	......	......	V	3889.24	4	......	......	V
3441.84	3	......	......	V	3889.33	4	......	......	V
3448.30	2	......	......	V	3899.93	20	8	4	II
3452.31	4	......	......	V	3918.10*	20	......	......	V E
3462.65	4	......	......	V E	3923.91	4	......	......	V E
3467.56	6	......	......	V	3931.36	10	......	......	V
3472.38	100	15	10	II	3951.81	12	4	......	III
3478.93	8	......	......	V E	3968.01	3	......	......	V
3479.28*	40	......	......	V E	4032.27†	6	4?	?	III ?
3484.71	1	......	......	V	4062.84	10	......	......	V
3495.75	10	......	......	V E	4080.44	8	......	......	V E
3497.16	8	......	......	V	4083.36	5	......	......	V
3497.49	150	20	12	II	4093.17*	40	......	......	V E
3505.23	100	......	......	V E	4113.58	3	......	......	V E
3523.02	60	12	4	II	4127.78	6	......	......	V E
3535.54	60	......	......	V E	4145.76	6	......	......	V
3536.62†	30	8	?	II ?	4162.40	5	......	......	V E
3552.70	20	......	......	V E	4162.68	4	......	......	V
3561.65	100	......	......	V E	4174.33†	50	15	5?	II
3567.36†	6	?	?	V ?	4177.50	4	......	......	V E
3569.03	50	......	......	V E	4206.57	5	......	......	V E
3599.87	8	......	......	V	4209.71†	8	1?	......	III ?
3616.89	30	8	4	II	4228.08	6	4	......	III
3630.86	8	4	2	II	4232.46	5	......	......	V E
3644.35	40	......	......	V E	4249.33	2	......	......	V E
3649.09	10	4	......	III	4260.96	8	......	......	V
3661.05	2	......	......	V E	4263.41	10	6	......	III
3665.36	6	......	......	V E	4272.84	8	......	......	V E
3672.28	6	......	......	V	4294.77	30	8	4?	II ?
3675.74	10	......	......	V	4318.13†	6	3?	?	III ?
3682.25*	200	30	20	II	4320.67	3	......	......	V E
3696.52	5	3	......	III	4330.27	8	......	......	V
3699.73	5	......	......	V E	4336.65	10	......	......	V E
3701.15	6	......	......	V E	4350.50	8	......	......	V E
3717.80	40	15	5	II	4356.29	20	—?	—?	V ?
3719.27	40	......	......	V E	4367.89	2	......	......	V E
3733.78	15	4	......	III	4370.92*	10	......	......	V E
3746.80	10	1	......	III	4417.35	8	......	......	V E
3768.25†	4	3	—?	III ?	4417.90	10	4	......	III
3777.64	50	10	8	II	4422.75	3	......	......	V E
3785.46†	30	—?	?	IV ?	4438.02	20	3	......	III
3793.37	20	......	......	V E	4457.35*	12	3?	......	III
3800.39†*	10	?	......	IV ?	4461.17	15	3	......	III
3811.76	8	3	......	III	4540.92	20	3	......	III
3820.74†	50	5?	?	III ?	4565.94	20	2	......	III
3830.01	6	......	......	V	4598.80*	25	4?	......	III ?
3849.17	25	......	......	V	4598.92*	20	......	......	V

TABLE I—*Continued*

λ (I.A.) (Meggers)	Arc Int.	Furnace Intensity		Class	λ (I.A.) (Meggers)	Arc Int.	Furnace Intensity		Class
		2900°	2600°				2900°	2600°	
4620.87....	25	2	......	III	5294.87†...	12	?	......	III ?
4655.19†...	30	3?	?	III ?	5298.06....	5	......	......	V E
4664.13....	5	......	......	V E	5309.68....	2	......	......	V
4699.01....	4	......	......	V	5311.60....	8	......	......	V E
4782.75....	8	......	......	V	5354.73....	8	5	......	III
4800.50....	25	4	3	II	5373.86....	20	15	2	II
4859.23....	4	......	......	V	5389.33†...	3	?	......	V ?
4934.44....	2	......	......	V E	5452.92†...	10	2?	......	III ?
4948.94....	3	......	......	V	5550.60†...	50	?	?	III ?
4975.25....	25	4	......	III	5552.12†...	40	?	?	III ?
5018.20....	8	8	2	II	5613.27....	10	2	......	III
5040.82....	10	......	......	V E	5719.18....	40	5	......	III
5047.45†...	15	5?	?	III ?	5890.45†...	2	?	......	V ?
5079.63....	2	......	......	V E	5902.94....	15	8	......	III
5157.96†...	6	?	?	?	5974.28†...	4	?	......	V ?
5170.18....	5	......	......	V	6098.67....	3	......	......	V
5181.86....	40	30	4	II	6185.13†...	5	4?	......	III ?
5243.99....	15	2	......	III	6248.96....	2	......	......	V E
5275.04....	4	2	......	III	6386.23†...	6	6?	?	III ?

NOTES TO TABLE I

λ	
2712.43	Moderately enhanced. *Zr* II λ 2712.41 not same line.
2751.81	May be blend with *Hf* I.
2758.76	Measured by writer. *Zr* λ 2758.82 on red edge.
2773.37	Weaker *Hf* II line to red.
2789.74	Weaker *Hf* II line to red.
2909.91	Moderately enhanced.
2924.61	Not *Zr* II λ 2924.64.
2929.63	Moderately enhanced.
2968.83	Weaker *Hf* II line to red.
3016.71 3016.83	Measured by writer. Doublet given by Meggers as λ 3016 78.
3016.93	Moderately enhanced.
3054.52	Moderately enhanced.
3063.77	Blend *V* in furnace.
3100.78	Blend faint *Hf* II line.
3110.88	Measured by writer.
3138.67	Measured by writer. Coincides *Zr* II λ 3138.68.
3162.57 3162.62	Blended in arc.
3164.39	Measured by writer. *Zr* λ 3164.32 to violet.
3217.30	Moderately enhanced.
3236.77	Measured by writer.
3247.66	Measured by writer. Close to *Cu* line.

λ	
3249.53	Blend *Ti* in furnace.
3255.29	Moderately enhanced.
3291.04	Coincides with hazy line in spark. Meggers' intensities indicate *Hf* II.
3317.99	Moderately enhanced.
3328.21	Moderately enhanced.
3358.95	Double.
3378.93	Double.
3384.70	Moderately enhanced.
3386.21	Measured by writer. Not *Ag*.
3394.58	Measured by writer. Moderately enhanced.
3428.36	Moderately enhanced.
3479.28	Moderately enhanced.
3682.25	*Ag* line to red.
3800.39	Faint *Hf* II line to red.
3918.10	Moderately enhanced.
4093.17	Moderately enhanced.
4370.92	Measured by writer.
4457.35	Blend *Ti* in furnace.
4598.80	Measured by writer. Doublet given by Meggers as λ 4598.86. Disturbed by carbon.
4598.92	

DISCUSSION

Features of the line spectrum.—The results here given, if used in connection with those of Meggers, serve to show the excitation required for the production of individual hafnium lines. In the range common to the two investigations, the observations are in close agreement. Lines which I have assigned to the neutral spectrum, through the comparison of furnace, arc, and spark, are given by Meggers as much weaker in the spark than in the arc; while in Meggers' list the lines I have classed as ionized are stronger in the spark than in the arc, or, in some cases, nearly equal in the two sources. From this relation between the two sets of data, the more extended table of Meggers may be used to classify the lines which I have not listed. The strong line λ 4093.17, which Meggers considers as neutral, does not appear in the furnace, and, I believe, on account of its high spark intensity should be placed among the enhanced lines. It belongs to a group in the region of shorter waves shown by the relative intensities of Meggers, confirmed by my spectrograms, to be enhanced in the spark much less than the majority of the enhanced lines. An origin of low energy-level in the ionized atom is thus indicated. The fainter enhanced lines appearing in the arc, usually much strengthened in the spark, are omitted from my list, as are numerous neutral lines too faint to be expected in the furnace spectrum. The furnace gives a number of lines, however, which are also among the weaker arc lines. This fact has justified the inclusion of neutral lines whose absence from the furnace and moderate intensity in the arc indicate that high excitation is required for their production. A large range of intensity is found among neutral lines in the arc, while in the furnace, probably on account of the small quantity of the substance and its high vaporization point, the lines are for the most part faint. The prominent hafnium lines, both neutral and ionized, are in the near ultra-violet. With some exceptions, such as λ 5181.86, the production of neutral lines in the furnace becomes increasingly difficult toward greater wave-length.

Band spectrum.—A set of bands occurring in the hafnium arc spectrum may be noted. These show well-defined structure, in all cases degraded toward the red. The more prominent heads have been measured by Meggers. The following list gives the head of shortest wave-length in each group.

λ	λ	λ
3236.09	3840.03	4252.05
3327.82	3970.06	5074.71
3654.26	4101.16	5698.04

The writer measured λ 3236 and λ 4101, the first of which is absent from Meggers' list and the second disturbed by a foreign line on his plates. The heads given above are usually the strongest in their respective groups, but the λ 4101 system has a stronger head at λ 4118.91.

These bands are in all cases absent from the spectrum of the vacuum furnace. As they appear in the arc in air when the metal is vaporized, the evidence is strong that they belong to the oxide spectrum.

Carnegie Institution of Washington
Mount Wilson Observatory
May 1929

Contributions from the Mount Wilson Observatory, No. 385
Reprinted from the *Astrophysical Journal*, Vol. LXX, pp. 160–194, 1929
Printed in the U.S.A.

ELEMENTS UNIDENTIFIED OR DOUBTFUL IN THE SUN

SUGGESTED OBSERVATIONS

By CHARLES E. ST. JOHN

ABSTRACT

Elements unidentified in the sun.—Argon, actinium, arsenic, gold, bismuth, bromine, chlorine, fluorine, mercury, iodine, iridium, krypton, masurium, neon, osmium, phosphorus, protoactinium, polonium, radium, rhenium, radon, selenium, tantalum, tellurium, thorium, uranium, xenon, and the rare earths, holmium, illinium, lutecium, terbium, and thulium.

Elements suggested for laboratory investigation.—Arsenic, iridium, osmium, phosphorus, tantalum, thorium, thallium, uranium and the rare earths. Study of these elements promises immediately useful information.

Data required.—(*a*) For immediate application to problems of identification we need accurate determinations of the wave-lengths of critical lines and a study of their relative intensities and appearance under varied conditions of excitation. (*b*) For general purposes we require precision wave-lengths throughout the spectral ranges of the different elements, preferably in vacuum, and analyses of the respective spectra

The identification and characteristic behavior of the Fraunhofer lines in the sun's spectrum deserve special attention and study, not only because the sun is of more immediate importance to us than any other star, but also because its position midway between the terrestrial laboratories and the stars is unique and therefore strategic. The intensity of radiation reaching the earth enables us to use instruments of observation and analysis equal to those in the laboratory and thereby furnishes the means of obtaining accurate data and testing quantitatively theories and assumptions. It was in anticipation of the advantages assured by a co-ordinated attack through laboratory, sun, and stars that the threefold organization at Mount Wilson arose.

In the preparation of tables of data on the solar spectrum astrophysicists of today have at hand methods and lines of attack undreamed of a generation ago. These may vary for individual elements, but for all there should be reasonable agreement in the position of solar and laboratory lines, so-called coincidence. We know now that exact coincidence is the exception and, when exact, points to possible errors of observation. As a rule, the departures from coincidence are positive for λ sun *minus* λ arc in vacuum and of the order of 0.01 A. Though close agreement in wave-length offers usually a first line of attack, this is not always the case. Not infrequently the approach has come through an analysis of the spectrum which has shown just what to look for and where to look; for example, the oxygen doublet in the infra-red.

Identifications of elements represented by few solar lines resting upon coincidences alone are subject to much uncertainty through accidental agreements in wave-length. In such cases considerations based upon atomic theory have been the determining factors.

Spectral lines are associated with the transitions of an atom between two energy-levels or spectroscopic terms which depend upon the configurations of the outer electrons. In the case of absorption the work required to raise the energy of the atom in its normal state to the lower of the two levels of the transition is the excitation potential for the line. It is measured in "volts," the "volt" being the energy acquired by an electron in falling through a difference of potential of 1 volt. For any element the absorption lines arising from transitions between the lowest and the next higher level, the resonance lines, are the strongest and the most probable to occur in the sun, provided they are in the region of the spectrum accessible to observation, viz. to the red of λ 2975 A. If these are not within the accessible region, then those from the next level are the most probable. The excitation potential is the important factor in determining the probability of the presence of a line in the spectrum.

The identification in the sun of the stronger lines of a multiplet facilitates the identification of the weaker members through the knowledge of their positions and relative intensities. It is a great gain to know for what to look and with what we need not bother. If the strong lines of a multiplet are absent or only weakly represented, the faint members may safely be neglected.

Fifty-eight of the 90 known elements appear with varying degrees of probability to be constituents of the sun's atmosphere (Table I). A brief examination of the elements not yet identified in the sun will indicate the possibilities for increasing the identified list and the new observational data most likely to prove of value for the purpose.

In the group of inert gases (Table II) the systematic decrease of the ionization and excitation potentials and the shift of the resonance region to longer wave-length with the increase of atomic number illustrate the progression so marked in the second half of columns IV–VIII in the periodic table and appearing later in Tables III, IV, and V.

For the inert gases the resonance lines begin far in the ultraviolet, and even for radon do not fall within the accessible region; and comparisons with solar absorption lines in the accessible regions (fifth column, Table II), do not show agreement in wave-length for any of these elements. The question of inexact data does not enter, for the wave-lengths of neon, argon, krypton, and xenon are known to the highest precision.[1] The non-appearance of these elements in the sun's spectrum is probably due to the combined effect of high excitation potential and very moderate abundance. The great majority of solar lines are due to the metals, and for them the mean

TABLE I

ELEMENTS IDENTIFIED IN THE SUN AND THEIR POSITION IN THE PERIODIC TABLE

(Unidentified Elements in Parentheses)

I	II	III	IV	V	VI	VII	VIII			
H	....	....	....	....	....	....	*He*			
Li	*Be*	*B*	*C*	*N*	*O*	(*F*)	(*Ne*)			
Na	*Mg*	*Al*	*Si*	(*P*)	*S*	(*Cl*)	(*A*)			
K	*Ca*	*Sc*	*Ti*	*V*	*Cr*	*Mn*	....	*Fe*	*Co*	*Ni*
Cu	*Zn*	*Ga*	*Ge*	(*As*)	(*Se*)	(*Br*)	(*Kr*)			
Rb	*Sr*	*Y*	*Zr*	*Cb*?	*Mo*	(*Ma*)	....	*Ru*	*Rh*	*Pd*
Ag	*Cd*	*In*	*Sn*?	*Sb*	(*Te*)	(*I*)	(*Xe*)			
Cs	*Ba*	*La**	*Hf*	(*Ta*)	*W*	(*Re*)	....	(*Os*)	(*Ir*)	*Pt*
(*Au*)	(*Hg*)	*Tl*?	*Pb*	(*Bi*)	(*Po*)	85	(*Rn*)			
87	(*Ra*)	(*Ac*)	(*Th*)	(*Pa*)	(*U*)	....	.....			

* RARE EARTHS

Ce	*Pr*	*Nd*	(*Il*)	*Sa*	*Eu*	*Gd*
(*Tb*)	*Dy*	(*Ho*)	*Er*?	(*Tu*)	*Yb*?	(*Lu*)

---

[1] Burns, Meggers, Merrill, *Bureau of Standards, Scientific Papers*, **14**, 765 (No. 329), 1919; Meggers, *ibid.*, **17**, 193 (No. 414), 1921.

excitation potential for neutral atoms is 1.319 volts, with a maximum, in the case of lead, of 5.771 volts. The maximum line intensity for lead is −2, the next to the faintest observable. The inert gases, with still higher excitation potentials, would need to be far more abundant than lead to produce even the faintest observable lines. Hence absence of their lines from the solar spectrum is not surprising and does not forbid their presence in the solar atmosphere with an abundance comparable to that in the earth.

TABLE II

INERT GASES

Atomic Number	Element	I.P.	Resonance Lines	Accessible Lines	E.P.	Identification
2	Helium	24.48	584.4	5875	20.871	*He*
10	Neon	21.47	735.95 743.73	3369–8495 55 lines	16.54	......
18	Argon	15.69	1048.21 1066.62	3948–8521 50 lines	11.50	......
36	Krypton	13.9	1164.90 1235.87	4273–7601 18 lines	9.9	......
54	Xenon	12.1	1295.65 1469.67	4500–4923 12 lines	8.2	......
86	Radon	....	2842.1* 2892.7*	4166.5† 4203.3†	....	......

* Strongest ultra-violet lines (S. Wolf, *Zeitschrift für Physik*, **48**, 790, 1928).

† Strongest and most persistent lines in the accessible region (T. Royds, *Philosophical Magazine*, **17**, 202, 1909; H. E. Watson, *Proceedings of the Royal Society*, A, **83**, 50, 1910).

For radon (radium emanation) accurate wave-lengths are not available. Radon is the most radioactive element and has an average life of 5.57 days.[1] It is an immediate product of radium, and its radioactive change evolves helium, polonium, and eventually lead. Unless in equilibrium with its mother-substances, it is rapidly dissipated; hence until thorium, uranium, and radium are detected in the sun, it would be vain to look for radon.

The remaining inert gas is helium. In spite of its high excitation potential of 20.871 volts, the helium line λ 5875 occurs in absorption in highly disturbed regions, and with other helium lines it is prominent in the flash spectrum. More surprising still is the presence of the enhanced line λ 4686 in the flash spectrum, requiring as it does an excitation of 72.57 volts. In view of its high excitation potential, it is obvious that helium must be present in abundance, as is indeed shown by the great height, 8000 km, to which it extends on photographs of the flash spectrum. The behavior of helium suggests causes of excitation in the sun's atmosphere not yet brought to light.

---

[1] F. Soddy, *Interpretation of Radium* (London, 1922), p. 113.

Passing to the left in the periodic table to the halogens, we find a similar situation (Table III). The resonance lines are in the inaccessible ultra-violet region, and only for fluorine and chlorine have arc lines of the next energy-level been identified. These, the most probable lines, are in the red and infra-red. Their excitation potentials are high in comparison with those of other non-metals represented in the sun by weak lines alone. They show no systematic agreement in position with solar lines, though occurring in spectral regions where agreements should be easily evident since the solar lines are not closely crowded. The arc wave-lengths have recently been measured to three decimals for fluorine[1] and to two places for chlorine.[2] Lines of bromine and iodine of the indicated excitation potential are theoretically possible in the visible region, but have not been observed.

TABLE III

HALOGENS

Atomic Number	Element	I.P.	Region of Resonance Lines	Most Probable Lines	E.P.
9..........	Fluorine	17.3	951–958	6239–6413 6774–6909 7256–7745	12.5
17..........	Chlorine	12.8	1335–1689	7980–8585 8948–9702	8.5
35..........	Bromine	11.4	1232–1633	....	7.5
53..........	Iodine	10.2	1234–2062	....	6.0

The data on band spectra of the halogens are too meager for profitable discussion. There is no evidence, and no present prospect of evidence, based on their spectra to show the presence of the halogens in the sun; nor are they found in the stars. In view of their abundance in the earth, their absence from the sun would be surprising. The failure to detect them is not inconsistent with their presence in the sun, for they would need to be very abundant in order to produce observable absorption lines in accessible spectral regions, as their excitation potentials are so high. The ozone in the upper reaches of the earth's atmosphere blocks appeal to the lines from the lowest energy-levels.

---

[1] H. Dingle, *Proceedings of the Royal Society*, A, **113**, 323, 1926; **117**, 407, 1928; T. L. de Bruin, *Amsterdam Academy Proceedings*, 30, 944, 1927; I. S. Bowen, *Physical Review*, **29**, 231, 1927.

[2] L. A. Turner, *Physical Review*, **27**, 401, 1926.

TABLE IV

OXYGEN GROUP

Atomic Number	Element	I.P	Resonance Lines	Accessible Lines	E.P.	Identification
8.........	Oxygen	13.56	1358	7774 8446	9.106 9.479	*O* Triplet *O* Doublet
16..........	Sulphur	10.31	1900	9224	6.496	*S* Triplet
34.........	Selenium	9.4	2050	....	6	....
52.........	Tellurium	8.7	2375	....	5.6	....
84.........	Polonium	....	Radioactive, average life 202 days			....

Of the oxygen group (Table IV), both oxygen and sulphur have been included as present in the sun's atmosphere. For selenium and tellurium the most probable lines would be farther to the red than for oxygen and sulphur, but nothing is known of their arc spectra in this region. McLennan, McLay, and McLeod[1] give one line of neutral tellurium in the ultra-violet at λ 3175.15 of intensity 3 on a scale of 20 R for the strongest resonance line λ 2142.75. There is an unidentified solar line at λ 3175.166 of intensity −3, giving, sun *minus Te* arc, +0.016 A, but without additional support this near coincidence for a single line can hardly be accepted as identifying it in the sun.

Polonium, being radioactive, would not be expected as long as thorium and uranium, the mother-elements, are unidentified, particularly in view of its short average life of 202 days.

---

[1] *Philosophical Magazine*, 4, 486, 1927.

The evidence for atomic nitrogen (Table V) in the sun's atmosphere is given by the three strongest lines of the $P-D^\circ$ quartet in the infra-red, λλ 8680.35, 8683.61, and 8686.38. These lines are from the next to the lowest energy-level, and within the errors of observation they agree in position with solar lines of intensities −2 to −1 not otherwise identified. Some doubt of the solar identification existed owing to the apparent absence of λ 8683 from the solar spectrum, but this has been dissipated, as the line has recently been measured upon a half-dozen spectrograms taken by Mr. Babcock in his extended investigation of the infra-red solar spectrum.

TABLE V

NITROGEN GROUP

Atomic Number	Elements	I.P.	Resonance Lines	Most Probable Lines	E.P.	Identification
7	Nitrogen*	14.2	1200	8680 8683 8686	10.0	*N*
15	Phosphorus	10.5	1781	9000–11,000	7	....
33	Arsenic	9.6	1972	3000	6.2	....
51	Antimony	8.35	2311.50	3100	2.024	*Sb*
83	Bismuth	7.25	3067.69	2989–4722	0.000	....

* C. C. Kiess, *Journal of the Optical Society of America*, **11**, 1, 1925; Merton and Pilley, *Proceedings of the Royal Society*, A, **107**, 411, 1925; Hopfield, *Physical Review*, **27**, 801, 1926; O. S. Duffenback and R. A. Wolfe, *Physical Review*, **34**, 409, 1929; S. B. Ingram, *ibid.*, p. 421, 1929.

For an element with the high excitation potential of nitrogen, viz., 10 volts, only a small fraction of its atoms in the sun's atmosphere would be excited to the energy states required for the production of its absorption lines. The presence in the solar spectrum of lines due to nitrogen implies therefore that the total amount is large. The abundance of nitrogen indicated in the sun is consistent with its abundance in the earth and its wide distribution in stars and nebulae.

The resonance lines of phosphorus[1] are in the far ultra-violet, and no arc lines are known in the visible region. There are, as for all of this group, possible lines in the infra-red. Dhavale identifies as phosphorus two lines in the infra-red with arc lines deduced from theory, but they have not been observed in the laboratory.

---

[1] Mohler and Foote, *Physical Review*, **15**, 321, 1920; Ruark, Mohler, Foote, and Chenault, *Bureau of Standards, Scientific Papers*, **19**, 463 (No. 490), 1924; M. O. Saltmarsh, *Philosophical Magazine*, **47**, 874, 1924; McLennan and McLay, *Transactions of the Royal Society of Canada* (3d ser.), **21**, sec. 3, 63, 1927; Dhavale, *Nature*, **123**, 799, 1929.

The remaining elements of the nitrogen group require a more detailed examination and will be considered in connection with Tables VI, VII, and VIII.

Only four arc lines of arsenic (Table VI) are known in the accessible region. The wave-lengths, except for λ 2990, are recent measures by Miss Ware on plates by Mr. King. The difference sun *minus* arc for λ 2990 is far too large to be accounted for by accidental errors of measurement. The residual sun *minus* arc for λ 3032 is consistent in sign and magnitude with its identification as arsenic. If the solar line is due to arsenic, it fixes a maximum intensity of −3 for arsenic lines in the sun, and λ 3119 should also be present. It would, however, fall midway between two solar lines, but so far from either that it should be possible to detect it, as in this region lines of the same solar intensity and still nearer to even stronger solar lines are given by Rowland. The available evidence for arsenic as a probable constituent of the sun's atmosphere does not appear strong enough to justify its inclusion, as it rests upon one out of four lines. A resurvey of this region of the solar spectrum under high dispersion would be necessary for a definite conclusion. It is known from other evidence that not all the faint lines have been recognized in this region, and

TABLE VI

ARSENIC*

Resonance Lines	Accessible Lines				Δλ Sun−Arc	Identifications
	Arc		Sun			
	λ I.A.	Int.	λ I.A.	Int.		
1972	2990.99	2	.861	−1	−0.129 A	....
			.101	0	+ .111	*Ni*
2349	3032.850	4	.868	−3	+ .018	....
2780	3075.320	2	.356	0	+ .036	$OH-Sc^{+}$
	3119.591	4	.505	3	− .086	*Fe*
			.679	1	+0.088	$OH-Cr$

* Ruark, Mohler, Foote, and Chenault, *Bureau of Standards, Scientific Papers*, **19**, 463 (No. 490), 1924.

the possibility that the line was missed holds the question still open.

The arc wave-lengths of antimony (Table VII) are measures from 1912. Though to three places and on the international system, they are of doubtful value, as the difficulties in such determinations were not at that time recognized as fully as later. Professor Kayser in his *Hauptlinien*[1] rounds them off to one and two places of decimals. Two of the three strong reversed lines show good agreement with solar lines of reasonable intensity, but for one the identification is questionable. Of the four weaker lines one is absent and three are masked or blended with other elements. The main evidence for the presence of antimony in the sun rests upon the near coincidence of the strong arc lines of low excitation—the *raies ultimes*—with solar lines of appropriate intensity and not otherwise identified. Wave-lengths of greater accuracy are desirable, particularly for the arc in vacuum.

TABLE VII

ANTIMONY*

Arc			Sun		Δλ Sun−Arc	Identification in Sun
λ I.A.	Int.	E.P.	λ I.A.	Int.		
3029.824	4R	2.024	.832	−2	+0.008 A	*Sb*
3232.537	4R	2.279	.548	−3N	+ .011	*Sb Raie ultime*
3267.497	4R	2.0204	.540	−3N	+ .043	*Sb? Raie ultime*
3383.150	3	....	......	....	....	....
3637.830	3	....	.874	4	+ .044	Masked by *Fe*
3722.787	3	2.024	.760	0	− .027	Masked by *Ce*
4033.562	3	....	.586	1	+0.024	Masked by *Mn*

* Ruark, Mohler, Foote and Chenault, *loc. cit.*, p. 476; McLennan and McLay, *loc. cit.*

In bismuth (Table VIII) the fine structure[2] is manifest to a high degree. This renders comparison with solar lines difficult. The resonance line λ 3067 should furnish the most decisive criterion for the presence of bismuth because of its low excitation, great intensity, accurate wave-length, and simplicity of structure—two equal components or reversal. The absence of this *raie ultime* seems to eliminate bismuth. The strong lines have six or more components spread over a range of 0.25 A, and the individual components are too weak to appear in the sun. In the case of narrow separations one would expect the components to form a broadish line, but of this there seems to be no evidence in the sun in the case of bismuth.

---

[1] H. Kayser, *Tabelle der Hauptlinien der Linien-spektra Aller Elemente*, 1926.

[2] Nagaoka and Mishima, *Proceedings of the Tokyo Imperial Academy*, 2, 249, 1926; Goudsmit and Back, *Zeitschrift für Physik*, 43, 321, 1927.

For elements giving rich arc spectra with few prominent lines the most probable lines to show in the sun are the strong absorption lines in the spectra of the under-water spark, as they arise from low energy-levels. As stated by Meggers and Laporte,[1] the characteristics of the under-water spark are: (*a*) All lines observed as "reversals" in arc emission spectra are always observed reversed in the under-water spark. (*b*) In so far as the temperature classification of emission lines has been studied in the electric furnace, it is evident that the lines ordinarily absorbed in under-water spark spectra are always the lines of lowest temperature class.

TABLE VIII

BISMUTH*

ARC			E.P.	SUN		Δλ SUN−ARC	IN SUN	REMARKS
λ I.A.†	Int.	Comp.		λ I.A.	Int.			
2989.045....	9R	2	1.410	.936 .196	0N −1	−0.109 + .151	*Sc* *Cr*$^+$	Under-water;‡ strong
2993.344....	9R	4	1.410	.355	−2	+ .011	.....	Under-water; weak
3024.646....	8R	6–12	1.906	.652	−2Nd?	+ .006	.....	Under-water; strong
3067.732....	9R	2 or R	0.000	.789	1	+ .057	.....	Under-water; very strong
3067.712§...	......	......	.....	....	....	+ .079	.....	*Raie ultime*
3397.208....	5R	6	1.906	.222	1	+ .014	*Fe*	Under-water; rev.
3397.216‖...	......	......	.....	....	....	+ .006	.....	....
3510.853....	6R	6	1.906	.847	5	− .006	*Ti*$^+$	Under-water; rev.
3510.899...	......	......	.....	....	....	− .052	.....	....
4722.190....	10	......	.....	.165	3	− .025	*Zn*	....
4722.542....	10	6	1.410	.468	−3	− .074	.....	....
4722.831....	10	......	.....	....	....	....	.....	Under-water; sharp
4722.501‖...	......	......	.....	.468	−3	−0.033	.....	*Raie ultime*

* Ruark, Mohler, Foote, and Chenault, *Bureau of Standards, Scientific Papers*, **19**, 482 (No. 490), 1924.

† Offerman, Dissertation, Bonn, 1920.

‡ L. and E. Bloch, *Journal de physique*, **3**, 309, 1922.

§ Measured as two components in the low density arc with wave-lengths ending in decimals .672 and .756; and as a reversed line in furnace with decimal .710 (King).

‖ Weighted mean of components.

The strongest lines in the spectra of osmium, iridium, and platinum are in the ultra-violet. Those in Table IX are the strongest lines in under-water absorption in the accessible region. There are no recent wave-length data for osmium and iridium. Those here used are from the *Handbuch der Spectroscopie* adjusted to the I.A. system. For platinum the recent measures are by McLennan and McLay.[1]

---

[1] *Physical Review*, **28**, 645, 1926.

The spectroscopic data show little if any evidence for osmium and iridium in the sun. The strong osmium line agrees in position with a solar line of intensity −3, but the solar line is identified with a ruthenium line (E.P. 0.000), and λ 3058, the line of lowest energy-level, is apparently absent. As ruthenium is represented by more than a score of lines, maximum intensity 0, the solar line at λ 3301.580 is probably due to ruthenium alone. For iridium the evidence is weaker still. For both elements the lack of accurate wave-length data leaves a factor of uncertainty. In the case of platinum the recent wave-length measures permit more definite conclusions. Of the four lines from the lowest energy-levels and strongest in under-water absorption, three agree in position with solar lines whose intensities match well the emission and absorption intensities. The fourth is possibly blended with the strong iron line.

TABLE IX

OSMIUM-PLATINUM GROUP

ATOMIC NUMBER	ELEMENT	λ I.A.	INTENSITY		E.P.	IN SUN		Δλ SUN−ARC	IDENTIFICATION
			E	Abs.		λ I.A.	Int.		
76........	Osmium	3018.059	4	10	.....	.983	−2N	−0.076	*Ni*
		3040.959	5	10	.....	.918	2	− .041	....
		3058.670	6	20	0.00	.707	0	+ .037	....
		3156.262	6	10	.....	.273	2	+ .011	*Fe*
		3262.308	6	10	.51	.354	1	+ .046	*Fe*
		3267.959	6	15	.....	.911	2	− .048	*Fe*$^+$
		3301.572	7	25	.....	.580	−3	+ .008	*Ru* E.P. 0.000
77........	Iridium	3068.90	4	6	.35	.947	−1	+ .05	....
		3220.81	8	5	.35	.776	−1	− .03	Persistent
						.836	−1	+ .03	....
78........	Platinum	2997.965	7R	30	.096	.965	0	.000	*Pt*
		3042.634	4R	10	.102	.663	3	+ .029	*Pt*? *Fe*
		3064.710	6R	40	.000	.696	1	− .014	*Pt*
		3301.859	10	5	0.811	.870	−3	+0.011	*Pt*

For thallium (Table X) there are no measures of wave-length later than 1904. The existing measures are to two decimal places and quite discordant. For the solar comparisons the means of arc and spark measures are used. Of the lines strong in the arc and in the under-water spark λ 3519 was identified by Rowland as *Tl*? and λ 3775 as *Tl*. The most persistent lines are λ 3775 and λ 5350, and for these the correspondence with solar lines of consistent intensity is within the errors of the measures. The other lines add little or nothing to the evidence. Thallium is, however, retained as probably present. Where a line was identified by Rowland and later evidence renders the identification doubtful, it has usually been retained, but questioned. Only in the lack of positive evidence or because of a more probable source for the line has an identification been rejected. The fine structure of λ 5350, a complex line,[1] has been much studied. The observed separations and relative intensities of the strong components are shown in Table XI.

---

[1] *Transactions of the Royal Society of Canada* (3d ser.), **20**, sec. 3, 201, 1926.

TABLE X

THALLIUM, ATOMIC NO. 81

ARC			UNDER-WATER* SPARK ABSORPTION	IN SUN		Δλ SUN−ARC	IDENTIFICATION
λ I.A.	Int.	E.P.		λ I.A.	Int.		
3229.77...........	10R	0.962	R sharp	.796	0	+0.026	*Fe*?
3519.24...........	10R	.962	R strong	.100	−3Nd?	− .140	....
				.392	−3	+ .159	....
3529.41...........	8R	.962	R strong	.355	−1	− .055	....
3775.74...........	10R	.000	R strong	.712	−2	− .031	*Tl*?
5350.50...........	10R	0.962	R strong	.505	−3N	+0.005	*Tl*?

* Bloch, *Journal de physique*, **3**, 309, 1922.

The positive identification of such complex lines in the sun would furnish the means of studying conditions in the sun's atmosphere from an unusual angle. For more certain identification of thallium in the sun, determinations of wave-lengths in vacuum are needed, together with further work on the conditions of excitation.

There remain in the main body of the periodic table the new elements, masurium and rhenium, for which our information is too meager; a few heavy elements, tantalum, gold, mercury, thorium, and uranium, for which precise wave-length data are lacking; and lastly, the strongly radioactive elements, radium, actinium, and protoactinium.

---

[1] Rowland, *Philosophical Magazine*, **36**, 67 n., 1893.

The arc spectra of tantalum, thorium, and uranium are very rich in lines, of which few are outstanding. Their spectra have not been analyzed, but it is probable from comparison with homologous elements that their excitation is low and that their persistent lines are in the observable region.[1] For them observations of spectra in the under-water spark offer the most promising means of identification.

In the case of gold, E.P. 4.60, and mercury, E. P. 4.65, the resonance lines are in the ultra-violet, λ 2427 and λ 2536, respectively. The present measurements of their wave-lengths in the accessible region are wanting in accuracy. Such as they are, they seem to furnish no evidence of the probable presence of these heavy elements in the sun, but as the presence of mercury has been suggested[2] as well as that of tantalum, thorium, and uranium, it is desirable that wave-length data of high precision be obtained for at least the important lines, in order that comparison with solar lines may yield unequivocal results.

TABLE XI

SEPARATION AND RELATIVE INTENSITY OF COMPONENTS OF THALLIUM λ 5350

Separation	Relative Intensities*		Authority
	Blue	Red	
0.12 A	1	0.50	Michelson
.21	1	.50	Perot and Fabry
.10	1	.75	Barnes
.114	1	.25	Janicki
0.11	1	0.35	Nutting

* Michelson, *Philosophical Magazine*, **34**, 280, 1892; Perot and Fabry, *Annales de chimie et de physique*, **16**, 115, 1899; Barnes, *Astrophysical Journal*, **19**, 190, 1904; Nutting, *ibid.*, **23**, 64, 1906; Janicki, *Annalen der Physik*, **19**, 36, 1906.

CONCLUSIONS

The preceding survey indicates the direction that efforts to widen our knowledge of the constituents of the sun and to narrow the list of the unrecognized elements may profitably take. Fortunately, the requirements for these objects run concurrently with those desired for the analysis of spectra, and results of laboratory observation are of equal importance to the physicist and to the astronomer. In recent years the progress in spectral analysis has been amazingly successful, but there still remain important elements whose spectra have so far failed to yield to it, and in great measure it is these same elements for which data are lacking for a definite examination of the composition of the sun's atmosphere. These spectra, because of their inherent difficulty, have naturally been left to the last, but, in view of past successes, it is not too much to hope that they will soon come within the pale of the conquered elements. There is great need for wave-lengths of the highest precision to replace the earlier approximate measures, but of equal, if not greater, importance is the investigation of the effects due to varying the conditions under which the spectra are produced in the laboratory. This has been a most fruitful line of attack to gain a foothold from which to storm the spectral citadel. Many such methods of attack are recognized and used, but there remains always the possibility of the discovery of a new method, and it behooves the investigator to be ever on the watch for what seem to be anomalous or unexpected effects, and to endeavor to relate them to conditions that favor their production.

---

[1] Russell, *Mt. Wilson Contr.*, No. 383; *Astrophysical Journal*, **70**, 11, 1929.

[2] Stratton, *Astronomical Physics* (London, 1925), p. 41.

The outstanding gaps and deficiencies in related solar and laboratory data have been given in detail. They are summarized below, together with suggested lines of attack for those elements whose investigation promises to yield the most immediate results capable of filling the gaps and removing the deficiencies.

SUMMARY

Osmium and iridium.—Known strong lines are in the accessible region. For these elements accurately determined wave-lengths of a limited number of lines would suffice for the immediate purpose of comparison with solar lines, but the measurement of the complete spectra is of increasing importance. Further observation of the solar spectrum in the ultra-violet is needed.

Tantalum, thorium, and uranium.—The spectra probably have unrecognized persistent lines in the accessible region. For their identification the under-water spark offers a promising means. Precise wave-length measures are lacking for all.

Phosphorus.—Investigations of the infra-red in the laboratory and in the sun are indicated as the most promising means of finding dependable evidence for phosphorus in the sun. Phosphor-bronze may prove advantageous for obtaining the arc spectrum.

Arsenic, antimony, bismuth, and thallium.—Re-examination of the solar spectrum in the extreme violet with high dispersion. Remeasurement of antimony, thallium, and bismuth spectra in the same region, preferably in vacuum, and a study of the relation of fine structure to excitation, in bismuth and thallium.

Rare earths.—These offer a very promising field of investigation. They are of astrophysical importance in the investigation of low levels in solar and stellar atmospheres. For five of them data are quite inadequate for comparison with the sun. They have been considered in a separate contribution.[1]

I take this opportunity to acknowledge my debt to Professor H. N. Russell for access to his manuscript in which he discusses the quantitative representation in the sun of the elements as identified in the *Rowland Revision*[2] recently compiled at Mount Wilson Observatory, and to Dr. I. S. Bowen, of the California Institute of Technology, for his helpful suggestions.

Carnegie Institution of Washington
Mount Wilson Observatory
August 1929

---

[1] St. John and Moore, *Mt. Wilson Contr.*, No. 364; *Astrophysical Journal*, **68**, 93, 1928.

[2] Revision of Rowland's Preliminary Table of Solar Spectrum Wave-lengths, *Carnegie Institution of Washington, Publications*, No. 396, 1928.

Contributions from the Mount Wilson Observatory, No. 386
Reprinted from the *Astrophysical Journal*, Vol. LXX, pp. 175–181, 1929
Printed in the U.S.A.

RONCHI'S METHOD OF OPTICAL TESTING

By J. A. ANDERSON and RUSSELL W. PORTER

ABSTRACT

1. *Ronchi's method.*—Light from a slit is brought to a focus by the lens or mirror to be tested. A short distance in front of (or behind) the focal plane is placed a line-screen having a spacing of 40–200 lines per centimeter, so oriented that the lines are parallel to the slit image. The shadow lines seen by the eye placed at the focus indicate clearly the characteristics of the wave surface as it leaves the lens or mirror. This method, which is described in Italian publications, is probably not so familiar to American readers as it deserves to be.

2. *Modification of Ronchi's method.*—Instead of a single slit, a line-screen illuminated by a frosted lamp or even by sky light may be used as the source, with the advantage that the illumination is so greatly increased that all observations can be made in a fully illuminated room. Also, for testing concave spherical mirrors, or lenses and paraboloids with parallel light, only one screen is required, one-half of which serves as the source, the other half as the observing screen. In this case the lines of the image are automatically parallel to those of the observing screen.

3. *A simple mounting* for the screen and light-source is described.

4. *Results of the examination* of a number of *lenses* and of a slightly defective concave *mirror* are given; these show that the method is fully as sensitive as the Foucault knife-edge test.

1. Of the many methods proposed for optical testing, two have come into very general use on account of their adequate sensitivity and simplicity in application. These are the Foucault knife-edge test and the Hartmann test. With either of these it is easy to observe an error of one-tenth of a wave-length in the wave surface as it leaves the principal plane of the instrument being tested, and under favorable conditions a considerably smaller error may be detected.

The knife-edge test is almost universally used by both amateur and professional opticians, because it requires only visual observations and practically no measurement. Consequently, it is qualitative rather than quantitative, although with a little practice the order of magnitude of the error can readily be estimated.

The Hartmann test, when used to the best advantage, requires one, or better two, photographs of the bundles of rays as they approach or depart from the focal plane and the subsequent measurement of the plates. It is, consequently, strictly quantitative and, for this reason, especially valuable to the user of an optical instrument who wishes to be fully aware of all its characteristics.

Several interference methods have been developed recently, among which may be mentioned those of F. Twyman[1] and A. A. Michelson.[2] In general, these methods require a rather complicated apparatus and a somewhat laborious series of observations. The results are, of course, highly accurate and strictly quantitative. About 1923 Vasco Ronchi announced a simple method of testing which is interferential in nature, but requires very little in the way of apparatus. The theory has been worked out by the discoverer,[3] and it is not the purpose of this communication to enter into that. We wish merely to call attention to a minor modification of his first published method and to some results which we have obtained in applying it to a few pieces of optical apparatus.

2. *Ronchi's method.*—In Figure 1 a slit S is illuminated by either white or monochromatic light from the source O, which, after passing through L, the lens to be tested, comes to a focus at F. A short distance in front of F is placed a coarse grating R, such as an ordinary half-tone screen, with its lines parallel to the slit S. If the eye is placed at or very near F, the lens will be seen as a bright circular disk crossed by a number of dark lines or bands, shown in Plates X and XI. The number of dark bands depends upon the distance from F to R, and is ordinarily equal to the number of lines on the screen R which fall within the light-cone from L. In some positions of R the bands are very faint, or appear to break up into a number of narrower bands; but in testing this is of no moment, for a position near F can always be found where they are well defined and of the proper number. If the lens is perfect, so that the light from all points on it comes to a focus precisely at F, the bands will appear perfectly straight and equidistant. But if a portion of the lens has a shorter focus, the light from this region comes to a focus between F and R, and the lines over it will be farther apart, while for a region of longer focus they will be closer together. If, however, R is placed outside the focus F, the phenomena are reversed, the area of shorter focus showing lines closer together than normal, and vice versa.

As an example, consider Plate X*f*, which shows the appearance of a concave spherical mirror when the screen *R* was placed 4.3 mm inside the center of curvature. Over a circular area in the center the bands are crowded together, thus indicating that the focus of this area is longer than that of the outer zone. The difference in the radii of curvature of the two portions was measured and found to be 0.016 inch. It is of interest to compute the resulting error for the central area. With the dimensions of the mirror given in a later section and $1\frac{1}{2}$ inches as the diameter of the central region, we find the maximum departure of the surface from the sphere defined by the outer zone to be one-sixth of a wave-length of green light.

---

[1] *Philosophical Magazine* (6), 35, 49, 1918.

[2] *Astrophysical Journal*, 47, 283, 1918.

[3] *La prova dei sistemi ottici*, Bologna, 1925. See also *Revue d'optique*, 5, 436, 1926.

3. *Modification of Ronchi's method.*—Ronchi found that the slit *S* need not be infinitely narrow, but may have a width such that its geometrical image is just equal to one of the opaque or transparent lines of the grating *R*. This suggested to us that for testing spherical mirrors at the center of curvature, or lenses and paraboloids with parallel light, the slit might be replaced by a portion of the screen *R*, backed by a lamp, as the source, while an adjacent portion would serve as the grating (see Fig. 2). Two distinct advantages are thus obtained: first, since light from many slits is used, the illumination is greatly increased; and, second, no adjustment for parallelism of slit and grating is required, since they are automatically parallel.

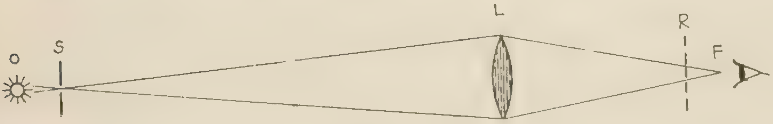

FIG. 1

4. *Apparatus and observations.*—The optical set-up is shown schematically in Figure 2, and a sketch of the apparatus in Figure 3. Light from a small frosted lamp bulb is reflected by a mirror through the grating to the mirror or lens under test. It then returns through the same grating and enters the eye. As shown in Figure 3, the light-source, reflecting mirror, and grating are mounted in a tube which can be racked toward and away from the object under test; further, the grating can be rotated about the axis of the tube. Scales are provided for measuring focal lengths and the rotation of the grating. The lamp is an ordinary 2-volt flash-light bulb, taking current from a

lighting socket through a transformer. It is worthy of note that no attempt was made to darken the room in which the experiments were carried on. In fact, part of the time they were made on a bench by a window with direct sunlight falling upon the apparatus.

In considering the drawings shown on Plates X and XI it must be borne in mind that the disk of the Ronchi pattern is not perfectly sharp around the entire circumference. Because of overlapping of the various diffraction orders, the right- and left-hand edges of the disks are more or less blurred, the amount depending on the coarseness of the grating used. The blurring does not, however, affect the interpretation of the Ronchi pattern and, because of the difficulty of reproducing it, has been omitted from the drawings. With this exception, the drawings are truthful representations of the phenomena observed.

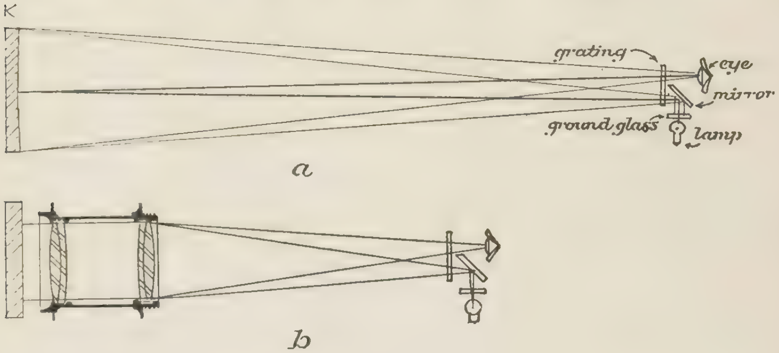

FIG. 2

Gratings of 100, 175, and 320 lines per inch were tried. That having the intermediate spacing was found the most satisfactory and was used throughout the tests. The mirror selected for examination is a spherical concave of $3\frac{3}{4}$-inch aperture and 36-inch radius of curvature. The surface is not perfect, but has a central area whose radius is 0.016 inch longer than that of the marginal region. Three drawings of the Foucault shadows for this mirror were first carefully made with the knife edge at and close to its mean center of curvature. These are shown in Plate IX with their apparent sections drawn below them. To anyone familar with the Foucault method of

PLATE IX

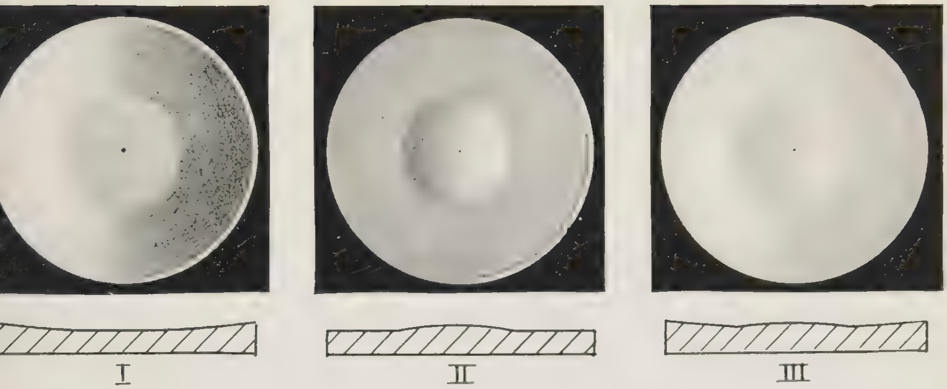

Appearance of a Slightly Imperfect Spherical Concave Mirror as Seen under the Foucault Knife Edge Test

I. Pinhole and knife edge at center of curvature of zone *A* (central area).
II. Pinhole and knife edge at center of curvature of zone *B* (marginal zone).
III. Pinhole and knife edge at mean curvature of zones *A* and *B*.

The knife edge is advancing from the left. The difference of radii of curvature of the two zones is 0.016 inch, *A* being the longer.

PLATE X

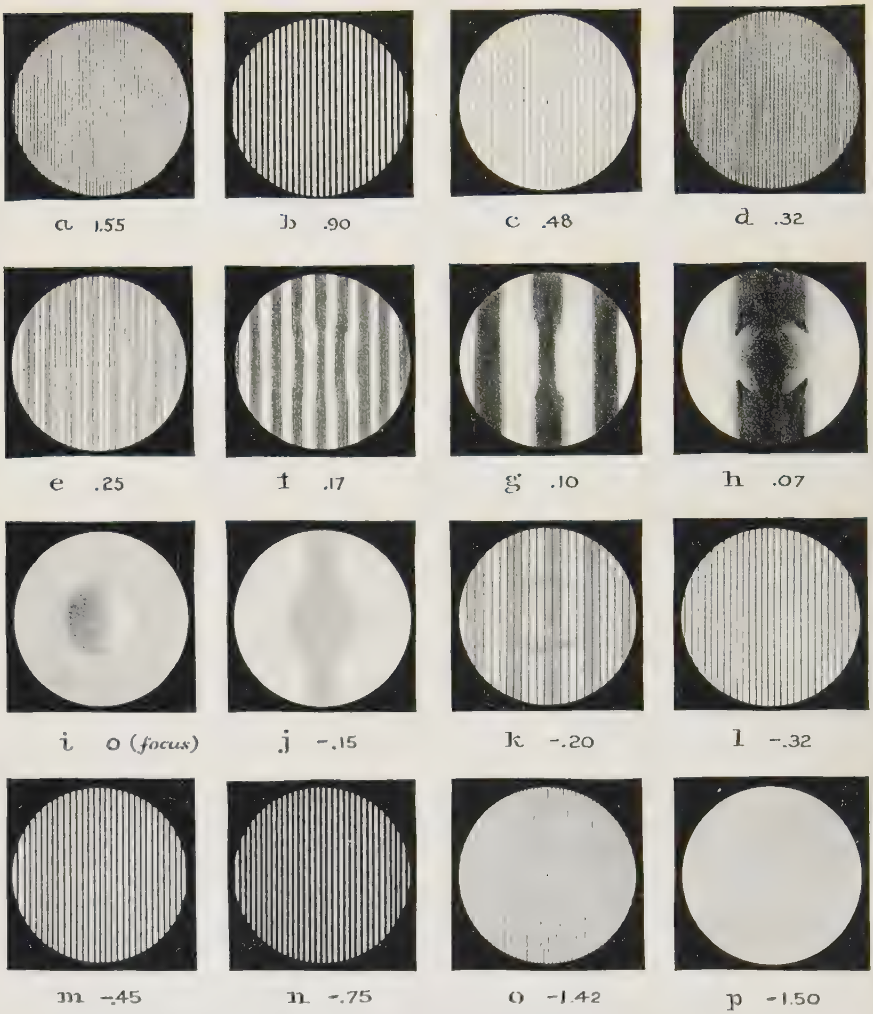

a 1.55
b .90
c .48
d .32
e .25
f .17
g .10
h .07
i 0 (*focus*)
j -.15
k -.20
l -.32
m -.45
n -.75
o -1.42
p -1.50

Appearance of Grating Patterns on a Concave Silvered Mirror, as Seen at Various Distances inside and outside the Center of Curvature. The Distances Are Given in Inches testing an optical surface, these drawings will give adequate information as to the characteristics of the mirror.

Plate X shows the series of Ronchi band patterns or images seen when the grating (175 lines per inch) is placed at various positions near the center of curvature of the mirror, the distance inside or outside the center being given in inches beneath each drawing.

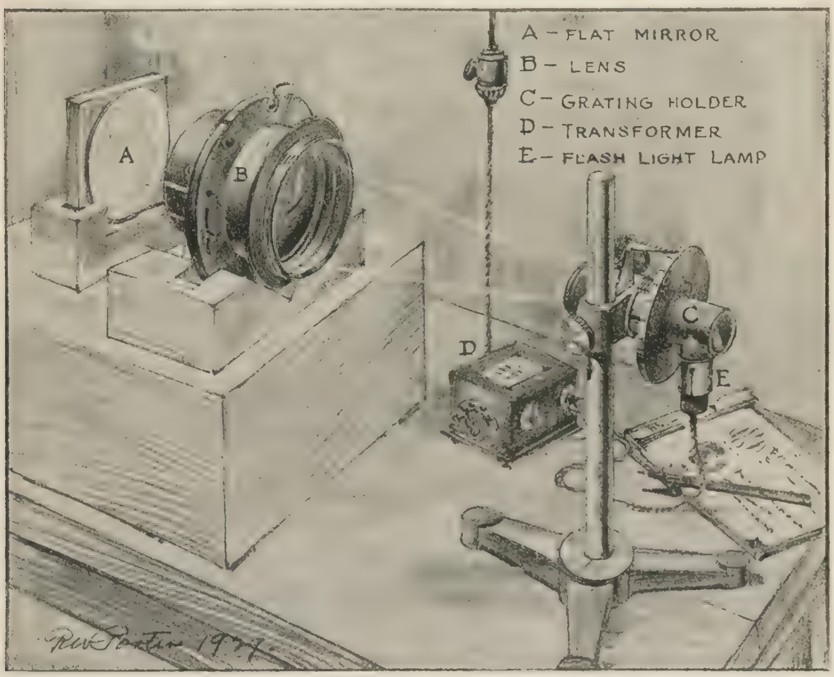

FIG. 3

Considered in order, *a* is the first noticeable pattern that appears as the grating is moved toward the center of curvature from the inside. The lines are faint and close together. At *b* another pattern appears with the lines more separated and intensely black. After another interval of confusion, *c* appears with the same separation as *b*, but with the faintness of *a*. At *d* the lines are crowded together again and are between *b* and *c* in intensity. The next pattern, *e*, shows a superposition of two line series, a coarse faint series of eight broad lines against about thirty-five sharp fine lines.

The grating now enters the region just inside the center of curvature which gives the most sensitive and satisfactory results for testing purposes. As the center is approached the bands spread out rapidly and reveal the features which indicate the character of the mirror surface. The positions illustrated are more or less arbitrary, as there are no intervals of confusion between *f* and *i* (center of curvature).

On passing outside the center of curvature the patterns appearing are those shown, and need no further description. After pattern *o* no more images appear, the mirror having a uniform surface, as at *p*. Returning to the region of greatest sensitivity, we note at *h* the peculiar appearance of the mirror's central area, the focal length of which is greater than that of the outer region. For this position of the grating (0.07 inch inside the center of curvature), the first wide band just covers the apparently raised central part of the mirror. Were this the only criterion for detecting surface errors, the interpretation would not be clear. But by moving the grating slightly nearer the center, the band continues to spread out until it covers the whole mirror; and if the grating is then shifted laterally so that the broadened band advances from the left, we see the shadow pattern *i*, which is exactly the appearance under the knife edge when the knife edge is at the center of curvature of the outer zone.

Hence for this particular position of the grating the shadows may be interpreted as in the "knife-edge test." The contour is determined by remembering that if the band advances from the *left* the resulting shadow models the surface of the mirror as though illuminated by light coming from the *right* at grazing incidence. On passing the center of curvature the first band appearing is very faint (*j*), and the additional bands rapidly fall off to a region of confusion.

Plate XI shows the results found by subjecting five different lenses to the Ronchi (or grating) test, with knife-edge shadows in the right-hand column for comparison. It should be remembered that these patterns are seen by the observer in color (secondary spectrum), while those obtained with a mirror are colorless.

The first test (*a*, *b*, *c*, *d*) is of a 4-inch telescope lens of ratio *f*/9. The lens at *a*, under the grating test, is uniform, like the knife-edge test at *d*, except that the left half is colored magenta and the right

PLATE XI

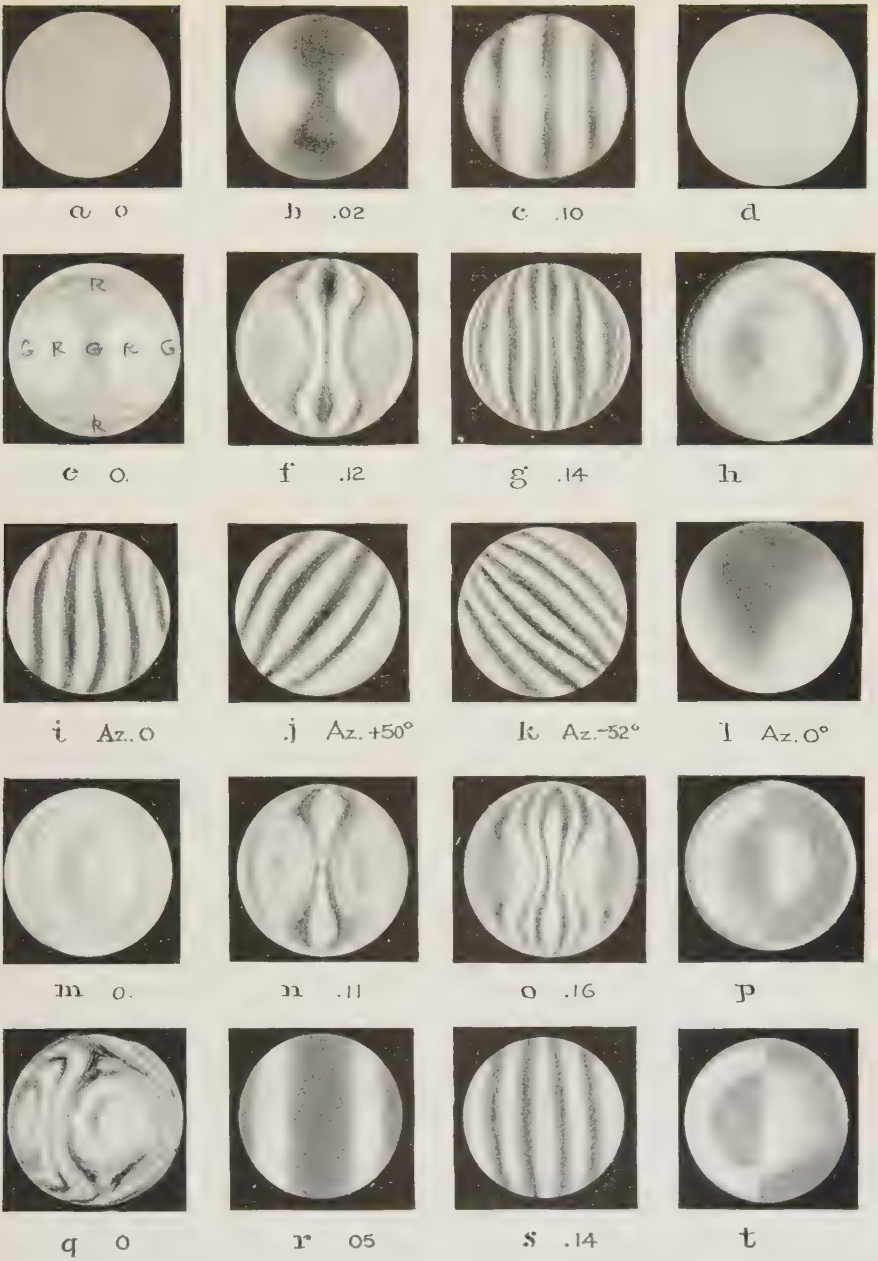

Grating Patterns Shown by Five Different Lenses. The Last Column Gives Knife-Edge Shadows for Comparison

half green. These colors are reversed if the broad band advances from the right. By moving the grating 0.02 inch inside the principal focus, *b*, the first band narrows to the dumbbell form shown, and this pattern is repeated in a less pronounced way as more bands appear (*c*). The grating test thus reveals a lack of achromatism as well as a slight amount of spherical aberration not evident in the knife-edge test.

The second lens (*e*, *f*, *g*, *h*) was a camera objective, *f*/4.5, of 3-inch aperture. Here is strikingly shown at *f* and *h* the difference in appearance between the grating and knife-edge shadows.

Astigmatism is beautifully shown in the group of patterns appearing in the third row. This was a lens of the Petzval type of 2½-inch aperture. With its lines vertical, the grating was placed so as to give *i*. Then, without changing its focal setting, the grating was rotated into the positions shown at *j* and *k*, giving four bands at *j* and six at *k*. The knife edge, when placed at the mean focus, confirms matters by showing the shadow *l*. The bands at *i*, *j*, and *k* strongly resemble the interference fringes produced by placing an astigmatic surface on one of pure revolution.

Another camera lens, *f*/4.5, aperture 3¾ inches (*m*, *n*, *o*, *p*), shows no trace of astigmatism and has characteristics similar to those shown in *e*–*h*. The appearance of this lens 10° off the axis is shown at *q*.

The results for the last photographic objective, *f*/5.6, aperture 2½ inches, shown in *r*, *s*, and *t*, indicate clearly the fine optical quality of this lens.

The line-screens used in the foregoing observations were photographic copies of a commercial half-tone screen.

Carnegie Institution of Washington
Mount Wilson Observatory
September 1929

Contributions from the Mount Wilson Observatory, No. 387
Reprinted from the *Astrophysical Journal*, Vol. LXX, pp. 207–236, 1929
Printed in the U.S.A.

THE RADIAL VELOCITIES OF 741 STARS

By W. S. ADAMS, A. H. JOY, R. F. SANFORD, and G. STRÖMBERG

ABSTRACT

This catalogue contains the *radial velocities* and *spectral types* of 741 stars observed at Mount Wilson with spectrographs of one-prism dispersion. The visual magnitudes range from 3.0 to 10.8, many faint dwarf stars being included.

The following *corrections* have been applied to the directly measured values: F, +0.5 km/sec.; G, 0.0; K, −0.9; M, −0.8.

Comparisons are made with 142 stars observed in common with the Lick Observatory, and 96 stars observed at the Dominion Astrophysical Observatory.

The *asymmetry* of stellar motions is shown in a striking way by the numerous stars of high radial velocity.

This catalogue of radial velocities contains the results for 741 stars observed at Mount Wilson during recent years with the spectrographs at the Cassegrain focus of the 60-inch and 100-inch reflectors. In all cases a dispersion of one prism has been used, but the prism employed in the spectrograph of the 60-inch telescope is of somewhat denser glass than the other and affords a larger scale. Cameras of 18-inch focal length are used in both instruments, supplemented in the case of the spectrograph of the 100-inch telescope by a 10-inch camera for observations on the fainter stars. The linear scale of the spectrograms ranges from 37 A to the millimeter at $H\gamma$ for the spectrograph on the 60-inch telescope with the 18-inch camera, to 76 A for the spectrograph on the 100-inch with the 10-inch camera.

Table I gives the results found for the radial velocities. The arrangement is the same as that in *Mt. Wilson Contribution*, No. 258.[1] The list contains stars ranging in visual magnitude from 3.0 to 10.8. The photographic magnitudes of many of the fainter stars reach 11.0. The brighter stars were observed for the double purpose of providing spectra suitable for determinations of absolute magnitude and parallax and of furnishing a comparison with the values for such stars measured at the Lick Observatory. The number of stars

---

[1] *Astrophysical Journal*, 57, 149, 1923.

TABLE I

Radial Velocities of 741 Stars

H.D.	Star	α 1900	δ 1900	m	Sp.	μ	No.	v	P.E.	Other Determinations	
										v	Auth.
								km/sec.	km/sec.	km/sec.	
....	Cin. 2S	$0^h\ 0^m.4$	+45° 15′	8.5	M0	$0''.858$	4	+ 1	±1		
87	Boss 2	0 0.6	+12 50	5.7	G5	.035	3	− 2.1	1.4	+ 2.6	V
603	22	0 6.2	−16 1	5.0	F4s	.280	4	+ 13.7	1.5	+15.0	L
787	25	0 7.1	−18 30	5.5	K5	.040	3	− 8.2	3.1	− 8.0	L
1014	30	0 9.4	− 8 20	5.4	M4	.060	2	− 6.0	0.5	− 2.4	L
1228	40	0 11.5	+ 1 18	7.3	M5	.022	4	− 7.9	1.6		
1317	45Br	0 12.3	+ 8 19	6.6	G1	.120	3	+ 32.0	1.2	+36.6	V
1671	57	0 15.9	+37 25	5.2	F2s	.078	3	+ 8.9	1.4	+ 9.5	L
1779	Cin. 35	0 17.0	−27 16	9.0	G1	.440	3	− 5	2		
1879	Boss 64	0 18.0	−16 30	6.6	M3	.041	3	− 22.3	2.3		
....	Cin. 41	0 19.3	−27 35	8.0	K4	.669	3	+ 6	1		
2806	Boss 98	0 26.4	+15 28	7.1	G9	.049	3	− 5.7	1.0		
2910	104	0 27.3	+19 45	5.5	K0	.138	3	− 11.5	1.1		
3125	112	0 29.4	− 5 6	7.0	G1	.082	3	+ 9.1	3.0		
3266A	βG.C. 322A	0 30.6	+29 27	7.9	G4	.449	5	− 49.5	1.5		
3266B	322B	0 30.6	+29 27	8.7	G6	.449	3	− 59	1		
3821	368Br	0 35.7	− 7 46	7.0	G3	.022	3	+ 4.7	0.8		
....	Cin. 90	0 38.2	+33 18	8.5	K6	.427	3	− 33	1		
4307	Boss 157	0 40.5	−13 25	6.1	F9	.200	3	− 12.8	0.6		
4568	167	0 42.6	+20 23	6.6	F8	.162	3	+ 3.4	1.4	− 1.0	V
4730	177	0 44.4	−14 6	5.8	K5	.135	3	+ 3.1	1.6		
5351	Cin. 122	0 50.4	+68 31	9.4	K6	.739	3	− 46	3		
6314	Boss 231	0 59.0	+39 27	6.7	A3n	.088	3	+ 5	1		
6734	251	1 2.9	+ 1 28	6.7	G5	.446	3	− 94.9	0.3	+12.4	V
6920	262	1 4.6	+41 33	5.7	F8	0.145	4	− 8.4	±0.9	−13.1	V

									km/sec.	km/sec.	km/sec.	
7218	Boss	275	$1^h\ 7^m.4$	+ 1° 57′	6.8	F5	0″.208	4	+ 3.2	±1.4		
7672		290	1 11.5	− 3 2	5.5	G4	.126	4	− 19.8	2.3		
7727		291	1 11.9	− 2 48	6.8	G0	.296	3	+ 8.0	1.9		
8126		303	1 15.6	+28 13	5.6	K5	.080	3	− 35.5	1.0		
8334		306	1 17.5	+ 1 12	6.5	M0	.069	4	− 15.7	2.3		
8491		310	1 18.9	+67 36	5.0	G9	.086	3	− 7.8	0.3	−12.0	L
8627	βG.C.	749Br	1 20.0	− 6 28	6.8	F0	....	3	+ 15.5	0.9		
8705	Boss	317	1 20.7	−15 7	5.2	K3	.043	3	− 20.8	1.2	−21.0	L
....	B.D. +59°	251	1 20.9	+59 46	8.5	B3	....	3	− 42	3		
8763	Boss	319	1 21.3	+18 43	5.6	G9	.076	4	− 41.2	1.2		
8779		320	1 21.3	− 0 55	6.5	G9	.049	3	− 6.6	1.3		
9352–3	B.D. +57°	320	1 27.0	+57 49	6.0	K0p	....	3	− 1.0	1.4		
9640	Boss	342	1 29.4	+17 57	6.0	M2	.088	4	− 26.4	1.7		
9670		344	1 29.7	+ 0 26	7.0	F8	.323	3	− 18.1	2.1		
9847	Cin.	216	1 31.0	−18 2	7.1	G1	.353	5	+ 7.5	1.4		
10113	Boss	361	1 33.9	+16 7	6.9	G5	.031	3	+ 4.5	1.4		
10164		367	1 34.3	+15 54	6.1	K1	.073	3	+ 18.7	1.5	+17.1	V
12292		455	1 55.5	− 9 0	5.7	M5	.086	3	+ 6.8	1.9		
12800		475	2 0.5	+71 5	6.7	F8	.389	3	+ 0.8	1.1	− 2.1	V
13137		481	2 3.4	+53 22	6.4	G5	.060	5	+ 10.5	0.8		
13174		483	2 3.7	+25 28	5.1	A7	.086	3	− 6	1	+ 3::	L
13325		491	2 5.1	+19 2	5.9	M3	.092	3	+ 60.3	2.6		
13452	βG.C.	1136Br	2 6.4	+53 46	8.1	A0	.010	4	+ 9	4		
13421	Boss	495	2 6.1	+ 8 6	5.7	F9	.174	3	− 16.7	1.3	−19.2	V
13468		496	2 6.5	− 2 18	6.0	G8	.026	3	+ 32.1	0.4		
13596		502	2 7.6	+14 49	6.0	M1	.100	4	+ 26.2	1.7		
13612		503	2 7.7	− 2 52	8.7	G3	.374	3	− 5	1		
13872		509	2 10.0	+24 35	5.6	F4	.120	3	− 44.3	0.4		
14411	B.D. − 3°	355	2 14.5	− 3 25	9.1	K5	.010	4	+ 39	1		
15089	Boss	550A	2 20.8	+66 57	4.6	cA4	0.015	2	+ 2	±1	+ 3.3	L

TABLE I—*Continued*

H.D.	Star	α 1900	δ 1900	*m*	Sp.	μ	No.	*v*	P.E.	Other Determinations	
										v	Auth.
								km/sec.	km/sec.	km/sec.	
....	Boss 550C	$2^{h}20^{m}.8$	+66° 57′	8.1	G4	0″.03	3	+ 10	±1		
15176..........	555	2 21.5	+31 21	5.8	G9	.046	4	− 38.0	1.7	−40.3	V
15596..........	568	2 25.4	+17 16	6.4	G5	.103	3	−116.0	2.8		
15652..........	570	2 26.0	−22 59	6.4	M2	.044	3	− 18.9	1.0		
16082–3........	585	2 29.9	+51 31	7.3	G1	.014	3	− 16.0	0.8		
16141..........	586	2 30.3	− 3 59	6.8	G1	.452	3	− 53.8	2.2		
16396..........	βG.C. 1346Br	2 32.9	+32 59	7.0	K2	....	3	− 3.8	1.4		
16480..........	1353Br	2 33.5	+14 25	7.3	K0	....	4	+ 0.8	1.6		
16647..........	Boss 607	2 35.0	+ 5 41	6.2	F2s	.050	5	+ 18.5	1.1	+16.7	V
16735..........	βG.C. 1376Br	2 35.9	+53 6	6.0	G8	.079	4	− 11.0	1.5		
17206..........	Boss 631	2 40.4	−19 0	4.6	F5s	.327	6	+ 23.6	1.1	+26.2	L
17245–6........	B.D. +43° 576	2 41.0	+43 50	6.7	F0s	....	3	− 13.7	0.5		
17459..........	Boss 635	2 42.9	+17 52	6.0	G8	.051	3	+ 47.8	1.4	+46.5	V
17660..........	Cin. 365	2 45.0	+15 19	9.2	K6	.510	5	− 26	2		
17785..........	βG.C. 1457S	2 46.1	+72 29	7.7	G0	.082	3	− 3.0	1.3		
18200..........	Cin. 379	2 50.3	+52 5	8.0	G6	.49	3	+ 32.8	1.8		
18449..........	Boss 670	2 52.9	+34 47	5.0	K2	.063	3	− 36.1	0.8	−36.0	L
18537..........	678	2 53.7	+51 57	5.4	B5	.043	3	− 2	3	− 3::	L
18633..........	682	2 54.6	− 2 52	5.5	B9	.017	5	+ 17	3	+24	L
18692..........	684	2 55.2	−25 40	5.6	A9n	.204	3	+ 21	1		
18803..........	689	2 56.5	+26 13	6.7	G5	.295	3	+ 15.6	1.2	+ 8.0	V
18907..........	693	2 57.3	−28 28	5.9	G5	.493	3	+ 31.7	2.5		
18975..........	βG.C. 1550Br	2 58.0	− 2 29	7.7	F7	....	3	+ 34.8	2.2		
20418..........	Boss 744	3 12.0	+49 44	5.1	B3	.041	6	+ 1	5	− 2::	L
21017..........	775	3 18.4	+24 22	5.7	K3	0.059	4	+ 13.1	±1.4	+11.7	V

									km/sec.	km/sec.	km/sec.	
21278	Boss	780	3h 20m.9	+48° 43′	4.9	B5	0″.032	6	+ 4	±2	+11	L
21531	Cin.	456	3 23.3	−20 10	8.2	M0	.603	4	+ 31.0	1.5		
21903	βG.C.	1747Br	3 26.8	+59 43	6.5	F2s	....	3	+ 20.5	0.3		
22468Ft	Boss	823Ft	3 31.7	+ 0 16	8.2	K6	.151	5	− 15	2		
23107	βG.C.	1827Br	3 37.4	+38 4	7.4	K4	.03	3	+ 15.6	1.0		
23108		1827Ft	3 37.4	+38 4	8.7	A5n	.03	3	+ 13	2		
23189	Cin.	499	3 38.2	+68 21	9.1	M1	.30	3	− 5	2		
23413	Boss	859	3 39.8	− 0 37	5.8	K5	.054	3	+ 69.3	2.0		
23480		865	3 40.4	+23 38	4.2	B5	.059	2	+ 13	1	+ 1::	L
23614		868	3 41.4	−12 25	4.6	M2	.069	3	+ 42.7	1.0	+45.7	L
23630		869	3 41.5	+23 48	3.0	B5p	.052	3	+ 14	6	+ 5	L
23850		877	3 43.2	+23 45	3.8	B8	.053	2	+ 6	5	+ 3:	L
23862		879	3 43.2	+23 50	5.2	B8p	.053	2	+ 14	1	+ 3:	L
23940		881	3 43.9	−30 28	5.6	G3	.243	3	+ 53.3	0.6		
24131		886	3 45.5	+34 3	5.7	B3	.011	4	+ 18	2		
24388		893	3 47.8	− 5 40	5.5	B8	.012	3	+ 15	4	+18:	L
24640		904	3 50.0	+34 47	5.5	B3	.020	3	+ 13	2	+25::	L
24834		912	3 51.8	−13 53	6.7	M2	.010	3	+ 38.0	1.4		
25570		935	3 58.5	+ 7 55	5.5	F2s	.159	3	+ 31.5	1.0	+36.0	L
25665	Cin.	546	3 59.2	+69 17	8.1	K2	.308	3	− 11	2		
26018		553	4 2.1	+76 2	8.8	K0	.25	6	+ 10	1		
26367	Boss	958	4 5.1	+85 17	6.7	F8	.038	6	− 47.0	1.4		
27176		991	4 12.5	+21 20	5.6	A8n	.112	5	+ 33	2		
....	B.D. +15°	609	4 12.6	+15 51	9.0	K4	....	5	+ 41	2		
27245	Boss	993	4 13.1	+60 30	5.7	M0	.122	3	+ 28.2	1.2		
27757	Cin.	580	4 17.8	+77 24	7.8	F9	.237	3	+ 38.0	0.1		
27991	Boss	1031	4 19.9	+15 43	6.4	F5s	.114	3	+ 38.7	0.9		
28034	B.D. +15°	624	4 20.4	+15 17	7.4	F7	.115	5	+ 41.1	2.0		
28226	Boss	1040	4 22.1	+21 24	5.7	A8n	0.118	5	+ 35	3	+35.7	V
....	B.D. +14°	699	4 22.1	+14 8	9.3	K3	....	3	+ 46	±2		

TABLE I—*Continued*

H.D.	STAR	α 1900	δ 1900	m	SP.	μ	No.	v	P.E.	OTHER DETERMINATIONS	
										v	Auth.
								km/sec.	km/sec.	km/sec.	
28424	B.D. +13° 688	$4^h23^m.9$	+13° 41′	7.8	G9	....	3	+ 94.4	±2.0		
28595	Boss 1057	4 25.4	+14 53	6.6	M3	0″.074	3	+ 38.0	0.2		
28704	1061	4 26.4	+42 51	6.1	A0n	.007	6	− 24	3		
28749	1063	4 26.8	− 0 16	5.0	K4	.003	3	+ 18.2	0.8	+16.2	L
....	B.D. +55° 900	4 27.9	+55 13	8.6	K4	.64	3	+ 50	2		
....	+14° 721	4 28.3	+14 57	8.5	K1	....	3	+ 37	1		
....	+14° 722	4 28.6	+14 46	8.7	K4	....	3	− 24	1		
29009	Boss 1070	4 29.0	− 6 57	5.7	B9	.012	6	+ 2	2		
29064	1071	4 29.4	− 8 26	5.4	M3	.035	3	− 10.3	1.3	−11.6	L
29065	1072	4 29.4	− 9 11	5.5	K5	.119	3	− 25.0	2.3	−27.4	L
29235	βG.C. 2274Br	4 31.1	+41 57	7.2	K2	.026	3	+ 16.7	0.9		
29364	2284N	4 32.4	+26 45	6.5	F2s	....	4	+ 3.9	2.8		
29775	Boss 1105	4 36.1	−19 52	4.5	M3	.094	3	− 32.3	2.1	−33.5	L
30020	1112	4 38.8	− 8 59	6.8	F1s	.044	3	+ 40.0	1.3		
30454	1129	4 42.8	+31 16	5.8	K1	.115	3	+ 22.0	0.4	+22.7	V
30504	1133	4 43.2	+37 19	5.1	K3	.046	2	− 22.7	0.2	−24.3	L
30834	1148	4 45.9	+36 32	5.0	K2	.026	2	− 15.9	0.2	−16.7	L
31865	βG.C. 2451S	4 54.2	+62 57	8.6	G4	.336	3	− 24	1		
32070	Cin. 646	4 55.5	+24 30	8.5	G2	.322	3	+ 29	1		
33664	Boss 1237	5 6.7	−11 58	5.9	M6	.051	3	+ 45.8	0.9		
33725	Cin. 674	5 7.1	− 9 13	8.0	K0	.57	4	+ 5.4	1.5		
....	Comp. α Aurigae	5 10.0	+45 44	9.8	M2	.437	3	+ 36	5		
....	B.D. +41°1154	5 13.0	+41 8	8.7	K0	....	3	+ 39	2		
35186	Boss 1292	5 17.9	+37 18	5.2	K5	.027	3	− 16.8	2.4	−20.0	L
35410	1300	5 19.4	− 0 59	5.2	G6	0.125	4	+ 22.3	±0.8	+20.0	L

									km/sec.	km/sec.	km/sec.	
35620	Boss	1311	5h21m0	+34° 23′	5.3	K4	0″.056	3	+ 30.6	±2.0	+31.0	L
35783	Cin.	693	5 22.1	+78 18	7.7	F3s	.258	3	+ 18.7	1.4		
36167	Boss	1327	5 24.6	− 1 10	5.0	M0	.028	4	+ 5.9	1.7	+ 7.9	L
36443	Cin.	706	5 26.6	+ 0 2	8.4	G5	.507	3	− 9	2		
....	βG.C.	2835Ft	5 30.5	+21 56	7.8	F7	.028	3	+ 25.2	1.4		
37269	Boss	1378	5 32.2	+30 26	5.5	A9n	.016	3	+ 4	2	+ 0.8	L, V
37603	βG.C.	2886Br	5 34.6	+15 18	6.7	F0n	....	4	+ 21.1	1.2		
37984	Boss	1407	5 37.3	+ 1 26	5.2	K1	.055	3	+ 85.2	1 7	+89.2	L
38014	Cin.	724	5 37.5	+ 2 39	8.8	K1	.54	3	+ 55	2		
38584	Boss	1425	5 41.8	+24 39	7.2	K4	.028	3	+ 15.6	0.4		
38604		1426	5 41.9	+39 30	6.9	G1	.024	3	+ 19.5	1.8		
38998	B.D. +27°	887	5 44.5	+27 39	7.7	M5	....	3	+ 27	1		
39019	Boss	1445	5 44.8	+14 17	5.7	K0	.035	3	+ 45.8	0.6	+44.7	V
39400		1458	5 47.2	+ 1 50	5.0	K2	.011	3	+ 10.4	0.9	+10.3	L
39425		1459	5 47.4	−35 48	3.2	K0	.397	3	+ 94.6	2.5	+89.1	L
39853		1470	5 50.1	−11 48	5.8	K4	.062	3	+ 87.0	1.3		
40002	B.D. +26°	1011	5 51.1	+26 51	8.0	K2	....	3	− 33	3		
40239	Boss	1479	5 52.5	+45 56	4 6	M3	.011	3	0.0	0.5	+ 0.9	L
40369–70		1485	5 53.2	+12 48	5 8	G5	.035	3	+ 11.0	1.7		
40959	βG.C.	3113Br	5 57.4	+27 39	8.8	G4	.42	3	− 2	1		
42042	Boss	1531	6 3.3	−19 9	5 5	M2	.063	6	+ 29.1	1.9		
42250	Cin.	769	6 4.5	+70 49	7.6	G6	.45	4	+ 25.6	2.4		
42618		772	6 6.6	+ 6 49	7.1	G4	.306	3	− 54.4	0.7		
43232	Boss	1570	6 10.0	− 6 15	4.1	K1	.021	3	− 3.4	1.0	− 5.2	L
....	Cin.	783	6 10.5	+25 15	9.1	K5	.48	3	+ 44	2		
44213	βG.C.	3319Br	6 15.5	+ 5 47	8.1	M4	....	3	+ 16	1		
44214		3319Ft	6 15.5	+ 5 47	9.8	A6n	....	3	+ 42	2		
44252	B.D. +22°	1294	6 15.6	+22 57	8.1	F4	....	4	+ 37.5	2.5		
44770	Boss	1611Ft	6 18.5	+ 4 39	6.5	F6s	.012	3	+ 16.3	0.4		
45018		1616	6 19.9	−25 31	5.7	M1	0.031	3	+ 33.2	±1.2		

TABLE I—*Continued*

H.D.	Star	α 1900	δ 1900	m	Sp.	μ	No.	v	P.E.	Other Determinations	
										v	Auth.
								km/sec.	km/sec.	km/sec.	
45416	Boss 1626	$6^{h}22^{m}1$	+ 0°22′	5.3	G8	0″011	3	+ 29.8	±2.3	+33.3	L, V
	Cin. 803	6 22.9	+27 5	8.7	K5	.50	3	− 47	1		
45951	βG.C. 3422Br	6 25.4	+17 0	6.2	K1	.089	4	+ 26.5	1.0		
46136	Boss 1650	6 26.5	+17 51	7.8	F6	.042	3	+ 0.2	0.7	− 0.5	V
46374	1663	6 27.9	+14 14	5.6	K1	.097	3	− 12.5	1.4		
	B.D. +17°1320	6 31.4	+17 38	9.5	M1	.88	3	− 59	2		
47127	Cin. 814	6 32.0	+12 16	7.6	G5	.292	6	+ 52.4	1.9		
47914	Boss 1707	6 35.8	+44 37	5.2	K5	.055	3	− 72.1	0.3	−75.8	L
48217	1715	6 37.2	− 9 4	5.3	Mo	.037	2	+ 1.6	2.0	+ 0.3	L
48250	1716	6 37.4	+59 33	4.9	A3n	.015	4	− 6	3	+ 7	L
49520	1748	6 43.7	+41 54	5.0	K3	.136	3	+ 60.8	1.3	+60.6	L
49618–9	1753	6 44.3	+59 34	5.4	Go	.047	3	+ 11.7	1.4	+13.1	L, V
49968	1760	6 45.9	+23 43	5.8	K5	.043	3	+ 39.7	2.0		
50635	1778Ft	6 49.0	+13 18	7.7	G5	.112	3	+ 25.4	1.8		
50692	1780	6 49.2	+25 30	5.8	Go	.042	3	− 11.8	0.7	....	
50806	1784	6 49.6	−28 24	6.0	G3	.524	4	+ 71.7	1.1		
51067	Cin. 840	6 50.8	+75 22	6.8	F8s	.265	3	+ 22.9	0.7		
52005	Boss 1803	6 54.5	+16 13	5.9	cK4	.018	3	+ 21.8	0.6	+21.4	V
52666	1808	6 57.0	− 5 35	5.4	M2	.009	3	− 0.8	2.5	+ 1.6	L
54046	Cin. 855	7 2.3	+15 41	7.5	F9	.231	4	− 12.7	2.3		
54100	856	7 2.5	+15 41	7.4	F8	.213	3	− 11.1	2.1		
55458	867	7 7.8	+25 11	8.4	K1	.451	3	− 51.8	0.9		
55751	Boss 1865	7 9.1	+ 3 17	5.6	K1	.030	3	+ 36.7	0.8		
56160	1878	7 10.8	−26 52	5.8	K5	.047	3	+ 14.2	2.1		
56618	1889	7 12.6	−27 42	4.8	M3	0.045	3	+ 43.4	±1.1	+40.6	L

									km/sec.	km/sec.	km/sec.	
	B.D.	+33°1505	$7^{h}13^{m}.0$	+33° 2′	9.3	M1	0″.57	3	− 61	±2		
57615	Boss	1918	7 17.0	−25 42	6.1	M5	.031	3	+ 23.1	0.9		
58461		1938	7 20.6	−13 33	5.8	A8n	.204	3	+ 7	2		
	βG.C.	4062Br	7 22.3	+50 11	8.2	G2	....	3	− 77	1		
		4062Ft	7 22.3	+50 11	8.7	G2	....	3	− 2	1		
58945		4065	7 22.7	+50 12	8.0	F4n	....	4	+ 14.7	2.9		
59604–5	B.D.	+ 8°1791	7 25.6	+ 8 46	7.2	F1s	....	4	+ 23.8	1.6		
60081	Boss	1975	7 27.7	+15 51	6.7	G9	.008	3	+ 55.8	1.0		
60437		1986	7 29.3	+46 24	5.8	M1	.047	3	+ 28.9	0.2		
	B.D.	+37°1748	7 31.6	+36 57	9.5	K5	0.87	3	− 8	1		
61421	Boss	2008	7 34.1	+ 5 29	0.5	F4	1.242	7	− 1.7	0.6	− 3	L
62285		2028	7 38.0	+26 1	5.4	Mo	0.034	3	+ 3.7	0.4	+ 1.8	L, V
	B.D.	+54°1175	7 40.8	+53 55	8.6	K6	.56	3	+ 2	2		
62902	Boss	2050	7 41.1	− 6 32	5.7	K5	.110	5	− 32.8	1.3		
63332		2057	7 43.2	+54 23	6.0	F6	.052	4	− 2.4	1.5		
63336		2058Br	7 43.3	−11 57	5.5	F5	.125	5	+ 26.0	1.4		
63700		2065	7 45.1	−24 37	3.5	Gop	.007	3	− 3.8	1.7	+ 3.9	L
63752		2068	7 45.4	− 8 56	5.8	K3	.014	3	− 7.4	1.7		
67458	Cin.	961	8 2.9	−29 6	6.9	Go	.546	3	− 19.2	1.8		
67501	βG.C.	4452Br	8 3.2	+32 31	6.7	F6	....	3	+ 11.4	0.4		
68146	Boss	2163	8 6.0	−13 30	5.6	F8	.235	3	+ 37.7	0.4		
68638	Cin.	971	8 8.1	+57 24	7.8	G5	.394	3	+ 17.7	1.3		
68744		973	8 8.7	+73 39	8.6	Go	.271	3	+ 52	1		
68788		974	8 8.8	+73 44	8.6	K1	.559	3	− 4	2		
68951	Boss	2186	8 9.7	+72 43	6.2	Mo	.027	3	+ 11.2	0.6		
	B.D.	+33°1694	8 18.9	+32 58	9.2	K6	.69	4	− 78	1		
71093	Boss	2232	8 20.4	+28 13	5.8	K2	.134	4	+ 23.8	1.4	+24.3	V
71153		2239	8 20.7	+24 52	7.6	F5	.093	3	+ 18.3	0.5	+17.7	V
71377		2248	8 22.0	−12 12	5.7	K2	.095	3	+ 65.0	2.7		
	B.D.	+46°1405	8 22.5	+46 15	9.4	K6	0.571	4	− 23	±1		

TABLE I—*Continued*

H.D.	Star	α 1900	δ 1900	m	Sp.	μ	No.	v	P.E.	Other Determinations	
										v	Auth.
								km/sec.	km/sec.	km/sec.	
71881	Cin. 996	$8^h24^m.6$	$+50°58'$	7.4	G0	$0''.376$	4	+16.7	±0.9		
71952	Boss 2260	8 25.1	+53 27	6.5	G8	.088	3	+44.1	1.7		
72094	2265	8 25.9	+18 26	5.6	M1	.087	3	+44.2	1.5		
72292	2271	8 26.9	+20 47	5.5	K5	.065	3	+25.3	0.4	+22.1	V
72626	βG.C. 4668m	8 28.8	−24 16	6.2	A5n	....	4	− 8	2		
73668	Cin. 1016	8 34.4	+ 6 8	7.8	G4	.326	3	−22.2	1.5		
73840	Boss 2315	8 35.3	−12 7	5.2	K5	.087	2	−12.5	0.5	−11.4	L
74000	B.D. −15°2546	8 36.2	−15 59	9.4	A9	.558	3	+200	5		
74137	Boss 2321	8 37.1	−15 35	5.0	G8	.099	4	− 3.4	2.1	− 1.8	L
75332	2364	8 44.3	+33 40	6.2	F7	.113	3	+ 4.6	1.2	+ 4.4	V
75700	B.D. +12°1927	8 46.3	+12 16	7.8	K0	....	3	− 4.9	1.9		
76219	Boss 2391	8 49.7	+28 19	5.2	G5	.041	3	+17.3	1.4	+17.2	L
....	B.D. +21°1947	8 52.1	+20 50	9.0	F3	.73	4	+36	1		
76644	Boss 2404	8 52.4	+48 26	3.1	A2n	.502	5	+ 9	3	+13	L
77175	βG.C. 4890N	8 55.8	+15 41	8.7	K6	.328	3	−13	1		
77353	Boss 2425	8 56.9	− 0 6	5.8	G9	.091	3	+73.7	1.7		
77408	Cin. 1070	8 57.2	+33 16	7.1	F5s	.40	3	+70.5	2.0		
77800	Boss 2434	8 59.6	+67 16	5.3	M0	.050	3	+18.7	0.4	+13.4	L
77938	C.D. −31°6877	9 0.3	−32 3	7.7	M5	....	3	− 3	1		
78235	Boss 2444	9 2.0	+30 3	5.4	G5	.028	3	−14.2	1.5	−12.6	L
78732	2456	9 4.7	− 8 23	5.7	G7	.036	3	+26.5	1.5		
79354	2474	9 8.4	+57 9	5.5	M0	.036	3	−31.2	1.9	−30.4	L, V
80024	2494Br	9 12.3	+35 47	5.8	A5	.058	5	+17	3	+25.4	V
80441N	βG.C. 5030N	9 14.8	+38 37	7.0	F4s	.047	3	+ 0.6	1.2		
80441S	5030S	9 14.8	+38 37	7.2	F2s	0.047	4	− 1.9	±1.1		

								km/sec.	km/sec.	km/sec.	
80499	Boss 2506	9h15m0	−11° 33′	4 9	G5	0″.021	3	− 5 8	±2.2	− 0.9	L
80536	2508	9 15.3	+25 35	7.3	G0	.160	3	− 38.6	1.8		
81809	2535	9 22 8	− 5 38	5.4	G1	.233	3	+ 52.3	1.2	+53.8	L
81937	2540	9 23.7	+63 30	3.8	A5n	.117	5	− 8	3	− 8	L
82087	2543	9 24.7	+34 6	6.0	G8	.065	6	+ 2.0	0.9	+ 1.4	V
82198	2546	9 25.5	+35 33	5.5	M1	.130	3	+ 37.7	1.0		
. . . .	B.D. +36°1970	9 25 8	+36 47	9.3	M2	.56	4	+ 21	3		
82309	βG.C. 5124Br	9 26.1	+20 27	7.4	G9	.118	3	− 10.6	2.4		
82522	Boss 2561	9 27 4	+36 56	6.4	K4	.059	3	− 17.4	1.5		
82621	2565	9 28.0	+52 30	4.6	A0	.073	5	+ 22	4	+20	L
82741	2570	9 28.8	+40 4	5.0	G5	.031	3	− 11.3	0.4	−11.9	L
82819	B.D. + 8°2243	9 29.4	+ 8 38	8.1	M4	.019	3	+ 45	2		
83069	Boss 2578	9 30.8	+31 37	5.7	M2	.044	3	− 17.9	1.5	−22.2	V
83489	2591	9 33.7	+69 42	5.7	K0	.093	3	− 9.0	1.8		
83506	2592	9 33.8	+72 42	5 4	G6	.042	3	− 16.5	1.5	−17.4	L
83754	2600	9 35.5	−13 53	5.0	B3	.031	3	+ 13	3	+17	L
83805	2601	9 35.8	+40 13	5.5	G5	.076	3	+ 32.4	1.7	+28.7	L
84035	Cin. 1153	9 37.1	+43 10	8.1	K5	.819	3	− 13.5	1.5		
84406	Boss 2617	9 39.9	+63 43	6.9	K0	.192	3	+ 7.5	1.9		
84453	2620	9 40.3	+45 35	6.8	K0	.155	3	− 43.8	2.1	−44.4	V
85029	2633	9 44.1	+40 6	6 8	M2	0.016	4	+ 8.6	1.5		
. . . .	Cin. 1167	9 46.2	−11 49	9 4	M2	1.848	4	+ 61	3		
. . . .	B.D. +63° 869	9 48.8	+63 16	8.7	M1	0.600	3	+ 10	1		
86012	Boss 2662	9 50.7	+32 51	6.6	F3s	.039	3	+ 9.1	0.5	+ 6.8	V
86513	2675	9 53.8	+30 7	5.9	G9	.112	3	− 0.1	1.8		
87443	βG.C. 5304Br	9 59.9	+31 35	7.9	A9n	.042	3	+ 20	1		
87696	Boss 2692	10 1.5	+35 44	4.5	A5	.054	3	− 14	2	−12:	L
88218	2704	10 5.2	−35 22	6.3	F9	.436	3	+ 40.9	0.7		
88547	2714	10 7.6	+ 5 7	5.9	G9	.059	3	+ 32.2	1.3		
. . . .	B.D. +10°2122	10 7.9	+10 4	9.2	K2	.626	3	− 17	±1		

TABLE I—*Continued*

H.D.	Star	α 1900	δ 1900	*m*	Sp.	μ	No.	*v*	P.E.	Other Determinations	
										v	Auth.
								km/sec.	km/sec.	km/sec.	
88742..........	Boss 2718	10^{h} $9^{m}0$	−32° 32′	6.4	G0	0.″356	3	+ 40.8	±0.4		
88986..........	2727	10 10.8	+29 11	6.5	F9	.108	3	+ 31.5	.7	+28.8	V
89056..........	2731	10 11.3	+14 14	5.7	M2	.035	3	+ 2.2	0.4		
89254..........	2735	10 12.7	− 7 34	5.4	F2s	.161	3	+ 20.7	2.3	+12.6	L
89269..........	2736	10 12.8	+44 33	6.7	G4	.311	3	− 10.5	1.1	− 6.9	V
89668..........	Cin. 1246	10 15.7	− 0 58	8.9	M0	.679	4	+ 35	2		
89777..........	B.D. −16°3030	10 16.5	−16 33	9.1	K1	.54	3	+ 44	3		
90254..........	Boss 2766	10 20.0	+ 9 18	5.9	M3	.045	5	− 20.3	1.3		
90277..........	2768	10 20.2	+34 18	4.8	F2	.107	3	+ 12.4	2.1	+13.7	L
90362..........	2770	10 20.7	− 6 33	5.8	M2	.189	3	+ 31.9	0.8		
....	B.D. +46°1635	10 25.5	+46 3	9.3	M0	.837	3	+ 25	3		
91550..........	Boss 2815	10 29.3	−23 14	5.3	K5	.009	2	− 3.9	0.5	− 5.3	L
91881..........	βG.C. 5491Br	10 31.6	−26 11	6.2	F2s	....	3	− 20.8	2.2		
92523..........	Boss 2844	10 35.9	+69 36	5.2	K4	.023	2	+ 1.7	1.7	− 0.6	L
....	B.D. +47°1806	10 38.1	+46 49	9.1	G0	....	3	− 15	2		
92940..........	+33°2022	10 38.8	+33 9	7.3	A9	.033	6	− 6	2		
92841..........	Boss 2858Br	10 38.2	+ 5 16	6.0	K2	.045	5	− 9.1	1.5	− 3.2	V
93257..........	2869	10 41.0	+19 25	5.6	K2	.099	3	− 6.3	0.7		
93291..........	2870	10 41.1	+14 43	5.6	G5	.152	3	+ 34.2	1.8		
94388..........	2902	10 48.6	−19 36	5.3	F5	.253	3	+ 0.8	1.9	− 4.5	L
94402..........	2903	10 48.6	− 1 36	5.7	G6	.094	3	+ 15.8	1.7		
94469..........	βG.C. 5599	10 49.2	+21 19	8.4	F1s	....	4	− 44	3		
94481..........	Boss 2906	10 49.3	−13 14	5.8	G4	.029	3	+ 4.9	0.9		
95241..........	2924	10 54.7	+43 27	6.1	F7	0.178	3	− 8.4	1.0	− 6.4	V
96074..........	B.D. +66° 697	10 59.8	+66 25	7.7	G5	....	4	− 10.5	±2.6		

									km/sec.	km/sec.	km/sec.	
....	βG.C.	5679Br	$11^h\ 2^m.1$	+53° 21′	7.1	F7	0″.044	3	− 36.6	±2.3		
96700..........	Cin.	1356	11 3.2	−29 38	6.5	G0	.546	3	+ 10.7	0.8		
97033..........		1359	11 5.3	+66 34	9.0	G6	.356	4	− 2	2		
97233..........		1364	11 6.5	−14 26	9.3	K6	.92	3	− 2	1		
97561..........	Boss	2967	11 8.4	+20 41	6.9	G3	.408	3	+ 44.9	1.7	+44.2	V
97605..........		2973	11 8.8	+ 8 36	5.9	K3	.130	3	+ 18.6	2.0	+15.8	V
....	Cin.	1375	11 12.2	− 1 26	9.0	M0	.53	3	+ 4	3		
99167..........	Boss	3002	11 19.6	−10 19	5.1	M1	.043	2	+ 5.1	0.2	+ 1.8	L
99196..........		3004	11 19.8	+11 59	6.0	K4	.116	4	+ 37.7	1.0		
99651..........		3020	11 22.8	− 1 9	6.3	G8	0.042	3	− 9.1	0.3		
....	Cin.	1412	11 23.3	+ 8 6	9.7	G8	1.16	3	+ 1	2		
99984..........	Boss	3028	11 25.1	+43 43	5.9	F2s	0.088	3	− 29.6	0.5		
99998..........		3029	11 25.2	− 2 27	5.1	K5	.026	3	+ 19.8	1.7	+18.5	L
100180..........		3032Ft	11 26.6	+14 55	8.4	M0	.387	4	− 10	1		
100563..........		3044	11 29.2	+ 3 37	5.8	F6	.215	3	+ 7.3	0.5		
101853..........		3083	11 38.3	+42 17	6.8	G8	.031	5	+ 3.9	0.8	+ 1.8	V
101933..........		3086	11 38.8	− 6 7	6.2	G9	.083	5	− 2.5	0.8		
102590..........	βG.C.	5926	11 43.5	+14 50	5.9	A6n	.12	3	+ 6	3		
102942–3..........	B.D.	+34° 2264	11 46.0	+33 56	6.1	F0s	....	3	+ 1.8	0.8	− 0.6	V
103026..........	Boss	3110	11 46.6	−30 16	6.0	F6	.310	3	+ 33.4	1.0		
103246..........	βG.C.	5951Br	11 48.3	+74 19	6.8	F7s	.090	3	− 35.3	1.3		
103484..........	Boss	3121	11 49.9	+ 9 0	5.6	G6	.030	3	− 9.1	0.5		
103596..........		3124	11 50.6	−27 55	6.1	K5	.032	3	+ 7.7	0.1		
103945..........		3128	11 53.1	+ 4 2	6.9	M4	.009	3	− 22.4	2.2		
104055..........		3132	11 53.9	+ 1 5	6.5	K3	.070	3	+ 11.4	1.6		
104216..........		3136	11 55.1	+81 25	6.4	M4	.068	3	+ 31.2	1.9		
104731..........		3148	11 58.5	−41 52	5.3	F5	.344	2	+ 38.1	0.0	+37.4	L
104755..........		3149	11 58.6	+ 6 7	6.5	F3s	.171	3	+ 1.6	0.9	+ 7.6	V
104800..........	Cin.	1492	11 59.0	+ 3 55	9.3	F9	.567	3	+ 11	3		
104985..........	Boss	3156	12 0.2	+77 28	6.0	G9	0.169	3	− 19.0	±0.8	−18.7	V

TABLE I—*Continued*

H.D.	Star		α 1900	δ 1900	m	Sp.	μ	No.	v	P.E.	Other Determinations	
											v	Auth.
									km/sec.	km/sec.	km/sec.	
....	B.D.	+28°2078	12h 1m1	+28° 3′	9.1	F6	0″.41	3	− 3	±1		
105390		+ 0°2897	12 3.0	+ 0 11	8.9	F6	....	4	− 19.4	1.4		
105702	Boss	3171	12 5.0	+ 6 22	5.7	cF4	.166	4	− 10.3	1.3	− 9.2	V
105791	Cin.	1515	12 5.6	+66 13	8.7	F2	.31	3	+ 66	2		
105963N	βG.C.	6064N	12 6.5	+53 59	7.5	K2	.221	4	− 9.5	0.8		
105963S		6064S	12 6.5	+53 59	7.7	G9	.221	3	+ 4.0	2.2		
106057	Boss	3181	12 7.1	+21 6	5.7	G7	.033	3	− 24.4	2.1	−25.8	V
106365	βG.C.	6082Br	12 9.1	+33 20	6.8	K2	.128	3	− 10.3	1.5		
107054–5	Cin.	1541	12 13.5	+30 49	6.1	A5n	.148	4	− 31	1		
107113	Boss	3204	12 13.9	+86 59	6.3	A8s	.210	3	− 6	1		
....	B.D.	+29°2279	12 14.5	+28 56	9.5	M2	.64	4	− 26	2		
107341	Boss	3212	12 15.2	+38 27	6.7	G6	.056	3	+ 4.9	0.4		
107325		3214	12 15.3	+27 11	5.7	K2	.138	3	− 9.7	0.9		
107465		3219	12 16.0	+58 25	5.7	K4	.083	3	− 41.3	1.0	−44.0	V
107612	B.D.	+17°2469	12 17.0	+17 17	6.6	A3s	....	4	+ 3	2		
107966	Boss	3231	12 19.3	+26 39	5.1	A2	.033	3	+ 3	2	− 2.5	L
108153	Cin.	1566	12 20.4	+32 26	9.3	K4	.468	3	− 20	3		
108225	Boss	3235	12 20.9	+39 34	5.2	G6	.086	4	− 4.1	1.1	− 2.8	L, V
108506		3247	12 22.7	− 4 4	6.0	Fon	.081	4	− 14.0	4.3		
108574	βG.C.	6179Br	12 23.3	+45 21	7.4	F8	....	3	− 0.1	0.4		
108575		6179Ft	12 23.3	+45 21	8.0	G2	....	3	+ 0.8	0.3		
108680	Boss	3252	12 24.0	− 1 53	7.6	M4	.049	3	− 35.7	0.7		
108767		3256	12 24.7	−15 58	3.1	A0	.251	3	+ 1	4	− 4:	L
108821		3259	12 25.1	−23 9	5.9	M0	.030	3	− 11.6	1.8		
108910		3264	12 25.7	− 3 31	7.1	K3	0.078	3	+ 83.9	±0.4		

								km/sec.	km/sec.	km/sec.	
....	B.D. + 9°2636	12ʰ26ᵐ3	+ 9° 22′	9.1	M1	0″.96	3	+ 21	±2		
109141..........	Boss 3273	12 27.4	−13 18	5.7	A0n	.154	3	− 1	1		
109628p..........	βG.C. 6216p	12 31.0	+11 57	8.5	F7	.300	5	+ 23	2		
109628f..........	6216f	12 31.0	+11 57	8.5	G0	.300	3	+ 17	1		
109742..........	Boss 3291	12 32.0	+17 38	5.8	K5	.050	3	− 8.0	0.8		
112943..........	Cin. 1661	12 55.2	− 2 10	9.1	M0	.73	3	− 13	1		
113101..........	1667	12 56.2	− 7 54	8.7	K0	.493	7	− 31	3		
113415..........	Boss 3387	12 58.4	−20 3	5.7	F8	.141	3	+ 33.5	1.5		
113865..........	B.D. +29°2365	13 1.4	+29 34	6.4	A4n	....	4	+ 2	1		
113848..........	Boss 3397	13 1.5	+21 41	6.0	F0n	.089	3	+ 1.9	0.8	− 1.1	V
114060Br..........	βG.C. 6393Br	13 2.9	+24 32	7.6	G5	.27	7	− 4.1	1.4		
114060Ft..........	6393Ft	13 2.9	+24 32	8.0	G7	.27	3	+ 0.5	1.5		
114094..........	B.D. + 4°2696	13 3.2	+ 4 19	9.5	G6	.54	3	− 57	3		
114300..........	+18°2696	13 4.6	+18 0	8.7	M0	.120	3	− 25	2		
114613..........	Boss 3421	13 6.5	−37 16	4.9	G3	.390	3	− 12.8	1.8	−15.8	L
114703..........	Cin. 1693	13 7.0	+68 2	8.8	K0	.75	4	− 13	2		
114692..........	C.D. −34°8720	13 7.0	−34 13	7.6	F7	.509	4	+ 1.3	1.6		
114729..........	Boss 3425	13 7.2	−31 20	6.7	G0	.380	4	+ 63.3	2.5		
114946..........	3430	13 8.8	−19 24	5.6	G4	.198	3	− 44.5	2.1		
115079..........	3435	13 9.7	−10 50	7.8	G3	.383	4	+ 7.1	1.3		
115478..........	3445	13 12.3	+14 12	5.4	K2	.027	3	− 27.2	0.9	−25.6	L
116303..........	3466	13 17.7	+44 26	6 4	A5s	.075	3	− 2	1		
116713..........	3477	13 20.3	−39 14	5.2	K0p	.203	3	+ 64.2	1.6	+69.4	L
116870..........	3481	13 21.4	−12 11	5.6	K5	.137	3	− 29.0	1.6		
116976..........	3482	13 22.1	−15 27	4.9	K1	.127	3	− 16.2	2.2	−13.7	L
117421..........	B.D. − 7°3631	13 25.0	− 8 5	9.6	F4	....	3	− 33	3		
117448..........	+70° 741	13 25.3	+70 39	7.5	K0	.039	5	− 28.5	2.1		
117697..........	+ 9°2773	13 27.0	+ 9 30	7.9	F8	.019	4	+ 8.6	1.7		
117939..........	C.D. −38°8635	13 28.7	−38 23	7.1	G4	.500	4	+ 86.8	2.2		
118036..........	βG.C. 6530Br	13 29.2	+ 0 12	7.4	K1	0.234	3	− 2.6	±0.7		

TABLE I—*Continued*

H.D.	Star		α 1900	δ 1900	m	Sp.	μ	No.	v	P.E.	Other Determinations	
											v	Auth.
									km/sec.	km/sec.	km/sec.	
118054..........	Boss	3507m	$13^{h}29^{m}.4$	−12° 42′	5.8	A2s	0″.067	4	− 20	±3		
119126..........		3533	13 36.3	+23 0	5.8	G5	.041	3	+ 5.5	1.1	+ 3.8	V
119217..........	B.D. + 0°3090		13 36.8	+ 0 24	9.3	M1	.545	3	+ 48	2		
119756..........	Boss	3544	13 40.0	−32 32	4.4	F1s	0.489	3	− 17.1	1.1	−14.9	L
....	Cin.	1784	13 40.2	+18 20	9.0	M1	1.86	4	+ 27	1		
120052..........	Boss	3553	13 42.0	−17 21	5.8	M2	0.065	3	+ 63.4	0.4		
120198..........		3561	13 42.9	+54 56	5.5	A2s	.015	5	− 5	2	− 5.3	V
120237..........	Cin.	1796	13 43.2	−35 12	6.5	F8	.57	3	+ 6.3	1.1		
120348..........	Boss	3568	13 43.9	+42 33	6.8	K2	.075	3	− 1.2	0.2		
120420..........		3570	13 44.1	+31 41	5.8	G7	0.043	3	+ 12.5	0.1	+10.5	V
120467..........	B.D. −21°3781		13 44.4	−21 36	7.9	K6	1.77	3	− 35.3	0.2		
120539..........	Boss	3573	13 45.0	+21 46	5.1	K4	0.017	2	− 1.7	0.5	− 3.1	L
121849..........	Cin.	1826	13 52.8	−33 30	8.4	G2	.59	3	+ 64	3		
121953..........		1828	13 53.7	+65 51	7.6	G2	.291	4	− 28.4	0.8		
122066..........	Boss	3607	13 54.4	−24 31	5.8	F2	.235	3	− 17.3	2.7		
....	B.D. +34°2476		13 54.8	+34 22	9.3	A5sp	.54	3	−164	2		
122408..........	Boss	3612	13 56.6	+ 2 2	4.3	A2	.032	5	− 4	4	− 5	L
123453..........	βG.C.	6725Br	14 2.6	−12 27	7.4	F4	.141	3	+ 14.1	1.0		
123934..........	Boss	3632	14 5.4	−15 50	5.1	M3	.027	3	+ 19.5	1.9	+17.6	L
124640Br.........	βG.C.	6776Br	14 9.7	+55 48	8.2	K6	.341	3	− 16	1		
124640Ft.........		6776Ft	14 9.7	+55°48′	8.5	K6	.341	3	− 18	2		
124679..........	Boss	3655	14 10.0	+10 34	5.4	G6	.172	3	+ 15.7	2.1	+17.0	L
124757..........	βG.C.	6780m	14 10.3	+ 3 35	7.0	F8	.194	5	− 44.8	1.2		
125040Br.........		6795Br	14 11.9	+20 35	6.4	F6	.181	3	− 10.1	1.3		
125140Br.........		6801Br	14 12.2	+57 7	8.5	G1	0.044	4	− 1	±1		

									km/sec.	km/sec.	km/sec.	
125140Ft	βG.C.	6801Ft	$14^{h}12^{m}.2$	+57° 7′	9.8	F0	0″.044	4	− 4	±2		
125560	Boss	3681	14 15.0	+16 46	5.0	K4	.155	3	− 8.1	0.4	− 7.3	L
125906	βG.C.	6837S	14 17.3	− 7 18	6.8	F8	0.125	3	− 34.8	1.5		
....	Cin.	1894	14 21.1	+24 6	9.0	M2	1.39	4	+ 14	2		
....		1895	14 21.1	+24 6	9.1	M2	1.40	5	+ 5	2		
126927	Boss	3711	14 23.4	− 6 27	5.7	K5	0.075	3	− 49.7	0.8		
127339	Cin.	1905	14 25.6	− 8 12	9.3	M1	1.26	3	− 27	2		
127506	B.D.	+36°2500	14 26.7	+35 53	8.2	K6	0.51	3	− 12	2		
127739	Boss	3721	14 28.0	+22 42	6.0	A9s	.133	5	− 12	2		
127930	βG.C.	6923Br	14 29.0	+49 38	7.8	F5s	....	3	− 4	1.1		
128165	Boss	3728	14 30.2	+53 20	7.4	K6	.316	3	+ 13.7	1.7		
....	Cin.	1920	14 30.9	+34 11	9.0	M0	.76	4	− 53	2		
128333	Boss	3733	14 31.2	+49 48	5.9	M1	.067	3	− 20.4	1.3		
128967	βG.C.	6949Br	14 34.9	+27 15	8.4	F1n	....	4	− 10.1	1.9		
129246–7	Boss	3752m	14 36.4	+14 9	3.8	A2n	.061	2	− 6	1	− 3:	L
129312		3753	14 36.7	+ 8 35	5.0	G0	.010	3	− 21.1	1.3	−22.6	L, V
129580Ft	βG.C.	6977Ft	14 38.2	+58 22	8.0	G4	.244	4	− 15.6	1.2		
....	B.D.	+ 6°2932	14 38.4	+ 6 15	9.5	G0	.93	3	−138	6		
129846	Boss	3764	14 39.8	+40 53	5.8	K3	.024	3	+ 16.6	1.1	+10.7	V
....	Cin.	1948	14 41.7	+16 56	8.9	K6	.97	4	+ 47.4	1.8		
130871		1960	14 45.5	+ 7 14	9.4	K5	.603	3	− 32	1		
130991	B.D.	−20°4107	14 46.0	−20 12	7.5	G8	....	3	− 7.1	1.1		
131111	Boss	3795	14 46.5	+37 41	5.5	G7	.231	4	− 64.8	1.8	−66.7	L, V
131316Br	βG.C.	7043Br	14 47.8	+45 1	8.0	F5s	....	3	− 27.8	2.6		
131473Br		7049Br	14 48.6	+16 6	6.4	F9	.017	3	+ 20.8	1.6		
132029Br		7065Br	14 51.7	+32 42	6.1	A3n	....	5	− 11	2		
132833	Boss	3828	14 56.1	− 2 22	5.7	M1	.048	4	− 15.2	1.7		
132933Br		3831Br	14 56.7	+ 0 15	5.9	M2	.030	3	− 35.7	0.6	−33.6	V
133029	B.D.	+47°2192	14 57.2	+47 40	6.2	A0	....	3	− 16	1	−12.6	V
133392	Boss	3841	14 59.1	+35 36	5.7	G8	0.050	3	− 26.2	±1.2		

TABLE I—*Continued*

H.D.	Star	α 1900	δ 1900	m	Sp.	μ	No.	v	P.E.	Other Determinations v	Other Determinations Auth.
								km/sec.	km/sec.	km/sec.	
134088	Cin. 2010	15^h $2^m.9$	−7° 31′	8.1	F8	0″.484	5	−59.2	±2.1		
....	2012	15 3.1	+25 18	9.2	M0	.961	3	−65	4		
134190	Boss 3856	15 3.4	+54 56	5.2	G5	.044	3	+15.7	1.3	+16.4	L, V
....	B.D. +32° 2547	15 3.6	+32 47	9.5	G0	.59	4	−63	3		
134285Br	βG.C. 7136Br	15 3.9	+2 4	7.8	F3s	....	3	+10.6	0.5		
134329	Boss 3858	15 4.0	−23 36	6.8	K5	.046	3	−14.1	3.2		
134320	3859	15 4.1	+26 41	5.7	K2	.029	3	+24.2	1.8	+18.3	V
134335	3860	15 4.2	+25 29	5.9	K1	.017	3	−17.6	1.3	−16.2	V
134987	3869	15 7.6	−24 56	6.4	G3	.401	3	+2.4	1.0		
....	B.D. −3° 3746	15 8.8	−3 26	9.2	M0	.69	3	−107	1		
135363	+76° 552	15 9.6	+76 34	9.2	K2	.211	3	−1	1		
135402	Boss 3881	15 9.8	+38 38	6.4	K1	.048	3	−62.5	2.4		
136136N	βG.C. 7212N	15 13.9	+44 10	8.5	G7	.034	3	−45	2		
136136S	7212S	15 13.9	+44 10	8.5	G5	.034	4	−17	2		
136138	Boss 3894	15 13.9	+20 56	5.7	G3	.045	3	−7.6	1.3		
136160Br	βG.C. 7210Br	15 13.9	+10 48	6.7	F5	....	3	−45.5	1.9		
136176	7214m	15 14.1	+27 12	6.6	F7s	0.117	3	−19.6	0.9		
....	B.D. −7° 4003	15 14.2	−7 21	9.8	M5	1.33	4	−30	2		
136526p	βG.C. 7226p	15 16.1	+31 3	8.7	F3	....	3	−43	1		
137443	Boss 3930	15 21.0	+63 42	5.8	K5	0.114	3	−47.3	1.7	−45.7	V
137704	3933	15 22.4	+34 41	5.9	K5	.120	3	−49.1	0.6	−47.9	V
137826	Cin. 2067	15 23.1	+66 54	9.0	G5	.28	4	−34	3		
138481	Boss 3945	15 27.3	+41 10	5.2	M0	.018	3	−7.6	1.1	−10.0	L
139153	3967	15 31.6	+39 21	5.4	M2	.029	4	−19.0	1.4	−19.2	L
139216	3969	15 31.8	+15 26	6.8	M6	0.011	5	−26.2	±2.1		

									km/sec.	km/sec.	km/sec.	
139307	Boss	3972	$15^h32^m.2$	+50° 2′	7.5	K5	0″.021	3	− 11.1	±0.8		
139669		3982	15 34.4	+77 41	5.3	K5	.044	3	− 26.5	1.9	−25.4	L, V
140027		3992	15 36.4	+16 21	6.0	G5	.033	4	+ 3.4	1.7	+ 3.2	V
140160		3993	15 37.1	+13 10	5.3	A0p	.044	4	+ 6	1		
140716		4003	15 40.0	+32 50	5.6	G9	.043	3	− 4.3	1.6	− 3.8	V
140901	Cin.	2109	15 41.0	−37 36	6.1	G5	.525	3	− 3.5	0.9		
141003	Boss	4009	15 41.6	+15 44	3.7	A1n	.091	5	+ 1.0	3	− 7	L
141513		4016	15 44.4	− 3 7	3.6	A0	.092	5	− 9	2	−11	L
141653		4021	15 45.1	+62 54	5.1	A2	.070	7	− 4	2	− 5	L
141680		4023	15 45.2	+ 2 30	5.3	G6	.064	5	− 2.5	1.0	− 3.7	L
142980		4060	15 52.6	+14 42	5.7	K3	.134	3	− 67.4	0.7	−69.4	V
143435		4069	15 55.3	+36 56	5.7	K5	.031	4	+ 10.4	1.1		
143553		4074	15 55.9	+ 4 42	5.9	G7	.081	3	− 3.6	0.6		
143787		4078	15 57.3	−25 35	5.1	K3	.080	3	− 38.5	0.8	−38.8	L
144087	βG.C.	7488Br	15 59.0	−11 10	7.4	G5	....	3	− 33.3	1.4		
144204	Boss	4085	15 59.5	+53 12	6.2	K5	.038	3	− 6.8	1.1		
145000		4102	16 3.6	+17 19	6.5	K1	.062	6	+ 38.0	1.2		
145675		4124	16 7.2	+44 5	6.5	G9	.336	3	− 5.0	1.2		
145958		4132S	16 8.6	+13 48	7.8	K0	.459	6	+ 17.7	1.5		
146698	B.D. +19°	3077	16 12.5	+19 5	7.6	K5	017	3	+ 9.4	0.7		
146834	Boss	4150	16 13.3	−19 58	6.4	G6	.026	8	+ 8.5	1.2		
147025		4154	16 14.2	+26 8	6.6	G4	.009	4	− 10.7	1.1	− 8.4	V
148048		4181	16 20.4	+75 59	5.0	A8n	.261	4	− 10	1	− 8	L, V
148211	Cin.	2193	16 21.3	−21 54	7.6	F8	.417	3	− 19.1	0.9		
148493	βG.C.	7636Br	16 23.4	+21 3	8.3	F9	.138	3	+ 8.9	0.5		
148604	Boss	4197	16 24.1	−14 20	5.8	G2	.025	3	− 31.9	0.7		
148605		4198	16 24.1	−24 54	4.9	B3	.028	3	− 2	4	− 5	L
148704	Cin.	2200	16 24.8	−38 48	7.5	K0	.563	3	− 59.1	0.6		
148783	Boss	4201	16 25.3	+42 6	5.0	M6	0.028	3	+ 3.5	1.0	+ 3.3	L
148980Br	βG.C.	7655Br	16 26.7	+ 5 39	7.6	A9	....	3	− 14	±2		

TABLE I—*Continued*

H.D.	Star	α 1900	δ 1900	m	Sp.	μ	No.		P.E.	Other Determinations	
										v	Auth.
								km/sec.	km/sec.	km/sec.	
149303Br	Boss 4214Br	$16^{h}28^{m}.8$	+45° 49′	5.6	A1n	0″.028	5	− 13	±3	−18.5	V
149303Ft	4214Ft	16 28 8	+45 49	8.2	F5	.028	4	− 16.9	1.6		
149957	Cin. 2217	16 32.9	+31 19	9.5	K6	.59	3	− 7	0		
....	B.D. +31°2877	16 33.4	+31 25	9.2	K5	....	3	− 20	1		
150379	Boss 4237	16 35.6	+ 4 24	6.9	A5n	.023	4	− 30	1		
151188	βG.C. 7748m	16 40.8	+43 41	8.3	K5	....	3	− 7	0		
151216	B.D. +33°2775	16 41.0	+33 30	8.8	K1	.059	5	− 16	2		
151482	+34°2839	16 42.5	+33 59	8.1	A3n	.02	6	+ 1	2		
151937	Boss 4279	16 45.3	+30 8	6.7	G7	.102	4	− 42.7	2.0		
152107	4284	16 46.3	+46 9	4.9	A4s	.076	3	− 4	1	+ 0.8	L
152334	4292	16 47.6	−42 11	3.8	K5	.266	2	− 15.3	0.4	−18.8	L
152326	4294	16 47.6	+24 49	5.2	K2	.016	3	− 15.5	1.1	−15.9	L
153301	βG.C. 7814Br	16 53.5	+15 18	7.8	G5	....	3	− 11.0	2.0		
153344	Boss 4317	16 53.8	+62 16	7.0	G2	.321	4	− 82.6	2.0		
....	B.D. +25°3173	16 54.1	+25 55	9.4	M2	.52	3	+ 11	4		
153834	Boss 4329	16 56.7	+22 47	5.7	K2	.030	3	+ 10.4	0.5	+11.0	V
153956	4330	16 57.5	+56 50	6.1	K2	.054	3	− 15.4	1.1		
154088	4333	16 58.1	−28 26	6.7	G8	.291	3	+ 17.2	1.8		
154228	4340	16 59.0	+13 45	5.9	A2s	.054	5	− 37	1		
154278	4341	16 59.3	+13 43	6.1	G7	0.135	4	+ 47.0	1.1		
154363	4342	16 59.8	− 4 54	7.9	M0	1.464	3	+ 28.2	0.5		
....	B.D. − 4°4226	17 0.0	− 4 55	9.3	M3	1.465	3	+ 30	4		
154733	Boss 4350	17 2.1	+22 13	5.7	K5	0.122	4	− 95.4	0.9	− 97.2	V
154759	βG.C. 7873Br	17 2.4	+47 6	8.1	K2	.046	3	− 52.9	0.4		
155644	Boss 4366	17 7.7	+10 42	5.6	M2	0.036	3	+ 25.3	±1.9		

								km/sec.	km/sec.	km/sec.	
155876	B.D. +45°2505	$17^{h}\ 9^{m}.2$	+45° 50′	9.6	M4	$1''.590$	4	− 19	±3		
	Cin. 2297	17 9.9	+42 28	9.4	M1	1.061	6	+ 6	3		
156681	Boss 4389	17 13.9	+10 58	5.3	K5	0.099	2	+ 42.7	0.2	+39.0	L
156890	βG.C. 7962Br	17 14.9	+60 49	6.7	A7n	.041	3	− 26	1		
157049	Boss 4400	17 15.9	+18 10	5.2	M2	.051	4	− 47.0	1.3	−46.1	L, V
157325	4408	17 17.5	+46° 20′	5.8	M0	.050	4	− 57.2	0.9		
157370	4409	17 17.8	+71 54	6.8	K2	.018	3	− 3.9	0.9		
157906Br	βG.C. 8009Br	17 21.0	+47 22	7.8	F6s	....	4	− 26.9	1.4		
157910	Boss 4422	17 21.0	+37 2	6.5	G5	.053	3	− 14.8	1.5	−18.2	V
158116Br	βG.C. 8017Br	17 22.4	+29 33	7.0	A8	....	4	− 25	1		
	Cin. 2326	17 22.9	+31 8	9.1	G7	.421	4	− 73	2		
158225	B.D. +31°3026	17 23.0	+31 21	7.0	F4	....	4	+ 0.1	0.8		
158226	Cin. 2328	17 23.0	+31 10	8.1	G0	.32	4	− 71	1		
159332	Boss 4446	17 29.0	+19 20	5.6	F5	.095	4	− 61.0	2.1		
159466	4451	17 29.8	+13 14	6.7	G4	.036	3	− 60.1	0.7		
161074	4486	17 38.4	+24 37	5.6	K5	.131	3	− 27.5	0.8	−28.0	V
161471	4492	17 40.6	−40 5	3.1	F6	.004	6	− 21.9	1.7	−26.7	L
161848	Cin. 2366	17 42.8	+ 4 59	9.0	K3	.70	3	− 93	2		
162076	Boss 4506	17 44.1	+20 36	5.8	G5	.022	3	− 28.6	1.1	−25.4	V
162555	4510	17 46.5	+29 21	5.6	G7	.049	3	− 13.7	0.4	−14.5	V
163608	B.D. +45°2621	17 51.8	+45 14	8.0	A0	.023	3	− 23	3		
163609	βG.C. 8242Br	17 51.8	+21 30	7.5	G3	....	3	− 32.5	1.7		
165625	Boss 4578	18 1.8	+22 13	5.3	M2	.023	5	− 19.8	1.1	−18.6	L, V
165945	B.D. −15°4832	18 3.3	−15 33	9.2	A4	....	4	− 16	2		
167618	Boss 4617	18 10.8	−36 48	3.2	M4	.216	3	+ 5.2	1.3	+ 0.1	L
168322	4624	18 13.9	+40 54	6.1	G3	.180	3	− 73.7	0.9		
168387	4626	18 14.3	+ 7 13	5.6	K2	.063	3	− 7.3	.9	− 8.7	V
168415	4627	18 14.4	−15 52	5.7	K5	.047	3	+ 30.1	.9		
168653	4634	18 15.9	+68 43	6.1	K0	.062	4	− 10.7	.8		
169110	4649	18 18.0	+23 14	5.7	M0	0.076	3	− 57.4	±0.8		

TABLE I—*Continued*

H.D.	Star	α 1900	δ 1900	m	Sp.	μ	No.	v	P.E.	Other Determinations	
										v	Auth.
								km/sec.	km/sec.	km/sec.	
169746	B.D.+ 43°2970	$18^{h}21^{m}1$	+43°51′	7.0	M2	....	3	− 46.7	±0.6		
170397	Boss 4675	18 24.1	−14 39	6.0	A2	0″022	4	− 16	2		
170740	4687	18 25.9	−10 52	5.8	B3	.031	3	− 13	1		
171115	4698	18 27.8	−24 6	5.7	K5	.018	3	− 14.6	1.3		
171586	βG.C. 8654	18 30.7	+ 4 51	6.7	A4p	.05	3	− 11	1		
171745	Boss 4708	18 31.3	+23 31	5.8	G7	.021	3	+ 16.4	1.6		
172546	4726	18 35.8	−23 56	6.1	A8	.043	3	+ 1	2		
172586Br	βG.C. 8721Br	18 35.8	+24 37	8.0	G5	....	3	− 32.0	2.1		
172713	Boss 4728N	18 36.6	+52 15	7.4	G0	.012	4	+ 17.8	1.9		
173460	4743	18 40.3	−22 30	5.8	K5	.026	4	− 3.1	1.1		
174224	βG.C. 8830	18 44.4	+16 8	8.1	F5s	.076	3	− 61.3	2.1		
....	Cin. 2463	18 44.5	+17 20	9.0	M0	.579	4	− 17	2		
174589	Boss 4773	18 46.1	− 3 26	6.0	A5n	.037	3	+ 12	2		
174980	4782	18 48.3	+73 58	5.4	G8	.081	3	+ 4.0	0.9	+ 2.8	L, V
175518	Cin. 2471	18 50.6	− 5 52	8.2	G8	.415	6	− 76.9	2.6		
176485	βG.C. 8954Br	18 55.3	+12 45	7.1	K5	.035	3	− 2.6	1.4		
176982	8986Br	18 57.6	− 0 51	7.9	G5	.131	3	− 11.2	1.2		
177095	Cin. 2487	18 58.0	−20 35	9.4	G2	.71	3	+ 78	2		
177483	Boss 4855	18 59.8	+52 7	6.4	G8	.029	3	+ 4.7	0.3		
177758	Cin. 2490	19 0.9	−12 2	7.1	F8	.422	3	− 2.5	1.3		
177749Br	βG.C. 9021Br	19 0.9	+ 6 24	6.9	F4	....	3	− 17.8	1.8		
178496	Cin. 2497	19 3.7	−21 37	8.7	G3	.468	4	− 42	1		
178770	Boss 4877	19 4.8	+39 0	7.6	M6	.007	3	− 17.2	0.4		
178911	βG.C. 9078Br	19 5.3	+34 26	6.5	G0	.191	3	− 41.7	1.3		
179406	Boss 4883	19 7.2	− 8 6	5.4	B3	0.017	3	− 15	±5	−19:	L

									km/sec.	km/sec.	km/sec.	
179484..........	βG.C.	9114A	19h 7m.7	+38° 37′	7.5	G4	0″.267	7	+ 27.4	±2.1		
179626..........	Cin.	2509	19 8.2	− 0 45	9.3	F4	.53	3	− 71	2		
180409..........	Boss	4901	19 11.3	−11 9	7.0	F6	.142	3	− 58.9	1.9		
180540..........		4903	19 11.8	−19 8	5.0	G6	.023	5	+ 15.3	3.3	+15.8	L
182477..........		4945	19 19.7	−14 6	5.8	K2	.086	3	− 34.6	1.8		
182900..........		4963	19 21.8	+12 49	5.8	F2s	.066	4	− 33.9	1.8		
182917..........		4966	19 21.9	+50 3	7.1	M7	.016	3	− 52.5	0.4		
183063S..........	βG.C.	9313S	19 22.7	−12 21	7.9	G4	....	3	− 22.0	0.6		
183473..........	B.D.+	42°3351	19 24.7	+42 33	8.6	G3	....	3	− 44	2		
183492..........	Boss	4977	19 24.8	+14 23	5.7	Ko	.049	3	− 40.9	1.7	−40.6	V
183630..........		4983	19 25.4	− 3 0	5.2	M1	.016	3	− 13.2	1.6	−10.4	L
....	B.D.+	35°3659	19 27.6	+35 58	9.5	Fos	.56	3	−172	2		
184268..........	Boss	4993	19 28.5	−24 4	6.7	Mo	.004	3	− 12.1	0.9		
184489..........	Cin.	2556	19 29.6	+ 4 21	10.5	M1	.58	3	− 52	2		
184860Br........	βG.C.	9434Br	19 31.3	−10 39	8.5	K5	.391	4	+ 68	2		
184853Br........		9439Br	19 31.3	+ 5 48	6.7	G6	....	3	+ 12.4	0.5		
....	B.D.+	44°3242	19 43.4	+44 49	9.2	M2	....	4	− 36	2		
187195..........	Boss	5053	19 43.5	−11 7	6.2	K5	.041	4	− 37.7	1.0		
187259..........		5055	19 44.0	+11 34	5.7	F1s	.011	3	+ 12.6	1.4		
187691..........		5065	19 46.2	+10 10	5.2	Go	.273	4	− 1.4	0.9	+ 0.7	L, V
187849..........		5069	19 47.0	+38 28	5.4	M2	.098	3	− 37.1	1.2	−39.4	L
188041..........		5074	19 48.1	− 3 22	5.6	A4sp	.016	3	− 19	2		
188088..........		5076	19 48.3	−24 11	6.3	K5	.431	4	− 7.5	1.6		
188262..........	B.D.+	16°4053	19 49.2	+16 31	7.6	F6	.008	4	− 0.9	1.1		
188326..........	Cin.	2596	19 49.5	+38 30	8.0	G5	.337	3	− 72	0		
188807..........		2599	19 51.8	−12 49	9.1	M1	.51	3	+ 3	2		
189037..........	Boss	5105	19 53.0	+52 10	4.8	Aon	.051	5	− 5	2	−17:	L
189063..........		5106	19 53.1	+60 33	7.3	M1	.012	4	− 23.0	1.6		
189245..........		5115	19 53.9	−33 58	5.7	F5	.337	3	− 15.2	2.4		
189763..........		5129	19 56.5	−27 59	4.6	M4	0.037	4	+ 6.8	±1.2	+11.5	L

TABLE I—*Continued*

H.D.	Star	α 1900	δ 1900	m	Sp.	μ	No.	v	P.E.	Other Determinations	
										v	Auth.
								km/sec.	km/sec.	km/sec.	
190147	Boss 5137	19h 58m.5	+49° 50′	5.3	G9	0″.018	3	+ 2.3	±0.9	+ 0.8	L, V
190608	5151	20 0.7	+19 42	5.3	K0	.083	4	− 40.1	1.1	−40.5	L, V
190713	5152	20 1.2	+64 21	6.6	G5	.047	3	+ 9.3	1.5		
190918	βG.C. 9916F	20 2.2	+35 31	7.7	O9	.51	4	− 4	1		
190960	Boss 5154	20 2.4	+76 12	6.3	M3	.059	3	− 67.4	2.6	−69.9	V
191174	5162Br	20 3.5	+63 36	6.2	A2s	.048	3	− 19	2		
191499	βG.C. 9949Br	20 5.0	+16 30	7.7	G9	.173	3	− 34.6	0.9		
192439	Boss 5183	20 9.7	+51 10	6.4	K1	.025	3	+ 12.6	.5		
192679Ft	βG.C. 10044Ft	20 11.0	+52 49	9.1	K2	.179	3	− 35	0		
192787	Boss 5193	20 11.5	+33 26	5.8	G6	.132	3	− 10.6	1.0		
192913	B.D.+27° 3668	20 12.3	+27 29	6.7	A2s	....	5	− 15	2		
193202	Cin. 2648	20 13.9	+76 55	9.3	M0	.46	3	− 2	5		
194258	Boss 5234	20 19.7	+68 34	6.0	M5	.042	5	− 43.6	1.2		
194640	Cin. 2657	20 21.5	−31 11	6.7	G6	.55	3	− 2.4	1.0		
195006	Boss 5248	20 23.7	−22 43	6.2	M1	.029	3	+ 55.2	1.1		
195068–9	5251	20 24.0	+49 3	5.7	F0s	.093	4	− 20.3	2.2		
195774	5271	20 28.2	+48 53	5.6	M2	.037	3	− 62.2	1.5	−66.0	V
196124	Cin. 2668	20 30.2	+ 5 47	8.7	K5	.44	4	− 32	1		
196180	Boss 5282	20 30.6	+14 20	4.7	A2	.038	3	− 28	2	−24	L
196758	5305	20 34.3	+ 0 8	5.4	G8	.094	3	− 45.4	1.9	−41.8	L
196852	5309	20 34.9	+29 59	5.9	G7	.090	3	+ 13.2	1.1	+12.4	V
196882	βG.C. 10404Br	20 35.1	+21 22	8.2	K3	....	5	−111	3		
196892	Cin. 2680	20 35.1	−19 8	8.6	F5	.440	4	− 30	3		
197684	βG.C. 10483Br	20 40.1	+11 57	6.7	A6n	....	3	− 11	2		
198542	Boss 5363	20 45.9	−27 18	4.2	M1	0.017	3	+ 4.5	±1.4	+11.4	L

									km/sec.	km/sec.	km/sec.	
199178	Boss	5380	20h50m4	+44° 0′	7.6	G4	0″.021	3	− 22.0	±1.0		
199345		5386	20 51.5	−10 5	5.7	K5	.021	3	− 33.1	1.6		
200004		5407	20 55.6	−13 55	6.6	G3	.005	3	+ 22.3	1.1		
....	Luyten	639	20 56.2	+39 41	9.7	M3e	.671	3	− 57	3		
200310	Boss	5414	20 57.7	+45 46	5.2	B3	.004	4	− 20	4	−20::	L
200497		5418Br	20 58.8	− 6 13	5.9	G2	.018	3	+ 0.6	1.0		
200914		5430	21 1.3	−25 24	4.6	Mo	.059	6	+ 29.4	1.5	+32.4	L
200968	βG.C.	10727	21 1.6	−14 19	7.2	Ko	.373	4	− 37.2	2.5		
201901	Boss	5448	21 7.4	−28 2	5.6	K5	.167	4	− 42.7	2.2		
201889	Cin.	2750	21 7.5	+23 45	8.0	F9	.460	3	−102.5	0.2		
202380	Boss	5458	21 10.2	+59 41	7.1	M2	.012	3	− 14.8	1.5		
202466		5462	21 10.9	− 9 38	6.8	M4	.012	3	+ 7.7	1.3		
202751	Cin.	2763	21 12.9	− 0 15	8.5	K6	.476	5	− 28	2		
203040		2770	21 14.6	−20 15	9.2	K6	.764	3	+ 21	1		
203291	Boss	5479	21 16.1	+ 6 56	6.0	M3	.044	3	− 22.8	0.6	−18.8	V
203475		5487	21 17.3	−23 6	5.7	Mo	.041	3	− 7.3	2.4		
203925		5504	21 20.1	+25 45	5.7	F1s	.039	3	+ 3.0	0.9	− 6.8	V
204129Br		5508Br	21 21.5	+79 55	8.1	F5s	.185	3	+ 28	2		
204139		5510	21 21.6	−21 38	6.0	K5	.037	3	+ 23.0	2.5		
204381		5513	21 23.0	−22 15	4.6	G5	.132	3	− 27.2	2.1	−22.0	L
205021Ft		5532Ft	21 27.4	+70 7	8.0	A3n	.012	4	− 18	3		
205114−5	B.D.+51°	3079	21 28.1	+52 11	6.2	Ko	....	3	− 26.3	0.2		
205855	Cin.	2808	21 33.0	− 2 45	8.8	K5	.566	3	+ 7	2		
206330	Boss	5567	21 36.3	+42 49	5.4	M1	.054	4	− 26.8	0.8	−27.7	L, V
206487		5572	21 37.3	+ 5 13	5.6	M2	.022	4	− 4.0	1.1		
206827		5588	21 39.7	+28 17	6.1	F8	.370	3	+ 16.5	1.1		
207491	Cin.	2833	21 44.1	+ 5 15	8.6	K6	.54	3	− 11	0		
207862Br	βG.C.	11302Br	21 46.9	+ 8 37	7.9	A8	....	3	+ 17	4		
208057	Boss	5627	21 48.5	+25 27	5.0	B3	.001	2	− 16	4	−21:	L
208063		5628	21 48.6	+55 19	7.3	A1s	0.045	4	− 6	±2		

TABLE I—*Continued*

H.D.	Star	α 1900	δ 1900	m	Sp.	μ	No.	v	P.E.	Other Determinations	
										v	Auth.
								km/sec.	km/sec.	km/sec.	
208074	B.D.+66° 1446	21^h48^m7	+66° 22′	8.3	F4s	0″.014	6	− 16	±2		
....	Luyten 680	21 50.8	+32 10	10.8	G1	.73	3	−178	0		
208552Br	βG.C. 11372Br	21 51.9	+15 41	8.3	F5	.039	3	− 21.9	0.6		
208742	Boss 5647	21 53.3	+79 5	6.8	M2	.029	3	− 15.8	1.6		
209761	5673	22 0.6	+26 11	5.9	K0	.048	4	− 21.0	1.5	−27.8	V
209772	5678	22 0.9	+62 38	5.5	M5	.052	3	− 3.8	0.8	− 3.7	L, V
209960	5685	22 2.0	+62 18	5.4	K5	.065	2	− 21.2	1.9	−20.9	L
209945	5686	22 2.0	+44 32	5.3	M0	.017	3	− 20.3	0.8	−23.8	L
210277	5697	22 4.2	− 8 2	6.6	G0	.458	4	− 23.6	1.4		
210302	5698	22 4.3	−33 2	5.1	F6	.447	3	− 14.2	0.5	−14.7	L
210354	5701	22 4.8	+32 41	5.6	G6	.092	3	− 6.2	1.8	− 4.7	V
210464	5708	22 5.5	−21 43	6.1	F6	.111	3	− 13.2	1.9		
....	Cin. 2889	22 5.9	+22 19	8.8	K3	.592	4	− 25	4		
210918	Boss 5725	22 8.5	−41 51	6.4	G0	.955	3	− 18.9	2.2		
211076	5731	22 9.5	+16 42	6.6	K4	.132	7	− 35.8	1.2		
....	βG.C. 11614	22 11.4	+30 55	9.3	F4s	......	3	− 9	3		
211833	Boss 5756	22 14.9	+62 18	6.0	K2	.051	3	+ 0.4	0.8	− 4.5	V
212010	5759	22 16.1	−22 6	5.4	K2	.089	3	+ 47.1	0.9	+48.1	L
212005Br	βG.C. 11657Br	22 16.1	+24 26	8.3	G6	.057	5	+ 2	1		
212391Br	Boss 5771Br	22 18.8	+66 12	6.7	G5	.042	4	− 3.2	2.1	− 1.5	V
213013Br	βG.C. 11741Br	22 23.4	+23 1	8.3	G7	......	3	− 19	1		
213013Ft	11741Ft	22 23.4	+23 1	8.8	K2	......	3	− 23	3		
213119	Boss 5797	22 24.1	+ 8 37	5.8	M0	0.062	3	− 34.1	0.4	−29.3	V
....	B.D. +53°2911	22 28.7	+53 16	9.5	M1	1.482	3	− 2	3		
213893	Boss 5820	22 29.5	+ 0 5	7.0	M1	0.089	4	− 88.7	±2.3		

								km/sec.	km/sec.	km/sec.	
214028	Boss 5825	22h30m.4	−17° 59′	6.8	K5	0″.057	3	− 8.5	±1.0		
....	B.D.+60° 2412	22 31.4	+60 17	9.0	K5	....	3	− 1	1		
214605–6	+68° 1319	22 34.3	+68 41	7.5	F4	....	3	+ 12.0	1.6		
214665	Boss 5843	22 34.7	+56 17	5.5	M4	.056	3	+ 10.9	0.5	+ 6.9	L, V
214966	5855	22 36.8	−29 53	6.4	M5	.030	4	− 9.1	1.1		
214995	5857	22 37.0	+14 0	6.1	G9	.096	4	− 25.2	1.3		
215318–9	5866	22 39.2	+80 52	6.9	G0	.024	3	+ 10.2	0.3		
215324	βG.C. 11930	22 39.2	+45 30	7.4	F5	.174	3	− 32.7	1.3		
215373	Boss 5869	22 39.6	+41 18	5.2	G5	.011	3	+ 12.6	0.8	+13.5	L
....	βG.C. 11943	22 40.5	+10 40	8.5	K5	....	3	+ 5	1		
215578	11952	22 41.2	+18 48	7.5	G8	.034	3	− 20.2	0.9		
....	B.D.+43° 4305	22 42.5	+43 49	9.5	M5e	.86	3	+ 2	2		
216172p	βG.C. 11997p	22 45.6	+68 2	7.2	F5s	.126	3	+ 3.1	1.2		
216172f	11997f	22 45.6	+68 2	7.2	F4s	.126	3	+ 1.5	0.5		
216397	Boss 5897	22 47.5	+42 47	5.2	M0	.106	6	− 16.2	0.6	−17.5	L
216991	B.D.+79° 758	22 52.0	+79 43	7.8	G8	....	3	− 11.8	0.8		
217701	Boss 5934	22 57.4	− 7 7	6.5	M2	0.039	3	− 8.1	2.4		
217987	Cin. 3014	22 59.4	−36 26	7.4	M2	6.900	4	+ 7.8	2.1		
218029	Boss 5943	22 59.7	+66 40	5.5	K3	0.033	3	− 4.7	1.2	− 7.9	L
218347	Cin. 3023	23 2.2	+15 44	9.3	F7	.170	3	− 22	1		
218452	Boss 5957	23 3.1	+45 51	5.6	K5	.030	3	− 6.6	0.9		
218739	βG.C. 12200Br	23 5.3	+47 26	7.0	G2	....	4	− 8.4	1.4		
218792	Boss 5971	23 5.7	+17 3	5.9	K4	.033	3	+ 0.6	0.9		
219127	βG.C. 12229Br	23 8.3	+39 28	7.4	A7n	.084	3	0	2		
219449	Boss 5981BC	23 10.7	− 9 38	9.0	K6	.367	4	− 26	2		
219576	5986	23 11.7	− 8 16	5.1	M5	.022	3	− 17.8	2.0	−14.8	L
219981	6003	23 15.1	+41 32	6.0	M0	.044	3	+ 3.1	2.3		
220009	6004	23 15.2	+ 4 50	5.2	G9	.100	3	+ 35.0	0.5	+39.7	L
220117	6008	23 16.1	+37 38	5.8	F4s	.139	3	− 10.0	1.9	− 9.1	V
220149Br	βG.C. 12317Br	23 16.4	+34 53	8.5	G9	0.023	4	+ 6	±1.5		

TABLE I—*Continued*

H.D.	Star	α 1900	δ 1900	m	Sp.	μ	No.	v	P.E.	Other Determinations	
										v	Auth.
								km/sec.	km/sec.	km/sec.	
220149Ft	βG.C. 12317Ft	$23^{h}16^{m}4$	+34° 53′	9.0	K2	....	4	− 35	±3		
220436	Boss 6017Br	23 18.6	− 9 1	7.0	G6	0″016	3	− 8.0	0.9		
220636–7	B.D.+76° 915	23 20.3	+76 58	7.9	F6	....	3	− 21.5	1.6		
220704	Boss 6026	23 20.8	−21 11	4.5	K5	.083	3	+ 13.0	1.3	+15.4	L
221615	6058	23 28.5	+21 57	5.5	M5	.036	3	+ 2.0	1.1	+ 2.1	V
221673	6059	23 29.0	+30 46	5.2	K4	.053	2	− 22.7	2.4	−24.2	L
221950	6067	23 31.3	+ 1 33	5.6	F2n	.125	4	+ 39.4	1.5		
222493	6081	23 36.0	−12 14	6.1	G7	.062	4	− 10.1	1.6		
222641	6086	23 37.3	+44 26	6.7	K5	.024	3	− 11.6	1.9		
222683	6088	23 37.7	+15 47	6.5	G7	.084	3	− 1.2	0.5		
222766	B.D.−8° 6177	23 38.3	− 8 27	9.7	G2	.64	3	− 98	2		
223047	Boss 6101	23 41.1	+45 52	5.1	Kop	.022	3	− 26.3	0.3	−24.5	L
223552	6117	23 45.4	+51 4	6.5	A9	.123	3	− 22	1		
223637	6121	23 46.2	+ 8 46	6.1	M2	.063	3	− 7.8	1.0	− 9.7	V
223718p	βG.C. 12601p	23 46.8	+37 21	7.0	F5s	....	3	− 19.9	2.0		
223718f	12601f	23 46.8	+37 21	7.0	F5s	....	3	− 17.8	2.5		
224062	Boss 6137	23 49.7	− 0 27	6.0	M5	.057	3	− 2.7	0.8		
224225	6143	23 51.0	−22 33	7.4	M2	.050	3	− 5.2	1.5		
224618	B.D.−17° 6856	23 54.2	−17 30	8.5	G5	....	3	− 44	2		
224758	Boss 6162	23 55.3	+26 22	6.4	F5s	.064	5	0.0	1.2		
224873	βG.C. 12696m	23 56.3	+39 4	8.6	K1	....	3	0	1		
224995	Boss 6174	23 57.3	+ 8 24	6.3	A3n	.004	7	+ 14	2		
225216	6184	23 59.5	+66 37	5.8	G8	0.102	3	− 26.6	0.3		
225213	Cin. 3161	23 59.5	−37 51	8.3	M3	6.112	4	+ 23	3		
225291Br	βG.C. 12736Br	23 59.8	+45 7	7.9	F8	0.031	4	− 17.5	1.4		
6	Boss 6188	23 59.9	− 1 3	6.3	G8	0.061	3	+ 14.2	±0.8		

in each spectral type based on our own classification is as follows: O, 1; B, 19; A, 71; F, 132; G, 193; K, 189; M, 136; total, 741.

A large proportion of the fainter stars are dwarfs with large proper motions. They were photographed with the 10-inch camera. The radial velocities of all such stars have been rounded off to even kilometers. The same procedure has been followed for stars of types B and A, observed with the 18-inch camera; but for other types the fractional part of the kilometer has been retained.

Soon after the publication of the *Catalogue of Stellar Radial Velocities* by the Lick Observatory a comparison was made between the results for all stars observed in common at the Lick and Mount Wilson Observatories. The systematic differences and average deviations for a single star in a total of 534 stars are as follows:

Type	No.	Mt. W.–Lick	Aver. Dev.
		km/sec.	km/sec.
B.	86	+0.51	4.9 (Good lines, 2.4)
A.	81	− .24	3.7 (Good lines, 3.0)
F.	73	− .52	2.08
G.	74	− .05	1.85
K.	162	+ .91	2.01
M.	58	+0.84	2.04

The greater dispersion used for the Lick spectrograms and the high order of accuracy attained in their measurement have led us to apply these values as corrections to the results derived from the low-dispersion Mount Wilson spectrograms for all stars of advanced spectral type. The differences are especially significant in types K and M, where they seem to be due mainly to the wave-lengths of some of the blended lines used on the plates of smaller scale. In the present list no correction has been applied to stars of types B and A, but for the remaining types the following values have been used throughout: F, +0.5; G, 0.0; K, −0.9; M, −0.8.

Our list contains 142 stars in common with the Lick Observatory *Catalogue*, some of which were used in the previous comparison, but many of which are new. There are also 96 stars in common with published lists from the Dominion Astrophysical Observatory at Victoria. The results of a comparison with these stars are shown in the table on page 406.

The average deviation for a single star for types F–M is 2.2 km/sec. when compared with the Lick values, and 2.3 km/sec. when compared with Victoria. In a few cases, especially among stars of type F, the size of the differences suggests the probability of variable velocity, but all values have been included in the comparison.

An interesting feature of the results, but one which would naturally be expected in a list containing so many stars of large proper motion, is the exceptional number of stars with high radial velocities. Corrected for the solar motion, twenty-six velocities exceed 70 km/sec., and seven exceed 100 km/sec. Two of the latter are for stars previously observed by Luyten. No exact count has been made of the number of velocities greater than 50 km/sec., but there are at least seventy. These stars show in a very marked way the asymmetry of stellar motions studied by Strömberg, the result being an almost complete absence of stars of large positive velocity in the northern sky between fifteen hours and two hours of right ascension.

Type	No.	Mt. W.–Lick	Type	No.	Mt. W.–Victoria
		km/sec.			km/sec.
B..........	15	+1.2	A.........	8	−0.6
A..........	20	−0.7	F.........	17	+1.6
F..........	12	+ .7	G.........	30	+0.3
G..........	28	− .7	K.........	26	+1.1
K..........	36	+ .5	M.........	15	+0.8
M..........	31	+0.1			

Six stars, two of which are fainter than the ninth magnitude, are shown by the radial velocities and proper motions to be members of the Taurus group. The mean value of their radial velocities is +39.1 km/sec. The faintest star photographically in the entire list is the distant companion of Capella, a dwarf star of type M2. In view of the low dispersion employed, its radial velocity, +36 km/sec., is in satisfactory agreement with the motion of the principal star, +30.2 km/sec. The components of seven Struve double stars show considerable disagreement in radial velocity. As they are mostly wide pairs it is probable that they are optical doubles. They appear in the *Catalogue* as β G.C. 3319, 4062, 6064, 7212, 12317, Boss 4101–2 and 4340–1.

Carnegie Institution of Washington
Mount Wilson Observatory
October 1929

Contributions from the Mount Wilson Observatory, No. 388
Reprinted from the *Astrophysical Journal*, Vol. LXX, pp. 265–311, 1929
Printed in the U.S.A.

THE SPECTROHELIOSCOPE AND ITS WORK

PART I. HISTORY, INSTRUMENTS, ADJUSTMENTS, AND METHODS OF OBSERVATION

By GEORGE E. HALE

ABSTRACT

The *spectrohelioscope* permits the *visual observation and analysis of the forms and motions of prominences at the sun's limb and of bright and dark flocculi on the disk.*

The *principle of the spectrohelioscope* was first suggested by Janssen in 1868, and successfully tried by Young in 1870 for observing the forms of prominences projecting beyond the limb, but was discarded by him when Zöllner and Huggins adopted a spectroscope with widened slit for this purpose. The spectrohelioscope was developed in 1924–1929 by Hale, who applied *high dispersion* to reveal *flocculi on the disk and a "line-shifter"* to vary the wave-length of the incident light during observation.

The inexpensive *instruments* described in this article, which comprise a horizontal *coelostat telescope* and *spectrohelioscope*, are suitable for a wide variety of observations. *Two oscillating slits* of easily variable amplitude or a *pair of square prisms* (Anderson's design) rotating before fixed slits may be used to give the *monochromatic* image of a portion of the sun, usually with the $H\alpha$ line.

The *adjustments* of the instruments are described in detail.

Methods of observing various types of prominences and flocculi and of analyzing their *forms* and *radial velocities* are then explained. Means of using the spectrohelioscope in conjunction with spectrographs or spectroheliographs are also described.

The possibility of obtaining the first rational explanation of many solar and geophysical phenomena by the aid of modern physics and chemistry, and the reciprocal advantages offered to these fundamental sciences through the study of matter acted upon by powerful forces in the atmosphere of the sun and sometimes apparently transmitted by solar eruptions to the higher atmosphere of the earth, place emphasis on the necessity of improving our methods of solar research. In previous papers I have described some of the unworked opportunities afforded by the spectrohelioscope, which is now easily within the reach of many amateur and professional observers. Even in the midst of a large city, under poor atmospheric conditions, it will yield valuable contributions in a field of astrophysics only partially explored and serve investigators in related sciences as a useful means of adding to their present laboratory facilities.[1]

As I have learned that several astronomers suppose the inexpensive instruments described in this paper to be intended chiefly for educational purposes, or merely to demonstrate the methods involved, I wish to correct this misapprehension. They are in fact instruments of research, capable of showing all of the phenomena described here as well as I can see them myself with my vertical spectrohelioscope, which in its present form is precisely equivalent, both mechanically and optically, to the spectrohelioscope illustrated in Plates XIV, XV, XVI, and XVII. The small coelostat also serves as well for these visual observations as the larger one needed for my work on solar magnetic fields and other investigations demanding very high dispersion.

ORIGIN AND DEVELOPMENT OF THE METHOD

Early history.—The well-known solar eclipse of August 18, 1868, following which Janssen in India and Lockyer in England succeeded for the first time in observing the spectra of prominences in full sunlight, needs no description in these pages. A few months later, while still in India, Janssen addressed to the Secretary of the Paris Academy of Sciences a letter which contains the essential principle of both the spectrohelioscope and the spectroheliograph. After referring to his observations with an ordinary spectroscope, he says that he was not satisfied with them and therefore devised a second method:

> Cette nouvelle méthode consiste, dans son principe, à isoler dans le champ spectral un des faisceaux lumineux émis par la protubérance, faisceau qui est déficient dans la lumière solaire, et à transformer ensuite les éléments linéaires des images protubérantielles dans les images elles-mêmes, par un mouvement rotatif assez rapide imprimé au spectroscope.[2]

---

[1] I have had so many inquiries regarding the construction, adjustments, and use of the spectrohelioscope that I have found it necessary to bring together in this single paper a variety of descriptions and illustrations, a few of which have appeared elsewhere, but are included here for the sake of clearness.

[2] *Comptes rendus*, 68, 94, 1869. See also p. 713 in the same volume.

The instrument subsequently built to accomplish this purpose has been described and illustrated by Millochau and Stefánik in this *Journal:*

> It consists of a direct-vision spectroscope, in which the collimating lens is movable between two screws, permitting the spectrum to be displaced slightly. At the focus of the telescope lens is a second slit, the two jaws of which can be independently adjusted and used to isolate the desired radiation. This slit is observed with a positive eyepiece. The spectroscope thus described is contained within a tube, which can be moved rapidly about its axis by means of a system of gears. This instrument thus constitutes a spectrohelioscope, and was intended for the visual study of the prominences; but by substituting a sensitive plate for the eyepiece it might be immediately transformed into a spectroheliograph. M. Janssen's apparatus embodies the principal characteristics of the spectroheliograph, although his idea did not receive practical application during a score of years.[1]

In a paper read before the Royal Saxon Academy of Sciences on February 6, 1869, Zöllner criticized Janssen's method and suggested a widened slit as preferable. After pointing out that an oscillating slit would be simpler and better than a rotating spectroscope, he discussed the principles involved in the use of an oscillating slit and a widened fixed slit, and concluded in favor of the latter (for the observation of prominences projecting against the sky):

> Nimmt man der Einfachheit halber an, die ganze Fläche, über welche sich der Spalt bei seiner Rotation oder Oscillation bewegte, wäre von der Protuberanz erfüllt, und setzt voraus, die Intensität des entstehenden Nachbildes wäre umgekehrt proportional jener Fläche (entsprechend einer gleichmässigen Ausbreitung des durch den ruhenden Spalt gehenden Lichtes über jene Fläche) so würde, unter Annahme der obigen drei Sätze, das Intensitätsverhältniss zwischen Grund und Protuberanz dasselbe bleiben, mag man
>
> Erstens, durch Oscillation des Spaltes die Helligkeit des Protuberanzgebildes herabsetzen und hierdurch die Helligkeit des superponirten Spectrums oder Grundes (nach 2) unverändert lassen oder mag man
>
> Zweitens, den ruhenden Spalt so weit öffnen, dass sich seine Oeffnung gerade über den Raum ausdehnt, über welchen sich im ersten Falle die Oscillation erstreckte. Hierdurch bleibt (nach 1) die scheinbare Helligkeit der Protuberanz unverändert, die des Grundes wird aber in demselben Verhältniss gesteigert wie sie vorher bei constantem Grunde abgeschwächt würde.
>
> Man würde daher unter den gemachten Voraussetzungen das beabsichtigte

---

[1] *Astrophysical Journal,* **24,** 42, 1906.

> Ziel viel einfacher auf dem zweiten Wege erreichen, wenn man stets dafür Sorge trüge, dass, der Blendung wegen, das intensive Licht des eigentlichen Sonnenkörpers nicht in den Spalt dringt.
>
> Der Spalt brauchte dann nur gerade so weit geöffnet zu werden, dass die Protuberanz oder ein Theil derselben in der Oeffnung erschiene.[1]

It will be observed that this reasoning is correct only when the oscillating narrow second slit, proposed by Janssen to isolate the line, is omitted. When used, it reduces the brightness of the continuous spectrum without affecting the brightness of the prominence, thus invalidating the first assumption of Zöllner.

On February 13, 1869, Huggins applied the wide-slit principle to the observation of the forms of prominences at the sun's limb.[2] Zöllner himself first utilized this method on July 1 of the same year,[3] and it was also adopted by Lockyer, Janssen, Secchi, Respighi, Young, and other solar observers.

In his *Contributions to Solar Physics* Lockyer remarked:

> At the very outset Janssen and myself attempted to accomplish this [i.e., to see the form of the prominences], Janssen by giving a rotary motion to a direct vision spectroscope, I by giving an oscillating motion to the slit, in which I was followed by Young, who afterwards expanded it.

He then went on to quote from Young (whose spectroscope with two oscillating slits is illustrated on p. 167 of Lockyer's book) and from Zöllner, to whom he gave the credit for devising the wide-slit method.

Young, who was the first American astronomer to apply the spectroscope to the observation of prominences, described in 1870 the first spectrohelioscope really capable of showing their forms projecting beyond the sun's limb (Janssen's apparatus was mechanically unsuitable for this, because of the rapid rotation required). After describing his new solar spectroscope, he continued as follows:

> The eye-piece of the instrument has an apparatus attached, which, however, thanks to the high dispersive power, I find unnecessary.
>
> It was early proposed by Janssen to use a vibrating or rotating slit in order

---

[1] *Berichte der K. Sächsischen Gesellschaft der Wissenschaften zu Leipzig*, **21**, 78, 1869.

[2] *Proceedings of the Royal Society*, **17**, 302, 1869. His reference to the use of a second slit between the prisms and the observing telescope was subsequently corrected.

[3] *Op. cit.*, **21**, 145, 1869.

> to make visible the form of a solar prominence, but as Zöllner has shown, the mere opening of the slit answers just as well, the light of the protuberance being diluted to precisely the same extent in either case.
>
> It occurred to me in connection with a suggestion of Professor Morton, that by interposing at the focus of the eye-piece a diaphragm which should move with the vibrating slit, the light of the neighboring portions of the spectrum might be cut off and this dilution avoided. Mr. Clark has devised and constructed a very beautiful mechanical arrangement by which this simultaneous and accordant motion of slit and diaphragm is effected by the rotation of the small fly-wheel shown in Fig. 1.
>
> But I find that although, seen in this way, the prominences appear very bright; yet the working of the apparatus always causes a slight oscillation of the equatorial, which interferes with the definition of details, and I prefer to work with the slit simply opened.[1]

In reviewing these articles, so long forgotten in the early literature of spectroscopy, one is struck by several points. Apparently, Zöllner's introduction of the convenient wide-slit method depended largely upon his failure to notice or appreciate the value of Janssen's proposed second slit for isolating the spectral line, which was also ignored by Lockyer. Young independently adopted a second slit, and was able to observe prominences with its aid. Nevertheless, he relinquished the possibilities afforded by his spectrohelioscope as soon as the fixed wide slit enabled him to see prominences outside the sun's limb. I can find no evidence that he ever looked for prominences on the disk with his oscillating slits, but in any event the linear dispersion of his spectroscope was insufficient to show any of them satisfactorily, unless of great intensity. The whole incident, like many others in the history of science, illustrates how a valuable principle may remain unused for decades, even when repeatedly published in widely read volumes.

It should be remembered, however, that it was not then a question of increasing the contrast, but of finding a means of seeing the forms and not merely the spectra of prominences projected against the comparatively faint dispersed light of the sky. The idea of setting the oscillating second slit on different parts of a line, and thus of employing the spectrohelioscope as a quick means of velocity analysis and for studies of the flocculi at different levels, apparently occurred to no one. As for prominences on the disk, although a few of exceptional intensity were seen there by Young and others with widened slit, the average prominence was evidently regarded as unattainable, so far as its form was concerned, when carried by the sun's rotation against the brilliant background of the photosphere. Secchi, however, gave voice in *Le Soleil* to a hope that must have been generally entertained:

---

[1] *Journal of the Franklin Institute*, **60**, 334, 1870.

> Ce qui serait à désirer maintenant pour faciliter encore davantage ces recherches, c'est la découverte d'un milieu parfaitement monochromatique pour les raies de l'hydrogène. On verrait alors l'image de ces flammes rouges comme on voit celles des taches. Ce milieu peut-il etre trouvé? Nous engageons les physiciens à diriger leurs recherches de ce coté.[1]

The spectrohelioscope accomplishes this purpose for limited areas and at the same time enables the wave-length of the transmitted light to be varied with the "line-shifter" or otherwise.

Recent progress.—Soon after we obtained on Mount Wilson the first spectroheliograms of the hydrogen flocculi with the $H\alpha$ line,[2] it occurred to me to try to observe their forms visually with the 30-foot spectroscope of the 60-foot tower telescope. This vertical spectroscope was of the Littrow type, with the slit in the optical axis of the tower telescope and an opening for a photographic plate at one side. Thus a second slit could be placed in the plate-opening in line with the first slit, an arrangement used when the instrument was employed as a spectroheliograph, either with a grating or with a large liquid prism mounted at the bottom of the 30-foot pit.

The distance between the slit centers is 6 inches, and it was a simple matter to mount in their place a circular brass disk, with its vertical bearing halfway between them. This disk was provided with a number of radial slits, which successively served in pairs as the first and second slits of a spectrohelioscope. As the first slit moved to the right, the corresponding $H\alpha$ line moved with the opposite slit at the same speed to the left, assuming the adjustments to be properly made and the field restricted so that only one pair of slits was illuminated at any time. Thus the observer, using a low-power posi-

---

[1] *Op. cit.* (2d ed.; Paris, 1877), **2**, 16.

[2] Hale, *Contributions from the Mount Wilson Observatory*, No. 26; *Astrophysical Journal*, **28**, 100, 1908.

PLATE XII

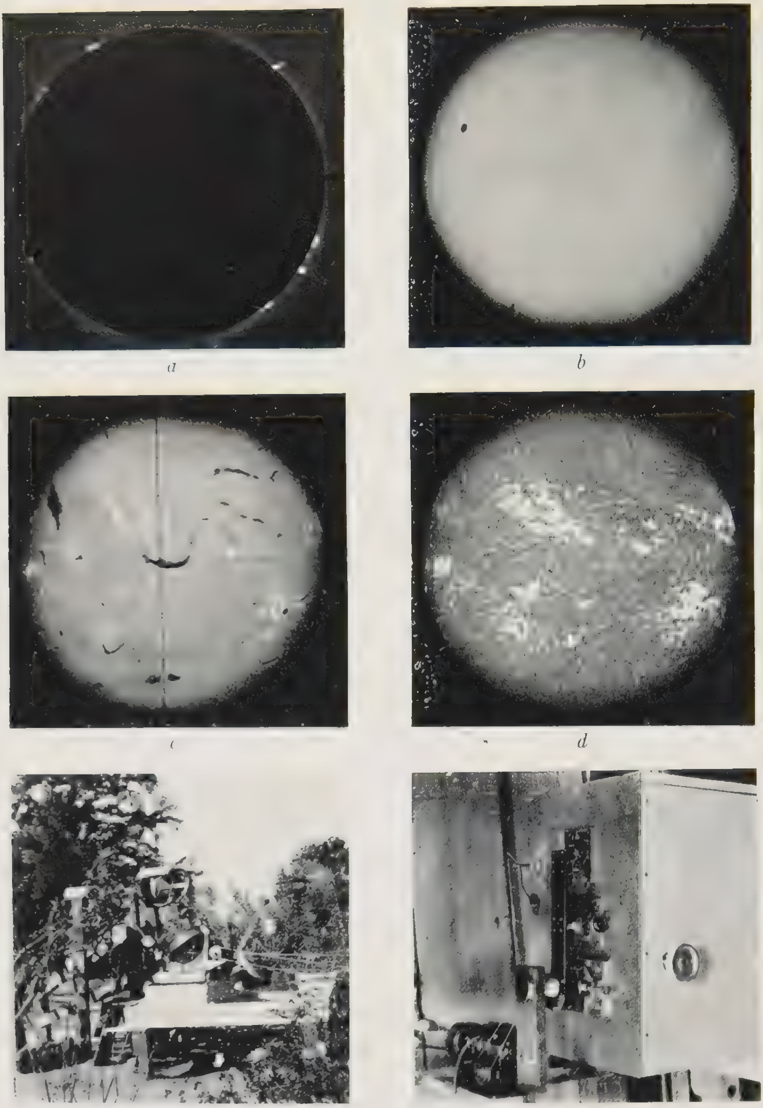

a. Prominences photographed with $H\alpha$ line, September 20, 1909
b. Direct photograph of the sun, July 31, 1927
c. Hydrogen flocculi, photographed with $H\alpha$ line, July 31, 1927
d. Calcium flocculi, photographed with K line, July 31, 1927
e. Coelostat temporarily used with 13-foot spectrohelioscope in 1924
f. Oscillating slits of 13-foot spectrohelioscope, 1924

tive eyepiece or a single lens focused on the second slits, should see a monochromatic image of a portion of the sun.

The method was feasible, but lack of time prevented me from determining the best spacing and width of slits, and thus from obtaining good results at that period. I kept the plan in mind, however, and after giving up the directorship of the Mount Wilson Observatory I decided to devote myself to its development. In the winter of 1923–1924 I accordingly set up in my garden in South Pasadena a coelostat telescope belonging to the Mount Wilson Observatory and a horizontal spectrohelioscope of 13 feet focal length (Plate XII *e, f*). This was of the type illustrated in the present article, but the (6-in.) grating and two concave mirrors were mounted in a long wooden box and the oscillating bar (used instead of a rotating disk) was provided at each end with a set of five slits, instead of the pair of single slits now employed. The wooden supports were unstable, and the mechanical parts rather crude. But by March, 1924, I had seen some dark hydrogen flocculi against the sun's disk and satisfied myself that when properly built the spectrohelioscope would prove a success.[1] Fortunately, I had chosen the diameter of solar image (2 in.), focal length of spectrohelioscope (13 ft.), and slit-width (0.003 in.) which I still find most suitable for use with the $H\alpha$ line in the brightest first-order spectrum of the gratings available (ruled with about 15,000 lines per inch).

When my Solar Laboratory, with a vertical coelostat telescope and the combined spectroscope, spectrohelioscope, and spectrograph shown in Plates XXV–XXVII, had been erected in Pasadena in 1925, it thus became merely a matter of transferring the same optical parts to their new and more substantial metallic mounting. Using at first the same oscillating bar with two sets of five slits (later reduced to a single pair of slits), I at once obtained excellent results. The prominences at the limb and the bright and dark flocculi all over the disk were easily seen, and by setting the second slit at different distances from the center of the $H\alpha$ line the variation of form and intensity with the wave-length and the radial velocities of the various parts of the prominences and flocculi could be quickly detected and compared.[1] The value of the spectrohelioscope for most of the purposes enumerated in the present paper then became apparent, and I decided to develop some of its possibilities, especially with the view of reducing its cost and thus rendering it more generally available.

---

[1] *Mt. Wilson Communication*, No. 87; *National Academy of Sciences Proceedings*, **10**, 361, 1924.

Before describing the instruments since constructed for this purpose I must refer to a form of spectrohelioscope proposed by the late Mr. Thomas Thorp sometime before his death in 1914, a blue-print of which has kindly been sent me by Mr. Buss. This instrument, consisting essentially of a short-focus direct-vision spectroscope with a Thorp grating replica, mounted within a rotating drum carrying a large number of slits, is admirably designed and should serve on an equatorial telescope for the observation of prominences beyond the limb. Its dispersion would be too low, however, for satisfactory observations of the flocculi, though it might show those of greatest intensity, including the brightest eruptions on the disk.

Another project for a spectrohelioscope was described and illustrated in 1924 by Mr. F. Stanley, who first tried some experiments with a rotating disk with radial slits in 1912.

> The instrument consists of a rotating disc (2) in which are cut a number of radial slits. The light which forms an image of the sun or other object comes to a focus on the rotating disc at (16). The light passes through the slit and is collimated by the object glass (3), and passes through the deflecting system (4) and (4′) and the pentagonal prism (5). The dispersing element (17) is a high dispersion compound prism which forms an image by means of the object glass (7) on the disc at position (17). This slit image will be in monochromatic light and will pass out through the slit at (17) into the observing eyepiece (13).
>
> When the instrument is in use, the disc (2) is rotated, by means of a pulley (15) and an electric motor, at a speed which will eliminate flicker, and the object is then seen in monochromatic light corresponding to that for which the compound prism is set. When light of a different wave-length is required, a suitable deflecting prism is interposed at (18). The degree of purity will, of course, depend on the width of slits employed. The deflecting prisms (4) and (4′) are used to correct small errors of deviation due to the dispersing prism (17) and are driven by suitable gearing to make one complete revolution as the entrance slit passes the object.[2]

---

[1] Hale, *Publications of the Astronomical Society of the Pacific*, **38**, 97, 1926; *Mt. Wilson Communication*, No. 97; *National Academy of Sciences Proceedings*, **12**, 286, 1926; *Nature*, July 3, 1926, Supplement; *ibid.*, **118**, 420, 1926; *ibid.*, **119**, 708, 1927.

[2] *Nature*, **114**, 683, 1924.

I prefer the simpler form of spectrohelioscope described in the present article, in which no revolving deflecting prisms are needed.

In a letter dated January 6, 1927, Mr. Evershed wrote me as follows:

> You may be interested to hear that I have recently made a spectrohelioscope attachment to my spectroheliograph, and have seen for the first time the dark prominences on the sun's disc. It is not so simple to construct as in your design, because the light coming from the prisms is reflected out at right angles near to the first slit, as in the sketch that I enclose, so that I have to construct a horizontal rocker with arms about a foot long and at right angles. This is pivoted over the mirror M2, and the end of each arm carries a vertical slit made of aluminium sheet. The whole is made as light as possible, and braced together to give rigidity, yet at any slight jarring in the running of the electric motor, such as happens when the joint in the belt runs over the small motor pulley, there is a tendency for the $H\alpha$ line to move slightly on the slit, and then one sees dark shadings moving over the portion of the sun's disc under observation. I hope to cure this defect eventually.

Evershed's spectroheliograph, it should be added, is of the Littrow type, of 16 feet focal length, provided with a 6-inch meniscus collimator lens and two very fine 45° prisms of the same aperture, used with a plane mirror behind them.

INEXPENSIVE INSTRUMENTS

A brilliant solar eruption, beautifully seen in all its changing forms on the sun's disk only a few days after my improved spectrohelioscope had been brought into use, and followed by a violent terrestrial magnetic storm,[1] emphasized for me the importance of establishing a chain of such instruments around the world. With their aid the sun could be kept under observation almost continuously, thus rendering practically certain the detection of all similar outbursts and greatly facilitating the study of their relationship to terrestrial phenomena. At present many of them are missed and progress is correspondingly slow.

The practicability of building small but efficient solar telescopes and spectrohelioscopes was soon proved by experiments with my larger instruments, and several designs were prepared, some of which have been briefly described.[1] The instruments illustrated in the present article embody later improvements and have been so satisfactory in performance that a more detailed description, including further information regarding their design, adjustment, and use, is due.[2]

---

[1] Hale, *Mt. Wilson Communication*, No. 97; *National Academy of Sciences Proceedings*, **12**, 286, 1926.

The necessary equipment, which in reality constitutes a small but efficient solar observatory, includes: (1) a telescope, which in its simplest and least expensive form comprises a coelostat, second mirror, and single lens; (2) a spectroscope, of about 13 feet focal length, of the reflecting or Littrow type; (3) a pair of oscillating slits or some other device for producing the necessary rapid relative motion of the slits and solar image.

The general arrangement of the telescope and spectrohelioscope is shown in Figure 1, from a sketch by Mr. Russell W. Porter. Figure 2, from a drawing by Mr. Nichols, of the Mount Wilson Observatory, gives the dimensions and relative positions of the piers. If made of concrete, "floated" on a bed of sand 6 inches thick, and not in direct contact with the floor, they will be stable and will not easily transmit vibrations. I may add, however, that I have also found heavy wooden boxes, filled with earth, to serve very satisfactorily as piers.

The telescope.—Mr. Porter's drawing of the coelostat, second mirror and lens (Plate XIII) is so clear in itself that little explanation is required. The mirror of the coelostat ($5\frac{1}{2}$ in. in diameter) and the second mirror ($4\frac{1}{2}$ in.) are made of ordinary plate glass, $\frac{1}{2}$ inch thick, with silvered front surfaces, plane to about a quarter of a wave. Glass is perfectly satisfactory in such a case; it would be a waste of expense to use fused silica for such small mirrors. The coelostat is driven by an ordinary (two-dollar) clock movement with escapement, as the intermittent motion is not perceptible under the low powers employed. The two slow motions for rotating or inclining the second mirror, thus bringing any part of the solar image upon the first slit of the spectrohelioscope, are shown here controlled by cords within reach of the observer, but these may be replaced by light rods

---

[1] Hale, *Nature*, **121**, 676, 1928; *Scientific American*, **140**, 302, 1929; *ibid.*, p. 436, 1929. See also *Amateur Telescope Making* (2d ed.), Part IX (Scientific American Publishing Co., 1928).

[2] Such instruments can be purchased from Howell & Sherburne, 88 N. Delacy Ave., Pasadena.

PLATE XIII

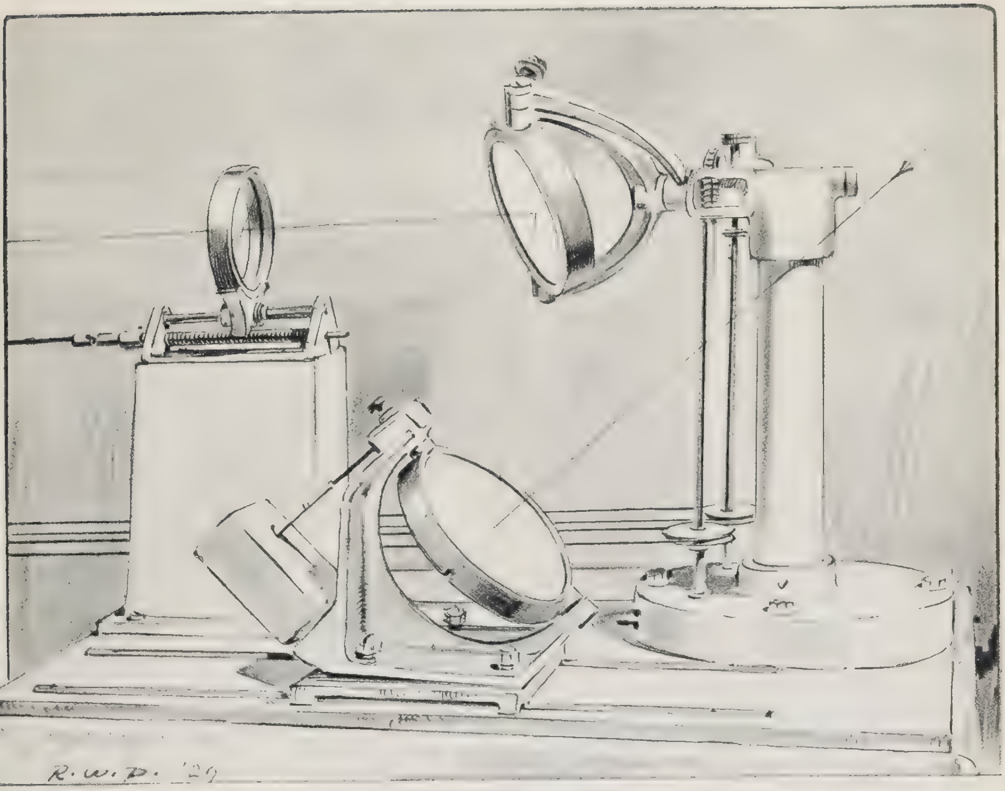

Coelostat, Second Mirror, and Telescope Lens

or tubes. The 4-inch single lens of 18 feet focal length can also b focused by the observer. A single lens serves perfectly for observa-

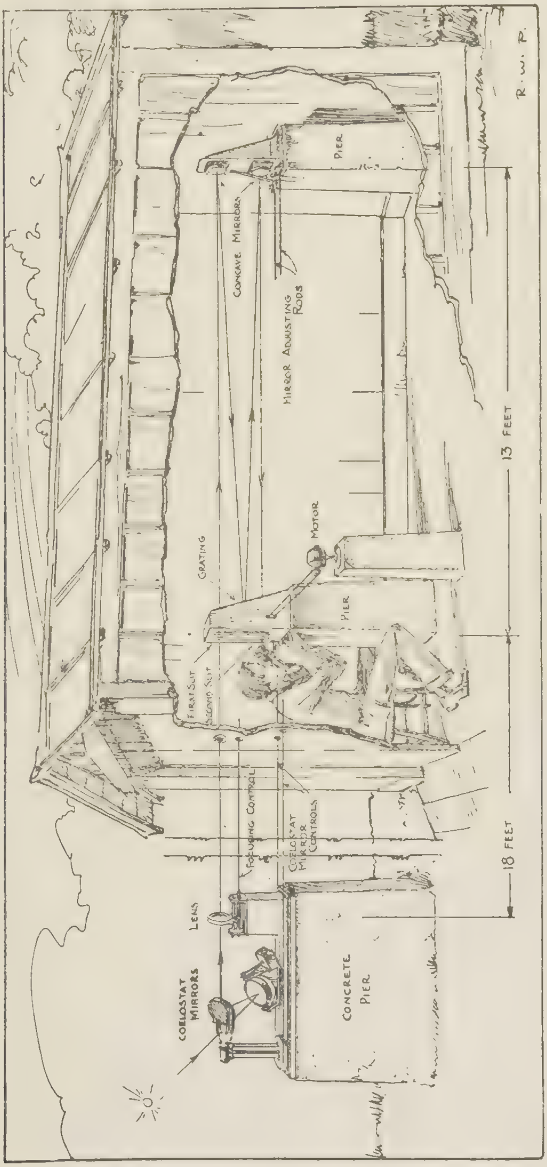

FIG. 1.—General arrangement of coelostat telescope and spectrohelioscope

tions with monochromatic light, but it is poorly adapted for drawings of the directly enlarged solar image, often needed to record the forms and positions of spots and faculae. Perhaps the simplest way to obtain such an enlarged image is to mount a 1- or 2-inch telescope with eyepiece within the building, at one side of the spectrohelioscope and making an angle of about 20° with it. By turning the second mirror so as to send a beam of parallel rays past one side of the 4-inch lens, instead of through it, this small telescope can be fed with sunlight and the enlarged solar image sketched upon paper fastened to a drawing screen fixed at the focus of the eyepiece.

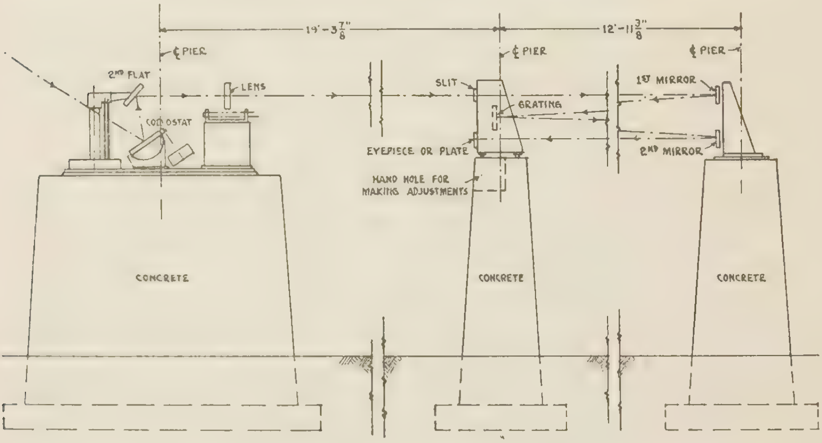

FIG. 2.—Concrete piers for coelostat telescope and spectrohelioscope

If desired, the coelostat, second mirror, and lens can be erected at the summit of a light steel tower and the beam sent vertically downward to the spectrohelioscope, mounted in a well in the earth beneath it. Such a tower telescope, with a small observing house at its base, takes little space and can be very cheaply built from standard materials. Or the coelostat, etc., can be placed on top of a building (if free from vibration) and the beam directed through a hole in the roof or down an open shaft.

I have not built a spectrohelioscope for attachment to an equatorial telescope, but this should not be difficult, especially if Anderson's rotating prisms (Plate XIX) are used instead of oscillating slits (to avoid vibration). A two-mirror or Littrow spectroscope of about

PLATE XIV

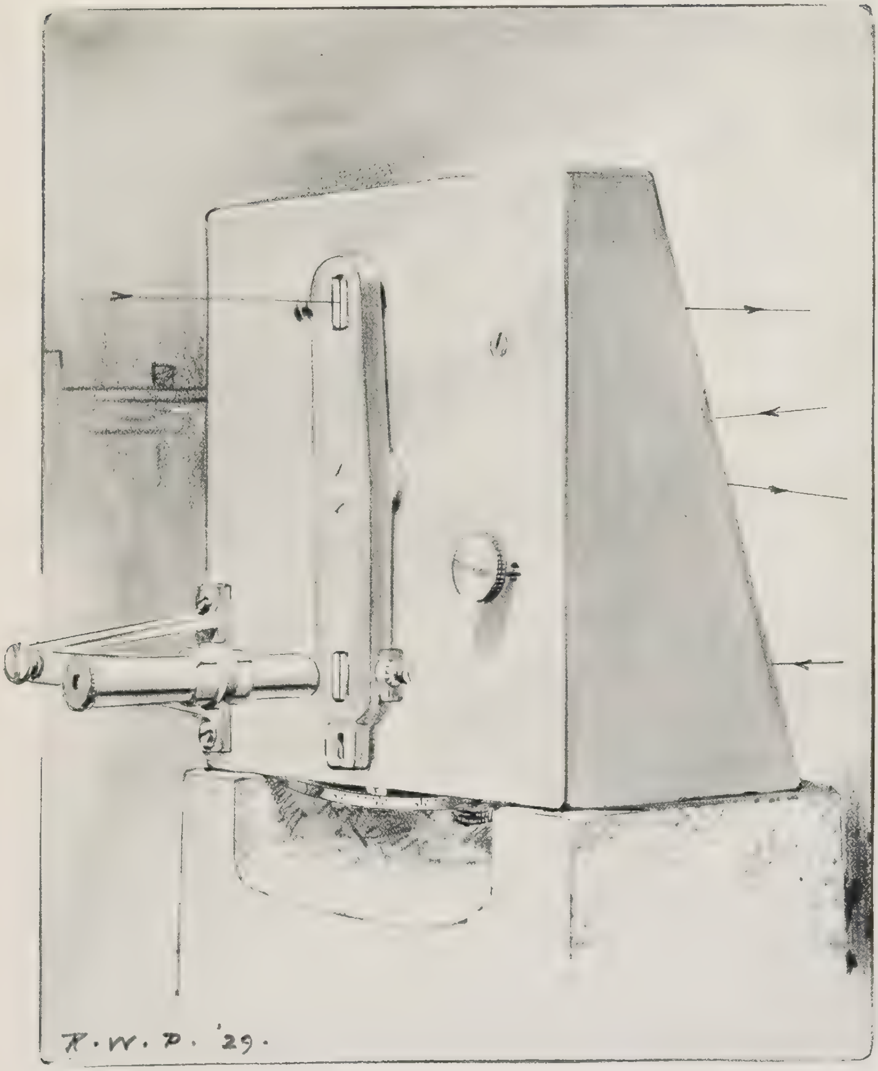

Oscillating Slits and Eyepiece of Spectrohelioscope

PLATE XV

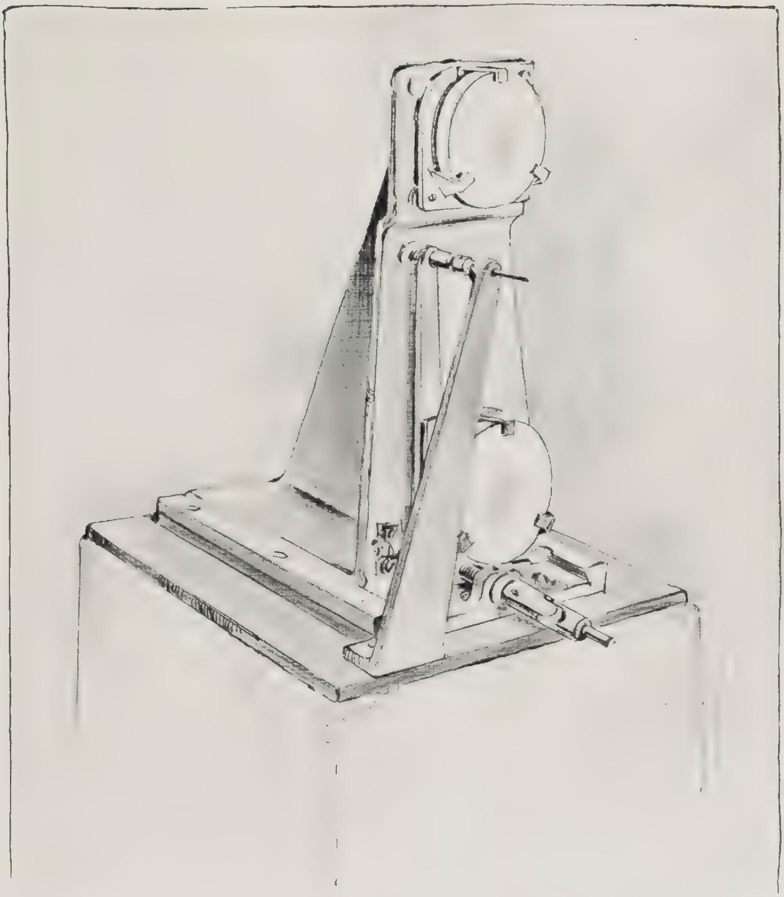

Concave Mirrors of Spectrohelioscope

PLATE XVI

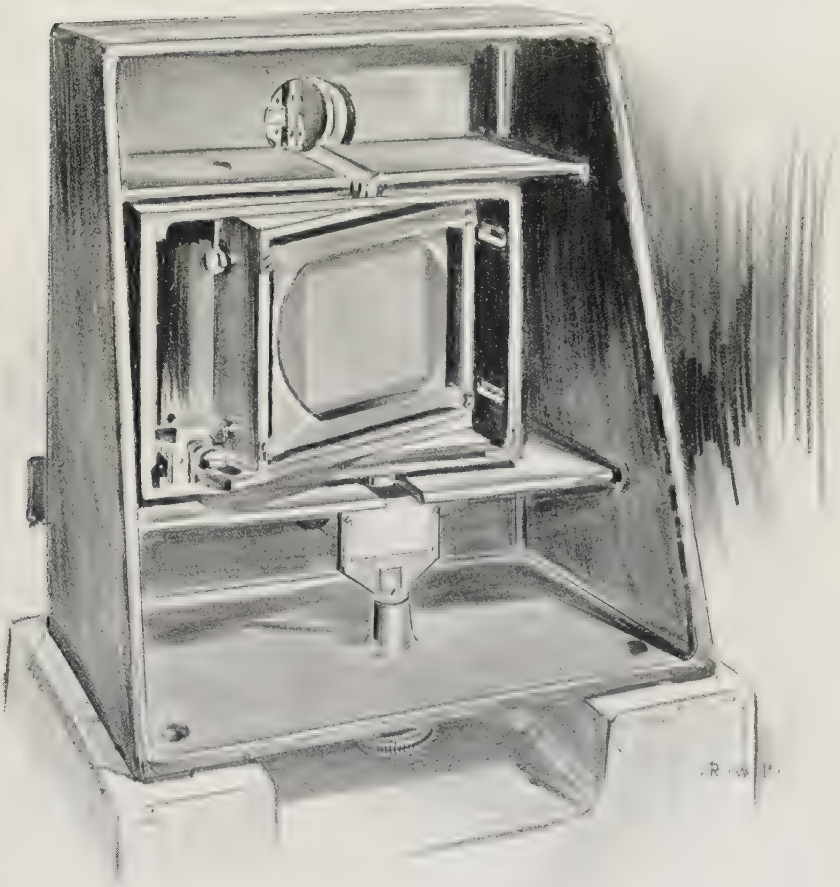

Grating Support and Line-Shifter

PLATE XVII

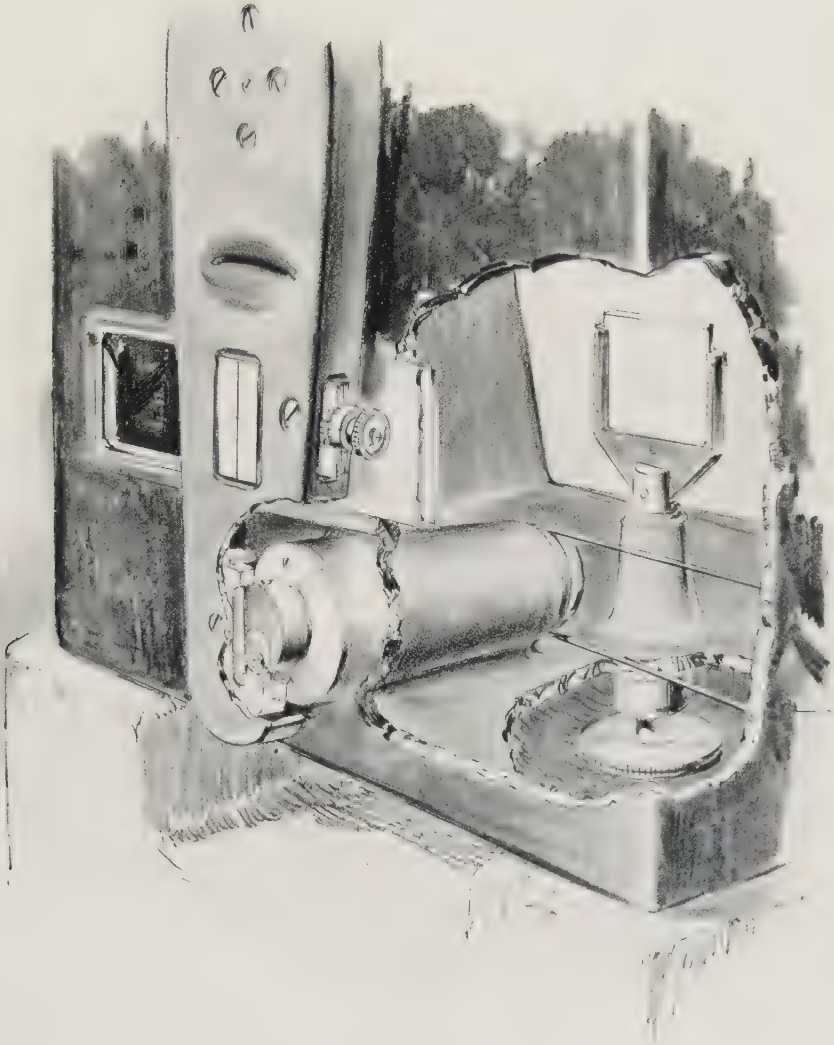

Second Slit, Driving Mechanism, and Line-Shifter

13 feet focal length, clamped to the telescope tube and receiving its light from the solar image by the aid of two right-angle prisms, would be needed in this case. The coelostat telescope and fixed spectrohelioscope are more convenient, however, and much less expensive.

The spectroscope.—If the angular dispersion used is assumed to be that of the first-order spectrum of an original plane grating ruled with about 15,000 lines per inch, a focal length of 13 feet will be found suitable for the spectroscope. This gives an $H\alpha$ line of sufficient width (about 0.008 in.) for use with first and second slits 0.003 or 0.004 inch wide. If narrower slits are employed, the dust lines are likely to be troublesome, even if the brightness of the spectrum is great enough. After trying focal lengths as short as 42¼ inches and as long as 75 feet, I can recommend 13 feet to anyone possessing such a grating as I have described, very bright in the first order.

As for the design of the spectroscope, I prefer that shown in Plates XIV, XV, XVI, and XVII. In this arrangement the rays diverging from the first slit fall on a spherical concave mirror 3 inches in diameter, which renders them parallel and returns them to the grating. This is rigidly mounted near the first slit, just below the diverging beam. The grating is set at such an angle as to return the spectrum to a second concave mirror exactly like the first and mounted below it. This is illuminated only by the region centering on the line employed (usually $H\alpha$), and as the upper (collimating) mirror is concealed from the observer by a suitable diaphragm, the intensity of the diffuse light entering the eye is greatly reduced, thus adding to the visibility of faint prominences or flocculi.

The lower concave mirror forms an image of the spectrum on the second slit, with which $H\alpha$ is brought into coincidence. The second slit is observed through a positive eyepiece (a single lens will usually suffice) having a magnifying power of from two to four diameters. Sunlight is excluded from the room by a tube, extending from the first slit to the opening in the wall. The darker the room the better one can see the structure of the solar atmosphere.

An alternative design for a spectrohelioscope, with slits horizontal instead of vertical, is shown in two previous articles.[1] This permits the use of slits with centers only 3½ inches apart, and consequently of a very light oscillating slit system. The chief idea of this spectrohelioscope was to simplify construction and reduce cost. I prefer the vertical slit arrangement, but the horizontal slit design is mentioned here because of its bearing on the possible substitution of a standard Littrow spectroscope for the two-mirror reflecting spectroscope adopted for both of the preceding instruments.

---

[1] Hale, *Nature*, **121**, 676, 1928; *Scientific American*, **140**, 302, 436, 1929.

Perhaps the simplest of all spectroscopes for the purpose in view is one of the Littrow type, in which a single crossed lens, with grating mounted behind it, is used instead of the two concave mirrors and grating mount already shown. The radius of curvature of the front surface of this lens should be equal to its focal length (13 ft.), thus returning the sunlight reflected from this surface to a focus on the first slit and keeping it out of the observer's eye. The light reflected from the more highly curved second surface produces another image of the first slit at a point on the same axis not far from the lens, where a small flat bar should be mounted to conceal it. The intensity of the white light scattered by the illuminated face of the grating naturally depends upon the grating employed and also upon the width of the first slit and the focal length of the spectroscope. I have seen the flocculi and the prominences beyond the limb fairly well with such a Littrow arrangement, but the contrast was less pronounced than with the double-concave-mirror form, which I therefore prefer.

Two prisms, with a plane mirror returning the dispersed beam through them, can be used in place of a grating. This equivalent of four prisms gives less dispersion in the $H\alpha$ region than the first order of a grating, unless glass of considerably higher refractive index than that at my disposal is available. I strongly recommend a grating, but it must be an original ruling, preferably of the 4-inch size (ruled area approximately $2\frac{1}{2}\times 3$ inches). Such gratings are obtainable from J. W. Fecker, 1954 Perrysville Avenue, Pittsburgh, Pennsylvania, and from Adam Hilger, Ltd., 75*a* Camden Road, London, N.W. 1, England. Thus far I have been unable to obtain a reflecting-grating replica good enough to meet the needs of the spectrohelioscope. I have also tested many transmission replicas without finding one of suitable quality. Nevertheless, I still hope that some improved method of copying gratings may ultimately be perfected.

Production of the monochromatic solar image.—The original Janssen-Lockyer method of observing the spectra of prominences, supplemented by the use of a wide slit to reveal their forms, serves admirably when it is only a question of reducing the brightness of the sky by the dispersion of the spectroscope. If, however, the sky were as bright as the sun's disk, the prominences, except in rare cases, would be rendered invisible by its overpowering brilliancy.

Professor Charles A. Young, one of the ablest and most experienced of solar observers, stated the case as follows in his well-known book, *The Sun:*

> In a few instances the gaseous eruptions in the neighborhood of a spot are so powerful and brilliant that with the spectroscope their forms can be made out on the background of the solar surface in the same way that the prominences are seen at the edge of the sun. In fact, there is probably no difference at all in the phenomena, except that only prominences of most unusual brightness can thus be detected on the solar surface.

Secchi's reference to the need of a method of observing prominences against the disk has already been quoted. Here, as the spectroheliograph first showed in 1903,[1] they usually appear as dark flocculi, because their comparatively cool gas absorbs the light of the hotter photosphere. Bright flocculi also occur, due to brighter hydrogen, usually found at lower levels. When these flocculi are intensely bright their forms can be made out roughly against the disk with a spectroscope by widening the slit, as already noted. Extremely dark flocculi may also be seen imperfectly in the same way, as Mr. Buss has shown; but these are exceptional cases. Most of the flocculi, bright or dark, disappear when the slit is widened sufficiently to include their forms. The weakening and disappearance of most of the lines of the solar spectrum, observed when the purity is decreased by widening the slit of a spectroscope, illustrate this effect. The spectrohelioscope retains the strong contrast given by a narrow slit, and thus renders visible the flocculi, both faint and intense, against the brilliant disk.[2] It also shows the prominences at the limb against a nearly black background. Moreover, as a narrow slit prevents the overlapping of images observed in white light with a wide slit, the spectrohelioscope renders visible the structure of sun-spots, which can be sharply seen with light from any part of the solar spectrum away from the dark line.

---

[1] Hale and Ellerman, *Publications of the Yerkes Observatory*, **3**, Part I, 1903; *Astrophysical Journal*, **19**, 41, 1904.

[2] The "motion forms" of Lockyer (*Contributions to Solar Physics*, Fig. 149), due to distortion of the hydrogen lines, are not to be confused with the true forms of the flocculi (see below, p. 437).

As we have seen, the spectrohelioscope may thus consist of a spectroscope of considerable dispersion, provided with a pair of oscillating slits and a "line-shifter" for varying the wave-length of the light transmitted by the second slit. As in the case of the spectroheliograph, however, a monochromatic image can be produced either by motion of narrow slits with respect to the solar image, or by motion of the solar image with respect to the slits. The chief difference between the two instruments lies in the fact that the spectroheliograph builds up its image gradually, slit-width by slit-width, by a slow motion of the slits or of the solar image with respect to the photographic plate, while the spectrohelioscope must reveal a considerable area of the sun at once to the eye, which obviously could not see the forms of the flocculi through slowly moving slits a few thousandths of an inch wide. Hence the rapid motion of the slits or of the solar image required for the spectrohelioscope.

I have tried successfully three systems of moving slits, as follows: (1) an oscillating bar carrying single slits at each end; (2) an oscillating bar carrying three or more slits at each end; (3) a rotating disk carrying many radial slits.

Three means of producing rapid motion of the solar image with respect to fixed slits have also been devised:

1. An oscillating plane mirror, so mounted in conjunction with a second plane mirror that the second slit can be viewed in another part of the same mirror system. This was suggested by Dr. Sinclair Smith.
2. A square prism of glass, mounted before each of the slits, rotating uniformly about an axis parallel to them. The portion of the solar image under observation reaches the first slit through one prism, while the resulting fixed monochromatic image is seen in an eyepiece focused through the other prism on the second slit. This device is due to Dr. J. A. Anderson.
3. An oscillating right-angle prism, mounted with its edge parallel to the slits and its hypotenuse surface normal to their plane. In this arrangement, previously used in somewhat different form on the spectroheliographs of our

60-foot and 150-foot tower telescopes at Mount Wilson, and now on that of my Solar Laboratory in Pasadena, the solar image moves at twice the speed of the prism.

All three of these devices for use with fixed slits are here supposed to be employed with a spectroscope in which the apparent motion of the solar image, as observed through the second slit, is opposite in direction to the actual motion of the solar image across the first slit. In this case, when looking at the second slit through an extension of the oscillating or rotating optical system that causes the motion of the solar image, the effect of this motion is exactly compensated and the monochromatic image appears at rest. The same devices can be adapted for use with spectroscopes of other types.

A more detailed consideration of several of these schemes may now be given.

Oscillating slits.—The simplest arrangement for the vertical-slit spectrohelioscope is a single pair of oscillating slits, as shown in Plate XIV. The bar supporting the slits is of sheet aluminum $\frac{1}{16}$-inch thick, hammered into shape over a suitable form. This bar is mounted on a conical bearing, resembling that of a jeweler's lathe, which permits all wear to be taken up for the purpose of eliminating vibration. The two slits are of simple design, one jaw being movable by a micrometer screw with divided head. The upper (first) slit is fixed on the bar, while the second slit can be rotated so as to make it exactly parallel to the $H\alpha$ line. This slit is also provided with small windows at top and bottom, permitting the upper and lower end of the line to be seen when the oscillating bar is at rest. In this way three adjustments can be effected: parallelism of the slit to the line, coincidence of slit and center of line when the circle of the line-shifter (see below) reads zero, and precisely equal motion of slit and line when the oscillating bar is moved (see "Adjustments").

The driving mechanism is shown in Plate XVII and Figure 3. A steel pin projecting from the face of a small brass disk driven by an electric motor of adjustable speed is so mounted that it can be moved toward or away from the center of the disk, thus permitting the amplitude of oscillation to be varied. This pin travels in a slot of adjustable width at the end of the oscillating bar. When properly made and adjusted the bar can be very rapidly oscillated without setting up troublesome vibration. The amplitude employed in my instruments is usually about $\frac{1}{4}$ inch, and the speed of the motor is regulated until the point of least flicker and vibration is found.

This driving device naturally involves a maximum slit velocity at the middle of an oscillation, slowing down to zero at each reversal of direction. Consequently the rectangular monochromatic image of a portion of the sun seen through the eyepiece focused on the second slit is brighter near the edges than at the center. In practice this is not objectionable. It can be reduced or completely eliminated, if desired, by multiple slits or revolving disks.

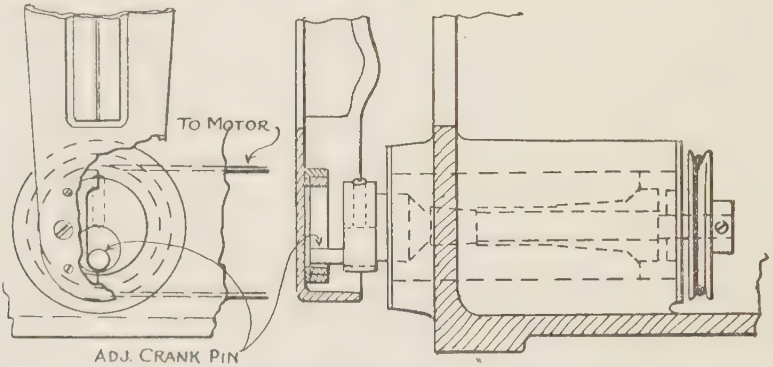

Fig. 3.—Driving mechanism for oscillating slits

The use at each end of the oscillating bar of three or more slits permits the rate of oscillation to be reduced (for the same degree of flicker) but calls for a fixed distance between consecutive slits, corresponding to invariable amplitude in the case of a pair of single slits. This distance must be slightly less than the width of a fixed window, or wide slit, mounted on the collimator axis just below the central position of the middle (oscillating) slit, so as to permit only one of the "first" slits to illuminate the collimator mirror at any moment. The amplitude of the oscillating bar must of course be increased sufficiently to bring all the slits successively into play. As for the slits themselves, they may be of fixed width (as in my first spectrohelioscope) or adjustable.[1] If a fixed window, such as that behind the first slits, is mounted centrally behind the second slits, a

---

[1] We have designed closely spaced adjustable slits of a very simple type.

PLATE XVIII

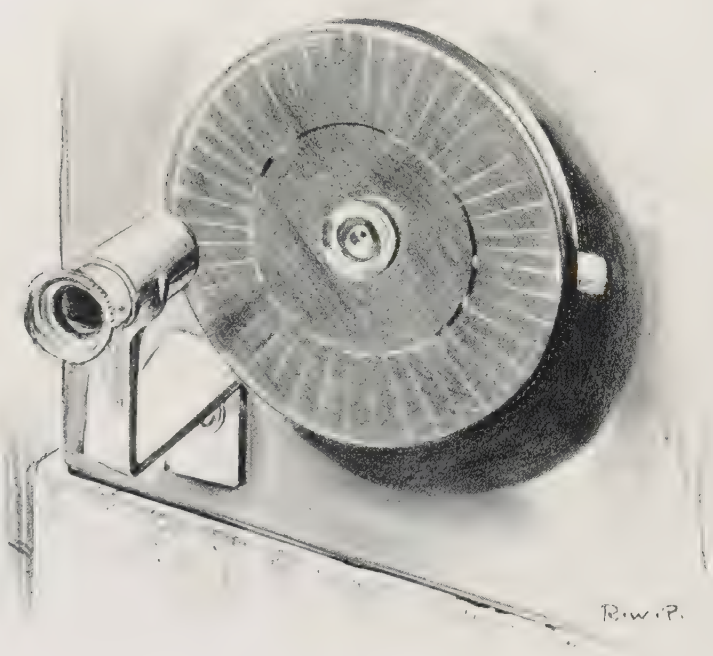

Spinning Disk with Radial Slits

single monochromatic image will be seen. If not, this image will be flanked on both sides by other images. If it be assumed that the central second slit falls on $H\alpha$, these supplementary images will be given by light from the continuous spectrum outside of $H\alpha$. Thus, if desired, the $H\alpha$ flocculi above a group of sun-spots may be seen simultaneously in the same field of view with the spots themselves. This is often convenient, especially if a window is used behind the second slits of such width and adjustment as to show an $H\alpha$ image beside only a single continuous-spectrum image of the spots. Obviously this could be obtained with a combination of a single first slit and a double second slit. However, the line-shifter permits such a quick transition from $H\alpha$ to a continuous-spectrum image that recently I have not often employed multiple slits.

In a spectroscope of great focal length, such as the 30-foot spectrograph of the 60-foot Mount Wilson tower telescope, the diffuse light from the grating and the inclination of the spectral lines with a Littrow spectrograph are so slight that one is tempted to use a rotating disk carrying many radial slits—an arrangement that appealed to me at the outset because of its simplicity and the complete absence of flicker. Recently I have obtained fairly good results in this way, even with a focal length of 13 feet. One of the disks, in which fifty radial slits were cut by Mr. Hitchcock on the face of a glass disk coated with silver or a uniform film of Duco paint, is shown in Plate XVIII.[1] This method, however, has several disadvantages compared with the oscillating bar and pair of single slits, among which the invariable slit-width and spacing and considerable inclination of the lines in certain spectroscopes may be mentioned. If I could afford the time I should nevertheless be inclined to develop it further, perhaps introducing adjustable slits and other changes. (I have already devised a simple optical method of bringing inclined spectral lines into precise coincidence with radial slits.)

Much more might be said regarding moving slits of various forms, especially those adapted for use with other kinds of spectroscopes. I must pass on, however, to the type of spectrohelioscope in which two fixed slits are employed, with devices for producing the necessary relative motion of the sun's image. On page 422 I have mentioned three of these, all of which could doubtless be made to give excellent results. Only one has been adequately developed, the ingenious scheme suggested by Anderson to give a monochromatic image completely free from the effects of flicker and instrumental vibration.

---

[1] The slits were cut on a Brown and Sharpe milling machine with a special tool. As the best spiral head is hardly accurate enough for spacing the slits, a divided circle with microscopes was employed.

Rotating prisms.—Plate XIX illustrates Anderson's device, in the form which I have adopted for the spectrohelioscopes built by the Mount Wilson Observatory and loaned to solar observatories widely distributed in longitude. Two rectangular prisms, square in cross-section, are mounted on a single shaft driven by a small electric motor. The upper prism receives the direct sunlight and transmits it to the first slit, on which the solar image is focused. Evidently the width of the area transmitted depends upon the width of the prism face and the index of refraction of the glass. As the prism rotates, this area is moved by the varying refraction across the slit and this process is repeated four times in each revolution. The second prism, rotating at the same speed, precisely compensates for the action of the first prism, and spreads before the eye a flicker-free monochromatic image of the area in question. When equipped with well-made prisms, accurately aligned, this admirable method gives beautiful results. The use of fixed slits simplifies the adjustment of the spectroscope, and the uniform rotation eliminates the dangers of vibration. It is true that with a single pair of prisms it is not possible to change the amplitude, which limits the brightness of the monochromatic image seen with a given slit-width. This can be done with oscillating slits, as already stated.[1] But for most purposes I can recommend Anderson's prisms, which are readily adaptable to existing Littrow spectroscopes.

Line-shifter.—Thus far we have considered the spectrohelioscope

---

[1] Since this article was put in type we have devised a simple attachment which will permit the amplitude of oscillating slits to be quickly varied while they are in motion. This will enable us to use a very small amplitude for the study of faint details on the dark center of $H\alpha$, and greatly to increase the amplitude (thus protecting the eye by holding down the brightness) when passing beyond the dark line on to the bright continuous spectrum. The same device, combined with a right-angle prism above the first slit for rotating the solar image, can also be used as a micrometer for measuring the dimensions of flocculi or their distance from sun-spots.

PLATE XIX

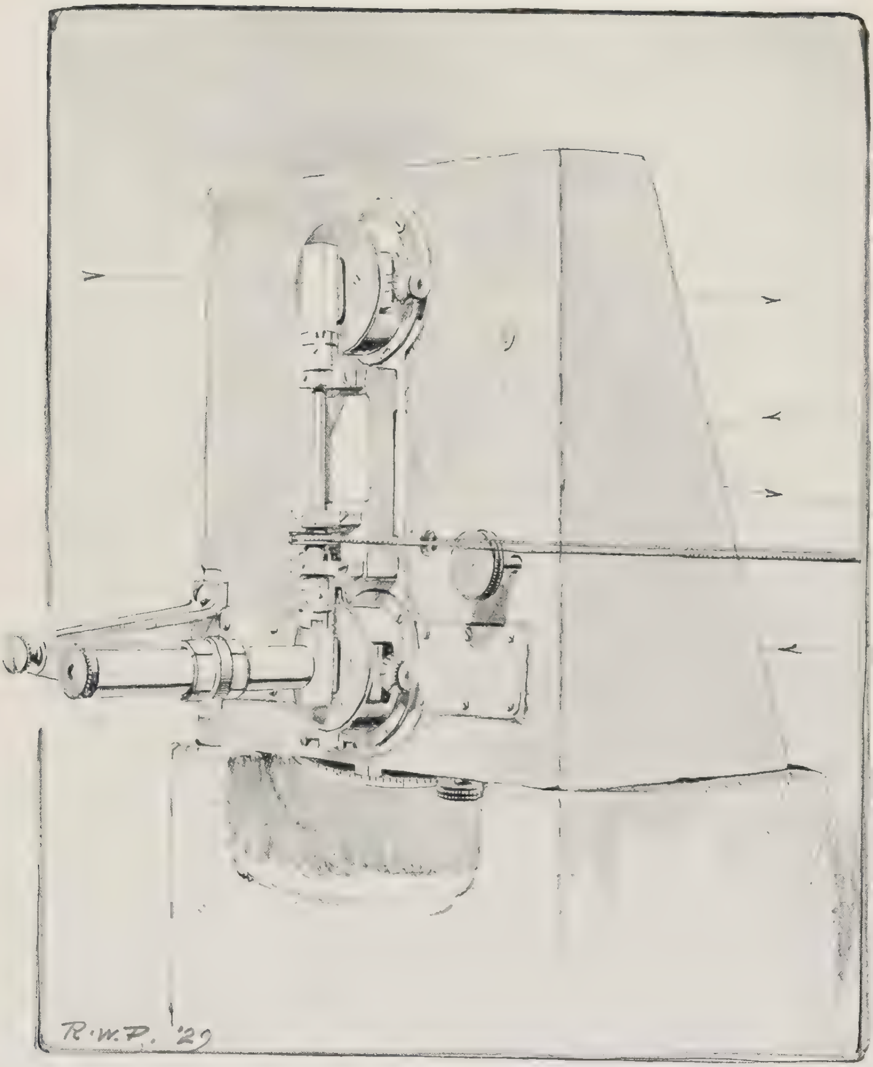

Anderson's Rotating Prisms, for Use with Fixed Slits

chiefly as a means of seeing directly such structure as is revealed photographically by a spectroheliograph with its second slit fixed at a given wave-length. The possibility of instantly varying the wave-length of the transmitted light while visual observations are in progress introduces a new and valuable element, applicable in the comparison of the forms of flocculi corresponding to different parts of the *Hα* line, the study of the relationship of the flocculi to neighboring sun-spots, the instant measurement of radial velocities, and the rapid velocity analysis of prominences and flocculi.

Any simple method of varying the relative position of the second slit and line may be employed. In my first spectrohelioscope the bearing that carried the oscillating bar was mounted on a support movable by means of a micrometer screw. Another method would be to move the first or second slit separately, most easily done when the Anderson prisms are employed. On the whole, however, I recommend the use of a piece of approximately plane-parallel glass, mounted just behind the second slit on a steel shaft, which is rotated by means of a milled head. Concentric with the shaft and milled head is a circular arc of 3¼-inch radius, with edge divided into degrees, or provided with a wave-length scale (shown in Plates XIV and XIX). The arc also carries near its circumference two adjustable brass stops, which can be clamped at any distance from the zero of the circle. The stops are sheathed with short pieces of rubber tubing, so as to prevent jar when the arc is moved rapidly back and forth between these limits. They permit the line-shifter to be employed like a "blink" comparator, facilitating the instant comparison of the forms or positions of prominences or flocculi corresponding to any part of the line with sun-spots or faculae seen by light from beyond its extreme boundaries. The adjustment and use of the line-shifter will be described more fully below.

INSTRUMENTAL ADJUSTMENTS[1]

Horizontal coelostat telescope.—1. Level the coelostat and adjust its polar axis to correspond with the latitude of the observing station.

---

[1] Most of these directions will be quite unnecessary to solar spectroscopists. They are given in detail because of the fact that several spectrohelioscopes are being erected or used by those who have had little or no experience in solar spectroscopic work. The directions refer to spectrohelioscopes with vertical slits.

2. Set the axis of the coelostat and the rails on which it slides in a north and south line.

3. See that the centers of the second mirror, the lens cell, the first slit of the spectrohelioscope, and the upper concave mirror lie on a horizontal north and south line.

4. Move the coelostat north or south until a beam of sunlight reflected from its mirror falls centrally on the second mirror. Start the clock and clamp the coelostat mirror at this position.

5. Put the lens in place at the central position of its run, which should be at a distance equal to its focal length for $H\alpha$ (about 18 ft.) from the first slit of the spectrohelioscope.

6. Turn the second mirror until the beam of sunlight falls centrally on the lens. The solar image should then be central on the first slit of the spectrohelioscope and the diverging beam from the slit (opened to 0.01 in. or more) should fall centrally on the upper concave mirror. Readjust, if necessary, to insure this coincidence.

7. Look at the solar image on the first slit through a piece of red glass and focus the lens by the screw until a sun-spot or the sun's limb is sharp on a piece of white paper held against the slit jaws.

Spectrohelioscope.—1. Set the casting that carries the slits and grating support with its face vertical and in an east-and-west plane; the axis about which the grating rotates should now be vertical; then fasten the casting firmly in place on the pier.

2. Make certain that the upper slit and the lines of the grating are also vertical.

3. Square up the casting supporting the concave mirrors and fasten it to the pier at the point where the distance of the silvered faces from the slits, at the middle of their run, is about equal to the focal length of the mirrors (about 13 ft.).

4. Incline the upper concave mirror by its adjusting screws until the beam of sunlight is reflected to the center of the grating.

5. Rotate the grating (unclamped) until the direct reflection (not one of the spectra) falls centrally on the lower concave mirror. If necessary tip the grating backward or forward in its cell until this adjustment is correct. Note that the brightest first-order spectrum should now appear on the wall to the right of the mirror. If this is not the case, invert the grating in its cell and readjust.

6. Adjust the lower concave mirror until a direct (white-light) image of the first slit falls exactly on the second or lower slit.

7. Reduce the intensity of the sunlight by means of a dark glass before the first slit and focus the concave mirrors by their screw until the image of the first slit, seen through a positive eyepiece focused on the widely opened jaws of the second slit, is sharply defined.

8. Rotate the grating until the deep red of the brightest first-order spectrum falls centrally on the lower concave mirror. As the grating is rotated the direct reflection and the spectra of the various orders should move along a horizontal line. If they do not, incline the grating in its cell by the side screws until the spectra move horizontally and then check up the other adjustments.

9. Narrow the first slit to a width of about 0.002 inch. The lines of the solar spectrum should now appear through the wide second slit. Refocus the concave mirrors (using a positive eyepiece magnifying ten diameters) until the narrowest lines are perfectly sharp on the slit jaws. The horizontal lines, caused by dust on the first slit, should also be sharp at the same focus.

10. Rotate the grating with the tangent screw until $H\alpha$, the broadest single line in the red, falls on the second slit.

11. Make the width of both the first and second slits 0.004 inch.

12. Put the plane-parallel glass plate (the line-shifter) in place behind the second slit with its face at right angles to the beam, where its circle reading should be zero.

13. Observe the $H\alpha$ line above and below the second slit through the small windows provided for the purpose and bring it into coincidence with the slit by means of the tangent screw of the grating. Rotate the second slit, if necessary, to make it exactly parallel to $H\alpha$.

14. If the spectrum is slightly too low or too high, tip the lower concave mirror by the fine screw provided for vertical adjustment.

15. If oscillating slits are used, move the slit-bar slowly by hand and see whether the $H\alpha$ line moves exactly with the second slit. If not, raise or lower the spectrum by the fine-adjustment screw on the lower concave mirror until line and slit, seen with a 10×-positive eyepiece, move precisely together. After completing these adjustments and checking them by noting (with widened first slit) whether

the beam is still central on both concave mirrors and grating, the instrument should be ready for the observation of prominences and flocculi. Before observing, however, a small screen (about $1\frac{7}{8}$ in. high) should be placed between the grating and the concave mirrors at such a point as to cut off the scattered sunlight which would otherwise be seen if the upper mirror were visible through the second slit. A position can be found where the screen will not intercept the beam between first slit, upper mirror, grating, lower mirror, and second slit.

16. Set the low power (2×) eyepiece opposite the center of the second slit, where the spectra passing through the windows at its extremities are not visible, and focus it sharply on the slit jaws. Run the motor at such a speed as to give a persistent monochromatic image of a portion of the sun about $\frac{1}{4}$ inch wide, sufficiently free from flicker and without troublesome vibration. Turn the line-shifter until the $H\alpha$ line is off the second slit. Move the solar image by the slow-motion cords or rods controlling the second mirror of the coelostat telescope until a sun-spot falls centrally on the first slit. An image of the spot in the red light of the continuous spectrum near $H\alpha$ should then be seen through the second slit and eyepiece. Focus the lens of the coelostat telescope until the spot appears through the eyepiece as black and distinct as possible. Turn the line-shifter back to the zero position, which should bring $H\alpha$ centrally on the second slit, thereby reducing the brightness of the solar image, now due to the hydrogen light of the solar atmosphere. Dark and bright flocculi, resembling those shown in several of the plates, should become visible on the sun's disk, the various parts of which can be examined by moving the solar image. Before studying their details, it is advantageous to become thoroughly familiar with the operation of the instrument by observing the bright prominences projecting beyond the sun's limb.

These can be examined by opening both of the oscillating slits to a width of 0.005 inch or more, and moving the sun's image so as to bring all parts of the circumference successively into the field of view. Select some bright prominence, refocus it as sharply as possible by moving the telescope lens with the screw, and turn the line-shifter. When the $H\alpha$ line moves off the second slit the prominence naturally disappears. Many prominences differ so slightly in radial velocity in their various parts that they may be equally well seen as a whole at any setting not too far from zero to exclude the bright central region of the $H\alpha$ line. The various types of flocculi, the study of their structure at various levels, and the analysis of "motion forms" due to marked differences of radial velocity are described below.

Anderson's rotating prisms.—When Anderson's rotating prisms are used with fixed slits, the $H\alpha$ line does not oscillate but remains at rest, and adjustment (15) becomes unnecessary. Instead, the following adjustments of the rotating prisms are required:

1. The two prisms (square in cross-section) are mounted in their cells at the ends of a steel shaft turning in bearings attached to a brass base plate. Place this in a beam of direct sunlight broad enough to cover both prisms.

2. Rotate the shaft slowly and watch the rectangular areas of sunlight as reflected successively from the four faces of one prism on a wall at least 10 or 12 feet distant. Mark on the wall the ends of one of these rectangles and fit the prism cell until the ends of the four rectangular reflections correspond in position, indicating that the axis of the prism coincides with the axis of the shaft. (This adjustment is made once for all by filing or scraping the three-point supports against which the prism-cell rests.)

3. Repeat for the second prism.

4. As the faces of the two prisms may not yet lie in the same plane, watch the rectangular areas and rotate one of the prisms until they correspond perfectly.

5. The first and second (fixed) slits of this form of spectrohelioscope are supported by a box casting, as shown in Plate XIX. Each slit is pivoted on a screw, and by releasing two clamping screws (from the rear) the slit may be rotated about its center. (The lower slit is also provided with another motion for lateral adjustment.) Set both slits in a vertical line.

6. Fasten the base plate carrying the shaft and prisms to the box casting, thus bringing one prism in front of each fixed slit.

7. Place the casting in front of a window, not in direct sunlight, with the prisms facing the window. (If the casting is already in posi-

tion on its pier, skylight may be reflected through the prisms with the aid of one or two large mirrors.)

8. Open the slits to a width of about 0.003 inch and look at the upper prism through the first slit from the rear. As the prisms are slowly rotated, their vertical corners can be seen as dark lines, momentarily cutting off part of the light as they pass the slits. If these lines are not exactly parallel to the upper slit, rotate this slit as described above until the light is cut off throughout its whole length at the same instant. Leave the prism in this position.

9. Look through the second or lower slit, and observe the line due to the corners of the lower prism through the small windows above and below the slit. If the coincidence is imperfect, move the slit laterally, or rotate it slightly until the light is cut off from both slits at the same instant when the prisms are turned.

10. Assuming the box casting, with slits and prisms in adjustment, in place on its pier, bring the solar image on to the first slit. Observe a narrow absorption line close to $H\alpha$ and notice that it makes a small angle with the second slit. Remove about half this angle by rotating the first slit and the balance by rotating the second slit. Set $H\alpha$ centrally on the second slit by rotating the grating (the line-shifter is assumed to be set at zero).

Line-shifter.—The line-shifter used on the horizontal spectrohelioscope described above is a plate of plane-parallel glass about 0.06 inch thick, mounted behind the second slit. When $H\alpha$ is set as nearly as possible on the center of the slit by the tangent screw of the grating, this glass plate is supposed to stand at right angles to the beam from the lower concave mirror; at this point the circle of the line-shifter should read zero. In practice, there is usually a slight correction to be applied to the zero reading, readily determined as follows:

1. Set the first and second slits at the widths to be used in observations with the spectrohelioscope (about 0.003 or 0.004 in. for the disk and the brighter prominences beyond the limb, and roughly twice this width for fainter, quiescent prominences). Observe the $H\alpha$ line through the small window above the second slit and rotate the line-shifter to the right until the most perfect coincidence of the slit with the center of the line is seen with an eyepiece or lens magnifying

about ten diameters. Note the circle reading. Repeat by rotating to the left, again noting the reading. Shift the eyepiece and repeat both right and left readings through the lower window. Their mean should obviously be practically the same as that for the top of the slit if line and slit are parallel. The mean of all four readings gives the zero correction for the middle of the slit. (A more precise method, not necessary in practice, would be to use a compound microscope, with filar micrometer, for settings on line and slit.)

TYPES OF HYDROGEN FLOCCULI

Before describing in detail the use of the line-shifter for the comparative study of phenomena at various levels in the solar atmosphere and the velocity analysis of moving gases, a brief statement regarding the types of hydrogen flocculi rendered visible by the spectrohelioscope may be of service. I have accordingly selected a number of spectroheliograms from the large collection of the Mount Wilson Observatory, which have been copied by Mr. Ellerman for reproduction, usually on a scale large enough to show the characteristic structure of the fields of force (when present). In this paper I shall describe the principal types of flocculi very briefly, but later some of their peculiarities will be more fully discussed in the light of recent observations with the spectrohelioscope.

The coarser structure of the hydrogen atmosphere, as revealed on spectroheliograms taken with the $H\alpha$ line, is shown in the small-scale photographs reproduced in Plate XII. These represent the 2-inch (52 mm) solar image photographed on Mount Wilson with the 13-foot spectroheliograph. An auxiliary slit, set on the continuous spectrum about $2\frac{1}{4}$ inches (57 mm) from the second slit centered on the $H\alpha$ line, gives a direct image of the photosphere and spots for comparison with the hydrogen image. In most cases the dispersion employed is 0.25 mm per angstrom at the $H\alpha$ line, and, as the second slit is generally 0.1 mm wide, only the central part of the dark line is used for these photographs.

The term "flocculi," which is not always used in the same sense by writers on astrophysics, should be clearly understood. In 1903 I suggested that all objects shown on spectroheliograms of the sun's disk taken with the lines of calcium, hydrogen, or other elements, be called by this name.[1] In the present paper this designation is employed in harmony with the original definition, which may be quoted here for the sake of clearness:

> The term "flocculi" is applied indiscriminately to all bright or dark clouds of vapor photographed in projection on the sun's disc, without distinction of level. In other words, a flocculus may be a mass of vapor in the reversing layer, or in the chromosphere, or in a prominence. For this reason we shall speak of calcium flocculi, hydrogen flocculi, etc.[2]

The determination of level is not always an easy task, and consequently a general term was adopted.

The flocculi photographed with the central part of the $H\alpha$ line are both bright and dark, as represented in Plate XII and other photographs. Bright flocculi are usually found in the spot zones, and are brightest and most conspicuous near the sun's limb and in the immediate vicinity of sun-spots (Plates XX, XXI*a*, and XXII). Quiescent bright flocculi, which change slowly in form, coincide approximately with the faculae and with the low-level bright flocculi photographed with the calcium lines H_1 or K_1. Differences in form are partly due to the absorptive effects of overlying dark flocculi. Active bright flocculi, which are often far brighter than the quiescent ones, change rapidly in form and intensity. They usually appear suddenly, close to active sun-spots, and sometimes become extremely brilliant and spread over large areas. These will be referred to later in a discussion of the use of the spectrohelioscope for the study of the relationship between solar and terrestrial phenomena.

Dark hydrogen flocculi are found on all parts of the disk, not merely in the sun-spot zones but often close to the poles. The more conspicuous ones are usually greatly elongated and have been called by Deslandres "filaments." Most of these represent or are closely associated with prominences, seen in projection on the disk as dark absorbing areas (Plate XXII*a*, *b*, *c*). Objects of this type generally change slowly in form unless they fall within the range of action of the fields of force, where they may often be seen with the spectrohelioscope as they are rapidly drawn into the vortices surrounding sun-spots.

---

[1] Hale and Ellerman, *Publications of the Yerkes Observatory*, **3**, Part I, 14, 1903; *Astrophysical Journal*, **19**, 42, 1904.

[2] Hale and Ellerman, *Astrophysical Journal*, **19**, 42, 1904.

PLATE XX

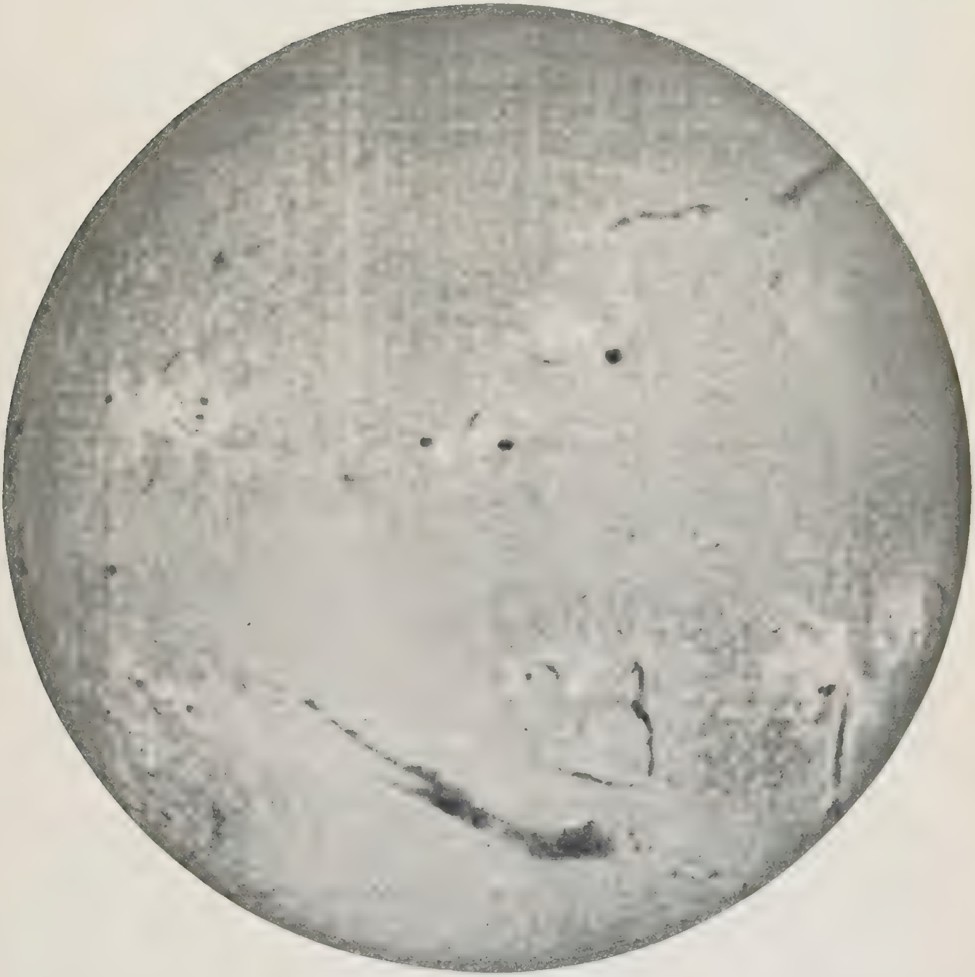

Bright and dark hydrogen flocculi. Enlarged from a small-scale spectroheliogram taken by Lewis Humason on February 17, 1926.

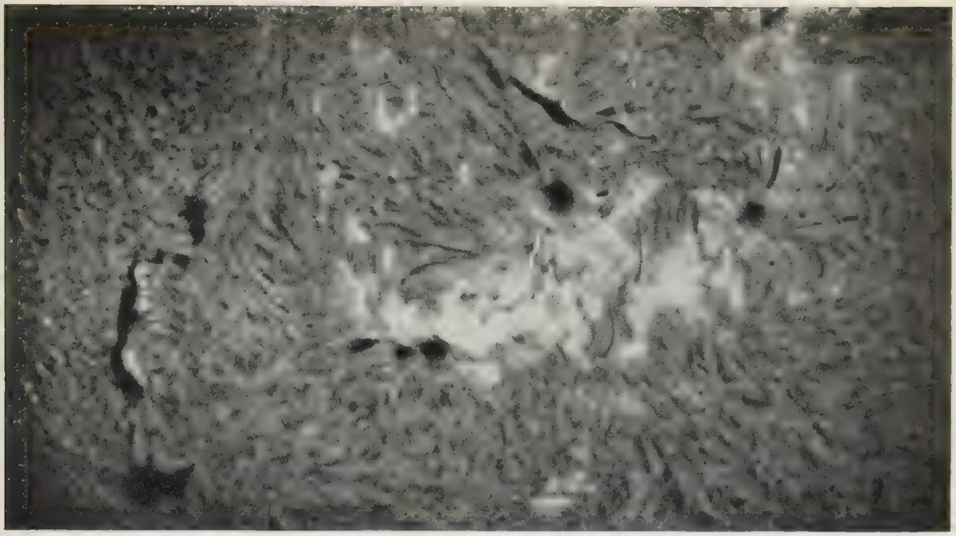

a.—Bright and dark hydrogen flocculi. From a spectroheliogram taken by A. H. Joy on July 11, 1917.

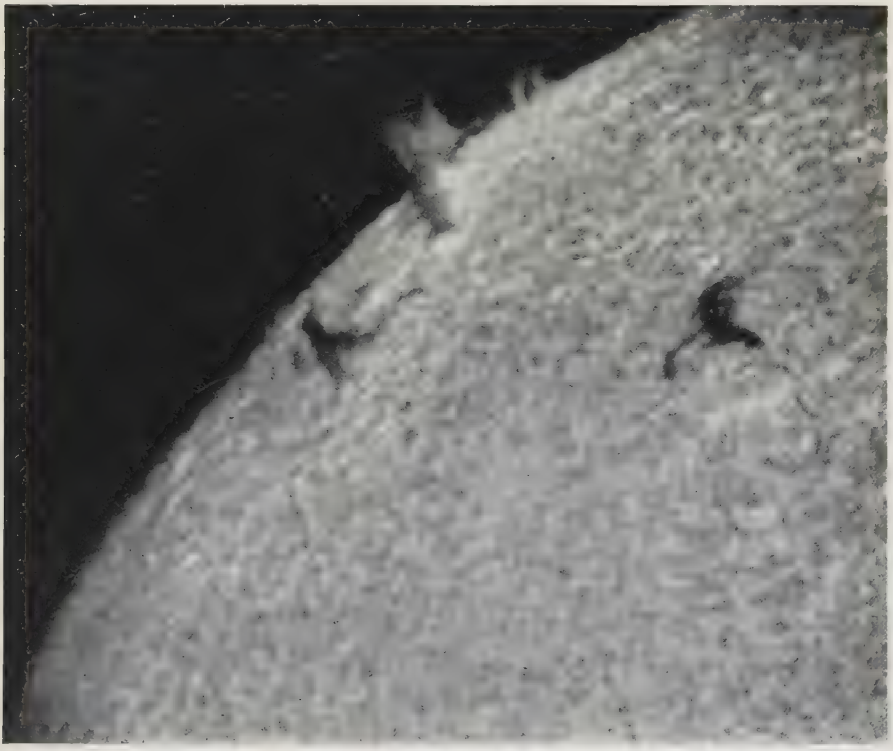

b.—Dark hydrogen flocculus, appearing as a prominence where it projects beyond the limb. From a spectroheliogram taken by S. B. Nicholson on June 16, 1916.

PLATE XXII

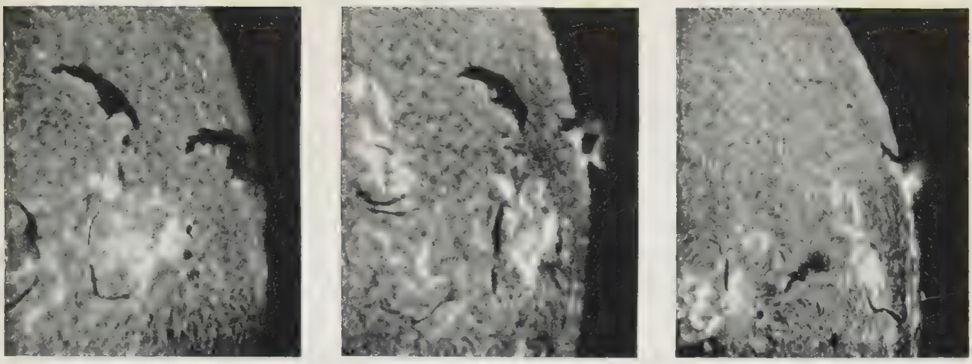

a *b* *c*

a, b, c.—Hydrogen flocculi photographed on three successive days. From spectroheliograms taken by A. H. Joy on June 27, 28, and 30, 1916.

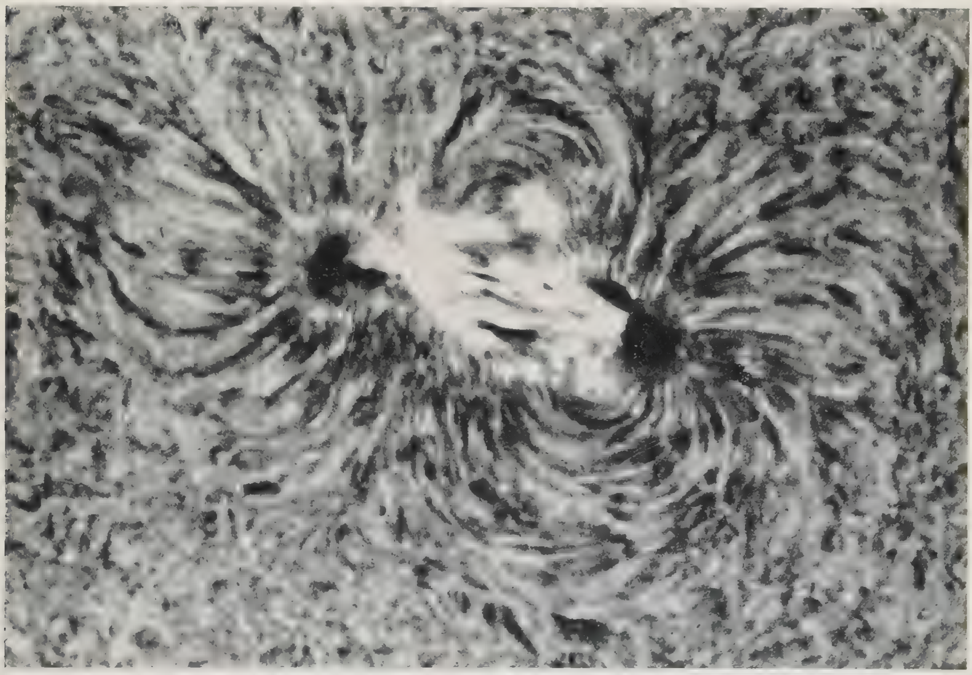

d.—Structure of hydrogen flocculi near large bipolar sun-spot group of August 30, 1924. From a spectroheliogram by Lewis Humason.

Active as well as quiescent dark flocculi are frequently observed, as would be expected from our knowledge of eruptive prominences. Many of them fail to appear as a whole on spectroheliograms because of their great radial velocity, which may displace parts of the *Hα* line to red or violet by an angstrom or more, and thus throw them off the second slit. Such flocculi are easily observed, however, with the spectrohelioscope and line-shifter, especially in association with active bright flocculi, from which they often rise as jets and arches. They sometimes develop suddenly near sun-spots, where their behavior gives valuable information regarding the nature of the fields of force.

It should be noted here that the distinction between bright and dark flocculi is somewhat arbitrary, as some flocculi that appear dark near the center of the sun would probably appear bright near the limb. Moreover, the hydrogen rising from bright flocculi often turns dark at a higher level.

The most interesting and perhaps the most significant structure in the solar atmosphere is that shown by the configuration of the dark hydrogen flocculi near sun-spots (Plates XXII*d*, XXIII*a*, and XXIV). When this structure was first detected on Mount Wilson in 1908 I ascribed it to the stream lines of extensive hydrodynamical vortices,[1] but subsequently Störmer investigated the hypothesis that it represented the lines of force of the magnetic fields in sun-spots.[2] The study of certain details of this structure with the spectrohelioscope is described below (p. 441).

HYDROGEN FLOCCULI AT VARIOUS LEVELS

The foregoing remarks apply to flocculi as shown by the spectroheliograph or spectrohelioscope with the second slit set centrally on the *Hα* line. It was long ago recognized, however, both by Deslandres and myself, that cross-sections of the solar atmosphere at various levels may be photographed by setting the second slit of the spectroheliograph at different distances from the center of the calcium and hydrogen lines. This conclusion has been fully confirmed by the work of Adams, Evershed, St. John, and others, and recently by Unsöld[1] on the basis of modern physical theory, in which the old conception of pressures of several atmospheres, increasing with the depth, has been abandoned. Very high dispersion, as pointed out in 1903,[2] and subsequently applied with admirable results by Deslandres and D'Azambuja,[3] is needed to isolate completely the H_3 or K_3 lines of calcium, which record the high-level dark calcium flocculi shown for the first time, with less contrast, on photographs taken with the lower dispersion of the Rumford spectroheliograph at the Yerkes Observatory.

---

[1] *Mt. Wilson Contr.*, No. 26; *Astrophysical Journal*, **28**, 100, 1908.

[2] *Mt. Wilson Contr.*, No. 109; *Astrophysical Journal*, **43**, 347, 1916.

The method described in the foregoing papers is illustrated in Plate XXIII*b*, *c*, *d*, *e*, *f*, which reproduces a series of photographs of the same region of the sun taken by my assistant, Mr. Hitchcock, with the 13-foot spectroheliograph of my Solar Laboratory in Pasadena on August 29, 1929. This instrument, which is described below (p. 449), is similar optically to the spectrohelioscope used in conjunction with it. Like the spectrohelioscope, it is provided with a line-shifter, and as the photographs were taken at settings of 0 ($H\alpha$ central on the second slit), -6, -10, -16, and -21, the structure shown at the decreasing levels is just what one would observe visually with the spectrohelioscope if its line-shifter (assuming the glass plate to be of the same thickness in both cases) were set at the same circle readings. As the flocculi in question were of the quiescent type, characterized by slow changes in form and small radial velocities, this illustration will serve to indicate the differences of structure, due chiefly to differences in level, which are very unlike those observed in active regions, marked by varying forms and high velocities, changing rapidly with time and from point to point at any given instant.

In cases of this kind, where the movements in the solar atmosphere are too gradual to produce important modifications of structure during the intervals involved, the spectroheliograph has the advantage of giving a permanent record for preservation and study. It often happens, however, that a far quicker and more flexible mode

---

[1] *Mt. Wilson Contr.*, No. 378; *Astrophysical Journal*, **69**, 275, 1929.

[2] Hale and Ellerman, *Yerkes Observatory Publications*, **3**, Part I, 17–19, 1903; *Astrophysical Journal*, **19**, 48, 1904.

[3] *Annales de l'Observatoire de Meudon*, **4**, 1910.

PLATE XXIII

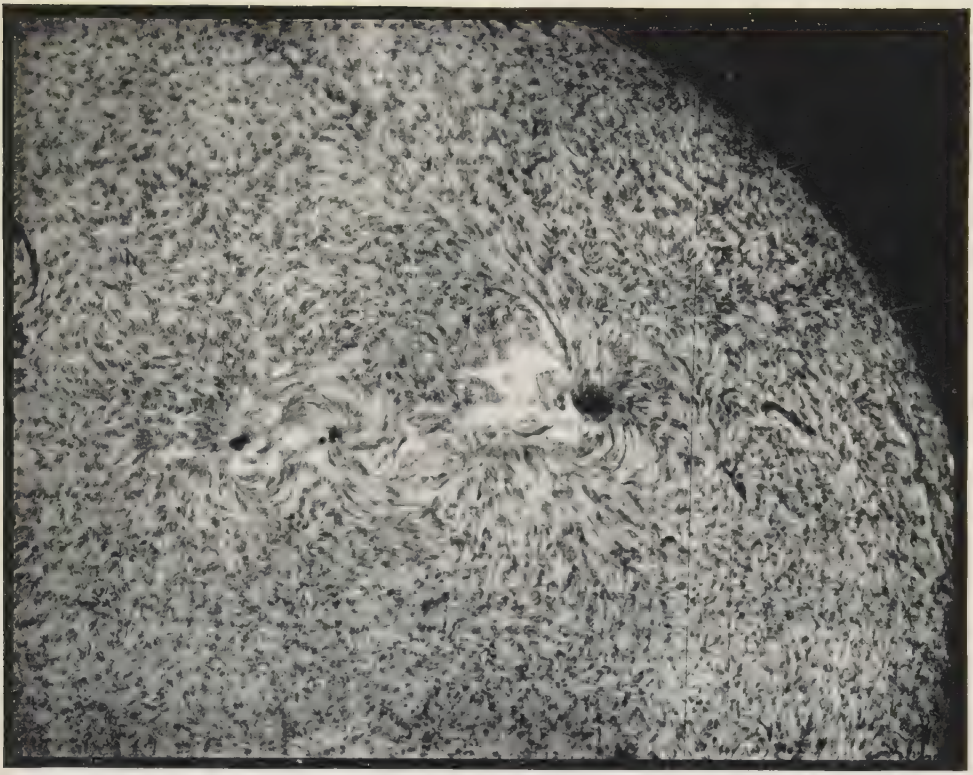

a.—Structure of hydrogen flocculi near sun-spots. From a spectroheliogram taken by Ferdinand Ellerman on January 5, 1917.

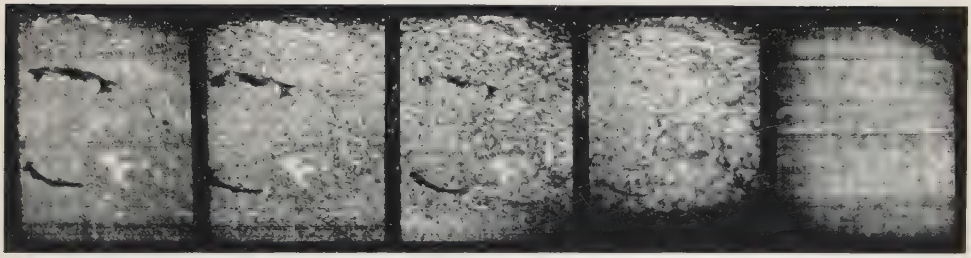

b (0, center of *Hα*)   *c* (−6)   *d* (−10)   *e* (−16)   *f* (−20)

b, c, d, e, f.—Same region of sun, as photographed by Hitchcock at center of *Hα* (*b*) and at increasing distances toward the violet on August 29, 1929.

of comparison is necessary to assure the recognition of phenomena otherwise certain to be overlooked or misinterpreted. The total exposure time for the five photographs reproduced in Plate XXIII was 25 minutes, making no allowance for the intervening instrumental adjustments.[1] With the spectrohelioscope the solar atmosphere at all of these levels and other intermediate ones, from the photosphere to the highest region attained by hydrogen, can be rapidly passed in review by a single quick turn of the line-shifter. Moreover, its adjustable stops permit the structure corresponding to any two levels to be instantly compared with the well-known precision of the Zeiss "blink"-micrometer and stereocomparator. By this method, or (less completely) by the use of two second slits (p. 425), we have the simplest and quickest means of detecting the relationship of the flocculi at any level to neighboring sun-spots.

I need not dwell at present on the structure of the flocculi at different heights, as this will appear more clearly in subsequent descriptions of particular cases.

ANALYSIS OF "MOTION FORMS"

The term "motion forms" is due to Lockyer, who first observed the distortion of the hydrogen lines in prominences and near sun-spots in 1869. His paper[2] and its addendum describe and illustrate reversed lines on the disk, the distortion of the $H\beta$ (F) in a prominence caused by cyclonic motion, and the varying appearances of this line in the following part of a long train of spots. In some places it disappeared entirely, or appeared as a bright line, at times greatly widened toward red and violet ("lozenges"), again widening only on one side, again as a widened bright line bounded on its red side by a dark line. Such distortions, which may assume fantastic shapes in striking contrast with the customary straight lines characteristic of a narrow slit, Lockyer named "motion forms." Symmetrical widening ("lozenges") he attributed to increased pressure, while the irregular displacements were ascribed to motion of the gas toward or from the earth. Even at this late date in solar spectroscopy, when

[1] Faster plates (giving less contrast) are now available.

[2] *Proceedings of the Royal Society*, **17**, 415, 1869. Reprinted in Lockyer's *Contributions to Solar Physics*, p. 488, where quotations on this subject from the papers of Young, Secchi, Rayet, Respighi, and others may also be found.

applying the new principles of modern physics, it is well worth while to re-read these early observations and those of Young, Secchi, Respighi, Rayet, Tacchini, Vogel, Zöllner, and others who took part in the spirited discussions of the period.

The introduction of photographic methods of recording solar spectroscopic phenomena was attended by many great advantages and some disadvantages. Rutherfurd and Rowland concentrated their attention on the spectrum of sunlight as a whole and made no attempt to deal with such localized phenomena as spots, faculae, or prominences. When these were attacked photographically in the early nineties, the new work absorbed so much time and attention that visual observations were somewhat neglected by those involved in it. Fortunately, however, the visual record of prominences and certain other solar phenomena has been maintained unbroken by observers in many countries. There is thus a large amount of literature open to those whose interest in the sun has recently been stimulated by advances in physics and chemistry.

The chief disadvantage of photography is that one proceeds more or less mechanically, making exposures without sufficient knowledge of the appearance of the flocculi at the moment, their exact position on the sun, or the critical periods of intense activity that characterize the most interesting phenomena. In work with the spectrograph, even if the slit is first set visually exactly at the points where line distortions are seen, their rapid changes in form, small size, and the effect of bad seeing in rendering them diffuse or causing them to oscillate across or along the slit may prevent the correct registration of their radial velocities. Some drawings by Young, showing the variation in form of the distorted $H\alpha$ line within a few minutes at the western edge of the penumbra of a large spot on September 22, 1870[1], indicate their rapid changes. But the best way to convince one's self of the value of the spectrohelioscope in analyzing such phenomena is to observe them simultaneously with this instrument and with a spectroscope, the narrow slit of which is set at the same position on the sun. The method I employ for this purpose is described on page 451.

---

[1] *Journal of the Franklin Institute*, 60, 338, 1870. Reproduced in Lockyer's *Solar Physics*, Fig. 173, p. 600.

I am not attempting to prove that the spectrohelioscope can take the place of the spectrograph, which gives measures of higher precision of such small line displacements as those due, for example, to the comparatively slow ascent or descent of gases in the solar atmosphere; nor does it compete with the velocity spectrograph, in the kind of work for which the latter is best adapted. The true function of the spectrohelioscope is to supplement these instruments, and also the spectroheliograph, not only by revealing many phenomena that would otherwise escape detection, but especially by the method of velocity analysis described below.

A motion form observed by myself in the great sun-spot group of February, 1892, shortly after the first photographs of calcium flocculi had been made with the Kenwood spectroheliograph, will serve to illustrate my meaning. The drawing reproduced in my paper shows a curved branch of $H\alpha$, extending toward the red and then bending downward to meet the dark absorption band caused by one of the spots of the group. It lasted only a few minutes, and I inferred that I was observing a varying mass of absorbing hydrogen, one extremity of which showed zero radial velocity while the other was moving rapidly downward toward the spot.[1] But I had no adequate means of determining its form or of studying its changes, both of which a spectrohelioscope would have supplied. Contrast this with some observations made with the latter instrument on August 15, 1926.

While examining the vortex structure associated with the large spot group then near the central meridian of the sun I noticed among other phenomena two slender, curved flocculi, both of which changed in appearance as the line-shifter was rocked back and forth. As the light in which they were observed varied in wave-length, the resulting effect was a shift of the position of maximum intensity along the curved flocculi. In fact, their dark heads were seen to advance toward the spot as the $H\alpha$ line moved across the second slit from its center toward the red. At a slit position completely outside of $H\alpha$ the curved flocculi had disappeared, but their extremities, like small black dots, were still visible, projected against the outer boundary of the penumbra. Another slender flocculus south of the preceding spot behaved in the same way.

---

[1] Hale, *Astronomy and Astrophysics*, **11**, 314, 1892; Crew, *ibid.*, p. 309.

Before giving the quantitative visual analysis of these effects, completed a few minutes later, let us consider how phenomena of this kind could be detected and interpreted in other ways. The spot in question was the preceding member of a bipolar group (Mount Wilson No. 2656) at 18° south latitude, then about 4° east of the central meridian. The 75-foot spectrograph of the 150-foot tower telescope on Mount Wilson showed it to be of north magnetic polarity, with a field strength on that day of 2800 gausses. The following spot was of south polarity, with a field strength of 2500 gausses. A direct photograph of the group was taken on Mount Wilson the same morning with the 60-foot tower telescope. From this, of course, no knowledge regarding the phenomena in the hydrogen atmosphere about the group could be derived, but it was useful in making the drawing (Plate XXIV*b*) showing the outline of the spots.

Two methods of observation other than the use of the spectrohelioscope might be employed in studying the flocculi associated with these spots. A series of photographs of the spectrum, taken at various points in the group, might register certain small projections from the *Hα* line, of varying form and length, in case the slit happened to lie in the right positions across the curved flocculi and also provided these slender objects were of sufficient width and intensity to appear on the negative, under the conditions imposed by the size of solar image, effects of vibration due to wind or other mechanical disturbances, the quality of the atmosphere, and the linear dispersion employed. Even if clearly registered, the measurement and interpretation of these motion forms would be a slow and tedious process.

On the other hand, a spectroheliograph might be employed to reveal the flocculi. My own spectroheliograph in Pasadena was not then ready for use, but I am fortunately able to give an enlargement of a photograph of the group (Plate XXIV*a*) made the same morning by Ellerman with the 13-foot spectroheliograph of the 60-foot tower telescope, which shows the curved flocculi and other structure in the hydrogen atmosphere. The slit was set at the center of *Hα*, but if Ellerman had known what phenomena were in progress and the posi-

PLATE XXIV

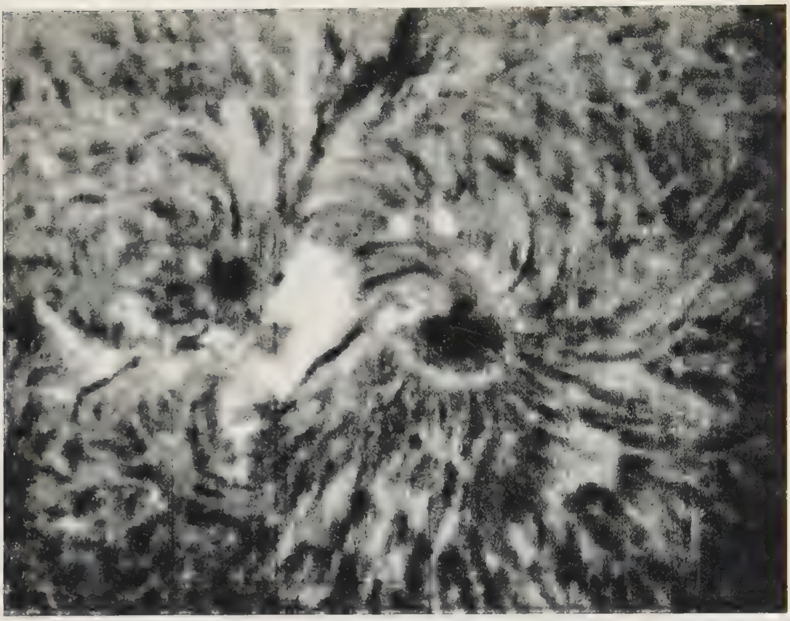

a.—Hydrogen flocculi surrounding the southern bipolar spot-group, Mt. Wilson No. 2656. Both vortices showed clockwise inflow, as illustrated for the preceding spot in (*b*). From a spectroheliogram taken by Ellerman on August 15, 1926.

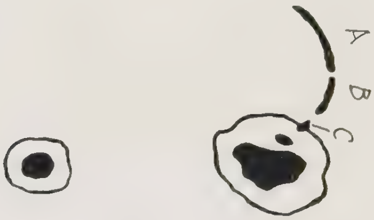

b.—Acceleration of the radial velocity of the inflowing hydrogen, shown by the line-shifter of the spectrohelioscope.

tions of the second slit required to register them, he might have obtained photographs of the effects described below; assuming, of course, that the demands of the various other solar observations of the daily program gave him time to do so. As it is, the spectroheliogram is of great value in showing the general structure of the field of force surrounding the spot group much more completely and accurately than I could have drawn it. The photograph also suggests the fact, proved beyond question by the spectrohelioscope, that the curved flocculi adjoining two spots marked by intense magnetic fields of opposite polarity both showed clockwise inflow—a point of prime importance in the interpretation of the nature of the forces in operation.

We may now turn to my visual work with the spectrohelioscope, in which the beautiful details of the $H\alpha$ flocculi were clearly seen, in spite of the fact that the atmospheric conditions in Pasadena were decidedly inferior to those a mile above me on Mount Wilson. One of these details, the curved flocculus shown in the sketch (Plate XXIV*b*), which was more intense than the others in the same region, was selected for observation. When the circle of the line-shifter indicated a radial velocity of +22 km/sec., only the outer part of the flocculus (*A* in Plate XXIV*b*) was visible. As the line was displaced farther to the violet, the flocculus seemed to move from *A* to *B*, the portion *B* corresponding to a velocity of +45 km/sec. When the second slit was about 1.1 A to the red of the center of $H\alpha$, corresponding to a velocity of about +50 km/sec., nothing remained visible of the flocculus except the black dot *C*, which was precisely on the edge of the penumbra. At still greater displacements the dot faded away and finally disappeared. The apparent advance of the flocculus toward the spot and the disappearance of all but the head were observed as often as the $H\alpha$ line was moved across the second slit from violet toward red.

It is interesting to note the accelerating radial velocities indicated by the successive slit positions, increasing from 22 km/sec. at a distance of 56,000 km from the center of the spot (*A*) to 45 km/sec. at a distance of 36,000 km (*B*) to about 50 km/sec. for a distance of 20,000 km, corresponding to the dot marking the inner extremity of the flocculus exactly on the outer edge of the penumbra (*C*). These values are not of the highest precision, but they cannot be far from the truth.

We at once recall the flow of prominences toward sun-spots,[1] as photographed in elevation at the sun's limb by Slocum with the Rumford spectroheliograph. Another series of calcium spectroheliograms of the prominences surrounding a large spot at the sun's limb on October 8, 1910, is also reproduced in his article on "The Attraction of Sun-Spots for Prominences."[2] Slocum directs attention to three bright knots on a long streamer, which gave velocities along the apparent trajectory of 16, 20, and 60 km/sec. at distances of 170,000, 130,000, and 75,000 km from the center of attraction. Pettit, who remeasured these plates, got velocities of 5, 8, and 44 km/sec., respectively. From these and other measures Pettit concludes: "Normally the matter about the spot is moving into it with accelerated velocities averaging about 35 km per second, sometimes reaching 100 km per second." Both Slocum and Pettit found that jets may be projected away from a spot at similar velocities, but Pettit[3] does not consider them to represent the normal condition. Evershed, on the contrary, in discussing his Kodaikanal observations of prominences, says: "No case has been found in which prominences were falling into sun-spots, but the reverse has several times been observed."[4] The difficulties involved are sufficiently indicated by these differences in opinion among experienced observers, but fortunately most of them are removed by the spectrohelioscope, in so far as the determination of the direction of flow and the radial velocity are concerned.

It is evident, however, that the observed radial velocity must depend upon the actual velocity along the true trajectory and the angle between this trajectory and the line of sight. If the trajectory is parallel to the solar surface, and the spot, as in the present case, is near the center of the sun, there will be no displacement of $H\alpha$, and the entire flocculus will be visible when the second slit of the spectroheliocope is set on the center of the line. Judged from the characteristic forms of prominences at the sun's limb, this is usually the condition of affairs at a considerable distance from a spot, though it often happens that at such a point the hydrogen is rising rapidly from below, thus producing a marked displacement of $H\alpha$ toward the violet when observed near the center of the sun. Nearer the spot, as the prominences at the limb discussed by Slocum and Pettit indicate, the trajectory makes an angle with the sun's surface ranging from small values up to 45° or even more. At the limb, the projection of the trajectory is often nearly a straight line over a great part of its length, and the increase in the radial component of the velocity observed on the disk as the spot is approached is probably due chiefly to the acceleration found by Slocum and Pettit. Sometimes, however, their limb photographs show that the tip of the inflowing prominence turns down close to the spot, and in spectroheliosopic observations made near the center of the disk this might account in such cases for an increase in the radial component of the velocity at this point, without a corresponding increase in the acceleration along the trajectory.

---

[1] It should be clearly understood, however, that Slocum's photographs represent three successive stages in the inflow of the tip of a prominence, whereas in the case illustrated in Plate XXIV the tip had already reached a point above the edge of the penumbra before the observations were begun. With a rather wide second slit, nearly the whole length of this curved flocculus (*A–C*) could be recorded in a single photograph, as shown in Plate XXIV*b*.

[2] *Astrophysical Journal*, **36**, 265, 1912.

[3] *Publications of the Yerkes Observatory*, **3**, Part IV, 1925.

[4] *Memoirs of the Kodaikanal Observatory*, **1**, Part II, 106, 1917.

The curved flocculus shown in Plate XXIV probably represents a prominence of moderate height projected against the disk. If we assume the trajectory to make an angle of 30° with the sun's surface, the corresponding velocities along the trajectory would be 44 km/sec. for the outer part of the flocculus (A), 90 km/sec. for the central part (B), and about 100 km/sec. for the tip (C).

The observation of August 15, 1926, proved to be typical, and it has been repeated in scores of cases, many of which will be described in detail in a later paper, where the bearing of these results on the work of St. John, Evershed, Fényi, Slocum, Pettit, and others will be discussed. In the present article I wish merely to make clear this new method of observation, in which the visibility of an object emitting approximately monochromatic light depends upon its radial velocity. The method evidently affords a valuable means of analysis, not merely of the hydrogen whirls but also of other important phenomena of the solar atmosphere. Noteworthy among these are the eruptive dark arches often seen with the spectrohelioscope. The following observation will suffice to show their nature.

On May 31, 1926, while observing spot No. 2571 (8° S., 20° E.) with the spectrohelioscope, I noticed a curious dark arch following the spot. The preceding end of this arch, which was seen when the second slit was on the violet side of *Hα*, seemed to rise from a small bright flocculus a short distance east of the spot. The central part of the arch, farther to the east, appeared when the slit was near the center of *Hα*, but its eastern extremity, where it seemed to curve back toward the surface of the sun, did not become visible until the slit was well beyond the boundary of *Hα* toward the red. Obviously we have here a dark arched prominence, rising with high velocity from a bright source near the sun-spot, pursuing a curved trajectory, the central part of which was nearly normal to the line of sight, and falling with high velocity at a point well to the east of its origin.

Since that date I have observed many of these arches and followed them across the disk until they were seen as high looped prominences projecting beyond the limb. They usually change rapidly in form and intensity but may be frequently renewed, sometimes from one point, again from another. In a bipolar spot-group three or four may often be seen at once, rising from a region of bright flocculi (such as that shown between the spots in Plate XXIV*a*) and falling at a distance, sometimes on the penumbra of one of the spots, sometimes elsewhere. When the radial velocities are high and the oscillating slits narrow, only a short section of an arch may be visible at a given position of the second slit on *Hα*. To show the whole arch, the line-shifter must be employed. As the line moves across the slit from violet to red, the maximum of intensity may be seen rising from the source of the ascending branch, passing along the trajectory, and running down the descending branch, which often seems to terminate in a rather definite dark head. The effect is of course different in different parts of the sun, because it depends upon the angle between the true trajectory and the line of sight. The appearance of such arches at the limb is illustrated in drawings by Young and others, and in many spectroheliograms. These looped prominences often appear intensely bright, even with the narrow slits of the spectrohelioscope employed for observations of the disk.

Another type of flocculus best observed with the spectrohelioscope is that which appears suddenly as a dark mass near large spots, often those of the bipolar type. If the spot group is near the center of the sun, the radial component of the ascending gas may be so great as to displace the hydrogen line an angstrom or more to the violet, thus completely excluding such flocculi from spectroheliograms taken with the second slit set at the normal position of $H\alpha$. As the line-shifter is turned from red to violet, these eruptive masses may be picked up visually and then watched as they are sucked toward the spots. I have observed very striking examples of this kind, which appeared about midway between the principal members of a bipolar group, at a considerable distance to one side of the line joining them. It is a fascinating sight to follow the disintegration of the flocculus and to trace the paths of its fragments as they are drawn asunder toward the two attracting centers. Some cases of this kind will be described in a later paper.

These applications of the spectrohelioscope will suffice to illustrate its advantages over the spectroheliograph when rapidly moving objects are under examination. Although I long ago recognized certain arches among the $H\alpha$ flocculi on spectroheliograms, and studied them by stereoscopic and other means in 1925, I could only suppose, but not prove, that the "bar magnet" structure of the fields of force might be due in part to them. In this study I made use of a series of spectroheliograms taken simultaneously with the second slit set on the red and violet sides of $H\alpha$, and inferred that their differences might be caused by motion of the gas along the arch. More can be learned in a few minutes, however, from such visual observations as I have just cited than from the comparison of many spectroheliograms, unless these are taken with the spectrohelioscope as a guide.

A word of caution regarding the use of the line-shifter for the study of moving gases should be added. In general, the chief criterion for distinguishing between effects due to differences in level and differences in velocity lies in comparing the structure and intensity of the flocculi on the red and violet sides of $H\alpha$. If at equal distances from the center of the line they differ materially, the asymmetry is probably due chiefly to the radial velocity of the gas, though other possible causes of asymmetry should not be forgotten. The most useful velocity effects are those of the progressive character just described, where the maximum of intensity runs along a flocculus, usually of the slender, curved type. It should be carefully noted in such cases, however, whether the observed displacement of the maximum of intensity with change of wave-length advances progressively from violet to red or whether, as occasionally happens, certain parts of a flocculus show maxima on both sides of $H\alpha$. The latter phenomenon is sometimes seen in (dark) eruptive flocculi, characterized by great widening of $H\alpha$ and by strengthening of its outer wings. Some cases of this sort will be described in a later paper.

ZEEMAN AND STARK EFFECTS

Imagine a Zeeman triplet, observed in the spectrum of a spark between the poles of a magnet. Along the lines of force only the two outer components of the triplet, circularly polarized in opposite directions, are visible. A quarter-wave plate and nicol, when properly adjusted, will quench either component. If the observation is made with a spectrohelioscope, an image of the spark will be seen in the light of the transmitted component, assuming it to be set on the second slit. If the quarter-wave plate is steadily rotated, this image will alternately appear and disappear.

It would be easy to devise a spectrohelioscope having a single first slit and two synchronous second slits that could be set at any reasonable separation in the spectrum. In this way the relative behavior in various parts of a spark or arc of the components of any two lines could be observed simultaneously with the aid of suitable polarizing apparatus and a compound eyepiece, bringing the monochromatic images due to the two lines into opposite halves of the same field of view. Various modifications of the arrangement, adapted for use at any angle with the lines of force, will suggest themselves to the reader. It is possible that such a substitution of a polarized image of the spark, visual or photographic, for the narrow spectral lines ordinarily observed, would assist in detecting slight variations of relative intensity otherwise likely to be overlooked. The same device might also be used, especially with a Lo Surdo tube, in certain laboratory studies of the Stark effect.

I am in doubt whether this method, even if applied with very high dispersion, can be used in the study of the magnetic fields of sun-spots or the general magnetic field of the sun.[1] In the former case, the general absorption in the spot and the weakness of the field just outside the penumbra and also in invisible spots may prevent tangible results. The weakness of the general magnetic field of the sun is also a serious obstacle. Moreover, the faintness of grating spectra of the highest dispersion, the comparatively low dispersion of prisms in the red, and the large scale of the solar image required stand in the way of success.

On the working hypothesis that appreciable electric fields, ordinarily too weak for detection in the solar atmosphere, might conceivably occur during certain stages of violent eruptive phenomena, I have frequently searched for them with the spectrohelioscope in active prominences and eruptive bright and dark flocculi. Assuming the electric field to be radial, the flocculi were usually observed near the sun's limb, with a nicol and half-wave plate, supported before the first slit. Sometimes a circular half-wave plate, rotated at any desired speed by an electric motor, was employed. In other cases I used a compound half-wave plate, made of narrow strips of mica. By moving this back and forth across the flocculus very slight differences in intensity could have been detected. The line-shifter was set so as to bring one of the outer edges of the greatly widened $H\alpha$ line upon the second slit.

While I have never been able to detect any differences of intensity clearly due to polarization effects, I believe that more observations should be made in this way. The phenomena of asymmetry in $H\alpha$ recently pointed out by Stark should also be borne in mind in these and other observations of the flocculi with the line-shifter.

It is evident that a spectrohelioscope with oscillating slits, rather than one having fixed slits with rotating prisms before them, should be employed in work of this kind, and that the polarization produced by the grating should not be overlooked.

---

[1] Hale, *Mt. Wilson Communication*, No. 97; *National Academy of Sciences Proceedings*, **12**, 286, 1926.

COMBINATION OF SPECTROGRAPH, SPECTROHELIOGRAPH, AND SPECTROHELIOSCOPE

A spectrohelioscope could easily be adapted to the photography of limited areas of the solar atmosphere; in fact, we have built and tested a special camera attachment for this purpose. But without the finest conditions of seeing and perfect fixity of the solar image during exposures, the results are inferior to those obtainable with a spectroheliograph, which also covers a much larger field. From the visual observations just cited, however, it is evident that a spectrohelioscope can be advantageously used as a guide to photography with a spectrograph or a spectroheliograph, as it reveals the position on the sun of the most interesting phenomena, the moments of active and significant changes, and the wave-lengths at which the second slit of the spectroheliograph must be set to record portions of flocculi or prominences moving with high radial velocities. I have therefore combined the two instruments in my Solar Laboratory, where the spectrohelioscope may also be used in conjunction with spectrographs of from 13 to 75 feet focal length.

The sunlight reflected from the 17½-inch coelostat mirror to the second mirror (also of 17½-in. aperture) at the summit of the low tower of my Solar Laboratory is sent vertically downward to the mirrors or lenses used to form solar images of diameters ranging from 2 to 16½ inches. In simultaneous work with the spectrograph or spectroheliograph and the spectrohelioscope the greater part of this beam falls on the large concave mirror on the left in Plate XXV, which is from a drawing by Porter of the combined instruments at the head of the 75-foot spectrograph well in the basement beneath the tower. This mirror returns the now converging rays to a convex mirror of fused quartz, which again reflects them downward to form a large solar image on the first slit of the spectrograph or spectroheliograph. Another portion of the same parallel beam is deflected by two plane mirrors in the tower to a single 6-inch lens of 18 feet focal length, which forms a 2-inch solar image on the first slit of the spectrohelioscope. The adjustments are such that when a given point on the

PLATE XXV

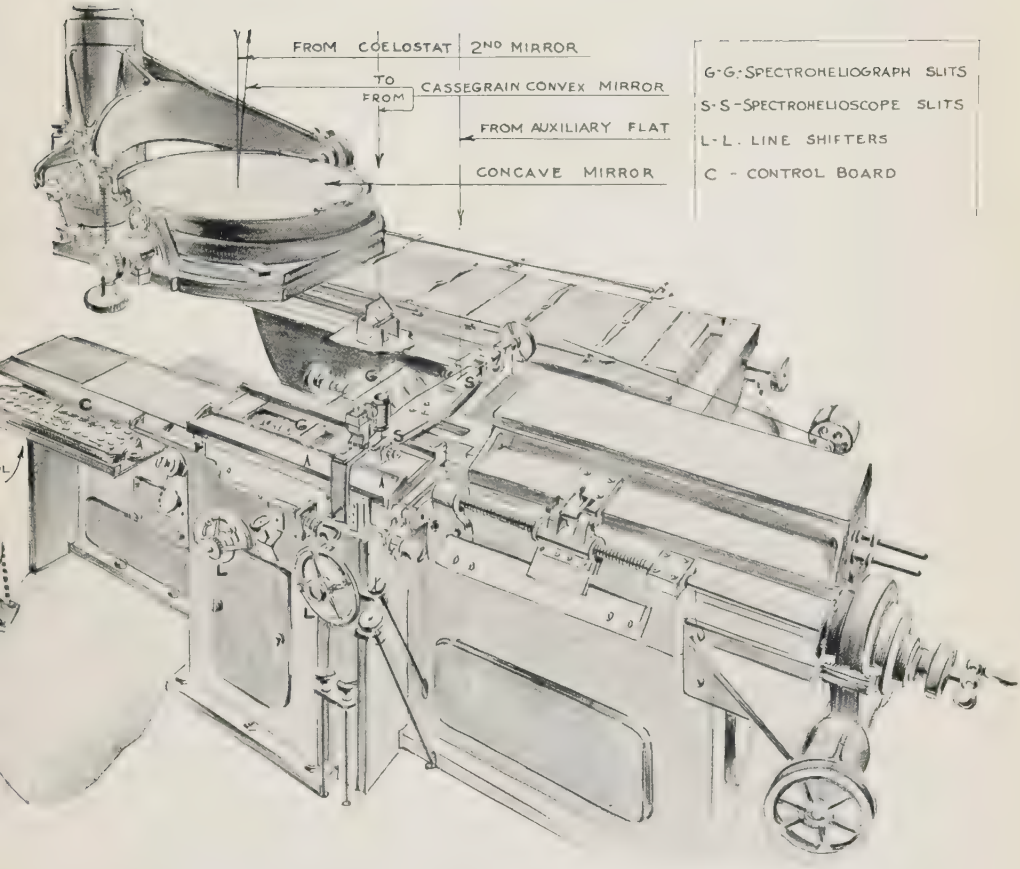

Combined Spectrograph, Spectroheliograph, and Spectrohelioscope

larger image is central on the slit of the spectrograph the same point on the smaller image is centered in the field of the spectrohelioscope. This adjustment remains good for all parts of the sun, because both images are moved at the same angular rate by the electric motors that control the position of the second mirror of the coelostat telescope.[1]

As arranged in Plate XXV, the spectroheliograph is merely a reflecting spectrograph of 13 feet focal length, with a right-angle prism mounted above its fixed first slit (G_1, beneath the prism), while its second slit (G_2) is also fixed in position during an exposure. The motion of the photographic plate across the second slit is produced by means of a screw driven by an electric motor (on a separate pier), while a lever (not shown in the drawing) connected with the plate-carriage moves the right-angle prism across the first slit at half the speed of the plate. This is a simple and effective device, giving $H\alpha$ spectroheliograms of excellent contrast. In the present arrangement I have purposely restricted the area photographed to $1\frac{1}{4}\times 2$ inches, though it can easily be increased to include a larger field. This is unnecessary in my case, because of the spectroheliographs in use daily for this purpose on Mount Wilson, and the fact that most of my present photographic records are confined to limited regions of a $3\frac{1}{2}$-inch solar image given by a mirror system not mentioned above.

The oscillating slits (S_1, S_2) of the spectrohelioscope, with their driving mechanism, are seen at the right of the spectroheliograph slits (G_1, G_2). The eyepiece[2] used for observing the spectrohelioscope image is in place above the second slit (S_2), and the dials of the two line-shifters (L_1, L_2) are also shown below. A microscope with micrometer eyepiece is used for setting the spectroheliograph slit G_2 on the center of $H\alpha$, after which the line-shifter L_1 of the spectroheliograph is employed in harmony with the indications regarding the most suitable wave-lengths afforded by the visual use of the spectrohelioscope and the line-shifter L_2. The control board for the electric slow motions appears at the left, while the long plate-holder for photographing spectra of high dispersion with the 75-foot (Littrow) spectrograph is shown beyond the slits.

---

[1] This precise correspondence of the two solar images is required only in the simultaneous use of the spectrograph and spectrohelioscope, as described on p. 451. It is of course affected by the introduction of the moving right-angle prism of the spectroheliograph.

[2] A periscopic eyepiece, permitting the observer to look horizontally while sitting in a chair, will also be available.

As for the optical arrangements within the well, only a brief description is needed here to supplement Porter's admirable drawings (Plates XXVI and XXVII). The slits, gratings, and line-shifter of the spectroheliograph are indicated from below in Plate XXVI, which shows the skeleton tube of the 75-foot spectrograph descending toward the bottom of the well from the 5-foot circular casting at the top. The solar rays diverging from the first slits meet the concave mirrors of 13 feet focal length (Plate XXVII), which render them parallel and return them to two plane gratings mounted below the circular casting (Plate XXVI). These send the $H\alpha$ region back to the second pair of concave mirrors shown in Plate XXVII, which form images of the $H\alpha$ line on the second slits of the spectroheliograph and spectrohelioscope, respectively, after passing through the parallel glass plates of the two line-shifters, only one of which is shown in Plate XXVI.

The spectroheliograph mirrors can be easily moved out of the way when it is desired to use greater linear dispersion. A pair of similar mirrors of 30 feet focal length can be employed at a lower level in their stead, or the light from the first slit can be sent to the 6-inch lens of 75 feet focal length, with large grating below it at the bottom of the well, which is chiefly used for the study of sun-spot spectra and the general magnetic field of the sun. The spectrohelioscope with its 2-inch solar image is also adapted for use in conjunction with this high dispersion spectrograph, for which a convex mirror in the tower above provides a solar image 16½ inches in diameter. Thus this combined equipment gives solar images and dispersions corresponding with those obtained on Mount Wilson with both the 60- and 150-foot tower telescopes, with the added facilities of the spectrohelioscope and the provision of a 3½-inch solar image, ordinarily preferable in Pasadena to a 6.7-inch solar image for photography with the spectroheliograph.

An independent spectrohelioscope, of the horizontal type described in the first part of this article, may also be used as a guide in work with a spectroheliograph. The advantage of my combined ar-

PLATE XXVI

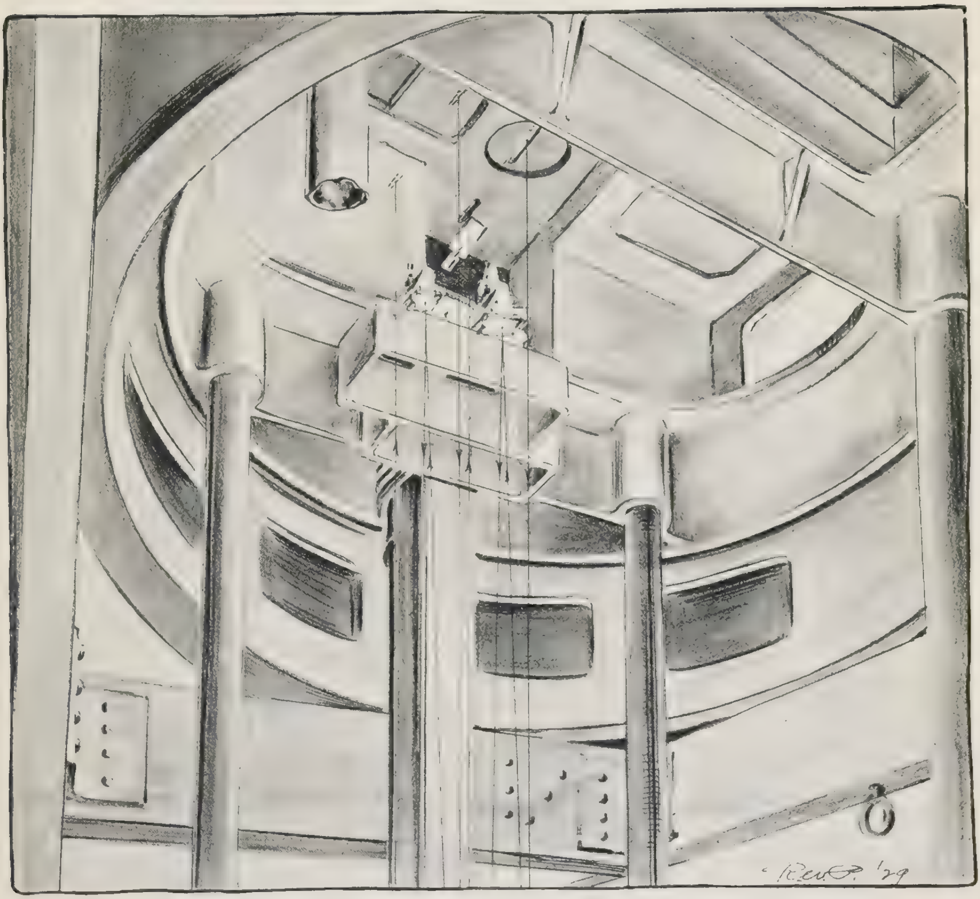

SLITS, GRATINGS, AND SKELETON TUBE OF COMBINED INSTRUMENTS SEEN FROM BELOW

PLATE XXVII

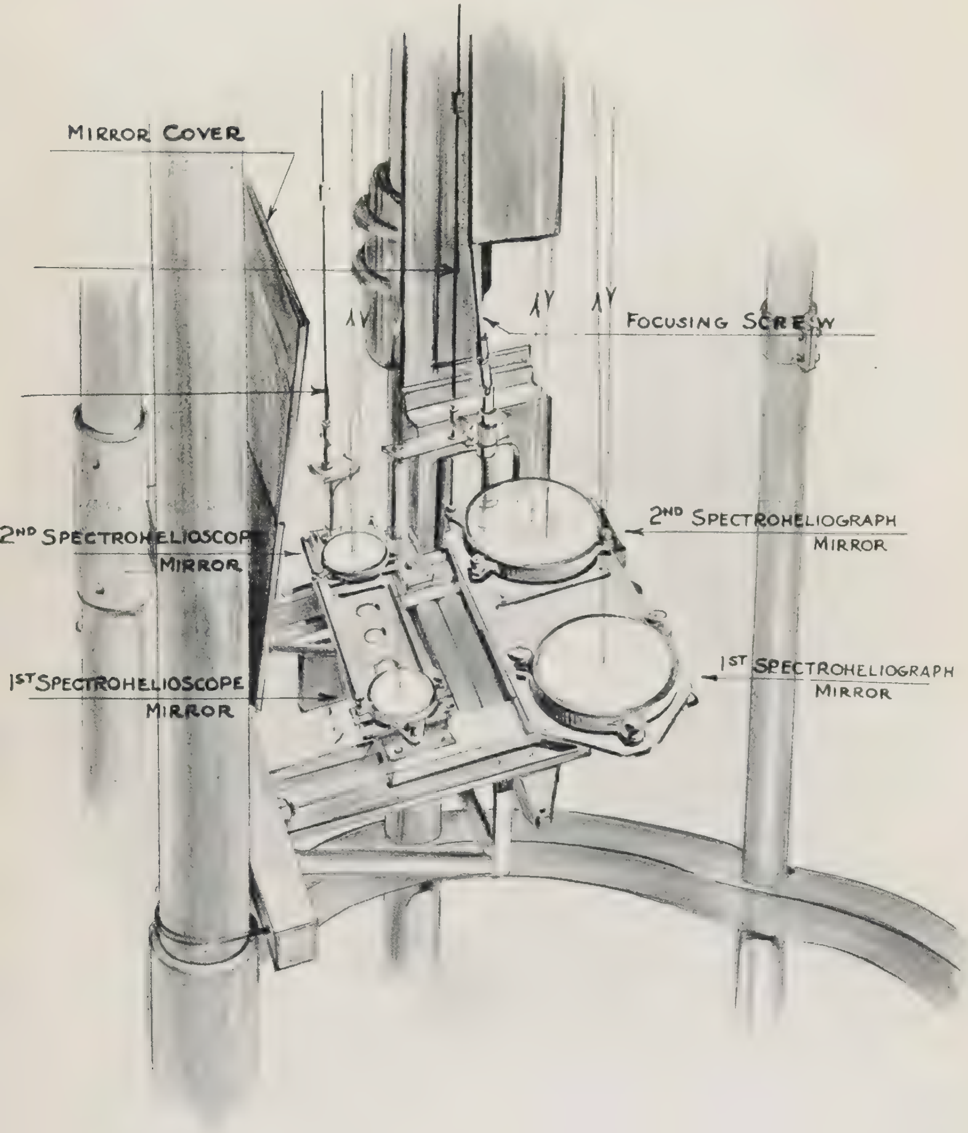
MIRROR COVER
FOCUSING SCREW
2ND SPECTROHELIOSCOPE MIRROR
2ND SPECTROHELIOGRAPH MIRROR
1ST SPECTROHELIOSCOPE MIRROR
1ST SPECTROHELIOGRAPH MIRROR

Concave Mirrors of Spectroheliograph and Spectrohelioscope

rangement appears in cases where it is desirable to bring a small region in the hydrogen atmosphere, otherwise invisible, exactly upon the fixed slit of a spectrograph; or, vice versa, to bring such an object as an invisible sun-spot, betrayed by visual observations of the oscillating Zeeman effect in the 75-foot spectrograph, into the center of the field of view of the spectrohelioscope, in order to learn whether the hydrogen at any level is appreciably affected above the magnetic field.

A word may be added regarding a compound eyepiece, not shown in the illustration, by means of which the (fixed) distorted $H\alpha$ line can be observed in half the field of view, while the other half shows the spectrohelioscope image of the same region. In this way the motion forms can be directly compared with the effects given by rotating the line-shifter.

SOLAR ERUPTIONS AND TERRESTRIAL PHENOMENA

In July, 1892, a brilliant eruption associated with a large sun-spot, followed the next day by an intense terrestrial magnetic storm, was photographed with the Kenwood spectroheliograph.[1] Since that time I have continued to hope that similar methods might permit the detection of all such eruptions and the determination of their exact relationship with auroras, magnetic storms, and other terrestrial phenomena. At present the spectroheliographs in England, France, Spain, Italy, India, and the United States serve this purpose in part, and a number of similar eruptions, also followed by magnetic storms, have been photographed at the Yerkes, Mount Wilson, Meudon, and Kodaikanal Observatories.[2] The large unfilled gaps in longitude and the impossibility of taking photographs at sufficiently short intervals nevertheless leave the solar record very incomplete, and further steps must be taken to amplify it.

On January 24, 1926, while testing my first spectrohelioscope between 11^h40^m and 12^h15^m P.S.T., I observed a bright eruption in and following the great spot-group then visible (latitude about 22° N.). Its form changed rapidly, and $H\alpha$ was so much distorted in places that the rapidly descending dark flocculi could be seen when the second slit was displaced far beyond the line toward the red. On January 25 the eruption, then extraordinarily brilliant, continued throughout the morning and most of the afternoon. The sodium lines D_1 and D_2 and the helium line D_3 were brightly reversed in the large spot. At certain points following the spot, D_3 appeared dark and greatly distorted toward the red. The next morning the great eruption seemed to be over, but at noon a small bright eruption was seen for a few minutes on the edge of the bridge in the large spot. On January 27 another small and short-lived eruption was seen near the large spot. Subsequently I learned from Professor Störmer that he observed at Oslo on the evening of January 26 the brightest (red) aurora he had seen for years. On January 26 the most intense magnetic disturbance in five years was recorded at the Royal Observatory, Greenwich. According to a note in *Nature* for February 6, "the disturbance commenced at 16½ h., rose to a considerable maximum, and subsided soon after 5 h. on the following morning."[1]

---

[1] Hale, *Astronomy and Astrophysics*, **11**, 611, 1892. Illustrated in my subsequent paper (*ibid.*, p. 917).

[2] Fox and Abetti, *Astrophysical Journal*, **29**, 40, 1909; D'Azambuja and Grenat, *L'Astronomie*, **40**, 489, 1926, and papers by Royds and Nicholson.

This observation, made while the spectrohelioscope was still in the experimental stage, convinced me of the importance of devising such inexpensive instruments as I have described in this paper, and arranging, if possible, for their co-operative use at widely distributed stations. At least seventeen of these instruments will soon be in operation, including two or more in England, one in Italy, one in Syria, one in Australia, one in New Zealand, one in Samoa, three in California, one in South Dakota, one in Michigan, one in Wisconsin, one in Illinois, two in Ohio, and one in New York. Several other spectrohelioscopes will also be installed at intermediate longitudes in the near future, and I therefore hope that within a short time a satisfactory scheme of observations may be in progress.

The spectrohelioscope is especially suited for this work because of the brief time needed to examine the whole disk of the sun and to detect signs of activity calling for vigilance on the part of the observer. Not only astronomers, physicists, and geophysicists, but also students of radio can advantageously join in our co-operative undertaking, because of the relationship that may exist between solar outbursts and radio transmission. The task of each observer will be a simple one. He will merely be asked to examine the sun several times a day, if possible at certain hours dependent upon his longitude, and to note the approximate position, area, and brightness of any exceptionally bright flocculi.

---

[1] Hale, *Mt. Wilson Communication*, No. 97; *National Academy of Sciences Proceedings*, **12**, 286, 1926.

Several other applications of the spectrohelioscope have been mentioned in previous articles,[1] including its use in connection with the classification of sun-spots, the study of the relationship between prominences and flocculi, and the investigation of the fields of force in the atmosphere of the sun. These will be discussed more fully in the detailed account of my visual observations of the hydrogen flocculi which will form the subject of a later paper.

In connection with the designing of the instruments described in this paper I owe my thanks to Messrs. Pease and Nichols, by whom most of the working drawings were prepared, and to Mr. L. R. Hitchcock, who has made many alterations and improvements and assisted me in the observations. I am also indebted to the members of the staff of the Mount Wilson Observatory who made the spectroheliograms, and to Mr. Russell W. Porter for the perspective drawings reproduced among the illustrations.

CARNEGIE INSTITUTION OF WASHINGTON
MOUNT WILSON OBSERVATORY
October 1929

---

[1] See Hale, *ibid.*, and *Nature*, **119**, 708, 1927.

Contributions from the Mount Wilson Observatory, No. 389
Reprinted from the *Astrophysical Journal,* Vol. LXX, pp. 312–318, 1929
Printed in the U.S.A.

THE UNIT CHARACTER OF MULTIPLETS

By CHARLES E. ST. JOHN

ABSTRACT

1. *Unit character of multiplets.*—Nine strong *Fe* multiplets in the violet with a range of line intensity within the multiplet of 2–40 give a red shift of +0.0104 A for strong and +0.0100 A for weak lines; 4 of medium strength with a range of line intensity of 1–6 give +0.0077 A for strong and +0.0074 for weak; 8 in the red with a range of line intensity of 1–9 give +0.0089 for strong and +0.0087 for weak lines. In a total of 154 lines *73 strong lines give +0.0094 A* and *81 weak lines +0.0092 A*. Lines on the main diagonal of the multiplet diagrams are taken as strong, on the side diagonals as weak.

2. The calculation of theoretical intensities, the calibration of the Rowland scale of intensities, the deduction of the number of atoms per square centimeter from line contours, and the equal red shift for the lines in a multiplet, whatever their intensity, imply in the sun *definite layers of maximum absorption.*

3. *Heights from flash spectra.*—Lines of mean intensity 6.5 in multiplets of maximum intensity 20–40 are higher by 400 km than lines of the same intensity in multiplets of maximum intensity 6–7, but owing to photographic errors are measured somewhat lower than the strongest lines in the multiplet.

Introduction.—It has been the practice in discussions of solar phenomena varying with line intensity, such as height, excitation potential, and solar rotation, to consider the intensities of individual lines in looking for correlations. It was thought that the absorbing layers of strong lines only were at great heights above the photosphere. Recent theories of the formation of absorption lines and their application to the quantitative determination of the constituents of the solar atmosphere seem to call for a reconsideration of the older view. The large number of normal *Fe* multiplets identified in the *Rowland Revision*[1] and the new and accurate wave-lengths[2] of the *Fe* lines in the vacuum arc furnish a body of data suitable for the purpose. It has been assembled and discussed in the present paper.

Red shift and line intensity.—The data for the strong *Fe* multiplets with maximum line intensity 10–40 and with low excitation potentials are assembled in section A of Table I. All measured lines are used, and the division between strong and weak lines within the multiplet is made by taking the lines on the main diagonal in the multiplet diagram as strong and those on the side diagonals as weak.

[1] *Publications of the Carnegie Institution of Washington,* No. 396; *Papers of the Mount Wilson Observatory,* **3,** 1928.

[2] Burns and Walters, *Publications of Allegheny Observatory,* **6,** 11, 1929.

The principles of selection are illustrated in the accompanying diagram where the lines on the main (left) diagonal form distinctly the stronger group. The lines on the weaker of the two side diagonals are not considered; λ 3940, because it is a blend with *Co;* λ 3917, because of the strong companion 0.06 A to the red; and λ 3898 for similar reasons. Although the average intensity of the lines on the main diagonal is 14.6 and on the side diagonal 7, the mean red displacement for the two groups of lines is the same. Nine strong and 4 weak multiplets in the violet and 10 of the strongest in the red have been treated in the same manner. The results are given in sections A, B, and C of Table I. The precision with which this like red displacement holds for lines of widely different intensities in multiplets is indicated by the fact that in a total of 154 lines 73 strong lines give $\Delta\lambda = 0.0094$ and 81 weak lines give $\Delta\lambda = 0.0092$ A, respectively.

MULTIPLET DIAGRAM FOR $A^5F-b^5D^\circ$, SHOWING RED DISPLACEMENTS FOR INDIVIDUAL LINES

($\Delta\lambda = \lambda$ sun *minus* λ vac.; unit=0.001 A)

	a^5F_5	a^5F_4	a^5F_3	a^5F_2	a^5F_1
$b^5D^\circ_4$	Int. = 25 λ 3820 Δλ = 10	7 3887 11	5 3940 *Fe, Co* 13		
$b^5D^\circ_3$		Int. = 20 λ 3825 Δλ = 10	8 3878 9	5 3917. Line (2) 0.06 A to the red	
$b^5D^\circ_2$			Int. = 10 λ 3834 Δλ = 10	6 3872 9	5 3898 *Fe, V.* Line (2) 0.08 A to the red
$b^5D^\circ_1$				Int. = 8 λ 3840 Δλ = 9	7 3865 10
$b^5D^\circ_0$					Int. = 10 λ 3849 Δλ = 10

Theoretical grounds.—The theoretical calculation of the relative intensity of any line in a multiplet is based upon the quantum numbers for all the lines in the multiplet and upon the correspondence principle. In calculating line intensities by the sum rule it must be applied, according to Ornstein and Burger,[1] to the squared amplitudes of "fictive radiators" which are assumed to represent or to be proportional to the number of atoms concerned in the production of the lines. This assumption was used by Russell, Adams, and Moore[1] in the calibration of the Rowland scale of intensities.

---

[1] *Zeitschrift für Physik*, **40**, 412, 1926.

In Unsöld's method[2] of deducing the number of atoms from line

TABLE I

RED SHIFT OF SOLAR LINES IN MULTIPLETS

($\Delta\lambda = \lambda$ sun *minus* λ vac.; unit $= 0.001$ A)

MULTIPLET	REGION	INTENSITY RANGE WITHIN THE MULTIPLET	ON MAIN DIAG.		ON SIDE DIAG.		E.P. IN VOLTS
			No. of Lines	$\Delta\lambda$	No. of Lines	$\Delta\lambda$	
A. Violet: Strong Multiplets							
$a^5F-a^5G^\circ$..........	3583–3647	4–20	5	8.4	4	8.8	0.93
$a^5D-a^5F^\circ$..........	3679–3748	6–40	4	9.2	3	9.7	.06
$a^5F-b^5F^\circ$..........	3687–3799	4–40	5	10.8	8	9.0	0.93
$a^3F-b^3D^\circ$..........	3815–3966	3–15	3	9.7	3	12.3	1.54
$a^5F-b^5D^\circ$..........	3820–3940	5–25	5	9.8	4	10.0	0.93
$a^5D-a^5D^\circ$..........	3824–3930	6–20	4	11.2	8	10.4	0.06
$a^3F-b^3F^\circ$..........	3969–4143	7–30	3	11.7	4	11.0	1.54
$a^3F-a^3G^\circ$..........	4147–4325	4–15	3	12.7	3	9.3	1.54
$a^3F-a^5G^\circ$..........	4337–4415	2–15	3	12.3	4	11.0	1.54
Means and totals	....	....	35	10.4	41	10.0	1.01
B. Violet: Multiplets of Medium Strength							
$a^3H-a^3H^\circ$..........	3619–3672	1–5	3	6.3	4	5.8	2.42
$a^3G-a^3H^\circ$..........	3937–4021	3–6	3	7.3	1	9.3	2.68
$a^5P-a^5P^\circ$..........	3943–4038	2–6	2	9.0	2	8.5	2.19
$a^5D^\circ-b^5F$..........	4565–4736	1–6	4	8.2	4	8.0	3.24
Means and totals	....	....	12	7.7	11	7.4	......
C. Red: Strong Multiplets							
$b^3F-b^3F^\circ$..........	6005–6322	1–7	3	10.5	3	6.8	2.57
$a^3H-a^3G^\circ$..........	6136–6344	4–9	2	8.5	3	8.0	2.43
$b^3F-b^3F^\circ$..........	6005–6322	1–7	3	10.5	3	6.8	2.57
$a^5P-b^5D^\circ$..........	6137–6430	3–6	3	6.8	6	8.1	2.19
$a^5P-a^5D^\circ$..........	6232–6411	3–8	3	7.7	4	7.8	3.63
$a^3P-a^3P^\circ$..........	6254–6478	2–7	2	10.5	3	11.0	2.38
$a^5F-a^7F^\circ$..........	6280–6625	1–8	4	7.9	3	10.5	0.93
$a^3H-a^5G^\circ$..........	6318–6593	2–8	3	10.8	2	12.0	2.42
$a^3G-b^3F^\circ$..........	6546–6806	1–6	3	11.2	2	10.5	2.72
Means and totals	....	....	26	9.3	29	8.8	......

---

[1] *Mt. Wilson Contr.*, No. 358; *Astrophysical Journal* **68**, 1, 1928.

[2] *Zeitschrift für Physik*, **44**, 793, 1927; **46**, 765, 1928.

contours, it is assumed that in a close doublet or triplet the "oscillating power," f, gives the proportion of atoms involved in a given transition and that the equal numbers N obtained for the individual lines represent the total number of atoms over one per square centimeter concerned in producing the lines of the multiplet.

These assumptions have no evident *raison d'être* unless they refer to the same body of absorbing material, and the observed equal red displacement for all lines in a multiplet puts the underlying assumptions upon a definite observational basis.

For the 9 strong multiplets (Table I, section A) the mean red shifts for lines ranging in solar intensity from 2 to 40 are equal. Since all the lines in a multiplet, whatever their intensities, give equal red displacements, it appears that the large red displacements characteristic of strong lines are not due, as sometimes stated, to an "intensity equation," according to which one measures strong and weak lines differently.

Data for multiplets in which the maximum line intensity is 6 are given in section B of Table I. The spectral region is approximately the same as for section A. The mean red displacements for lines in these multiplets, ranging in solar intensity from 1 to 6, are also equal, but definitely smaller than those of section A. Thus the lines of intensity 6 in section A give a mean for the group of 0.0102 A, while lines of the same intensity in section B give a mean of 0.0077 A. We can therefore no longer speak of the red shift of a line of intensity 40, 10, or 6 per se, but only of the lines in a 40-multiplet, a 10-multiplet, or a 6-multiplet where 40, 10, and 6 are the maximum intensities in the separate multiplets.

Heights from flash spectra.—It has been the practice to group the heights of all lines of the same solar intensity and to assume that the mean is the height reached by the corresponding gaseous layers in the sun's atmosphere, for example, for lines of intensity 6. It is evident from sections A and B of Table I that lines of intensity 6 in a 40-multiplet show larger red displacements than lines of intensity 6 in a 6-multiplet, and that the 6's in a 40-multiplet have a much lower excitation potential than the 6's in a 6-multiplet. Do the former also originate in a higher layer? The question is answered by the data in Table II.

TABLE II

HEIGHTS FOR LINES OF LIKE INTENSITY IN MULTIPLETS OF DIFFERENT STRENGTHS

1	2	3	4	5	6	7	8
MULTIPLET	MAX. INT. IN MULTIPLET	LINE	INT.	Δλ	HEIGHT	ON MAIN DIAGONAL	
						Δλ	Height in Km
A. Lines of Intensity 6–7 in Strong Multiplets							
$a^5D-a^5F^\circ$....	40	3733.332	7	12.0	....	8.8	1125
		3745.912	6	10.0	....	....	....
$a^5D-a^5D^\circ$....	20	3824.454	6	9.0	1000	....	....
		3878.583	7	9.0	1200	11.0	1190
		3895.669	7	11.0	1000	....	....
$a^5F-b^5D^\circ$....	25	3865.535	7	9.5	900	....	....
		3872.506	6	8.5	700	10.5	1250
		3887.061	7	8.5	600	....	....
		3940.892	5	11.5	600	....	....
$a^3F-b^3F^\circ$....	30	4005.256	7	10.5	800	11.5	950
Means...	....	3839.537	6.5	10.2	850	10.4	1100
B. Lines of Intensity 6–7 in Medium Multiplets							
$a^5F^\circ-x^3G$....	7	3716.452	7	8.0	400	7.3	450
$a^5P-a^5D^\circ$...	6	3807.546	6	6.0	500	8.5	500
$a^3G-a^3H^\circ$...	6	3956.688	6	9.0	....	8.2	....
$a^5P-c^5P^\circ$....	6	3974.766	6	6.0	500	2.7	550
		3977.752	6	9.0	....	....	....
$a^5D^\circ-b^5F$....	6	4736.783	6	8.0	400	8.2	....
Means...	....	3878.330	6.2	7.7	450	8.0	500
C. Lines of Intensity 3–5 in Strong Multiplets							
$a^3F-b^3D^\circ$....	15	3888.526	5	10.0	....	10.3	850
$a^5F-b^5D^\circ$....	25	3940.892	5	11.5	600	10.0	1250
$a^5F-b^5F^\circ$....	40	3727.636	4	14.5	500	10.0	1000
$a^3F-a^3G^\circ$....	15	4147.677	4	6.0	400	11.0	750
$a^3F-b^3D^\circ$....	15	3966.075	3	10.0	500	10.3	850
Means...	....	....	4.2	10.4	500	10.3	1175

TABLE II—*Continued*

1	2	3	4	5	6	7	8
MULTIPLET	MAX. INT. IN MULTIPLET	LINE	INT.	Δλ	HEIGHT	ON MAIN DIAGONAL	
						Δλ	Height in Km
D. Lines of Intensity 3–5 in Weak Multiplets							
$a^5F^\circ - c^5D$....	5	4084.503	5	10.0	400	8.5	400
$b^3P - d^3D^\circ$...	5	4134.687	5	8.0	500	7.5	480
$b^3F - c^3F^\circ$....	4	3779.433	4	....	500	....	500
$b^3P - b^3P^\circ$....	4	4154.507	4	6.0	500	6.7	500
$b^3F - b^3G^\circ$...	3	4011.416	3	6.0	350	5.3	350
Means...	....	....	4.2	7.5	430	7.0	465

The first and second columns of Table II give the multiplet and its maximum intensity; the third and fourth, the individual lines and their intensity; the fifth and sixth, the displacement to the red and the heights for the lines considered; and the seventh and eighth, like data for the lines on the main diagonal. Sections A and B supply one set of comparisons and sections C and D a second set. The mean intensity of the lines considered in the first set is 6.4 and in the second 4.2. The spectral regions are approximately the same.

Lines in strong multiplets. Since the lines in a multiplet originate in the same absorbing layer, the images on flash-spectrum plates are images of the same crescent but made by radiations of widely different intensities. The densities of the images depend upon the strength of the lines and upon the sensibility and threshold value of the photographic plate. The heights of the weak lines estimated from these images will be too low; the deficit for them should increase with increased difference of intensity between the weak and strong lines, and for lines of relative intensity 3–40 it should be larger. The observations show that the lines of mean intensities 6.5 and 4.2 in multiplets of strength 15–40 have heights of 850 and 500 km, respectively, while for lines on the mean diagonal the height is $\approx$ 1100 km. The red displacement is, however, the same for all.

Lines in weak and strong multiplets.—Since the absorbing layers for strong multiplets are higher than for weak multiplets, the heights for lines of the same solar intensity measured on flash-spectrum plates should on the whole be greater for the strong multiplets. The observations in the third and fourth columns of the summary of Table II show just this, and not only this, but also that the red displacement for high ($\approx$ 1100 km) absorbing layers is larger than for low ($\approx$ 500 km) layers; namely, 0.0103 and 0.0076 A in the mean.

SUMMARY OF DATA IN TABLE II

1	2	3	4		5	
Set	Mean Int. of Compared Lines	Strength of Multiplet	Lines Compared		Lines of Main Diag.	
			$\Delta\lambda$ A	Height in Km	$\Delta\lambda$ A	Height in Km
1................	6.5	20–40	0.0102	850	0.0104	1100
	6.2	6–7	.0077	450	.008	500
2................	4.2	15–40	.0104	500	.0103	1175
	4.2	3–5	0.0075	430	0.007	465

The results for lines of equal solar intensity show that intensity is not the sole cause controlling height in flash spectra, as lines of the same intensity in strong and weak multiplets give heights of 850 and 450, and 500 and 430 km, respectively, the difference being due to the different elevations of the absorbing layers.

Envoy.—The unit character of multiplets places correlations depending on line intensity upon a new basis and suggests a review of former findings. This has been done for the observations on the outflow from spots[1] and for the data on red displacement and relativity.[2] In both cases the results are more consistent and the conclusions strengthened.

Carnegie Institution of Washington
Mount Wilson Observatory
November 1929

---

[1] *Mt. Wilson Contr.*, No. 69; *Astrophysical Journal*, **37**, 322, 1913.

[2] *Mt. Wilson Contr.*, No. 348; *Astrophysical Journal*, **67**, 195, 1928.

Contributions from the Mount Wilson Observatory, No. 390
Reprinted from the *Astrophysical Journal*, Vol. LXX, pp. 319–330, 1929
Printed in the U.S.A.

EXCITATION POTENTIAL IN SOLAR PHENOMENA

By CHARLES E. ST. JOHN

ABSTRACT

1. *Excitation potential fixes the relative heights of the effective absorbing layers* above the photosphere. High values of excitation potential require the stronger fields of excitation obtaining near the photosphere in order to excite the needed number of atoms to the energy-levels of absorption (Table I).

2. *Low heights* above the photosphere of absorbing layers for *multiplets with high excitation potential* are shown by correlating excitation potential with outflow from spots, heights from flash spectra, red displacement, and line intensity, in graphs 1, 2, 3 of Figure 1.

3. The absorbing layers for *intersystem lines* of a given excitation potential are *nearer* the photosphere than those for *normal lines* of the same excitation potential (Table V). The low transition probability for intersystem lines requires the greater abundance of atoms obtaining at the higher pressure near the photosphere.

4. *Excitation potential determines* (1) the possibility and relative probability of the occurrence of a line in the sun's spectrum; (2) the relative heights of absorbing layers above the photosphere; (3) in connection with transition probability, the maximum line intensity in a multiplet; and (4) the temperature classification (Table VI).

5. *Small changes in the energy-level of the higher term* are associated with profound changes in the character of the lines and furnish the basis for a fundamental classification (Table VII).

Introduction.—The importance of excitation potential in showing the relative heights above the photosphere of the absorbing layers in which different Fraunhofer lines originate was noted by the writer in *Mount Wilson Contribution* No. 348.[1] The conclusion (Abstract) was that any one of five methods may be used to allocate the relative levels of origin: (1) solar rotation, (2) Evershed effect, (3) flash spectra, (4) excitation potential, (5) deviations from relativity predictions. In the paragraph on titanium the subject was further discussed. At that time the relation between heights and excitation potential was obtained by forming groups of lines of the same solar intensity and comparing their heights with the corresponding excitation potential. In *Contribution* No. 389[2] it was shown that the multiplet acts as a unit, that the lines in a given multiplet have important characteristics in common, among them equal displacements to the red, whatever the line intensities may be.

---

[1] *Astrophysical Journal*, 67, 195, 1928.

[2] *Ibid.*, 70, 312, 1929.

Accordingly, in the present paper the multiplet is treated as the unit. The basic data are the red displacement, λ sun *minus* λ vac., the velocity of outflow from spots, and the heights in the reversing layer obtained from flash spectra for the normal multiplets of neutral iron. These define the characteristics of the individual multiplets with which the excitation potentials in the *Rowland Revision*[1] are compared. A multiplet will be designated as a 30-multiplet, a 6-multiplet, etc., the numerals giving the maximum line intensity in the multiplet.

Height of absorbing layers.—Eddington in a paper on "The Formation of Absorption Lines"[2] finds that the lines giving the lowest emergent radiation, the blacker lines, refer to absorbing layers at the least optical depth, and that the weaker lines are to be referred to layers at greater depths; for example, for moderately strong lines, $\tau \approx 0.16$, and for weak lines, $\tau \approx 0.58$. Data showing the height of absorbing layers above the photosphere are presented in Table I.

The multiplets and their spectral regions are given in the first column of Table I. The line intensity, number of lines, λ sun *minus* λ vac., Evershed effect, height, and excitation potential are shown in the second, third, fourth, fifth, sixth, and seventh columns, respectively. The data in the fourth, fifth, and sixth columns indicate relative heights above the photosphere.

It has long been recognized that the red displacement of solar absorption lines is greater for lines originating in the upper levels of the sun's atmosphere. The fourth column shows that the red displacement for lines in the first section of the table is 0.0112 A, while for lines of like intensity and wave-length the red displacement as shown in the second section of the table is 0.0092 A. The velocity of horizontal outflow from sun-spots for lines in the reversing layer increases with depth, in this case from 0.42 to 0.84 km/sec., as shown in the fifth column. The sixth column shows the height of the reversing layer for the two groups of lines from measures of their reversals in the flash spectrum. These all march with excitation potential in such a way as to indicate that lines due to transitions from high energy-levels originate in low layers of the sun's atmosphere.

---

[1] *Publications of the Carnegie Institution of Washington*, No. 396; *Papers of the Mount Wilson Observatory*, **3**, 1928.

[2] *Monthly Notices*, **89**, 627–629, 1929.

Excitation potential depends upon the configuration of the electrons in the atom and not upon the position of the atom. The magnitudes in the fourth, fifth, and sixth columns change with excitation potential, and are to be regarded as functions of the excitation potential, which is the fundamental physical characteristic.

TABLE I

CORRELATION OF EXCITATION POTENTIAL, RED SHIFT, OUTFLOW FROM SPOTS, AND HEIGHT

($\Delta\lambda=\lambda$ sun *minus* λ vac.; unit=0.001 A)

Multiplet, Region	Int. of Line	No. of Lines	$\Delta\lambda$	Evershed Effect in Km/Sec.	Height* in Km	E.P.
A. Pressure Class *a*						
$a^5F-a^5D^\circ$	4	1	14.0	....	500	1.007
5269−5506	5	4	10.8	....	450	0.988
	6	3	8.7	....	570	.975
	7	2	12.5	....	650	.932
	8	2	13.0	....	500	0.933
Means and totals	6	12	11.2	0.42 out	575	0.967
B. Pressure Class *d*						
$a^5D^\circ-b^5D$	3	3	7.5	....	315	3.242
5208−5393	4	2	9.0	....	375	3.260
	5	2	8.5	....	375	3.246
	6	2	9.0	....	300	3.260
	7	1	12.0	....	....	3.199
$a^5G^\circ-y^5F$	5	2	7.0	....	425	4.324
5367−5424	6	3	11.7	....	350	4.375
$a^5G^\circ-(wy)$ 5364	5	1	8.0	....	300	4.294
$a^5G^\circ-(vy)$ 5393	6	1	11.0	....	400	4.302
Means and totals	5	17	9.2	0.84 out	350	3.752

* Mitchell, *Astrophysical Journal*, **38**, 407, 1913.

According to current views, equal line intensities imply equal numbers of atoms in the respective excited states. To attain approximate equality between the 8-multiplet (Table I, A; E.P. 0.967) and the multiplets 5-7, the lines having mean excitation potential 3.752 volts must originate where the field of excitation is stronger—that is, nearer the photosphere, hence in a deeper-lying portion of the reversing layer. This is shown by the summarized data taken from the fourth to the seventh columns of Table I and given in Table II.

This view is in harmony with findings in the furnace.[1] Lines of class *a* (low E.P.) appear at the lowest temperature, and lines of class *d* (high E.P.) only at the highest temperature, if at all. The enhanced lines of high ionization potential are quenched by adding to the furnace an element, such as caesium, of the lowest-known ionization potential. In the sun and in the furnace, the atoms which are activated by the least energy appropriate the major portion of the available supply.

TABLE II

SUMMARY

SECTION	4	5	6	7
	λ Sun *minus* λ Vac. A	Outflow from Spots in Km/Sec.	Height in Km	Excitation Potential
A.	0.0112	Vel. = 0.42	575	0.967
B.	0.0092	Vel. = 0.84	350	3.752

Excitation Potential and Line Intensity.—The inverse relation between excitation potential and height of the absorbing layers above the photosphere for multiplets of various strengths appears with distinctness from the correlation between excitation and line intensity. The mean excitation potentials for multiplets of different strengths, such as a 5-multiplet, a 4-multiplet, etc., are plotted as ordinates and the line intensities as abscissae in graph 1, Figure 1. The highest excitation potential corresponds to the weakest lines. Lines of intensity −1 and −2 appear at heights of 250 km in flash spectra, and lines of intensity −3 rise so slightly above the photosphere that they do not show at all.

---

[1] King, *Mt. Wilson Contr.*, No. 66; *Astrophysical Journal*, **37**, 234, 1913; *Mt. Wilson Contr.*, No. 233; *Astrophysical Journal*, **55**, 380, 1922.

Excitation potential and outflow from spots.—The relation of excitation to spectral region and to outflow from spots shows again how it acts as an index of the relative levels of the absorbing layers.

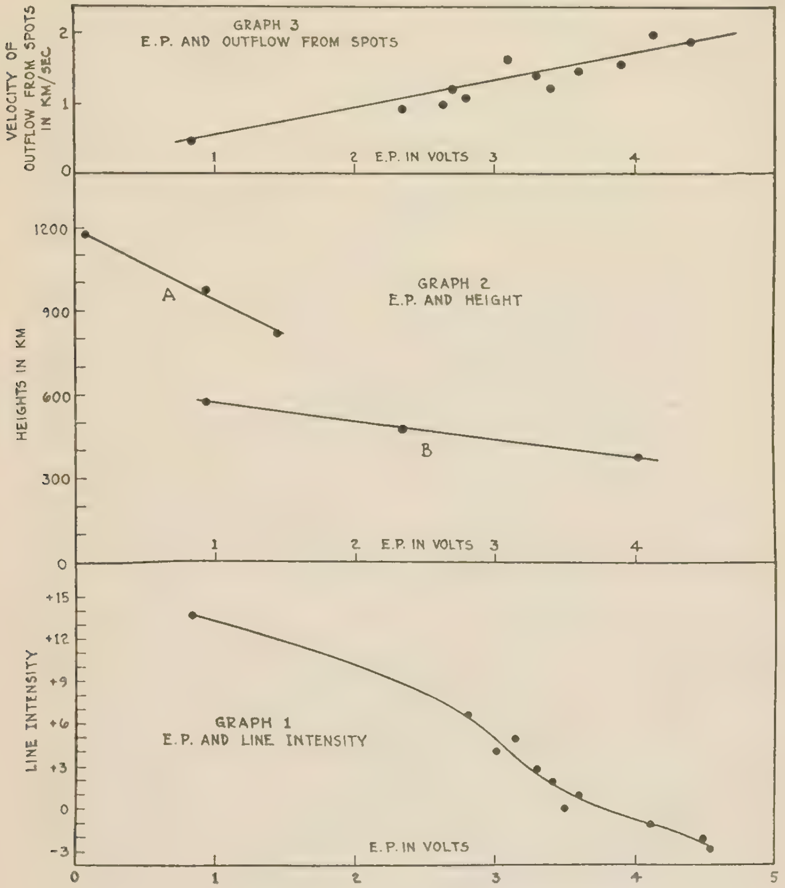

FIG. 1.—Conditions determined by excitation potential

The data are given in Table III. The numbers in the first column are the intensities of the strongest line in the multiplet, and in the second column the mean excitation potential from all multiplets of a given intensity. The third and fourth columns contain in the upper line the mean excitation potential for the two spectral regions, and in the lower line the corresponding velocities of outflow from spots in km/sec. The fifth and sixth columns give the excitation potentials for the even and odd terms.

An absorption line can be produced only when the atom is already excited to the lower energy state of the transition which produces the line. The excitation potentials of the first column are divided into energy-levels for the even and odd states. For each intensity group the excitation potential of even terms is the lower, which accounts for the predominance of absorption lines in the solar spectrum from even energy-levels. The seventh column gives the east-wind velocity at two levels.

TABLE III

Excitation Potential, Spectral Region, Outflow from Spots, Even and Odd Terms

1	2	3	4	5	6	7
Int. of Multiplet	Mean E.P.	E.P. to Violet of λ 5000 and Outflow	E.P. to Red of λ 5000 and Outflow	Even Terms	Odd Terms	Winds in the Sun
15–40	0.83	0.83 0.24	No lines	0.83	None	200 km/hour at height of 1100 km
6–7	2.80	2.35 0.9	3.40 1.2	2.47	4.20	100 km/hour at height of 650 km
5	3.15	2.65 1.0	3.89 1.5	2.91	3.97	
4	3.03	2.77 1.1	3.61 1.5	2.69	4.11	
3	3.29	2.68 1.2	3.90 1.6	2.15	4.36	
2	3.43	3.28 1.4	4.22 2.0	2.53	4.13	
1	3.60	3.11 1.7	4.42 1.9	2.73	4.15	Photosphere

The third and fourth columns show that the excitation potential increases to a striking degree in passing from the violet to the red, and also that this increase keeps step with the velocity of outflow from spots. As this velocity increases with decrease of height above the photosphere, the higher excitation potential in the red means lower level for the absorbing layers in the red.

In my original paper[1] on outflow from sun-spots it appeared that the velocity of outflow for lines of solar intensity 6, 5, 4, etc., in the red was approximately 0.4 km/sec. greater than for lines of the same intensity in the violet, and the difference was interpreted as evidence that the corresponding absorbing layers corresponding to the red lines were nearer the photosphere. The average change in velocity per Rowland unit of intensity was 0.2 km/sec. The average increase in velocity of outflow on passing from the violet to the red, column 4 *minus* column 3, is 0.4 km/sec., which means, as before, that a line of intensity 6 in the red is at the level of a line of intensity 4 in the violet. The effect is too large to be attributed to changes in the Rowland scale of intensities.[2]

TABLE IV

Excitation Potential an Index of Height

Max. Int. 15–40		Max. Int. 6–7		Max. Int. 5		Max. Int. 4		Max. Int. 3		Max. Int. 2	
E.P.	Ht. in Km	E.P.	Ht. in Km	E.P.	Ht. in Km	E.P.	Ht. in Km	E.P.	Ht. in Km	E.P.	Ht. in Km
0.06	1170	2.04	550	2.46	575	2.27	465	2.47	390	2.44	388
0.96	980	3.80	400	3.80	380	4.18	390	4.13	365	4.21	338
1.24	875	......	......	......	......	......	......	......	......	......	.....

The positive correlation coefficient between excitation potential and velocity of outflow from spots is shown by graph 3 in Figure 1, where the abscissae are volts and the ordinates are velocities of outflow. High excitation potential means, then, low heights for the absorbing layers and should show a negative correlation coefficient with heights above the photosphere.

Excitation potential an index of height.—The data in Table IV were obtained by dividing the excitation potentials for each multiplet group into low and high groups and taking the corresponding heights from flash spectra.

---

[1] *Mt. Wilson Contr.*, No. 69; *Astrophysical Journal*, **37**, 322, 1913.

[2] Russell, Adams, and Moore, *Mt. Wilson Contr.*, No. 358; *Astrophysical Journal*, **68**, 1, 1928.

Graph 2 in Figure 1, besides showing a negative correlation between excitation potential and heights, brings to light somewhat surprising differences in distribution of *Fe* absorbing layers. The discontinuity between sections A and B is real and was foreshadowed by the gap at the high-intensity end of the graph in Figure 1. Three energy-levels only are represented by *Fe* lines at great heights above the photosphere: a^5D, a^5F, and a^3F with the excitation potentials 0.06, 0.96, and 1.54 volts. All the multiplets[1] represented in this high layer originate in these three energy-levels, the total number of lines being 88. All others of the 3157 lines identified with normal iron in the *Rowland Revision* are found below this level. The discontinuity between sections A and B, graph 2, Figure 1, implies a region in the sun's atmosphere, about 300 km in extent, in which no lines due to neutral iron originate. With the present data it is probably pushing the interpretation too far to take seriously the result that a difference of 1 volt in excitation potential means a difference in level of 40 km.

The heights for multiplets of a given excitation potential may be approximately obtained from section B, graph 2. For example, there are six strong multiplets with excitation potentials of 2.19–3.60 volts and of strengths 7–10. If these are arranged in groups of three with mean excitation potentials 2.35 and 3.0, the heights according to the graph are 490 and 450 km; as observed, they are 453 and 425 km.

Intersystem combinations.—Up to this point only normal multiplets of neutral iron have been considered. The conclusion is that high excitation potential indicates low level of the absorbing layer. Intersystem combinations may be compared with normal combinations by the data in Table V. The first column gives the excitation potential; the third, the line intensity; the fifth, sixth, and seventh, the velocity of outflow from spots, the height from flash spectra, and the pressure in the sun's atmosphere. Sections A and B give the data for intersystem and normal combinations having the same energy-level. The fourth, fifth, and sixth columns give criteria for level. These show that the absorbing layer for the intersystem lines is far below that for normal lines. Intersystem combinations mimic normal combinations having higher excitation potentials. For example,

---

[1] Included in the spectral region to the red of λ 3585 remeasured for the *Rowland Revision.*

TABLE V

INTERSYSTEM AND NORMAL COMBINATIONS

(λ sun *minus* λ vac. $= \Delta\lambda$; unit $= 0.001$ A)

1	2	3	4	5	6	7
Multiplet E.P.	Lines	Intensity	$\Delta\lambda$	Outflow from Spots in Km/Sec.	Height in Km	Pressure Atm.
			A. Intersystem Combinations			
$a^5D-a^7P^\circ$:						
0.051	4206.704	3	60.0	....	400	....
.000	4216.193	3	8.0	....	400	....
.110	4232.736	2	9.0	....	400	....
.087	4258.324	2	9.0	1.56	400	....
0.051	4291.475	2	9.0	1.08	500	....
$a^5D-a^7F^\circ$:						
0.000	4347.244	1	9.0	0.96	....	....
.000	4375.946	6	14.0	....	500	....
.051	4389.256	2	8.0	....	500	....
.051	4427.319	5	7.0	....	600	....
.087	4435.158	2	8.0	....	....	....
.087	4461.662	4	7.0	....	500	....
0.121	4483.750	4	10.0	....	400	....
0.058	4343.814	3.0	8.7	1.20	460	$\approx 10^{-3}$
			B. Normal Combinations			
$a^5D-a^5D^\circ$:						
0.000	3824.444	6	9.0	....	1000	....
.051	3856.383	8	10.0	....	1600	....
.000	3859.924	20	10.5	....	1600	....
.087	3878.583	7	8.5	....	1200	....
.051	3886.296	15	12.0	....	1600	....
.110	3895.669	7	17.0	0.3	1200	....
.087	3889.721	8	17.0	....	1000	....
.110	3906.492	10	12.0	0.24	750	....
.121	3920.271	10	13.0	....	1000	....
.051	3922.925	12	11.5	....	1200	....
.110	3927.935	8	14.0	....	1000	....
0.087	3930.310	8	11.0	....	1000	....
0.072	3889.182	9.3	11.9	0.27	1175	$\approx 10^{-6}$

the intersystem lines with excitation potential 0.058 given in the second column of Table V behave like normal lines with excitation

3 volts (graphs 1–3, Fig. 1). The transition probability in intersystem combinations is low, as shown by the relative intensity 1–3 for the lines in the second column of sections A and B. The transition probability being low, the production of lines of intensity 5–6 requires that large numbers of atoms be at disposal. These are supplied by the relatively high pressure at the lower level indicated in the seventh column.

Effects depending upon energy-level.—Changes in energy-level are concerned in a number of observations that at first sight do not seem to be intimately related to them, but of which they are the *vera causa*. Energy-level serves as a kind of "barometer"; when it changes, other effects follow which may be regarded as functions of it. The second, fourth, and fifth columns of Table VI give essential data, namely, excitation potential, energy-level of the high term, and pressure class.

TABLE VI

FACTORS FIXED BY ENERGY-LEVEL

LINES	E.P.	MULTIPLET	LEVEL OF HIGH TERM	PRESSURE CLASS
				$E<$ Energy-Level $<E_2$ of Higher Term
3906.492.......	0.110	$a^5D_1-a^5D^\circ_1$	3.269	$2.432<$ Class $a<4.012$
3906.270.......	1.478	$a^3F\ -b^3F^\circ_3$	4.588	$4.012<$ Class $b<5.123$
3997.403.......	2.176	$a^3G_4-a^3H^\circ_5$	5.802	$5.123<$ Class $d<6.790$
5415.199.......	4.354	$a^5G^\circ_4-54W_3$	6.632	$6.605<$ Class $e<6.790$

A. Excitation potential determines:

1. The probability of the occurrence of a line in the sun's spectrum. The lower the excitation potential the higher the probability. For *Fe* lines the range in excitation potential is from 0.000 to 5.064.

2. The position of the absorbing layer:

E.P.	Height in Km
0.06......................	1100–1200
1.54......................	850– 950
2.716......................	450– 500
5.064......................	250

3. In combination with transition probability, the maximum intensity in the multiplet:

E.P.	Maximum Intensity
0.06	40
1.54	30
2.716	8
5.064	2

4. The temperature class, which changes by 1 unit for a change of 0.72 volt in excitation potential.[1]

B. The energy-level of the higher terms in the combination determines the pressure class, a function of the electronic configuration in the atom in the higher energy state. The four pressure classes are as sharply differentiated as the energy states and include all *Fe* lines identified in multiplets. Classes *a*, *b*, and *d* were proposed by Gale and Adams[2] from the pressure coefficients; class *e*, by St. John and Miss Ware[3] from its negative pole effect. Their connection with the energy-level of the higher term was recently established by Babcock.[4] Data showing the significance of changes in the high-level term are given in the third, fifth, and sixth columns in Table VII.

Small changes in excitation potential have comparatively little effect, but small changes in the energy-level of the higher terms may completely alter the character of the spectral lines. Lines λ 5065 and λ 5090 are produced by transitions from the same lower term $b^5F_3^\circ$ to levels of 6.675 and 6.662 volts, respectively. By this change of 0.013 volt the character of the line is reversed. Line λ 5065 is asymmetrical to the violet and shorter at the pole of the arc than in the center; line λ 5090 is asymmetrical to the red and longer at the pole of the arc. One temperature class represents a fifty-fold greater change in excitation potential. The pressure classification apparently depends upon profound changes in the atom, and by this criterion it is fundamental.

Conclusion.—Five indices of relative levels of the absorbing layers in the sun's atmosphere have been considered. All agree in the order of levels. In historical sequence they are heights from flash spectra, solar rotation, outflow from spots, red displacement of Fraunhofer lines, and excitation potential. In order of precision, because of its exact determination, excitation potential comes first; then, depending upon precision of observation and weight of accumulated data, follow in order red displacement of Fraunhofer lines, outflow from spots, solar rotation, and heights from eclipse spectra, the last being affected by photographic errors.

---

[1] *Mt. Wilson Contr.*, No. 350; *Astrophysical Journal*, **67**, 259, 1928.

[2] *Mt. Wilson Contr.*, No. 58; *Astrophysical Journal*, **35**, 10, 1912.

[3] *Mt. Wilson Contr.*, No. 61; *Astrophysical Journal*, **36**, 14, 1912.

[4] *Mt. Wilson Contr.*, No. 350; *Astrophysical Journal*, **67**, 240, 1928.

TABLE VII

EFFECTS PRODUCED BY CHANGES IN THE ENERGY-LEVEL OF THE HIGHER TERM

Line	Int.	E.P.	Multiplet	High Term	Pressure Class*	T Class*
5065.030...	3	4.238	$b^5F^\circ_3-c^3G_4$	6.675	*e* Asymmetrical to violet Pole-effect negative Pressure coeff. moderate Very high temp. lines	V
5090.782...	5	4.238	$b^5F^\circ_3-61W_3$	6.662	*d* Asymmetrical to red	IV
3305.974...	4	2.188	$a^5P_2-c^5P^\circ_3$	5.251	*d* Pole-effect positive Pressure coeff. large High temp. lines	III
4292.296...	2	2.188	$a^5P_2-c^5F^\circ_2$	5.064	*b* Generally symmetrical	
3849.979...	10	1.007	$a^5F_1-b^5D^\circ_2$	4.213	*b* Pressure coeff. medium Medium temp. lines	II
5434.536...	5	1.007	$a^5F_1-a^5D^\circ_0$	3.278	*a* Always symmetrical Pressure coeff. small Low temp. lines	I

* Defined in the *Rowland Revision*, pp. x–xi of Introduction.

The energy-levels of the low and high terms in multiplets play distinct rôles. The low term, for example, determines the temperature class; the high term founds the pressure classification upon profound changes in the electron configuration within the atom. Intersystem combinations mimic the behavior of normal combinations with higher excitation potential.

CARNEGIE INSTITUTION OF WASHINGTON
MOUNT WILSON OBSERVATORY
November 1929

END OF VOLUME XVII

INDEX TO VOLUME XVII

Nos. 371 to 390

AUTHORS

PAGE

Abbot, C. G.—Energy Spectra of the Stars 193

Adams, Walter S., A. H. Joy, R. F. Sanford, and G. Strömberg—The Radial Velocities of 741 Stars 377

Anderson, J. A., and Russell W. Porter—Ronchi's Method of Optical Testing 369

Babcock, Harold D.—Revision of the Value of *e/m* Derived from Measurements of the Zeeman Effect 79

Bowen, I. S. *See* Russell, Henry Norris

Epstein, Paul S.—Conference on the Michelson-Morley Experiment . 17

Hale, George E.—The Spectrohelioscope and Its Work: Part I. History, Instruments, Adjustments, and Methods of Observation . . 407

Hedrick, E. R.—Conference on the Michelson-Morley Experiment . 17

Hubble, Edwin—A Spiral Nebula as a Stellar System, Messier 31 . 99

Joy, Alfred H. *See* Adams, Walter S.; Merrill, Paul W.

Kennedy, Roy J.—Conference on the Michelson-Morley Experiment . 17

King, Arthur S.—The Electric-Furnace Spectrum of Hafnium . . 343

Lorentz, H. A.—Conference on the Michelson-Morley Experiment . 17

Merrill, Paul W.—The Spectrum of B.D.+11°4673 213

Merrill, Paul W., and Alfred H. Joy—Spectroscopic Observations of R Virginis 263

Michelson, A. A.—Conference on the Michelson-Morley Experiment . 17

Miller, Dayton C.—Conference on the Michelson-Morley Experiment 17

Osgood, Thomas H.—Photographic Observations of Some Double Stars 1

Porter, Russell W. *See* Anderson, J. A.

Russell, Henry Norris—On the Composition of the Sun's Atmosphere 271

Russell, Henry Norris, and I. S. Bowen—Is There Argon in the Corona? 85

PAGE

St. John, Charles E.—
  Elements Unidentified or Doubtful in the Sun 353
  Excitation Potential in Solar Phenomena 463
  The Unit Character of Multiplets 455
Sanford, Roscoe F.—The Spectrum and Radial-Velocity Variation of RU Camelopardalis 9
Sanford, Roscoe F. *See* Adams, Walter S.
Strömberg, Gustaf. *See* Adams, Walter S.
Unsöld, Albrecht—
  On the Physical Interpretation of Spectroheliograms 173
  On the Thermal Excitation of Atoms in the Reversing Layer of the Sun 185
  A Spectroscopic Determination of the Pressure in the Calcium Chromosphere: An Experimental Test of Milne's Theory 155

SUBJECTS

Argon, in solar corona, 85
Atmosphere, solar, composition, 271
Atoms, thermal excitation in reversing layer of sun, 185
Chromosphere, calcium, spectroscopic determination of its pressure, 155
Coronal lines, attributed to argon, 85
Double stars. *See* Stars, double
Electric-furnace spectrum, of hafnium, 343
Electron charge, revised value of e/m from measurements of Zeeman effect, 79
Elements, in the sun, unidentified or doubtful, 353
Energy spectra, of stars, 193
Excitation potential, in solar phenomena, 463
Hafnium, electric-furnace spectrum, 343
Messier 31, spiral nebula as stellar system, 99
Michelson-Morley experiment, conference held at Mount Wilson Observatory, 17
Milne's theory, experimental test, 155
Multiplets, unit character, 455
Nebula, spiral, as stellar system, 99
Optical testing, Ronchi's method, 369
Potential, excitation, in solar phenomena, 463
Radial velocities, of 741 stars, 377
Radial-velocity variation, of RU Camelopardalis, 9
Ronchi's method of optical testing, 369
Spectra, energy, of stars, 193
Spectroheliograms, physical interpretation, 173
Spectrohelioscope, history, instruments, adjustments, methods of observation, 407
Spectrum, electric-furnace, of hafnium, 343
———, of B.D.+11°4673; 213
———, of RU Camelopardalis, 9
Spiral nebula as stellar system, Messier 31; 99
Stars, double, photographic observations, 1
———, energy spectra, 193
———, radial velocities and spectral types, 377
———, variable, radial-velocity variation of RU Camelopardalis, 9
———, ———, spectroscopic observations of R Virginis, 263
Stellar systems, Messier 31; 99
Sun, composition of atmosphere, 271
———, excitation potential in various phenomena, 463

Sun, thermal excitation of atoms in reversing layer, 185
———, unidentified or doubtful elements, 353
Variable stars. *See* Stars, variable
Velocities, radial, of 741 stars, 377
Velocity, radial, variation, of RU Camelopardalis, 9
R Virginis, spectroscopic observations, 263
Zeeman effect, measurements used to revise value of e/m, 79

522.19 C28 V17

a39001 006937299b

522 19 C28 V17
MOUNT WILSON OBSERVATORY CONTRIBUTION

INSERT BOOK
MASTER CARD
FACE UP IN
FRONT SLOT
OF S.R. PUNCH

MASTER CARD

GLOBE 90144-0

UNIVERSITY OF ARIZO
LIBRARY